



Wright, Pamela Burnby (2013) *The immunopathogenesis of ankylosing spondylitis*. PhD thesis.

<http://theses.gla.ac.uk/4882/>

Copyright and moral rights for this work are retained by the author

A copy can be downloaded for personal non-commercial research or study, without prior permission or charge

This work cannot be reproduced or quoted extensively from without first obtaining permission in writing from the author

The content must not be changed in any way or sold commercially in any format or medium without the formal permission of the author

When referring to this work, full bibliographic details including the author, title, awarding institution and date of the thesis must be given

Glasgow Theses Service
<http://theses.gla.ac.uk/>
theses@gla.ac.uk

The Immunopathogenesis of Ankylosing Spondylitis

Pamela Burnby Wright
BSc (Hons)

Submitted in fulfilment of the requirements for the degree of
Doctor of Philosophy

College of Medical, Veterinary and Life Sciences
Institute of Infection, Immunity and Inflammation
University of Glasgow

December 2013

Abstract

The Spondyloarthritis (SpA) are a group of genetically and pathophysiologically related diseases. Ankylosing spondylitis (AS), the prototypic SpA family member, is a systemic inflammatory disease primarily affecting the axial skeleton, characterised by sacroiliitis and bone formation, promoting joint inhibition. AS is highly heritable; approximately 90% of AS susceptibility is defined by an individual's genetic background, to which the MHC class I molecule HLA-B27 contributes approximately 30%. This association was discovered 40 years ago, yet the pathogenic role of HLA-B27 remains elusive.

Dendritic cells (DCs) belong to the myeloid lineage and as the principal antigen presenting cells (APCs) of the immune system, activate naïve T cells and contribute to the balance between activation and suppression of the immune response. If affected by HLA-B27, DCs are therefore likely to contribute to the T cell-mediated aspects of AS pathogenesis. Studies in our laboratory, using HLA-B27 transgenic (HLA-B27 TG) rats, have revealed HLA-B27-mediated effects on DC populations. The affected DCs induce abnormally high levels of IL-17 production from T cells; CCR6⁺ IL-17-secreting cells appear to be important in driving pathology both in the HLA-B27 TG rats and in AS patients. We therefore aimed to perform the first characterisations of the phenotype and functions of DCs and other myeloid populations purified directly from AS patients, to understand their role in AS pathogenesis.

Analyses of circulating myeloid populations revealed that AS patients have a reduced proportion of the CD1c-expressing blood DCs, offset by an increase in CD14⁻ CD16⁺ mononuclear cells. Interactions between CD14⁻ CD16⁺ mononuclear cells and CD4⁺ T cells generated high levels of IL-6 secretion, required for the generation of Th17 cells. CD14⁻ CD16⁺ mononuclear cells also induced T cells to express CCR6, and may therefore contribute to pathology by promoting Th17 responses. Interestingly, our data also indicate that APCs of mucosal origin may make a significant contribution to the systemic inflammation observed in AS patients. These observations give new insights into the pathogenic mechanisms in AS.

Abstract	2
Acknowledgements	8
Author's declaration	10
List of abbreviations	11
Chapter 1: General introduction	16
1.1 Spondyloarthritides	17
1.1.1 Ankylosing spondylitis	18
1.1.2 Genetics of ankylosing spondylitis.....	20
1.1.3 Involvement of the immune response.....	22
1.2 T cells	23
1.2.1 T cell populations	23
1.2.2 Effector CD4 ⁺ T cell phenotypes.....	25
1.2.3 Cytokines.....	28
1.2.4 Chemokines and their receptors.....	31
1.3 Dendritic cells	34
1.3.1 What is a dendritic cell?.....	34
1.3.2 Human myeloid cell classification	35
1.3.2.1 DCs.....	35
1.3.2.2 Blood CD1c ⁺ DCs.....	36
1.3.2.3 Blood CD141 ⁺ DCs.....	36
1.3.2.4 Blood pDCs.....	37
1.3.2.5 Monocytes	37
1.3.2.6 CD16 ⁺ mononuclear cells.....	38
1.3.2.7 Lymphoid tissue DCs	41
1.3.2.8 Non-lymphoid tissue DCs	42
1.3.3 DC development.....	43
1.3.3.1 cDCs.....	43
1.3.3.2 pDCs.....	44
1.3.4 DC function.....	45
1.3.4.1 Antigen presentation and T cell priming.....	45
1.3.4.2 CD141 ⁺ DCs.....	49
1.3.4.3 CD1c ⁺ DCs.....	51
1.3.4.4 CD14 ⁻ CD16 ⁺ mononuclear cells.....	52
1.3.4.5 pDCs.....	53
1.3.5 Rat DC classification	54
1.3.6 Murine DC classification	55
1.3.7 Comparing DC populations between species	56
1.4 Intestinal immune system	57
1.4.1 Intestinal DCs	58
1.4.2 Intestinal macrophages.....	60
1.4.3 AS and the intestinal immune system	62
1.5 Ankylosing spondylitis	62
1.5.1 Inflammation associated with ankylosing spondylitis.....	62
1.5.2 Animal models of SpA and immune pathogenesis	63
1.5.3 Immunopathogenesis of AS/SpA	65
1.6 Molecular pathogenesis of AS	67
1.6.1 Molecular mimicry	67
1.6.2 Cell surface HLA-B27 dimer formation.....	69
1.6.3 ER stress	71
1.7 Immunopathogenesis of AS	73
1.7.1 Cytokines	73
1.7.2 T cells	75
1.7.3 Myeloid cells	76
1.7.4 Peripheral tissue.....	77
1.7.5 Treatment of AS.....	78
1.7.5.1 Therapeutic categories used in the management of AS	78

1.7.5.2	Assessment of disease activity	79
1.7.5.3	Effectiveness of therapeutics	80
1.8	Hypotheses and aims	80
Chapter 2:	Materials and Methods	82
2.1	Patient blood samples	83
2.2	Intestinal samples	83
2.3	Cell culture medium	85
2.4	Blood collection	85
2.5	PBMC isolation	85
2.6	Flow cytometry and monoclonal antibodies.....	86
2.6.1	Surface staining	86
2.6.2	FACS cell sorting	88
2.6.3	Intracellular cytokine staining.....	88
2.7	Naïve T cell isolation	89
2.8	Carboxyfluorescein succinimidyl ester (CFSE) staining	90
2.9	Allogeneic mixed leukocyte reaction (MLR)	90
2.10	Cytospins and H&E staining	91
2.11	Annexin V staining	91
2.12	Synovial fluid processing	91
2.13	Isolation of RNA.....	92
2.14	Generation of cDNA.....	93
2.15	Quantitative real time PCR	93
2.16	Luminex	94
2.17	Elisa	94
2.18	Cell survival assay	95
2.19	Human colonic and small intestine cell isolation	95
2.20	Histology.....	96
2.21	Statistics.....	96
Chapter 3:	Characterisation of blood mononuclear cell populations.....	98
3.1	Introduction.....	99
3.2	Patient characteristics.....	99
3.3	Identification of peripheral blood DC subsets.....	102
3.4	Quantification of DC and monocyte subsets in AS patients and HCs.....	105
3.4.1	cDCs and pDCs	105
3.4.2	CD14 ⁻ CD16 ⁺ mononuclear cells.....	108
3.5	Identification and quantification of blood monocytes	111
3.6	DC morphology.....	114
3.6.1	Cell viability.....	118
3.7	Maturation status of DCs and monocytes in AS patients and HCs.....	121
3.8	Further characterisation of DCs and monocytes	121
3.8.1	Monocytes.....	124
3.8.2	DCs	124
3.8.3	CD14 ⁻ CD16 ⁺ mononuclear cells.....	124
3.8.4	CD115 expression on blood mononuclear cells	127
3.9	Expression of zDC by circulating myeloid populations	127
3.10	Discussion	131
Chapter 4:	Role of T cells in AS pathogenesis.....	143
4.1	Introduction.....	144
4.2	Patient characteristics.....	144
4.3	T cell subsets in peripheral blood	147
4.4	Chemokine receptor expression on circulating T cells.....	151
4.5	T cell phenotype and cytokine secretion	155
4.6	Plasma cytokines in AS patients.....	160
4.7	Discussion.....	165
Chapter 5:	Synovial Fluid	175

5.1	Introduction.....	176
5.2	Patient characteristics.....	176
5.3	Synovial fluid mononuclear phagocytes	177
5.3.1	cDCs and monocytes.....	177
5.3.2	Plasmacytoid DCs	178
5.4	Surface phenotype of cDCs and monocytes	181
5.5	Quantification of cDCs	184
5.6	CD4 ⁺ T cells and chemokine receptor expression.....	184
5.7	Blood and SF cDC and pDC populations.....	187
5.8	Differences in cytokine profile between blood and SF	188
5.9	Discussion.....	191
Chapter 6: Functional characterisation of circulating DCs.....		198
6.1	Introduction.....	199
6.2	Patient characteristics.....	199
6.3	Induction of T cell proliferation.....	200
6.4	Upregulation of chemokine receptors	205
6.5	Induction of T cell responses	208
6.6	Assessment of cell survival.....	212
6.7	ER stress in circulating myeloid populations	213
6.8	Role of myeloid A20 expression in AS.....	216
6.9	Discussion.....	220
Chapter 7: Comparisons between patient characteristics and immunological parameters 227		
7.1	Introduction.....	228
7.2	Patient Characteristics	228
7.3	Correlative analyses.....	230
7.4	The influence of disease severity.....	231
7.5	Effect of inflammation on immunological parameters.....	234
7.6	Disease treatment protocols and plasma cytokines	238
7.7	Influence of extra-articular disease manifestation	238
7.8	DC related correlations	240
7.9	Discussion.....	245
Chapter 8: Intestinal Phagocytes.....		252
8.1	Introduction.....	253
8.2	Patient characteristics.....	254
8.3	Isolation of intestinal phagocytes.....	255
8.4	Identification of intestinal cDCs.....	262
8.5	Steady state vs inflammation	267
8.6	Expression of CCR2 by intestinal DC populations	267
8.7	Intestinal macrophages.....	270
8.8	Macrophages in inflammation	271
8.9	<i>In vivo</i> turnover of intestinal macrophages	274
8.10	Discussion	276
Chapter 9: Final discussion		285
9.1	General discussion.....	286
9.2	Conclusion	289
References.....		290

TABLE 1.1: CLASSIFICATION OF INFLAMMATORY AND T CELL ASSOCIATED CYTOKINES AND GROWTH FACTORS.....	29
TABLE 1.2: CHEMOKINE FUNCTION	33
TABLE 1.3: SURFACE RECEPTOR EXPRESSION OF MONOCYTES AND CD14 ⁻ CD16 ⁻ MONONUCLEAR CELLS	39
TABLE 1.4: HUMAN DC CLASSIFICATION	40
TABLE 1.5: COMPARISON OF HUMAN AND MURINE DC POPULATIONS.....	56
TABLE 1.6: DRUGS USED IN THE MANAGEMENT OF AS.....	79
TABLE 1.7: ASSESSMENT OF DISEASE SEVERITY AND THERAPEUTIC RESPONSE	79
TABLE 2.1: LIST OF MONOCLONAL ANTIBODIES USED FOR FLOW CYTOMETRY.....	86
TABLE 2.2: PRIMERS USED FOR QRT-PCR.....	94
TABLE 3.1: CLINICAL CHARACTERISTICS OF PATIENTS AND HEALTHY CONTROLS	100
TABLE 4.1: PATIENT CHARACTERISTICS FOR T CELL ANALYSIS	145
TABLE 5.1: PATIENT CHARACTERISTICS FOR SF ANALYSIS.....	176
TABLE 6.1: PATIENT CHARACTERISTICS FOR DC FUNCTION EXPERIMENTS.....	199
TABLE 7.1: CLINICAL CHARACTERISTICS OF AS PATIENTS AND HEALTHY CONTROLS	228
TABLE 7.2: IMMUNOLOGICAL PARAMETERS ASSESSED FOR CORRELATIVE ANALYSES.....	230
TABLE 8.1: PATIENT CHARACTERISTICS FOR INTESTINAL TISSUE SPECIMENS.....	254

FIGURE 1.1: ASAS CRITERIA FOR SPA CLASSIFICATION.....	18
FIGURE 1.2: PROGRESSION OF ANKYLOSING SPONDYLITIS	19
FIGURE 1.3: HUMAN CD4 ⁺ T CELL SUBSETS	25
FIGURE 1.4: HUMAN CD4 ⁺ T CELL PHENOTYPES	27
FIGURE 1.5: HUMAN CHEMOKINE RECEPTOR PROMISCUITY	31
FIGURE 1.6: IMMUNOLOGICAL SYNAPSE BETWEEN DC AND CD4 ⁺ NAÏVE T CELL.....	49
FIGURE 1.7: DIAGRAM DEPICTING ER STRESS PATHWAYS.....	72
FIGURE 2.1: PATIENT DATA COLLECTION SHEET	84
FIGURE 3.1: GATING STRATEGY FOR THE IDENTIFICATION OF BLOOD MONOCYTES AND DCs.....	103
FIGURE 3.2: PDCs IN PERIPHERAL BLOOD	104
FIGURE 3.3: ENUMERATING DCs IN AS PATIENTS	106
FIGURE 3.4: ENUMERATION OF PDCs AND DC SUBSETS IN AS PATIENTS AND HCs	107
FIGURE 3.5: CHANGES IN HC BLOOD DC AND MONONUCLEAR CELL PROPORTIONS OVER TIME.....	109
FIGURE 3.6: GATING STRATEGY FOR CD16 ⁺ SLAN ⁻ AND CD16 ⁺ SLAN ⁺ CELLS.....	110
FIGURE 3.7: COMPARISON OF CD16 ⁺ CELLS BETWEEN AS PATIENTS AND HCs.....	112
FIGURE 3.8: IDENTIFICATION OF MONOCYTES IN PERIPHERAL BLOOD.....	113
FIGURE 3.9: QUANTIFICATION OF BLOOD MONOCYTE SUBSETS.....	115
FIGURE 3.10: COMPARISON OF DC MORPHOLOGY BETWEEN AS PATIENTS AND HCs	116
FIGURE 3.11: COMPARISON OF ACTIVATED DC MORPHOLOGY BETWEEN AS PATIENTS AND HCs	117
FIGURE 3.12: SURVIVAL OF CDC SUBSETS AFTER OVERNIGHT INCUBATION AND FLOW CYTOMETRY SORTING	119
FIGURE 3.13: SURVIVAL OF PDC SUBSETS AFTER OVERNIGHT INCUBATION AND FLOW CYTOMETRY SORTING	120
FIGURE 3.14: CO-STIMULATORY MOLECULE EXPRESSION ON CDC AND MONOCYTE SUBSETS	122
FIGURE 3.15: EXPRESSION OF DC CO-STIMULATORY MOLECULES – CD40, CD80 AND CD86.....	123
FIGURE 3.16: SURFACE PHENOTYPE OF CD14 ⁺ CD16 ⁻ AND CD14 ⁺ CD16 ⁺ MONOCYTES.....	125
FIGURE 3.17: EXPRESSION OF CD11B, CD64, CD135 AND CX3CR1 ON DC SUBSETS.....	126
FIGURE 3.18: SURFACE PHENOTYPE OF CD16 ⁺ SLAN ⁻ AND CD16 ⁺ SLAN ⁺ MONONUCLEAR CELLS.....	128
FIGURE 3.19: SURFACE EXPRESSION OF CD115 ON DC AND MONOCYTE SUBSETS.....	129
FIGURE 3.20: ZBTB46 (zDC) EXPRESSION BY DC AND MONOCYTE SUBSETS	130
FIGURE 4.1: IDENTIFICATION OF PERIPHERAL BLOOD T CELL SUBSETS.....	148
FIGURE 4.2: COMPARISON OF T CELL SUBSETS IN AS PATIENTS AND HCs.....	149
FIGURE 4.3: COMPARISON OF CD25 ⁺ T CELL SUBSETS IN AS PATIENTS AND HCs.....	150
FIGURE 4.4: DETECTION OF CHEMOKINE RECEPTOR EXPRESSION ON CD4 ⁺ T CELLS.....	152
FIGURE 4.5: EXPRESSION OF CCR4, CCR6 AND CXCR3 ON T CELL SUBSETS	153
FIGURE 4.6: EXPRESSION OF CCR9 AND CCR10 ON T CELL SUBSETS.....	154
FIGURE 4.7: CCR4 AND CCR6 EXPRESSION IN AS PATIENTS AND HCs	156
FIGURE 4.8: CXCR3 EXPRESSION IN AS PATIENTS AND HCs.....	157
FIGURE 4.9: CCR9 AND CCR10 EXPRESSION IN AS PATIENTS AND HCs	158
FIGURE 4.10: SECRETION OF IL-17A AND IFN γ FROM PERIPHERAL BLOOD CD4 ⁺ TcRAB ⁺ T CELLS.....	159
FIGURE 4.11: QUANTIFICATION OF IL-17A AND IFN γ SECRETING CD4 ⁺ TcRAB ⁺ T CELLS.....	161
FIGURE 4.12: CCR6 EXPRESSION ON CYTOKINE SECRETING CD4 ⁺ TcRAB ⁺ T CELLS.....	162
FIGURE 4.13: PRESENCE OF T HELPER CYTOKINES IN AS PATIENT AND HC PLASMA	163
FIGURE 4.14: PRESENCE OF INFLAMMATORY CYTOKINES AND GROWTH FACTORS IN AS PATIENT AND HC PLASMA.....	164

FIGURE 5.1: IDENTIFICATION OF CD141 ⁺ AND CD1c ⁺ SYNOVIAL FLUID DC SUBSETS	179
FIGURE 5.2: PRESENCE OF CD16 ⁺ CD11c ⁺ MONONUCLEAR CELLS AND SLAN SUBSETS IN SF	180
FIGURE 5.3: pDCs PRESENT IN AS PATIENT SF	182
FIGURE 5.4: EXPRESSION OF CD11b AND CD86 BY SF CDC AND MONOCYTE SUBSETS	183
FIGURE 5.5: QUANTIFICATION OF SF CDC SUBSETS	185
FIGURE 5.6: CD4 ⁺ T CELLS INFILTRATE AS SYNOVIUM AND EXPRESS CCR4 AND CCR6	186
FIGURE 5.7: COMPARISON OF CDCs AND pDCs BETWEEN PERIPHERAL BLOOD AND SF	189
FIGURE 5.8: COMPARISON OF CYTOKINE LEVELS IN AS PLASMA AND SF	190
FIGURE 6.1: INDUCTION OF T CELL PROLIFERATION BY BLOOD DC/MONOCYTE SUBSETS	202
FIGURE 6.2: T CELL PROLIFERATION INDUCTION BY HC AND AS BLOOD DC/MONOCYTE SUBSETS	203
FIGURE 6.3: COMPARISON OF T CELL PROLIFERATION BY BLOOD DC/MONOCYTE SUBSETS	204
FIGURE 6.4: ABILITY OF HUMAN BLOOD DCs/MONOCYTES TO INDUCE T CELL HOMING MARKERS	206
FIGURE 6.5: CCR6 INDUCTION BY HC AND AS BLOOD DC/MONOCYTE SUBSETS.....	207
FIGURE 6.6: CXCR3 INDUCTION BY HC AND AS BLOOD DC/MONOCYTE SUBSETS.....	209
FIGURE 6.7: SECRETION OF T CELL-ASSOCIATED CYTOKINES FOLLOWING MLR	210
FIGURE 6.8: SECRETION OF INFLAMMATORY CYTOKINES AND GROWTH FACTORS FOLLOWING MLR	211
FIGURE 6.9: SURVIVAL OF CDC AND MONOCYTE SUBSETS ISOLATED FROM AS PATIENTS AND HCS	214
FIGURE 6.10: SURVIVAL OF AS PATIENT AND HC CD1c, CD16 AND MONOCYTE POPULATIONS	215
FIGURE 6.11: EXPRESSION OF ER STRESS GENES IN CIRCULATING CD1c ⁺ DCs	217
FIGURE 6.12: EXPRESSION OF ER STRESS GENES IN CIRCULATING CD16 ⁺ MONONUCLEAR CELLS	218
FIGURE 6.13: MYELOID EXPRESSION OF A20 IN AS PATIENTS AND HCS	219
FIGURE 7.1: T CELL PROPORTIONAL CORRELATIONS WITH DISEASE SEVERITY	232
FIGURE 7.2: CD4 ⁺ T CELL CHEMOKINE PROFILE CORRELATIONS WITH DISEASE SEVERITY	233
FIGURE 7.3: IMMUNOLOGICAL CORRELATIONS RELATED TO DISEASE SEVERITY AND IL-23p19	235
FIGURE 7.4: INFLUENCE OF INFLAMMATION ON ACTIVATED CD4 ⁺ T CELL CHEMOKINE PROFILES	236
FIGURE 7.5: CCR9 ASSOCIATION WITH INFLAMMATION	237
FIGURE 7.6: INFLUENCE OF DISEASE TREATMENT STRATEGIES ON CYTOKINES AND CHEMOKINES	239
FIGURE 7.7: INFLUENCE OF EXTRA-ARTICULAR MANIFESTATIONS ON IMMUNOLOGICAL PARAMETERS	242
FIGURE 7.8: INFLUENCE OF CLINICAL AND IMMUNOLOGICAL FACTORS ON CD141 ⁺ DCs	243
FIGURE 7.9: INFLUENCE OF AGE ON DC POPULATIONS IN AS PATIENT AND HCS	244
FIGURE 8.1: INITIAL GATING STRATEGY FOR IDENTIFICATION OF INTESTINAL PHAGOCYTE SUBSETS.....	257
FIGURE 8.2: CLEAVAGE OF CX3CR1 AND CD16 BY ENZYMATIC DIGESTION	258
FIGURE 8.3: MARKER EXPRESSION IS DEPENDENT ON ENZYMATIC DIGESTION CONDITIONS.....	260
FIGURE 8.4: SURFACE MARKER EXPRESSION FOLLOWING ENZYMATIC DIGESTION.....	261
FIGURE 8.5: IDENTIFICATION OF CD14 ⁻ CD16 ⁺ INTESTINAL MONONUCLEAR CELLS	263
FIGURE 8.6: LINEAGE EXCLUSION NOT REQUIRED FOR THE IDENTIFICATION OF INTESTINAL CDCs	264
FIGURE 8.7: IDENTIFICATION OF INTESTINAL CDC SUBSETS	266
FIGURE 8.8: HISTOLOGY OF COLONIC TISSUE FROM AN ULCERATIVE COLITIS PATIENT.....	268
FIGURE 8.9: EXPRESSION OF CCR2 BY CDC SUBSETS FROM STEADY STATE AND INFLAMED COLON	269
FIGURE 8.10: IDENTIFICATION OF INTESTINAL MACROPHAGES IN HEALTHY COLON	272
FIGURE 8.11: MACROPHAGES IN STEADY STATE AND CROHN'S DISEASE.....	273
FIGURE 8.12: MACROPHAGE SUBSET PROLIFERATION POTENTIAL FROM HC AND INFLAMED COLON.....	275
FIGURE 9.1: ROLE OF DCs IN DISEASE PATHOGENESIS	287
FIGURE 9.2: IMMUNOPATHOGENESIS OF AS.....	289

Acknowledgements

Firstly, I would like to thank my supervisor, Simon Milling, for all of his support over the last four years. He has supported and encouraged me throughout my PhD and I really appreciate the belief he has shown in me. He also never gave up on my writing regardless of how much there was. I also really appreciate all the time he dedicated to thoroughly reading and correcting my thesis. Thanks for all you have done.

I would also like to extend my thanks to Prof Allan Mowat for all his advice throughout my PhD and during my undergrad. Your admiration of St. Mirren is also much appreciated. To Professor Iain McInnes, thank you for giving me the opportunity to participate in the Oliver Bird programme, it has been such a rewarding experience. To Diane, your help over the last four years has been endless and without your constant aria set-up for me on Tuesday mornings I could not have performed the majority of my experiments, so thank you. Jim and Shauna thanks for all your technical expertise and help throughout my PhD, especially with the human tissue sections. To Ashley G and Darren, thanks for all your experimental advice but most importantly your friendship.

I am extremely grateful to Dr David McCarey and Dr Anne McEntegart, and all the other doctors and nurses involved in running of the AS clinic at the GRI, for their continuous collection and supply of patient samples. Without your help, I could not have done my PhD. And to that, thanks to all the patients for supplying their blood! My PhD has relied heavily on the generosity of numerous “healthy” controls from within the department, of which there are too many name, but if I have taken your blood, not personally, then thanks very much! I need to extend my sincere thanks to several very generous people who have given up their time to help me, no matter of how busy they were, to take blood from willing donors: Ananda Mirchandani, Hannah Bayes, Neil Ritchie, Sharon Irvine, Marina Frleta, Jagtar Nijjar and everyone else who donated their time. I can't put into words how grateful I am.

Next, I would like to thank all of my current and past lab members for their support, encouragement and help over the last few years. Special mentions go to Yvonne and Elinor; your help and kindness fostered my desire to do a PhD. Thanks for all the laughs and songs about Andy Murray as well! And to all the current lab members (Mowlings), I apologise for my mood swings and grumpiness over the last four years, and especially the final few months. You have all become great friends, and I could not have asked to work

with a better group of people. This includes the honorary Mowlings, Ananda and Ashley G! To the Millings, thank you for all your support, advice and banter – I could not have got through the last four years without it. Lotta, Vuk and Calum, thank you so much for reading my thesis! I know it was hard going but I really appreciate it. To Lotta especially, thanks for all your extra help with the formatting of my thesis, without you I would have gone insane!! Steph, we have done this together and despite your fascination with lowering my chair I could not have asked for a better bench partner!! Also to Lotta and Steph, thanks for being my drinking and crazy dancing partners! To Charlie and Calum, thanks for your constant and unwavering help throughout all the years, both in terms of scientific discussion, assistance, friendship and alcohol consumption! I genuinely don't think I could have done it without you.

There are too many people to mention but thanks to everyone in the GBRC for their friendship and support over the last few years. I need to specially thank Felix and Carolyn for all their emotional support and friendship during my undergraduate and PhD. Thanks for being my travelling buddy Felix! I also need to thank Martin for his constant support and encouragement; it really does mean a lot. To all the amazing people that have become my friends through swimming I thank you, I don't think I would have stayed sane without you. Special mentions go to Kirsty H, Claire, Jeanna, Kirsty McW, Adam and the rest of the guys I have trained with over my 8 years at university!! Also thanks to everyone at NAASC, especially Sharon and the Hughes for the laughs and support!

What can I say about Kate and Charlie: no matter where we all end up we will always remain great friends. You are both such amazing people and I will never forget all the random trips we went on, drunken nights out and movie nights in (with you both falling asleep!). Thanks for being awesome and for everything that you have done for me, love you!

And finally to my family; the Wrights, the Websters and all, words can't describe how lucky I feel to be part of this family. Your support and love is unwavering and I could not have got through this without you all. However, I need to say special thanks to mum, dad, Caroline and John. Thanks for putting up with my grumpiness and tears, especially over the last few months, I love you all very much. And to mum and dad, thanks for reading parts of my thesis; you have always been there for me when I needed you! And now you can have the real me back!

Author's declaration

I declare that, except where explicit reference is made to the contribution of others, that this thesis is the result of my own work and has not been submitted for any other degree at the University of Glasgow or any other institution.

Signature: Printed name: Pamela Wright

List of abbreviations

A

Ab	Antibody
Ag	Antigen
AK2	Adenylate kinase 2
ALDH	Aldehyde dehydrogenase
ANOVA	Analysis of Variance
APC	Antigen presenting cell
ANTXR2	Anthrax toxin receptor 2
AS	Ankylosing Spondylitis
ASAS	Assessment of Spondyloarthritis International Society
ASDAS	Ankylosing spondylitis disease activity score
ATF	Activating transcription factor
ATG16L1	Autophagy-related protein 16-1

B

β 2m	β 2-microglobulin
BASDAI	Bath ankylosing spondylitis disease activity index
BASFI	Bath ankylosing spondylitis functional index
BASMI	Bath ankylosing spondylitis metrology index
Batf3	Basic leucine zipper transcription factor, ATF-like 3
Bcl-6	B-cell lymphoma 6 protein

Bio	Biotin
BiP	Binding immunoglobulin protein
BM	Bone Marrow
BMDC	Bone marrow derived dendritic cell
BMP	Bone morphogenetic protein

C

CARD9	Caspase recruitment domain-containing protein 9
CD	Cluster of differentiation
CD	Crohn's disease
cDC	Conventional dendritic cell
cDNA	Complementary DNA
CDP	Common DC progenitor
CFSE	Carboxyfluorescein succinimidyl ester
CHOP	CCAAT/enhancer binding protein (C/EBP), epsilon
CLA	Cutaneous leukocyte-associated antigen
CLIP	Class II-associated invariant chain peptide
CLEC9A	C-type lectin domain family 9, member A
CLP	Common lymphoid progenitor
CMP	Common myeloid progenitor
ConA	Concanavalin A
CRP	C-reactive protein

CSF-1	Colony stimulating factor 1	F	
CT	Cholera Toxin	FACS	Fluorescence activated cell sorting
CTL	Cytotoxic T lymphocyte	FAE	Follicle associated epithelium
CTLA-4	Cytotoxic T lymphocyte antigen 4	FBS	Fetal bovine serum
CXCR	CXC-chemokine receptor	FCS	Fetal calf serum
D		FITC	Fluorescein isothiocyanate
DAPI	4',6-diamidino-2-phenylindole	Flt3	Fms-like tyrosine kinase
DC	Dendritic cell	Flt3L	Fms-like tyrosine kinase ligand
DCML	Dendritic cell, monocyte, B and NK lymphoid deficiency	FOXP3	Forkhead box protein P3
DC-SIGN	Dendritic cell-specific intercellular adhesion molecule-3-grabbing non-integrin	FSC	Forward scatter
DMARDs	Disease modifying anti-rheumatic drugs	G	
DNA	Deoxyribonucleic acid	GALT	Gut-associated lymphoid tissue
DR3	Death receptor 3	GM-CSF	Granulocyte macrophage colony-stimulating factor
E		GPCR	G-protein coupled receptor
EAE	Experimental autoimmune encephalomyelitis	GWAS	Genome wide association study
E. coli	Escherichia coli	H	
EDTA	ethylenediaminetetraacetic acid	HC	Healthy control
ELISA	Enzyme-linked immunosorbent assay	hi	High
ER	Endoplasmic reticulum	HIV	Human immunodeficiency virus
ERAD	ER-associated degradation	HLA-B27 TG	HLA-B27 transgenic rats
ERAP1	ER aminopeptidase 1	HSCs	Hematopoietic stem cells
ESR	Erythrocyte sedimentation rate	I	
		IBD	Inflammatory bowel disease

IBP	Inflammatory back pain	K	
ICAM1	Intracellular adhesion molecule 1	KIR	Killer-cell immunoglobulin-like receptor
ID2	Inhibitor of DNA binding 2	KO	Knock out
IDO	Indoleamine 2,3-dioxygenase	L	
IEC	Intestinal epithelial cell	LC	Langerhans cell
IEL	Intraepithelial lymphocyte	LFA-1	Lymphocyte function-associated antigen 1
IFN	Interferon	LIN	Lineage markers
Ig	Immunoglobulin	LN	Lymph node
IL	Interleukin	lo	Low
ILF	Isolated lymphoid follicle	LP	Lamina propria
ILT	Immunoglobulin-like transcript	LPMC	Lamina propria mononuclear cell
iNOS	Inducible nitric oxide	LPS	Lipopolysaccharide
int	Intermediate	M	
IRE1 α	Inositol requiring enzyme 1 α	mAb	Monoclonal antibody
IRF	Interferon regulatory factor	MACS	Magnetically activated cell sorter
IRGM	Immunity-related GTPase family M protein	MAPK	Mitogen-activated protein kinase
ITAM	Immunoreceptor tyrosine-based activation motif	M-CSF	Macrophage colony stimulating factor
ITIM	Immunoreceptor tyrosine-based inhibition motif	MDP	Monocyte-DC progenitor
iTregs	Inducible regulatory T cells	MHC	Major histocompatibility complex
J		MIP-1 α	Macrophage inflammatory protein 1 α
Jak	Janus kinase	MLN	Mesenteric lymph node
jSpA	Juvenile Spondyloarthritis	MLR	Mixed leukocyte reaction
		MMP	Matrix metalloproteinase

moDCs	Monocyte-derived dendritic cells	PERK	Protein kinase RNA-like endoplasmic reticulum kinase
MP	Mononuclear phagocyte	PGE2	Prostaglandin E2
MPO	Myeloperoxidase	PIP2	Phosphatidylinositol-4, 5-bisphosphate
mRNA	Messenger RNA	PI3K	Phosphoinositide 3-kinase
N		PLC	Peptide loading complex
Necl2	Nectin and nectin-like molecule 2	pLN	Popliteal lymph node
NFAT	Nuclear factor of activated T-cells	PP	Peyer's patch
NFκB	Nuclear factor-kappa beta	PRR	Pattern recognition receptor
NK	Natural killer	PsA	Psoriatic Arthritis
NOD	Non-obese diabetic	PSGL-1	P-selectin glycoprotein 1
NSAIDs	Non-steroidal anti-inflammatory drugs	PsSpA	Psoriatic Spondyloarthritis
nTreg	Natural regulatory T cells	Q	
O		qRT-PcR	Quantitative real time-PCR
OA	Osteoarthritis	R	
P		RA	Rheumatoid arthritis
PAMP	Pathogen associated molecular pattern	RALDH	Retinaldehyde dehydrogenase
PB	Peripheral blood	RBC	Red blood cell
PBMC	Peripheral blood mononuclear cell	ReA	Reactive arthritis
PBS	Phosphate buffered saline	RetA	Retinoic acid
PcR	Polymerase chain reaction	RNA	Ribonucleic acid
pDC	Plasmacytoid dendritic cell	RORγt	RAR-related orphan receptor γt
PE	Phycoerythrin	ROS	Reactive oxygen species
PerCP	Peridinin-chlorophyll-protein	RPMI	Roswell Park Memorial Institute-1640 medium

S		TBP	Tata-box binding protein
SA	Streptavidin	TCM	Central memory T cell
SCID	Severe combined immunodeficiency	TcR	T cell receptor
SD	Standard deviation	T _{EM}	Effector memory T cell
SED	Sub-epithelial dome	TF	Transcription factor
SEM	Standard error of the mean	T _{FH}	Follicular T helper cell
SF	Synovial fluid	TG	Transgenic
SFMC	Synovial fluid mononuclear cell	TGF	Transforming growth factor
SI	Small intestine	Th	T helper cell
SIJ	Sacroiliac joint	TLR	Toll-like receptor
SILP	Small intestinal lamina propria	TNF α	Tumour necrosis factor α
SIRP α	Signal-regulatory protein α	TNFSF15	Tumour necrosis factor (ligand) superfamily, member 15
SLAN	6-sulfo LacNAc	Treg	T regulatory cell
SLE	Systemic lupus erythematosus	TSLP	Thymic stromal lymphopoietin
SLO	Secondary lymphoid organ	U	
SNP	Single nucleotide polymorphisms	UC	Ulcerative colitis
SpA	Spondyloarthritis	UPR	Unfolded protein response
SpA-IBD	Spondyloarthritis associated with inflammatory bowel disease	uSpA	Undifferentiated spondyloarthritis
SSC	Side scatter	V	
STAT	Signal transducers and activators of transcription	VEGF	Vascular endothelial growth factor
T		VIPR	Vasoactive intestinal polypeptide receptor
TAP	Transported associated with antigen processing	Vit D3	Vitamin D3
Tbet	T-box transcription factor	W	
		WT	Wild-type

Chapter 1: General introduction

1.1 Spondyloarthritides

The spondyloarthritis (SpA) family of diseases is heterogeneous but shares many genetic and pathophysiological features. Originally, SpA was considered a variant of the well-known and characterised disease rheumatoid arthritis (RA) (1). However, Moll et al recognised the need for further classification of these rheumatoid factor negative diseases, subsequently termed “seronegative spondarthritis” (1). Ankylosing spondylitis (AS) is the prototypic and most studied SpA family member (1-3). Since the original Moll and Wright description, there have been various classification criteria, with the most recent classification by the Assessment of SpondyloArthritis international Society (ASAS) assigning the following diseases as SpA family members: AS, psoriatic arthritis (PsA), reactive arthritis (ReA), arthritis associated with inflammatory bowel disease (SpA-IBD), undifferentiated SpA (uSpA), juvenile SpA (jSpA) and acute anterior uveitis. Diseases of the SpA family share several physiological characteristics including spondylitis, sacroiliitis, peripheral arthritis, enthesitis, uveitis, psoriasis and inflammatory bowel disease (IBD) (1, 2, 4, 5). Disease comorbidities may additionally affect tissues including the heart, lungs and kidneys (6).

The ASAS classification criteria subdivide SpA patients into two groups according to whether they have dominant axial (axial SpA) or peripheral (peripheral SpA) joint disease (7, 8). These groups are not exclusive, as patients assigned to the axial SpA group may develop peripheral joint involvement. As there was a recognition that many patients with axial SpA did not have radiographic sacroiliac changes meeting the modified New York criteria for AS (7, 8), the ASAS axial SpA was developed to incorporate both patients with AS and those with non-radiographic axial SpA. Patients can be classified with axial SpA through either an imaging or a clinical arm (Figure 1.1). For the imaging arm, patients require chronic back pain, evidence of sacroiliitis on imaging (x-ray or MRI) and at least one other SpA feature. Alternatively, patients without the required radiographic evidence of sacroiliitis can still be classified with axial SpA via the clinical arm for which they require chronic back pain, a positive HLA-B27 and at least 2 other specified SpA features which include uveitis, psoriasis and IBD. The ASAS criteria are outlined in Figure 1.1.

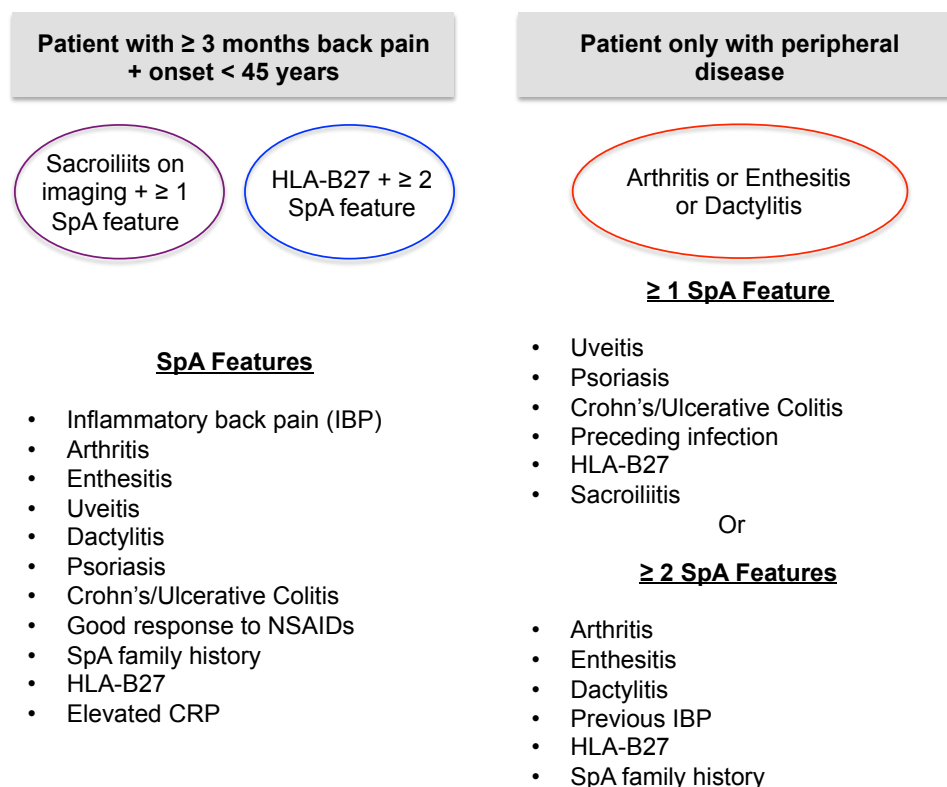


Figure 1.1: ASAS criteria for SpA classification

Adapted from Rudwaleit et al, describing the classification criteria for patients with axial disease, either AS or non-radiographic axial SpA (left) and those presenting only with peripheral/extra-articular symptoms (right) (7). Sacroiilitis on imaging is defined through use of x-ray and MRI. IBP = inflammatory back pain. ASAS = Assessment of SpondyloArthritis international Society. SpA classification criteria from 2011 onwards.

Patients with peripheral arthritis and/or enthesitis and/or dactylitis but no axial disease can fulfil the ASAS criteria for peripheral SpA if they meet a number of other specified SpA features which include HLA-B27 positivity, IBD and clinical uveitis (Fig. 1.1). Despite these advancements regarding clinical characterisation of SpA, this remains a heterogeneous group and the aetiology and pathogenesis of this disease remain elusive.

1.1.1 Ankylosing spondylitis

Ankylosing Spondylitis (AS) is a chronic inflammatory disease belonging to the SpA family (9). AS affects 0.1 to 1.4% of the global population (4). AS susceptibility is highly influenced by an individual's genotype, with around 95% of AS sufferers expressing the MHC Class I molecule HLA-B27 (4). AS primarily affects the axial skeleton and is characterised by spinal inflammation, particularly sacroiilitis, bone formation and joint damage (4). As shown in Figure 1.2, severe spinal changes and loss of spinal function are associated with AS.



Figure 1.2: Progression of Ankylosing Spondylitis

This picture highlights the postural changes associated with AS disease progression. This figure was adapted from Little et al (10).

AS is associated with IBD, uveitis and psoriasis with 10%, 25% and 10% of AS patients presenting with these extra-articular manifestations respectively (11, 12). Furthermore, approximately 50% of AS patients display evidence of subclinical intestinal inflammation (4, 13). Characteristic of all SpA family members is the development of enthesitis; inflammation associated with entheses, the sites of tendon or ligament adhesion to bone (5, 14). Approximately 25% of patients are thought to display evidence of peripheral enthesitis (15). Enthesitis and subsequent erosion of the associated bone in AS patients leads to joint ossification (syndesmophyte growth), contributing to the development of AS (16). The details of the relationship between inflammation and pathological changes in bone formation are currently under debate (17, 18). Several studies report a disconnection between inhibition of inflammation using of anti-tumour necrosis factor α (TNF α) treatment, and prevention of structural progression (19, 20). In contrast, anti-TNF α treatment has been shown to slow bone formation in AS patients, and Maksymowych et al observed a preference for bone formation to occur at sites of inflammation (21, 22). Despite this uncertainty regarding the relationship between inflammation and bone formation, the wide range of extra- and articular manifestations in addition to axial involvement indicate the complexity of this disease.

Despite the fact that the biological processes involved in AS development and disease perpetuation remain unclear, several therapeutic agents have shown efficacy in approximately 60% of patients (23). The current most effective therapy is TNF α blockade, but this is only partially successful in reducing disease symptoms, including inflammation

(11). Furthermore, this so-called “biological therapy” remains ineffective for a large proportion of AS patients. The unknown aetiology and pathogenesis of AS partially contribute to the paucity of disease-specific therapies and the ineffectiveness of current therapeutics.

1.1.2 Genetics of ankylosing spondylitis

All SpA family members are linked through their association with the MHC Class I molecule, HLA-B27 (3). However, the role of HLA-B27 in disease development is still not clear. Two seminal papers in 1973 first described the association between AS and HLA-B27 (24, 25). In the study by Brewerton et al 96% of patients, compared to 4% of HCs, expressed HLA-B27 (24). Of the Caucasian European population, approximately 8% carry the HLA-B27 gene, and 0.5% of HLA-B27⁺ individuals develop AS (11). The frequency of HLA-B27 in the general population differs according to ethnicity and geographical location (4, 11). Given that the relationship between AS and HLA-B27 is one of the strongest genetic associations described (11, 26), it is not surprising that HLA-B27 tissue typing is used as a diagnostic marker in suspected AS patients, and is included in the ASAS classification criteria (Figure 1.1).

The association between AS and HLA-B27 is complex; several HLA-B27 haplotypes are associated with disease (27). There are over 50 coding subtypes of HLA-B27 (11, 27), the majority of which are too rare to be comprehensively assessed for disease association (11, 28). However at least 12 subtypes exhibit strong associations with AS development (11). To be specific, HLA-B*2701-08, HLA-B*2710, HLA-B*2714-15 and HLA-B*2719 all confer AS disease susceptibility (11, 29-35). European cohorts are dominated by the HLA-B*2702 and HLA-B*2705 subtypes (HLA-B*2705 is most prevalent); these subtypes are equally associated with SpA (29, 36). In Asian populations, HLA-B*2704 is the dominant HLA-B27 variant, and has been shown to have a stronger AS association than HLA-B*2705 (28). Not every HLA-B27 subtype associated with AS is necessarily pathogenic. Early studies indicated that HLA-B*2709 was protective against AS, however more recent investigations have refuted this (11, 27, 37, 38). Although HLA-B27 expression is strongly associated with SpA, it accounts for less than 50% of the genetic risk associated with disease (11). In fact, the HLA-B27 contribution may be as low as 20-30% (4).

The genetic background of AS patients contributes approximately 90% to disease susceptibility (11, 27). Other MHC genes may exhibit association with AS, including

HLA-B60 and HLA DR1 (28), but their importance is thought to be minor. Multiple genes outside the MHC region contribute to the genetic make-up of AS patients. For instance, single nucleotide polymorphisms (SNPs) within the interleukin-23 receptor (IL-23R) gene and the IL-23 signalling molecule STAT3 are also associated with AS (11, 27, 28, 39-42). Interestingly, the IL-23R polymorphisms associated with AS additionally confer susceptibility to IBD (43) and psoriasis (44), two common extra-articular manifestations of AS patients. Given the close relationship between IBD, psoriasis and AS, it was interesting to note that the IL-23R AS susceptibility association was not due to the concurrent development of these extra-articular manifestations (27, 39). Therefore, IL-23R polymorphisms may inextricably link AS, IBD and psoriasis. Despite this clear association between IL-23R polymorphisms and SpA, the mechanism by which IL-23R SNPs drive SpA remain undetermined.

Another AS susceptibility gene additionally identified through genome-wide association studies (GWAS) was the endoplasmic reticulum aminopeptidase gene, ERAP1 (11, 27, 28, 39, 40). The ERAP1 SNP in AS patients is restricted to HLA-B27⁺ individuals (45). This ERAP1 SNP may reduce the activity of the ERAP1 protein, which is involved in MHC class I peptide loading and cleavage of cytokine receptors, including IL-1RII (28, 46). However, the importance of these functions in AS pathogenesis have still to be elucidated (27). Interestingly, no associations between IBD, psoriasis and ERAP1 have been identified (11, 28).

The role of the killer cell immunoglobulin-like receptors (KIRs), expressed on cytotoxic natural killer (NK) cells, in relation to AS susceptibility has been investigated recently (11). KIRs, principally KIR3DL1 and KIR3DL2, recognise a specific epitope causing “differential NK cell activation” in response to cells expressing B*2708 (11), one of the HLA-B27 alleles strongly associated with AS susceptibility (11, 30). Furthermore, Chan et al observed an upregulation of KIR3DL2 expression on SpA NK cells and CD4⁺ T cells (47). Therefore, given this association between KIRs and AS, at a genetic and immunological level, these receptors may be involved in AS pathogenesis.

Through the GWAS studies, several other candidate genes influencing AS susceptibility were identified: Anthrax toxin receptor 2 (ANTXR2) and TNF (ligand) superfamily, member 15 (TNFSF15) (11, 28). The ANTXR2 gene encodes the capillary morphogenesis protein – 2 (11, 28, 40). TNFSF15 is a ligand for death receptor 3 (DR3), a member of the TNF superfamily. Binding of TNFSF15 to DR3 has been shown to induce proliferation of

Th17 cells, a subtype of T cells associated with the pathogenesis of AS (48, 49). Interestingly, TNFSF15 is also associated with Crohn's disease (CD) (50).

AS is additionally associated with SNPs of the IL-1 gene complex, especially IL-1R2 and CARD9 (11, 28, 39, 40). These SNPs may further support the involvement of Th17 cells in AS pathogenesis, as CARD9 is involved in Th1 and Th17 differentiation (11, 51). Overall, many of the genetic associations identified through the use of GWAS studies have highlighted a potential role for several immune pathways in the development and/or pathogenesis of this disease. Specifically, associations were observed between AS and the IL-23R/Th17 axis, antigen presentation, the innate arm of the immune system and the Th1 pathway. The exact mechanisms by which many of these AS associated genes influence development of this disease remain unknown. However, these newly identified associations have prompted and directed research into understanding their role in AS pathogenesis. Several of the resultant proposals will be discussed below.

1.1.3 Involvement of the immune response

The genetic signature of AS implicates cells of the immune system in the pathogenesis of disease, particularly CD4⁺ T cells and the dendritic cells (DCs) that activate them. The immune system orchestrates the host's defence mechanisms directed towards invading pathogenic organisms, through the mobilisation of effector immune cells. Regulatory immune processes also prevent potentially damaging responses to self-antigen and harmless bacteria (commensals). The balance between immunity (pathogenic antigen) and tolerance (commensals/food) is essential for maintaining homeostasis.

The immune system is comprised of two branches. The innate immune system encompasses cells and molecules that respond first. This rapid response functions to eradicate potentially harmful antigens and secretes molecules that initiate inflammation and cell recruitment. In contrast, the adaptive immune response comprises antigen-specific populations of T cells and B cells and is essential for the generation of long-lived immunological memory, on which vaccine efficacy relies. Failure to regulate these innate and adaptive responses may result in the development of chronic inflammation and autoimmune disease. An understanding of some of the components of the immune system is necessary before the pathogenesis of AS can be investigated.

1.2 T cells

T cells are an effector immune population of the adaptive immune response. Specific T cell populations co-ordinate the defence mechanisms required to eradicate and protect against pathogens through the secretion of immunomodulatory hormones known as cytokines, through their ability to lyse infected cells, and by promoting the activation and differentiation of B cells. T cells also regulate the immune response, inhibiting aberrant immune responses against self-antigen and commensal bacteria.

1.2.1 T cell populations

T cells, which express the CD3 molecule, can be subdivided into two types dependent upon their expression of the glycoproteins CD4 and CD8. In addition, T cells can be further subdivided based on their expression of the T cell receptor (TcR) composed of either $\alpha\beta$, or $\gamma\delta$ subunits. The majority of $CD4^+$ and $CD8^+$ T cells express TcR $\alpha\beta$ (52). TcRs are highly polymorphic and bind to a restricted set of major histocompatibility complex (MHC) molecules, complexed to short self- or pathogen-derived peptides, in addition to commensals, food antigen and allergens. During their development, cells each expressing their own unique TcR, are selected based on their capacity for binding MHC: peptide complexes in the thymus (53). Once selected, $CD4^+$ T cells interact with MHC class II molecules, whilst $CD8^+$ T cells interact with MHC class I expressing cells (53). Therefore, T cells exiting the thymus display a vast repertoire of antigen-specific TcRs able to mediate protection against a multitude of potential pathogens (54).

Antigen-inexperienced T cells are known as naïve T cells. Naïve $CD4^+$ T cells in humans express the molecules CD45RA, CD62L, CD27 and lack expression of CD45RO (55, 56). They recirculate throughout secondary lymphoid organs (SLOs), due to their expression of CD62L (57-59), until they are activated by an antigen-presenting cell (APC) expressing the correct MHC: peptide complex. This constant recirculation of T cells increases the probability that these specific T cell: APC interactions will occur. Following activation, $CD4^+$ and $CD8^+$ T cells differentiate into effector populations that participate in primary and secondary immune responses (immunological memory), becoming activated, regulatory and memory T cell populations. Activated $CD4^+$ T cells in humans are identified predominantly through their expression of intermediate levels of the interleukin-2 receptor (IL-2R), CD25 (60-63). Furthermore, $CD25^+$ activated T cells upregulate CD45RO and lack expression of CD45RA (64). Activated cells, directed by their

interaction with the antigen-specific APC, home to the tissue from which the APC originated and execute their effector functions. Activated CD8⁺ T cells secrete granules that can lyse cells in a contact dependent manner. CD4⁺ T cells contribute to the immune response primarily through their secretion of immune-active soluble molecules, called cytokines. Through cytokine expression, they drive the activation of surrounding cells and cell recruitment. Furthermore, T cell: APC interactions result in the differentiation of specific CD4⁺ activated T cell phenotypes, which will be discussed in more detail below.

Prevention of aberrant responses directed against self-antigen or commensal bacteria is partially achieved through the function of regulatory T cells (Tregs). During the process of thymic selection, natural Tregs (nTregs) are generated. These are identified through their expression of the transcription factor forkhead box P3 (FOXP3), high levels of CD25, cytotoxic T-lymphocyte-associated protein 4 (CTLA-4), transforming growth factor β (TGF- β 1) and tumour necrosis factor receptor 2 (TNFR2) (65-68). The suppressive functions of nTregs are mediated through secretion of immunomodulatory cytokines including TGF β and IL-10, in addition to contact dependent mechanisms potentially mediated by a combination of CTLA-4 and TGF- β 1 (66, 67, 69). Peripheral naïve CD4⁺ T cells can also differentiate into Treg populations following APC interaction: inducible Tregs (iTregs) express CD4, CD25 and FOXP3 and are dependent upon TGF β for their development from naïve T cells *in vivo* (70). A subset of iTregs that exert their immunosuppressive functions through secretion of IL-10 are often referred to as Tr1 cells (71, 72). Overall Tregs, regardless of their site of induction or mode(s) of action, function to control and inhibit aberrant immune responses.

Induction of the adaptive response is central to the development of immunological memory. Memory permits rapid, specific, improved adaptive responses towards previously encountered antigen. In humans, memory cells are identified by their expression of low levels of CD45RA and CD25, and high expression of CD45RO (73). Functionally distinct memory T cell populations can be differentiated based on their homing capabilities: central memory cells (TCM) express CCR7, enabling peripheral lymph node homing, whilst effector memory cells (TEM) are CCR7⁻ permitting their migration to peripheral tissues (74, 75). TEM retain the ability to rapidly secrete effector cytokines following antigen exposure, whilst TCM are thought to differentiate into effector cells following restimulation (74, 75). Classification of human CD4⁺ T cell populations is depicted in Figure 1.3.

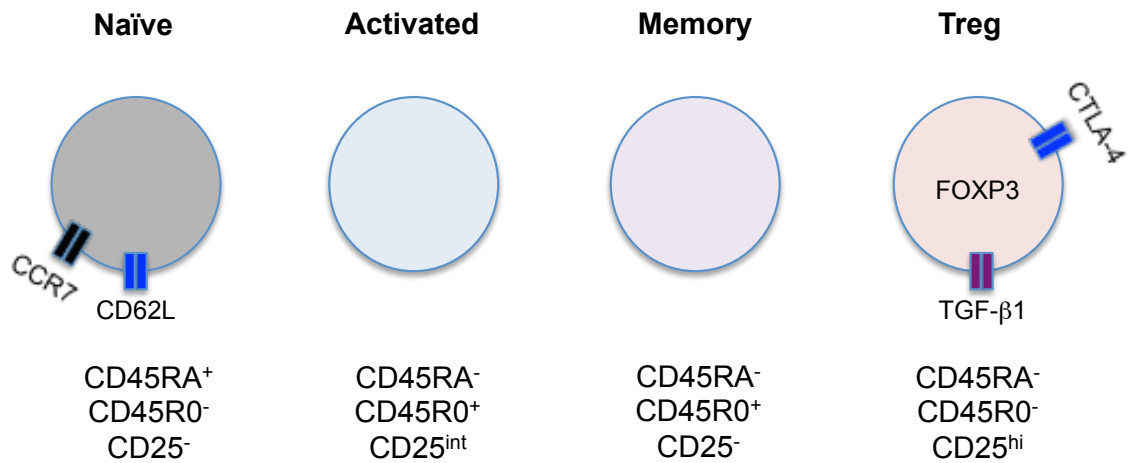


Figure 1.3: Human CD4⁺ T cell subsets

Four populations of human CD4⁺ T cells exist in human blood. Recirculating CD4⁺ naïve T cells express CCR7, permitting entry into secondary lymphoid organs. Following APC stimulation, cells that upregulate CD25 and lose CD45RA can be subdivided into activated and regulatory (Treg) subsets. Regulatory T cells are further identified through their expression of FOXP3, CTLA-4 and TGF-β1. Following clearance of antigen, memory cells persist and upon re-stimulation induce a rapid, efficacious immune response.

1.2.2 Effector CD4⁺ T cell phenotypes

Following activation, naïve CD4⁺ T cells develop into effector cells (Fig. 1.4) that home to peripheral tissues or SLOs and contribute to the immune response. The immune system has evolved to respond to a vast array of potential pathogens, each requiring a different effector response. These include pathogenic bacteria and viruses, parasitic multicellular organisms, neoplastic cells, food antigens, and commensal bacteria. In 1986, Mossman and Coffman first described the differentiation of murine CD4⁺ helper T cell (Th) cells into populations with the ability to secrete different cytokines. These populations were called Th1 and Th2 (76). Equivalent human Th populations were identified in 1991 (77). Originally Th1 and Th2 populations were defined on the basis of their secretion of specific cytokines and their differential capacity to support specific types of B cell responses (76). The Th1 subset secretes interferon γ (IFN γ), IL-2 and granulocyte macrophage colony-stimulating factor (GM-CSF) (77, 78). In contrast, Th2 cells produce IL-4, IL-3, IL-5 and IL-13 (76, 77, 79). Furthermore, Th1 cells are preferentially able to kill intracellular pathogens, whilst Th2 cells mediate expulsion of extracellular pathogens (80-82). Mature Th1 and Th2 cells have a distinct set of genes that transcriptionally regulate their phenotype and function. The majority of studies investigating Th differentiation were performed using mice, however human studies have confirmed many of these observations. Th1 differentiation requires upregulation of the transcription factors signal transducer and activator of transcription 4 (STAT4), STAT1 and T-box expressed in T

cells (T-bet) (83-85). Signalling through the TcR and IL-12R mediate activation of STAT4, and upregulate the IL-12R β 2 on T cells, promoting induction of a Th1 phenotype (86-88). The primary sources of IL-12 in this setting are thought to be two types of APC: dendritic cells (DCs) and macrophages (89). In addition to IL-12, IL-27 and IFN γ additionally promote the differentiation and proliferation of Th1 cells (90-93).

A different form of transcriptional regulation is employed for the differentiation of Th2 cells. STAT6, GATA binding protein 3 (GATA-3), c-Maf and nuclear factor of activated T-cells (NFAT) are the major transcription factors involved in promotion of the Th2 phenotype (94-97). IL-4, the dominant cytokine inducer of Th2 cells inhibits the upregulation of IL-12R β 2 on dividing CD4⁺ T cells, upregulates IL-4R α and activates the transcription factor STAT6 thereby promoting the differentiation of Th2 cells (92, 94, 98, 99). The interaction between transcription factor STAT5 and IL-2 has been reported to promote a Th2 phenotype through regulation of IL-4 signalling (100). The source of IL-4 within SLOs remains unclear, however mast cells, eosinophils, basophils and activated Th2 cells have all been shown capable of IL-4 production (101). In addition to their differential transcriptional and functional phenotypes, Th1 and Th2 cells actively inhibit the generation of the opposing subset. For example, secretion of IL-10 by Th2 cells inhibits the secretion of IL-12 by macrophages, thereby blocking Th1 differentiation (102). In contrast, IL-12 actively inhibits expression of GATA3 within dividing cells, consequently inhibiting the generation of the Th2 subset (98). Given the nature of these counter-regulatory processes, following naïve CD4⁺ T cell activation, the resulting mature Th1 or Th2 CD4⁺ populations secrete either IFN γ (Th1) or IL-4 (Th2).

More recently, several murine disease models highlighted a role for IL-17-secreting CD4⁺ T cells in disease pathogenesis (103-105). These observations led to the identification of a third CD4⁺ effector T cell subset designated Th17 cells (106). Th17 cells secrete IL-17A, IL-17F, IL-22, IL-6 and tumour necrosis factor α (TNF α) and express the IL-23R (105, 107). Differentiation of murine Th17 cells is dependent upon IL-6 and TGF β (108), although IL-1 β may substitute for TGF β in humans (107, 109). The master transcriptional regulators of Th17 cells are ROR γ t and STAT3 (109-111). IL-23 has been shown to promote the survival and not the differentiation of Th17 cells (112). Studies have found Th17 differentiation to be independent of STAT1, STAT4, STAT6 and T-bet (106). Th17 cells are now considered to be an independent lineage of CD4⁺ effector T cell that may contribute to host defence against extracellular pathogens and/or autoimmune disease (113, 114). Th17 and Th1 differentiation appear to be counter-regulatory. The Th1 associated

cytokine IFN γ inhibits development of Th17 cells through downregulation of the IL-23R (106). Unlike Th1 and Th2 cells, the stability of Th17 cells *in vivo* is unclear. IL-17-secreting CD4⁺ T cells under inflammatory conditions have been shown to acquire Th1 attributes, including IFN γ secretion (115-118). Furthermore, given that murine Th17 and Treg differentiation both involve the cytokine TGF β , a reciprocal relationship between these opposing inflammatory and regulatory effector cells may exist. In the presence of inflammation, IL-6 may promote Th17 generation, whilst under steady-state conditions retinoic acid (RetA) has been shown to inhibit IL-6 production and the associated Th17 induction (108, 119, 120). Overall, human Th17 cells represent a distinct lineage of CD4⁺ T cells, require ROR γ t, IL-6 and IL-1 β for their development and are thought to participate in immunogenic immune responses that may contribute to the development or perpetuation of inflammatory diseases.

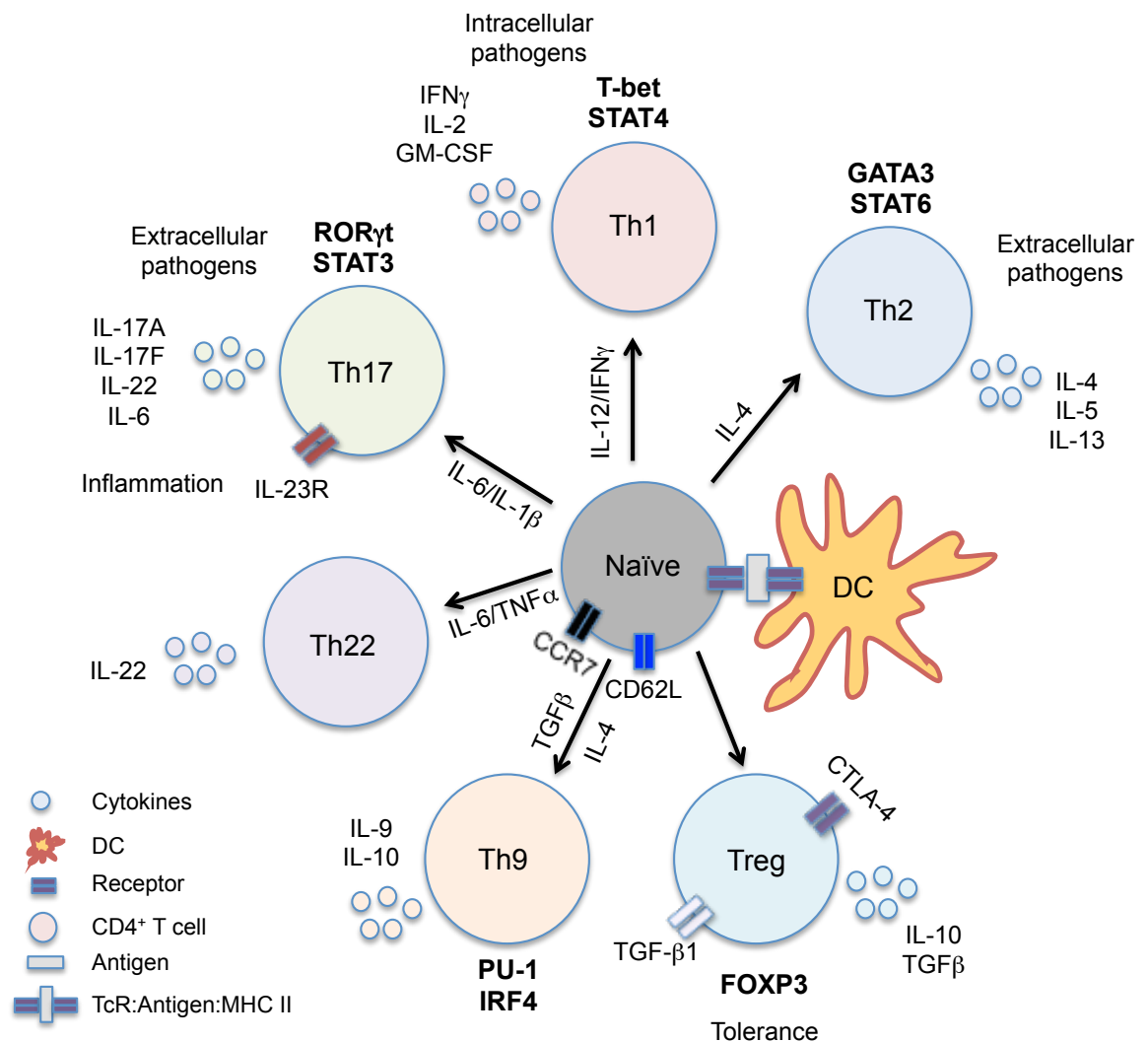


Figure 1.4: Human CD4⁺ T cell phenotypes

Human CD4⁺ effector populations can be subdivided into five populations: Th1, Th2, Th9, Th17 and Th22. Each population is defined by their cytokine secretion profile. This diagram describes

the functions of the individual populations and the molecules involved in their differentiation. Following the interaction between APCs and naïve CD4⁺ T cells in SLOs, under specific conditions Tregs can be generated in the periphery in order to control immune responses. Adapted from Jiang et al (121). DC = dendritic cell, TcR = T cell receptor. Transcription factors for each effector CD4⁺ T cell population are in bold.

In recent years, two further CD4⁺ effector T cell subsets have been identified: Th9 and Th22 cells. Th9 cells were ascribed their name through their preferential secretion of IL-9, in addition to IL-10 (122, 123). They were generated *in vitro* in the presence of TGFβ and IL-4 and were observed to promote chronic inflammation, despite their secretion of IL-10 (122). The transcription factors PU-1 (124) and interferon regulatory factor 4 (IRF4) (125) regulate Th9 development. Th9 cells have been identified and are increased in the blood of allergic patients compared to healthy controls (126). This CD4⁺ effector population is thought to promote allergic and inflammatory responses whilst enhancing tumour killing (126, 127).

Th22 cells, as their name suggests secrete IL-22. Th17 cells and NK cells also secrete IL-22, however in contrast to the Th17 subset, Th22 cells do not secrete IL-17 (121, 128, 129). The transcription factors involved in the generation of Th22 cells have yet to be determined, however Th22 cells have been generated *in vitro* through co-culture with a population of APC called plasmacytoid DCs (pDCs). Their development was dependent upon IL-6 and TNFα (130). This effector population may be involved in skin-associated immune responses (128-130).

CD4⁺ T cells interact with B cells within SLOs facilitating their production of antibodies (131). This specific CD4⁺ T cell population, referred to as follicular T-helper cells (T_{FH}) promote B cell activation and function and germinal centre formation (121). Tfh cells are thought to represent an independent CD4⁺ T cell lineage regulated by the transcription factor (TF) B-cell lymphoma 6 (Bcl-6) and the cytokines IL-6 and IL-21 (132, 133). Long-term humoral immunity is thought to be dependent on this interaction between B and Tfh cells (121).

The contribution of these CD4⁺ effector populations to AS pathogenesis will be discussed below.

1.2.3 Cytokines

Immunomodulatory hormones, cytokines or interleukins (IL) are small molecules secreted or expressed by numerous immune populations, often in response to specific stimuli (134).

Cytokines are composed either of a solitary polypeptide chain or dimeric polypeptides and perform their functions in an antigen non-specific manner (135). Cytokines are pleiotropic in their functional activities: cell activation and recruitment, alteration of barrier homeostasis, haematopoiesis, differentiation and function of immune populations. They also influence the generation of immunogenic and tolerogenic immune responses. Cytokines mediate the majority of their functions through engagement of their specific receptor. Depending on receptor expression, and on the particular function of the receptor-expressing cells, these small molecules can act either in an autocrine, paracrine or endocrine manner. Currently, 36 interleukins have been described and are designated IL-1 through to IL-36 (136, 137). Furthermore there are several additional cytokine families distinct from the interleukin nomenclature including the interferon (IFN) and TNF receptor families (135). Cytokines can be categorised on the basis of their structure, class of binding receptor, function and source. To provide context for their potential role in AS development, I have categorised several cytokines according to their role in the immune system (Table 1.1). Given their functional promiscuity, several cytokines belong to multiple categories. For example, IL-6 and IL-1 β are involved in the recruitment and activation of immune populations, and therefore contribute to the inflammatory response. Murine and human studies have also identified a requirement for IL-6 in the differentiation of Th17 cells (108, 138), and IL-1 β drives the differentiation of human Th17 cells (109).

Numerous cytokines that contribute to inflammation and AS pathogenesis, in the context of this study, are described in Table 1.1.

Table 1.1: Classification of inflammatory and T cell associated cytokines and growth factors

Cytokines were subdivided according to their involvement in inflammation, T cell differentiation or function, and cell development (growth factors). The predominant sources and functions of the listed cytokines are provided. Th1 – T helper 1 cell, Th2 = T helper 2 cell, Th17 = T helper 17 cell, Treg = regulatory T cell, DCs = dendritic cells, TNF α = tumour necrosis factor α , GM-CSF = granulocyte macrophage-colony stimulating factor, Flt3L = FMS-like tyrosine kinase 3 ligand.

Classification	Cytokine	Source	Function	Reference
Inflammation	IL-1 β	Monocytes	Th17 differentiation, cell proliferation and inflammation	(109, 139)
	IL-6	Monocytes, Fibroblasts, Endothelial cells	Cell activation and recruitment, Th17 differentiation	(109, 140)

	TNF α	Macrophages, Monocytes, Neutrophils, T cells, NK cells	Inflammation, cell activation and recruitment	(141)
T cells	IL-4	Th2, Basophils, Neutrophils, Eosinophils	Th2 differentiation, Ab production, inflammation	(99, 142)
	IL-5	Th2, Mast cells	B cell and Eosinophil function	(77, 143)
	IL-10	Treg, Monocytes, Th2	Inhibit immune responses, immune cell differentiation	(144)
	IL-12	Macrophages, DCs	Th1 differentiation, cytokine induction, growth factor	(145)
	IL-13	Th2, CD8 ⁺ T cells	Inflammation, Ab switching, Allergy	(146)
	IL-17A	Th17 CD4 ⁺ T cells	Cell activation, Cytokine induction	(147)
	IL-17F	Th17 CD4 ⁺ T cells	Inflammation, Cytokine induction	(148)
	IL-22	Th17, Th22	Tissue repair, Anti-microbial defence	(149)
	IL-23	Macrophages, DCs	Th17 survival and differentiation	(150)
	IFN γ	T cells, NK cells	Viral infections, cell recruitment, immune cell function	(151)
	TGF β	Macrophages, T cells, B cells, endothelial cells, keratinocytes, chondrocytes	Treg differentiation, inflammation, wound repair, cell function	(152)
Growth Factors	GM-CSF	T cells, Macrophages	Myeloid cell development, Inflammation	(153)
	Flt3L	T cells	Haematopoiesis, DC development	(154, 155)

1.2.4 Chemokines and their receptors

Chemokines are another form of immunomodulatory hormone that direct leukocyte migration, a process known as chemotaxis. Similar to cytokines, chemokines are small molecules that exert their functions through binding to cell surface receptors. Four chemokine families have been described. They are classified by structural differences relating to the location of the first two cysteine residues, forming CC, CXC, XC and CX3C families (156). The first chemokine to be described was designated IL-8, now known as CXCL8 (156, 157). In 2006, 46 human chemokines and 18 interacting receptors had been identified (158). The discrepancy between the number of chemokines and the chemokine receptors highlights the redundancy and promiscuity within the chemokine system (Fig. 1.5) (159).

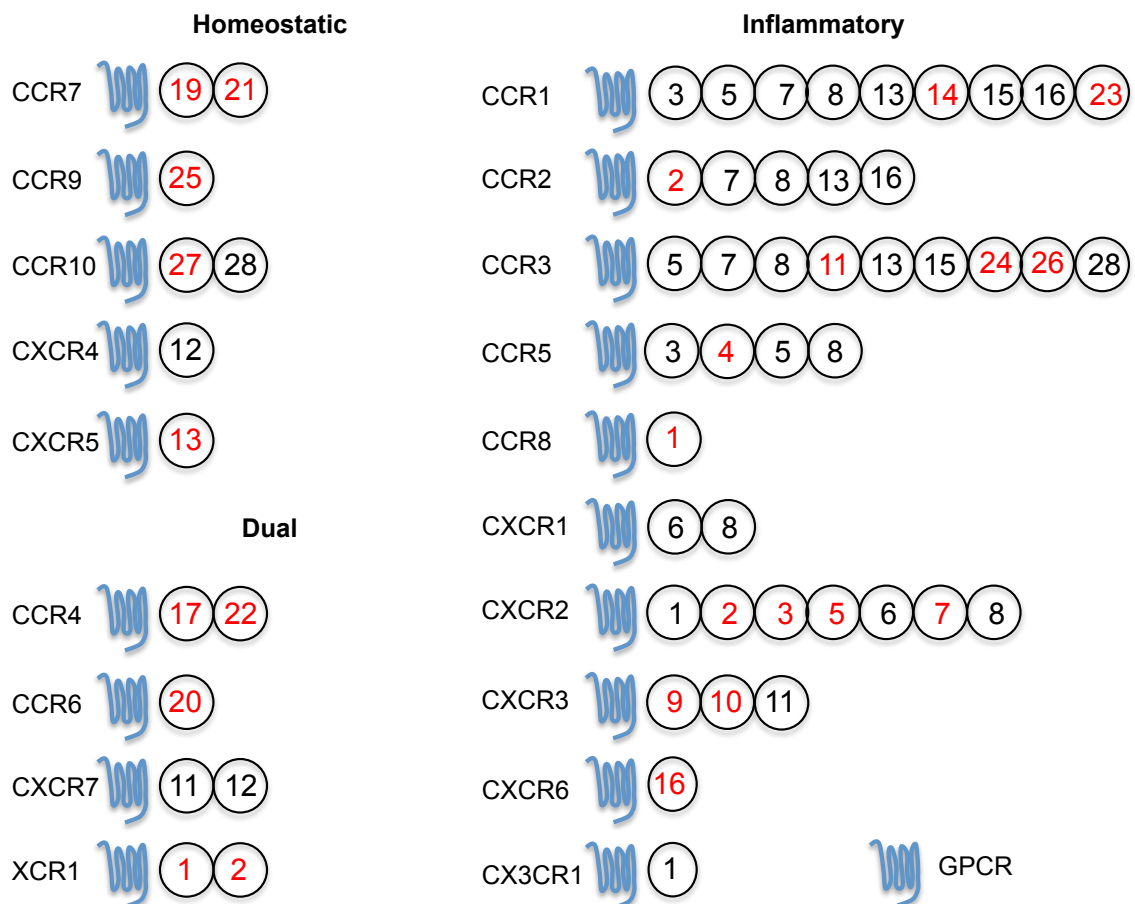


Figure 1.5: Human chemokine receptor promiscuity

Diagram depicting chemokine ligand and receptor promiscuity. Receptor: ligand partnerships are classified as either homeostatic or inflammatory. In certain circumstances, the function of the ligands may be both homeostatic and inflammatory; these are classed as having dual function. Chemokines are depicted only by their number: for example, CCR7 binds to CCL19 and CCL21. The name of the receptor indicates the class of both receptor and ligand. Chemokines in red have unique binding capacity to the specific receptor. Chemokines in black bind multiple receptors. Diagram adapted from Zlotnik et al, 2006 and Moser et al, 2001 (158, 160).

In addition to their structural categorisation, chemokines can be classified as either homeostatic or inflammatory (160-162). Homeostatic chemokines, including CCL19 (ELC) and CCL21 (SLC) are expressed locally within SLOs or peripheral tissue. Their primary functions are to organise lymphoid structures to facilitate the adaptive immune response and, under steady state conditions, recruit immune populations to peripheral tissues to maintain homeostasis (160, 161). In contrast, inflammatory chemokines, including CCL5 (RANTES) and CCL3 (MIP-1 α), permit and direct migration of cells towards sites of inflammation, allowing their participation in the ongoing immune response (160). Cells actively migrate in response to engagement of chemokine with specific receptors on their surface. These seven transmembrane G-protein coupled receptors (GPCRs) activate numerous signalling pathways, resulting in directional cell migration. GPCRs are composed of an extracellular N-terminus, permitting chemokine binding, and an intracellular C-terminus, providing a platform for the intracellular signalling molecules (163-165). Following binding, chemokines induce activation of the receptor-associated G proteins, phosphatidylinositol-4, 5-bisphosphate (PIP2) and the subsequent signalling pathways including phosphatidylinositol-3 kinase (PI3K), Rho and Ras family members and the mitogen activated protein kinase (MAPK) pathway (166, 167). GPCR signalling can be prevented by the administration of Bordetella pertussis toxin. Use of this technique has demonstrated the involvement of the Gi family of G proteins in chemokine signalling (168, 169). Phosphorylation of these signalling molecules induces activation of STAT transcription factors and mediates cell migration (166). In addition to activation of the JAK/STAT pathway, intracellular calcium levels are increased causing protein kinase C activation mediating signal transduction (168). Proteins of the Rho and Ras family, activated following chemokine binding, enable changes to cell structure allowing active migration (168, 170). Chemokine receptor nomenclature (CC, CXC, XC and CX3C) is identical to that described for chemokines (156). The relationship between chemokines and their receptors and the redundancy of the chemokine system is depicted in Fig 1.5.

The chemokine receptor profile of immune populations often referred to as an “address code”, influences migration to a particular tissue destination. For example, CCR10 expression mediates homeostatic migration to the small intestine (171, 172), whilst CCR4 is required for migration to the skin under steady state and inflammatory conditions (173-175). Within Peyer’s patches (PPs), CCR6 is required for migration of DCs to the subepithelial dome, necessary for efficient capture of intestinal antigen (176). A murine study by Wurbel et al, reported an increased susceptibility to the induction of intestinal

inflammation in CCR9 knock-out (KO) mice compared to wild-type (WT) controls (177). Thus, the chemokine receptor profile of immune populations mediates their migration to and within specific SLOs and peripheral tissue, and is required for the effective generation and control of immune responses. The relationship between chemokine receptors, their expression, tissue migration, function, and association with the specific T cell phenotypes described in section 1.2.2 is presented in Table 1.2.

Table 1.2: Chemokine function

Expression of homeostatic and T cell phenotype-associated chemokine receptors (158, 160, 178). Sites of migration or chemokine: chemokine receptor interactions are provided. SLOs = secondary lymphoid organs, BM = bone marrow and TFH = follicular T helper cells.

Receptor	Expression	Tissue	T cell phenotype
CCR4	T cells	Thymus, Skin, SLOs	Th1, Th2, Treg
CCR6	T cells, B cells	Intestine, Skin, SLOs	Th17, Treg
CCR7	T cells, Thymocytes	Thymus, SLOs	
CCR9	T cells, B cells, Thymocytes	Small Intestine, Thymus	
CCR10	T cells	Intestine, Skin	
CXCR3	T cells	Inflamed tissue	Th1
CXCR4	T cells, B cells, Thymocytes	BM, SLOs, peripheral tissue	
CXCR5	T _{FH} , B cells	SLOs	T _{FH}
CXCR7	Hematopoietic cells	Thymus, SLOs, peripheral tissue	
XCR1	CD141 ⁺ DCs		

As depicted in Table 1.2, several chemokine receptors are expressed by specific T cell phenotypes. For instance, CXCR5 expression by T_{FH} is required for effective B cell stimulation and antibody production (179). Expression of this chemokine receptor mediates trafficking of T_{FH} cells to the B cell follicle (179). The T cell associated chemokine receptors can be used for the identification of effector populations. For example, CCR6 expression is reported to be restricted to the Th17 CD4⁺ effector population (180, 181) whilst CXCR3 is commonly associated with the Th1 phenotype (182, 183). Expression of CCR3, CCR4 and CCR8 are frequently associated with Th2 cells (160, 182, 183). However, whether these phenotype-associated chemokine receptors are required for T cell function, similar to CXCR5 and T_{FH} cells, remains unclear. Overall, the

chemokine receptor profile of immune populations can infer migration patterns, cell phenotype and subsequent function.

1.3 Dendritic cells

1.3.1 What is a dendritic cell?

Dendritic cells (DCs) are haematopoietic cells of the myeloid lineage that reside in peripheral tissues and SLOs. Langerhans cells (LCs), a skin-resident DC population, were first described by Paul Langerhans in 1868 (184). However, it was not until the 1970s that seminal papers by Steinman et al further characterised this tissue resident population (185, 186). The morphological appearance of this myeloid population contributed to their classification as DCs; they constantly protract and retract pseudopods or “dendrites” (185). DCs are highly proficient in their ability to stimulate T cell proliferation and have been described as the principal APCs of the immune system (186). Given their location at sites of environmental exposure to antigens and immune response induction (SLOs), and their ability to prime the adaptive immune system, DCs represent a significant link between the innate and adaptive branches of the immune system. Broadly speaking, DCs are the primary migratory subset responsible for communicating signals from the peripheral environment to SLOs where they direct lymphocyte differentiation. Consequently, DCs are involved in maintaining immune homeostasis through regulation of immunity and tolerance. Under steady state conditions, immature DCs sample their environment and actively acquire antigen. DCs are unique in their ability to migrate from peripheral tissue to SLOs via afferent lymphatics, unlike macrophages that also belong to the myeloid lineage (187, 188). Following entry to SLOs they form complex interactions with antigen-specific T cells and direct their differentiation. During migration and in the absence of inflammatory stimuli, DCs adopt a semi-mature phenotype and are able to induce differentiation of Tregs and consequently promote tolerogenic responses (189-192). Paradoxically, DCs are also essential for the induction of protective immunogenic responses directed against pathogenic organisms. Consequently, in the presence of inflammatory stimuli, migrating DCs upregulate co-stimulatory and major histocompatibility (MHC) molecules, allowing efficient antigen presentation and induction of active immunity against pathogenic organisms (184). Overall, DCs represent the bridge between innate and adaptive immunity and are specialised in their ability to influence immune response induction.

In mice and men, DCs can be subdivided into two fundamental populations: conventional DCs (cDCs) and plasmacytoid DCs (pDCs). cDCs are the prototypic DC in terms of morphology, function and location as described above. pDCs, as will be discussed in greater depth below, may appear morphologically similar to cells of the lymphoid lineage (193). Among DCs, pDCs are unique in their ability to secrete high concentrations of type I IFNs in response to viruses (194). pDCs are classified as a subset of DC based on their ability to stimulate proliferation of naïve T cells, the hallmark function of DCs (195).

To date, three human DC-related syndromes have been reported. Dendritic cell, monocyte, B and NK lymphoid deficiency syndrome (DCML), caused by a mutation of the GATA-binding factor 2 results in the complete eradication of blood DCs, tissue cDCs, monocytes, B cells, NK cells, and myeloid and lymphoid progenitors. DCML patients suffer from severe bacterial and viral infections and develop distinct forms of cancer (196, 197). Mutations of the IRF8 gene lead to an increase in circulating granulocytes, accompanied by a reduction in blood monocytes and DCs, dermal DCs and reduced IL-12 production (198). Again, these patients suffer from severe bacterial and viral infections (198). The final DC syndrome involves a mutation of a phosphotransferase involved in nucleotide homeostasis called adenylate kinase 2 (AK2) (199). These patients develop a form of severe combined immunodeficiency (SCID): reticular dysgenesis (199). Weakened development of nucleated cells is characteristic of this disorder, and Emile et al have recently found Langerhans cells to be deficient in AK2 patients (199).

Understanding the roles of DCs in human immunity is complicated by several factors: tissue localisation affects functional specialisation; DCs and macrophages are often misidentified; there are difficulties associated with obtaining human tissues; and the numbers of recovered cells are often low. In addition, DCs in tissues have become specialised, leading to the generation of numerous DC subpopulations. I will compare human, rat and mouse DC populations to allow comparisons between animal and human studies that may contribute to the understanding of AS pathogenesis.

1.3.2 Human myeloid cell classification

1.3.2.1 DCs

Identification of human peripheral DC populations has been hindered due to the difficulties faced in obtaining human tissues and sufficient numbers of cells. Consequently the majority of human DC profiling has been performed on mature circulating blood

populations. These DCs account for approximately 1% of blood leukocytes (200). Initial phenotypic analyses of human DCs relied on their high expression of MHC II and CD11c, their lack of several lineage markers including CD3 and CD19, and their ability to prime naïve T cells (186, 200, 201). While the use of several additional human DC markers has permitted further characterisation of human DC subsets (200, 202, 203), precise identification of human DCs still requires use of multiple surface markers.

There are two main populations of human DCs (202): pDCs and cDCs. pDCs were identified by their CD123⁺ CD45RA⁺ CD68^{hi} MHC II⁺ CD11c⁻ phenotype (202, 204, 205). When immature, pDCs have a distinctive lymphoid-like morphology; they are circular with large nuclei (204). Upon activation these cells develop processes and adopt the typical “dendritic” DC morphology (202, 204). Survival, activation and maturation of pDCs, which is IL-3 dependent, facilitates their ability to prime naive T cells (202).

A surface phenotype of CD123⁻ CD45RO⁺ CD11c^{hi} MHC II⁺ CD68^{lo} was initially used to identify cDCs. Unlike pDCs, they mature in the absence of external growth factors (202, 204, 205). Many investigators have since shown that human cDCs can be further subdivided into at least 2 populations, based on the expression of surface antigens: BDCA-1 (CD1c)⁺, and BDCA-3 (CD141)⁺ DCs (200, 202, 203, 206).

1.3.2.2 Blood CD1c⁺ DCs

CD1c⁺ DCs, which express the BDCA-1 antigen, belong to the myeloid lineage. They express the myeloid specific markers CD13 and CD33 (202, 207). As CD1c⁺ DCs represent approximately 0.6% of human peripheral blood mononuclear cells (PBMCs) (208), they are the dominant circulating DC population in humans. Furthermore, it has been reported that blood CD1c⁺ DCs account for approximately 20-50% of total CD11c⁺ cells (209). CD1c⁺ DCs express greater levels of the DC-specific intracellular adhesion molecule-3-grabbing non-integrin (DC-SIGN), IL-1R and Langerin compared to CD141⁺ DCs (210). CD1c⁺ DCs express a variety of Toll-like receptors (TLRs) including TLRs 1-4, 6-8 and 10 that are involved in pathogen recognition (200, 210, 211).

1.3.2.3 Blood CD141⁺ DCs

Similar to the CD1c⁺ population, CD141⁺ (BDCA-3) DCs belong to the myeloid lineage and express the myeloid lineage specific markers CD13, CD33 and CD11c (207). They represent an extremely small proportion of human blood leukocytes, comprising 0.03-

0.05% of PBMCs (200, 203, 207). Consequently, CD141⁺ DCs account for 3% of the circulating cDC pool (212). This small DC population has been shown to preferentially express TLR3 and TLR 10 (210, 213) but also express numerous other TLRs including TLR 1, 2, 6 and 8 (200, 210). Further surface phenotypic characterisation identified that nectin-like molecule 2 (Nect2), C-type lectin domain family 9, member A (CLEC9A) and XCR1 are uniquely expressed by this DC subset (212, 214, 215).

1.3.2.4 Blood pDCs

Blood pDCs lack the myeloid specific lineage markers CD11c, CD13 and CD33 (195, 216). Furthermore, they lack expression of molecules associated with lymphocytes, monocytes and granulocytes (CD3, CD14, CD15, CD19 and CD56). They can however be identified through their unique expression of CD303 (BDCA-2), CD304 (BDCA-4), CD123 (IL-3R α) and CD45RA (202, 217). pDCs are the second largest DC population in blood, representing approximately 0.3% of total PBMCs (217). In contrast to other human DCs, they have been shown to express a “pre-T-cell receptor alpha chain” commonly associated with lymphocytes (193, 208, 218). pDCs express a unique TLR panel, including high levels of the intracellular TLRs 7 and 9, highlighting their involvement in anti-viral defence (210, 219). Human CD303⁺ pDCs additionally express Immunoglobulin-like transcript 7 (ILT7) (220, 221). They predominantly reside within blood and lymphoid tissues and enter lymph nodes via the blood circulation (222).

1.3.2.5 Monocytes

Monocytes are a relatively large myeloid circulating blood leukocyte population (10%) (223, 224). Monocytes give rise to resident intestinal macrophages (225) and in animal and human studies have been reported to develop into DCs under inflammatory conditions (226-230). However the contribution of monocytes to intestinal DCs under steady state and inflammatory conditions has recently been disputed (225). In humans, 90% of human monocytes express CD11c and MHC II (207, 231). Previously, monocytes have been defined based on the expression of CD16 and CD64 (232), and divided into CD16⁺ CD64⁺, CD16⁺ CD64⁻, CD16⁻ CD64⁺, and CD16⁻ CD64⁻ populations. In some analyses, CD64 was not used in monocyte subset identification. (233). However, without addition of anti-CD64 it is not possible to distinguish CD64⁺ macrophages from CD64⁻ DCs (234). Recent studies have used CD14 and CD16 to identify three populations of human blood monocytes: CD14⁺ CD16⁻ (235), CD14⁺ CD16⁺ (236) and CD14⁻ CD16⁺ subsets (237). The CD14⁻ CD16⁺ population will be discussed separately below. CD14⁺ CD16⁻ “classical”

monocytes account for approximately 85% of circulating monocytes, whilst CD14⁺ CD16⁺ monocytes are the smallest population (5%) (237). There are several surface phenotypic differences between these monocytic populations: CD14⁺ CD16⁻ monocytes express CD11c, MHC II, CCR2, CD62L, and low levels of CX3CR1 whilst CD14⁺ CD16⁺ monocytes express CD11c, MHC II, CX3CR1, lymphocyte function-associated antigen 1 (LFA-1) and lack expression of CCR2 and CD62L (Table 1.3) (238).

1.3.2.6 CD16⁺ mononuclear cells

The CD14⁻ CD16⁺ human mononuclear population represents approximately 7% of blood monocytes (237). Classification of these cells as a monocytic population remains controversial. A proportion of the MHC II⁺ CD11c⁺ CD14⁻ CD16⁺ cells express 6-sulpho LacNAc (SLAN), historically termed M-DC8⁺ cells due to the specific binding of the M-DC8 monoclonal antibody (239, 240). SLAN is a carbohydrate modification of the P selectin ligand, P selectin glycoprotein ligand 1 (PSGL-1) (239). PSGL-1 binds to P selectin on endothelial cells and platelets and mediates cell rolling and adhesion (241-243). These original studies classified this SLAN⁺ subset as a third blood DC subset based on their morphology, ability to present antigen and subsequently activate naïve T cells and induction of antigen-specific cytotoxic lymphocyte (CTL) responses (240). However several groups report that regardless of SLAN expression, CD14⁻ CD16⁺ mononuclear cells represent a third monocytic population, involved in the surveillance of blood vessels and absent from peripheral tissues under steady state conditions (229, 237, 244). The functions of these SLAN⁺ and SLAN⁻ populations will be discussed in greater detail below. Regardless of their classification, CD14⁻ CD16⁺ mononuclear cells are smaller and of lower granularity than both CD14⁺ monocyte populations (237). They lack expression of the cutaneous lymphocyte antigen (CLA), expressed on all other DC subsets, and express low levels of the myeloid marker CD33 (209, 237). Furthermore, it has been reported that CD14⁻ CD16⁺ mononuclear cells express lower levels of both CD11b and CD163, surface molecules identifying cells belonging to the myeloid and macrophage/monocyte lineages respectively (237, 245).

Both CD14⁺ CD16⁺ monocytes and CD14⁻ CD16⁺ mononuclear cells have higher levels of CX3CR1 expression than CD14⁺ CD16⁻ monocytes (237). Murine monocytes can be subdivided into two populations on the basis of CX3CR1 expression, a chemokine receptor for the membrane-bound ligand fractalkine (229). CX3CR1 is expressed on cells committed to the myeloid lineage, including macrophages and some DCs (229, 246, 247).

Based on surface phenotypic markers and functional analysis, Ly6C⁺ CX3CR1^{lo} and Ly6C⁻ CX3CR1^{hi} murine monocytes are thought to be equivalent to the human CD14⁺ CD16⁻ and CD14⁻ CD16⁺ populations respectively (229, 237, 248). However, given that the CD14⁻ CD16⁺ population is heterogeneous, containing SLAN⁻ and SLAN⁺ cells, the true classification of this population remains highly contentious (237, 239).

CD14⁻ CD16⁺ mononuclear cells circulate through blood vessels (237). However SLAN⁺ cells, a subset of this mononuclear population, have been reported to reside within healthy human skin (249, 250). Furthermore, SLAN⁺ cells are present in inflamed tissues including tonsil, skin, Peyer's patches (PPs) and CD ileal mucosa (249-252).

Circulating CD14⁻ CD16⁺ mononuclear cells and both putative CD14⁺ monocyte populations express TLRs 1, 2 and 4-9, although the former population expressed lowest levels of TLR 5 and TLR 7 (237). Furthermore, each population differs in their expression of multiple chemokine, scavenger and cytokine receptors (Table 1.3). In addition, CD14⁻ CD16⁺ mononuclear cells have been reported to express receptors for C5a and C3a, complement mediators (239).

Table 1.3: Surface receptor expression of monocytes and CD14⁻ CD16⁻ mononuclear cells

Differential expression of chemokine, scavenger and cytokine receptors by CD14⁺ CD16⁻ and CD14⁺ CD16⁺ monocytes, and CD14⁻ CD16⁺ mononuclear cells.

Population	Chemokine Receptors	Scavenger receptors	Cytokine Receptors
CD14⁺ CD16⁻	CX3CR1 ^{lo} , CCR1 ^{hi} , CCR2 ^{hi} , CCR3 ⁺ , CCR5 ^{hi} , CCR9 ^{lo} , CXCR4 ^{hi}	CD68 ⁺ , CD209 ⁺ , CD36 ^{hi} , CD163 ^{hi} , CXCL16 ^{lo}	IFN γ R1 ⁺ , IFN γ R2 ⁺ , IL-2R γ ^{lo} , IL-6R ⁺ , IL- 10R α ^{lo} , IL-12R β 1 ^{lo} , IL-17R α ^{hi}
CD14⁺ CD16⁺	CX3CR1 ^{int} , CCR1 ^{hi} , CCR2 ^{lo} , CCR3 ⁺ , CCR5 ^{hi} , CCR9 ^{lo} , CXCR4 ^{lo}	CD68 ⁺ , CD209 ⁺ , CD36 ^{int} , CD163 ^{lo} , CXCL16 ^{lo}	IFN γ R1 ⁺ , IFN γ R2 ⁺ , IL-2R γ ^{hi} , IL-6R ⁺ , IL- 10R α ^{hi} , IL-12R β 1 ^{hi} , IL-17R α ^{int}
CD14⁻ CD16⁺	CX3CR1 ^{hi} , CCR1 ^{int} , CCR2 ⁻ , CCR3 ⁺ , CCR5 ^{lo} , CCR9 ^{lo} , CXCR4 ^{lo}	CD68 ⁺ , CD209 ⁺ , CD36 ^{lo} , CD163 ⁻ , CXCL16 ^{hi}	IFN γ R1 ⁺ , IFN γ R2 ⁺ , IL-2R γ ^{hi} , IL-6R ⁺ , IL- 10R α ^{hi} , IL-12R β 1 ^{hi} , IL-17R α ^{int}

Overall, human blood contains two populations of bona fide monocytes: CD14⁺ CD16⁻ and CD14⁺ CD16⁺ subsets, and a CD14⁻ CD16⁺ mononuclear population. Approximately 50% of the CD14⁻ CD16⁺ cells express SLAN, resulting in a degree of dubiety relating to the classification of this population, which represents either a third blood DC or a third blood monocyte population.

A summary of the surface marker expression and location of CD1c⁺ and CD141⁺ cDCs, pDCs and CD14⁻ CD16⁺ mononuclear cells is provided in Table 1.4.

Table 1.4: Human DC classification

Cell surface antigen expression on CD1c⁺ and CD141⁺ cDCs, CD303⁺ pDCs and CD16⁺ mononuclear cells.

Cell population	Surface Phenotype	Location
CD1c (BDCA-1⁺)	MHC Class II CD11c CD1c (BDCA-1) CD13 CD33 DC-SIGN IL-1R LANGERIN CD4 CD45RO CLA CD2 DEC-205 ^{lo} CD62L CD11b	Blood, lymphoid and peripheral tissue.
pDC (BDCA-2/4⁺)	MHC Class II CD123 CD303 (BDCA-2) CD304 (BDCA-4) CD45RA ILT7 CD68 CD4 CLA DEC-205 ^{int} CD62L	Blood and lymphoid tissue. Rare pDCs found in peripheral tissue.

CD141 (BDCA-3⁺)	MHC Class II CD11c CD141 (BDCA-3) CD13 CD33 CLEC9A XCR1 CD4 CD45RO CLA Necl2 DEC-205 ^{hi} CD62L CD11b ^{lo}	Blood, lymphoid and peripheral tissue.
CD14⁻ CD16⁺	MHC Class II CD11c CD14 SLAN ^{+/-} CD33 CD4 CD16 CD62L ⁻ CX3CR1 ^{hi} CD163 ⁻ CD11b ^{lo} CD36 ^{lo} CCR2 ⁻	Mainly found in blood. SLAN ⁺ cells in skin inflamed tonsil, PPs, and ileal mucosa.

1.3.2.7 Lymphoid tissue DCs

Human DCs were first identified in the kidney as MHC II⁺ interstitial cells (253). Following this discovery, DCs were subsequently identified in several lymphoid and non-lymphoid organs. Splenic DCs have been shown to reside within the subcapsular zone, T cell areas, marginal zone and B cell follicles (254, 255). Poulin et al have described 3 human splenic DC subsets: CLEC9A⁻ CD141⁻ CD303⁻ equivalent to the CD1c⁺ population, CLEC9A⁻ CD141^{int} CD303⁺ pDCs and a CLEC9A⁺ CD141⁺ DC subset (203). Even though equivalent blood DC populations exist, the splenic DC populations are present at a higher frequency, with cDCs and pDCs representing 1% and 0.1% of total splenic cells respectively (254). The majority of splenic DCs express CD11c and HLA-DR and are reportedly immature given their lack of CD83 expression (254, 255).

pDCs (CD1a⁻ CD3⁻ CD4⁺ CD8⁻ CD123⁺) are the major thymic DC population and undergo maturation upon CD40 and IL-3 stimulation (208, 256-260). The surface phenotype of thymic pDCs is similar to that of the equivalent blood population; CD45RA⁺ CD13^{lo}

CD33^{lo} (258). In contrast, a subset of thymic pDCs expressed CD2, CD5 and CD7 (261, 262). Despite representing the minor DC population, HLA-DR⁺ CD11c⁺ myeloid thymic DCs have been identified and can be subdivided based on their CD11b expression (259, 260). Thymic DCs were identified within both the cortex and medulla regions, with a significant proportion of DCs residing at the cortico-medullary junction indicating potential involvement in negative selection (259, 260).

Before widespread use of the newly identified DC specific antigens by Dzionek et al (202), five populations of tonsil resident DCs were identified according to their expression of HLA-DR, CD11c, CD13 and CD123 (263): HLA-DR^{hi} CD11c⁺ CD83⁺; HLA-DR^{int} CD11c⁺ CD13^{lo} CD45RA⁺ CD2⁺; HLA-DR^{int} CD11c⁺ CD13^{hi} CD45RA⁻ CD2⁻; HLA-DR^{int} CD11c CD123⁻; and HLA-DR^{int} CD11c⁻ CD123⁺ populations. However the functions of these DC populations were not assessed, preventing confirmation that these populations each represent bona fide DCs. More recently, using more up-to-date human DC markers, a recent publication by Segura et al identified and functionally characterised CD141⁺, CD1c⁺ and pDC thymic resident DC populations (264).

Again, using up-to-date human DC markers, several lymph node (LN) DCs have been identified. These LN DC populations will consist of recently arrived migratory populations, alongside resident LN populations. Comparison of skin-draining LNs with tonsil-resident DCs enabled identification of several populations of skin-migrating DC populations: Langerhans DCs (HLA-DR⁺ CD11c⁺ CD1a⁻ CD206⁻), CD1a⁺ DCs (HLA-DR⁺ CD11c⁺ CD1a⁺ CD206⁺) and a CD206/CD209 expressing DC population (265). LN-resident DCs were similar to blood DCs: pDCs, CD141⁺, and CD1c⁺ cDCs (265). As in the thymus pDCs were the dominant LN DC subset, with CD1c⁺ DCs being the dominant myeloid DC population (265). LN resident DCs expressed low levels of CD83 indicating immaturity (265).

From these data we can infer that tissue equivalents of blood CD141⁺ and CD1c⁺ cDCs and CD303⁺ CD304⁺ pDCs exist in several human lymphoid tissues, including the thymus and spleen.

1.3.2.8 Non-lymphoid tissue DCs

Langerhans cells (LCs - MHC II⁺ CD11c⁺ CD207⁺ CCR6⁺) and dermal DCs (MHC II⁺ CD11c⁺ CD1c⁺ CCR2⁺ DC-SIGN⁺) were initially described as the two cDC populations residing in human skin (266, 267). However, it is now clear that dermal DCs can be

divided based on their expression of CD14 and CD1a (266-268). Human pDCs (BDCA-2⁺ DC-SIGN⁺) have been identified in healthy human dermis. However, in contrast to the thymus, pDCs are a minor skin resident DC population (269).

The intestine, exposed to the greatest antigenic load, has been shown to contain CD1c⁺ and CD141⁺ DCs; both populations lack CD1a expression (270). A recent study by Dillon et al identified HLA-DR⁺ CD11c⁺ CD1c⁺ DCs in human colonic and small intestinal tissue (271). CD1c⁺ DCs represent a larger leukocyte population in the lamina propria (LP) compared to peripheral blood (271). Furthermore, LP CD1c⁺ DCs possessed a more activated phenotype compared to their blood counterparts through elevated levels of CD86, CD83, CD40 and HLA-DR expression (271). Another report has identified CD141⁺ DCs in human PPs, MLN and LP (272). Several studies have reported an absence of pDCs from colonic mucosa (270, 271, 273). To align with murine studies, discussed below, CD103⁺ and CD103⁻ DC subsets have been identified in human mesenteric LNs (MLNs) and intestinal tissue (274-276). Furthermore, CD103⁺ DCs could be subdivided based on the expression of CD141 and signal-regulatory protein α (SIRP α). Two populations were observed: CD141⁻ SIRP α ^{hi}, and CD141⁺ SIRP α ^{lo/-} (275).

Lung CD1c⁺ and CD141⁺ cDCs have recently been characterised: HLA-DR⁺ CD11c⁺ CD1c⁺ CD11b⁺ CX3CR1⁺ SIRP α ⁻ and HLA-DR^{lo} CD11c^{lo} CD141⁺ CD11b⁻ CX3CR1⁻ SIRP α ⁻ (277). Interestingly, CD141⁺ lung DCs appear to represent a larger proportion of DCs compared to their blood counterparts (277). Similar populations have additionally been identified in the kidney through the use of humanised mice (272). However, these studies suggest that lung DC populations lack CD103 expression (272). Immature pDCs (HLA-DR⁺ CD123⁺) have been identified in human lung (278).

As in lymphoid tissues, CD141⁺ and CD1c⁺ DC populations can be identified in several non-lymphoid tissues including the skin, intestine and lung. However, in contrast to lymphoid tissue and blood, pDCs represent a minor DC population in non-lymphoid tissue.

1.3.3 DC development

1.3.3.1 cDCs

cDCs are hematopoietic cells belonging to the myeloid lineage. Under steady state conditions they are continuously replaced by BM derived precursors. Monocytes have been shown not to be the precursors for steady state DCs as was originally thought, at least

within the intestine (225, 230, 279). cDCs have a relatively short life span, in contrast to pDCs (279, 280). The majority of work on DC development has come from murine studies, however some human data has been reported (222, 281, 282). Hematopoietic stem cells (HSCs) in the BM have the potential to develop into progenitors for both the myeloid or lymphoid lineages, the common myeloid progenitor (CMP) and the common lymphoid progenitor (CLP) respectively (222, 283). CMPs represent the first stage in myeloid lineage commitment. $CD34^+ CD38^+ IL-3R\alpha^{lo} CD45RA^-$ cells that lack numerous lineage markers are suggested to represent human CMPs (281). Following commitment to the CMP stage, Flt3L and colony stimulating factor 1 (Csf-1), also known as macrophage colony-stimulating factor (M-CSF), are involved in the differentiation of the CMP to the macrophage DC progenitor (MDP) (222, 284, 285). The MDP can give rise to either monocytes that exit the BM and enter the circulation or to the common DC progenitor (CDP) (222). The transition from MDP to CDP is dependent upon Flt3L, STAT3 and PU.1 (222), with the CDP now being restricted to the subsequent development of DCs, both cDCs and pDCs (286, 287). Under the influence of Flt3L and the transcription factor PU.1, CDPs differentiate into pre-cDC that exit the BM, circulate in blood and seed lymphoid and peripheral tissues, where they develop *in situ* into mature cDC populations (222, 288). Macrophages and pDCs do not develop from pre-cDCs *in vivo* (230, 289). Based on this linear commitment model, HSCs give rise to CMPs that subsequently become limited in their potential for cell development through their differentiation into MDPs and subsequently CDPs. CDPs have the ability to generate pDCs and cDCs, controlled by specific transcription factors and cytokines. Pre-cDCs represent the final progenitor in the differentiation of HSCs to cDCs. However, Ishikawa et al. report that human CMPs and CLPs can give rise to identical populations of DC, although CLPs may be less efficient than CMPs (290). In addition to circulating cDC precursors that seed tissues and differentiate *in situ* (288), circulating mature DC populations exist in human blood (209). The precise role of these circulating blood DCs in the immune response remains undetermined.

1.3.3.2 pDCs

The precise development pathway of human pDCs remains undetermined. pDCs were originally thought to develop from lymphoid precursors egressing the BM, due to their lack of expression of myeloid cell antigens including CD33 and CD11c (205). To support their lymphoid origin, genetic defects of the lymphoid exclusive transcription factor Spi-B have been reported to inhibit pDC development, whilst cDCs remained unaffected (291,

292). Furthermore, pre-TcR α and λ 5, markers of immature lymphocytes, are expressed on the surface of murine pDCs (293). In the mid 2000s, it was shown that human pDCs could be generated from both CLPs and CMPs. However pDCs, like cDCs, showed a tendency to be generated through CMPs (282). Development of human and murine pDCs has been shown to be augmented by Flt3L, as was described for cDCs (294-296). Subsequent identification of the conserved pDC specific TF E2-2 indicates a distinct developmental pathway from cDCs (297). This pDC specific TF is involved in the regulation of Spi-B, CD303, IL-7 and IRF7 (297). The current consensus regarding pDC development involves a shared pathway with cDCs, and has been characterised through the use of murine adoptive transfer studies. Similar to cDCs, BM HSCs give rise to CMPs and subsequently MDPs (222) under the control of numerous TFs. As previously mentioned, human progenitor candidates have been identified (222, 281). Under the control of Flt3L, STAT3 and PU.1 MDPs develop into CDPs that can give rise to mature pDCs, dependent upon E2-2 (297), that enter the circulation and migrate to lymphoid tissues (222).

1.3.4 DC function

DCs are the principal APCs of the immune system and act as a bridge between the innate and adaptive branches. Maintenance of tissue homeostasis is at least partially controlled by DC populations specialised for their surrounding environment.

1.3.4.1 Antigen presentation and T cell priming

Following the identification of DCs in 1973, Steinman et al characterised this population as potent inducers of T cell proliferation (186). Immature DCs reside in peripheral tissues where they survey their environment. They acquire antigen, migrate to SLOs, and induce immunogenic or protective responses (184). Additionally, DCs resident in lymphoid tissues act as sentinels of the immune system (184). In the immature state, DCs are proficient at internalising and processing antigen through several distinct mechanisms (298-301). Antigen uptake is an active DC process and occurs via macropinocytosis, engulfment and endocytosis, mediated through a variety of surface receptors (298). Macropinocytosis is a continuous non-specific mechanism whereby soluble antigen is captured through rearrangement of the DC cytoskeleton, specifically membrane ruffling and formation of vesicles (298, 300). In contrast, the process of endocytosis lends a degree of specificity to DC antigen uptake (300). This process is mediated through the expression of several cell surface receptors: Fc γ and Fc ϵ receptors, the mannose receptor, and DEC-205 (298). For example, human LCs residing in the epidermis enhance their ability to

acquire IgE associated antigen through elevated surface expression of FcεR1 (302). Following uptake, the complete FcR: antigen complex is degraded for antigen presentation (298). This process additionally permits capture of large antigens (298, 302).

Blood DCs express both CD64 (FcγRI) and CD32 (FcγRII) that actively mediate antigen phagocytosis (303). It should be noted that whilst recent studies have shown CD64 expression to discriminate between macrophages and DCs, with macrophages expressing high levels of CD64, DCs can also express low levels of this Fc receptor (225, 234).

Mannose receptors are highly expressed on the surface of DCs and mediate the internalisation of numerous glycoproteins (298, 300). Following capture, receptor: antigen complexes are internalised, resulting in antigen delivery to cytoplasmic endosomes for trafficking and degradation, allowing recycling of the surface receptor (298). DEC-205 is a surface membrane receptor, related to the macrophage mannose receptor, involved in receptor-mediated endocytosis (304). Following antigen binding, the receptor is internalised by vesicle formation and transferred to the antigen processing compartment (304). Additionally, DCs appear able to engulf apoptotic bodies that may result in the generation of tolerogenic responses to self or cross-presentation and activation of targeted immune responses to harmful antigen (305).

Regardless of the route of antigen uptake, T cells require the antigen to have been processed by the DC and presented, as epitopes, on the cell surface bound to MHC (306). Intracellular antigen is classically presented to CD8⁺ T cells via MHC I molecules whilst extracellular antigen is associated with MHC II molecules and CD4⁺ T cells responses. Surface MHC I is expressed on the majority of nucleated cells (307) whilst MHC II expression is restricted to APCs. Antigen processing for the MHC I pathway occurs in the cytosol via proteasome targeted degradation of endogenous proteins, often through ubiquitination, resulting in the generation of short peptide sequences (308, 309). Following proteasome-mediated antigen degradation, peptides are transported into the endoplasmic reticulum (ER) by the transporter associated with antigen processing (TAP) whereupon they are clipped by ER aminopeptidases (310-312). TAP constitutes part of the “peptide loading complex” (PLC) situated within the ER, composed of several molecules including MHC I, β2 microglobulin (β2m), tapasin and ERp57 (311, 313). MHC I molecules, when associated with the PLC bind high affinity antigenic peptides, whereupon the MHC I: β2m: antigen complexes are released from the PLC and translocate to the cell surface (311).

In contrast to the MHC I processing pathway, the endocytic pathway is the site of antigenic peptide binding to MHC II molecules (311, 314). Following extracellular capture, antigen is continuously degraded by vesicle-mediated proteolysis. Antigen is then transported through a pathway of increasingly acidic and proteolytically active vesicles known as early endosomes, late endosomes and lysosomes (315). MHC II molecules are generated in the ER, where they are stabilised through their association with the invariant chain (CD74) and transported to the endosome pathway (311, 316, 317). MHC II entry into late endosomes results in cleavage of CD74, with only a peptide residing within the MHC II binding groove remaining. This peptide is termed the class II-associated invariant chain peptide (CLIP) (318). CLIP removal by a glycoprotein called DM mediates binding of antigenic peptides, generated through cathepsin-induced degradation, into the MHC II binding groove (319). MHC II molecules bound to high affinity antigen are subsequently transported to the cell surface.

Under specific circumstances, including viral infections, exogenous antigen may be processed and presented by the MHC I pathway resulting in the DC induction of cytotoxic CD8⁺ T cell responses (307, 320). This immunological process is termed cross-presentation and is essential for effective clearance of multiple intracellular pathogens. DC subset specialisation relating to cross-presentation has been reported and will be discussed in more detail below.

Following antigen processing and receipt of maturation signals, DCs down-regulate their expression of Fc receptors, including CD64 (303), and reduce their macropinocytic uptake. DC maturation is associated with a reduction in their ability to capture antigen (298). Accompanying this downregulation of phagocytic uptake, mature DCs upregulate expression of their surface co-stimulatory molecules and MHC: antigen complexes and alter their chemokine receptor profile. These adaptations change DC function from environmental sampling (immature DCs) to T cell stimulation and immune response induction (mature DCs).

DCs carrying antigen migrate from tissue to the T cell zone of SLOs, tissues that orchestrate interactions between DCs and antigen specific T cells. This migration process, either via blood or lymphatics is CCR7 dependent (321). The subsequent interaction between DCs and T cells is mediated through MHC: antigen complexes and the TcR. This interaction involves the development of a molecular structure called the immunological synapse (322, 323). Adhesion molecules including LFA-1 (T cell) bind to intracellular

adhesion molecule 1 (ICAM1 - DC), CD4 and CD8 are also involved in the initial connection and stabilisation of the interaction between T cells and DCs (322). If antigen-specific T cells recognise the cognate MHC: antigen complex on the surface of the DC (signal 1), their migration is inhibited and the resulting synapse leads to the activation and maturation of both the DC and the T cell. This synapse is composed of TcR: MHC complexes surrounded by an intricate network of co-stimulatory molecules (signal 2), including CD28 engaged by CD80/CD86 expressing DCs, and adhesion molecules (324). TcR: MHC engagement, when sustained for several hours in the presence of co-stimulatory molecule binding, leads to the activation of phosphatidylinositol 3-kinase (PI3K) and release of intracellular calcium stores (325, 326). These pathways drive changes to the cells expression profiles within a few hours (327). Maintenance of the synapse is dependent upon TcR-driven signals and permits production of IL-2 for T cell survival and proliferation (326). T cell proliferation occurs within 24-48 hours following immunological synapse formation. Synapse abrogation may result from the engagement of cytotoxic T-lymphocyte antigen 4 (CTLA-4), expressed on T cells, with the DC expressing CD28 ligands CD80 and CD86 (326). Following the DC: T cell interaction, the majority of DCs die *in situ* by apoptosis (328).

DCs play an important role in the induction of both immunogenic and tolerogenic immune responses. Peripheral DCs acquiring apoptotic cells in the absence of exogenous “danger” signals, may retain their immature profile and induce tolerance through promotion of Treg differentiation (329). However, more recent evidence suggests that tolerogenic responses require a degree of DC maturation, at least upregulation of MHC and co-stimulatory molecules (190). DCs involved in tolerance induction are thought not to secrete IL-12 (189, 190, 330). These tolerance-inducing DCs are said to be “semi-mature”. It is also possible, however, that distinct populations of DCs may be specialised for the induction of tolerogenic responses. Murine studies have suggested that CD8 α ⁺ DCs may preferentially induce tolerance (329, 331) whilst similar observations have been reported for human CD141⁺ DCs (332). However, CD8 α DC deficient mice are not deficient in their generation of Tregs (333, 334). Alternatively, indoleamine-pyrrole 2,3-dioxygenase (IDO) expressing DCs have been reported to mediate inhibition of T cell responses (335). Another school of thought involves the class of danger signal received by the migrating DCs. TNF α stimulated DC have been shown to induce IL-10 secreting T cells, in contrast to those stimulated with LPS (330). These data suggest that specific stimuli may affect DCs ability to promote either tolerance or immunity. However, the precise mechanisms

and signal(s) required for the induction of tolerance versus immunity remain to be determined.

An illustration of the DC: CD4⁺ T cell interaction, and the immunological synapse, is shown in Figure 1.6.

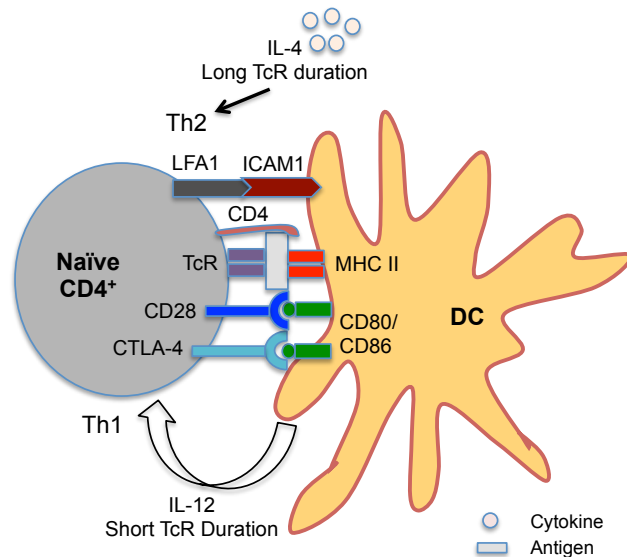


Figure 1.6: Immunological synapse between DC and CD4⁺ naïve T cell

Depiction of the molecules involved in the immunological synapse that occurs between DCs and naïve antigen-specific CD4⁺ T cells in SLOs. The synapse is stabilised through the interaction of co-stimulatory molecules and adhesion molecules. DC secretion of IL-12 during TcR engagement skews Th differentiation to a Th1 phenotype. Alternatively, TcR signalling in the presence of IL-4 is required for Th2 differentiation. Figure adapted from (325).

The defining feature of DCs is their ability to stimulate naïve T cell proliferation and direct the subsequent immune responses. However, this is a rather simple definition. Environmental conditioning, DC subsets and exogenous stimuli all add complexity to this process. The specialised functions of DC subsets will be discussed below.

1.3.4.2 CD141⁺ DCs

Of blood myeloid populations, CD141⁺ DCs express the highest levels of TLR3 (200). Stimulation of isolated blood DCs with the TLR3 ligand Poly I:C, identified CD141⁺ DCs as the preferential inducers of IFN γ -secreting CD4⁺ T cells and secretors of IFN β (200). IFN β promotes the cross-presenting properties of DCs (200, 336, 337). Following TLR3 stimulation, CD141⁺ DCs express high quantities of several molecules belonging to the MHC I antigen processing pathway, including TAP 1 and TAP 2, and were more effective at cross-presentation than CD1c⁺ DCs (200). However, under steady state conditions, it is

important to note that CD141⁺ and CD1c⁺ blood DCs are both capable of cross-presentation (200).

CLEC9A is exclusively expressed on CD141⁺ human DCs. Murine studies report CLEC9A to be involved in the identification of necrotic cells and cross-presentation of antigens derived from these cells (338). Blood CD141⁺ DCs have been found to be capable of cross-presentation to CD8⁺ T cells following ingestion of necrotic cells (200, 212, 339).

Skin and blood-derived CD141⁺ DCs excel in the ability to cross-present soluble antigen (340). Similar to the data from Jongbloed et al, skin CD141⁺ DCs only exhibited this characteristic following TLR3 stimulation (200, 340). In addition to IFN β , CD141⁺ DCs additionally secreted elevated levels of IL-12p70, IFN α , IFN λ , TNF α and CXCL10, in contrast to CD1c⁺ DCs (200, 340-342). Given the role of IL-12p70 in the generation of Th1 cells, and their preferential capacity for cross-presentation under inflammatory conditions, these results indicate that CD141⁺ DCs may preferentially induce Th1 responses and excel at cross-presentation (200).

In contrast to the studies described above, skin-resident CD141⁺ DCs have been shown to be potent secretors of the regulatory cytokine IL-10, and to express high levels of the immunoregulatory receptor immunoglobulin-like transcript 3 (ILT3) (332). The apparent regulatory phenotype of this population was supported by several additional observations: CD141⁺ skin DCs inhibited T cell proliferation in an IL-10-dependent manner; and they induced CTLA-4 expression on interacting CD4⁺ T cells, shown to represent functionally viable Tregs *in vivo* (332). However, the DC population used in these studies expresses CD14, and may therefore not represent true tissue equivalents of blood CD141⁺ DCs. Notably, CD141⁺ CD14⁻ skin-resident DCs assessed by Haniffa et al efficiently induced CD4⁺ and CD8⁺ effector T cell proliferation (340). While it is possible that, human DCs may functionally adapt in response to tissue-specific environmental conditioning, further analysis is required to fully elucidate the functional characteristics of this cross-presenting population.

Basic leucine zipper transcription factor, ATF-like 3 (Batf3) and IRF-8 are TFs involved in the development of murine CD8 α ⁺ DCs (343-345). Human CD141⁺ DCs express both Batf3 and IRF-8 (200, 203). Consequently, both their ability to cross-present antigen and their TF regulation indicate that human CD141⁺ DCs are equivalent to murine CD8 α ⁺ DCs. This relationship will be discussed in more detail below.

1.3.4.3 CD1c⁺ DCs

Blood CD1c⁺ DCs express TLR4, unlike CD141⁺ DCs (211). Following TLR4 stimulation via *Escherichia coli* (E.coli), CD1c⁺ DCs predominantly secrete IL-10 and IDO, accompanied with low levels of TNF α , IL-6 and IL-12 (211). Supporting a potential regulatory role for this circulating population, CD1c⁺ DCs have also been shown to suppress T cell proliferation in an IL-10 dependent manner (211). However, another study found CD1c⁺ DCs to be the dominant producers of the pro-inflammatory cytokine IL-8 following TLR stimulation (346).

Isolated lung and blood CD1c⁺ DCs induce CD103 expression on interacting CD8⁺ T cells in a TGF- β 1 dependent manner (347). CD103 binds to E-cadherin and retains effector and memory T cells within epithelia (347, 348). Consequently, lung CD1c⁺ DCs may promote expression of CD103 on interacting CD8⁺ T cells and promote their accumulation within epithelium, thus enhancing clearance of viral pathogens (347).

Environmental conditioning may promote maintenance of intestinal homeostasis. Retinoic acid (RetA) is one of several molecules thought to contribute to this process (119, 349, 350). A specific subset of murine intestinal DCs (CD103⁺) are reported to secrete high levels of RA, resulting in the induction of gut-homing T cells and Treg differentiation (119, 349-351). Until recently, equivalent human DC populations had not been identified. Sato et al found blood CD1c⁺ DCs, when compared to the CD141⁺ subset, express elevated levels of the retinaldehyde dehydrogenase 2 (RALDH2) enzyme responsible for the conversion of retinal to RetA, (352). This expression was accompanied by an increase in aldehyde dehydrogenase (ALDH) activity following stimulation (352). In addition to circulating CD1c⁺ DCs, mesenteric lymph node (MLN) CD103⁻ DCs showed similar levels of ALDH activity compared to the CD103⁺ population (352). These MLN results are different from the findings of murine studies (119, 349, 350). When the functional consequences of this ALDH activity in human blood DCs was assessed, CD1c⁺ DCs induced expression of the gut-homing molecule α 4 β 7 and secretion of the Th2-associated cytokines IL-4, IL-5 and IL-13 (352). These data suggest that CD1c⁺ DCs may drive mucosal Th2 and Treg responses.

Alternatively, CD1c⁺ DCs have recently been shown capable of promoting Th17 differentiation (277). Blood, lung and small intestinal CD1c⁺ DC express higher levels of the TF interferon regulatory factor 4 (IRF4) than other myeloid populations and IRF4 was

required for the differentiation of the CD1c⁺ population (277). IRF4 may therefore be important for the survival or proliferation of CD1c⁺ DCs (277). Compared to the CD141⁺ population, lung CD1c⁺ DCs were the major producers of IL-23 (277), previously shown to promote the survival of Th17 cells (112). Furthermore, these IL-23-secreting lung resident CD1c⁺ DCs preferentially promoted the differentiation of IL-17A⁺, and IL-17⁺ IFN γ ⁺ CD4⁺ T cells (277). Therefore lung-resident CD1c⁺ DCs may promote Th17 responses.

Taken together these results suggest that CD1c⁺ DCs might adapt to the surrounding environment and are capable of inducing different immune responses in different contexts.

1.3.4.4 CD14⁻CD16⁺ mononuclear cells

Classification of CD14⁻CD16⁺ mononuclear cells either as a DC or monocyte subset remains unclear, partly due to the presence of SLAN⁺ and SLAN⁻ subpopulations. Regardless of the classification, the function of this subset has been addressed by several groups and is discussed below.

Blood monocytes were initially divided into two subsets: CD14⁺CD16⁻ and CD14⁺CD16⁺ cells. In 2010, CD16⁺ monocytes were further subdivided into two populations: CD14⁺CD16⁺, and CD14⁻CD16⁺ populations (237). Much of the initial phenotyping of CD14⁻CD16⁺ mononuclear cells was performed when they were included within the original CD14⁺CD16⁺ population. Following TLR 2 and 4 stimulation, CD14^{+/-}CD16⁺ monocytes were observed to be the dominant TNF α -producing monocyte population under steady state and inflammatory conditions (244, 353). In addition to their proinflammatory function, CD14^{+/-}CD16⁺ monocytes excel in the uptake of antigen by Fc γ mediated phagocytosis, due to their CD16 (Fc γ RIII) expression (354).

However, following separation of CD16⁺ monocytes into CD14⁺CD16⁺ monocytes and a CD14⁻CD16⁺ mononuclear population, the proinflammatory profile was attributed to the CD14⁺CD16⁺ monocyte population (237). This population has subsequently been shown to be expanded in disease (355). Functional analyses of the newly defined CD14⁻CD16⁺ mononuclear population suggested homology with the murine Ly6C^{lo} patrolling monocyte subset (248, 356). Human CD14⁻CD16⁺ mononuclear cells do not enter tissues under steady state conditions but actively patrol blood vessel endothelium in a LFA-1 dependent manner (237). CD14⁻CD16⁺ mononuclear cells were in fact found to be refractory to TLR stimulation, unlike CD14⁺CD16⁺ monocytes (237). However, this population was capable

of TNF α , IL-1 β and CCL3 production following viral, TLR 7 or TLR 8 stimulation (237). Response to TLR 7 and 8 stimulation appears to be characteristic of CD14 $^-$ CD16 $^+$ mononuclear cells (237, 249, 252, 357). Unlike both CD14 $^+$ monocyte populations, CD14 $^-$ CD16 $^+$ mononuclear cells exhibited poor phagocytic capacity (237). These CD14 $^-$ CD16 $^+$ cells appear to be functionally distinct from both CD14 $^+$ monocyte subsets and appear refractory to TLR stimulation.

Despite this classification of three blood monocyte populations, the CD14 $^-$ CD16 $^+$ “population” is heterogeneous for the marker SLAN (M-DC8), previously used to isolate a “third” DC population (240). Also, CD16 $^+$ “monocytes” have the potential to develop into migratory DCs and transmigrate through epithelium (358). In the studies described above by Cros et al suggesting endothelial surveillance, the SLAN subsets were not individually assessed.

The functional attributes of CD14 $^-$ CD16 $^+$ SLAN $^+$ cells will now be described, and they will be subsequently referred to as SLAN $^+$ cells. In contrast to the findings by Cros et al, SLAN $^+$ cells secrete proinflammatory cytokines upon TLR stimulation: IL-1 β , IL-6, IL-12, IL-23, TNF α , macrophage inflammatory protein 1 α (MIP-1 α) and MIP-1 β (249, 346, 359). Following co-culture with T cells, SLAN $^+$ cells induce differentiation of Th17 and Th1 cells, observed to secrete more IL-17, IL-22, IFN γ and TNF α than T cells induced by CD1c $^+$ DCs (249, 359). SLAN $^+$ DCs also secrete IL-12 and TNF α in response to TLR 7 and TLR 8 stimulation (252, 357). These findings suggest that upon activation SLAN $^+$ cells promote the immune response through secretion of proinflammatory cytokines and the differentiation of Th1 and Th17 cells.

A final reported function of SLAN $^+$ cells relates to their interaction with NK cells. TLR 4 stimulated SLAN $^+$ cells enhance expression of the activation marker CD69 on interacting NK cells (360). This cellular activation was reciprocal and promoted IFN γ secretion in an IL-12-dependent manner (360). Furthermore, Th1 differentiation was promoted through DC: NK crosstalk (360). Overall, SLAN $^+$ cells appear to orchestrate immune responses through their interaction with other hematopoietic cells.

1.3.4.5 pDCs

Circulating pDCs enter inflamed LNs and secrete large quantities of type I IFNs, in response to viral infections, after TLR 7 and TLR 9 engagement (194, 361, 362). This IFN response to viral infections is the prototypic function of pDCs. In addition to the role of

type I IFNs in viral clearance, pDCs can promote the differentiation of memory and effector cells (363), T cell survival (364) and CD8⁺ T cell function (365). Furthermore, pDCs produce an array of cytokines and chemokines following TLR stimulation, other than type I IFNs, which can functionally influence immune populations associated with both the adaptive and innate arms of the immune response. These cytokines include: IL-6, IL-8, TNF α , CCL3, CCL5 and CXCL10 (366, 367).

Human pDCs that have been directly isolated from patients are reported to possess low antigen presenting capabilities (220). However, following stimulation by viruses or TLR ligands, pDCs are capable of direct antigen presentation to CD4⁺ T cells (368) and cross-presentation (369), thereby adopting a similar functional role to cDCs (220).

1.3.5 Rat DC classification

Rats are used as transgenic models for many autoimmune and chronic diseases including SpA, creating the need to understand rat DC biology. The animal models used to understand the pathogenesis of SpA will be described in more detail below. Rat studies rely on identification of DCs through expression of the surface markers CD11c, MHC Class II and CD103 (370). Rat DCs can then be further differentiated based on their CD4 and SIRP α (CD172a) profile (370).

DCs in the rat intestine have been extensively studied. They were initially divided into two subsets: - CD4⁻ CD172a⁻ and CD4⁺ CD172a⁺, with the latter population accounting for 50-60% of DCs migrating from the intestine in lymph and reportedly having greater antigen processing and presentation capabilities (370, 371). CD4⁺ CD172a⁺ DCs were originally thought to be a precursor for the CD4⁻ CD172a⁻ population, however their similar turnover rates *in vivo* have led to the rejection of this hypothesis (371). The CD4⁻ CD172a⁻ DC population has been reported to possess tolerogenic properties, taking up apoptotic cells and migrating to T cell areas of SLOs (372). However, more recent analysis has shown that these DCs did not preferentially induce differentiation of Tregs (373). Analysis of CD11b expression allowed further subdivision of rat intestinal DCs. CD103⁺ MHC II⁺ migrating DCs could be divided into CD172a^{hi} CD11b^{lo}, CD172a^{int} CD11b^{hi}, and CD172a^{lo} CD11b^{int} populations (374). The CD172a^{hi} CD11b^{lo} subset secretes the highest levels of IL-12p40 and IL-6 following TLR activation (374, 375).

Two major splenic DC subsets have been identified: the CD4⁺ CD172a⁺ CD5⁺ MHC II⁺ subset is the minor population, accounting for approximately 10% of total splenic DCs. CD4⁻ CD172a⁻ CD11b⁻ CD5⁻ MHC II⁺ cells represent the major DC population (376). Rat pDCs (CD4⁺ MHC II⁺ CD3⁻ CD11b⁻) express a variety of lymphoid and myeloid antigens including CD172a, CD5, CD90 and CD200 (377). This subset produces vast quantities of type I IFN following TLR 7 and TLR 9 stimulation (377).

1.3.6 Murine DC classification

All murine cDCs express CD11c and MHC II. cDC precursors (pre-cDCs) seed peripheral and lymphoid tissue where DCs develop *in situ*. In lymphoid tissue, murine cDCs can be subdivided into two populations on the basis of CD8 α and CD11b expression: CD11c⁺ MHC II⁺ CD8 α ⁺ XCR1⁺ CD11b^{-/lo} CD172a⁻ (CD8⁺ DCs) and CD11c⁺ MHC II⁺ CD8 α ⁻ XCR1⁻ CD11b⁺ CD172a⁺ (CD11b⁺ DCs) (222). CD8⁺ DCs are the minor lymphoid resident population, express high levels of the Flt3L receptor CD135, proliferate in response to Flt3L and are diminished in Flt3L^{-/-} mice (222, 284, 378). Development of this population is dependent upon the TF Batf3 and inhibitor of DNA binding 2 (ID2) (334, 379-382). CD8⁺ DCs excel in the cross-presentation of antigens, MHC I presentation, and are the main source of IL-12 (343, 379, 383-385). Furthermore, this population captures apoptotic cells and subsequently induces tolerogenic responses (331, 386).

The CD11b⁺ DC population is the most abundant lymphoid DC population and is also responsive to Flt3L (222, 284, 378). Development of CD11b⁺ DCs is dependent upon the TFs RelB, Notch RBP-J and IRF4 (222, 387, 388). CD11b⁺ DCs are believed to chiefly process antigen through the MHC II pathway, partially through their higher expression levels of the MHC II machinery than CD8⁺ DCs (222, 383).

In peripheral tissues, several DC subsets have been categorised based on CD103 and CD11b expression: CD103⁺ CD11b⁻ CD8^{+/-} XCR1⁺ CLEC9A⁺ CX3CR1⁻ (CD103⁺ CD11b⁻), CD103⁺ CD11b⁺ CD8⁻ XCR1⁻ CLEC9A⁻ CX3CR1⁻ (CD103⁺ CD11b⁺), CD103⁻ CD11b⁺ CD8⁻ XCR1⁻ CLEC9A⁻ CX3CR1⁺ (CD103⁻ CD11b⁺) and CD103⁻ CD11b⁻ CX3CR1⁻ (CD103⁻ CD11b⁻) DCs have been identified in the intestinal lamina propria (LP) and intestinal afferent lymphatics (222, 389). The CD103⁺ CD11b⁻ and CD11b⁺ DC subsets dominate the majority of peripheral tissues, accounting for approximately 1-5% of leukocytes (222). The proportions change in different tissues. For instance, CD103⁺ CD11b⁺ DCs dominate the small intestinal mucosa (389). Peripheral tissue CD103⁺

CD11b⁻ and lymphoid CD8⁺ DC subsets are thought to be related in terms of function (cross-presentation) and origin (334, 380).

pDCs are mainly found within the circulation or lymphoid tissues. They can be identified as CD11c^{lo} MHC II^{lo} CD45⁺ CD4⁺ B220⁺ Ly6C⁺ CD172a⁺ CLEC9A⁺ cells (222). In response to TLR 7 or TLR 9 stimulation they secrete large quantities of type I IFNs (390-392), as described above for human pDCs.

1.3.7 Comparing DC populations between species

Recently, human and murine DC subsets have been compared. CD141⁺ DCs are considered equivalent to the mouse CD8⁺ DCs (200, 203, 212, 340, 393). Despite the fact that these subsets share similar functional (cross-presentation), phenotypic (CLEC9A, Necl2 and XCR1) and developmental similarities (Batf3), CD141⁺ DCs do not express CD8 (394). In addition, rat CD172a^{lo} lymph-migrating DCs are presumed equivalents of human CD141⁺ DCs and murine CD8⁺ DCs based on their shared uptake of apoptotic material (372) and TLR3 expression (375).

Murine CD11b⁺ DCs share a similar genetic transcriptional profile to human CD1c⁺ DCs (393). For example, genes similarly expressed by LN resident CD11b⁺ and CD1c⁺ DCs include those involved in the inflammatory response, MHC II processing pathway and nuclear factor kappa-light-chain-enhancer of activated B cells (NF-κB) signalling (393). Murine and human pDCs were additionally found to be genetically and functionally related and were distinct from all cDC populations (194, 361, 362, 390-393). Table 1.5 describes the relationship between lymphoid tissue murine and human DC populations.

Table 1.5: Comparison of human and murine DC populations

Common functional, phenotypic and developmental similarities exist between several human and murine DC populations. These are depicted in table 1.5. TF = transcription factors and Ag = antigen.

Human	Murine	Phenotype	Function	TF
CD141⁺	CD8 ⁺ /CD103 ⁺	CD11c ⁺ MHC II ⁺ XCR1 ⁺ CLEC9A ⁺ Necl2 ⁺ CD11b ^{lo}	Cross-presentation, tolerance	Batf3, IRF8, Flt3
CD1c⁺	CD11b ⁺	CD11c ⁺ MHC II ⁺ CD11b ⁺ SIRPα ⁺	MHC II Ag presentation, (Th17 induction?)	Flt3, IRF4

CD303⁺ pDC	B220 ⁺ pDC	TLR 7, TLR 9, MHC II ⁺	Type I IFN production following TLR 7/9 stimulation	Flt3, E2-2, Spi-B
----------------------------------	-----------------------	--------------------------------------	--------------------------------------------------------------	----------------------

1.4 Intestinal immune system

Control of immunogenic and tolerogenic immune responses is of great importance in the intestine because of the high antigenic load and the deleterious consequences of inappropriate immune activation. The intestine, composed of the stomach, small intestine (SI), caecum, large intestine (colon) and rectum, harbours commensal bacteria, food antigens, and pathogenic bacteria. Specifically, the human intestine is occupied by approximately 10^{14} microorganisms (395). Consequently, the intestinal immune system has had to adapt to continuous exposure to innocuous and harmful antigen, in order to prevent the development of aberrant immune responses whilst remaining responsive to harmful pathogens (396). Inflammatory bowel disease (IBD), either in the form of Crohn's disease (CD) or ulcerative colitis (UC), results from the breakdown of intestinal homeostasis and occurs in approximately 1 in 500 individuals (397). Furthermore, patients suffering from chronic inflammatory diseases, including AS, commonly experience symptoms of IBD as an extra-articular manifestation of their disease (4, 13). Therefore, elucidating the pathways involved in intestinal homeostasis and inflammation may aid development of new therapeutics for both IBD and AS.

To respond to the largest antigenic load in the body, the intestinal immune system has adapted structurally and functionally to deal with the numerous, contrasting antigens and stimuli (395). The intestinal immune system comprises the largest body surface area (400m^2), enhanced through site specific development of villi (396). Secondly, the intestinal mucosa is separated from the lumen by a single layer of epithelium that is coated in a thick layer of mucus (395). Furthermore, this barrier secretes several antigenic peptides that maintain barrier function and act as a primary defence mechanism (395). In addition, there is continuous transport of mucosal IgA to the luminal surface (3g/day), this IgA aids the clearance of bacteria to maintain barrier homeostasis (395). The intestine harbours a larger population of T cells than any other tissue, with 60% of all T lymphocytes thought to reside here (396, 398). Within the intestinal mucosa, several discrete lymphoid organs reside, often in close proximity to the lumen and the associated antigen. These are referred to as the gut-associated lymphoid tissue (GALT), which consists of Peyer's patches (PPs),

mesenteric lymph nodes (MLNs) and isolated lymphoid follicles (ILFs) (396). These SLOs mediate intestinal immune responses and are structurally adapted to meet the demands associated with the intestinal environment. For example PPs composed of distinct T and B cell areas, exist within the submucosa and are separated from the external environment by a single layer of epithelium known as the follicle-associated epithelium (FAE) (396). Scattered throughout this layer exist specialised epithelial cells involved in the uptake and transportation of antigen, called M cells (396). Within PPs, antigen-specific T and B cell activation occurs *in situ*, whereupon these lymphocytes egress the PP and migrate back to the intestinal mucosa to perform their regulatory or immunogenic functions (396). In addition to these organised structures, T lymphocytes reside within the lamina propria (LP) and intestinal epithelium (intraepithelial T lymphocytes - IELs) (396). The majority of intestinal lymphocytes are refractory to exogenous stimuli and are phenotypically appear to be effector populations that secrete cytokines including IFN γ and IL-4 (396, 399, 400). The majority of IELs are CD8⁺ T cells expressing the CD8 $\alpha\alpha$ homodimer, in contrast to circulating CD8 $\alpha\beta$ ⁺ T cells, and have been shown to possess cytolytic activity (401, 402). In addition to the cells described above, the intestinal immune system contains a complex, unique system of mononuclear phagocytes, described in more detail below.

1.4.1 Intestinal DCs

Given the central role of DCs in the induction of immune responses, understanding how intestinal tissue homeostasis is achieved requires an understanding of the functions of intestinal DCs.

Within the human intestine reside several cDC populations, defined on the basis of CD141 and CD1c expression (270, 271, 403). pDCs are reported to be relatively rare within the intestinal mucosa (270, 271, 273). The precise function of these subsets remains relatively obscure, due to the difficulties in isolating these populations from human intestinal mucosa. A study by Dillon et al has examined the functions of peripheral blood (PB) and LP CD1c⁺ DCs, to assess the impact of intestinal environmental conditioning on DC function (271). Under steady state conditions LP DCs, compared to those isolated from PB, show elevated levels of several activation markers (CD40, CD83 and CD86) and cytokines including IL-6, IL-10 and TNF α (271, 404). However, human intestinal DCs have also been reported to express low levels of numerous activation markers, highlighting need for further investigation (404, 405).

Cytokines are involved in the regulation of both intestinal inflammation and homeostasis. TNF α is pro-inflammatory, but also inhibits IL-12 and IL-23 production (406, 407). Inhibition of myeloid IL-10 signalling through deletion of STAT3 leads to enhanced IL-12 production and intestinal inflammation (408, 409). Subsequently, IL-6 and IL-10 have been shown to be involved in barrier homeostasis (410, 411). A variety of immune and endothelial cells secrete these cytokines, highlighting a potential role for LP DCs in tissue homeostasis through their cytokine profile. Furthermore, LP CD11c⁺ DCs appeared refractory to TLR 4 and TLR 5 stimulation, with low expression levels of both TLRs (271, 404). This intestinal TLR hyporesponsiveness replicates findings reported in several murine and rat intestinal DC studies (375, 412). Furthermore, LP CD1c⁺ DCs' capacity to secrete IL-23 was only induced following TLR 7 and 8 stimulation, whilst IL-10 was upregulated in response to TLR 2 activation (271). Therefore the activation and function of this LP DC population may be mediated by intestinal conditioning and TLR stimulation. However the precise functions of human intestinal CD1c⁺ and CD141⁺ DC populations remain to be fully elucidated.

The interaction of the intestinal environment with myeloid populations has been shown to be important in mediating cell function in both murine and human studies. Intestinal DCs are unique in their ability to induce α 4 β 7 and CCR9 on interacting T cells, promoting migration and homing of effector T cell populations to the intestine (171, 172, 413). Human intestinal DCs may preferentially induce Th2 type immune responses, promoted through the expression of thymic stromal lymphopoietin (TSLP) by gut epithelial cells (414). This intestinal DC conditioning is important for tissue homeostasis as TSLP expression is reduced on epithelial cells isolated from CD patients. In turn, this may affect DC function and thus perpetuate inflammation as epithelial cell: DC crosstalk enhances DC secretion of the immunoregulatory cytokine IL-10 (414). This Th2 bias of human intestinal DCs is recapitulated in several murine studies where CD103⁺ intestinal DCs preferentially secreted IL-10 and induced Th2 responses (415, 416). However, murine intestinal CD103⁺ CD11b⁺ DCs have recently been shown to be the primary inducers of the Th17 phenotype (275). In addition, murine intestinal lymph or MLN CD103⁻ DCs appear capable of the induction of IFN γ -secreting and IL-17-secreting CD4⁺ T cells (349, 389, 417).

As stated above, IgA is abundant within the intestine and is plays important roles in the clearance of pathogens and preventing commensal organisms breaching the intestinal

barrier (395, 418). Intestinal DCs are more proficient at promoting B cell IgA class switching and IgA production than other lymphoid DC populations (418, 419).

In addition to Th2 induction, IL-10 secretion, TLR hyporesponsiveness, IgA secretion and barrier maintenance, intestinal DCs have a specialised ability to direct Treg differentiation. Murine intestinal CD103⁺ DCs are specialised for the induction of FOXP3⁺ CD4⁺ T cells, with or without the addition of exogenous TGFβ (119, 349, 351). Intestinal Treg differentiation was found to be dependent upon RetA production, with MLN CD103⁺ DCs expressing RALDH2 (349). This Treg induction is at the expense of Th17 differentiation (119). Thus, as a consequence of environmental conditioning, murine intestinal DCs, or at least a specific DC subset, preferentially induce tolerogenic responses through priming of Tregs in the presence of TGFβ and RetA. An equivalent human Treg inducing DC subset has not yet been identified; although human CD103⁺ small intestinal LP DCs can induce FOXP3⁺ Tregs, the capacity for CD103⁻ DCs to induce Tregs was not assessed in this study (420). Isolated human CD103⁻ MLN DCs are reported to develop ALDH activity following stimulation with 1α,25-dihydroxyvitamin D3 (Vit D3), GM-CSF and RetA (352). In contrast, CD103⁺ DCs isolated from both human and murine LP have been shown to express IDO, implicated in Treg generation (421).

Little is known about how human intestinal DCs are affected by inflammation. Under inflammatory conditions, expression of TLR 2 and TLR 4 is upregulated on intestinal DCs (404) and accumulation of activated DCs has been observed within inflamed tissue (405, 422). The functions and detailed phenotypes of these populations have, however, not been assessed.

Overall, intestinal DCs in both mice and men are conditioned by the intestinal environment to prevent aberrant responses to commensal bacteria and food antigens whilst remaining capable of inducing targeted immunogenic immune responses. Whether these differential functions are mediated by unique subsets, changes in environmental conditioning or a combination of both factors remains to be determined in humans.

1.4.2 Intestinal macrophages

Like DCs, macrophages are phagocytes critical for intestinal tissue homeostasis. Under steady state conditions human intestinal macrophages lack expression of the monocyte marker CD14 (423-426). However, CD14⁺ macrophages infiltrate inflamed mucosa, and

secreted pro-inflammatory cytokines including TNF α and IL-23 (427). Advances in flow cytometry have enabled identification of two populations of human intestinal macrophage: CD14^{lo}, and CD14^{hi} (225). In addition to CD14, human intestinal macrophages express CD11c, MHC II, CD13, CD33 and low levels of co-stimulatory molecules (423, 424, 426, 428). Much of the functional characterisation of intestinal macrophages has been performed in the mouse. Murine macrophages are defined as MHC II⁺ CD11c⁺ F4/80⁺ CD64⁺ CX3CR1^{int/hi} (225, 234). These CX3CR1-expressing cells extend dendrites into intestinal lumen, perhaps representing another method of antigen capture (429, 430). Intestinal macrophages have several regulatory and homeostatic functions, including maintenance of epithelial barrier function through secretion of IL-10 and prostaglandin E2 (PGE2) (225, 431, 432), and regulation of Treg survival and function *in situ* (433).

Following uptake and degradation of antigen, human intestinal macrophages do not secrete the pro-inflammatory hormones commonly associated with other tissue-resident macrophage populations (434). Specifically, human intestinal macrophages lack respiratory burst activity following stimulation with PMA or opsonized zymosan (435). However, this deficiency was overcome in IBD (435). Low expression of numerous pattern recognition receptors (PRRs) including CD14, CD64 and CD123 (IL-3R) and the signalling molecule MyD88 are thought to contribute to the differential functional capacity of intestinal macrophages (424, 436). However, human intestinal macrophages have been shown to express numerous TLRs (TLR 2-9) (426, 436). Control of murine intestinal macrophage pro-inflammatory activity is maintained by environmental conditioning through TGF β (436), and by expression of several inhibitory receptors including CD200R1 (437). However, intestinal macrophages in CD200R mice exhibit normal phenotype and function (438).

Some reports suggest that discrete monocyte populations independently gave rise to resident and inflammatory macrophage populations. Specifically, murine Ly6C^{lo} and Ly6C^{hi} monocytes generate resident and pro-inflammatory macrophages respectively (279). However, it has recently been shown that Ly6C^{hi} macrophages generate both resident (CX3CR1^{hi}) and pro-inflammatory (CX3CR1^{int}) intestinal macrophage populations *in situ* (225, 439). A similar macrophage differentiation process has been postulated for human intestinal CD14^{lo} (resident) and CD14^{hi} (pro-inflammatory) macrophage populations. The pro-inflammatory CD14^{hi} macrophages expand during CD (225, 427).

Overall, resident macrophages are refractory to exogenous stimuli and promote tolerogenic responses and homeostatic processes through Treg and epithelial barrier maintenance. However, during inflammation pro-inflammatory macrophages dominate the intestinal mucosa and secrete pro-inflammatory molecules including IL-23 and TNF α . Further characterisation of these populations in human intestinal mucosa is required.

1.4.3 AS and the intestinal immune system

Intestinal inflammation is inextricably linked to AS pathogenesis. AS patients often suffer from extra-articular disease manifestations; with approximately 10% of AS patients concurrently diagnosed with IBD, commonly in the form of CD (11, 12). Of patients initially diagnosed with CD alone, 54% of HLA-B27⁺ individuals subsequently develop AS in comparison to only 2.6% of HLA-B27⁻ CD patients (440). In addition to those AS patients clinically diagnosed with IBD, at least 50% of AS patients show signs of subclinical intestinal inflammation (4, 11, 13). AS patients with IBD are associated with increased disease severity, as measured by function and disease activity (441-443). Together, these data indicate that disruption of intestinal homeostasis may contribute to the clinical and pathological features of AS.

Further supporting a role for intestinal inflammation in SpA pathogenesis, a rat model of SpA failed to exhibit gut and joint pathology in the absence of intestinal flora, whilst skin inflammation was unaffected (444). These findings provide evidence for the interplay between the intestinal environment, specifically the gut flora, and SpA development. However, the presence and colonisation of several intestinal bacterial species did not differ between AS patients and healthy controls (445). Elucidation of the immune pathways involved in this interaction may improve the understanding of AS pathogenesis.

1.5 Ankylosing spondylitis

1.5.1 Inflammation associated with ankylosing spondylitis

The tissues most afflicted by inflammation in AS include the sacroiliac joints (SIJ), sites of tendon/ligament attachment (entheses), axial skeleton, peripheral joints, intestine and the eyes (446). For several of these tissues the inflammatory infiltrate has at least partially been described.

Inflammation in AS is believed to first occur within the SIJs (446). This inflammation is associated with reduced BM cellularity, loss of synovium and cartilage, enthesitis and bone (syndesmophyte) formation (447). Synovitis is succeeded by pannus and connective tissue formation, leading to the destruction of local cartilage and bone (447). Following these destructive processes, bone formation occurs, leading to loss of joint function as is shown in Figure 1.2 (447, 448). Entheses are commonly believed to be the location for the initial inflammatory infiltrate (14, 16, 449, 450), however this claim has also been refuted by some (446, 447). The inflammatory infiltrate associated with AS SI joints has been characterised and is dominated by CD3⁺ T cell of both CD4⁺ and CD8⁺ lineages, fibroblasts, and CD14⁺ macrophages (451, 452). Furthermore, all infiltrating populations express elevated transcriptional levels of TNF α (451). CD3⁺ T cells and macrophages (CD68⁺) also dominate the cellular infiltrate in synovial inflammation (453). Similarly, HLA-DR^{hi} CD163⁺ TNF α ⁺ macrophages preferentially infiltrate both the synovial membrane and colonic LP of SpA patients (454, 455).

In addition to the characterisation of the inflammatory infiltrate associated with the axial skeleton, articular and extra-articular tissues, the populations associated with enthesal inflammation have been described, where macrophages appear to dominate and very few infiltrating lymphocytes are observed (456). However, BM cellular infiltrate at sites of entheses mostly contain lymphocytes, with CD8⁺ T cells being the abundant population (457). Within affected joints, blood vessel formation may promote infiltration of inflammatory populations (452). These results indicate that both branches of the immune system, innate and adaptive, are involved in the pathogenesis of AS.

Despite a relative abundance of information about inflammatory tissue infiltrate, the functional contributions of these immune populations to disease pathogenesis remain poorly understood. Much of what is known has been generated using animal models.

1.5.2 Animal models of SpA and immune pathogenesis

The HLA-B27 transgenic rats (HLA-B27 TG) have been the most important model for understanding the immunopathogenesis of SpA. Rats over-expressing the human HLA-B*2705 and associated β 2-microglobulin (β 2m) genes (458) spontaneously develop a range of symptoms including intestinal inflammation, peripheral arthritis, uveitis and skin inflammation (444). This model has proved extremely useful in unravelling several key components regarding the pathogenesis of SpA disease, much of which will be discussed

in greater detail below. This model has recently been adapted by increasing the $\beta 2m$ copy number/cell (459). Interestingly, this alteration enhances the severity of peripheral arthritis and promotes development of axial bone formation, spondylitis and enthesitis (459). In contrast to HLA-B27 TG rats, colitis failed to develop in this SpA model, both in terms of histological analysis and presence of diarrhoea (459).

Murine SpA models have been described. $TNF^{\Delta ARE}$ mice develop several SpA symptoms including IBD, peripheral arthritis, enthesitis, spondylitis and sacroiliitis (460, 461). This model relies on an induced deletion within the AU-rich elements of the TNF gene, leading to an increase in TNF production under steady state conditions in both the haematopoietic and stromal compartments (460, 461). Human TNF TG mice have additionally been observed to develop peripheral arthritis and bilateral sacroiliitis through matrix metalloproteinase (MMP) mediated bone erosion (462). These models indicate that TNF α can drive a range of pathologies, resembling SpA.

Immunisation of specific mouse strains, including BALB/c, with human cartilage proteoglycan leads to the development of arthritis, and progressive erosion and formation of bone resulting in complete ankylosis of the SIJs (463). This murine model is of interest because it has been argued that AS associated enthesitis results from aberrant responses directed against cartilage (460, 464).

A model developed to assess the processes of bone formation characteristic of AS involves co-habiting DBA/1 mice from separate litters at 2 months post-weaning (465). These mice develop ankylosis, particularly of the hind limbs and have enabled identification of several bone morphogenetic proteins (BMPs) involved in pathogenic bone formation (465, 466). Furthermore, *ank/ank* mice developed for the study of ankylosis development and progression are generated through mutation of the *ank* gene, encoding a pyrophosphate transporter, resulting in loss of function (460, 467).

A recent murine model provides a mechanism by which IL-23 may drive enthesitis in AS and SpA. Systemic administration of IL-23, via minicircle technology, to the murine B10.RIII strain resulted in the development of enthesial inflammation within peripheral and axial joints (468). Furthermore, this murine model developed psoriasis and enthesial bone formation (468). IL-23 was shown to mediate these destructive effects partially through activation of an enthesial resident IL-23R⁺ CD3⁺ CD4⁻ CD8⁻ T cell population

(468). This model has provided insights into the potential mechanisms relating IL-23 and SpA development.

1.5.3 Immunopathogenesis of AS/SpA

Studies using animal models of SpA have shaped investigations aimed at understanding the pathogenesis of human disease. One such study identified a dominant role for CD4⁺ T cells, but not CD8⁺ T cells, in the pathogenesis of disease. These observations were surprising, given the contribution of HLA-B27, an MHC class I gene, to disease development. Several lines of evidence in the HLA-B27 TG rats now support a role for CD4⁺ T cells, and not CD8⁺ T cells, in disease development. CD4⁺ T cells infiltrate colonic tissues of HLA-B27 TG rats (469). Compared to CD8⁺ T cells, CD4⁺ T cells isolated from HLA-B27 TG rats and transferred into nude recipients, cause more severe disease (470). Furthermore, adult thymectomy or antibody-mediated depletion of CD8⁺ T cells failed to inhibit the development of arthritis and colitis in the HLA-B27 TG rat model (471). Additionally, a loss of function deletion in the CD8 α gene did not affect the onset or severity of disease symptoms (472). Overall these data suggest that SpA development, at least in the HLA-B27 TG rat model, is CD4⁺ T cell mediated.

T cell priming is dependent upon the interaction of naïve T cells with professional APCs. The importance of this interaction in SpA pathogenesis was highlighted through the use of athymic HLA-B27 TG rats. In this model, development of colitis was dependent upon the interaction between T cells and an HLA-B27-expressing APC (473). Furthermore, HLA-B27 TG BM transfer into non-TG rats was efficient for disease transfer, highlighting the involvement of haematopoietic cells in disease development (474). Disease did not develop following T cell transfer into non-TG recipients (473). Subsequently, several studies have focused on the role of DCs, as the principal APC, in disease development.

Initial studies found that HLA-B27 TG DCs, predominantly splenic DCs, were deficient in their ability to stimulate T cells (475, 476). Contributing to this deficiency was the fact that fewer DC: T cell conjugates formed when HLA-B27 was expressed on the DC (476). Subsequent investigations found impairment of immunological synapse formation between HLA-B27 TG DCs and CD4⁺ T cells compared to HLA-B7 TG controls (477, 478). A reduction in the frequency of T cell Ca⁺ signalling events following interaction with HLA-B27 TG DCs was also observed (478). It has been suggested that interference of HLA-B27 with co-stimulatory molecule engagement may partially account for this insufficient

interaction and that this may contribute to aberrant CD4⁺ T cell priming and subsequent inflammation (478).

Proteomic analysis of HLA-B27 TG DCs identified upregulation of proteins related to the MHC class I processing pathway and the unfolded protein response (UPR) (477). The involvement of the UPR in AS pathogenesis will be discussed in detail below. In contrast, numerous “cytoskeleton-reorganising” proteins were downregulated in HLA-B27 TG DCs (477). Consequently HLA-B27 TG DCs were less motile than non-TG controls. The HLA-B27 TG DCs also displayed alterations to cell morphology and a reduction in their expression of surface MHC II (477). The authors argue that these factors could contribute to the impaired immunological synapse formation and the reduction in number of DC: T conjugates, leading to aberrant T cell priming and perpetuating disease development.

Relating to the T cell priming aspect of DC function, HLA-B27 TG rats have a higher proportion of activated CD4⁺ T cells in MLN and popliteal LNs (pLN) compared to WT littermates (479). Within these LNs, the proportions of IL-17A⁺, TNFα⁺ and IL-17A⁺ TNFα⁺ CD4⁺ T cells were expanded in HLA-B27 TG rats (479). *In vitro* experiments demonstrated that HLA-B27 TG splenic DCs preferentially drive differentiation and maintenance of Th17 cells in a contact dependent manner (479). Furthermore, IL-17⁺ mononuclear cells have been identified in the synovium of HLA-B27 TG rats, but are absent from non-TG controls (479). Thus, IL-17-secreting cells appear to be involved in the pathogenesis of SpA, in HLA-B27 TG animals.

An alternative explanation for the aberrant immune response observed in these rats has been proposed. HLA-B27 TG rats lack a specific migratory intestinal DC subset, compared to WT littermates and HLA-B7 TG controls (480). This DC deficiency was systemic in HLA-B27 TG rats (480). This “missing” subset of CD172a^{lo} DCs (CD103⁺ MHC II⁺ CD11b^{int} CD172a^{lo}) (480) has been reported to possess tolerogenic properties (372) and is analogous to the human CD141⁺ and murine CD8⁺ DC populations. This population has further been shown to be susceptible to apoptosis, providing a mechanism for the loss of this subset in HLA-B27 TG rats (477). The remaining HLA-B27 TG DCs were more activated, expressing higher levels of CD25, but did not display differences in the induction of naïve T cell proliferation (480). However, BM-generated DCs from HLA-B27 TG rats were susceptible to cell death, and had an impaired capacity to drive T cell proliferation, whilst selectively promoting differentiation of IL-17-secreting cells (480). Th17 and Th1 cells are reported to be expanded in the colonic LP of HLA-B27 TG rats

(481). Overall, data from animal models suggest involvement of DCs and T cells in the pathogenesis of SpA.

However, this SpA animal model has several disease-associated limitations that must be considered when relating HLA-B27 TG rat model findings to human disease: in order to develop disease symptoms, HLA-B27 TG rats have to express an extremely high HLA-B27 and $\beta 2m$ copy number. To be exact, in the original 33-3 strain on a Fischer background (F344), 55 HLA-B*2705 and 66 $\beta 2m$ genetic copies per cell had to be introduced to induce symptom development (458). The genetic profile of SpA family members is not solely reliant on HLA-B27 expression as several other genes including IL-23R and STAT3 elicit disease susceptibility (39). Furthermore there is little conclusive evidence to suggest involvement of spinal disease in terms of entheses inflammation in HLA-B27 TG rats, a hallmark symptom of AS (458, 482).

1.6 Molecular pathogenesis of AS

1.6.1 Molecular mimicry

Numerous attempts have been made to understand the causes of AS, yet no definitive trigger has yet been identified. In the past, associations between infection and AS pathogenesis have been suggested. For instance, *Klebsiella-enterobacter* species have been reported to show a degree of immunological cross-reactivity with HLA-B27⁺ lymphocytes (483). Furthermore, 93% of inflamed AS patients were infected with *Klebsiella-enterobacter* (483). In addition, levels of *anti-Klebsiella pneumoniae* antibodies in AS patients' serum and SF and were elevated compared to healthy controls and RA patients (484, 485). Evidence suggests that the intestine may be the primary source of *Klebsiella* infection in AS patients, and it is argued that it is the principal microbial cause of AS pathogenesis (485). However, several investigators have failed to establish an association between *Klebsiella* infections and AS pathogenesis (486). Subsequently, the role of microbial infection and AS aetiology remains unclear.

Other contributions of molecular mimicry to AS pathogenesis have been described. Molecular mimicry involves mistaken immune targeting of self-antigens; immune responses directed against bacterial antigens can target self-antigen bearing similar peptide sequences. In the context of AS, HLA-B27 may present arthritogenic peptides derived from host proteins to CD8⁺ T cells, resulting in the development of chronic inflammation

and/or autoimmune disease. The *Klebsiella pneumoniae* nitrogenase reductase enzyme has been reported to share amino acid homology with HLA-B*2705 molecules (487). Furthermore, *Klebsiella* pullulanase enzymes share amino acid sequences with HLA-B27 molecules (488). These observations hint that direct recognition or molecular mimicry associated with *Klebsiella* species might be involved in the pathogenesis of AS.

Further supporting a role for molecular mimicry in disease development, a self HLA-B27 derived peptide has been identified as a natural ligand for several specific B27 subtypes highly associated with AS: HLA-B*2702, HLA-B*2704 and HLA-B*2705 (489). In conjunction, this peptide shows sequence homology with *Chlamydia trachomatis* (489), suggesting potential for cross-reactivity and disease perpetuation. Cartilage and bone derived peptides have additionally been suggested to bind to HLA-B27 (490), again supporting the capacity for the generation of autoimmunity.

Self-antigen derived from vasoactive intestinal peptide receptor 1 (VIPR1) shares homology with the Epstein-Barr virus protein, pLMP2. Following binding to HLA-B*2705 this may elicit activation of autoreactive T cells (491, 492). Similar responses were not generated following binding to the HLA-B*2709 subtype, not commonly associated with AS susceptibility (491, 492). Binding of antigenic peptides to AS-susceptible HLA-B27 subtypes may therefore promote disease pathogenesis.

The HLA-B27 molecule has 6 pockets capable of binding antigenic peptides, with the B pocket being the favoured region for determining the epitope presentation repertoire of HLA-B27 (11). This B binding pocket may be involved in arthritogenic peptide recognition, initiating joint specific disease (11). To support this, only a single amino acid substitution from aspartate to histidine is responsible for the different disease susceptibility profiles of the HLA-B*2705 and HLA-B*2709 subtypes; only HLA-B*2705 confers a disease association. This mutation occurs within the binding region of the MHC class I molecule, suggesting a possible role for arthritogenic peptide presentation due to the alterations in peptide binding. While it has been argued that HLA-B*2705 presentation of a unique set of peptides may initiate disease development, HLA-B*2709 AS patients have now been identified, weakening the plausibility of this hypothesis of arthritogenic peptides and molecular mimicry. Furthermore, HLA-B27 is an MHC Class I molecule and therefore conventionally presents antigens to CD8⁺ T cells. Animal models have discounted a role for CD8⁺ T cells in disease pathogenesis (470, 471). Together, these observations refute a role for arthritogenic peptide presentation and molecular mimicry in AS development.

Indeed, a specific HLA-B27 restricted antigen has yet to be discovered (493). However, further studies investing arthritogenic peptides are still being performed.

1.6.2 Cell surface HLA-B27 dimer formation

As described in section 1.3.4.1, MHC class I molecules such as HLA-B27 are associated with $\beta 2m$ and are expressed on the cell surface for interaction with $CD8^+$ T cells (494). However, HLA-B27 shows a tendency to form atypical disulphide-bonded heavy chain homodimers (HLA-B27₂), which are expressed on the cell surface (495-497). These homodimers are not extra- or intracellularly complexed to $\beta 2m$ (497). This unusual conformation is mediated through an unpaired cysteine residue occurring at position 67 and is believed to occur during endosomal processing by two distinct pathways (495, 496). Intracellular homodimers are formed in the ER but do not traffic to the surface, whilst homodimers expressed on the cell surface may arise from unstable heterodimers on the surface or located within the endosomal recycling compartments (496). Promoting the capacity for homodimer formation, HLA-B27 molecules are more likely to form complexes in the absence of TAP or tapasin, compared to other MHC class I molecules, enhancing the likelihood of HLA-B27 heterodimer instability (494, 498).

Receptors for these atypical surface HLA-B27₂ molecules have been identified on lymphocytes, monocytes, DCs and NK cells (499, 500). HLA-B27₂ receptors include killer cell immunoglobulin-like receptor 3DL1 (KIR3DL1), KIR3DL2 and immunoglobulin-like transcript 4 (ILT4) (500). HLA-B27₂ molecules do not exhibit binding to the inhibitory immunoglobulin-like receptor (LILRB1 or ILT2) (499, 500). Furthermore, KIR3DL2 is a ligand for HLA-B27₂ surface molecules but not HLA-B27 heterodimers (496). KIR engagement of MHC class I molecules has been shown to prevent activation-induced cell death (AICD) of NK and T cells (47, 501). Subsequently, KIR activation may promote the survival of the leukocyte populations leading to the perpetuation of the inflammatory response. To this end, HLA-B27₂-expressing APCs have been shown to stimulate the proliferation and survival of activated KIR3DL2⁺ CD4⁺ T cells capable of IL-17 secretion (495).

SpA patients express these atypical HLA-B27₂ molecules along with their receptors, specifically KIR3DL1 and KIR3DL2 (500). KIR3DL2⁺ NK cells and CD4⁺ T cells have shown to be expanded in the peripheral blood and SF of SpA patients compared to healthy controls (47, 495). Furthermore, peripheral blood NK cells isolated from SpA patients

exhibited elevated cytotoxicity activity and activation compared to those isolated from healthy controls (47). These data indicate preferential HLA-B27₂ binding in AS patients, leading to abnormal cell activation and inflammation (47).

In addition, KIR3DL2-expressing CD4⁺ T cells isolated from SpA peripheral blood upon stimulation preferentially secrete elevated levels of IL-17A, IFN γ and TNF α compared to B27⁻ controls (495). The proportion of circulating KIR3DL2⁺ IL-17-secreting cells is increased in SpA patients compared to healthy controls (495). This population has been shown to be enriched for IL-23R-expressing cells, with SpA patients again having a greater proportion of circulating IL-23R⁺ KIR3DL2⁺ CD4⁺ T cells, compared to healthy controls (495). These populations were further enriched within inflamed joints compared to peripheral blood (495). These data indicate that SpA patients have an increased proportion of circulating and tissue-resident KIR3DL2⁺ Th17 cells, shown to proliferate in response to HLA-B27₂ molecules highlighting an additional role for HLA-B27₂ in AS pathogenesis.

Investigation of HLA-B27₂ surface molecules has been hampered through a lack of specific antibodies. However several antibodies have recently been identified to bind these homodimers, including the HD6 monoclonal antibody (502, 503). Given the abnormalities of DC function in rat models of SpA, and the expression of MHC class I molecules on APCs, the expression of HLA-B27₂ molecules has been assessed on DCs. HLA-B27₂ surface expression on monocyte-derived DCs was intensified following cell activation and appeared transient in nature (504). However, no difference was observed in homodimer expression between AS patients and healthy controls (505).

Current data suggest that KIR3DL2 ligation, through binding of HLA-B27₂, may promote cell activation and cytokine release, with a higher proportion of KIR3DL2⁺ CD4⁺ IL-17A-secreting T cells being observed in SpA patients. These cells may perpetuate disease pathogenesis. While the formation of HLA-B27₂ molecules and generation of free heavy chains is not restricted to those HLA-B27 subtypes associated with AS susceptibility (506), β 2m dissociation from surface HLA-B27 heterodimers is more frequent in AS-associated HLA-B27 subtypes (507). Expression of these HLA-B27₂ molecules *in vivo*, in healthy controls and AS patients remains to be established. In addition, any HLA-B27₂ molecules formed in the ER that fail to reach the cell surface may be involved in a process termed ER stress, described below. Therefore HLA-B27₂ molecules may promote inflammation in AS patients through several pathways.

1.6.3 ER stress

A separate hypothesis regarding the mechanism of AS development relates to the propensity for HLA-B27 to form intracellular homodimers within the ER (496). This protein misfolding leads to the accumulation of HLA-B27 molecules within the ER (508, 509). It has been reported that approximately 70% of newly synthesised HLA-B27 heavy chains are misfolded within the ER (508, 509). This unique propensity for HLA-B27 to misfold within the ER is supported by several observations: HLA-B27 heavy chains have an increased tendency to enter the ER-associated degradation pathway (510); extended interactions with the ER chaperone molecule, binding immunoglobulin protein (BiP) have been observed; HLA-B27 protein folding and maturation is retarded compared to HLA-B7 (511, 512). BiP is an ER chaperone molecule that binds to newly created proteins following ER translocation and forms stable interactions with misfolded proteins (508). This tendency for HLA-B27 to misfold within the ER is unique amongst MHC Class I molecules (508).

ER homeostasis relies on the generation of stable protein complexes following protein influx, and the expulsion of misfolded proteins through endoplasmic-reticulum-associated protein degradation (ERAD) (508). Following sufficient aggregation of misfolded proteins, homeostasis is lost and ER stress pathways are initiated. These pathways are collectively known as the unfolded protein response (UPR) (508). The function of the UPR is to restore ER homeostasis through restoration of the protein folding, secretion and degradation pathways (508). Several proteins are responsible for the transduction of stress signals from the ER to the nucleus, to initiate the UPR: inositol requiring enzyme 1 α (IRE1 α), pancreatic ER eIF2 α kinase (PERK) and activating transcription factor 6 α (ATF6 α) (513). Under homeostatic conditions, BiP is bound to the nuclear sensors inhibiting UPR activation (508). A diagram depicting the major ER stress pathways is shown in Fig. 1.7. The UPR initiates several pathways to restore homeostasis including induction of chaperone molecule generation (514, 515), promotion of ERAD (516) and autophagy activation (517, 518). If ER stress cannot be overcome, then apoptosis often ensues, accompanied by the release of pro-inflammatory factors including IL-6 and TNF α (493, 498, 508). The UPR can also stimulate pro-inflammatory responses to repair damage caused by UPR induced cell death (519). Therefore, given the propensity for HLA-B27 to misfold and the biological responses associated with subsequent UPR activation, the roles of these pathways have been investigated both in AS and in animal models of SpA.

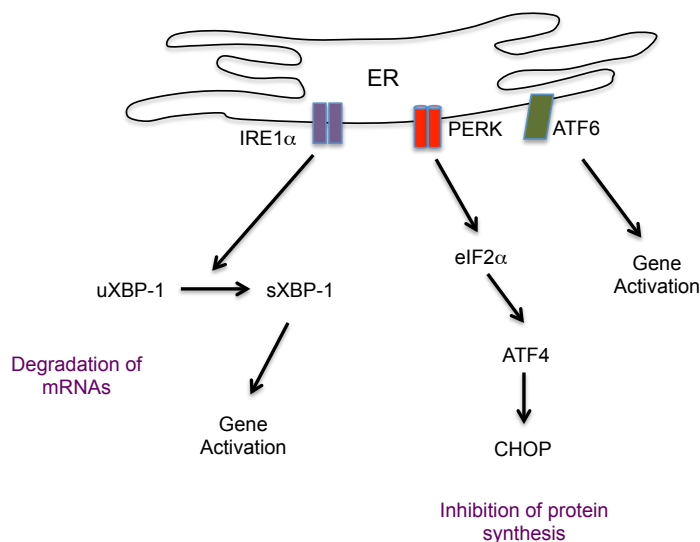


Figure 1.7: Diagram depicting ER stress pathways

Pathways involved in the transmission and activation of ER stress and the unfolded protein response. uXBP-1 = unspliced XBP-1, sXBP-1 = spliced XBP-1.

BM-derived macrophages from HLA-B27 TG rats exhibited elevated levels of BiP, CHOP and spliced XBP-1 expression, suggesting activation of the UPR. This pathway was promoted through IFN γ exposure (520). The HLA-B27 TG rat model that expresses increased levels of β 2m did not exhibit similar activation of the UPR pathway, and displayed reduced HLA-B27 misfolding (459). These observations support the relationship between HLA-B27 misfolding and UPR activation. However, the overexpression of β 2m, despite a reduction of UPR activation, increased disease severity in terms of spondylitis and arthritis (459). Intestinal inflammation was severely diminished in this model, suggesting that HLA-B27 misfolding may be most important for SpA related intestinal inflammation (459). Consistent with this hypothesis, UPR over-activation has been observed in intestinal tissue isolated from UC and CD patients (521).

Further investigations have highlighted differences in cell susceptibility to HLA-B27 misfolding. Cells of the myeloid lineage, specifically macrophages, are more susceptible to HLA-B27 misfolding than isolated splenocytes, following cytokine exposure (522). Given this apparent myeloid propensity for ER stress, UPR activation and the inflammatory consequences of this pathway have been studied in greater detail in BM-derived macrophages. Following LPS and IFN γ stimulation, upregulation of the UPR in HLA-B27 TG BM-derived macrophages via BiP and XBP-1 splicing was observed (481). Activation of the UPR subsequent to HLA-B27 misfolding was observed to enhance IL-23 production (481). CD11b/c⁺ cells isolated from the LP of HLA-B27 TG rats showed selective upregulation of BiP and IL-23 and IL-12 secretion (481). Overall, HLA-B27 misfolding

may result in ER stress and UPR activation, and may augment TLR-4 induced IL-23 secretion by myeloid cells.

Despite evidence from animal models, described above, implicating a role for ER stress and UPR activation in the pathogenesis of SpA, similar observations have not been observed in human disease. Monocyte-derived macrophages from AS patients stimulated with IFN γ and LPS did not exhibit upregulation of BiP or CHOP (523). Another study failed to detect a difference in BiP expression or XBP-1 splicing in monocyte-derived DCs and circulating lymphocytes isolated from AS patients (505).

Intestinal samples from AS patients, CD patients and healthy controls were analysed for activation of the UPR and autophagy pathways. LP mononuclear cells failed to exhibit upregulation of the UPR pathway, although XBP-1 unspliced was upregulated in LP mononuclear cells (LPMCs) isolated from the chronically inflamed ileum of AS patients (524). In contrast, several autophagy associated genes were upregulated in response to misfolding in the chronically inflamed ileum of AS patients: autophagy-related protein 16-1 (ATG16L1), immunity-related GTPase family M protein (IRGM) and microtubule-associated proteins 1A/1B light chain 3A (MAP1LC3A) (524). Inhibition of the autophagy pathway in AS and CD patients and healthy controls reduced IL-23 secretion from LPMCs (524). Inhibition of the UPR did not replicate these IL-23-related observations (524). These findings reject a role for UPR activation and ER stress induction in human disease. However, HLA-B27 misfolding in AS patients may induce activation of the autophagy pathway enhancing IL-23 production, contributing to the elevated levels of IL-23 in AS and CD patients (524).

1.7 Immunopathogenesis of AS

The direction of many human AS studies have been influenced by the findings from the animal models described above. Consequently, many AS studies focus on serum cytokines and circulating T cells.

1.7.1 Cytokines

Serum isolated from AS patients and HCs is often analysed to determine the cytokine profile of AS patients. In terms of pro-inflammatory cytokines, TNF α and IL-8 have been found to be elevated in AS patients (525-527). Anti-TNF α therapies have shown a certain

degree of efficacy in disease inhibition, as discussed below, supporting a role for these inflammatory hormones in disease pathogenesis. The remaining cytokines associated with disease include those associated with the Th17 phenotype. For instance, the primary cytokine released by Th17 cells, IL-17A, has been found to be upregulated in AS patients compared to healthy controls in numerous studies (49, 181, 527-529). IL-6 promotes differentiation of Th17 cells in humans (107, 109) and has additionally been found to be upregulated in the serum of AS patients compared to healthy controls (49, 525-527). Furthermore, IL-6 expression correlated with markers of inflammation: erythrocyte sedimentation rate (ESR) and C-reactive protein (CRP), and spinal function (525, 526). However anti-IL-6 therapy (Tocilizumab) recently failed to show efficacy through inhibition of IL-6 engagement to the IL-6R (23).

Supporting a role for the hypothesis that AS is a Th17 mediated disease, Th17 effector cytokines IL-6, IL-22, IL-23 and TNF α are upregulated in AS patient serum (49, 527-530). Furthermore, recombinant IL-23 has been shown to preferentially enhance IL-17 secretion by patient peripheral blood mononuclear cells (PBMCs) (528). However, a study by Wendling et al failed to detect upregulation of the IL-12/23 p40 subunit in patient serum, although IL-12/23p40 concentration was elevated in AS patient SF (531). However, current data indicates systemic upregulation of Th17-associated cytokines in AS. Supporting a Th1 circulating phenotype of AS patients, IFN γ and IL-2R levels are reported to be elevated in serum (526, 532). IL-12p70, secreted by DCs and macrophages, and required for Th1 induction, has been reported to be elevated in patient serum compared to healthy controls (49). The role of Tregs in AS pathogenesis remains controversial, as will be discussed below; however several immunomodulatory molecules have been found to be upregulated in AS patient serum: IL-10 and TGF β (49, 532). Overall, the serum of AS patients contains a vast array of immunogenic (Th17 and Th1) and tolerogenic (Treg) associated cytokines, which may influence disease pathogenesis.

Patient serum cytokine data predominantly implicate Th17 cells and TNF α in the pathogenesis of disease, however the cellular sources and functions of these cytokines have not yet been elucidated in AS.

1.7.2 T cells

As described in section 1.2.2, numerous circulating T cell phenotypes have been identified in humans including Th1, Th2, Th17, Th22 and Tregs. In addition, several unusual T cell populations and CD8⁺ T cells have been studied in AS.

A population of cytotoxic CD3⁺ CD4⁺ CD57⁺ CD28⁺ T cells is increased in AS patients compared to HCs. Further phenotypic analyses found this population to secrete IFN γ and perforin upon activation, sharing a phenotypic and functional likeness with NK cells. This population increased in response to inflammation, as measured by ESR (533).

A higher proportion of CD8⁺ IL-4⁺ regulatory T cells are also observed in AS patients compared to HCs (534). However, the functional attributes of this circulating population have not yet been elucidated. Classical CD8⁺ populations have been studied, with no difference being observed between AS patients and healthy controls (535).

A higher proportion of circulating IL-23R⁺ T cells in AS patients compared to HCs has been observed, with the majority γ/δ T cells (536). These cells were found capable of IL-17 secretion and may represent a source of IL-17 contributing to the elevated serum levels in AS patients (536).

AS patients have been shown to have elevated proportions of circulating activated T cells compared to healthy controls (535, 537). Several studies have focused on Th17 cells and Tregs given their role in inflammatory disease and tolerance respectively. Correlating with the upregulation of Th17 associated cytokines (IL-17, IL-22, TNF α , IL6 and IL-23) in patient serum, several studies support the involvement of Th17 cells in disease pathogenesis (181, 527, 530, 535, 538, 539). The circulating Th17 cells express CD4, CD45RO, CCR6 and CCR4 (181). Despite this, several studies reject the idea that circulating Th17 cells contribute to AS pathogenesis (536, 540). However, the overwhelming majority of studies suggest a contribution of Th17 cells to AS pathogenesis, given that cytokines they secrete are upregulated in patient plasma and that they expand in AS patient blood.

IL-22-secreting T cells (Th22) (181, 530) are increased in the blood of AS patients, as in other inflammatory diseases including RA, psoriasis and SLE (129, 530, 541, 542). In addition, Th1 and Th2 cells are reportedly increased in AS patient plasma compared to healthy controls, although these observations remain disputed (181, 527, 535). In terms of

activated circulating T cell populations, AS patients appear dominated by the Th17 and Th22 pathogenic populations.

Similar to the studies described above investigating the phenotype of circulating T cells in AS patients, data on the proportions of circulating Tregs is controversial. Numbers of Tregs, predominantly identified through their expression of FOXP3, may be increased (527, 538), decreased (539, 543) or unchanged (540) compared to healthy controls. Furthermore, CCR4⁺ CD4⁺ T cells are elevated in AS patients and may represent a regulatory population given their observed correlation with IL-10 serum levels (532). Clearly, the role of Tregs in AS pathogenesis requires further investigation.

1.7.3 Myeloid cells

Only three studies have investigated the function of myeloid derived cells in AS pathogenesis, albeit through the generation of monocyte-derived DCs (moDCs). Firstly, proteomic analysis of AS patient monocytes revealed an increase in proteasome associated proteins, and molecules associated with TLR signalling, vascular endothelial growth factor (VEGF) and integrin pathways (544). This data set suggests alterations to the function of circulating monocytes in terms of their response to exogenous signalling and antigenic processing.

CD14⁺ monocytes isolated from blood and grown in the presence of IL-4 and GM-CSF for approximately 7 days are termed moDCs. Many DC based studies exploit this technique, given the relative ease of generating large numbers of moDCs, and subsequently compare those generated from patients and healthy controls. DCs generated under these conditions are thought to replicate the phenotype and function of inflammatory DCs (545). Using this system, moDCs isolated from AS patients express lower levels of MHC II under resting conditions, although the functional consequences of this observation have yet to be determined (546, 547). Despite this apparent down-regulation of MHC II, no difference in the expression of co-stimulatory molecules including CD80, CD86 and CD83 has been observed (546, 547). Furthermore, in comparison to healthy controls, AS patient moDCs did not differ in their secretion of IL-23 following TLR 7, 8 and 3 stimulation and did not differ in their baseline cytokine production (547). Overall moDCs generated from AS patients have similar functions to those isolated from healthy controls. The phenotype and functions of *in vivo* DC and macrophage populations have not been assessed in AS.

1.7.4 Peripheral tissue

Investigations in AS have focused on the intestine, facet joints and SF. Pathological changes at these sites in AS patients are termed extra-articular manifestations. Understanding the immunological pathways involved in the perpetuation of inflammation at these sites can aid the understanding of the relationship between these extra-articular sites, peripheral joints and AS development and pathogenesis.

SF, more commonly associated with RA, isolated from AS patients has been shown to contain a higher proportion of CD4⁺ FOXP3⁺ Tregs compared to RA patients and AS patient blood (540, 548). These SF Tregs possess suppressive activity, inhibiting proliferation and cytokine production from effector CD4⁺ populations (548). However, another study noted that following isolation, SF Tregs failed to secrete IL-10, IL-2, IFN γ or TNF α (549). Overall, these data suggest that Tregs are present within SF and may inhibit effector T cell populations.

IL-17⁺ cells, predominantly myeloperoxidase (MPO) positive cells and CD15⁺ neutrophils, are increased in the facet joints of AS patients compared to osteoarthritis (OA) (540). These data are consistent with IL-17 involvement in disease pathogenesis, and also highlight a potential role for the innate immune response through secretion of IL-17. This study further characterised SF Th17 cells and observed no difference compared to OA samples (540). Furthermore, subchondral BM isolated from AS patients has been shown to contain a higher proportion of IL-23⁺ cells compared to OA patients, again involving MPO⁺ cells, however macrophages and DCs additionally contributed to this IL-23 signature (550).

As described throughout this introduction, there is a strong association between AS and the intestinal environment. SpA symptoms do not develop in HLA-B27 TG rats raised under germ-free conditions, at least 50% of AS patients show evidence of intestinal inflammation, and 54% of IBD sufferers expressing HLA-B27 eventually develop AS (4, 13, 440, 441). Unsurprisingly therefore, the intestinal environment of AS patients has been studied in some detail.

Within the SI of AS patients, an increase in IL-23, IL-32 and TGF β mRNA transcripts has been observed compared to healthy controls (551, 552). Infiltrating cells with myeloid morphology and Paneth cells are responsible for producing this IL-23 (551). Perhaps

contradicting the systemic involvement of Th17 cells, IL-17A, IL-6, TNF α and IL-1 β levels were relatively low compared to CD patients and HCs (551). Furthermore, IL-4 and IL-5 levels were elevated, suggesting intestinal Th2 polarisation in AS patients (551).

AS patients who developed chronic ileal inflammation showed elevated transcript levels of FOXP3 and the regulatory associated cytokines IL-2, TGF β and IL-10 within the small intestine (552, 553). The increase in intestinal CD4⁺ IL-10-secreting Tregs may contribute to the levels of these cytokines (553). Specifically, there was a 5 fold increase in intestinal Tregs in AS patients compared to HCs, with 70-80% secreting IL-10 (553). Furthermore, blocking IL-10 promoted Th17 polarisation in LPMCs isolated from AS patients (553). These data suggest that functional Tregs within the intestine of AS patients may be actively inhibiting the expansion or development of Th17 cells in an IL-10-dependent manner.

Given the increase in circulating Th22 cells in AS patients, and their association with inflammatory disease, the role of intestinal IL-22 has been investigated in AS. Within the inflamed small intestine of AS patients, there was a selective expansion of the IL-22-secreting CD3⁻ CD56⁺ NKp44⁺ NK cell subset in AS patients compared to healthy controls (554). No difference was observed in the IFN γ -producing CD3⁻ CD56⁺ NKp46⁺ NK subset (554). Accordingly, IL-22 levels were increased within intestinal tissue isolated from AS patients (554). Overall, IL-22 and IL-23 appear to dominate the cytokine profile of intestinal inflammation in AS patients whilst functional Tregs are expanded within this environment, presumably to dampen the ongoing inflammatory response.

1.7.5 Treatment of AS

1.7.5.1 Therapeutic categories used in the management of AS

The treatment of AS has developed over recent years to include biological therapy, disease-modifying antirheumatic drugs (DMARDs) and non-steroidal anti-inflammatory drugs (NSAIDs). The biological therapies, NSAIDs and DMARDs commonly used in the treatment of AS are listed in Table 1.6. Biological therapies in AS are currently restricted to those targeting and inhibiting TNF α . They act to prevent TNF α engagement of the TNF receptor by binding to circulating TNF α .

NSAIDs are moderately effective in the treatment of AS and are often the first course of disease treatment (4). Patients in whom NSAIDs fail to control symptoms progress,

depending on disease symptoms, to DMARD or biological therapy (4). However, DMARDs are not effective for the treatment of AS patients presenting with axial symptoms (23, 555, 556).

Table 1.6: Drugs used in the management of AS

Drugs commonly used in the treatment of AS can be subdivided into three categories: NSAIDs, DMARDs and biologics. Examples are listed in the table.

Categories	Examples
NSAID	COX-2 inhibitors, Ibruprofen, Naproxen, Etodolac, Diclofenac, Etoricoxib
DMARD	Sulphasalazine, Methotrexate, Azathioprine
Biologic	Adalimumab, Etanercept, Infliximab

1.7.5.2 Assessment of disease activity

In order to assess disease status, progression and therapeutic effectiveness, AS patients undergo several immunological and physiological tests. Levels of systemic inflammation are routinely determined by erythrocyte sedimentation rate (ESR) and C-reactive protein (CRP). To assess disease activity and joint function, several distinct tests may be performed. These are outlined in Table 1.7.

Table 1.7: Assessment of disease severity and therapeutic response

Four tools, either in the form of a questionnaire or performed by a clinician, contribute to assessment of disease activity in AS.

Functional Assessment	Output	Score
Bath AS Disease activity index (BASDAI)	Questionnaire to assess pain, fatigue and stiffness	0-10
Bath AS metrology index (BASMI)	Clinical measurements to determine axial function	0-10
Bath AS functional index (BASFI)	Questionnaire to assess functional limitations and patient mentality	0-10

Bath AS patient global score (BAS-G)	Patient assessment of disease impact over time	0-10
---------------------------------------------	------------------------------------------------	------

1.7.5.3 Effectiveness of therapeutics

The effectiveness of biological therapy on AS patient disease activity is continually assessed. Furthermore, several studies have focused on the patient immunological profile following anti-TNF α treatment in order to elucidate the pathways involved in disease progression and the *in vivo* mechanisms underlying the response to blocking TNF α .

Anti-TNF α has been shown to slow radiographic progression (22, 557, 558). Etanercept, amongst other anti-TNF α blockers, led to improvements in disease activity through BASDAI assessment, CRP, ESR and axial function (531, 559-561). In one study, anti-TNF α therapy reduced BASDAI scores by 70% (561).

With regards to the immunological response, circulating levels of several cytokines including IL-6, IL-17A, IL-23 and TNF α have been reduced following biological therapy (539, 561). However, TNF α blockers do not appear to inhibit IL-12/23p40 secretion (531). Associated with these alterations to the cytokine profile of AS patients following biological therapy, the proportion of activated T cells (537), Th1 (527) and Th17 (527, 539) subsets returned to baseline levels. Furthermore, the numbers of circulating Tregs and serum TGB β increase in response to anti-TNF α treatment, supporting a shift from immunogenic to tolerogenic responses in AS patients. However, one study disputes this hypothesis with the observation that the proportion of CD8 $^+$ T cells and IFN γ^+ and TNF α^+ CD4 $^+$ T cells increased following anti-TNF α treatment (562).

Despite these advances in disease treatment, approximately 50% of patients remain unresponsive to current therapeutics (4, 23) highlighting the need for further investigation of the pathways involved in disease pathogenesis to guide development of future therapeutics.

1.8 Hypotheses and aims

Investigations using animal models of SpA suggest a role for DCs in the pathogenesis of SpA. Specifically, we observed a systemic DC defect in the HLA-B27 TG rat model of

SpA, with the CD103⁺ MHC II⁺ CD11b^{int} CD172a^{lo} subset absent from intestinal lymph and MLNs (480). The absence of this reportedly tolerogenic DC subset (372) supported the differentiation and maintenance of a Th17 type immune response, characterised through the preferential secretion of IL-17 by CD4⁺ T cells cultured with HLA-B27 TG BM-derived DCs (480). Furthermore, no studies have yet investigated the phenotype and functions of circulating DC populations in AS patients. Therefore the aim of my thesis was to study the phenotype and function of circulating DCs in AS, directly *ex vivo*, to elucidate any potential role in the development or perpetuation of AS.

Based on previous work from our laboratory we hypothesised that the human CD141⁺ DC population, equivalent to the CD11b^{int} CD172a^{lo} rat DC population, would be absent or significantly reduced in AS patients compared to HCs. We also hypothesised that the remaining AS patient DCs would subsequently induce aberrant immune responses through the generation of pathogenic T cells, as in the HLA-B27 TG rats. In order to test these hypotheses we identified and analysed the proportions of circulating DCs (chapter 3) and assessed their ability to induce T cell proliferation and chemokine receptor expression (chapter 6). Furthermore, we characterised the circulating T cell profile of AS patients (chapter 4) in order to identify the T cell populations dysregulated with disease, and permit inferences regarding the ongoing *in vivo* DC: T cell priming events. We also set out to elucidate the immunological mechanisms involved in the perpetuation of peripheral disease in AS patients, specifically the SF (chapter 5) and the intestine (chapter 8). The immune populations involved in AS pathogenesis were subsequently assessed for their relationship with patient clinical parameters (chapter 7). By performing these experiments, we hoped to elucidate the immunological pathways involved in disease development and perpetuation, with the hope of identifying future molecules or cellular populations that could be targeted for much-needed future AS therapeutics.

Chapter 2: Materials and Methods

2.1 Patient blood samples

Patients were recruited from the rheumatology clinic run by Dr David McCarey and Dr Anne McEntegart at the Glasgow Royal Infirmary. All patients had been clinically diagnosed with AS and had consented to donating blood or synovial fluid (SF) samples to this project. For each patient the following information was collected (Figure 2.1): Spinal disease levels (identification of sacroiliitis, peripheral arthritis and spinal disease – cervical, thoracic and lumbar), extra-articular manifestation diagnoses (presence of IBD, uveitis, arthritis and psoriasis), HLA-B27 status, inflammatory markers (ESR and CRP), disease duration, disease score (bath ankylosing spondylitis disease activity index (BASDAI) and ankylosing spondylitis disease activity score (ASDAS)) and disease treatment protocol. Categories of treatment protocol included: non-steroidal anti-inflammatory drugs (NSAIDs); disease modifying anti-rheumatic drugs (DMARDs); and biological therapy. The patient samples were predominantly collected under the ethical application titled “Institute of Infection, Immunity and Inflammation Research Tissue Bank” (REC reference: 11/S0704/7). Healthy controls (HCs) were recruited from within the Institute of Infection, Immunity and Inflammation at the University of Glasgow. Each individual gave informed consent and completed consent forms that complied with the ethical application entitled “Acquisition of healthy donor peripheral blood to provide normal values to allow interpretation of disease states in terms of immune system function” granted by the College of Medical, Veterinary & Life Sciences Ethics Committee for Non-Clinical Research Involving Human Subjects. Initially, no restrictions were set on the age of HCs, however as the project progressed only individuals ≥ 30 years of age were recruited. Restrictions on participation included: age, disease status and a bias towards male participation was encouraged to control more closely for the characteristics of the AS patient population.

2.2 Intestinal samples

Small intestinal and colonic samples were obtained from the National Health Service Greater Glasgow and Clyde (NHSGGC) Biorepository. Excess tissue samples were collected during intestinal surgery under the Biorepository NHSGGC ethics application entitled “Mononuclear phagocytes in intestinal tissues”,

Information on ankylosing spondylitis patients who have blood sent to university for testing

Date

Affix patient label here

Sacroileitis only...**MRI**....

Peripheral arthritis...No.....

Spinal disease(which levels)

.....**Not known**.....

.....

Other coexisting clinical diagnoses

IBD	<input type="checkbox"/>
Uveitis	<input type="checkbox"/>
Psoriasis	<input type="checkbox"/>

HLA B27 status(+/-/unknown)...**+ve**.

ESR...**4**..... CRP...**0.3**.....

Onset of symptoms...**2007**..... Year diagnosis made ...**2009**.....

BASDAI score...**2.76**.....

ASDAS...**0.7**.....

Spinal VAS score.....**2**.....

Treatment

NSAIDs.....**Diclofenac**.....

DMARD.....**Nil**.....

Biologic therapy.....**Nil**.....

Figure 2.1: Patient data collection sheet

Data sheet used to collect clinical data during clinic or from patient files for every AS patient participating in this study through donation of blood samples.

application number 65. Patient consent was gained for every sample processed. Samples were collected from the pathologist at the Southern General Hospital, Glasgow and stored

in sterile PBS on ice until used. Patient information for every sample was provided. Clinical parameters collected included: sex, age, ethnic group, disease type, smoking status, alcohol consumption, reason for and type of surgery, current medication, blood pressure, previous medical history including previous surgeries and any other relevant donor information.

2.3 Cell culture medium

Cells were cultured in 10% complete media (R10) consisting of: Roswell park memorial institute (RPMI) 1640 medium supplemented with 10% fetal calf serum (FCS), 2mM L-Glutamine, 100U/ml penicillin, 100µg/ml streptomycin and 50µM 2-mercaptoethanol (Invitrogen, UK).

2.4 Blood collection

Whole blood was collected in green 6ml vacutainer lithium/heparin tubes (BD Biosciences). All venepuncture procedures were carried out by qualified medical practitioners based at the Glasgow Royal Infirmary (AS patients) or at the clinical facility in the British Heart Foundation (BHF) building at the University of Glasgow (HCs). Blood was processed within 2 hours of sample collection.

2.5 PBMC isolation

To isolate peripheral blood mononuclear cells (PBMCs), 10ml of whole blood was layered on top of 4ml of histopaque – 1077 (Sigma-Aldrich, Poole, UK) and spun at 2,100rpm for 20 minutes at room temperature, with no brake being applied. For optimal separation, both blood and histopaque should be at room temperature before processing. This gradient generates 5 layers: - plasma, PBMCs, histopaque, granulocytes and red blood cells. Aliquots of plasma (1.5ml) were stored at -80°C for subsequent analysis. The PBMC layer was harvested and washed twice in FACS buffer: PBS (Gibco, Life Technologies, Paisley, UK), 2% FCS and 2mM EDTA (Sigma-Aldrich), at 1,500rpm for 5 minutes at 4°C. Cells were counted and resuspended at $2-5 \times 10^6$ cells/ml of R10 or FACS buffer.

2.6 Flow cytometry and monoclonal antibodies

2.6.1 Surface staining

Cells were spun down in 6ml FACS tubes (BD Biosciences, UK) at 1,500rpm for 5 minutes. Supernatant was removed and cells incubated with Fc block (5µl - eBioscience) for 10 minutes at 4°C. Without washing, cells were incubated with fluorescently labelled antibodies for a further 25 minutes at 4°C in the dark. Cells were washed in FACS buffer, again at 1,500rpm for 5 minutes. Supernatant was removed. If a biotinylated antibody had been used in the antibody cocktail a streptavidin step was required. Under these circumstances, 200ul of fluorescently labelled streptavidin mix was added to the appropriate tubes and incubated at 4°C in the dark for 20 minutes. In the final 5 minutes of the streptavidin step or main antibody step, 3ul of DAPI (50ng/ml - Invitrogen) or 20µl of 7AAD (Biolegend) was added to all sample tubes to stain dead cells. All antibodies were subsequently washed off in 2ml of FACS buffer by centrifuging at 1500rpm for 5 minutes at 4°C. Cells were resuspended in 200µl of FACS buffer and run on the BD LSR II (BD Biosciences) or MACS Quant analyser (Miltenyi Biotec). All data analyses were performed using FlowJo software (Tree Star Inc., USA - versions 8.8.4 or 9.2). Antibodies used for flow cytometry are listed in Table 2.1.

Table 2.1: List of monoclonal antibodies used for flow cytometry

Primary antibodies were conjugated to various fluorochromes: FITC, PE, PE-CY5, PERCP, PE-CY7, APC, APC-CY7, AF700, V450, V500, BV421 and BV605. Several antibodies used in my staining panels were biotin conjugated and therefore I used several streptavidin conjugates including PERCP, PE-CY7, V450, BV421, BV605 and Q-DOT 605. m = mouse, r = rat.

Marker	Clone	Isotype	Source	Conc.	Conjugate
CD3	UCHT-1	mIgG1k	Biolegend	1:40	FITC
CD4	OKT4	mIgG2b	Biolegend	1:200	Biotin
CD8	HIT8a	mIgG1k	Biolegend	1:200	Biotin
CD1c	AD5-8E7	mIgG2a	Miltenyi Biotec	1:10	APC
CD11b	ICRF44	mIgG1k	Biolegend	1:20	APC
CD11c	B-Ly6	mIgG1k	BD Biosciences	1:20	PE-CY5/V450
CD14	M5E2	mIgG2a	Biolegend	1:40	FITC/AF700
CD15	W6D3	mIgG1k	Biolegend	1:40	FITC
CD16	3G8	mIgG1k	Biolegend	1:40	PE-CY7

CD19	H1B19	mlgG1k	Biolegend	1:40	FITC
CD25	BC96	mlgG1k	Biolegend	1:40	PE
CD33	WM53	mlgG1k	Biolegend	1:40	APC
CD40	5C3	mlgG1k	Biolegend	1:10	APC
CD45	HI30	mlgG1k	Biolegend	1:40	BV510
CD45RA	HI100	mlgG2b	Biolegend	1:20	APC-CY7
CD56	MEM-188	mlgG2a	Biolegend	1:40	FITC
CD64	10.1	mlgG1k	Biolegend	1:40	APC
CD69	FN50	mlgG1k	Biolegend	1:40	PE
CD80	2D10	mlgG1k	Biolegend	1:40	APC
CD86	IT2.2	mlgG2b	Biolegend	1:10	APC
CD103	B-ly7	mlgG1k	eBioscience	1:40	PE-CY7
CD115	12-3A3-1B10	rlgG2a	eBioscience	1:200	Biotin
CD123	6H6	mlgG1k	Biolegend	1:20	PE-CY5
CD135	BV10A4H2	mlgG1k	Biolegend	1:10	APC
CD141	1A4	mlgG1k	BD Biosciences	1:20	PE
CD163	GH1/61	mlgG1k	Biolegend	1:200	Biotin
CD172a	SE5A5	mlgG1k	Biolegend	1:200	Biotin
CD206	15-2	mlgG1k	Biolegend	1:10	PE
CD209	eB-h209	rlgG2ak	eBioscience	1:40	PE-CY7
CD303	AC144	mlgG1	Miltenyi Biotech	1:40	PE
CD304	AD5-17F6	mlgG1	Miltenyi Biotech	1:40	PE
CCR2	48607	mlgG2b	R + D Systems	1:20	PE
CCR4	1G1	mlgG1k	BD Biosciences	1:40	APC
CCR6	11A9	mlgG1k	BD Biosciences	1:20	APC
CCR9	248621	mlgG2a	R + D Systems	1:5	APC
CCR10	314305	rlgG2a	R + D Systems	1:10	APC
CXCR3	G025H7	mlgG1k	Biolegend	1:40	APC
CX3CR1	2A9	rlgG2b	MBL	1:10	PE
Annexin V			BD Biosciences	1:50	PE
FOXP3	PCH101	rlgG2a	eBioscience	1:10	FITC
HLA-B27	HLA-ABC-m3	mlgG2a	AbD Serotec	1:100	FITC

HLA-B7	BB7.1	mIgG1	AbD Serotec	1:100	FITC
IFNγ	4S.B3	mIgG1k	Biolegend	1:40	FITC
IL-17A	BL168	mIgG1k	Biolegend	1:40	PE
IL-23R	218213	mIgG2b	R + D Systems	1:20	APC
Ki67	B56	mIgG1	BD Biosciences	1:200	APC
MHC II	L243	mIgG2a	Biolegend	1:40	APC-CY7
RORγt	AFKJS-9	rlgG2b	eBioscience	1:200	PE
SLAN	DD-1	mIgM	Miltenyi Biotec	1:20	Biotin
TcR$\alpha\beta$	IP26	mIgG1k	Biolegend	1:40	PE-CY7

2.6.2 FACS cell sorting

PBMCs were processed as described above. Cells were counted, resuspended at 2×10^6 cells/ml in 10% complete media and left at 4°C overnight. Cell sorting was performed the day following PBMC isolation. Cells were re-counted before continuing with the FACS staining protocol. Cells were separated into sterile FACS tubes, washed in FACS buffer and incubated with Fc block for 10 minutes at 4°C. Without washing, cells were subsequently incubated with 400 μ l of the appropriate antibody mix for a further 25 minutes at 4°C, in the dark. The cells were washed in FACS buffer, again at 1,500rpm for 5 minutes. If a biotinylated antibody had been used in the main antibody cocktail, then a streptavidin step was required. If this was the case, 400 μ l of the streptavidin mix was added to the appropriate tubes and incubated at 4°C in the dark for 20 minutes. On occasion, DAPI (50ng/ml) was added to sample tubes to stain dead cells for 5 minutes. All antibodies were then washed off in 2ml of FACS buffer by centrifuging at 1,500rpm for 5 minutes at 4°C. Cells were then resuspended in FACS buffer at 2×10^6 /ml and run on the FACS Aria. Sorted cell subsets were collected in sterile 6ml FACS tubes containing 2ml of 10% complete media. After sorting, a purity check was performed for every subset, except CD141⁺ DCs where too few cells were available.

2.6.3 Intracellular cytokine staining

Cells were resuspended in sterile FACS tubes at 2-3 $\times 10^6$ cells/ml of 10% complete media. To measure steady state cytokine production, cells were incubated with Brefeldin A (10 μ g/ml, Sigma-Aldrich) and monensin (1 μ M, Biolegend, UK) or Brefeldin A, monensin, phorbol 12-myristate 13-acetate (PMA, 1 μ M, Sigma-Aldrich) and ionomycin (1 μ M,

Sigma-Aldrich) for stimulated samples. All samples were incubated at 37°C for 4.5 hours in the dark. After incubation, cells were washed in FACS buffer. Surface staining was performed as described in the FACS staining description (section 2.6.1). After washing off all antibodies in FACS buffer, cells were resuspended in 1ml of fix/perm buffer (eBioscience intracellular staining kit). Cells were then incubated at room temperature for 30 minutes before being washed twice in 2ml of 1x PERM buffer at 1,500rpm, 4°C for 5 minutes. Supernatant was removed and 10µl of Fc block was added to every tube and incubated in the dark at 4°C for 5 minutes. Without washing, and in 1x PERM buffer, antibodies were added directly to the appropriate tubes and incubated at 4°C, in the dark for a further 45 minutes. Following incubation, cells were washed twice in 2ml of 1x PERM buffer at 1,500rpm, 4°C for 5 minutes. Cells were then run on the LSR II instrument.

2.7 Naïve T cell isolation

PBMCs from whole blood are isolated as described above. Naïve CD4⁺ T cells were isolated from the PBMC fraction using a Naïve CD4⁺ T Cell isolation kit II (Miltenyi Biotec). Cells were washed in FACS buffer at 1,500rpm for 5 minutes at 4°C. Cells were then resuspended in 40µl/10⁷ cells of MACS buffer (PBS, 0.5% FCS and 2mM EDTA) and 10µl/10⁷ cells of naïve CD4⁺ T cell biotin antibody cocktail II (containing antibodies against CD8, CD14, CD15, CD16, CD19, CD25, CD34, CD36, CD45RO, CD56, CD123, CD235a, HLA-DR and TcRγ/δ). Cells were then mixed and incubated for 10 minutes at 4°C, following which they were washed using 2ml/10⁷ cells of MACS buffer at 1,500rpm for 5 minutes. Supernatant was then completely removed. Cells were subsequently resuspended in 80µl/10⁷ cells of MACS buffer and 20µl/10⁷ cells of anti-biotin microbeads. Cells were incubated for 15 minutes at 4°C and then washed in 2ml/10⁷ cells of MACS buffer as previously described. Cells were resuspended in 500µl of MACS buffer and placed on ice until ready for separation. To separate the naïve T cells, magnetic separation with LS columns (Miltenyi Biotec) was performed. LS columns were washed with 3ml of MACS buffer, to which the sample was then applied. The column was then washed 3 times with 3ml of MACS buffer. The flow through from the sample and the subsequent washes were collected together and this contained isolated naïve CD4⁺ T cells. Cells were counted and resuspended at 20,000 cells/ml of R10.

2.8 Carboxyfluorescein succinimidyl ester (CFSE) staining

Cells to be stained with carboxyfluorescein succinimidyl ester (CFSE; Invitrogen) were first washed in PBS to remove all culture supernatant. Subsequently, $\leq 10^7$ cells were resuspended in 1ml of PBS. For cell counts $> 10^7$, volumes were scaled up appropriately. To this, 1 μ l/ml of a 5mM stock of CFSE was added (final concentration - 5 μ M). Cells were incubated at room temperature, in the dark, for 3 minutes whilst shaking. After staining, cells were washed immediately in 10% complete media at 1,500rpm for 5 minutes at 4°C. Cells were then recounted and resuspended in R10.

2.9 Allogeneic mixed leukocyte reaction (MLR)

Individual cell subsets from HCs and AS patients: CD1c⁺ and CD141⁺ DCs, CD16⁺ mononuclear cells and CD14⁺ monocytes, were isolated using the FACS Aria. The DCs were then resuspended at the following concentrations: CD141⁺ - 1500, CD1c⁺ - 12000, CD16⁺ - 24000 and CD14⁺ monocytes - 24000 (number of cells/100 μ l). Doubling dilutions of each DC/monocyte subset except CD141⁺ DCs were performed in a round bottomed 96 well tissue culture plate (Corning, USA) using 10% complete media. Isolated naïve CFSE⁺ T cells, from another HC, were resuspended at 20,000 T cells/100 μ l in 10% complete media. To every co-culture well, 100 μ l of CFSE⁺ naïve T cells were added. As controls, T cells and DCs were also plated out separately, with T cells alone being stimulated with 10 μ g concanavalin A (Sigma-Aldrich). MLRs were incubated at 37°C and 5% CO₂ for 5 days, in the dark. After 5 days, the 96 well plate was spun down at 1,500rpm for 5 minutes. To analyse cytokine production from these co-cultures, 100 μ l of supernatant was transferred to a fresh 96 rounded well plate, sealed and stored at -20°C. The remaining cells were washed twice in FACS buffer at 1,500rpm, 4°C for 5 minutes. Fc block was added to every well with cells left to incubate at 4°C for 10 minutes. Without washing, cells were incubated with 50 μ l of the cocktail composed of antibodies specific for CD4, CD25 and either CCR6 or CXCR3. Cells were incubated with the antibodies for 30 minutes at 4°C in the dark. Antibodies were washed off using FACS buffer and 50 μ l of streptavidin cocktail was added to all appropriate wells for 20 minutes at 4°C in the dark. Again, DAPI was added in the final 5 minutes of the streptavidin step to identify dead cells. After staining, all antibodies were washed off. Cells were subsequently transferred to 6ml FACS tubes and analysed on the BD LSR II.

2.10 Cytospins and H&E staining

Cells to be analysed by cytopins were individually sorted using the FACS aria. Approximately 30,000 cells were resuspended in 200µl of PBS. Slides were labelled and cells were applied to the slide using the funnel/filter card/harness apparatus. Cells were spun at 450rpm for 6 minutes. Cells were then left to air dry at room temperature. For hematoxylin and eosin (H&E) staining, the Rapid Romanowsky (RA Lamb) staining kit was used. Polysine slides (VWR International) are immersed in fixative, followed by hematoxylin and eosin staining for 30 seconds. The slides were washed in distilled water and left to dry at room temperature. Once completely dry, a drop of DPX mountant (VWR International) was applied, allowing attachment of a cover slip that is further fixed in place using nail polish. Cells and pictures were taken using a light microscope and cell[^]B software (Olympus, UK).

2.11 Annexin V staining

To identify cells undergoing early apoptosis, Annexin V staining was performed. Cells were counted and transferred to 6ml FACS tubes. After washing the cells in FACS buffer, the protocol for extracellular FACS staining was carried out as described above (section 2.6.1). Following extracellular staining, cells were washed twice in cold PBS followed by a wash using 1x annexin binding buffer (diluted in PBS, BD) at 1,500rpm, 4°C for 5 minutes. Supernatant was removed and the PE-conjugated annexin V antibody (BD) was added directly to the cells (used at 1:50) and incubated at room temperature in the dark for 15 minutes. 200µl of 1x annexin V binding buffer was added to every tube while samples remained on ice. Samples were run on the LSR II within an hour of staining.

2.12 Synovial fluid processing

Synovial fluid (SF) samples were transferred into 50ml centrifuge tubes and spun at room temperature for 10 minutes at 2,100rpm. Supernatants were aliquoted and stored at -80°C for analysis. If a cell pellet was present, cells were resuspended in a 50:50 mix of 10% complete media and PBS. Intense pipetting was occasionally required to disintegrate the pellet. A histopaque gradient was used to isolate SF mononuclear cells (SFMCs): - 10ml of the cell suspension was layered carefully onto 4ml of histopaque 1077. All reagents were at room temperature. Tubes were centrifuged at 2,100rpm, room temperature for 20

minutes. The SFMC layer was then isolated and processed as described in the PBMC isolation protocol (section 2.5).

2.13 Isolation of RNA

After cell suspensions had been generated, cells were washed in PBS to remove culture supernatant and spun at 13,000rpm for 10 minutes. Supernatant was completely aspirated and cells were resuspended in buffer RLT (Qiagen). The volume of RLT added was dependent upon cell number and RNA extraction kit to be used: for samples containing $\leq 100,000$ cells, cells were resuspended in 75 μ l of buffer RLT and stored at -20°C. RNA was extracted using the RNeasy micro kit (Qiagen) for these samples. However for samples containing $\geq 100,000$ cells, 350 μ l of buffer RLT was used to lyse the cell pellet and with the RNeasy mini kit used to extract RNA. All samples were stored at -20°C until RNA was to be extracted. The kit-specific protocols were followed but are described briefly as follows: cell suspension was lysed using QIAshredder spin columns (Qiagen) and spun at 13,000rpm for 2 minutes using a bench top centrifuge. To this, 1 volume of 70% ethanol was added, mixed thoroughly, transferred to an RNeasy (mini kit) or RNeasy MiniElute spin column (micro kit) and spun for 15 seconds at 10,000rpm. After which, flow-through was discarded. Columns were washed with 350 μ l of buffer RW1 at 10,000rpm for 15 seconds. On column DNase digestion was then carried out by adding 10 μ l DNase I stock and 70 μ l buffer RDD (previously mixed) directly to the spin column membrane for 15 minutes at room temperature. If using the RNeasy mini kit, the column was washed three times, first with 350 μ l of buffer RW1 for 15 seconds at 10,000rpm followed by two washes (15 seconds/2 minutes) with 500 μ l of buffer RPE. For the RNeasy micro kit, the third wash is replaced with addition of 500 μ l of 80% ethanol to the spin column followed by centrifugation for 2 minutes at 10,000rpm. Following this, the MiniElute spin column was centrifuged at 13,000rpm for 2 minutes with the lid open to dry the membrane. For both kits, the final step involved the spin columns being placed in a fresh collection tube and RNase free water being added to the spin column - 14 μ l (RNeasy micro) or 30 μ l (RNeasy mini), incubated at room temperature for 5 minutes and spun for 1 minute at 10,000rpm. RNA was then stored at -20°C in 1.5ml collection tubes until cDNA was to be generated. The concentration of RNA (ng/ μ l) was measured using a nanodrop (Amersham Biosciences) immediately before cDNA generation.

2.14 Generation of cDNA

To generate cDNA, the SuperScript First-Strand Synthesis System for RT-PCR kit (Invitrogen, UK) was utilised, using approximately 18ng of RNA. The manufacturers protocol for cDNA synthesis using Oligo (dT) was followed. Briefly, cDNA generation was carried out in 0.2ml eppendorfs or in a 96 well PCR plate. Each sample requires a minus reverse transcriptase (RT) control and a fully transcribed sample. The first step requires the generation of a master mix. For every sample (sample or minus RT control) the following are required: 1µl of 10nM dNTP mix, 1µl of 0.5µg/µl oligo(dT)₁₂₋₁₈ primer, the volume of RNA required to generate 18ng cDNA (≤5µl) and DEPC-treated water to give a final volume of 10µl. Using a TProfessional thermocycler (Biometra), samples were incubated at 65°C for 5 minutes followed by a 1 minute incubation at 4°C. The second master mix was generated during this incubation, containing the following for every sample: 2µl of 10x RT buffer, 4µl 25mM MgCl₂, 2µl of 0.1M DTT, 1µl of RNaseOUT (40U/ml) and either 1µl SuperScript II RT (sample) or 1µl DEPC-treated water (minus RT control). Following addition of the second master mix, samples were subjected to the following incubations: 42°C for 52 minutes followed by 70°C for 15 minutes with samples subsequently held at 4°C. At this point, 1µl of RNase H is added to every tube and incubated at 37°C for 20 minutes. The samples are then stored at -20°C.

2.15 Quantitative real time PcR

Gene expression was determined by quantitative reverse transcription polymerase chain reaction (qRT-PcR) using Brilliant III Ultra Fast SYBR qRT-PcR Master Mix (Agilent). Reactions were performed in MicroAmp Fast Optical 96-well reaction plates (Applied Biosystems). Reagents for each reaction include: 10µl SYBR green, 0.4µl primer mix, 0.3µl reference dye (diluted 1:500 with DEPC-treated water, 30nM final concentration), 8.3µl DEPC-treated water and 1µl of cDNA (diluted 1:5 with DEPC-treated water). Plates were covered with an optical adhesive cover (Applied Biosystems) and centrifuged at 400G for 1 minute. Plates were analysed using a 7500 Fast Real-Time PCR System machine (Applied Biosystems). PCR protocol: 95°C incubation for 10 minutes followed by 40 cycles composed of 15 seconds at 95°C followed by a 60°C incubation for 1 minute. Melt curves were performed for each experiment to determine primer suitability and assess PcR performance. Samples were assayed in triplicate with expression levels normalised to TATA binding protein (TBP). Results analysed and presented using the $2^{-\Delta C(t)}$ method.

Table 2.2: Primers used for qRT-PCR

Gene	Forward	Reverse	Ref
ATF4	GACCACGTTGGATGACACTTG	GGGAAGAGGTTGTAAGAAGGTG	(521)
ATF6	TCAGACAGTACCAACGCTTATGC	GTTGTACCACAGTAGGCTGAGA	(521)
A20	AAGAAACTCAACTGGTGTGCGAGAA	TGCCGTCACCGTTCGTT	(563)
BiP	TGCTTGATGTATGTCCCCTTA	CCTTGTCTTCAGCTGTCACT	N/A
EIF2α	GCTCTTGACAGTCCGAGGAT	CATTGCCCCAGGCAAACAAG	(521)
PERK	TGCCTGGCTCGAAGCACCCAC	TGGTGCATCCATTGGGCTAGGA	(521)
TBP	AGACCTTCCTGTTTACCCTTG	TAGCTGTGGGTGACTGCTTGG	N/A
sXBP-1	AGACAGCGCTTGGGGATGGAT	CCTGCACCTGCTGCGGACTC	(521)
uXBP-1	AGACAGCGCTTGGGGATGGAT	CCTGCTGCAGAGGTGCACGTAG	(521)
zDC	GAGCTTTGGGACACAGGACAC	TGTGCAAAGTTGCAAGCAGTA	N/A

2.16 Luminex

To measure cytokine levels in plasma and culture supernatants, a custom-made Luminex from R & D systems was used. The following cytokines were assayed: IL-1 β , IL-4, IL-5, IL-6, IL-10, IL-17, GM-CSF, IFN γ and TNF α . The luminex kit protocol was followed. Briefly, plasma samples were diluted 1:4 with the specific calibrator diluent with culture supernatants analysed neat. The luminex plate was washed with the appropriate buffer and liquid was removed using a vacuum. All cytokine microparticles were mixed with 50 μ l being added to every well. To the microparticles, 50 μ l of standard or sample was added to the appropriate wells and allowed to incubate on a shaker for 3 hours at room temperature. The plate was then washed 3 times using wash buffer. Liquid was again removed under vacuum. To every well 50 μ l of biotin antibody cocktail was added and left to incubate at room temperature on a shaker for 1 hour. The wash step was repeated, after which 50 μ l of streptavidin PE was added to every well and again incubated at room temperature for 30 minutes. The plate was washed 3 times and following liquid removal, 100 μ l of wash buffer was added to every well and the plate was left on the shaker for 5 minutes to disperse microparticles before being run using the Bio Plex 200 system luminex plate reader (Bio-Rad, CA, USA). Cytokine levels were extrapolated from the standard curve.

2.17 Elisa

Several cytokines measured were not available in the Luminex format. Therefore I performed several enzyme-linked immuno sorbent assays (ELISA) to test for cytokines including Flt3L, IL-23 and IL-12p70 (R&D systems). The protocol involved adding

appropriate volumes of assay diluent and standard or sample to a pre-coated ELISA plate according to the plate plan. Samples were incubated for 2 hours at room temperature. Plates were washed with the appropriate wash buffer, with the conjugate (200µl) subsequently added to every well and incubated for 2 hours at room temperature. Plates were washed again, and incubated for 30 minutes with the appropriate substrate solution. Stop solution (50µl) was added to every well and developed for 20 minutes. The plate was then read at 450nm using an MRX microplate reader (Dyn-ex technologies, USA).

2.18 Cell survival assay

DC subsets were sorted using the FACS Aria. The cells were washed in PBS and resuspended at 1×10^6 cells/ml of PBS. Cells from a HC and an AS patient sample were stained with either CFSE (5µM) as previously described, or the eFlour V450 proliferation dye (eBioscience). If eFlour V450 proliferation dye was used, cells were stained with 10µM (final concentration) for 10 minutes in the dark with intermittent shaking. After staining, cells were washed in FACS buffer and re-counted. Cells were resuspended at the following cell concentrations per 100µl of 10% complete medium: CD1c – 30,000 or 40,000 cells, CD16 – 40,000 or 50,000 cells, monocytes – 100,000 cells. Cells isolated from a HC and an AS patient were mixed together 1:1 in 96 well round bottomed culture plates. An aliquot from each well was analysed on the BD LSR II for analysis at the 0 hour time point. Cells were incubated at 5% CO₂ and 37°C for 24 hours or 48 hours. After, co-culture cells were harvested and analysed using the BD LSR II.

2.19 Human colonic and small intestine cell isolation

To isolate cells from patient surgical samples, a protocol was adapted from one developed for the isolation of cells from murine intestinal samples by the laboratory of Professor Allan Mowat. For surgical specimens, the fat and muscle layers were removed before processing. The muscle layer, for some experiments was digested in the same manner as colonic and small intestinal tissue. Samples were first transferred to 50ml falcons (Greiner Bio-one) containing HBSS (Gibco) supplemented with 2% FCS. Tissue was cut into 0.5cm sections and kept in 2% FCS/HBSS on ice until digestion. Tissue was vigorously shaken; the supernatant discarded, and resuspended in 20ml of 2mM EDTA/HBSS (pre-warmed) to remove the epithelial layer. For colonic specimens, the tissue was placed in a shaking incubator at 37°C for 15 minutes before being shaken vigorously again and supernatant

discarded. Tissue was then washed in HBSS (pre-warmed). This step was repeated a total of three times. For small intestinal samples, tissue in 20ml of 2mM EDTA/HBSS was placed at 37°C in a shaking incubator for 30 minutes before being shaken vigorously, supernatant discarded and washed in HBSS (pre-warmed). This was followed by a second incubation, similar to that described above but of only 15 minutes duration. After the final EDTA step, cells were washed in HBSS and resuspended in 20ml of pre-warmed 10% complete media containing the following enzymes: Collagenase VIII (1mg/ml, Sigma-Aldrich), Collagenase D (1.25mg/ml, Roche Diagnostics GmbH, Mannheim, Germany), Dispase (1mg/ml, Gibco) and DNase (30µg/ml, Roche). Tubes were then placed in a shaking incubator (37°C) for 45 minutes; additional vigorous shaking was performed every 10 minutes to aid digestion. The supernatant was then passed through a 100µM cell strainer (BD Falcon). Any remaining undigested tissue was returned to the tube, 20ml of fresh enzyme mix was added and returned to the shaking incubator (37°C) until tissue was completely digested. Again tubes were shaken vigorously every 10 minutes. Supernatant removed after 45 minutes was filtered through a 40µM cell strainer (BD Falcon) and centrifuged at 1,500rpm for 5 minutes. Supernatant was discarded and cells were resuspended in FACS buffer and kept on ice. After the remaining tissue was fully digested, supernatant was filtered as previously described, centrifuged and resuspended in FACS buffer. After cell suspensions were combined, cells were counted and left on ice until use.

2.20 Histology

A number of human small intestinal and colonic samples were fixed in 10% neutral buffered formalin for 24 hours. Jim Reilly and Shauna Kerr, histology technicians within the Institute of Infection, Immunity and Inflammation at the University of Glasgow, processed the samples and performed H&E staining. Sections were then viewed using a light microscope and pictures were taken using the cell^B software (Olympus).

2.21 Statistics

Results are presented with +/- standard error of the mean (SEM) or standard deviation (SD). Data were analysed using either a Student's t test or a Mann Whitney, followed by a Bonferroni post test using GraphPad prism (San Diego, CA, USA). Statistical tests were performed as described in figure legends. For patient correlative data, linear regression,

Kruskal Wallis Spearman correlative tests were performed with Dunn multiple comparisons post test. Values of $p < 0.05$ were considered statistically significant.

Chapter 3: Characterisation of blood mononuclear cell populations

3.1 Introduction

Human dendritic cells (DCs) are often identified based on the expression of MHC II, lack of common lineage markers and their ability to stimulate naïve T cells (200, 201, 208). Recent advances in surface phenotyping and cell isolation have enabled the characterisation of several human DC subsets circulating in peripheral blood (207-209). However, application of these experimental developments is severely lacking in some areas of human research. One such area involves the analysis and quantification of human DC subsets in patients with ankylosing spondylitis (AS). Due to the involvement of DCs in directing and controlling immune responses, and given that our previous work indicated a role for DCs in SpA development using the HLA-B27 transgenic (HLA-B27 TG) rat model (480), it was important to fully characterise the role of DCs in human AS, with a view to improving future disease therapies. Therefore, the aim of the project was to contribute to the understanding of AS pathogenesis by investigating differences in the frequency and phenotype of human DC subsets, conventional (cDC) and plasmacytoid (pDC), between patients with AS and healthy controls (HCs). In addition, other related inflammatory cells, including monocytes were investigated for the purposes of comparison.

3.2 Patient characteristics

AS patients were recruited from the clinics at the Glasgow Royal Infirmary run by Dr David McCarey and Dr Anne McEntegart. Patient information regarding disease severity, treatment and duration was collected and is summarised in Table 3.1, together with information about HCs used in the study.

Due to the nature of the disease, the majority (75.5%) of AS patients used in this study were older, male participants. In order to control for this, the majority (58.6%) of recruited HCs were also male (Table 3.1). Furthermore, all patients at time of analysis presented with long-standing disease, with minimum disease duration being 7 years (Table 3.1). Unfortunately, samples from newly diagnosed patients (<2 years) were not received during this study.

Table 3.1: Clinical characteristics of patients and healthy controls

For the analysis of cDC and pDC blood populations, 45 AS patients and 29 HCs were used. Patient characteristics were collated and are summarised below. Information for some clinical parameters were not available for all patients. Percentages represent proportion of all patients used in the study. Spinal disease was assessed based on the presence or absence of cervical, thoracic and lumbar involvement. Levels were categorised based on the number of sites involved: 1 site = level 1, 2 sites = level 2 and 3 sites = level 3. Combination therapy consists of DMARD and NSAID treatment. N/A = Not applicable. Mean \pm SD is shown.

	AS Patients	Healthy Controls
Age (yrs)	54.87 \pm 12.2	40.66 \pm 12.5
Sex – Male/Female	34/9	17/12
Disease Duration (yrs)	28.8 \pm 12.5	N/A
B27 – Pos/Neg (% B27⁺)	41/4 (91%)	6/23 (21%)
BASDAI	4.09 \pm 2.27	N/A
BASMI	4.18 \pm 2.48	N/A
ESR (mm/hr)	14.62 \pm 13.19	N/A
CRP (mg/L)	6.89 \pm 9.17	N/A
Bilateral Sacroiliitis – No. (%)	30 (66.7%)	N/A
Spinal disease		
Absent – No. (%)	4 (8.9%)	N/A
Level 1 – No. (%)	9 (20%)	N/A
Level 2 – No. (%)	6 (13.3%)	N/A
Level 3 – No. (%)	5 (11.1%)	N/A
Extra-articular Disease		
IBD – No. (%)	3 (6.7%)	N/A
Uveitis – No. (%)	4 (8.9%)	N/A
Psoriasis – No. (%)	3 (6.7%)	N/A
Arthritis – No. (%)	8 (17.8%)	N/A
Medication		
DMARDs – No. (%)	1 (2.2%)	N/A
NSAIDs – No. (%)	18 (40%)	N/A
Combination – No. (%)	2 (4.4%)	N/A
Biologics – No. (%)	7 (15.6%)	N/A

On average, patients presented with mid-range disease scores, (BASDAI 4.09, BASMI 4.18) measured on scales of 0-10 and 0-10 respectively (Table 3.1). Alongside disease score, two factors relating to inflammation were examined – erythrocyte sedimentation rate (ESR) and C-reactive protein (CRP). When describing a HC population, ESR and CRP levels were considered normal if below 10 (Dr David McCarey, personal communication). AS patients used in this study had average ESR and CRP values of 14.62 and 6.89 respectively (Table 3.1). Therefore, the AS patients in our cohort showed evidence of ongoing inflammation but not to the extent observed in other inflammatory diseases including rheumatoid arthritis (RA) (564). Involvement of the axial skeleton and SIJs are characteristic of AS, and can lead to joint deformity. Based on magnetic resonance imaging (MRI) and X-rays, patients are assessed for the presence of vertebral fusion or structural changes within the cervical, thoracic and lumbar regions of the spine, in addition to the presence of unilateral or bilateral sacroiliitis. Approximately 70% of patients presented with evidence of bilateral sacroiliitis (Table 3.1). For the remaining 15 patients, data regarding presence of sacroiliitis was not recorded or available, although two patients that were assessed displayed a total lack of SIJ involvement. Within this patient cohort, spinal disease affecting one area of the spine (Level 1 – Table 3.1), predominantly within the cervical and lumbar regions, was most prevalent.

AS is commonly associated with the presence of extra-articular disease manifestations including IBD, uveitis, psoriasis and arthritis. The most common comorbidity in the study cohort was the presence of peripheral arthritis (approximately 20% - Table 3.1). The 18 incidences of extra-articular disease manifestations are attributable to 15 individuals. The patients with two comorbidities all presented with peripheral arthritis in addition to IBD, uveitis or psoriasis. The final aspect to be considered when analysing data obtained from patient cohorts relates to the contribution of disease treatments. Common therapies in this cohort included disease-modifying anti-rheumatic drugs (DMARDs), non-steroidal anti-inflammatory drugs (NSAIDs) and biological therapies (Biologics - Table 3.1). The most common therapy (40%) was through administration of NSAIDs, including ibuprofen, co-codamol, diclofenac and etoricoxib. 15% of patients were receiving biological therapy, predominantly in the form of etanercept and adalimumab. Only two patients were receiving combination therapy involving both DMARDs and NSAIDs. All experiments involving DC characterisation in the blood of AS patients and HCs involve either all or subgroups of the individuals described in Table 3.1. Relationships between experimental findings and disease parameters will be described and discussed in Chapter 7.

3.3 Identification of peripheral blood DC subsets

DCs represent around 0.5-1% of peripheral blood mononuclear cells (PBMCs). To identify cDC subsets, a suitable gating strategy was devised (Fig. 3.1). A staining panel described by Jongbloed et al (200) was used at the outset, and altered for specific experiments when required (Fig. 3.1A). Firstly, doublets and dead leukocytes were excluded from analysis. Due to the paucity of DCs in blood, it is advantageous to exclude large cell populations not required for analysis, in addition to those cells expressing similar surface markers to DCs. Lineage markers included CD3 (T cells), CD14 (monocytes), CD15 (neutrophils), CD19 (B cells) and CD56 (NK cells). Cells lacking expression of all lineage markers were analysed for expression of the DC markers, CD11c and MHC II. Cells co-expressing CD11c and MHC II can be subdivided into three distinct subsets based on the expression of CD141 (BDCA-3) and CD16 (Fig. 3.1A): CD141⁺ CD16⁻ (CD141⁺ DCs), CD141⁻ CD16⁻ and CD141⁻ CD16⁺ populations. The CD141⁻ CD16⁻ DCs are the only subset to express CD1c and are henceforth referred to as CD1c⁺ DCs (Fig. 3.1A). To further characterise and identify these cell populations, CD14 expression was assessed. CD14 is a marker of human monocytes, which can also co-express CD11c and MHC II. Both DC subsets (CD1c⁺ and CD141⁺) and the CD14⁻ CD16⁺ mononuclear population lacked or expressed negligible levels of CD14, in comparison to the CD14⁺ CD16⁻ classical monocytes (Fig. 3.1B). Using this gating strategy it is possible to clearly identify and isolate two DC subsets (CD141⁺ and CD1c⁺ DCs) and one mononuclear cell population (CD16⁺ CD14⁻).

To complement the investigation of cDC subsets in AS patients, pDCs were also studied. To identify pDCs, doublets, dead cells and lineage positive cells were excluded, and pDCs were identified through co-expression of CD123, CD303 (BDCA-2) and CD304 (BDCA-4 - Fig. 3.2A). Cells lacking expression of all lineage markers (LIN⁻), whilst co-expressing CD123⁺ and MHC II⁺ were further analysed for the expression of CD304 (Fig. 3.2A). All CD123⁺ MHC II⁺ CD304⁺ cells were classified as pDCs. Activation can affect cell morphology (545), so the size and granularity profiles of pDCs in AS patients and HCs were compared (Fig. 3.2B). No difference in morphology was observed. In addition, CD123⁺ MHC II⁺ cells from both HCs and AS patients expressed comparable levels of the pDC marker CD303 (Fig. 3.2C), whereas CD123⁻ MHC II⁺ cells did not express it, further identifying CD123⁺ cells as pDCs.

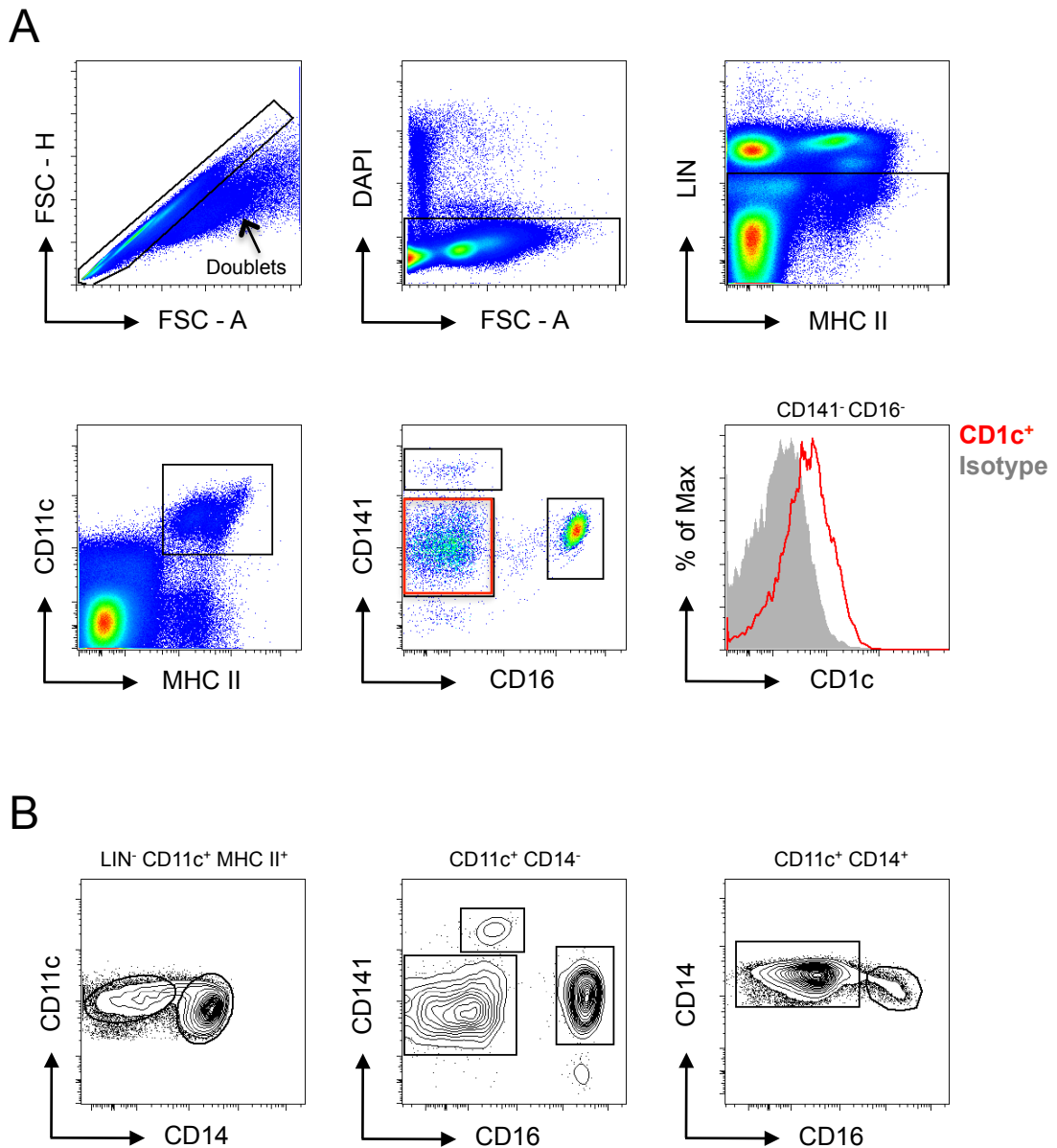


Figure 3.1: Gating strategy for the identification of blood monocytes and DCs

Dendritic cells (DCs) were identified in the peripheral blood of HCs and AS patients through the expression of several cell surface markers. **(A)** Doublets were excluded using the FCS-H vs FSC-A gate. DAPI⁺ dead cells were excluded and live cells were subdivided on the expression of LIN markers (CD3, CD14, CD15, CD19 and CD56) and MHC II. DCs are LIN⁻ CD11c⁺ MHC II⁺. This population was subdivided into CD14⁻ CD16⁺ mononuclear cells and CD141⁺ (BDCA-3) and CD1c⁺ (BDCA-1) DCs. The CD141⁻ CD16⁻ DC population expresses CD1c – histogram (right). **(B)** LIN⁻ CD11c⁺ MHC II⁺ cells were subdivided on CD14 expression. The CD14 negative fraction contains CD141⁺ and CD1c⁺ DCs in addition to the CD14⁻ CD16⁺ mononuclear population based on CD141 and CD16 expression. CD14⁺ monocytes resided in the CD14⁺ fraction.

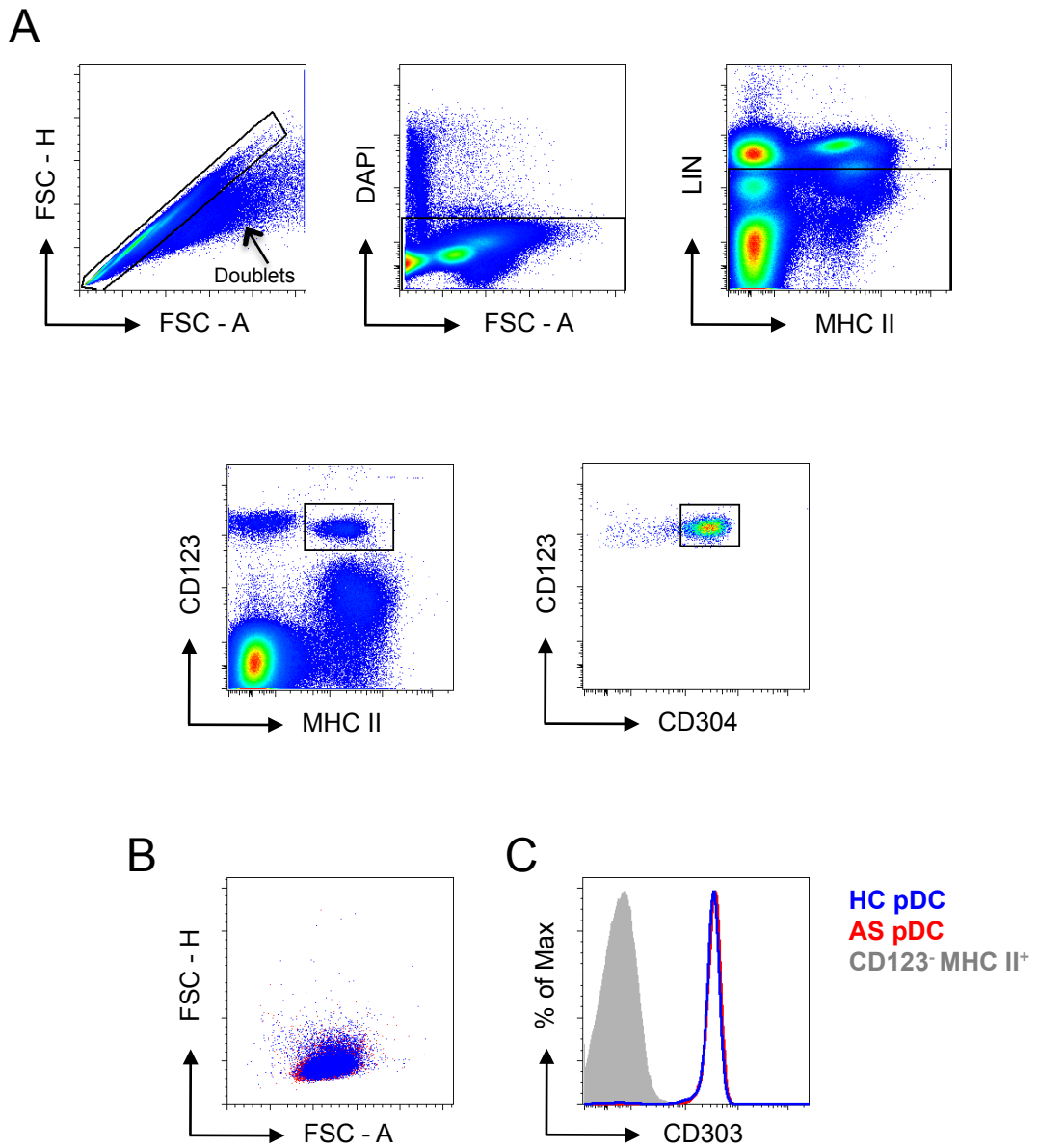


Figure 3.2: pDCs in peripheral blood

Gating strategy used to identify plasmacytoid dendritic cells (pDCs) in peripheral blood of HCs and AS patients. **(A)** Doublets were excluded using the FCS-H vs FSC-A gate. DAPI⁺ dead cells were excluded. Live cells were subdivided on the expression of LIN markers (CD3, CD14, CD15, CD19 and CD56) and MHC II. Human pDCs co-express MHC II, CD123 and CD304 (BDCA-4). **(B)** pDCs in HCs and AS patients have identical FSC-A and SSC-A profiles. **(C)** Human pDCs in HCs (blue) and AS patients (red) uniformly express CD303 (BDCA-2). CD303 expression was compared to CD123⁻ MHC II⁺ cells (grey shaded histogram), including CD11c⁺ MHC II⁺ cDCs.

3.4 Quantification of DC and monocyte subsets in AS patients and HCs

3.4.1 cDCs and pDCs

My aim was to investigate the role of cDCs and pDCs in AS pathogenesis. The gating strategies developed for cDCs (Fig. 3.1A) and pDCs (Fig. 3.2A) were therefore used to quantify these populations in AS patient and HC blood. Initially, total numbers of PBMCs per ml of blood were compared between HCs and AS patients, and a significant increase in the number of PBMCs in AS patients was observed (Fig. 3.3A). Due to the strong genetic association between HLA-B27 and AS, HLA-B27 involvement was assessed in relation to PBMC number. No effect of HLA-B27 expression on PBMC numbers in AS patients or HCs was observed (Fig. 3.3A). The proportions of total cDCs (CD1c⁺ and CD141⁺ subsets) in the blood of AS patients and HCs were also compared (Fig. 3.3B and 3.3C). The CD16⁺ mononuclear population was excluded from the total cDC analysis, as the classification of these cells remains controversial. A slight trend towards fewer DCs as a percentage of live cells in AS patients was observed, however, this was found not to be statistically significant ($p=0.0545$ – Fig. 3.3C). No difference was observed in the proportion of cDCs when analysed as total cell number/ml of blood. Furthermore, HLA-B27 expression appeared to have no effect on the proportion of total DCs found in AS patients or HCs (Fig. 3.3C). However, this study was not sufficiently powered to fully understand the function of HLA-B27 with respect to these immunological parameters.

Our laboratory has previously shown that HLA-B27 TG rats lack the tolerogenic CD172a^{lo} DC subset within intestinal lymphatics and MLNs (480). Initially it was hypothesised that CD141⁺ DCs, the human equivalent of the tolerogenic CD172a^{lo} rat DCs, would be deficient in AS patients compared to HCs. No significant difference in the proportion of CD141⁺ DCs between HCs and AS patients was observed, in terms of the percentage of CD11c⁺ MHC II⁺ DCs, percentage of total live cells, or total cell number/ml of blood (Fig. 3.4A). However, in AS patients CD1c⁺ DCs represented a significantly lower proportion of total CD11c⁺ MHC II⁺ cells than in HCs (Fig. 3.4B). This difference was not reflected as proportion of total live cells or absolute cell number (Fig. 3.4B). This significant reduction of CD1c⁺ DCs could represent the slight decline in total DCs observed in AS patients (Fig. 3.3C and Fig. 3.4B). Initial evaluation of pDCs showed no significant difference between HCs and AS patients in terms of percentage of live cells and total cell number (Fig. 3.4C). Overall, my data suggests that there are only slight differences in the proportions of blood

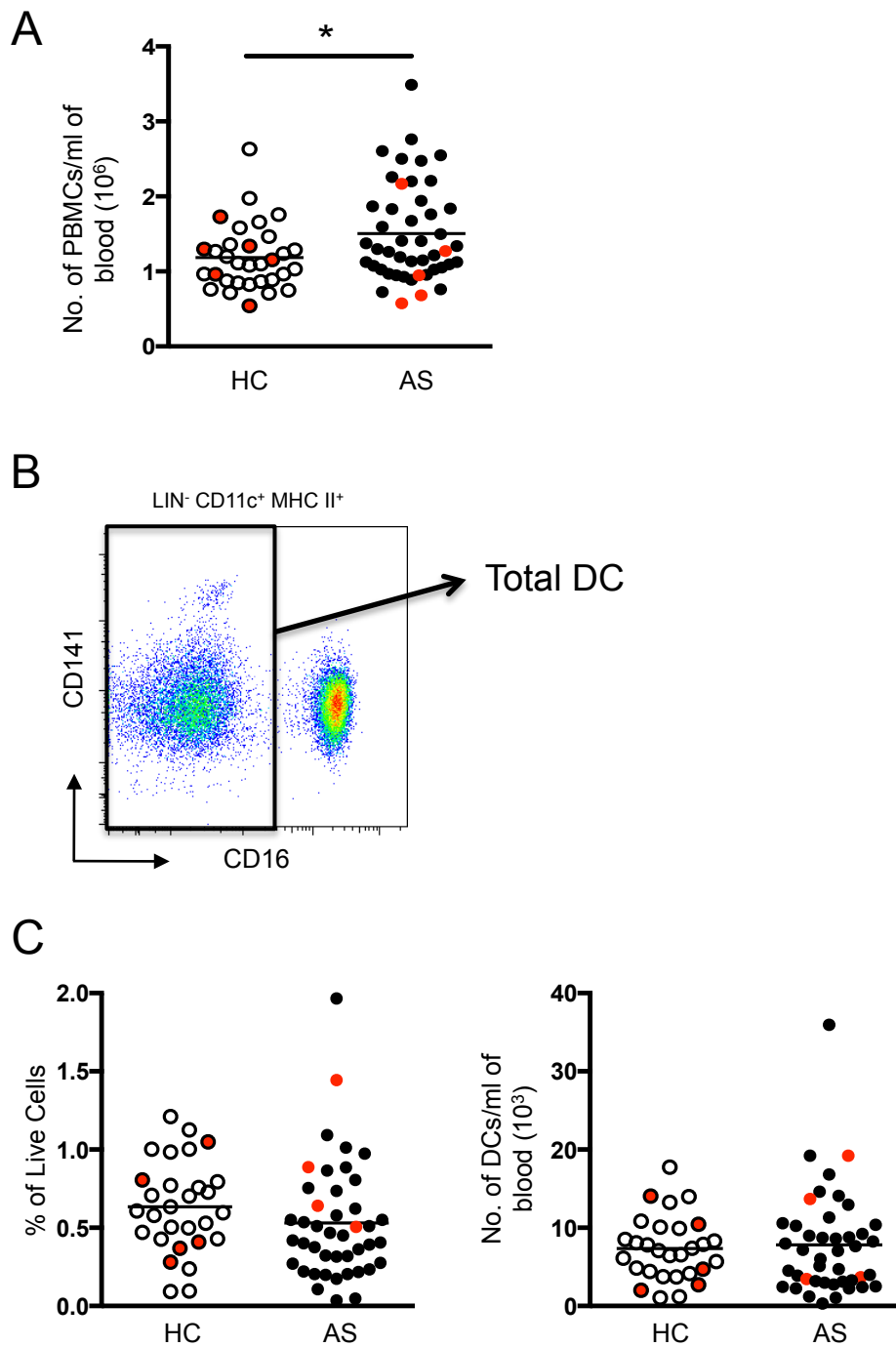


Figure 3.3: Enumerating DCs in AS patients

Number and frequency of blood DCs in AS patients and HCs. (A) Number of PBMCs/ml of blood was enumerated in AS patients and HCs. 33 HCs and 47 AS patients were used for analysis. (B) Of the LIN⁻ (CD3, CD14, CD15, CD19 and CD56) CD11c⁺ MHC II⁺ population, CD141⁺ and CD1c⁺ (CD141⁻ CD16⁻) cells were combined to analyse total DCs. (C) Proportion of total DCs as percentage of live cells (left) and total cell number/ml of blood ($\times 10^3$ – right). 29 HCs and 43 AS patients were compared. Data analysed by Mann-Whitney test, * = $p < 0.05$. HC red dots = B27⁺ individuals, AS red dots = B27⁻ patients. All graphs show mean.

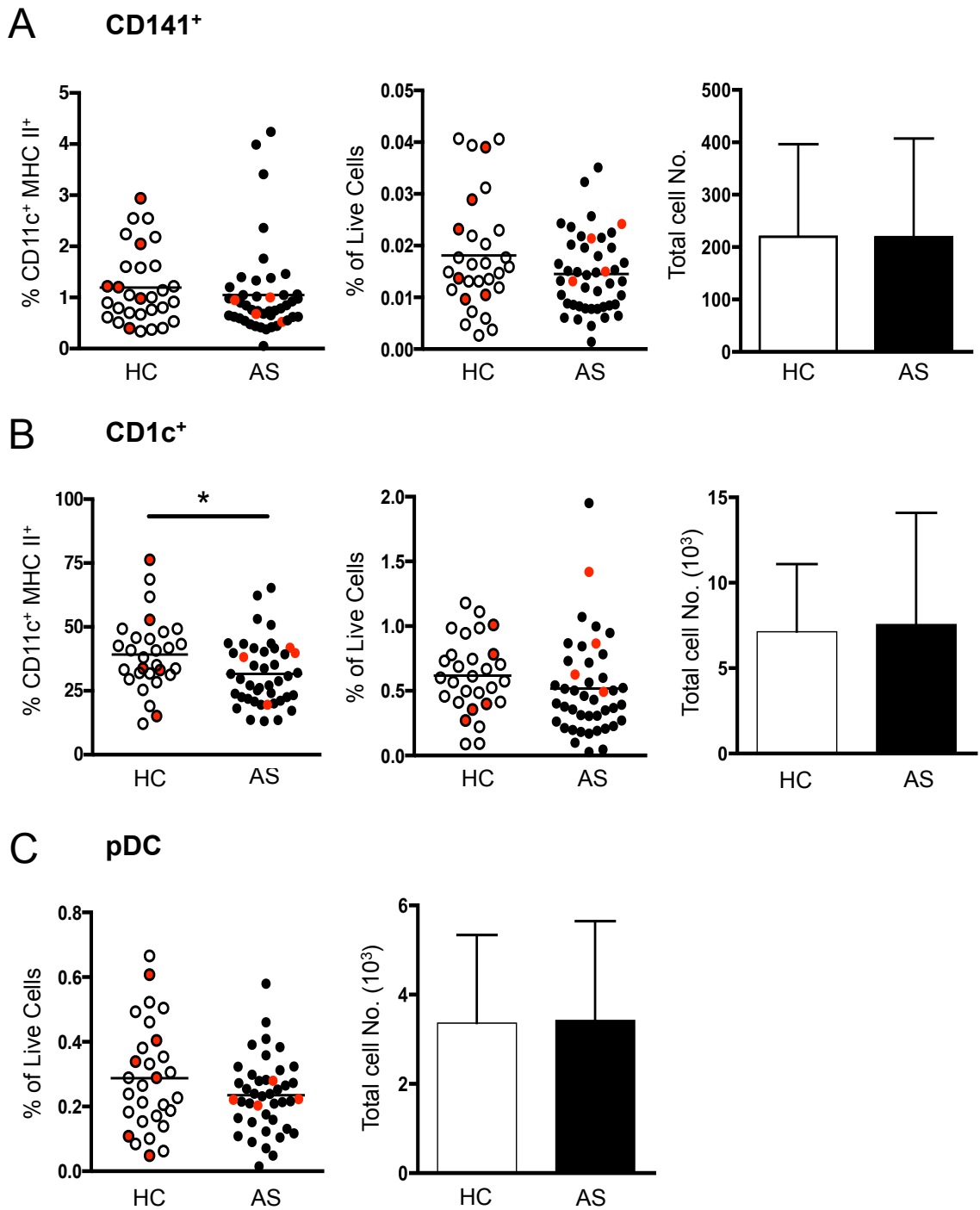


Figure 3.4: Enumeration of pDCs and DC subsets in AS patients and HCs

Comparison of blood CD141⁺ DCs, CD1c⁺ and pDCs between AS patients and HCs. **(A)** Analysis of AS patient and HC CD141⁺ DCs (30 HCs/45 AS patients) represented as % of CD11c⁺ MHC II⁺ cells (left), % of live cells (centre) and total cell number/ml of blood (right). **(B)** Proportion of CD1c⁺ DCs (29 HCs/43 AS patients) represented as % of CD11c⁺ MHC II⁺ cells (left), % of live cells (centre) and total cell number (10³)/per ml of blood (left) between HCs and AS patients. **(C)** pDCs compared between HCs (n=29) and AS patients (n=43) as % of live cells (left) and total cell number (10³)/per ml of blood (right). HCs shown in open circles/bars, AS patients depicted by filled circles/bars. All graphs show mean. Mann-Whitney statistical used, * = p<0.05. HC red dots = B27⁺ individuals, AS red dots = B27⁻ patients. Graphs show mean + SD.

DCs between HCs and AS patients, with a significant, proportional reduction in the major blood DC population (CD1c⁺ DCs) in AS patients. Additionally, no difference was observed when comparing the few HLA-B27⁻ and HLA-B27⁺ AS patients or HCs for all DC subsets analysed in terms of percentage of total CD11c⁺ MHC II⁺ cells and live cells (Fig. 3.4).

Circulating DC proportional analyses of AS patients and HCs revealed a large deviation around the mean for each cohort (Fig. 3.3 and 3.4). Given this considerable variation in DC proportions, two HCs were analysed over time to assess cDC subset stability (Fig. 3.5). A HC with an initial low ratio of CD1c⁺ DCs: CD16⁺ mononuclear cells (15.1%: 84.5%) was re-assessed 6 months after initial characterisation (Fig. 3.5A). Proportions of CD11c⁺ MHC II⁺ subsets remained relatively stable over time, with the CD1c⁺: CD16⁺ cell ratio after 8 months equating to 20.9%: 77.1% (Fig. 3.5A). Additionally, DC proportions of a second HC with an initial high ratio of CD1c⁺: CD16⁺ cells (45.8%: 51.7%) were assessed 18 months later (Fig. 3.5B). At the later time point there was a slight shift towards the CD16⁺ mononuclear population, with a ratio of 32.2%: 62.6% (CD1c⁺ DCs: CD16⁺ mononuclear cells – Fig. 3.5B). From this very small dataset, it appears that the proportion of CD1c⁺: CD16⁺ cells remains relatively stable over time.

3.4.2 CD14⁻ CD16⁺ mononuclear cells

The CD14⁻ CD16⁺ mononuclear population is not homogeneous. In a recent publication, Cros et al define three blood monocyte subsets (237) - CD14⁺ CD16⁻, CD14⁺ CD16⁺ and CD14⁻ CD16⁺ - based on surface marker expression and subsequently their functional roles in immune responses have been described (229, 353, 565, 566). This “third” CD14⁻ CD16⁺ monocyte subset equates to our CD14⁻ CD16⁺ mononuclear population. However, classification of this CD14⁻ CD16⁺ mononuclear cell population remains controversial. CD14⁻ CD16⁺ cells have recently been shown to be heterogeneous for M-DC8 (237, 240), which is also known as 6-sulfo LacNAc or SLAN, as it will be referred from here onwards. In some samples, the gating strategy used in Fig. 3.1 was altered to accommodate staining for SLAN (Fig. 3.6). LIN⁻ live, single cells were analysed for CD14 expression (Fig. 3.6A), and CD14 negative cells that expressed both CD11c and MHC II were subdivided into the three myeloid populations, as defined in Fig. 3.1A. Subsequently, the CD14⁻ CD16⁺ mononuclear cell population can be separated into two distinct subsets based on the expression of SLAN (Fig. 3.6A). Levels of SLAN expression on the CD16⁺ subset appeared similar for both HCs and AS patients (Fig. 3.6B).

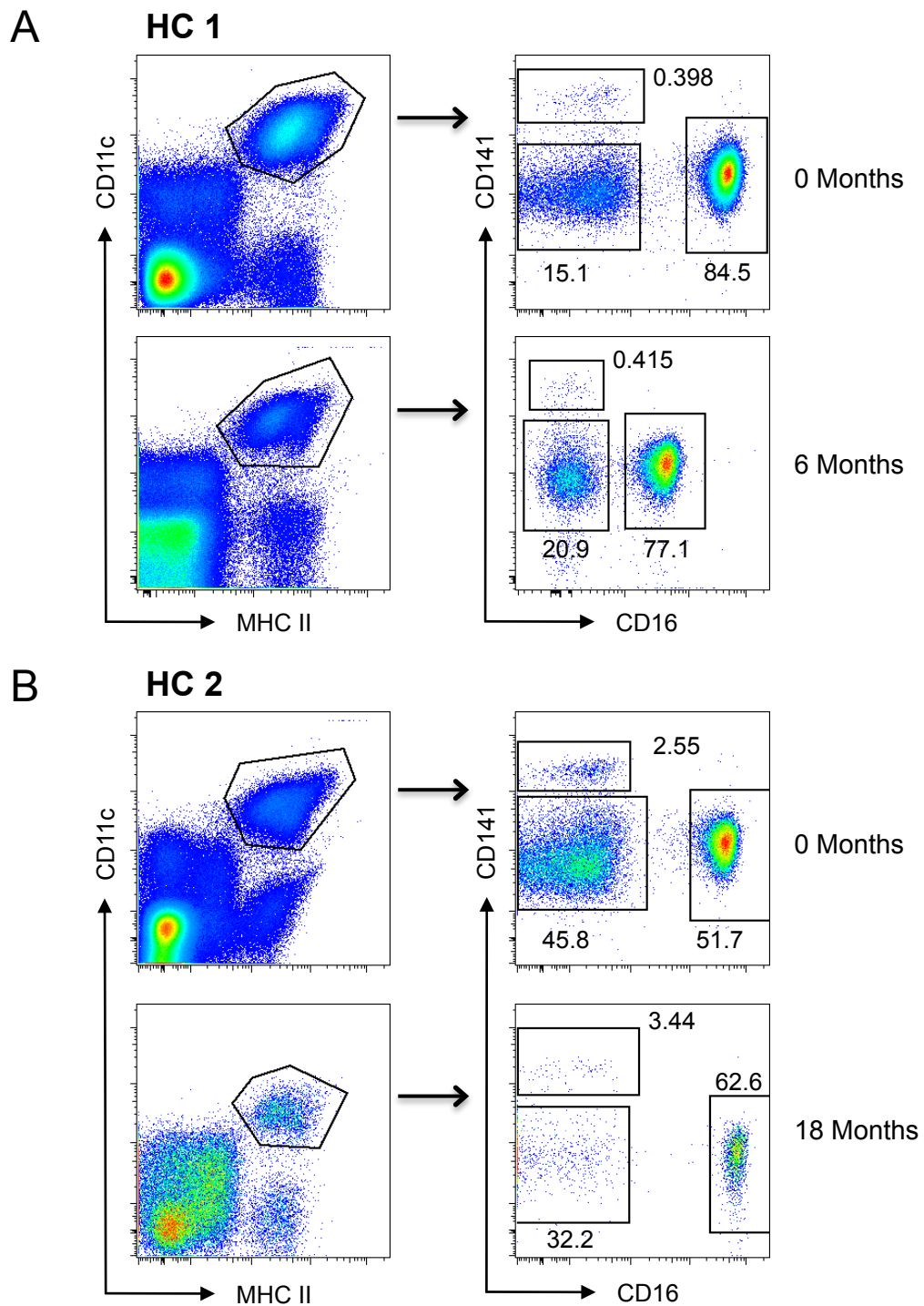


Figure 3.5: Changes in HC blood DC and mononuclear cell proportions over time

DCs and mononuclear cells in blood from two HC donors were analysed at two different time points to estimate the stability of DC proportions over time. **(A)** HC DCs were compared at 0 months (top) and 6 months (bottom). LIN⁻ CD14⁻ CD11c⁺ MHC II⁺ cells were subdivided based on the expression of CD141 and CD16. Numbers represent the proportions of the 3 subsets depicted in the right hand plots, as a percentage of total CD11c⁺ MHC II⁺ cells. **(B)** HC DCs were compared at 0 months (top) and 18 months (bottom), using the strategy in A. Gating strategy used in Fig. 3.1A was used for this analysis.

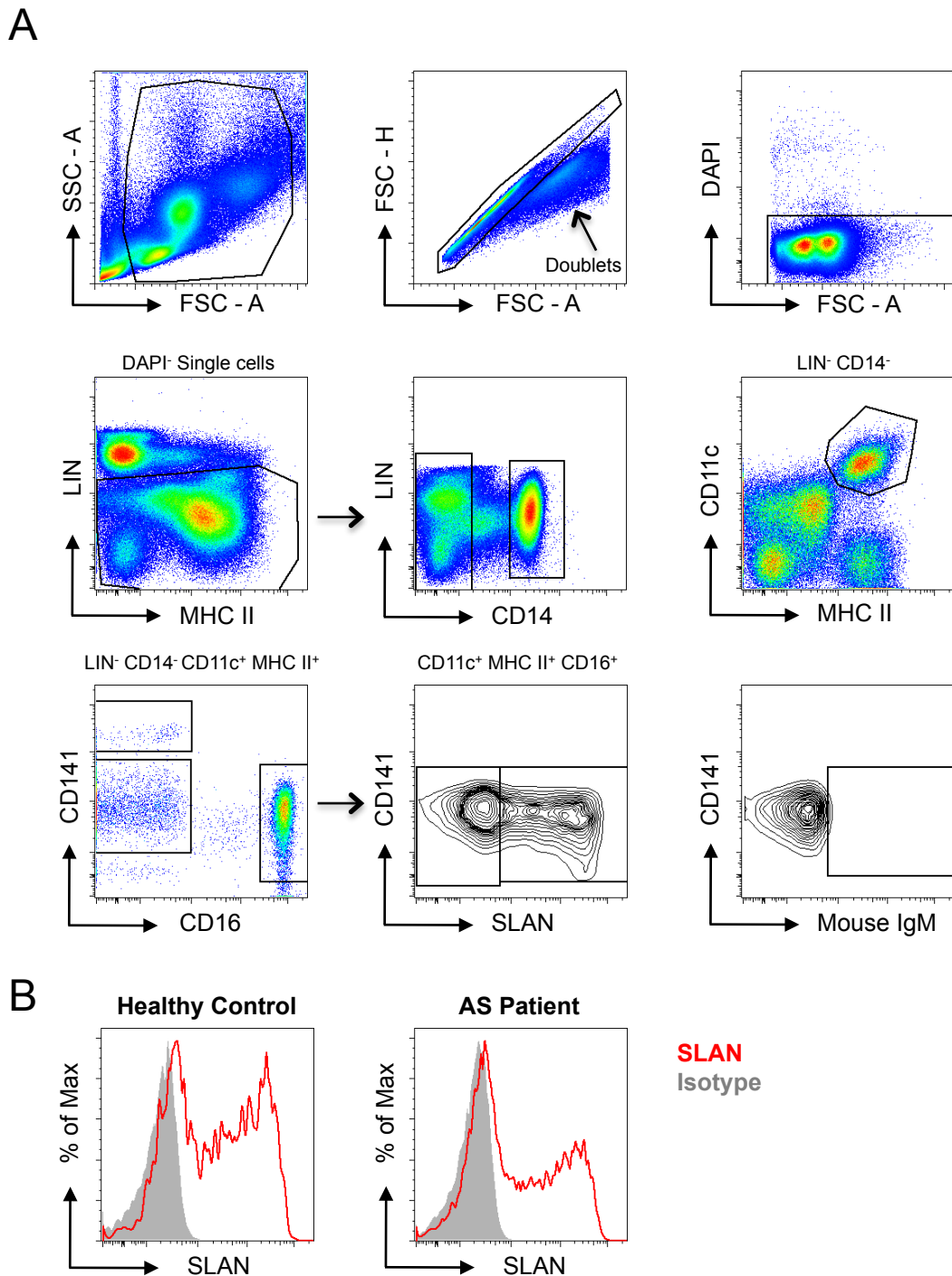


Figure 3.6: Gating strategy for CD16⁺ SLAN⁻ and CD16⁺ SLAN⁺ cells

Peripheral blood DCs and monocytes were identified by the expression of several cell surface markers. **(A)** FSC-A vs SSC-A gate is used to exclude dead cells. Doublets are excluded by FCS-H vs FSC-A. Remaining dead cells (DAPI⁺) are excluded and live cells subdivided on the expression of LIN markers (CD3, CD15, CD19 and CD56) and MHC II. LIN⁻ CD14⁺ cells are classical monocytes. CD14⁻ CD11c⁺ MHC II⁺ cells are divided into CD141⁺ DCs, CD1c⁺ DCs and CD16⁺ cells that are either CD16⁺ SLAN⁻ or CD16⁺ SLAN⁺. The SLAN⁺ gate is set based on the isotype control. **(B)** Representative histograms of a HC and AS patient sample showing SLAN expression on live LIN⁻ CD11c⁺ MHC II⁺ CD14⁻ CD16⁺ cells. Isotype in grey filled histograms (monoclonal Mouse IgM), and SLAN expression depicted in red.

Using the gating strategies described in Fig. 3.1A and Fig. 3.6A, the proportions of total CD14⁻ CD16⁺ mononuclear cells, CD16⁺ SLAN⁺ and CD16⁺ SLAN⁻ subsets were compared between AS patients and HCs (Fig. 3.7). A trend towards an increase in the proportion of CD11c⁺ MHC II⁺ CD16⁺ cells was observed (Fig. 3.7A), but this did not reach statistical significance (p=0.0552). Furthermore, this trend towards increased CD16⁺ cells was not observed as percentage of live cells or total cell number (Fig. 3.7A). Additionally, when the CD16⁺ SLAN⁺ and SLAN⁻ subsets were analysed separately, no differences were detected between AS patients and HCs in terms of proportion or cell number of CD16⁺ SLAN⁺ (Fig. 3.7B) and CD16⁺ SLAN⁻ cells (Fig. 3.7C). Additionally, HLA-B27⁻ AS patients and HLA-B27⁺ HC individuals were highlighted to see if this phenotype would be associated with any changes in cell populations, however no patterns were detected (Fig. 3.7). Overall, slight variations in the proportions of blood DC and mononuclear cell populations were observed in AS patients – specifically AS patients have a reduced proportion of circulating CD1c⁺ DCs accompanied with a trend towards an increase in the CD14⁻ CD16⁺ mononuclear population.

3.5 Identification and quantification of blood monocytes

Due to the role of monocytes in inflammation and their possible contribution to the DC pool in non-lymphoid tissues during inflammatory responses (225, 234), it was important to study blood monocyte subsets in AS patients and HCs. The gating strategy used in Fig. 3.1 was modified to accommodate monocyte subsets. LIN⁻ live single cells co-expressing CD11c and MHC II could be subdivided into four subsets, classified as CD14⁺ CD16⁻ (A) and CD14⁺ CD16⁺ (B) monocytes, CD14⁻ CD16⁺ (C) mononuclear cells and cDCs (D – Fig. 3.8A). The presence of the CD1c⁺ and CD141⁺ cDC subsets in population D was confirmed by flow cytometry (Fig. 3.8B). Additionally, the CD14⁻ CD16⁺ subset was shown to be heterogeneous for SLAN and represents the CD16⁺ mononuclear population described in previous figures (Fig. 3.8C).

Blood monocyte subsets are often depicted as a “waterfall” (237) based on the expression of CD14 and CD16, as shown in the gating strategy in Fig. 3.8A. Representative plots depicting this monocyte waterfall in HCs and AS patients are shown in Fig. 3.9A. Consistent with previous publications (236, 237, 567, 568), CD14⁺ CD16⁻ monocytes represent the major blood monocyte subset accounting for approximately 80-85% of CD11c⁺ MHC II⁺ blood monocytes. Next, the CD14⁻ CD16⁺ heterogeneous population contributes around 10% to the monocyte pool, with the CD14⁺ CD16⁺ monocytes

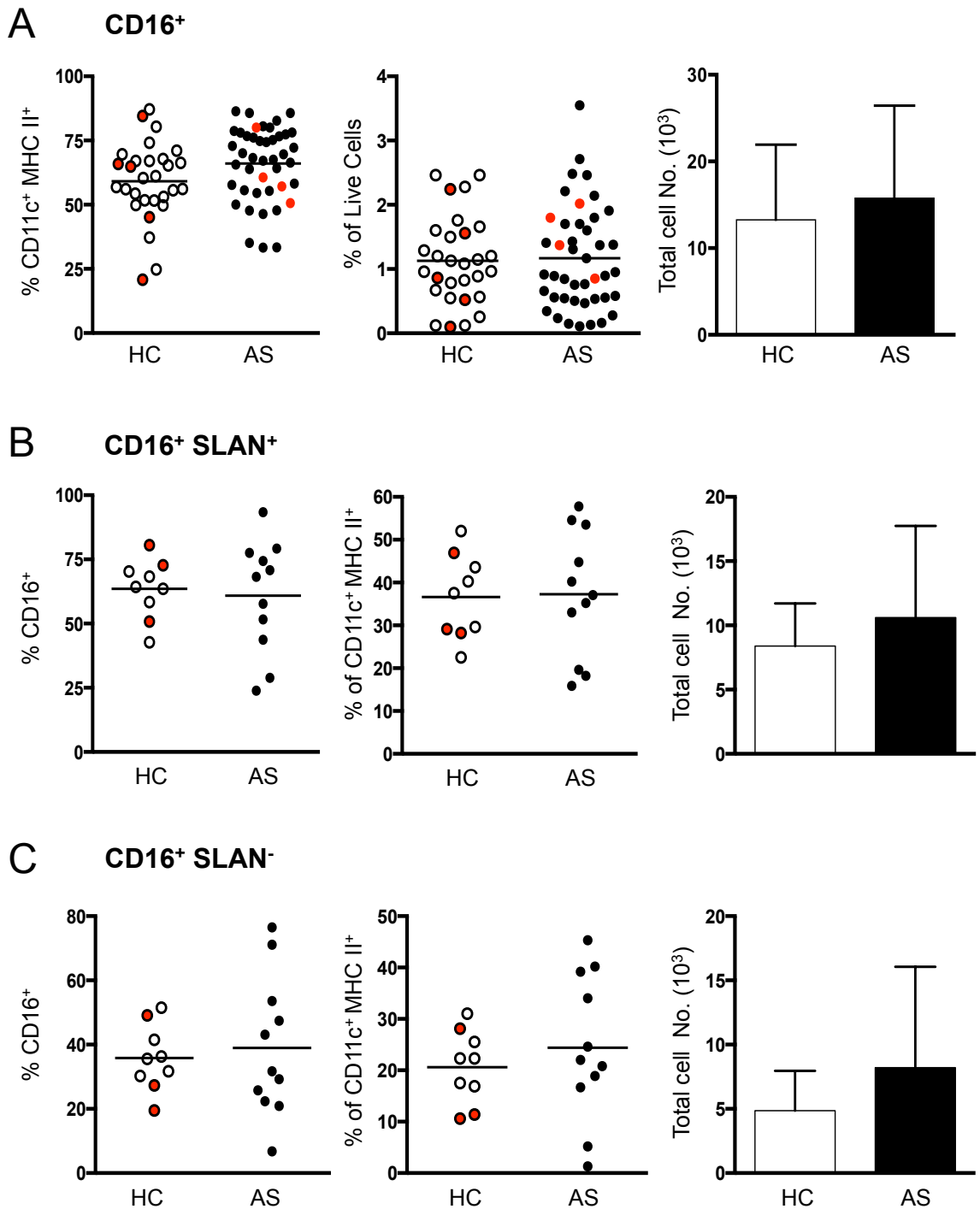


Figure 3.7: Comparison of CD16⁺ cells between AS patients and HCs

Comparison of CD11c⁺ MHC II⁺ CD14⁻ CD16⁺ cells and SLAN⁻ and SLAN⁺ subsets between AS patients and HCs. **(A)** Analysis of single DAPI⁻ LIN⁻ CD11c⁺ MHC II⁺ CD16⁺ cells from HCs and AS patients; % of CD11c⁺ MHC II⁺ population (left), live cells (centre) and total cell number (10³)/ml of blood (right). 29 HCs and 43 AS patients were used for this analysis. This CD16⁺ CD11c⁺ MHC II⁺ population was then divided into CD16⁺ SLAN⁺ **(B)** and CD16⁺ SLAN⁻ **(C)**. Percentage of CD16⁺ CD11c⁺ MHC II⁺ (left) and % of total CD11c⁺ MHC II⁺ CD14⁻ cells (right) were calculated for 9 HCs and 11 AS patients. Each point represents one individual. HC red dots = B27⁺ individuals, AS red dots = B27⁻ patients. Graphs represent mean + SD.

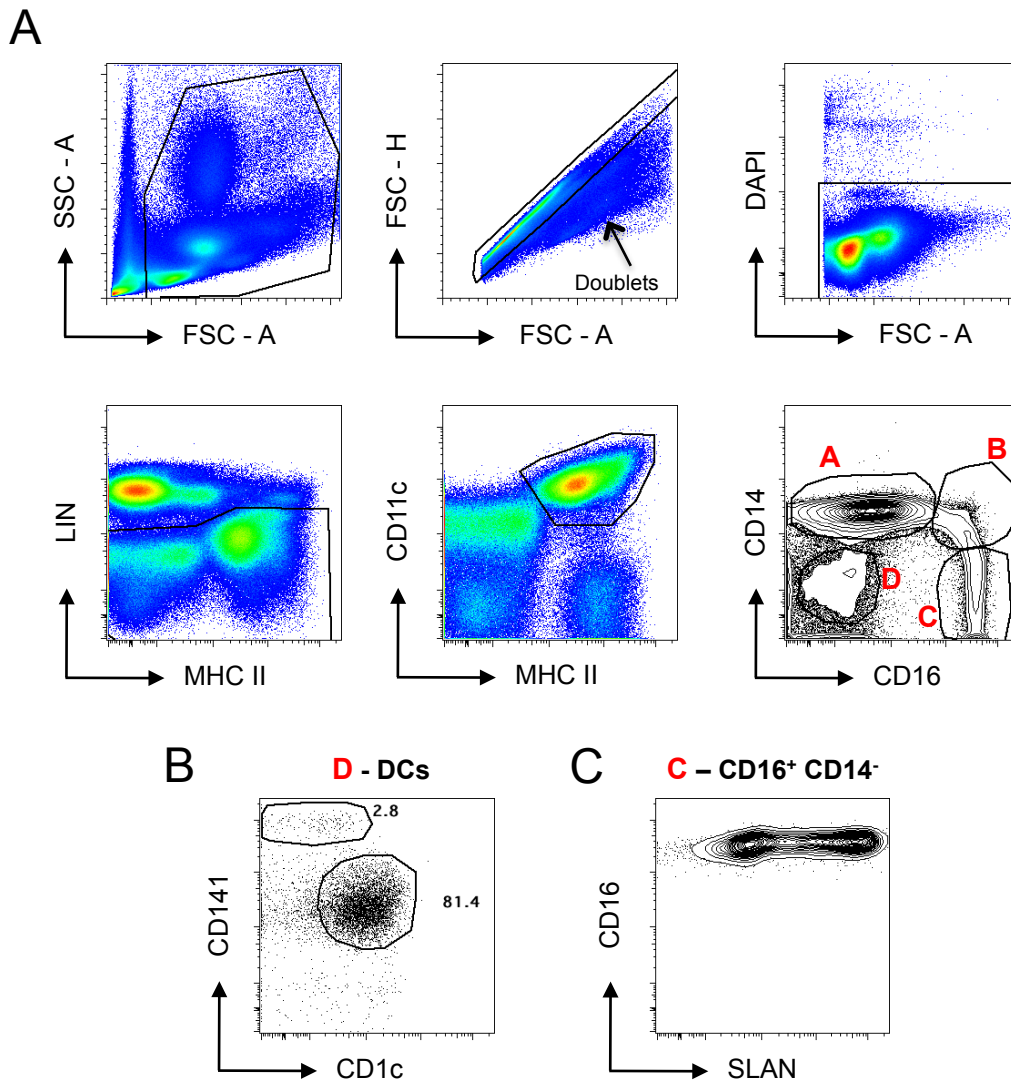


Figure 3.8: Identification of monocytes in peripheral blood

Identification of monocyte subsets from peripheral blood. **(A)** Initially, live cells and doublets were excluded using FSC-A vs SSC-A, FSC-H vs FSC-A and DAPI⁻ gates. Live cells (DAPI⁻) were subdivided on the expression of LIN markers (CD3, CD15, CD19 and CD56) and MHC II. Total CD11c⁺ MHC II⁺ LIN⁻ cells were separated on CD14 and CD16. Four populations (A, B, C and D) were identified. **(B)** The CD14⁻ CD16⁻ population (D) is predominantly composed of blood CD1c⁺ and CD141⁺ DCs. This population is heterogeneous for SLAN, and represents the CD11c⁺ MHC II⁺ CD14⁻ CD16⁺ population described earlier **(C)**.

representing the smallest monocyte subset (5%, Fig. 3.9A). Comparative analyses of the proportions of blood monocyte subsets between AS patients and HCs revealed no significant differences, with the CD14⁻ CD16⁺ population consisting of both SLAN⁻ and SLAN⁺ cells (Fig. 3.9A). Furthermore, no significant differences between AS patients and HCs were observed in terms of percentage of live cells or total cell number/ml of blood (Fig. 3.9B).

3.6 DC morphology

To further characterise the DC populations, peripheral blood DC subsets and CD14⁻ CD16⁺ mononuclear cells were sorted by flow cytometry to analyse cell morphology. Cytospins were prepared and cells were stained with hematoxylin and eosin (H & E) to identify any differences in cell morphology and associated structures between HCs and AS patients. Representative pictures of CD141⁺ DCs (Fig. 3.10A), CD1c⁺ DCs (Fig. 3.10B), pDCs (Fig. 3.10C) and CD14⁻ CD16⁺ mononuclear cells (Fig. 3.10D), containing SLAN⁺ and SLAN⁻ subsets, were taken and analysed. Interestingly, all blood DC subsets and CD14⁻ CD16⁺ mononuclear cells possessed lobulated nuclei, often associated with neutrophils (Fig. 3.10). In contrast, isolated pDCs (LIN⁻ CD123⁺ MHC II⁺ CD304⁺) were lymphoid in appearance, with large spherical nuclei and minimal cytoplasm. CD141⁺, CD1c⁺ and CD16⁺ subsets all possessed ruffled membranes, however there was little evidence of dendrite formation immediately following isolation from peripheral blood (Fig. 3.10A/B/D). DCs, when first discovered in 1973, were given their name due to the presence of characteristic dendrites (185). However, based on the cell structure representations depicted in Fig. 3.10, no dendrite formation was detected on cells directly isolated from peripheral blood. As activation can affect cell morphology, it was decided to investigate whether cell stimulation would induce morphological changes, with particular reference to dendrite formation. Interestingly, 18-hour lipopolysaccharide (LPS) stimulation of all CD11c⁺ MHC II⁺ subsets induced dramatic changes in nuclear morphology (Fig. 3.11A-C), with the nuclei for each subset changing from a lobulated shape to a round, compact structure (illustrated with arrows in Fig. 3.11B). In addition, all subsets developed cytoplasmic inclusions and dendrites (Fig. 3.11B). Despite these changes, no differences in cell morphology were observed between AS patients and HCs.

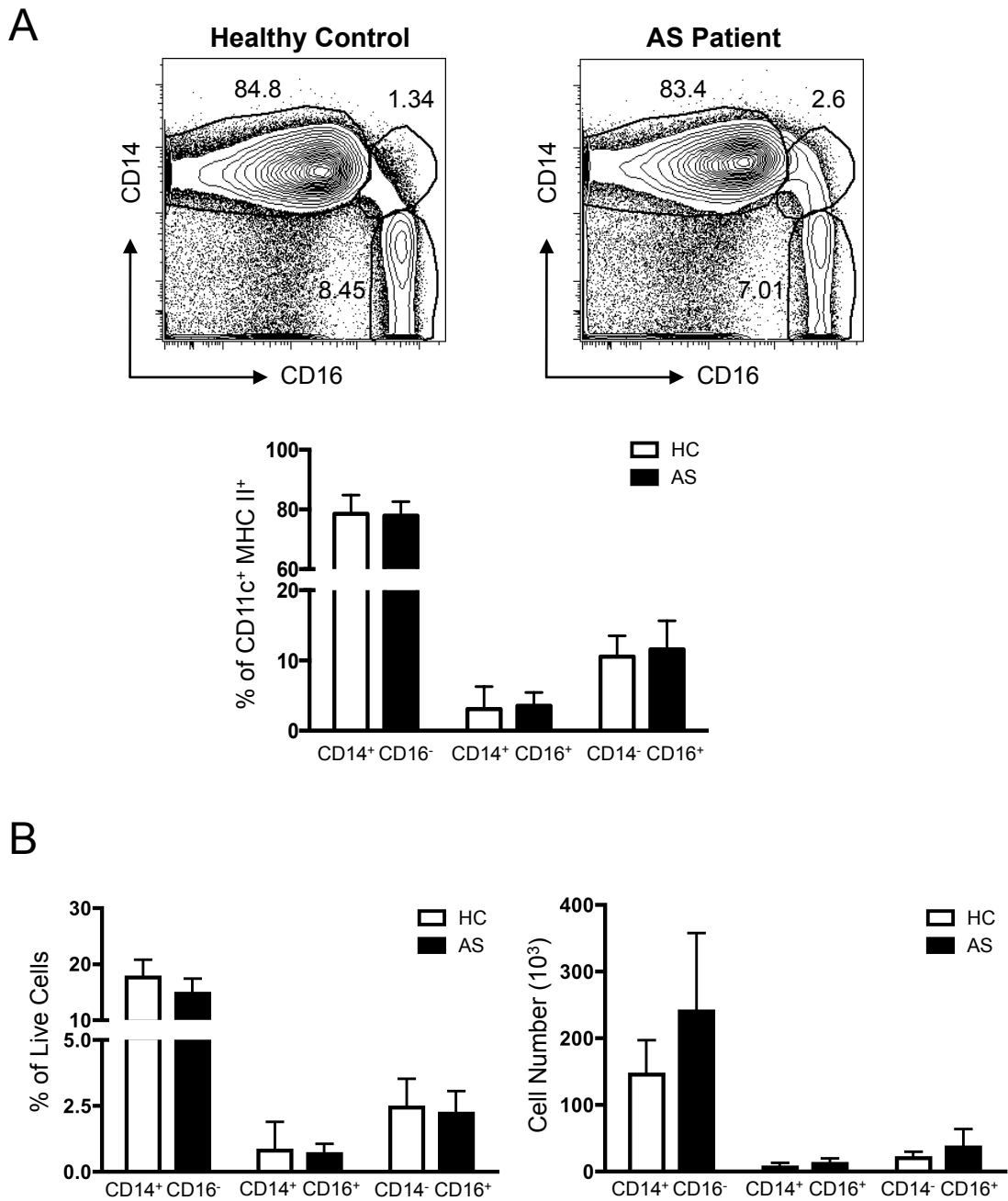


Figure 3.9: Quantification of blood monocyte subsets

Comparison of blood monocyte subsets in healthy controls (HC) and AS patients (AS). The gating strategy described in Fig. 3.8 was used to quantify proportions of CD14⁺ CD16⁻, CD14⁺ CD16⁺ and CD14⁻ CD16⁺ mononuclear cell populations. **(A)** Examples of monocyte “waterfall” FACS plots generated for a HC (left) and an AS patient (right). Quantification of subsets as proportion of CD11c⁺ MHC II⁺ cells (A). Numbers associated with the contour plots represent the proportion of CD11c⁺ MHC II⁺ cells. **(B)** The proportion of live cells (left) and total cell number (right) for each subset is depicted. Cell number is represented as no. of cells per ml of blood (10³). All graphs show mean + SD.

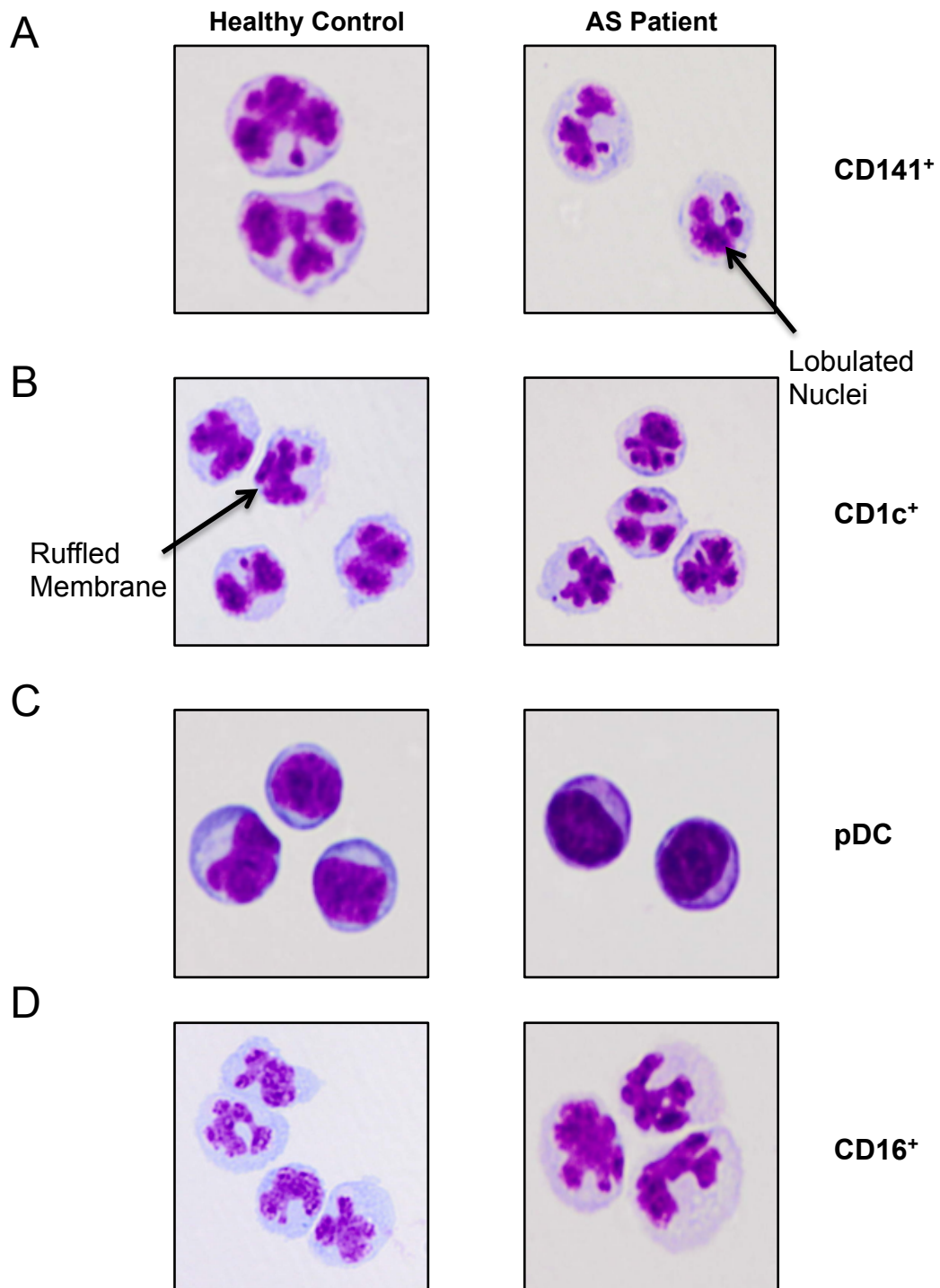


Figure 3.10: Comparison of DC morphology between AS patients and HCs

DC subsets were flow sorted from AS patients and HCs by using the gating strategy described in Fig. 3.1. Cytospins of purified populations were stained with hematoxylin and eosin. Representative pictures generated for CD141⁺ DCs (**A**), CD1c⁺ DCs (**B**) and pDCs (**C**) from an HC (left) or AS patient (right). (**D**) Cytospins for the heterogeneous CD11c⁺ MHC II⁺ CD14⁻ CD16⁺ population, containing both SLAN⁻ and SLAN⁺ subsets. DC-associated cellular features, including lobulated nuclei and ruffled membranes are highlighted.

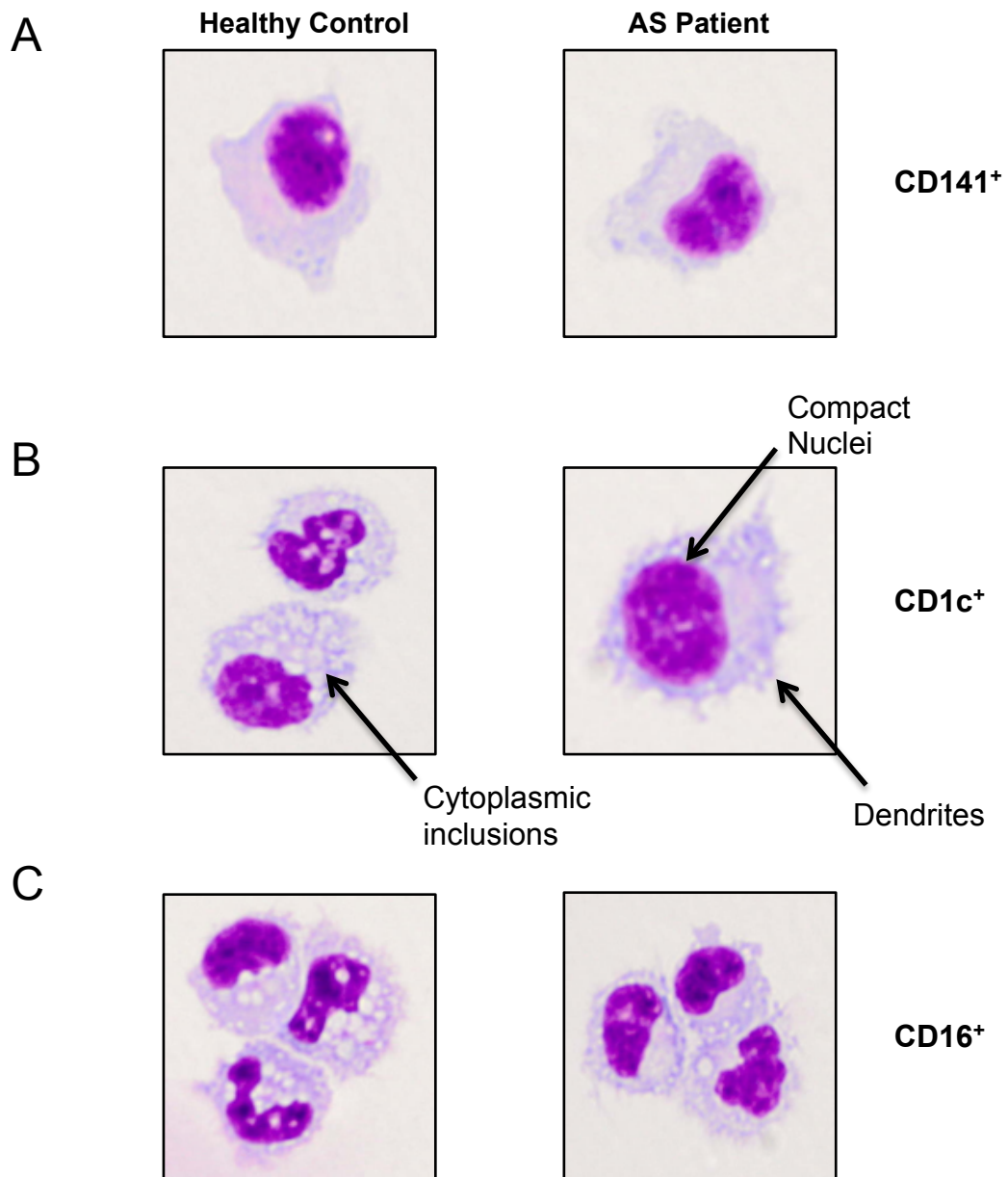


Figure 3.11: Comparison of activated DC morphology between AS patients and HCs

DC subsets from peripheral blood of AS patients and HCs were sorted by flow cytometry, using the gating strategy described in Fig. 3.1. Cells were stimulated with 100ng/ml of LPS for 18 hours. Representative pictures generated for CD141⁺ DCs (**A**) and CD1c⁺ DCs (**B**) from a HC (left) and an AS patient (right) are shown. (**C**) Cytospins for the heterogeneous population of CD11c⁺ MHC II⁺ CD14⁻ CD16⁺ cells, containing both SLAN⁻ and SLAN⁺ subsets. Compact nuclei, dendrite formation and the presence of cytoplasmic inclusions are highlighted by the black arrows.

3.6.1 Cell viability

The unusual lobulated nuclear morphology of DC subsets isolated straight from peripheral blood was unexpected and it was hypothesised that these cells could be undergoing apoptosis. Following initial studies, all cell-sorting experiments were carried out the day following cell isolation, with samples stored at 4°C overnight. Thus, it was important to confirm whether the DC morphology depicted in Fig. 3.10 was true, or if it was due to cells undergoing apoptosis after overnight incubation. Therefore, survival of cDCs was assessed and compared under four conditions using an annexin V survival assay: cells freshly isolated from blood; cells isolated and then sorted immediately; cells isolated and left overnight at 4°C; and cells that were isolated, incubated at 4°C overnight and then sorted using flow cytometry. LIN⁻ cells co-expressing CD11c and MHC II were classified as total cDCs for this experiment (Fig. 3.12A). Annexin V and DAPI were used to assess cell viability with individual single stains (Fig. 3.12B) being used to set the relevant gates. DAPI⁺ Annexin V⁺ cells were classed as dead. The proportions of dead and apoptotic cells were then compared (Fig. 3.12C). Less than 3% of cells died in every condition (Fig. 3.12C). Furthermore, no significant differences were observed, with relation to cells going under apoptosis, between those isolated fresh or stored overnight (4% vs 3.1%); or between those flow sorted directly after isolation or those stored overnight and then isolated (0.18% vs 0.76% - Fig. 3.12).

A similar experiment was performed to assess cell survival of pDCs. The gating strategy used to assess pDC viability is shown in Fig. 3.13A. As before, pDCs were identified as LIN⁻ MHC II⁺ CD123⁺ CD304⁺ cells (Fig. 3.13A). The same protocol as used for cDCs was adopted for pDC survival analysis. DAPI and Annexin V singles (Fig. 3.13B) were used to set individual gates, with DAPI⁺ Annexin V⁺ cells again being classified as dead cells. For every condition, approximately 1% of cells were DAPI⁺ Annexin V⁺, indicating that pDCs are viable following overnight incubation and cell sorting (Fig. 3.13C). With regards to apoptosis, approximately 2-3% of pDCs were apoptotic under all conditions (Fig. 3.13C). It was therefore concluded that those cDCs and pDCs that remained after an overnight incubation at 4°C and the subsequent cell sorting protocol were viable for subsequent experiments. Therefore the unusual morphology of human blood DCs cannot be attributed to granulocytic cellular infiltration or cell death.

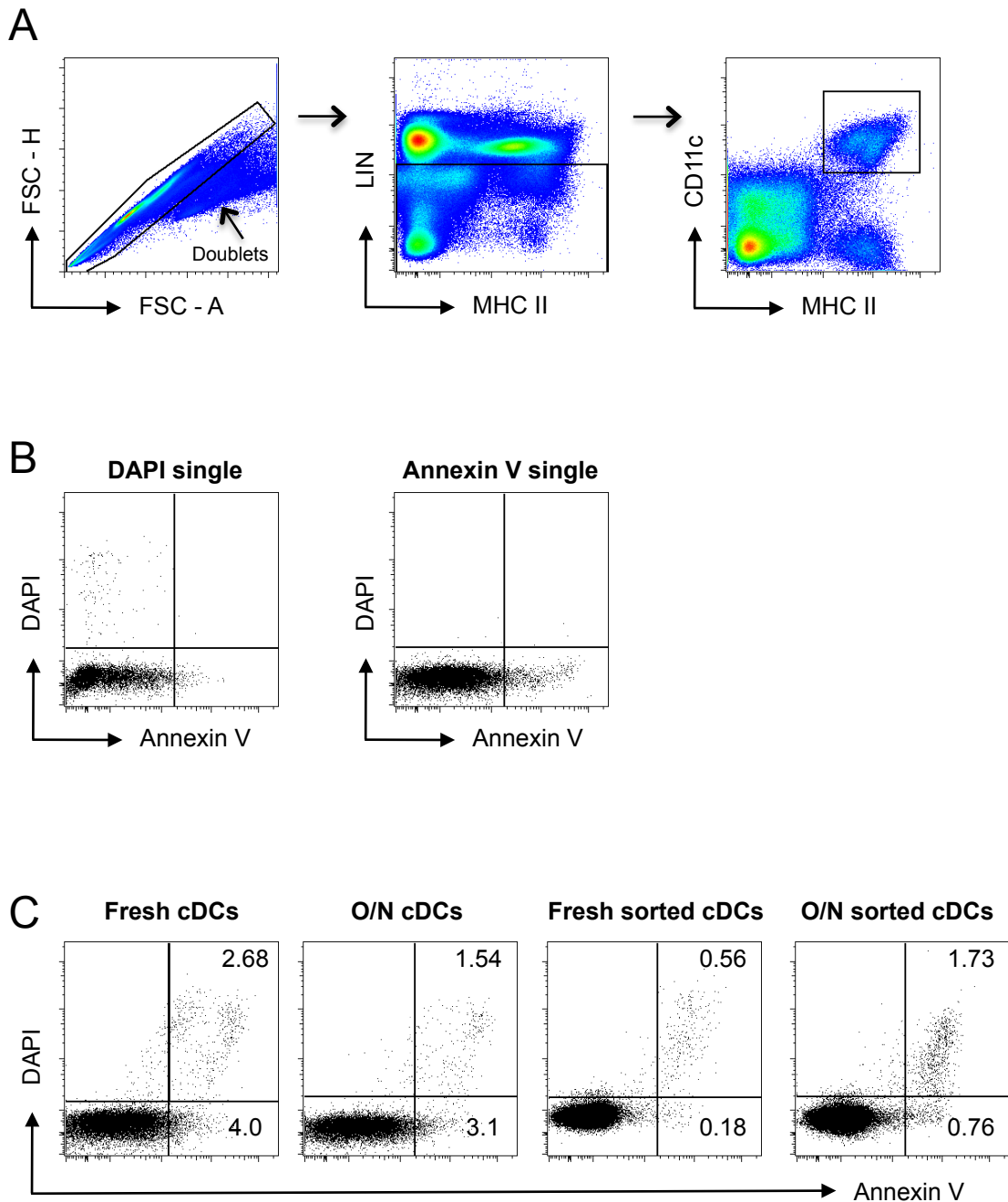


Figure 3.12: Survival of cDC subsets after overnight incubation and flow cytometry sorting

Cell survival was not affected by overnight (o/n) incubation or flow cytometric sorting. **(A)** Gating strategy to identify DCs. Initially doublets were gated out (left) and single LIN⁻ cells (centre) were analysed for expression of CD11c and MHC II (right). **(B)** DAPI single- (left) and Annexin V single-stained samples (right) were used to set the appropriate gates. **(C)** Proportion of DAPI⁺ Annexin V⁺ CD11c⁺ MHC II⁺ cells were compared between freshly isolated cells (left), cells left at 4°C o/n (centre – left), freshly isolated cells after sorting (centre – right) and o/n cells after sorting (right). Numbers represent proportion of DAPI⁺ Annexin V⁺ CD11c⁺ MHC II⁺ cells (dead cells), and DAPI⁺ Annexin V⁺ CD11c⁺ MHC II⁺ cells (apoptotic). LIN = CD3, CD14, CD15, CD19 and CD56.

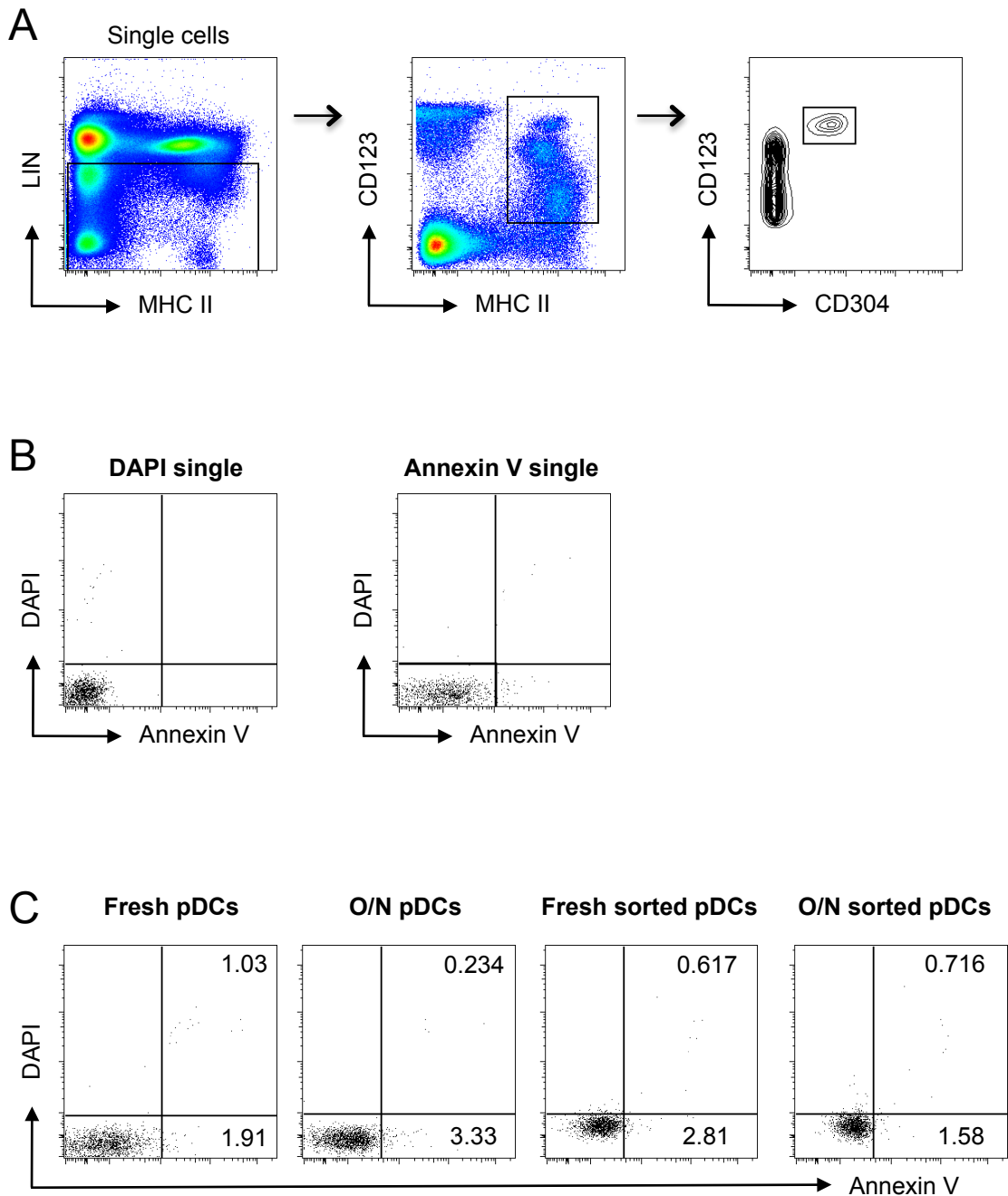


Figure 3.13: Survival of pDC subsets after overnight incubation and flow cytometry sorting

Cell survival of pDCs was not affected by overnight (o/n) incubation or flow cytometric sorting. **(A)** Gating strategy to identify pDCs. Singlet LIN⁻ cells (left) were analysed for CD123 and MHC II expression (centre). pDCs are CD123⁺ MHC II⁺ CD304⁺ (right). **(B)** DAPI single- (left) and Annexin V single-stained samples (right) were used to set the appropriate analysis gates. **(C)** Proportions of DAPI⁺ Annexin V⁺ CD304⁺ CD123⁺ cells were compared between freshly isolated cells (left), cells left at 4°C o/n (centre – left), freshly isolated cells after sorting (centre – right) and o/n cells after sorting (right). Numbers represent proportion of DAPI⁺ Annexin V⁺ CD123⁺ CD304⁺ cells, and DAPI⁻ Annexin V⁺ CD123⁺ CD304⁺ cells (apoptotic). LIN = CD3, CD14, CD15, CD19 and CD56.

3.7 Maturation status of DCs and monocytes in AS patients and HCs

While DCs migrate from tissue via lymphatics to lymph nodes to activate naïve T cells resulting in the induction of T cell responses, they undergo several phenotypic changes in order to facilitate changes in cell function. During DC migration in response to foreign antigen, surface molecules involved in antigen presentation and co-stimulation are upregulated, including MHC II, CD80, CD86 and CD40 (569). Thus, the activation status of circulating cells can infer detail regarding cell maturation, function and migration. Therefore we set out to assess the expression of CD40, CD80 and CD86 on the surface of CD141⁺ and CD1c⁺ DCs, CD14⁺ CD16⁻ and CD14⁺ CD16⁺ monocytes and the CD14⁻ CD16⁺ SLAN^{+/-} mononuclear populations. Representative histograms of co-stimulatory molecule expression on CD1c⁺ cDCs is shown in Fig. 3.14A. Furthermore, representative histograms depicting co-stimulatory molecule expression on CD14⁺ CD16⁻ monocytes are depicted in Fig. 3.14B. Quantification of co-stimulatory molecule expression was subsequently performed for 5 HCs and 8 AS patients (Fig. 3.15). No differences in expression of CD40 (Fig. 3.15A), CD80 (Fig. 3.15B) or CD86 (Fig. 3.15C) between AS patients and HCs were observed for any of the myeloid populations analysed. However, differences existed between myeloid subsets. CD141⁺ DCs expressed higher levels of CD40 compared to their CD1c⁺ counterparts, with the converse applying for CD86. The SLAN⁺ and SLAN⁻ CD14⁻ CD16⁺ subsets did not differ in their expression of CD40 and CD86, although CD86 was expressed at higher levels compared to both cDC subsets. The CD14⁺ CD16⁺ monocytes expressed higher levels of CD40 and CD86 compared to CD14⁺ CD16⁻ monocytes (Fig. 3.15). CD86 expression on both monocyte populations was similar to that of the CD14⁻ CD16⁺ SLAN⁺ and SLAN⁻ subsets. CD80 expression was minimal on all cell populations (Fig. 3.15B). Overall, no difference was observed between AS patients and HCs in terms of co-stimulatory molecule expression on DCs, monocytes and CD14⁻ CD16⁺ mononuclear populations.

3.8 Further characterisation of DCs and monocytes

To further characterise myeloid cell subsets in AS patients and HCs, it was important to look at expression of several key surface markers. The aim of this characterisation was to further understand the identity of several cell subsets and the inter-relationship between subsets.

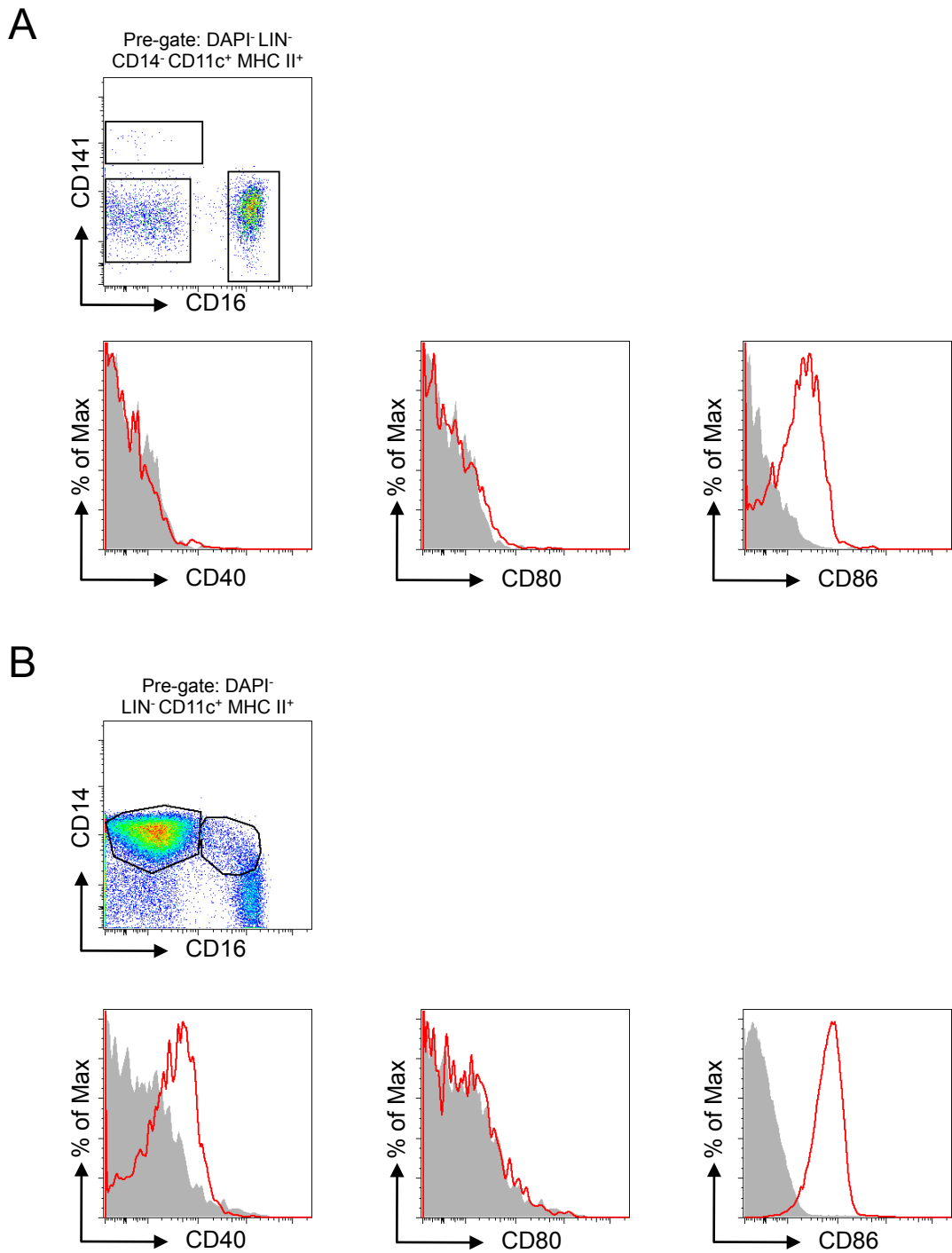


Figure 3.14: Co-stimulatory molecule expression on cDC and monocyte subsets

Expression of CD40, CD80 and CD86 on blood cDC and monocyte subsets. **(A)** cDC subsets and CD16 mononuclear cells (DAPI⁻ LIN⁻ CD14⁻ CD11c⁺ MHC II⁺ - top) were analysed for expression of CD40, CD80 and CD86. Representative histogram plots are shown for CD1c⁺ DCs (bottom). **(B)** CD14⁺ CD16⁻ and CD14⁺ CD16⁺ monocytes (top) were studied for the expression of the activation molecules CD40, CD80 and CD86. Representative histograms depicting CD40, CD80 and CD86 expression on CD14⁺ CD16⁻ monocytes (bottom). Isotypes are shown in shaded grey histograms with marker shown in red.

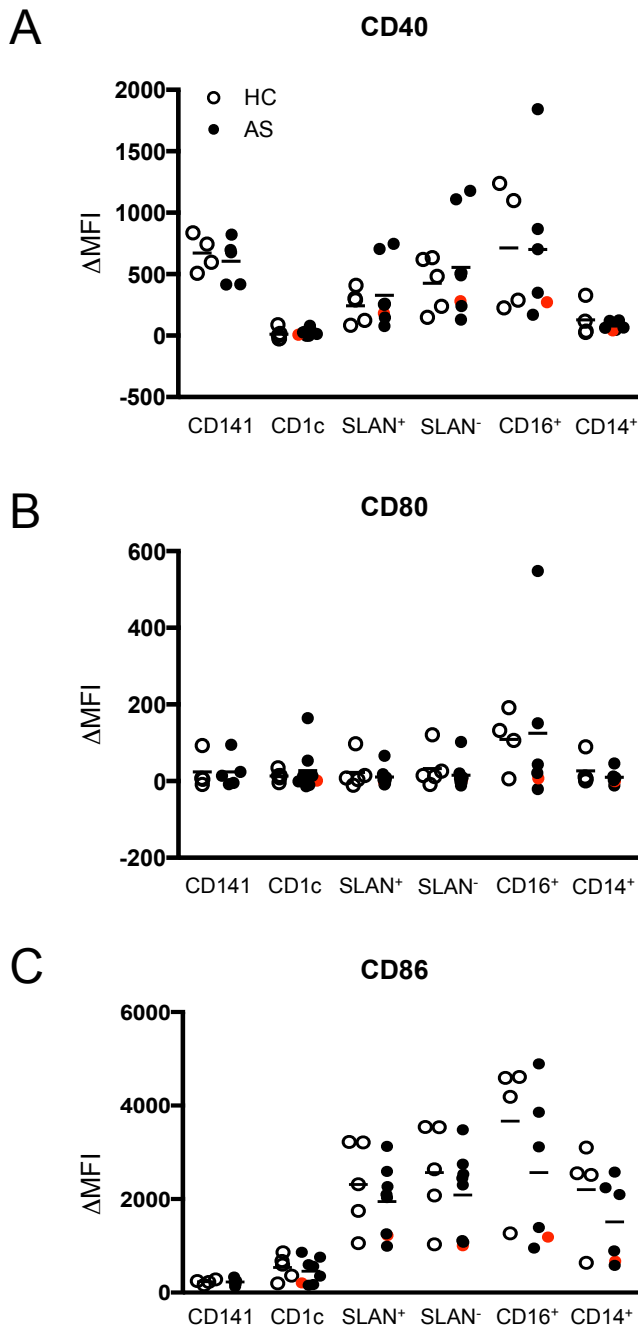


Figure 3.15: Expression of DC co-stimulatory molecules – CD40, CD80 and CD86

Comparison of CD40, CD80 and CD86 on blood cDC and monocyte subsets between AS patients and HCs. Level of CD40 (**A**), CD80 (**B**) and CD86 (**C**) on cDC and monocyte subsets for AS patients (filled circles) and HCs (empty circles). Subsets analysed: CD141⁺ (CD141) and CD1c⁺ DCs (CD1c), CD14⁻ CD16⁺ SLAN⁺ (SLAN⁺) and CD14⁻ CD16⁺ SLAN⁻ (SLAN⁻) mononuclear cells, CD14⁺ CD16⁺ (CD16⁺) and CD14⁺ CD16⁻ (CD14⁺) monocyte subsets. Expression was assessed by Δ MFI: geometric mean of marker expression – geometric mean of subset isotype. AS red dot = B27 patient. All graphs show mean. 5 HCs and 8 AS patients were used for analysis.

3.8.1 Monocytes

To clarify the differences between monocytes and DCs, the surface marker profile of both CD14⁺ monocyte subsets - CD14⁺ CD16⁻ and CD14⁺ CD16⁺ - was assessed. In humans, CD11b and CD64 are predominantly expressed on monocytes and macrophages. In conjunction, CX3CR1 can be used to identify monocyte subsets in both mice and men (229). Both monocyte subsets expressed high levels of CD11b (Fig. 3.16A), CD64 (Fig. 3.16B) and CX3CR1 (Fig. 3.16C), and at relatively similar levels. However direct comparison of these markers, especially CD11b and CD64, is difficult due to differences in background isotype staining. As expected, both monocyte subsets were negative for the DC marker CD135 (Fig. 3.16D).

3.8.2 DCs

CD141⁺ and CD1c⁺ DC subsets isolated from a HC were subsequently analysed for the surface expression of CD11b, CD64, CD135 and CX3CR1, compared to the appropriate isotype-matched negative control for each cell subset (Fig. 3.17). CD141⁺ DCs were found to lack expression of CD11b and CD64 (Fig. 3.17A/B). However, CD1c⁺ DCs expressed intermediate levels of both these markers (Fig. 3.17A/B), when compared to CD14⁺ CD16⁻ monocytes (Fig. 3.16A/B). Based on the surface phenotype of the DC subsets described so far, it was no surprise that the CD141⁺ DCs lacked CX3CR1 expression whilst the CD1c⁺ DCs expressed intermediate levels of this molecule (Fig. 3.17C). CX3CR1 levels on CD1c⁺ DCs were described as intermediate given the high levels of CX3CR1 expression observed on CD14⁺ monocytes (Fig. 3.16C). As stated previously, CD135 is a marker commonly associated with DC subsets and their progenitors (286, 570-572). Interestingly, CD135 was predominantly expressed on the CD141⁺ DC subset, with little expression being detected on the CD1c⁺ DC subset (Fig. 3.17D). Overall, CD141⁺ and CD1c⁺ DC subsets differed in their expression of the surface markers analysed. CD141⁺ DCs lacked expression of the monocyte/macrophage markers CD11b, CD64 and CX3CR1, but expressed CD135 (Fig. 3.17). In contrast, CD1c⁺ DCs did not express CD135 but did display intermediate levels of CD11b, CD64 and CX3CR1 (Fig. 3.17), compared to blood monocytes (Fig. 3.16).

3.8.3 CD14⁻ CD16⁺ mononuclear cells

Due to the heterogeneity regarding SLAN expression within the LIN⁻ CD11c⁺ MHC II⁺ CD14⁻ CD16⁺ population, expression of the same surface markers described above were

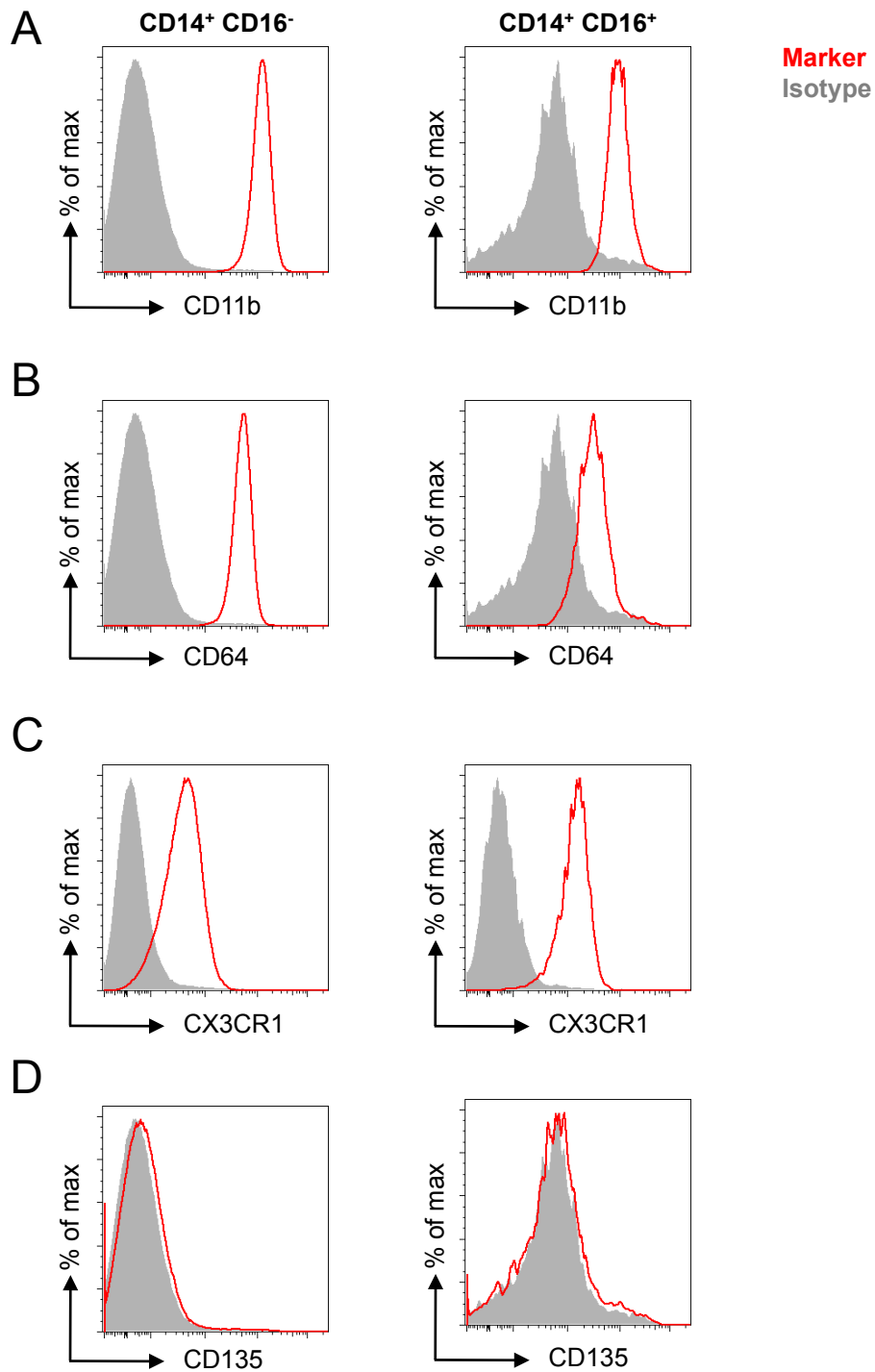


Figure 3.16: Surface phenotype of CD14⁺ CD16⁻ and CD14⁺ CD16⁺ monocytes

PBMCs were isolated from peripheral blood of a healthy control, and CD14⁺ monocyte subsets were analysed for expression of CD11b (**A**), CD64 (**B**), CX3CR1 (**C**) and CD135 (**D**). The appropriate isotype control – Mouse IgG1κ (CD11b, CD64 and CD135) and Rat IgG2b (CX3CR1) are represented in grey filled histograms. Marker expression is depicted in red for each monocyte subset. Expression of these markers on CD14⁺ CD16⁻ (left) and CD14⁺ CD16⁺ (right) monocytes is presented. Gating strategy described in Fig. 3.6A was used for this analysis.

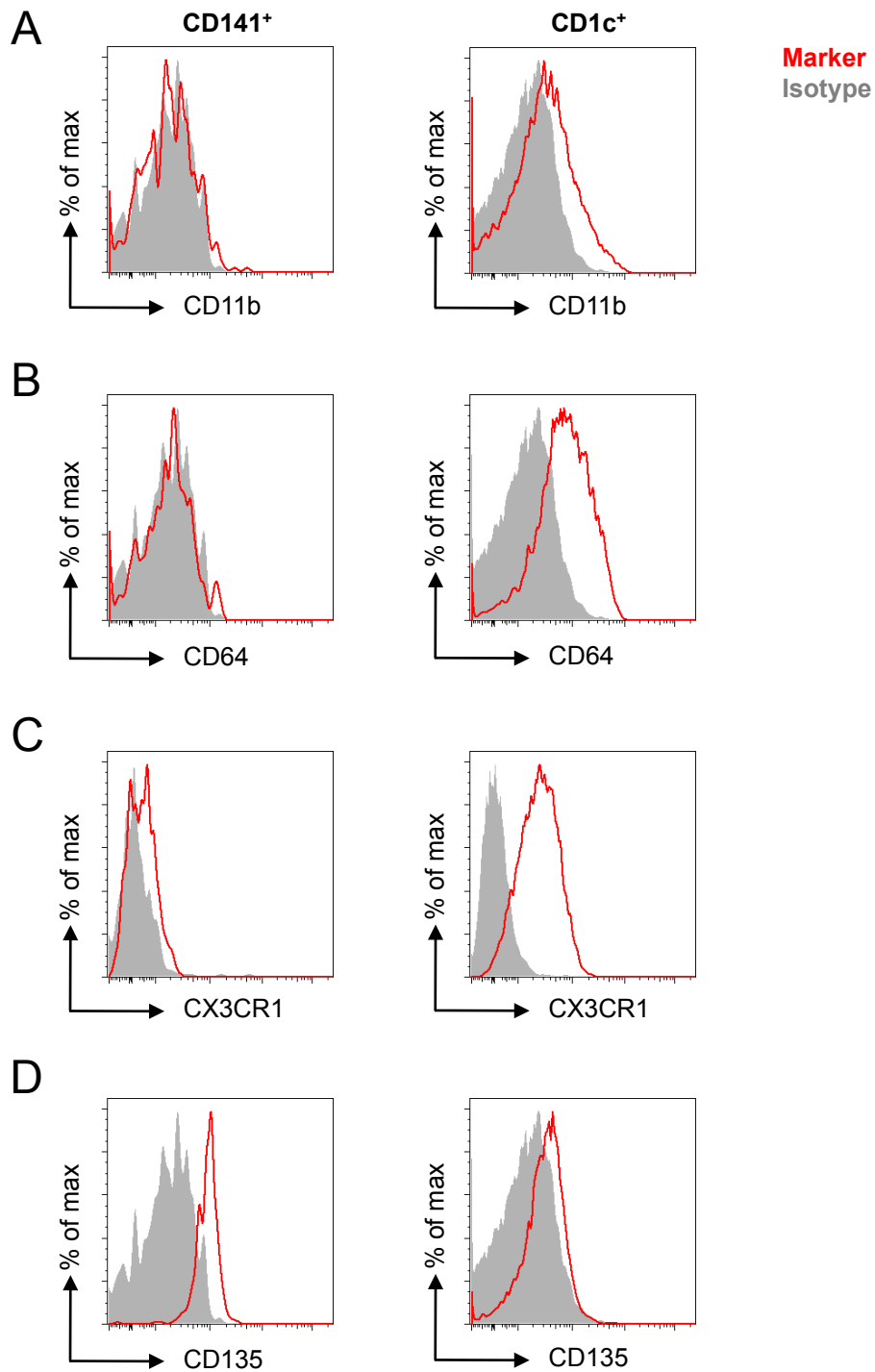


Figure 3.17: Expression of CD11b, CD64, CD135 and CX3CR1 on DC subsets

PBMCs were isolated from peripheral blood from a healthy control and analysed for the expression of several surface markers including CD11b (**A**), CD64 (**B**), CX3CR1 (**C**) and CD135 (**D**). The appropriate isotype controls – Mouse IgG1 κ (CD11b, CD64 and CD135) and Rat IgG2b (CX3CR1) are shown in the grey filled histograms. Marker expression is depicted in red for each DC subset. Expression of these markers on CD141⁺ DCs (left) and CD1c⁺ DCs (right) is depicted above. Gating strategy described in Fig. 3.6A was used for this analysis.

investigated for both SLAN⁻ and SLAN⁺ subsets. Both subsets expressed CD11b at intermediate levels (Fig. 3.18A) when compared to CD14⁺ monocytes (Fig. 3.16A). CD11b expression was slightly lower on the CD16⁺ SLAN⁺ subset than the CD16⁺ SLAN⁻ population (Fig. 3.18A). CD64 was expressed at intermediate levels on both SLAN subsets (Fig. 3.18B) in comparison to monocytes (Fig. 3.16B). CX3CR1 was expressed homogeneously on total CD14⁻ CD16⁺ cells (Fig. 3.18C). Both CD16⁺ SLAN⁻ and CD16⁺ SLAN⁺ subsets lacked expression of CD135 (Fig. 3.18D), unlike conventional CD141⁺ DCs (Fig. 3.17D). Overall, CD16⁺ SLAN⁻ and CD16⁺ SLAN⁺ mononuclear cells had a very similar profile of surface marker expression for CD11b, CD64, CX3CR1 and CD135. Although CD16⁺ SLAN⁺ cells had slightly lower levels of CD11b expression than CD16⁺ SLAN⁻ cells, this difference would be insufficient to distinguish between the two subsets based on this analysis.

3.8.4 CD115 expression on blood mononuclear cells

CD115, through its interaction with CSF-1 is critical for macrophage function and survival (573, 574). When cDC subsets were assessed for CD115 expression, it was noted that the CD141⁺ population completely lacked CD115 expression, whilst the CD1c⁺ subset was heterogeneous for this marker (Fig. 3.19A). Additionally, monocyte subsets were analysed for the expression of CD115 (Fig. 3.19B/C). Progression along the monocyte “waterfall” from population A to C (Fig. 3.8A) was accompanied by an increase in CD115 expression. CD14⁺ CD16⁻ lacked detectable surface CD115, whilst the CD14⁺ CD16⁺ monocyte population expressed intermediate levels of this molecule. The majority of the CD14⁻ CD16⁺ population homogeneously expressed high levels of CD115 (Fig. 3.19B/C).

3.9 Expression of zDC by circulating myeloid populations

Recently, expression of the transcription factor *Zbtb46* (zDC) has been reported to be specific to the DC lineage, thereby allowing separation of monocytes/macrophages and DCs (575). Due to the uncertainty regarding the identity of the CD14⁻ CD16⁺ population (monocyte or DC), zDC expression was tested on CD14⁺ CD16⁻ monocytes, CD14⁻ CD16⁺ mononuclear cells and CD1c⁺ DCs (Fig. 3.20A) by qRT-PCR. All subsets tested were compared to CD14⁺ CD16⁻ monocytes, as they had previously been shown to lack expression of this transcription factor (575). CD1c⁺ DCs expressed high levels of zDC, confirming their identity as a putative cDC subset (Fig. 3.20A). Expression of zDC on the heterogeneous population of CD14⁻ CD16⁺ cells was found to be minimal and similar to

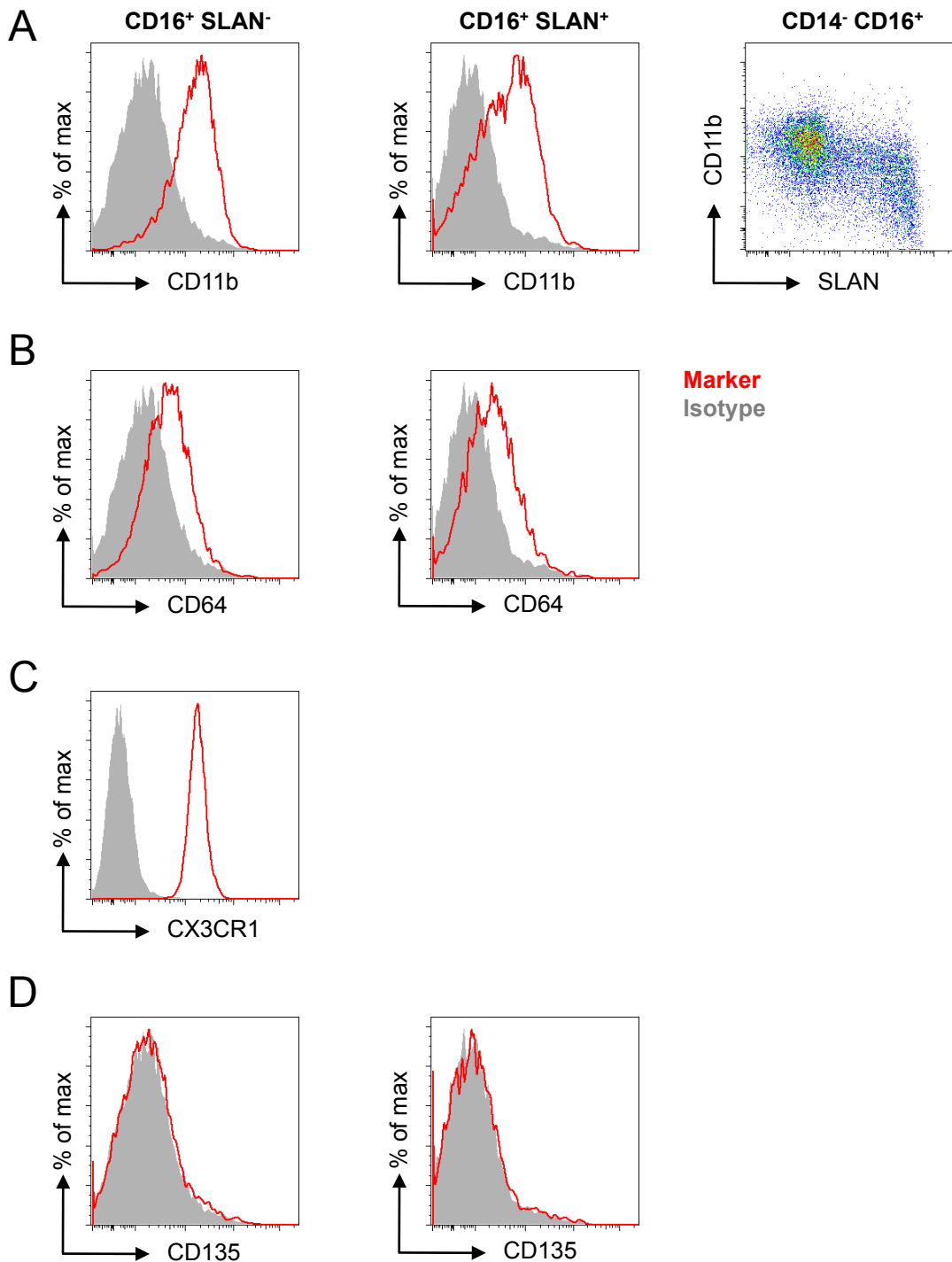


Figure 3.18: Surface phenotype of CD16⁺ SLAN⁻ and CD16⁺ SLAN⁺ mononuclear cells

PBMCs were isolated from peripheral blood of a HC and CD16⁺ mononuclear subsets were analysed for the expression of several surface markers. **(A)** Histograms showing CD11b expression on SLAN⁺ and SLAN⁻ CD16⁺ subsets. FACS plot of SLAN and CD11b expression on total CD14⁻ CD16⁺ cells. **(B)** Histograms show expression of CD64 on CD16⁺ subsets. **(C)** Expression of CX3CR1 on total CD11c⁺ MHC II⁺ CD14⁻ CD16⁺ cells. **(D)** Expression of CD135 on CD16⁺ subsets. The appropriate isotype controls – Mouse IgG1κ (CD11b, CD64 and CD135) and Rat IgG2b (CX3CR1) are shown in the grey filled histograms. Marker expression is depicted in red. Gating strategy described in Fig. 3.6A was used for this analysis.

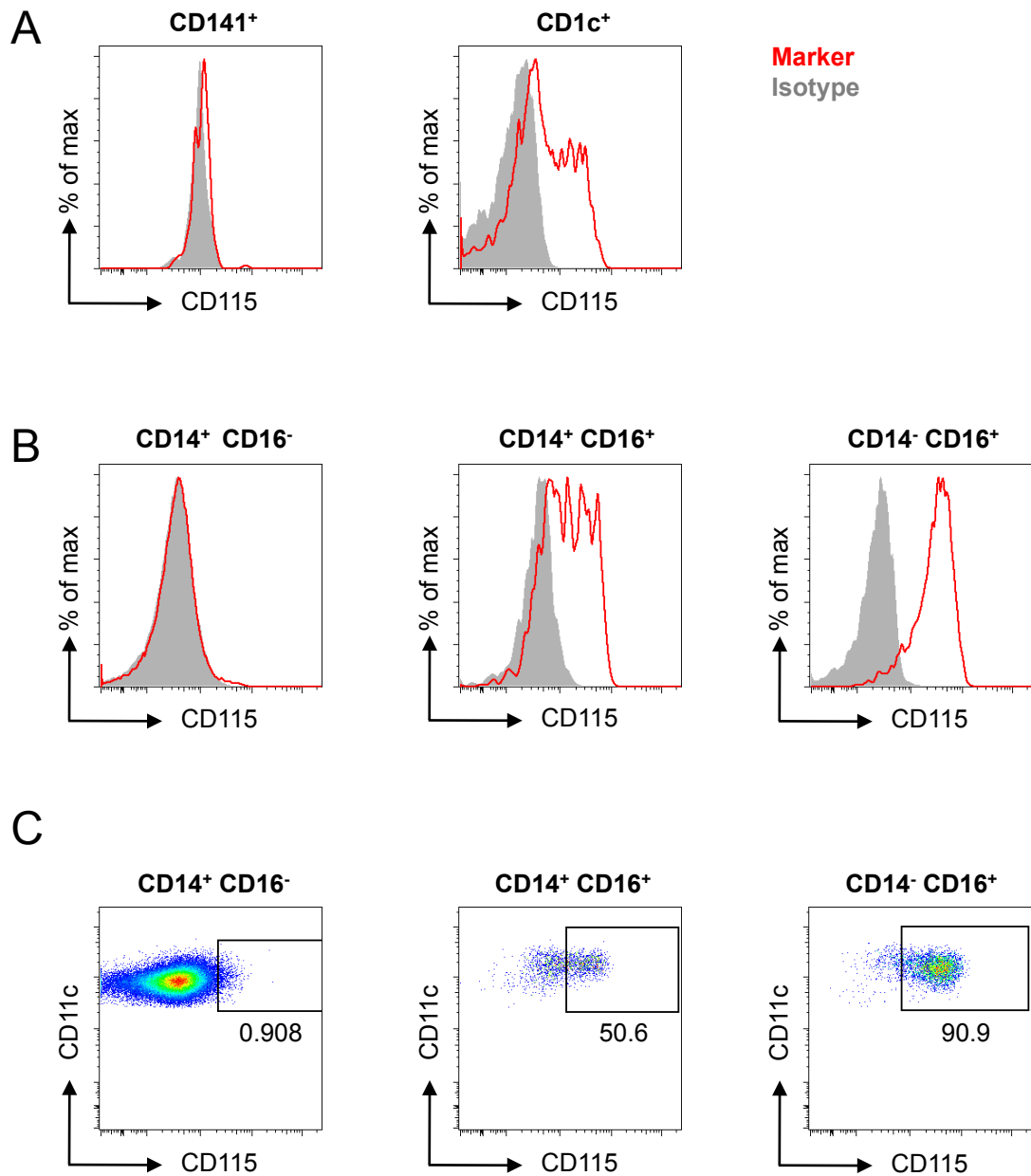


Figure 3.19: Surface expression of CD115 on DC and monocyte subsets

PBMCs were isolated from peripheral blood of a HC. CD11c⁺ MHC II⁺ cell subsets were analysed for the expression of CD115. **(A)** Histogram plots showing CD115 expression on CD141⁺ (left) and CD1c⁺ (right) DC subsets. **(B)** CD115 expression on mononuclear cell subsets – CD14⁺ CD16⁻ (left), CD14⁺ CD16⁺ (centre) and CD14⁻ CD16⁺ (right). **(C)** Representative FACS plots of CD115 expression on CD14⁺ CD16⁻ (left), CD14⁺ CD16⁺ (centre) and CD14⁻ CD16⁺ (right) cell subsets. Numbers represent percentage of parent population. Isotype control (Rat IgG2aκ) is represented by the grey solid histograms. Marker expression is depicted in red for each subset. Gating strategy described in Fig. 3.1A was used for analysis.

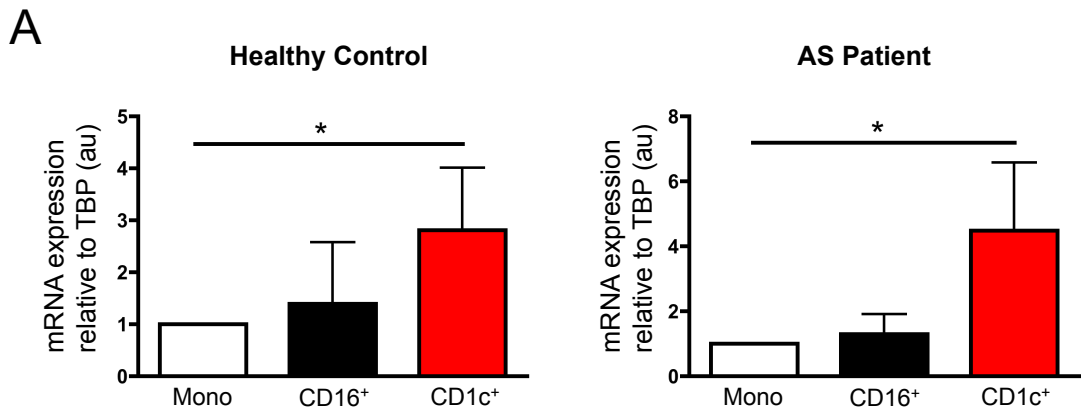


Figure 3.20: Zbtb46 (zDC) expression by DC and monocyte subsets

PBMCs were isolated from peripheral blood of HCs and AS patients; DC/monocyte subsets were flow sorted for qRT-PcR analysis of Zbtb46 (zDC) expression. **(A)** Quantification of zDC expression in HCs (left) and AS patients (right) in CD14⁺ monocytes, CD1c⁺ DCs and CD14⁻ CD16⁺ mononuclear cells. Monocytes were used as the reference subset (1) and mRNA expression is relative to the endogenous control, TATA binding protein (TBP). Data were analysed using a Mann-Whitney test. * = p<0.05. Error bars show mean + SD, au = arbitrary units.

that observed for CD14⁺ CD16⁻ monocytes (Fig. 3.20A). No difference in subset zDC expression was observed between AS patients and HCs (Fig. 3.20A). However, due to the discovery of the heterogeneity within the CD14⁻ CD16⁺ population, it was important to characterise zDC expression by CD16⁺ SLAN⁻ and CD16⁺ SLAN⁺ subsets. Unfortunately, this experiment did not work and will have to be repeated to establish zDC expression on both subsets of CD14⁻ CD16⁺ mononuclear cells.

3.10 Discussion

Inadequate tools and markers available for identification of DCs initially hampered their quantification and functional assessment in disease pathogenesis. Due to the location, function and diversity of DC populations, understanding their involvement in disease induction and pathology may enable improved development of disease therapeutics. Human DC biology has advanced through the identification of several human DC specific markers and utilisation of gene arrays permitting cross-species analysis (202, 203, 209, 210, 393, 576). Analysis of DC populations in chronic and autoimmune diseases, has led to their exploitation for use in disease specific targeted therapies. To date, patients have been shown to successfully tolerate DC therapy, although efficacy of these therapies remains uncertain (577-579). However, recent advances in generating human tolerogenic DCs have shown promise for future treatment strategies in RA (580).

Functional assessment and quantification of DCs has been performed for several diseases including RA and systemic lupus erythematosus (SLE) (217, 581-585). To the best of my knowledge, not one paper has been published examining the function and phenotype of peripheral blood DC subsets in AS *ex vivo*. Previous studies have relied on the generation of monocyte-derived DCs (moDCs) (546, 547). In these studies, blood monocytes are cultured *in vitro*, predominantly in the presence of GM-CSF and IL-4 to generate moDCs. These cultures generate large cell numbers for analysis and overcome the difficulties associated with isolating rare populations. The *in vitro* generated AS patient and HC moDCs were assessed functionally with regard to: cytokine secretion and maturation status. Robbins et al have shown that GM-CSF-cultured *in vitro* derived moDCs are more representative of monocytes/macrophages than of DCs (393). Therefore, moDCs do not sufficiently represent *in vivo* human DC populations. To investigate the properties of bona-fide DCs, AS patient and HC DC populations were examined *ex vivo*. It was predicted that there would be differences between AS patient and HC DCs because of the recently identified systemic DC defect in HLA-B27 TG rats, a model of spondyloarthritis (SpA)

(480). HLA-B27 TG rats lacked a specific subset ($CD172a^{lo} CD11b^{int} CD103^{+}$) of intestinal DCs, whilst the remaining DC populations preferentially induced Th17 responses (479, 480). Additionally, this missing $CD172a^{lo}$ population has previously been shown to possess tolerogenic properties (372). Therefore, DCs in HLA-B27 TG rats may be involved in the development of SpA through loss of tolerance. Accordingly, detailed functional and phenotypic analyses of AS patient DCs may improve the understanding of this chronic inflammatory disease.

For blood DC analysis, all or a fraction of 45 AS patients and 29 HCs were used. Patient clinical parameters including disease severity (BASDAI and BASMI), inflammation status (ESR and CRP), spinal disease levels, extra-articular tissue involvement and disease treatment protocols were collated and are portrayed in Table 3.1. AS is historically associated with young males (4), and the patient cohort corresponds with this assessment with 75% being male. The average age of the patient cohort was approximately 55 years, and would therefore initially appear to contradict the link between AS and young males. However, typical disease duration was approximately 30 years signifying early disease onset. Most patients expressed HLA-B27 (91%); this MHC I molecule provides the strongest genetic association of any inflammatory disease (11, 26). Characteristics of the study cohort include mid-range disease scores and low levels of the inflammatory markers ESR and CRP (Table 3.1). These features support the notion that AS is a disease associated with low levels of chronic spinal inflammation and bone formation, rather than severe inflammatory infiltrate as is observed in RA (564). Patients presented with various levels of spinal disease (sacroiliitis and/or bony changes within spinal regions), with approximately 30% of patients presenting with extra-articular disease. The presence of individual extra-articular manifestations may affect circulating immune populations, however this cohort is insufficiently powered to assess this hypothesis. Furthermore, disease treatment regimens and levels of inflammation may affect the immunological profile of patients. For example, anti-TNF α treatment has been reported to increase circulating myeloid DCs in the blood of AS patients (586). These correlations will be analysed and discussed in chapter 7.

Using the patient and HC cohorts described in Table 3.1, the initial aim was to identify and enumerate circulating DC and monocyte populations. In blood, several populations of mononuclear cells were detected, including two cDC subsets, $CD141^{+}$ and $CD1c^{+}$ DCs (Fig. 3.1); two monocyte populations, $CD14^{+} CD16^{-}$ and $CD14^{+} CD16^{+}$ (Fig. 3.1); pDCs (Fig. 3.2A) and a $CD14^{-} CD16^{+}$ mononuclear population (Fig. 3.6). Classification of the

CD14⁻ CD16⁺ mononuclear population remains contentious, and it is often referred to as the third blood monocyte population in humans (231, 236, 237, 354, 587). However, this subset is not homogeneous as approximately 60% express the historical DC marker M-DC8 or SLAN (Fig. 3.7B) (237, 239, 240, 588). Throughout this thesis I will try to address the heterogeneity of this population through phenotypic analyses, with the hope of elucidating the identity of this subset.

AS patients had significantly more PBMCs per ml of blood compared to HCs (Fig. 3.3A). This finding can perhaps be attributed to the inflammatory environment associated with disease development. Compared to HCs, a trend towards a reduced proportion of total cDCs (CD141⁺ and CD1c⁺ subsets) was observed in AS patients, although this did not reach significance (Fig. 3.3.C). Several groups have reported reduced proportions of circulating DC in diseased individuals. One such disease is RA, in which the reduction in circulating DCs was attributed to enhanced recruitment to the inflamed synovium, where DCs are thought to contribute to disease pathogenesis through IL-23p19 secretion and induction of Th17 responses (217, 582). The study carried out by Jongbloed et al compared only 12 RA patients and HCs in addition to excluding CD141⁺ cDCs from their myeloid DC analysis (217). These discrepancies prevent direct correlation of these studies, however results presented here suggest that the proportion of total circulating cDCs did not differ dramatically between AS patients and HCs.

Given the reported importance of DCs in driving disease pathology in diseases such as RA and our observations in the HLA-B27 TG rat model, it was not prudent to rule out a potential role for DCs in AS pathogenesis based on total cDC analysis alone. As discussed, circulating cDCs can be subdivided into two subsets on the basis of their expression of CD141 and CD1c. The MHC II⁺ CD103⁺ CD11b^{int} CD172a^{lo} DC subset in rats is equivalent to the CD141⁺ human DC subset. As previously shown, this migrating intestinal population was absent from intestinal lymph of HLA-B27 TG animals (480). Loss of this tolerogenic population promoted generation of Th17 responses (480). It was therefore hypothesised that compared to HCs, the CD141⁺ cDC subset would be reduced or absent in AS patients. The obtained results, however, led to rejection of this hypothesis as no differences either in proportion or number of CD141⁺ cells between AS patients and HCs were detected (Fig. 3.4A). This population accounts for approximately 0.02% of live PBMCs, and thus given the rarity of this blood population, slight changes may be difficult to detect.

The original hypothesis was formed on the basis of lymph migrating and MLN resident populations in HLA-B27 TG rats. As blood was the only tissue available for this study, it is still possible that tissue resident CD141⁺ DCs are deficient in AS patients. The presence of mature circulating blood DCs in mice and rats remains controversial (Vuk Cerovic, unpublished results) (207, 390), again hindering direct comparison of our human and rat observations. Future studies could isolate and investigate the role of intestinal CD141⁺ DCs in human disease. Another consideration relates to the suitability of HLA-B27 TG rats for assessing AS pathogenesis. Although these animals develop SpA-like symptoms, their degree of spinal involvement is minimal (458). Consequently, this model may not adequately replicate human disease, especially that of AS. Although it is not possible to ignore the chance that CD141⁺ cDCs may be diminished within afflicted tissues such as the intestine, these data show that circulating CD141⁺ DCs were not diminished in AS patients, allowing rejection of the hypothesis at the present time.

The major blood cDC population (CD1c⁺ DCs, ~95%) was significantly reduced in AS patients, as proportion of CD11c⁺ MHC II⁺ cells (Fig. 3.4B). This observation was not reflected when presented as total cell number or proportion of live cells. The reduction as proportion of CD11c⁺ MHC II⁺ may reflect expansion of the other LIN⁻ CD14⁻ CD11c⁺ MHC II⁺ population: CD14⁻ CD16⁺ mononuclear cells. This will be discussed in depth later. However, to complete the thorough characterisation of circulating DC subsets, pDCs were enumerated. No significant difference was observed between AS patients and HCs in terms CD123⁺ CD304⁺ pDCs (Fig. 3.4C). Therefore, due to observations in the HLA-B27 TG rat model and their role in the induction and skewing of immune responses, cDCs and not pDCs became the focus of the project. Consequently, pDCs were not included in subsequent analyses regarding maturation and functional assessment. Therefore future studies are required to elucidate the role of pDCs disease pathogenesis.

Initial results suggest that some cDC populations are altered in AS patients. For these analyses, patient clinical parameters were not considered, but clinical and immunological correlative analyses were performed and are discussed in Chapter 7. That being said, the effect of HLA-B27 on immunological parameters was assessed throughout this study. Even though the genetic association between AS and HLA-B27 was described 40 years ago (24), the role of this gene in disease pathogenesis still remains elusive. Thus, the aim was to identify any relationship between HLA-B27 expression and frequency of blood DC populations. Unfortunately this study was not sufficiently powered to draw any definitive conclusions regarding HLA-B27 involvement, as only 6 HLA-B27⁺ HC individuals and 4

HLA-B27⁻ AS patients were included. Despite this, no obvious patterns regarding HLA-B27 involvement and blood DC parameters were observed (Fig. 3.4 and 3.5). Larger patient and HC cohorts would be required to fully assess the role of HLA-B27 expression in disease pathogenesis and circulating myeloid populations.

Quantification of AS patient and HC blood DCs highlighted a high degree of variation within both cohorts. This is an unfortunate yet unavoidable aspect of working with clinical samples. Within the HC cohort, the proportion of CD1c⁺ DCs as percentage of CD11c⁺ MHC II⁺ cells ranged from 12% to 76%. This variation prompted a study where cDC proportions were monitored over time in individual blood donors. Proportional analysis of CD141⁺ and CD1c⁺ DCs and CD14⁻ CD16⁺ mononuclear cells was performed using two HC individuals. These results suggest that populations do not vary drastically over time (Fig. 3.5). Given that proportions appear relatively stable over time, above and below average cell subsets proportions may not be attributable to underlying or unknown infections, exercise or stress. Taken together, the variation within both cohorts may not be attributable to inflammation. However, as only two HCs were used for this analysis, further experiments should be performed to validate these observations. Furthermore, comparative analysis of AS patient samples over time was not performed. Given the clinical and immunological parameter variation within the patient cohort, it would be of interest to assess DC proportions over time.

As stated above, classification of the CD14⁻ CD16⁺ mononuclear population is controversial. A significant proportion (60%) of CD14⁻ CD16⁺ mononuclear cells express the surface marker SLAN or M-DC8 (Fig. 3.7B). SLAN⁺ cells are reported to possess DC-like morphology (239, 240, 588). The majority of SLAN⁺ cells expressed CD16 whilst lacking expression of CD1c, CD14, CD19, CD56, CD2 and CD83. SLAN⁺ CD16⁺ cells were capable of stimulating T cells in a mixed leukocyte reaction (MLR), presenting antigen via recall responses and promoting cytotoxic T cell responses to a greater extent than CD14⁺ monocytes (240). Recently, SLAN⁺ cells have been reported to be principal producers of IL-12p70, IL-1 β and IL-23p19 following TLR stimulation, with several groups suggesting a role for this pro-inflammatory, Th1 associated DC population in psoriasis and SLE pathogenesis (249, 252, 359). These findings support the premise that CD14⁻ CD16⁺ SLAN⁺ cells are a distinct subset of circulating DCs. Principal component analysis (PCA) performed by Cros et al showed clustering of total CD14⁻ CD16⁺ mononuclear cells, regardless of SLAN expression (237). These results appear to contradict the supposition that SLAN⁺ cells are distinct from their SLAN⁻ counterparts.

Importantly though, CD14⁻ CD16⁺ cells expressed a discrete set of genes in comparison to CD14⁺ CD16⁻ and CD14⁺ CD16⁺ cells (237). These differentially expressed genes included scavenger receptors (CXCL16 and CD163) and apolipoproteins (237). These data suggest that the CD14⁻ CD16⁺ cells express a distinct set of genes, differentiating them from CD14⁺ CD16⁻ and CD14⁺ CD16⁺ monocytes. Consequently, CD14⁻ CD16⁺ cells may represent a different stage of monocyte differentiation. In support for this statement, the murine equivalents of the CD14⁻ CD16⁺ mononuclear population (Ly6C^{lo} monocytes) have been recently reported to be derived from the murine equivalent of CD14⁺ CD16⁻ monocytes (Ly6C^{hi} monocytes) under steady state conditions (589).

Alternatively, the CD14⁻ CD16⁺ cells may not represent a third blood monocyte population. In addition to PCA analysis, Cros et al functionally assessed these subsets *in vivo*. Purified monocytes and total CD14⁻ CD16⁺ mononuclear cells were transferred into Rag2^{-/-} Il2rg^{-/-} CX3CR1^{-gfp} mice (237). CD14⁻ CD16⁺ cells were observed to attach and migrate along blood vessel endothelium (237). The authors concluded that human CD14⁻ CD16⁺ mononuclear cells were equivalent to the “patrolling” Gr1⁻ murine monocyte subset (237). Whilst performing this surveillance function, CD14⁻ CD16⁺ cells were functionally distinct from CD14⁺ CD16⁻ monocytes in terms of ROS production, MPO and lysozyme expression and phagocytosis uptake (237). Of note CD14⁻ CD16⁺ mononuclear cells phagocytosed particles less efficiently than CD14⁺ CD16⁻ monocytes (237). Taken together these results suggest that CD14⁻ CD16⁺ mononuclear cells are functionally distinct from CD14⁺ CD16⁻ blood monocytes. In contrast to Hansel et al, Cros et al found blood CD14⁻ CD16⁺ cells to be somewhat anti-inflammatory (237, 249, 252). Despite these recent publications, classification of CD14⁻ CD16⁺ mononuclear cells, either as a DC or monocyte population, remains uncertain. Given the functional and phenotypic heterogeneity of the CD14⁻ CD16⁺ mononuclear population, SLAN⁺ and SLAN⁻ cells may reflect different stages of monocyte maturation. Alternatively, the CD14⁻ CD16⁺ population may contain both DCs (SLAN⁺) and monocytes (SLAN⁻). Chapter 6 concentrates on the functional capabilities of DCs, CD14⁺ CD16⁻ monocytes and CD14⁻ CD16⁺ mononuclear cells isolated from AS patients and HCs.

Given the involvement of the CD14⁻ CD16⁺ mononuclear population in RA and SLE pathogenesis, and the observation that CD1c⁺ DCs were significantly reduced in AS patients as proportion of CD11c⁺ MHC II⁺ cells, CD14⁻ CD16⁺ mononuclear cells were identified and enumerated in AS patients and HCs (249, 252, 359). No difference in the proportion of SLAN⁺ and SLAN⁻ subsets was observed between AS patients and HCs (Fig.

3.7). However, a trend towards increased proportions of circulating total CD14⁻ CD16⁺ mononuclear cells in AS patients was observed. CD14⁻ CD16⁺ cells are identified within the LIN⁻ CD14⁻ CD11c⁺ MHC II⁺ population, together with CD141⁺ and CD1c⁺ DCs. Therefore, the reduction in CD1c⁺ DCs, as proportion of CD11c⁺ MHC II⁺, may be counterbalanced by an increase in CD14⁻ CD16⁺ mononuclear cells. Consequently, AS patients may have an increased proportion of circulating CD14⁻ CD16⁺ mononuclear cells compared to HCs. Published reports have not yet reached consensus regarding the pro- or anti-inflammatory properties of this population, and thus it would be important to study the functions of these cells to establish whether they could have a role in AS disease pathogenesis.

Monocytes are rapidly recruited to sites of inflammation where they contribute to the immune response through secretion of pro-inflammatory cytokines (237, 238, 359, 590). Additionally, monocytes are believed by some to contribute to the tissue DC pool under steady state and inflammatory conditions (226, 228, 591-593). Again this topic is highly contentious with recent studies disputing this supposed monocyte function (225, 234). Much of this confusion results from use of overlapping markers used to identify DCs and macrophages. As discussed previously, *in vitro* moDCs have been utilised for AS DC phenotypic and functional analyses. Given the importance of monocyte functions in the immune response, and their exploitation for DC analysis in AS studies, CD14⁺ CD16⁻ and CD14⁺ CD16⁺ monocytes in AS patients and HCs were identified and enumerated. No differences were observed in the proportions of either monocyte subset between AS patients and HCs (Fig. 3.9), which has not previously been reported in AS. Overall, these results suggest that changes in the frequencies of circulating blood monocytes do not change with AS disease pathology. Assessing monocyte and tissue resident macrophage function in AS patients and HCs may however provide important information regarding monocytes and disease pathogenesis.

Overall, we have observed small changes to the proportion of circulating myeloid populations in AS patients. Compared to HCs, AS patients have a reduced proportion of CD1c⁺ DCs that may be counterbalanced by CD14⁻ CD16⁺ mononuclear cells. Consequently, these populations may be involved in disease pathogenesis given their reported functions *in vivo*. Functional assessment of both populations will be presented and discussed in Chapter 6.

Murine DCs were initially characterised by Ralph Steinman in 1973 as adherent cells that constantly extend and retract processes (dendrites) and possessed large “contorted” nuclei (185). Based on these observations, the morphology of circulating myeloid populations in AS patients and HCs was characterised (Fig. 3.10). These experiments could additionally aid classification of CD14⁻ CD16⁺ monocytes based on their morphological appearance. Unfortunately, SLAN⁺ and SLAN⁻ subsets were not individually purified for this experiment. Both DC subsets (CD141⁺ and CD1c⁺) uniformly possessed lobulated nuclei, commonly associated with granulocytes. However, as the majority of granulocytes are removed from blood leukocytes during the density gradient stage of blood separation, and through exclusion of lineage positive cells (including CD15 and CD56) during cell sorting we can reject the possibility of granulocyte contamination contributing to the unusual morphological appearance of these myeloid populations. Steinman et al referred to DCs as possessing “contorted” nuclei (185). Therefore the “lobulated” nuclei most likely represent previously described DC morphologic characterisations. However, given their unusual appearance and the potentially harsh methods used to isolate immune populations, it was possible that cell death was contributing to these morphological characteristics. However cell death and apoptosis, assessed by annexin V and DAPI staining, were minimal following cell isolation (Fig. 3.12). Therefore, lobulated nuclei can be considered characteristic of live human circulating DCs. In support, several papers have published similar findings regarding blood cDC morphology (202, 594). Despite the unusual morphology of blood DCs, no differences between AS patients and HCs were seen. However, morphological assessment in terms of dendrite formation and number of cytoplasmic granules was not performed, and consequently, it is possible that there are subtle morphological differences between AS patient and HC DCs.

Morphological analysis was additionally performed for CD14⁻ CD16⁺ mononuclear cells and pDCs. Interestingly, CD14⁻ CD16⁺ mononuclear cells possessed similar morphology to that of blood cDC populations (Fig. 3.9D). Unfortunately morphology of SLAN⁺ and SLAN⁻ subsets was not individually assessed. These experiments did not enable exclusive classification of CD14⁻ CD16⁺ as a DC or monocyte population based on morphology alone, although it was notable that the appearance of CD14⁻ CD16⁺ cells closely resembled that of blood cDCs. In contrast, pDCs were similar to lymphocytes in morphology with large nuclei and little surrounding cytoplasm (Fig. 3.9C). Similarly, no morphological differences between AS patients and HCs for CD14⁻ CD16⁺ mononuclear cells and pDCs were observed.

Cell migration from peripheral tissue to lymph nodes is often associated with maturation and alterations to the cellular phenotypic and functional attributes. Therefore, myeloid cell morphology was assessed following cell activation: overnight culture in the presence of LPS (Fig. 3.11). Following activation, cell nuclei contracted generating a more compact structure, dendrites were extended and cytoplasmic inclusions could be identified, supporting previous observations (595). Overall, activation altered the morphology of CD141⁺ DCs, CD1c⁺ DCs and CD14⁻ CD16⁺ mononuclear cells. These data suggest that cell morphology adapts to the surrounding environment.

As previously mentioned, the maturation status of DCs may influence whether the induced immune response is pro-inflammatory or tolerogenic. Upregulation of co-stimulatory molecules is associated with immunogenic responses, whilst semi-matured DCs are thought to promote tolerogenic responses (184, 190, 329, 596, 597). Given the importance of cell maturation in DC: T cell priming, assessment of DC maturation in AS patients and HCs was measured through expression of the co-stimulatory molecules CD40, CD80 and CD86 (Fig. 3.15). Expression of these co-stimulatory molecules was additionally assessed on CD14⁻ CD16⁺ SLAN^{+/+} mononuclear cells and the two CD14⁺ monocyte subsets. CD40, CD80 and CD86 expression was comparable between AS patients and HCs for all populations. These results indicate that myeloid populations in AS patients are unlikely to favour tolerogenic or immunogenic responses. However, these experiments were performed on circulating populations, and given the previously discussed dubiety surrounding blood DC function, these findings may not be indicative of tissue resident myeloid cell maturation. Therefore, analysis of tissue resident DC subsets may be more informative, with regards to the immune responses being induced at sites of inflammation. In turn these experiments could illuminate the function of individual populations in disease pathogenesis. That being said, co-stimulatory molecule expression on DC subsets was assessed using only 5 HCs and 8 AS patients. However, one study analysing moDCs in AS patients and HCs similarly found no difference in the expression of CD40 and CD86 (546), supporting our observations.

Despite no differences being observed with regards to the cell maturation status of AS patient and HC myeloid populations, several differences were detected between individual cell populations (Fig. 3.15). DC subsets expressed similar levels of CD80 and CD86. However the CD141⁺ DC subset expressed significantly elevated levels of CD40 compared to CD1c⁺ DCs. CD40-CD40L DC: T cell interactions are important for the induction of CD8⁺ T cell responses (598). Therefore, preferential expression of CD40 by CD141⁺ DCs

supports their function as the principal cross-presenting DC population (200, 212, 340). In contrast to cDCs, monocytes and CD14⁻ CD16⁺ mononuclear cells expressed high levels of CD86. This result suggests that circulating monocytes achieve a higher activation status than that of DCs under steady state and inflammatory conditions, potentially reflecting their differential roles in the propagation of immune responses.

To further characterise the five myeloid populations of interest (DCs, monocytes and CD14⁻ CD16⁺ mononuclear cells), several surface markers related to cell function and lineage commitment were analysed. CD135, the receptor for FMS-like tyrosine kinase ligand 3 (Flt3L) controls development and expansion of DCs *in vivo* (571, 572, 599). Expression of CD135 was restricted to CD141⁺ cDCs (Fig. 3.16). These results are obtained from one HC individual, and should be repeated. However, this differential CD135 expression could infer involvement of distinct progenitors and growth factors for the generation of CD141⁺ and CD1c⁺ DCs. Murine CD103⁺ DCs express higher levels of CD135 compared to their CD11b/CD1c⁺ counterparts (380). CD141⁺ DCs are thought to be equivalent to murine lymphoid CD8⁺ DCs and non-lymphoid CD103⁺ DCs (212, 340). Therefore, CD135 expression on human DC subsets mirrors that of their equivalent murine DC populations. This data could suggest that Flt3L is not required for the generation or maintenance of CD1c⁺ DCs. However, both CD141⁺ and CD1c⁺ DCs have been previously reported to be generated *in vitro* using CD34⁺ progenitor cells cultured in the presence of Flt3L, and furthermore both subsets have been shown to expand following *in vivo* Flt3L administration (203, 214, 571, 572, 600). Therefore the role of Flt3L in CD1c⁺ DC generation and maintenance remains undetermined.

CD115, the receptor for CSF-1, is involved in the development of the macrophage lineage and is essential for their survival and function (Fig. 3.19) (573, 574). As for murine CD11b⁺ DCs, CD115 expression was restricted to the CD1c⁺ subset (380). These results suggest that several CD1c⁺ DC characteristics are associated with the monocyte/macrophage lineage. Overall CD135 and CD115 were expressed on CD141⁺ and CD1c⁺ DCs respectively. As stated above, these results could suggest utilisation of alternative precursors for the generation of CD141⁺ and CD1c⁺ DCs. However, further investigation is required. Characterisation of human circulating DC precursors, in addition to CD34⁺ haematopoietic stem cells may aid characterisation of human DC development.

CD11b, CD64 and CX3CR1 are surface markers often used to identify and discriminate between monocyte/macrophage and DC populations. CD11b in mice and men is

predominantly expressed on cells of the myeloid lineage including DCs and macrophages (222, 573), and all subsets except CD141⁺ DCs expressed CD11b, albeit at different levels (Fig. 3.16, 3,17 and 3.18). Lack of CD11b on CD141⁺ DCs corroborates an original study published by Dzionek et al, and supports their distinction from all other myeloid populations (202). CD64 expression, used to differentiate macrophages and monocytes from DCs in mice and men (225, 234, 601), was similar to that of CD11b. CD64 and CD11b expression on CD1c⁺ DCs further suggests a close relationship with the monocyte/macrophage lineage. In comparison to CD14⁺ monocytes, CD14⁻ CD16⁺ mononuclear cells expressed lower levels of both CD64 and CD11b. This variation in marker expression may support the hypothesis that CD14⁻ CD16⁺ mononuclear cells represent a differentially matured blood monocyte subset. However, these experiments are insufficient to fully address the classification of CD14⁻ CD16⁺ mononuclear cells.

CX3CR1 is expressed on monocytes, DCs and macrophages (246, 602). Examination of HC circulating myeloid populations revealed that CD141⁺ cDCs completely lacked expression of CX3CR1. Based on the expression of CX3CR1, CD11b, CD115 and Flt3L, CD141⁺ DCs therefore represent putative DCs. CX3CR1 was homogenously expressed on all other myeloid subsets assessed. Given the association between CD115 and the monocyte/macrophage lineage, it was therefore surprising that CD14⁺ CD16⁻ monocytes were deficient in CD115 expression. This observation disputes a previous publication where CD115 was found to be highly expressed on both CD14⁺ monocyte populations (238, 565). Despite the same antibody clone being used in both experiments, the discrepancy between these results remains unexplained. CD115 was expressed at intermediate levels on CD14⁺ CD16⁺ monocytes, with highest levels being observed on CD14⁻ CD16⁺ mononuclear cells. However, caution should be taken when interpreting these results as all surface phenotyping analyses were performed only once.

Recently, several surface markers and transcription factors have been identified that may allow discrimination between myeloid populations (575, 603-605). One such transcription factor is Zbtb46 (zDC), shown to be DC specific in mice and men (575, 603). zDC expression was assessed on CD14⁺ CD16⁻ monocytes, total CD14⁻ CD16⁺ mononuclear cells and CD1c⁺ DCs (Fig. 3.20), which was expected to clarify lineage commitment of the CD14⁻ CD16⁺ mononuclear population. In both HCs and AS patients, CD1c⁺ DCs expressed high levels of zDC, confirming that these cells are part of the DC lineage. Therefore, despite their association with the macrophage lineage in terms of surface marker expression, zDC expression confirms these cells as putative DCs. CD14⁺

monocytes and CD14⁻ CD16⁺ mononuclear cells expressed three to four times lower levels of zDC than CD1c⁺ DCs. CD141⁺ DCs could not be assessed due to poor yields after purification but have previously been reported to express zDC to similar levels of CD1c⁺ DCs (575, 603). These results suggest that CD14⁻ CD16⁺ mononuclear cells do not belong to the cDC lineage. However, as previously discussed, CD14⁻ CD16⁺ mononuclear cells are heterogeneous for SLAN expression, with CD16⁺ SLAN⁺ cells reported to represent a third blood DC population (240). Unfortunately, zDC expression of SLAN subsets was not performed. In order to clarify the debate regarding lineage commitment of CD14⁻ CD16⁺ cells, zDC expression on individual subsets should be performed. If CD14⁻ CD16⁺ SLAN⁺ cells do indeed represent a third DC population, they would be expected to express similar levels to that of CD1c⁺ DCs.

In conclusion, AS patients appear to have a slightly altered immunological profile compared to HCs in terms of the circulating myeloid populations. A slight but significant reduction in circulating CD1c⁺ cDCs was counterbalanced by an increase in circulating CD14⁻ CD16⁺ mononuclear cells. However, this increase was not associated with preferential expansion of either SLAN⁻ or SLAN⁺ subsets. As different functional properties have been attributed to the CD14⁻ CD16⁺ mononuclear population (237, 249, 252, 359), further clarification regarding identity and functional characterisation of this population is required to fully understand their role in disease pathogenesis. Based on previous functional characterisations, I hypothesise that the CD14⁻ CD16⁺ population contains both monocytes (SLAN⁻) and DCs (SLAN⁺). However to test this hypothesis, several functional and transcriptional analyses would have to be performed on the individual subsets, including: naïve T cell proliferation, antigen presentation, cytokine production and zDC expression. In addition, these data also suggest that despite CD141⁺ and CD1c⁺ cells represent putative DC populations, the ontogeny of these populations may be distinct. These findings could have important implications for DC-based therapies.

As stated previously, a defining feature of DCs is their ability to stimulate naïve T cells leading to the induction of specific immunogenic or tolerogenic immune responses. Consequently, analysis of T cell subsets and their expression of chemokine receptors can indicate the type of immune response induced following DC: T cell interaction. Furthermore, these studies can provide information relating to the site(s) of disease induction and perpetuation. Therefore in the next chapter, circulating AS patient and HC T cells were analysed in terms of activation status and chemokine receptor expression.

Chapter 4: Role of T cells in AS pathogenesis

4.1 Introduction

DCs interact with T cells to orchestrate protective or tolerogenic immunity. Following DC: T cell crosstalk, T cells migrate to the tissue from which the interacting DC migrated. Within this tissue, they perform a variety of functions: they secrete cytokines that direct and control the immune response; they induce cell death in neighbouring cells; or they may inhibit aberrant responses. These functions depend on the phenotype of T cell subsets induced at priming (60, 80), and these consequently define the profile of the resulting immune response. When immune responses are not appropriately controlled, aberrant responses to self or harmless antigens can cause disease. Characterisation of these disease-causing T cell responses can provide knowledge about pathogenic pathways and can be beneficial to the generation of new treatment strategies. Published work relating to AS and T cells focus on the identification and characterisation of Th1, Th2, Th17 and Th22 CD4⁺ T cell subsets circulating in the blood of patients. Many of these studies suggest pathogenic roles for Th17 and Th22 T cells in disease development (181, 495, 527, 530). This focus on CD4⁺ T cells in AS patients is due to the results obtained from animal models of SpA. These results exclude involvement of CD8⁺ T cells in disease development, despite their role in responding to antigen presented on MHC class I molecules such as HLA-B27. CD8⁺ T cells, in the HLA-B27 transgenic rat model, are insufficient to transfer disease to nude recipients, whilst inhibition of CD8⁺ T cell responses did not inhibit SpA progression (470-472). Although CD8⁺ T cells are not a primary focus for AS research, IL-4⁺ CD8⁺ T cells are found at increased frequencies in AS patients (606). Despite much research, consensus relating to the pathogenic functions of T cells in AS has not yet been reached. Consequently, I set out to examine the proportions of naïve, memory, activated and regulatory T cells in the blood of AS patients, and to address some of their functions, through examination of their cytokine secretion and chemokine receptor expression profiles.

4.2 Patient characteristics

AS patients were recruited from the Glasgow Royal Infirmary Ankylosing Spondylitis clinic run by Dr David McCarey and Dr Anne McEntegart. The results described in this chapter use all or a fraction of the participants whose information is depicted in Table 4.1. Many of the patients used for blood DC analysis were also assessed for T cell subsets and

are therefore included in the clinical information provided below. Clinical parameters assessed included disease duration, severity and treatment.

Table 4.1: Patient Characteristics for T cell analysis

For T cell analysis, 27 AS patients and 14 HCs were used. Patient and HC data were collated and tabulated below. Some patient records were incomplete or unavailable, and therefore, percentages represent proportion of total patients used in the study. Spinal disease levels were classified based on the number of sites involved: cervical, thoracic and/or lumbar: 1 site = level 1, 2 sites = level 2 and 3 sites = level 3. Combination therapy refers to those patients receiving both DMARDs and NSAIDs. N/A = Not applicable. Mean \pm SD.

	AS Patients	Healthy Controls
Age (yrs)	54.96 \pm 11.5	49.7 \pm 10.2
Sex – Male/Female	24/3	9/4
Disease Duration (yrs)	28.6 \pm 12.8	N/A
B27 – Pos/Neg (% B27⁺)	24/3 (89%)	1/13 (7%)
BASDAI	3.65 \pm 2.3	N/A
BASMI	4.3 \pm 2.71	N/A
ESR (mm/hr)	12.52 \pm 10.9	N/A
CRP (mg/L)	5.99 \pm 5.16	N/A
Bilateral Sacroiliitis – No. (%)	19 (94.7%)	N/A
Spinal disease		
Absent – No. (%)	5 (29.4%)	N/A
Level 1 – No. (%)	5 (29.4%)	N/A
Level 2 – No. (%)	3 (17.65%)	N/A
Level 3 – No. (%)	4 (23.56%)	N/A
Extra-articular Disease		
IBD – No. (%)	1 (4.76%)	N/A
Uveitis – No. (%)	4 (19.05%)	N/A
Psoriasis – No. (%)	2 (9.52%)	N/A
Arthritis – No. (%)	2 (10.53%)	N/A
Medication		
DMARDs – No. (%)	0 (0%)	N/A
NSAIDs – No. (%)	11 (68.75%)	N/A
Combination – No. (%)	1 (6.25%)	N/A
Biologics – No. (%)	4 (25%)	N/A

Due to the overlap between the groups, many of the patient characteristics for blood cDC analysis are similar to this T cell patient cohort. The majority of AS patients were HLA-B27⁺ (89%) and male, and the average age was 55 years. HCs were also predominantly male but were slightly younger with an average age of 50 years, and the majority (93%) were HLA-B27⁻. Again, disease was longstanding in patients with an average duration of 28.6 years. Unfortunately, within this patient cohort, no newly diagnosed (<2 years) patients were included, which might have allowed comparison of immunological parameters at onset of disease with those patients experiencing long term, chronic disease. Disease severity was determined through BASDAI and BASMI assessment, whilst levels of inflammation were assessed using ESR and CRP levels. BASDAI (0-10) and BASMI scores (0-10) averaged 3.65 and 4.3 respectively. Inflammatory marker values below 10 are considered normal for the Glasgow general population (Dr David McCarey, personal communication). Consequently, this patient cohort can be considered as mildly inflamed, with average values of 12.52 and 5.99 for ESR and CRP respectively. Similar to the blood DC patient cohort, information relating to levels of spinal disease was not consistently available. Of the 27 patients used for analysis, 18 patients (66.7%) presented with bilateral sacroiliitis whilst 1 patient completely lacked evidence of sacroiliitis. For the remaining 8 patients, data were not recorded. Likewise, information about the degree of spinal disease (bony changes or fusion within the cervical, thoracic or lumbar regions of the spine) was not always available; these details were only available for 17 out of 27 patients. Patients presenting with complete absence of spinal disease or only one affected site were most abundant. As described previously, AS patients often present with extra-articular manifestations: IBD, uveitis, psoriasis and peripheral arthritis. Within this cohort, 8 patients presented with extra-articular disease, with uveitis being the most common amongst them. One patient had developed two extra-articular manifestations: uveitis and peripheral arthritis. Disease treatment was the final clinical parameter considered for the patient cohort, with treatment strategies subdivided into four groups: DMARDs, NSAIDs, combination (DMARD + NSAID) and biological therapy. As for the blood DC group, NSAIDs were the most common form of treatment (69%) while 23% of patients were receiving biological therapy. The potential effects of these clinical factors on patient immunological parameters will be discussed in more depth in Chapter 7. All, or a subset of these patients were used for the following T cell analyses, which will focus on the phenotype and functions of T cells in AS patients.

4.3 T cell subsets in peripheral blood

To identify CD4⁺ T cell subsets in the blood of AS patients, the gating strategy depicted in Fig. 4.1A was used. First, cell debris was gated out based on the FSC vs SSC profile. Subsequently, doublets and dead (DAPI⁺) cells were excluded from further analysis. CD4⁺ TcRαβ⁺ cells were then subdivided into 4 subsets based on expression of CD25 and CD45RA (Fig. 4.1A): CD45RA⁺ CD25⁻, CD45RA⁻ CD25⁻, CD45RA⁻ CD25^{int} and CD45RA⁻ CD25^{hi}. To further characterise these CD4⁺ T cell subsets, cells were additionally stained for the CD4⁺ Treg transcription factor FOXP3, which controls Treg development and function (607). The results were consistent with published data, showing that all CD45RA⁻ CD25^{hi} cells expressed FOXP3 (Fig. 4.1B), whilst the majority of CD45RA⁻ CD25^{int} cells lacked FOXP3 expression. The CD4⁺ TcRαβ⁺ CD45RA⁻ CD25^{hi} cells were therefore considered to be Tregs. Thus, based on expression of CD45RA, CD25 and FOXP3, our CD4⁺ T cell subsets were classified as naïve (CD45RA⁺ CD25⁻), memory (CD45RA⁻ CD25⁻), activated/effector (CD45RA⁻ CD25^{int}) or Treg (CD45RA⁻ CD25^{hi} FOXP3⁺) populations (Fig. 4.1C).

Following identification of four CD4⁺ T cell subsets, the proportions of total circulating CD4⁺ TcRαβ⁺ T cells as well as the individual T cell subsets were compared between AS patients and HCs. No difference in the proportion of total CD4⁺ TcRαβ⁺ T cells between AS patients and HCs was observed, in terms of percentage of live cells or cell number/ml of blood (Fig. 4.2A). The individual subsets were analysed in terms of percentage of CD4⁺ TcRαβ⁺ cells, percentage of live cells and absolute cell number/ml of blood. Again, no significant differences were seen between AS patients and HCs for naïve (Fig. 4.2B), memory (Fig. 4.2C), activated (Fig. 4.3A) and Treg (Fig. 4.3B) populations. In blood, naïve CD4⁺ T cells represented the major population, comprising 45-50% of total CD4⁺ TcRαβ⁺ T cells, activated (CD45RA⁻ CD25^{int}) CD4⁺ T cells represented approximately 25% of this T cell pool, and memory T cells and Tregs (CD45RA⁻ CD25^{hi}) contributed approximately 15% and 5% respectively (Fig. 4.2 and 4.3). In addition to analysing the proportions of CD4⁺ T cell subsets, the aim was to investigate whether HLA-B27 expression affects the T cell profile observed in AS patients and HCs. However, too few samples of HLA-B27⁺ HCs and HLA-B27⁻ AS patients were available to power this aspect of the study. Data from these individuals are highlighted in red (Fig. 4.2 and 4.3).

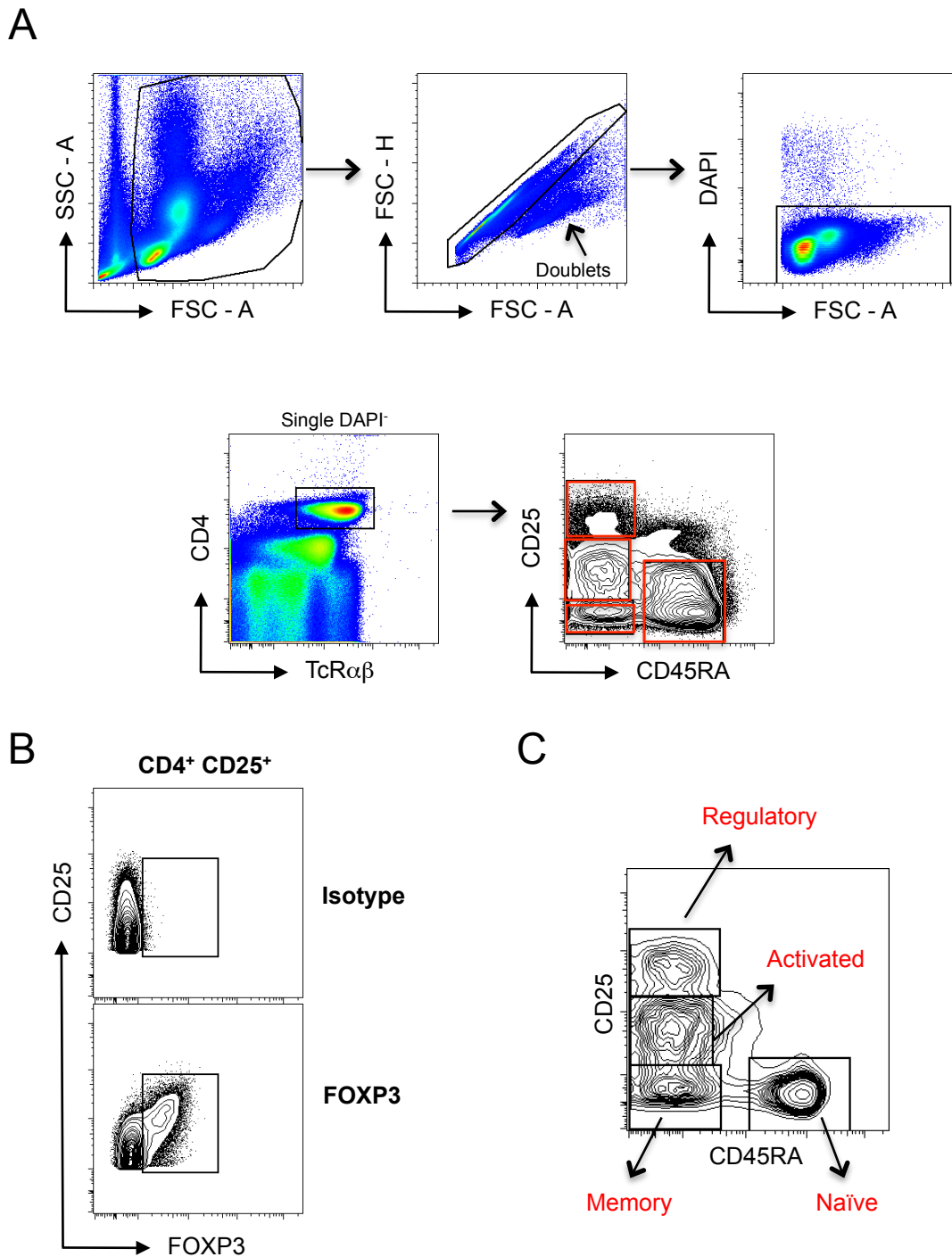


Figure 4.1: Identification of peripheral blood T cell subsets

Four T cell subsets can be identified in peripheral blood. PBMCs were isolated using Ficoll gradient, with cells identified by flow cytometry. **(A)** Gating strategy used to identify CD4⁺ T cells. First, doublets and dead cells (DAPI⁺) were excluded from analysis. Single live cells (top, right) were analysed for expression of CD4 and TcRαβ (bottom left), with CD4⁺ TcRαβ⁺ cells being subdivided into four subsets based on CD25 and CD45RA expression (bottom, right). **(B)** FOXP3 expression on live CD4⁺ TcRαβ⁺ CD25⁺ CD45RA⁻ T cells. Gate based on isotype. **(C)** Identification of four T cell subsets – activated (CD25^{lo} CD45RA⁻), naïve (CD25^{lo} CD45RA⁺), memory (CD25^{hi} CD45RA⁺) and regulatory T cells (CD25^{hi} CD45RA⁻). Arrows highlight the individual T cell subsets.

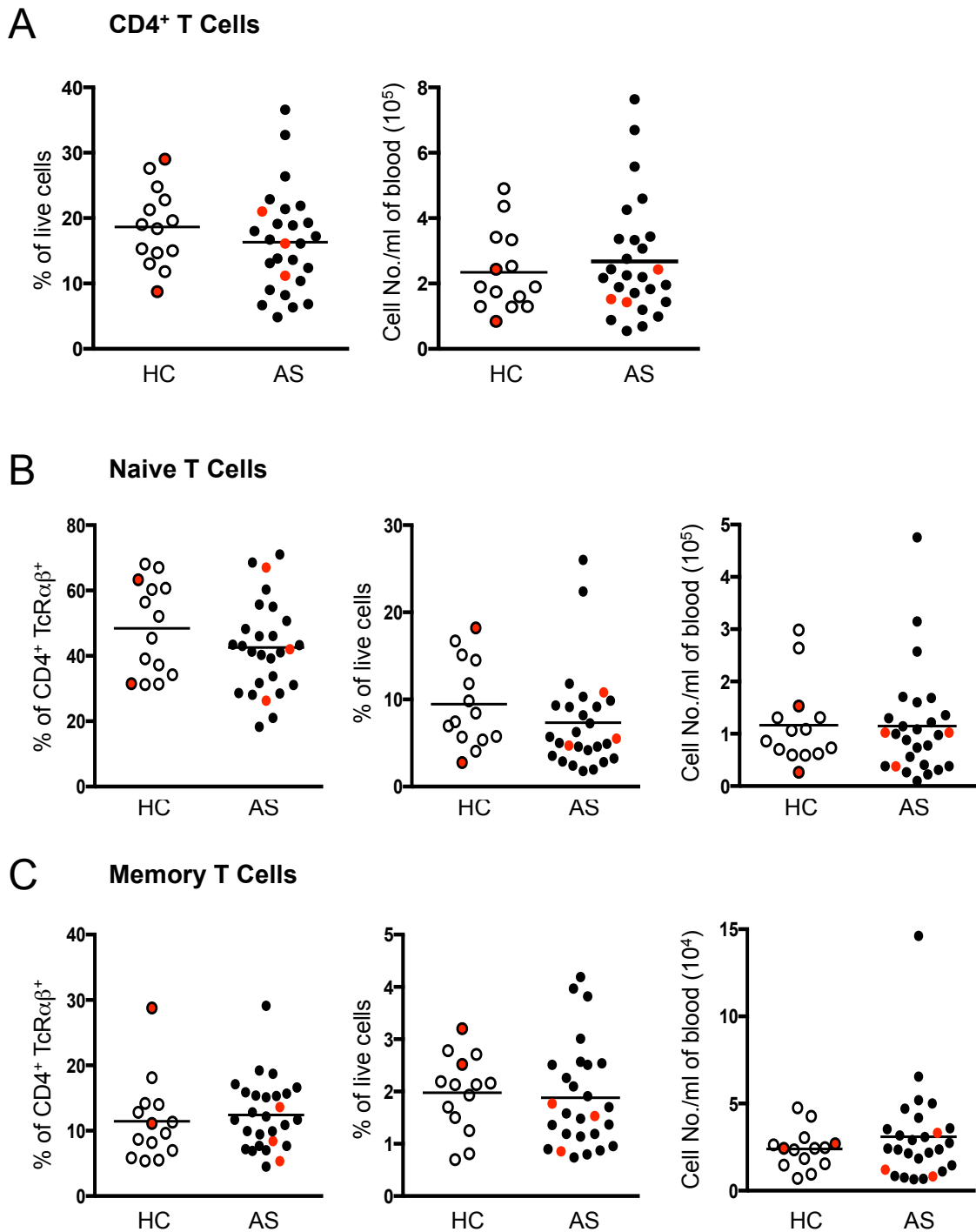


Figure 4.2: Comparison of T cell subsets in AS patients and HCs

No differences in the proportions of total, naïve and memory CD4⁺ T cell subsets between HCs (empty circles) and AS patients (filled circles). **(A)** % of live cells (left) and no. of CD4⁺ TcRαβ⁺ T cells/ml of blood (10⁵ - right) for AS patients and HCs. **(B)** Analysis of naïve CD4⁺ T cells (CD25⁻ CD45RA⁺) in terms of proportion of CD4⁺ TcRαβ⁺ T cells (left), % of live cells (centre) and no. of cells/ml of blood (10⁵ - right) in AS patients. **(C)** Quantification of memory CD4⁺ T cells (CD25⁺ CD45RA⁻) in terms of proportion of CD4⁺ TcRαβ⁺ T cells (left), % of live cells (centre) and no. of cells/ml of blood (10⁵ - right). All graphs show mean. HC red dots = B27⁺ individuals, AS red dots = B27⁺ patients. HC = 14, AS = 27.

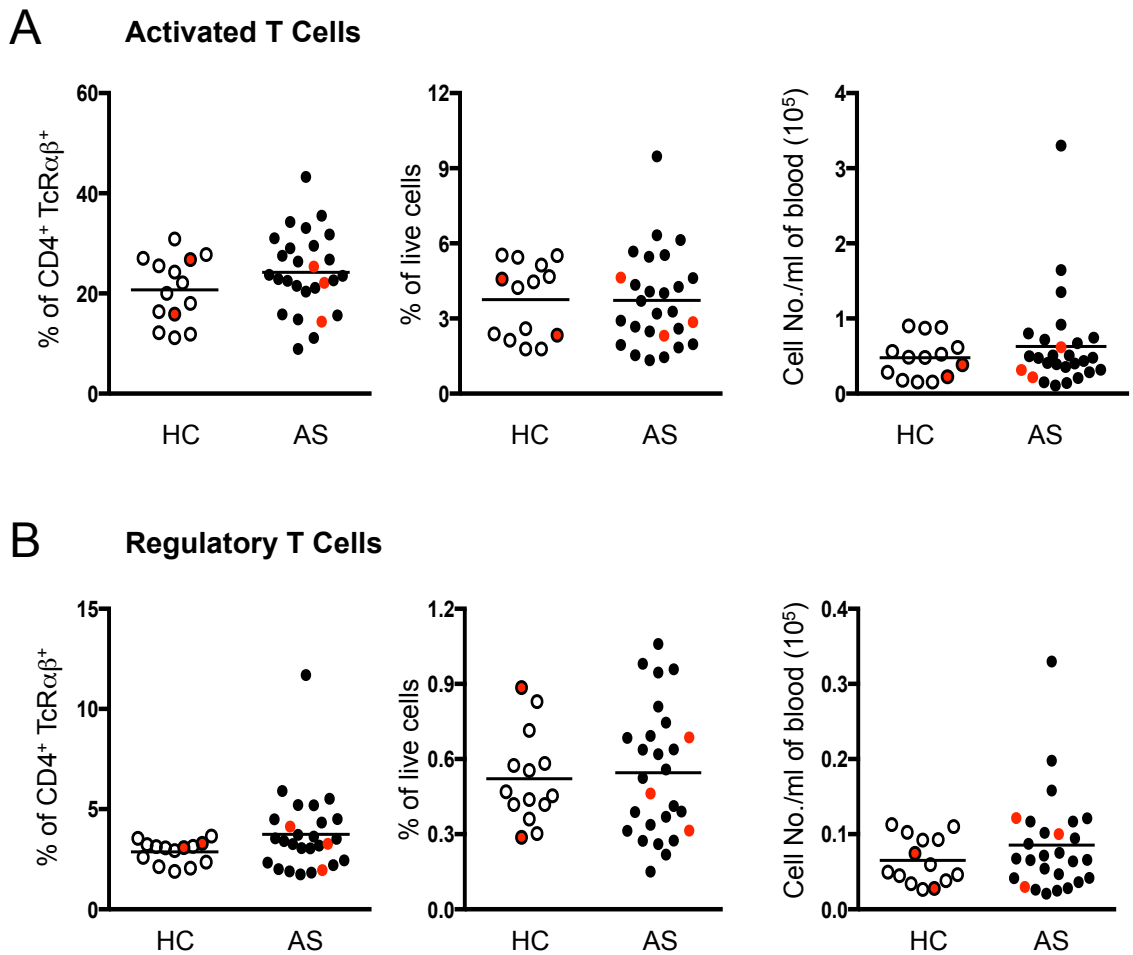


Figure 4.3: Comparison of CD25⁺ T cell subsets in AS patients and HCs

AS patients (filled circles) have similar frequencies of activated and regulatory T cells compared to HCs (empty circles). **(A)** Analysis of activated CD4⁺ T cells (CD25^{lo} CD45RA⁻) in terms of proportion of CD4⁺ TcRαβ⁺ T cells (left), % of live cells (centre) and no. of cells/ml of blood (10⁵ – right). **(B)** Quantification of regulatory CD4⁺ T cells (CD25^{hi} CD45RA⁻) in terms of proportion of CD4⁺ TcRαβ⁺ T cells (left), % of live cells (centre) and no. of cells/ml of blood (10⁵ – right). All graphs show mean. HC red dots = B27⁺ individuals, AS red dots = B27⁻ patients. HC = 14, AS = 27.

4.4 Chemokine receptor expression on circulating T cells

Following activation, chemokine receptors are upregulated on the surface of T cells, directing their migration to specific tissues. When a T cell encounters and interacts with a DC in a lymph node, it is “instructed” to return to the tissue from which the DC originated (172, 413, 608, 609). For example, intestinal DCs instruct T cells to return to the intestine by inducing expression of the gut homing markers CCR9 and $\alpha 4\beta 7$ (171, 172). Thus, analysing the array of chemokine receptors expressed on the surface of T cells makes it possible to deduce what tissues these cells are likely to migrate towards. An example of chemokine receptor staining is shown in Fig. 4.4A. The gating strategy described in Fig. 4.1 was implemented and $CD4^+ TcR\alpha\beta^+ CD45RA^- CD25^{int}$ activated T cells were analysed for expression of CCR4 (Fig. 4.4A). The CCR^+ gate was set using the appropriate isotype control antibodies for each $CD4^+$ T cell subset.

Expression of the chemokine receptors CCR4, CCR6, CCR9, CCR10 and CXCR3 were assessed in this study for the four T cell populations shown earlier. CCR9 promotes migration to the small intestine (171, 172); CCR10 induces migration of lymphocytes to mucosal sites and skin whilst CCR4 is the major promoter of skin migration (173-175, 610-612). CCR6 is expressed by mucosal lymphocytes, cells migrating to sites of inflammation and DCs residing in Peyer’s patches (176, 180, 613). In addition to directing cell migration, several chemokine receptors are associated with specific T cell effector types. For example, CCR6 is used as a surrogate marker for Th17 cells (180, 181), while CXCR3 is predominantly expressed on Th1 cells and promotes migration to inflammatory sites (182, 183, 614). This panel of chemokine receptors was chosen given their associations with tissues involved in disease pathology (skin, intestine and joint) or expression on disease associated T cell phenotypes (Th1 and Th17). Expression of CCR4, CCR6, CXCR3, CCR9 and CCR10 on activated, memory, regulatory and naïve T cells isolated from a HC are shown in Fig. 4.5 and 4.6. A significant proportion of all T cell populations, except naïve T cells (Fig. 4.5D), were found to express CCR4, CCR6 and CXCR3 (Fig. 4.5). Strikingly, the majority of Tregs expressed CCR4 (Fig. 4.5C). A fraction of naïve $CD4^+$ T cells expressed CXCR3 (Fig. 4.5D). Few $CCR9^+$ cells were detected (Fig. 4.6). CCR10 expression followed the pattern of CCR4, CCR6 and CXCR3, with a proportion of all subsets except naïve T cells expressing this mucosal/skin homing chemokine receptor (Fig. 4.6). Expression of the above-mentioned chemokine receptors were compared between AS patients and HCs. CCR4 was expressed at similar proportions on activated, memory, naïve and Treg subsets in AS patients and HCs (Fig. 4.7). When

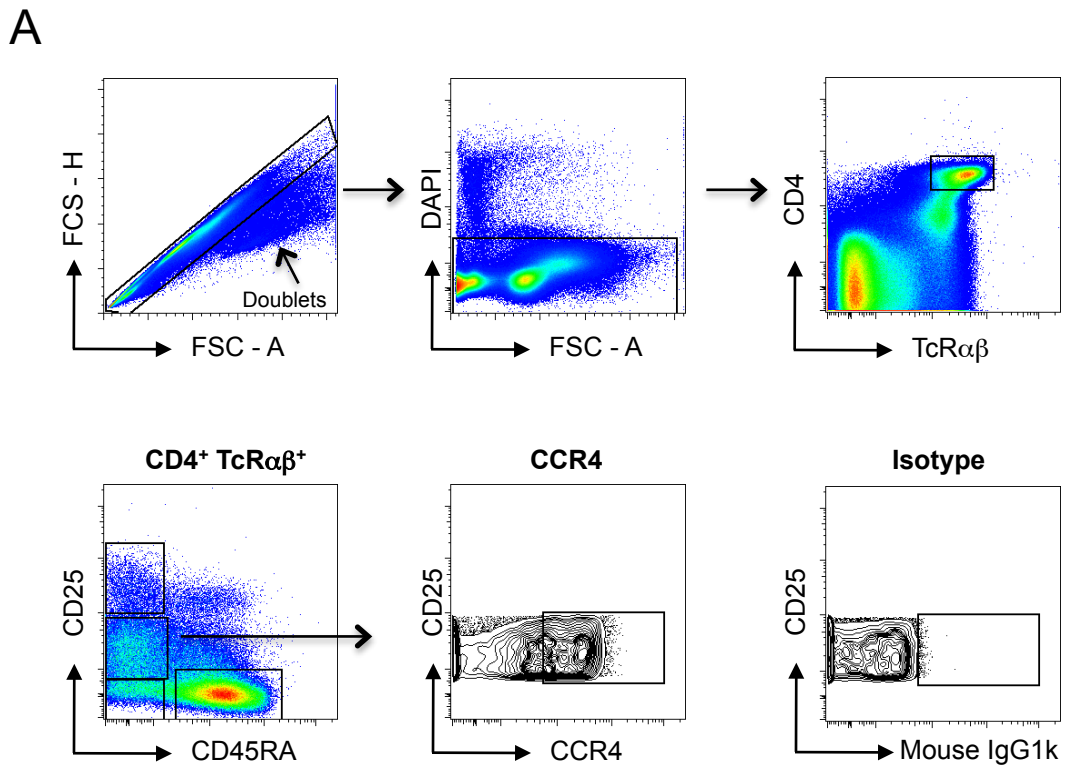


Figure 4.4: Detection of chemokine receptor expression on CD4⁺ T cells

Identification of chemokine receptor (CCR) expression on CD4⁺ T cells. **(A)** To identify T cell subset CCR expression, doublets and dead cells (DAPI⁺) were excluded from further analysis. Single live cells (top centre) were analysed for expression of CD4 and TcRαβ (top right), with cells co-expressing both markers being subdivided into four subsets based on CD25 and CD45RA expression (bottom left). As an example of CCR expression, CD25^{lo} CD45RA⁺ activated T cells were analysed for expression of CCR4 (bottom centre). CCR4 gate was set based on the isotype (bottom right).

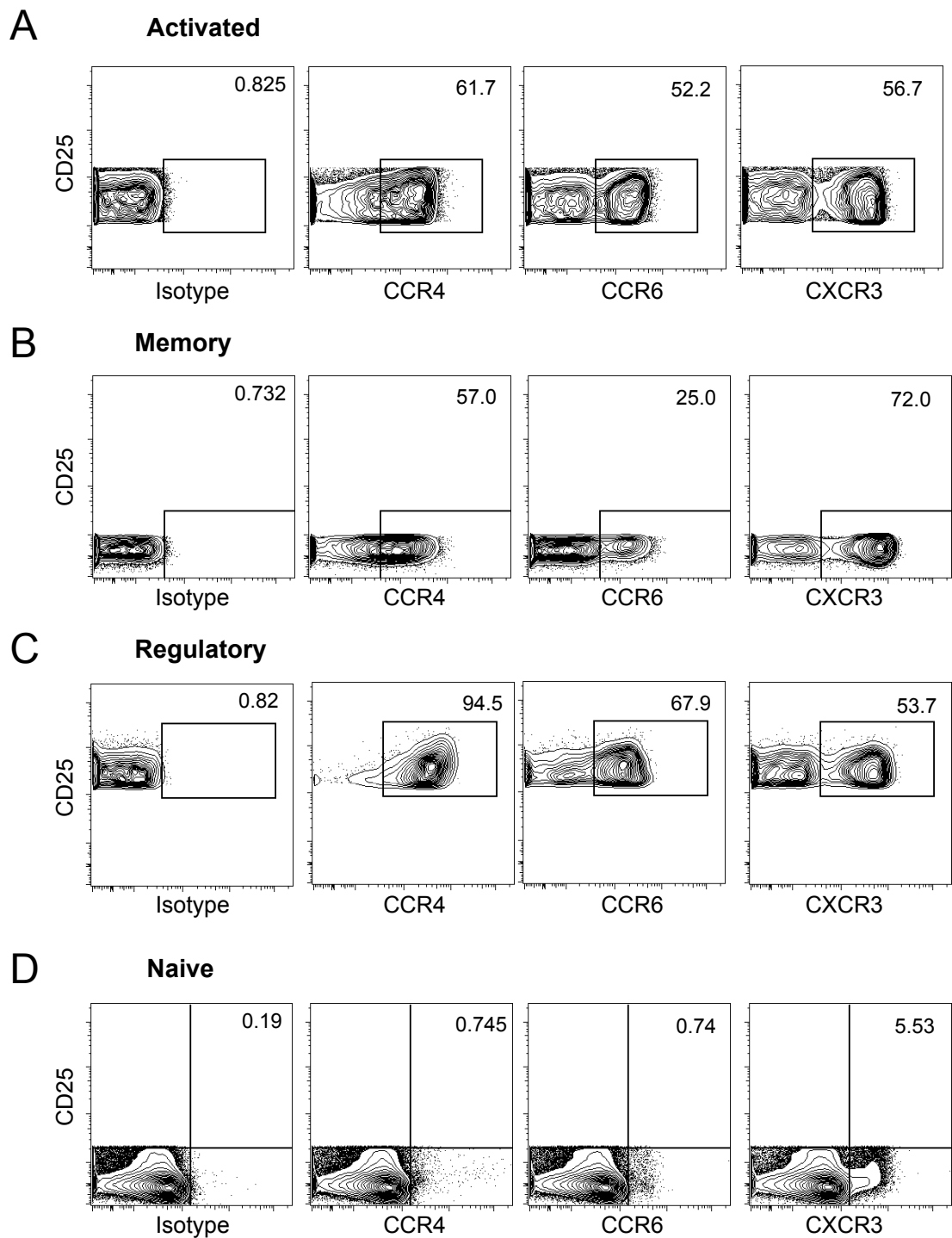


Figure 4.5: Expression of CCR4, CCR6 and CXCR3 on T cell subsets

Representative chemokine receptor (CCR) staining on HC blood T cell subsets. Single DAPI⁻ CD4⁺ TcRαβ⁺ cells were subdivided into 4 T cell subsets and CCR⁺ expression was analysed. Activated (**A**), memory (**B**), regulatory (**C**) and naïve (**D**) T cell subsets were analysed for the expression of the chemokine receptors CCR4 (centre, left), CCR6 (centre, right) and CXCR3 (right). Gates for each individual CCR were set using the isotype plot (left). Numbers represent proportion of CCR⁺ T cells. Activated = CD25⁺ CD45RA⁻, memory = CD25⁻ CD45RA⁻, regulatory = CD25^{hi} CD45RA⁻ and naïve = CD25⁻ CD45RA⁺. Isotype for all CCRs was mouse IgG1k.

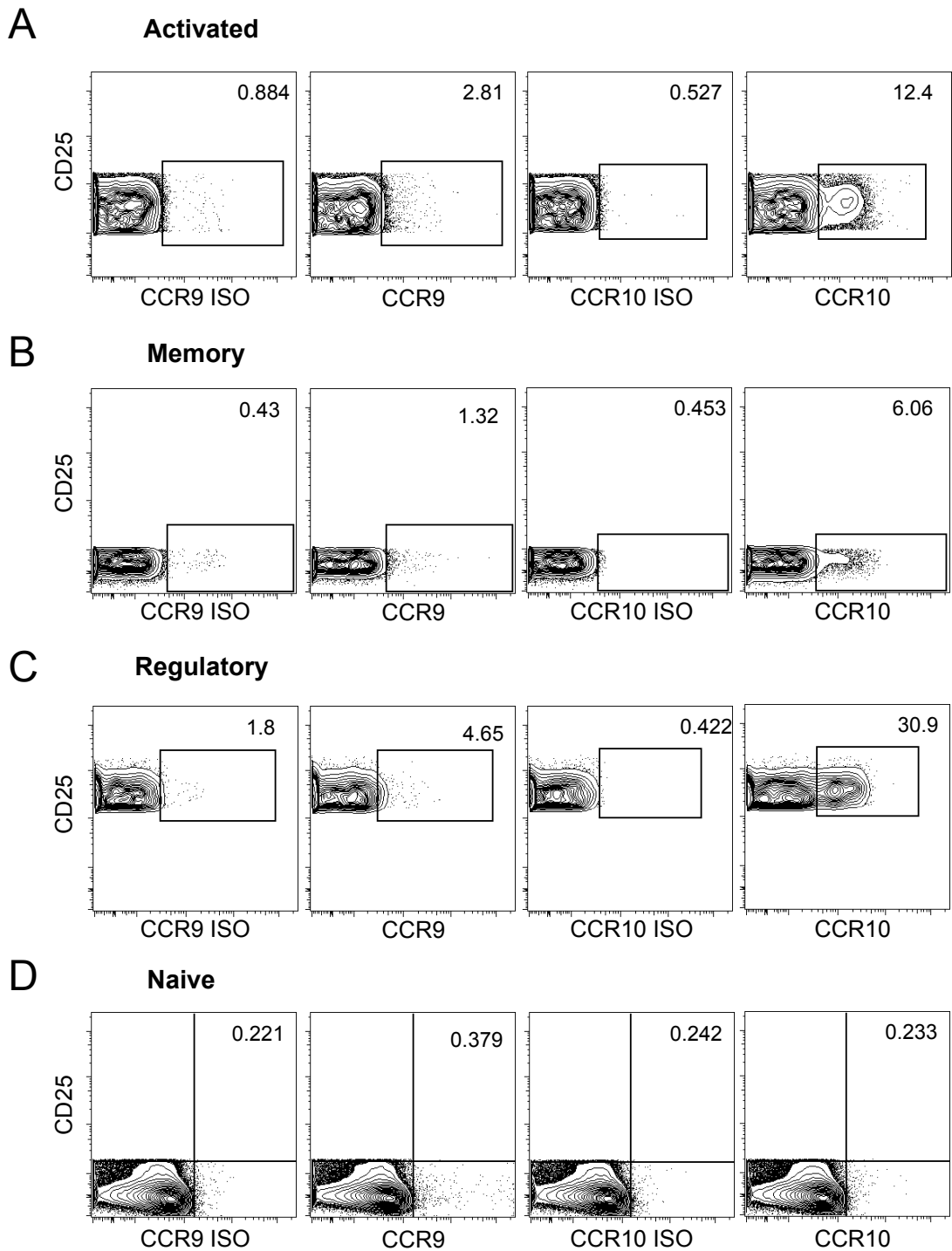


Figure 4.6: Expression of CCR9 and CCR10 on T cell subsets

Representative chemokine receptor (CCR) staining on peripheral blood T cell subsets from a HC. Single DAPI⁻ CD4⁺ TcRαβ⁺ cells were subdivided into 4 T cell subsets and CCR⁺ expression was analysed. Activated (**A**), memory (**B**), regulatory (**C**) and naïve (**D**) T cell subsets were analysed for expression of the chemokine receptors CCR9 (centre, left) and CCR10 (right). Gates for CCR9 were set using the specific isotype plot (left – Rat IgG2a). Gates for CCR10 were set using the specific isotype gate (centre, right – mouse IgG2a). Numbers represent proportion of CCR⁺ T cells. Activated = CD25⁺ CD45RA⁻, memory = CD25⁻ CD45RA⁻, regulatory = CD25^{hi} CD45RA⁻ and naïve = CD25⁻ CD45RA⁺. Numbers represent proportion of CCR⁺ T cells.

percentage of CCR⁺ CD4⁺ TcRαβ⁺ cells, live cells and the CCR⁺ cell number/ml of blood were all analysed, interestingly, CCR6 and CXCR3 were differentially expressed in AS patients, compared to HCs (Fig. 4.7 and 4.8). The proportion of CCR6⁺ CD45RA⁻ CD25^{int} (activated) T cells was significantly increased in AS patients compared to HCs (Fig. 4.7A). However, the percentage of CCR6⁺ T cell among live cells and the absolute number of CCR6⁺ CD45RA⁻ CD25^{int} T cells per ml of blood did not differ between AS patients and HCs (Fig. 4.7). In contrast, CXCR3 was expressed on a significantly smaller percentage of activated and memory T cells in AS patients, with a reduced proportion of CXCR3 memory T cells also being observed when represented as a percentage of live cells (Fig. 4.8A and 4.8B). No difference in the proportion of CCR9⁺ and CCR10⁺ expressing CD4⁺ T subsets was observed between AS patients and HCs, expressed as either % of total CD4⁺ T cells (Fig. 4.9A), % of live cells (Fig. 4.9B) and cell number (Fig. 4.9C). Expression of chemokine receptors on HLA-B27⁺ HCs and HLA-B27⁻ AS patients was compared but no conclusions could be drawn due to insufficient numbers of samples.

4.5 T cell phenotype and cytokine secretion

The expression of particular chemokine receptors is associated with specific T cell phenotypes. To corroborate above findings relating to chemokine receptor expression in AS patients, where differential expression of CCR6 and CXCR3 was observed on CD4⁺ TcRαβ⁺ T cells, we investigated cytokine production by CD4⁺ TcRαβ⁺ T cells in the blood of AS patients and HCs. The gating strategy used in these experiments was identical to that described in Fig. 4.1. Cytokine production was assessed by intracellular staining 4.5 hours after stimulation with PMA and ionomycin in the presence of brefeldin A and monensin (protein secretion inhibitors). Unstimulated CD4⁺ T cells produced barely detectable quantities of cytokines (Fig. 4.10A). Following stimulation, cells were analysed for the production of IL-17A and IFNγ. These cytokines are diagnostic for specific T cell phenotypes: IL-17A is produced by Th17 cells, known to express CCR6; IFNγ is the signature cytokine of Th1 cells, thought to preferentially express CXCR3 (180, 181, 183). Gates for analysis were set using specific isotype controls (data not shown). Staining for IL-17A and IFNγ on stimulated CD4⁺ T cells identified 3 subsets of cytokine producing T cells: IFNγ⁺ IL-17A⁻, IFNγ⁻ IL-17A⁺ and double-producing IFNγ⁺ IL-17A⁺ CD4⁺ T cells (Fig. 4.10B). To identify non-CD4 cytokine producing cells, total single live cells from a HC were also assessed for IFNγ and IL-17A production (Fig. 4.10C). The majority of IL-17A producing cells were CD4⁺ (0.007% vs 0.173% - Fig. 4.10C). In contrast, a larger proportion of IFNγ⁺ CD4⁻ cells were present in HC blood (5.18% vs 23.4% - Fig. 4.10C).

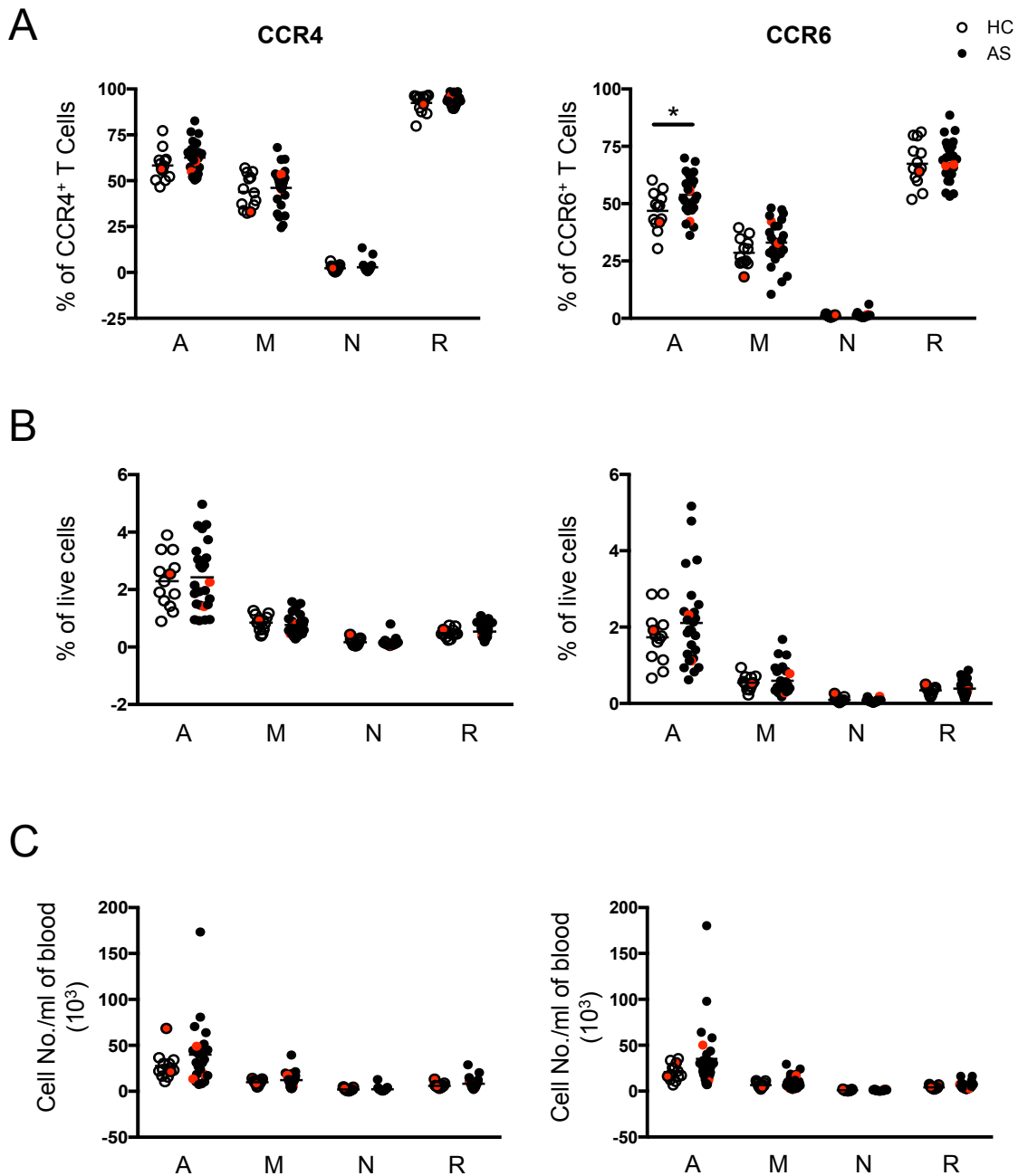


Figure 4.7: CCR4 and CCR6 expression in AS patients and HCs

A greater proportion of activated T cells isolated from AS patients (filled circles) express CCR6 compared to HCs (empty circles). Quantification of CCR4 and CCR6 expression on activated (A), memory (M), naïve (N) and regulatory (R) T cell subsets in AS patients and HCs. **(A)** The proportion of CCR4⁺ (left) and CCR6⁺ (right) CD4⁺ TcRαβ⁺ T cell subsets in AS patients and HCs. The % of live cells **(B)** and total number of CCR⁺ cells/ml of blood **(C)** were also compared between AS patients and HCs for CCR4 (left) and CCR6 (right). Graphs show mean. HC red dots = B27⁺ individuals, AS red dots = B27⁻ patients. Students unpaired T test (A, right), * p<0.05. 13 HCs and 25 AS patients were used for analysis.

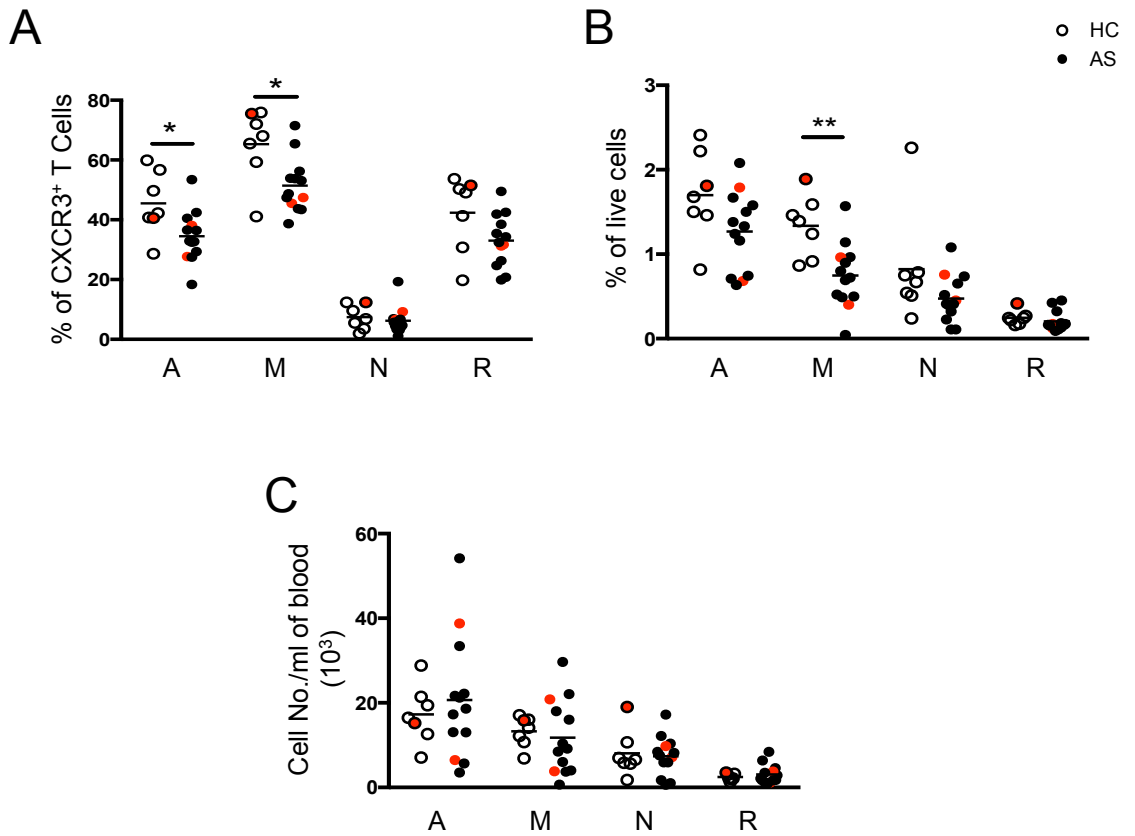


Figure 4.8: CXCR3 expression in AS patients and HCs

CXCR3 expression is differentially expressed in AS patients (filled circles) compared to HCs (empty circles). Expression of CXCR3 was assessed on activated (A), memory (M), naïve (N) and regulatory (R) T cells in the blood of AS patients and HCs. **(A)** Proportion of CXCR3⁺ CD4⁺ TcRαβ⁺ T cell subsets in AS patients and HCs. The % of live cells **(B)** and total number of CXCR3⁺ cells/ml of blood **(C)** were compared between AS patients and HCs for each T cell subset. All graphs show mean. HC red dots = B27⁺ individuals, AS red dots = B27⁻ patients. Students unpaired T test or Mann-Whitney non-parametric test used where appropriate, * p<0.05. 7 HCs and 13 AS patients were used for analysis.

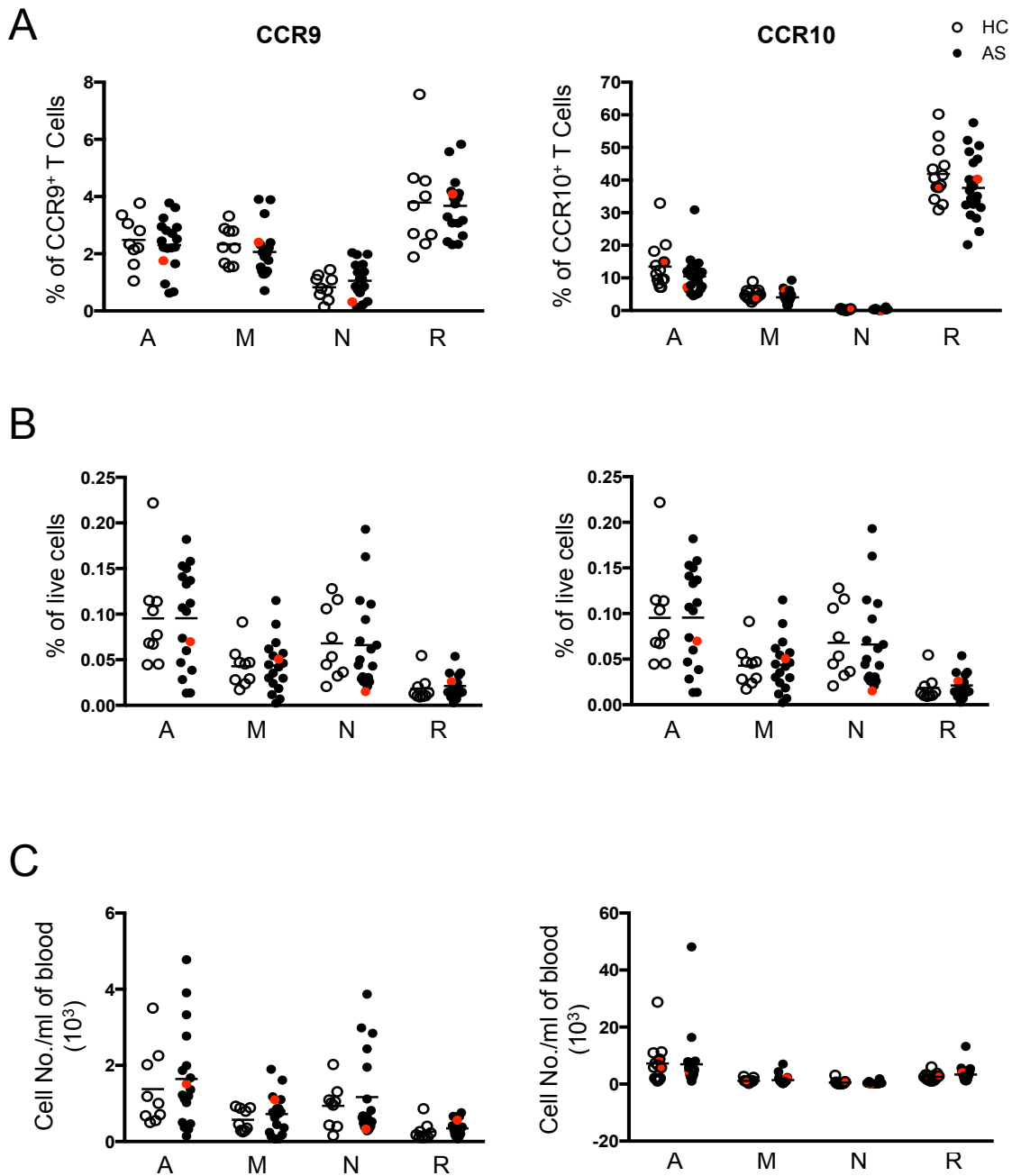


Figure 4.9: CCR9 and CCR10 expression in AS patients and HCs

No difference in CCR9 and CCR10 expression on CD4⁺ T cells between AS patients (filled circles) and HCs (empty circles). Activated (A), memory (M), naive (N) and regulatory (R) T cell subsets were assessed for the expression of CCR9 and CCR10. **(A)** The proportion of CCR9⁺ (left) and CCR10⁺ (right) CD4⁺ TcRαβ⁺ T cell subsets in AS patients and HCs. The % of live cells **(B)** and total number of CCR⁺ cells/ml of blood **(C)** were also compared between AS patients and HCs for CCR9 (left) and CCR10 (right). All graphs show mean. HC red dots = B27⁺ individuals, AS red dots = B27⁻ patients. CCR9 – 9 HCs and 13 AS patients, CCR10 – 18 HCs and 24 AS patients used for analysis.

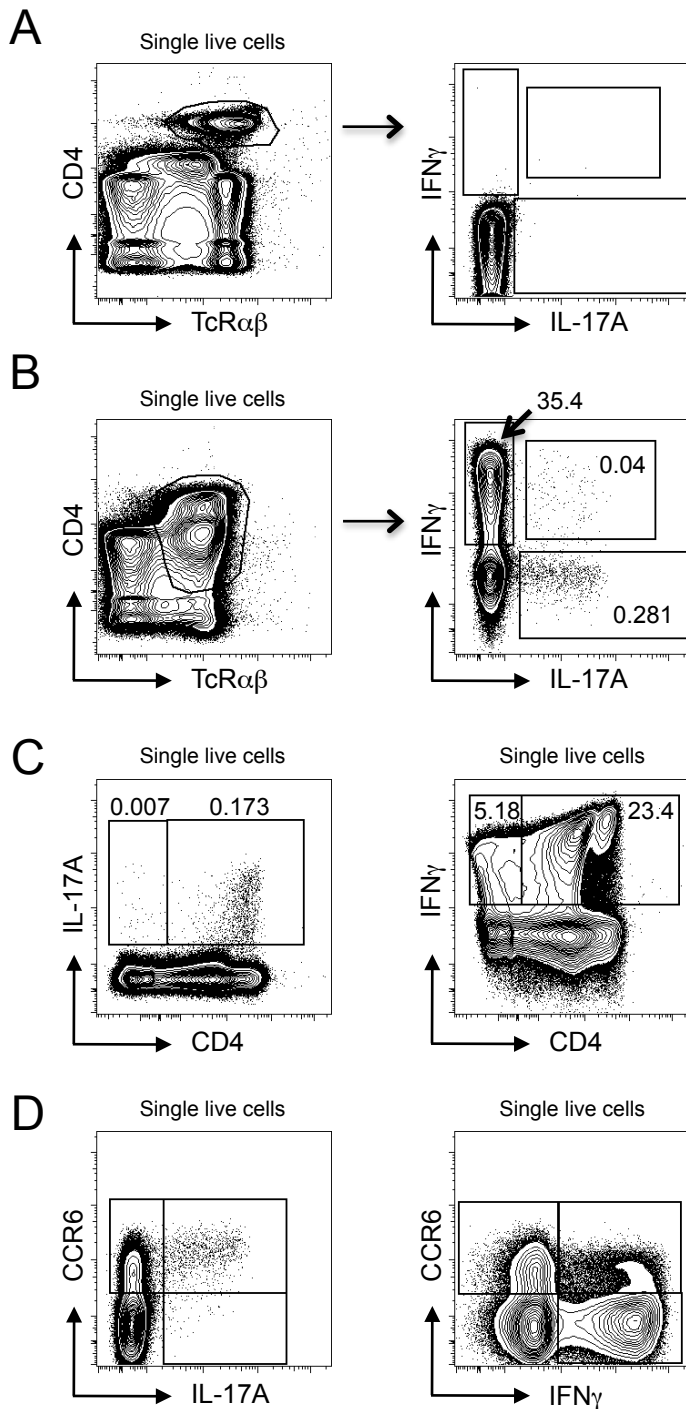


Figure 4.10: Secretion of IL-17A and IFN γ from peripheral blood CD4 $^+$ TcR $\alpha\beta$ $^+$ T Cells

CD4 $^+$ TcR $\alpha\beta$ $^+$ cells can secrete IL-17A and IFN γ after 4.5 hour stimulation with PMA and ionomycin. Unstimulated (**A**) and stimulated (**B**) CD4 $^+$ TcR $\alpha\beta$ $^+$ were analysed for expression of IL-17A and IFN γ after 4.5 hour incubation at 37°C, 5% CO $_2$. Gating strategy used to identify CD4 $^+$ TcR $\alpha\beta$ $^+$ T cells is described in Fig. 4.1A. IL-17A $^+$, IFN γ $^+$ and IL-17A $^+$ IFN γ $^+$ secreting T cells were identified following PBMC stimulation. Percentages are proportion of CD4 $^+$ TcR $\alpha\beta$ $^+$ cells. (**C**) IL-17A (left) and IFN γ (right) cytokine secretion by total CD4 $^+$ and CD4 $^-$ single DAPI $^-$ cells. Percentages represent proportion of live cells. (**D**) Representative plots showing IL-17A (left) and IFN γ (right) secretion by CCR6 $^+$ and CCR6 $^-$ cells. Gates were set based on isotype controls.

In addition to detecting cytokine production from $CD4^+ TcR\alpha\beta^+$ cells, expression of CCR6 on the cytokine-producing cells was assessed. IL-17A secreting cells predominantly expressed CCR6, while $IFN\gamma^+ CD4^+$ T cells were largely CCR6⁻ (Fig. 4.10D).

Quantification of cytokine producing cells revealed that AS patients appeared to have a higher proportion of $CD4^+ IL-17A^+$ T cells compared to HCs in terms of percentage of live cells, proportion of $CD4^+ TcR\alpha\beta^+$ T cells and cell number (Fig. 4.11A, 4.11B and 4.11C). The proportion of $CD4^+ IFN\gamma^+$ and $CD4^+ IFN\gamma^+ IL-17A^+$ T cells were assessed, however no differences in the frequencies of these populations were observed between AS patients and HCs (Fig. 4.11A/B/C). Although AS patients may have a lower proportion of circulating $IFN\gamma$ -secreting cells, compared to HCs (Fig. 4.11A/B). Unfortunately, due to insufficient numbers of samples, statistical analysis could not be performed and thus it is not possible to draw any definitive conclusions from these data sets. However, a trend towards increased circulating $IL-17A^+ CD4^+$ T cells in AS patients was observed. Quantification of CCR6 expression on cytokine producing cells confirmed the initial observations; AS patients seemed to have a greater proportion of CCR6⁺ cells expressing IL-17 (Fig. 4.12A). The majority of $IL-17A^+ CD4^+$ T cells (~85%) expressed CCR6, in both HCs and AS patients (Fig. 4.12B). However, statistical analysis could not be performed on these data sets due to insufficient numbers of data points. In contrast to IL-17A secreting cells, only 8% of $IFN\gamma^+ CD4^+ TcR\alpha\beta^+$ in both AS patients and HCs expressed CCR6 (Fig. 4.12C). Interestingly, the majority (~85%) of $IFN\gamma^+ IL-17A^+ CD4^+$ T cells expressed CCR6, matching the proportion of $IL-17A^+$ T cells (Fig. 4.12D).

4.6 Plasma cytokines in AS patients

Cytokines influence the immune response through diverse interactions with cells, and thus analysis of plasma cytokines in AS patients may reveal mechanisms involved in disease pathogenesis. Accordingly, we measured cytokines and growth factors attributed to T cell subsets (Th1, Th2, Th17 and Tregs) and inflammation in the plasma of HCs and AS patients. We were able to detect $IFN\gamma$, IL-10, IL-4, IL-5, IL-17A, IL-23p19, IL-1 β , IL-6, TNF α and Flt3L (Fig. 4.13 and 4.14). In addition, levels of GM-CSF and IL-12 were measured but both cytokines fell below limit of detection. Of the cytokines produced by helper T cell subsets, only IL-4 (Th2) and IL-23p19 (Th17) were differentially expressed between AS patients and HCs. IL-4 was downregulated in AS patients (Fig. 4.13A), whereas levels of circulating IL-23p19 were significantly higher in AS patients than in HCs (Fig. 4.13B). However, it should be noted that plasma levels of all the cytokines

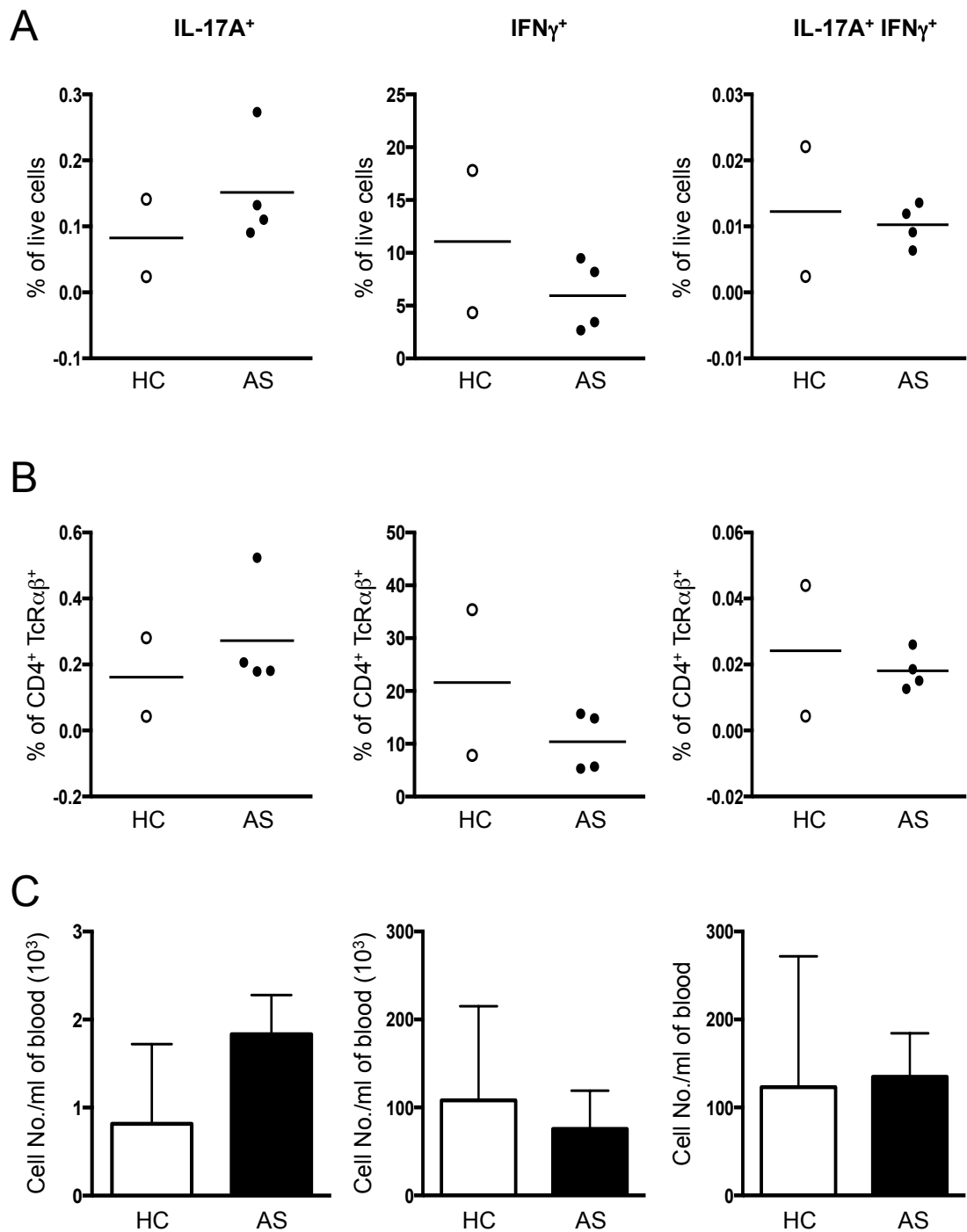


Figure 4.11: Quantification of IL-17A and IFN γ secreting CD4⁺ TcR $\alpha\beta$ ⁺ T Cells

Comparison of intracellular IL-17A and IFN γ stores in CD4⁺ TcR $\alpha\beta$ ⁺ T cells isolated from AS patients and HCs. The proportion of IL-17A⁺ (left), IFN γ ⁺ (centre) and IL-17A⁺ IFN γ ⁺ (right) secreting CD4⁺ TcR $\alpha\beta$ ⁺ T cells in terms of % of live cells (**A**), % of CD4⁺ TcR $\alpha\beta$ ⁺ T cells (**B**) and total cell number/ml of blood (**C**) for AS patients (filled circles/bars) and HCs (empty circles/bars) were assessed. For all data sets, 2 HCs and 4 AS patients were collated from two independent experiments. Error bars represent mean + SD.

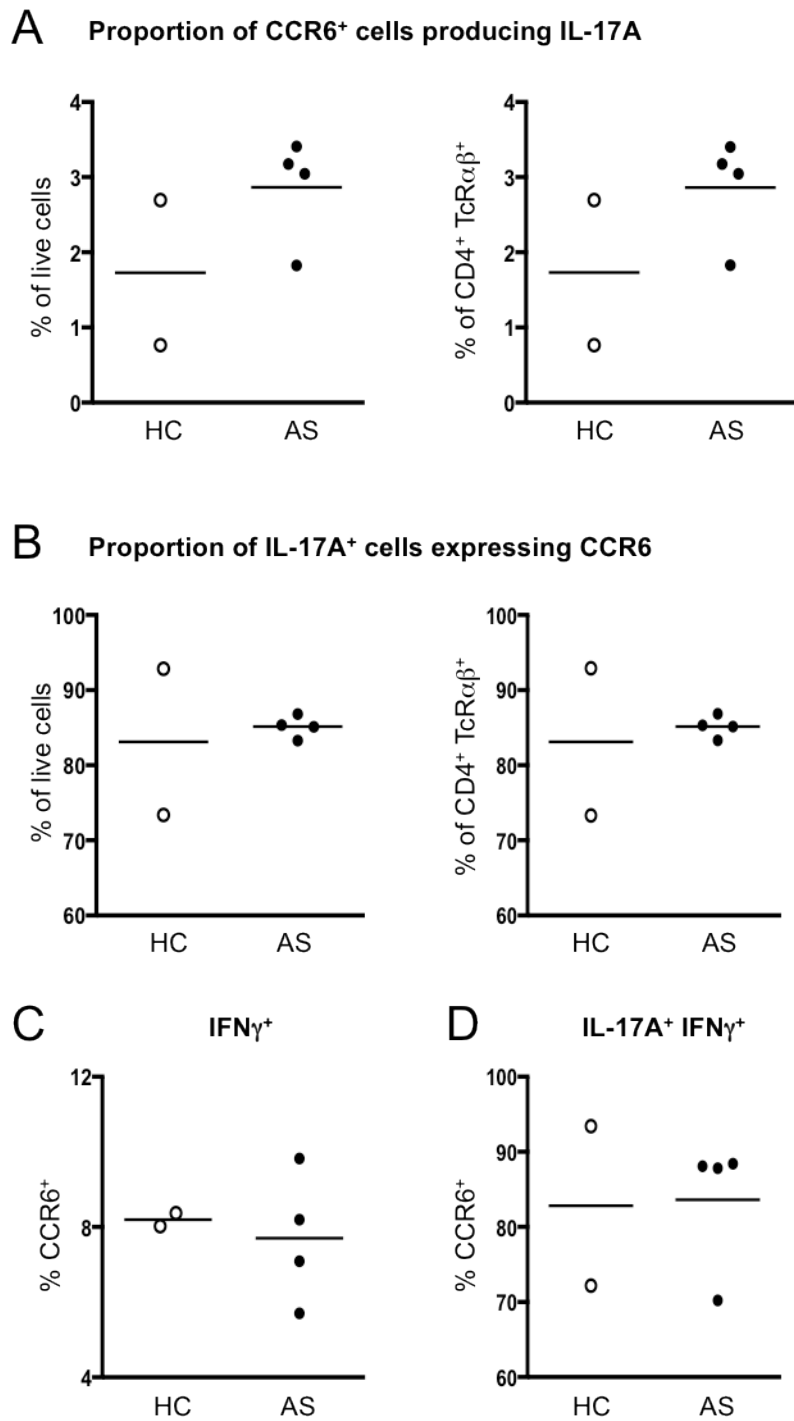


Figure 4.12: CCR6 expression on cytokine secreting CD4⁺ TcRαβ⁺ T Cells

CD4⁺ TcRαβ⁺ T cells producing IL-17A predominantly express CCR6. **(A)** Proportion of CCR6⁺ T cells secreting IL-17A were compared between AS patients (filled circles) and HCs (empty circles) in terms of % of live cells (left) and % of CD4⁺ TcRαβ⁺ T cells (right). **(B)** Proportional analyses of AS patient and HC IL-17A⁺ secreting T cells expressing CCR6, in terms of % of live cells (left) and % of CD4⁺ TcRαβ⁺ T cells (right). Percentage of CD4⁺ TcRαβ⁺ IFN γ ⁺ **(C)** and CD4⁺ TcRαβ⁺ IL-17A⁺ IFN γ ⁺ **(D)** T cells from AS patients and HCs that co-express CCR6. All graphs show mean.

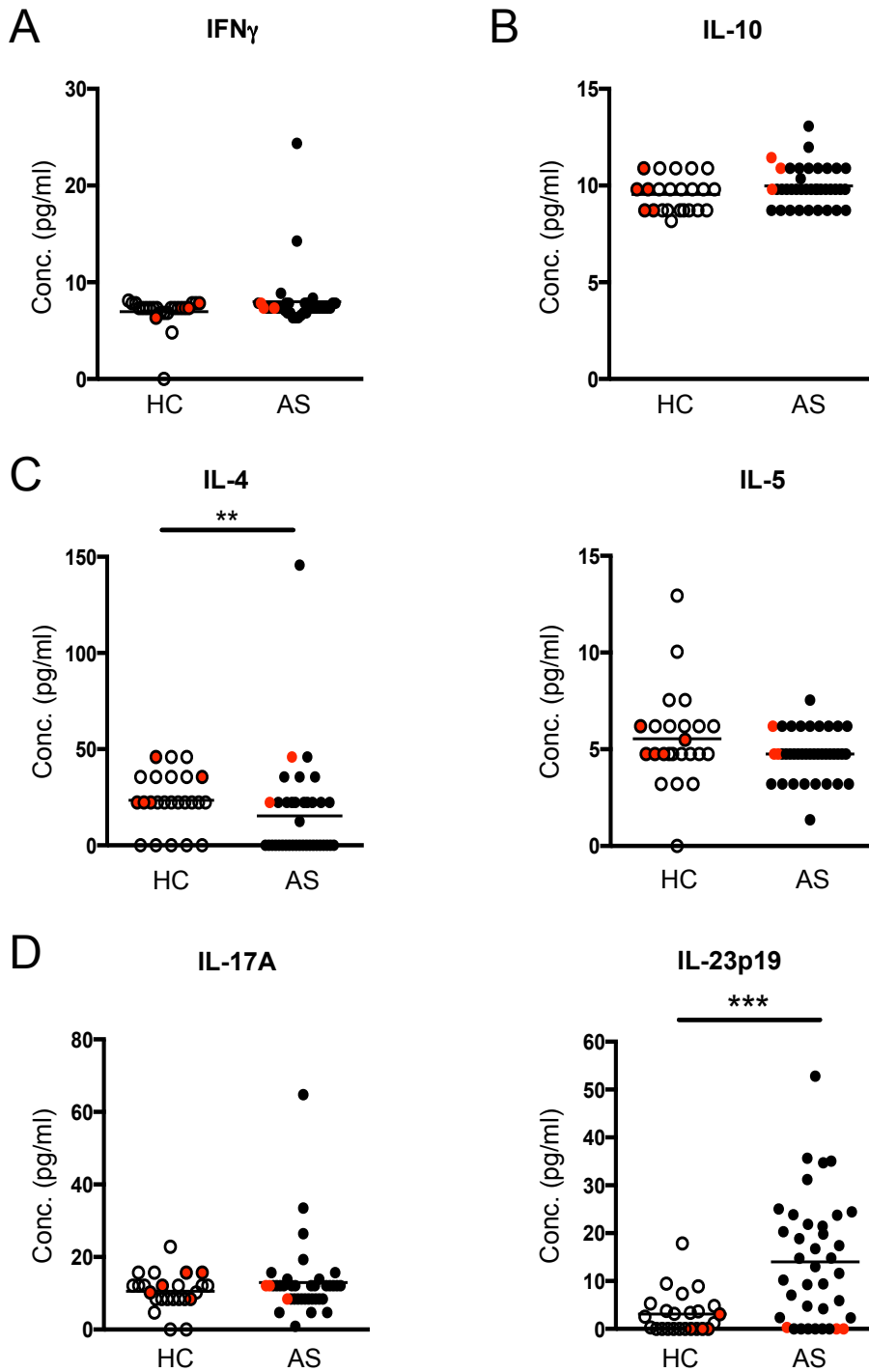


Figure 4.13: Presence of T helper cytokines in AS patient and HC plasma

Plasma cytokines associated with Th1, Th2, Th17 and regulatory T cells in AS patient and HC plasma were measured by luminex or ELISA. Levels of the Th1 associated cytokine IFN γ (A) and the regulatory cytokine IL-10 (B) in AS patient (filled circles) and HC (empty circles) plasma. (C) Th2 cytokines – IL-4 (left) and IL-5 (right) were detected in AS patient and HC plasma. (D) The Th17 associated cytokine profile of AS patients and HC plasma was assessed – IL-17A (left) and IL-23p19 (right). HLA-B27⁺ HC individuals and HLA-B27⁺ AS patients are highlighted in red. ** p = < 0.01 and *** p = < 0.001, by Mann Whitney T tests.

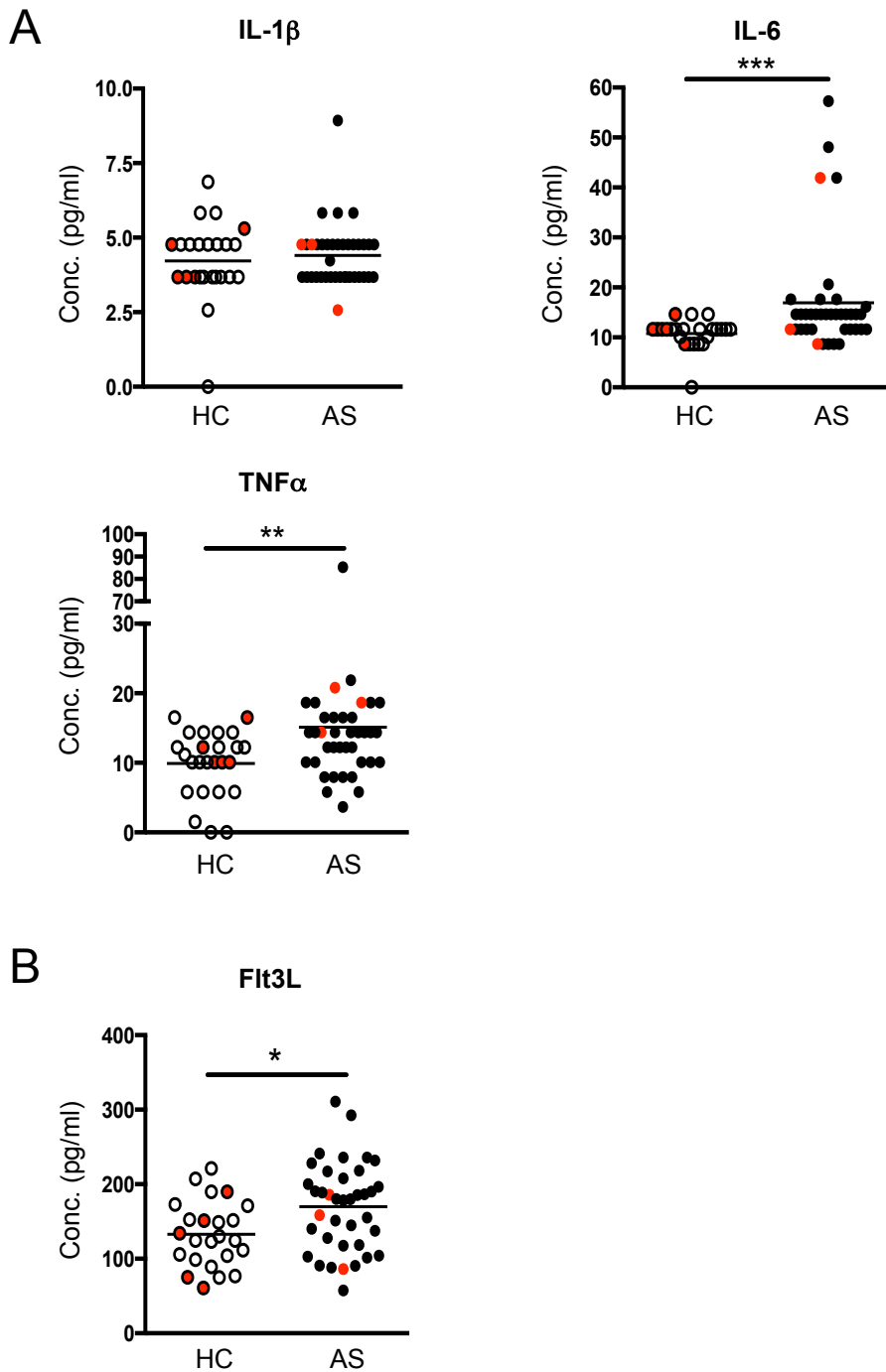


Figure 4.14: Presence of inflammatory cytokines and growth factors in AS patient and HC plasma

Plasma cytokines associated with inflammation and haematopoiesis in AS patients and HCs were analysed. **(A)** Analysis of IL-1 β (top left), IL-6 (top right) and TNF α (bottom) in AS patient and HC plasma. Cytokines were measured by Luminex. **(B)** The haematopoietic growth factor – Flt3L – was measured in plasma isolated from AS patients and HCs using ELISA. HLA-B27⁺ HC individuals and HLA-B27⁻ AS patients are highlighted in red. * $p < 0.05$ and ** $p < 0.01$. A Mann Whitney T test was used for TNF α analysis, whilst an unpaired students T test was used for Flt3L analysis. All graphs show mean.

measured – IFN γ (Th1), IL-10 (Tregs), IL-4 and IL-5 (Th2) and IL-17A and IL-23p19 (Th17) – averaged below 50pg/ml (Fig. 4.13). Two cytokines indicative of inflammation, IL-6 and TNF α , were upregulated in AS patient plasma compared to HCs (Fig. 4.14C). Plasma IL-1 β levels were similar in AS patients and HCs (Fig. 4.14A). Again, concentrations of all inflammatory associated cytokines averaged below 50pg/ml (Fig. 4.14A). Plasma Flt3L was significantly upregulated in AS patients (170pg/ml) compared to HCs (130pg/ml - Fig. 4.14B). The relationship between HLA-B27 expression and plasma cytokine levels was assessed and is depicted in Fig. 4.13 and Fig. 4.14. However, too few HLA-B27⁺ HCs and HLA-B27⁻ AS patients were available; this aspect of the study had insufficient power to assess the relationship between HLA-B27 expression and plasma cytokine concentrations.

Overall, no differences were noted in proportions of naïve, activated, memory and regulatory T cell subsets between AS patients and HCs. However, a significantly higher proportion of activated T cells from AS patients expressed the Th17-associated chemokine receptor CCR6, and a lower proportion of both memory and activated T cells from AS patients expressed the Th1-associated CXCR3 chemokine receptor. Furthermore, these data also indicate that AS patients have a higher proportion of circulating CCR6⁺ IL-17A producing CD4⁺ T cells. Furthermore, we observed higher levels of the Th17-associated cytokines IL-23p19, IL-6 and TNF α in AS patients. All together these data suggest a role for Th17 cells, in accordance with published data.

4.7 Discussion

In this chapter, the phenotypic and functional properties of peripheral blood CD4⁺ T cell subsets in AS patients were investigated. The majority of studies examining the role of T cells in AS have focused on quantifying circulating CD4⁺ T cell subsets (Tregs and Th17 cells), T cell activation, antigen reactivity and plasma cytokines (530, 537, 543, 549, 615, 616). Several studies have focused on alternative T cell populations including $\gamma\delta$ T cells (536) and CD8⁺ T cells (534, 617). This bias towards the study of CD4⁺ T cells originates from a number of influential reports. Initially, athymic HLA-B27 TG rats were shown to develop SpA-like symptoms following transfer of T cells, where CD4⁺ T cells were more efficient than CD8⁺ T cells (470). Not only did this paper highlight a role for T cells in disease induction, but it also identified CD4⁺ T cells to be more pathogenic than CD8⁺ T cells. This result was surprising given that HLA-B27 is a MHC class I molecule classically involved in antigen presentation to CD8⁺ T cells and the strong genetic link between AS

and HLA-B27. These results have been confirmed more recently when eradication of CD8 $\alpha\beta^+$ T cells by thymectomy, antibody depletion or use of CD8 $\alpha^{-/-}$ rats failed to inhibit disease progression (471, 472). Despite intensive efforts trying to identify the role of CD4 $^+$ T cells in the disease pathogenesis, no consensus regarding their role has yet been reached. Several studies indicate involvement of pathogenic Th17 cells in disease development (495, 527, 530, 539, 618) although this is disputed by others (540, 553). Overall, the exact role of Th17 cells in AS pathogenesis remains to be determined. Until now, no detailed analysis of circulating naïve, activated, memory and regulatory T cell subsets has been performed in AS patients. With the aim of generating a greater understanding of AS immunopathogenesis I performed phenotypic and functional analyses of CD4 $^+$ T cell subsets.

The majority of the patients in this study were male and HLA-B27 $^+$. AS is often described as a disease predominantly affecting young males, with approximately 95% of patients expressing HLA-B27 (4). Therefore our small patient cohort is representative of European AS patients. Patient characteristics here are similar to those in Chapter 3, due to some patient overlap and recruitment of patients from the same AS clinic. HC cohort parameters were sufficiently similar to those of AS patients to permit comparative analyses. AS patient disease severity scores and levels of inflammatory markers were relatively low; AS is not often associated with severe systemic inflammation (564). The majority of patients had developed bilateral sacroiliitis, with 45% exhibiting signs of spinal disease. However, data regarding spinal disease was not available for 10 patients, making correlations between spinal disease severity and immunological factors very difficult. Approximately 40% of patients had developed extra-articular manifestations, with uveitis being the most widespread. Excluding patients for whom extra-articular disease manifestation data was not available, 20% of our patient cohort suffered from uveitis. Sampaio-Barros et al report that of their cohort, 15% of AS patients were diagnosed with uveitis (619, 620). However, our study was insufficiently powered to draw any definitive conclusions regarding the prevalence of IBD, psoriasis, uveitis and peripheral arthritis.

Treatment strategies, previously shown to affect immunological factors (539, 586, 621, 622), must be considered when working with patient cohorts. Similar to our blood DC cohort, the majority of patients were receiving treatment with NSAIDs. However, information regarding disease treatment was available for only 60% of patients. Despite these shortcomings, the effect of these individual clinical parameters will be assessed and discussed in Chapter 7.

Using the patient and HC cohorts described above, the proportions of blood T cell subsets were analysed. Given that many patients exhibit a degree of inflammation, we hypothesised that AS patients would have a higher proportion of circulating CD4⁺ T cells compared to HCs. Naïve, memory, activated and regulatory T cell subsets were identified in AS patients and HCs based on the expression of CD45RA, CD25 and FOXP3 (Fig. 4.1). No differences were observed in the proportions of any of the T cell subsets between AS patients and HCs (Fig. 4.2 and 4.3). Furthermore, the total number of circulating CD4⁺ T cells was not increased in AS patients (Fig. 4.2A). Consequently, we can disprove our hypothesis. Very few published studies in AS have quantified the proportions of these T cell subsets. The only study to have performed similar analyses is that by DeJaco et al (623), where no difference in the proportion of blood naïve, memory, activated and regulatory CD4⁺ T cell subsets in the blood of AS patients compared to HCs was observed (623). Of note, they and others identified a population of “chronically stimulated” memory CD4⁺ T cells (CD3⁺ CD4⁺ CD28⁻ CD57⁺) that represented a larger population in AS patients compared to HCs (533, 623). These “chronically stimulated” memory CD4⁺ T cells were described to contribute to disease pathogenesis through their accumulation within inflamed tissue and secretion of IFN γ and pathogenic granules (623). In this study however, this effector CD4⁺ T cell population was not investigated.

Several studies have investigated the proportion and function of Tregs in AS pathogenesis. Some have reported a reduction of circulating Tregs in AS patients, whilst others, including ourselves failed to identify any difference in Treg proportions between AS patients and HCs (543, 549, 623, 624). To complicate matters further, one group observed an increase in circulating Tregs in AS patients (553). These discrepancies may partially be attributed to the use of small patients cohorts, inconsistent use of surface markers including CD25, CD127 and FOXP3, and variation in the antibody clones used to identify CD4⁺ Treg populations. Data presented here suggests that circulating Tregs are not affected in AS and therefore may not contribute to disease pathogenesis. However, accumulation of this immunosuppressive subset at sites of inflammation, including SF and the intestine, may remain important in disease pathogenesis. Supporting this hypothesis, functional Tregs have been reported to represent a larger proportion of the leukocyte population in SF compared to that in blood (548, 549). Furthermore, Ciccia et al observed significant increases in the proportion of intestinal Tregs identified in AS patients presenting with chronic ileal inflammation compared to HCs (553). These Tregs were found to secrete large amounts of IL-10 and suppress T cell proliferation *ex vivo* (553). These results suggest that functional Treg responses are occurring within inflamed peripheral tissues to

suppress inflammation. Overall, compared to HCs we observed no difference in the proportion of total circulating CD4⁺ Tregs in AS patients. However, recent publications suggest that functional Tregs reside within sites of inflammation in AS patients (548, 553), and may represent candidates for the development of future therapeutics. Expansion of these populations *in vivo* may lead to the inhibition of the pathogenic immune response.

In addition to the quantification of individual circulating T cell subsets, one of the aims was to investigate the influence of HLA-B27 expression on the immunological profile of AS patients. Unfortunately the study was insufficiently powered to test this objective, having too few HLA-B27⁻ patient samples and too few HLA-B27⁺ HC samples (Fig. 4.2 and 4.3). However, Wu et al were unable to identify differences between HLA-B27⁻ (n=37) and HLA-B27⁺ (n=12) HC individuals in terms of circulating Treg proportions (624). In contrast, Poddubnyy et al found that anti-TNF α naïve HLA-B27⁺ patients had a lower proportion of IL-10⁺ CD8⁺ T cells compared to HLA-B27⁻ patients. Therefore, HLA-B27 expression may affect the development of IL-10 secreting cells (625). These data suggest that HLA-B27 expression may affect specific cellular aspects of the immune profile of AS patients, highlighting the need for larger studies to functionally assess the role of HLA-B27 in disease development.

Overall, we were unable to identify any differences in the proportions of circulating naïve, memory, activated and Treg populations in AS patients, consistent with the findings by Dejaco et al (623). Therefore, we can conclude that T cell proportions are not quantitatively affected in AS patients despite the ongoing disease processes. Patient clinical parameters may influence our analysis of blood cell populations in AS patients. In fact, one study in RA reported that blood CD4⁺ CD25^{hi} Tregs negatively correlated with CRP, highlighting the importance of evaluating these clinical/immunological relationships (626). Detailed analysis of these relationships will be discussed in Chapter 7.

Several groups have investigated the involvement of T cells in AS pathogenesis through analyses of their function and effector phenotype (Th1/Th2/Th17/Treg/Th22) (181, 470, 480, 495, 530, 537, 586). To corroborate these studies, the function and migration patterns of CD4⁺ T cells in AS patients and HCs were investigated. Following DC: T cell interactions, chemokine receptors are upregulated on the surface of antigen specific T cells. The array of chemokine receptors induced on the T cells promotes directed migration to specific tissues where they exert their functions, resulting in the promotion of immunogenic or tolerogenic immune responses. Furthermore, expression of chemokine

receptors, given their association with specific Th cell phenotypes, can indicate the T cell subsets involved in disease pathogenesis. Published data examining the chemokine receptor profile of AS patients T cells has focused on CCR4 and CCR6 expression. CCR4 induces T cell migration to the skin, a tissue commonly affected in AS patients (173, 175). CCR4 is proposed to be involved in cell migration to rheumatic joints, as is CXCR3 (627). CCR6 is often studied due to its use as a surrogate marker for IL-17 secreting Th17 cells (180, 181). In order to identify alterations to the migration patterns of AS patient T cells, expression of CCR4, CCR6, CCR9, CCR10 and CXCR3 were assessed on T cells. Circulating memory, activated and regulatory T cell populations from HC expressed all the chemokine receptors analysed (Fig. 4.5 and 4.6). Strikingly, the majority (~95%) of Tregs expressed CCR4, the highest expression of any chemokine receptor studied (Fig. 4.7A). This finding supports published studies where $CD4^+ CD25^{hi} FOXP3^+$ T cells specifically expressed high levels of CCR4 (628, 629). This characteristic feature of Tregs may permit migration into and surveillance of the skin epithelial barrier, the largest organ in the body. However Tregs additionally express high levels of CCR6, suggesting that circulating T cells express an array of chemokine receptors mediating their migration to a multitude of tissues, mediated by chemokine engagement. In contrast to memory, activated and regulatory subsets, naïve $CD4^+$ T cells lacked expression of all chemokine receptors, except CXCR3 (Fig. 4.5 and 4.6). CXCR3 is thought to be rapidly upregulated on naïve T cells following activation. Therefore the small population of $CXCR3^+ CD45RA^+ CD25^-$ naïve T cells may represent newly activated T cells. The absence of chemokine receptors prevents directed tissue migration, allowing naïve T cells to recirculate through and survey lymphoid tissues in a CCR7 dependent manner (630-632). CCR9 expression on all subsets was minimal, perhaps suggesting that only a small proportion of T cells in the blood home to the gut.

Comparison of chemokine receptor expression on AS patients and HCs revealed no differences in expression of CCR4, CCR9 and CCR10 on any of the $CD4^+$ T cell subsets (Fig. 4.7 and 4.9). Accordingly, these results suggest that the migration of $CD4^+$ T cells toward tissues including the skin and intestine are not altered in AS patients. This observation was surprising given that the skin and intestine represent common sites of extra-articular inflammation in patients. Furthermore, these results appear to contradict the hypothesis that the intestine is a site of induction in SpA (4, 440, 444, 480). However, parameters measured in blood do not necessarily reflect pathological processes occurring in peripheral tissues, and therefore based on these results alone it is only possible to conclude that mucosal-homing primed cells do not appear to be increased in the blood of

AS patients. Also no differences were detected in the frequency of CD4⁺ T cells expressing CCR4 (Fig. 4.7). This observation contradicts previously published reports where the frequency of CCR4⁺ CD4⁺ T cells was upregulated in blood of AS patients compared to HCs (532, 624). Differences in antibody clone, gating strategies and patient cohorts could account for these different results. It would be interesting to analyse co-expression of chemokine receptors in the future to further define the complete chemokine receptor profile of T cells in AS patients and HCs.

In contrast to CCR4, CCR9 and CCR10, both CCR6 and CXCR3 were differentially expressed on circulating AS CD4⁺ T cells compared to HCs. Activated T cells from AS patients expressed significantly elevated levels of CCR6 compared to HCs (Fig. 4.7A). CCR6 promotes migration of cells to inflamed tissues including the skin and the intestine (180). Inflammation in AS patients often occurs within the spine, SIJs and extra-articular tissues. Therefore, one could predict that CCR6 mediates cell migration to these sites. Furthermore, CCR6 is often expressed by Th17 cells (180, 181). Confirming this relationship, the majority of IL-17A⁺ cells expressed CCR6 (~85% - Fig. 4.12B). Given the increase in circulating CCR6⁺ CD4⁺ T cells, the capacity of CD4⁺ T cells to secrete IL-17A was investigated. Indeed, a trend towards a higher proportion of IL-17⁺ CD4⁺ T cells in AS patients was seen (Fig. 4.11). However, only 2 HCs and 4 AS patients were used, and thus this experiment will need to be repeated before firm conclusions can be drawn. In addition, examination of other Th17-associated molecules such as expression of RORγt, IL-17F and IL-22 by CCR6⁺ T cells would complement the investigation of Th17 cells in AS.

The higher proportion of circulating CCR6⁺ CD4⁺ T cells, with the ability to secrete IL-17, may represent circulating Th17 cells, thought to be pathogenic in AS (495, 527, 530, 539). Several groups have previously reported increased Th17 proportions in the blood of AS patients, supporting my observations (527, 530, 538, 539, 633). Only two reports have addressed the contribution of Th17 cells within extra-articular tissue of AS patients. Ciccia et al were unable to detect any significant Th17 polarisation in AS patient intestinal tissue (551), but, interestingly, compared to HCs they observed expansion of IL-10-secreting Tregs in the intestine of AS patients (551, 553). These results suggest that the intestinal environment of AS patients supports the generation of Tregs that subsequently control Th17 responses. Retinoic acid (RetA) has previously been shown to promote generation of Tregs at the expense of Th17 cells and therefore may contribute to the phenomenon described by Ciccia et al (119, 551, 553). Consequently, it would be interesting to analyse

RetA levels in AS and HC intestinal tissue and further assess the impact of intestinal Th17 and Treg populations in AS pathogenesis. However in the study conducted by Ciccia et al, a proportional comparison of intestinal Th17 cells between AS patients and HCs was not performed (553). The second study investigating peripheral Th17 cells involved use of tissue isolated from the facet joints of AS patients. Appel et al observed an increase in IL-17⁺ cells within these facet joints, despite the absence of circulating Th17-phenotype T cells (540). These experiments identified neutrophils and MPO positive cells to be the main producers of IL-17 (540). Therefore, within the joints of AS patients the secretion of IL-17 from innate leukocytes may be involved in the pathogenesis of AS. However, the role of Th17 cells and IL-17 in disease pathogenesis especially within the extra-articular tissues requires further investigation.

In contrast to our findings regarding CCR6 expression on CD4⁺ activated T cells, a significant reduction was observed in the frequency of CXCR3⁺ activated and memory T cells in AS patients compared to HCs (Fig. 4.8). This phenomenon has not been reported before in AS. CXCR3 is associated with the Th1 phenotype and migration of cells to inflamed tissues (182, 183, 614). A reduction in CXCR3⁺ CD4⁺ T cells accompanied with an increase in circulating CCR6⁺ CD4⁺ T cells could suggest a shift in T cell phenotype from Th1 to Th17 in patients. Thus, these observations support a role for Th17 cells in the pathogenesis of AS. Alternatively, loss of circulating CXCR3⁺ cells may not just represent a shift in T cell phenotype: given the propensity for CXCR3 to induce migration to inflammatory sites, activated and memory CXCR3⁺ cells may accumulate within inflamed tissues. To support this hypothesis, CXCR3 has previously been shown to induce SF cell migration in juvenile idiopathic arthritis (JIA) patients (634). Analysis of CXCR3⁺ cells within inflamed tissues, expression of Th1 associated cytokines, and assessment of the induction of CXCR3⁺ T cells following DC: T cell interactions could further elucidate the role(s) of CXCR3⁺ T cells in AS pathogenesis. Partially addressing this question, we analysed the proportions of circulating IFN γ -secreting CD4⁺ T cells in AS patients, the prototypic Th1-associated cytokine (Fig. 4.11). We hypothesised that production of this cytokine would be reduced in patients given the downregulation of CXCR3 expression. However, compared to HCs, no difference was observed in the proportion of IFN γ ⁺-secreting CD4⁺ T cells between AS patients and HCs (Fig. 4.11). However due to insufficient sample numbers, we cannot irrefutably exclude the possibility that proportions of IFN γ -secreting cells differ between AS patients and HCs. A power calculation can be performed to calculate the minimum sample size required to ensure confidence in our observations. With respect to the frequency of IFN γ ⁺ CD4⁺ T cells in AS patients and HCs,

using a power calculation we determined the sample size required to identify potential differences between our cohorts. As proportion of live cells, 7% and 11% of CD4⁺ IFN γ ⁺ cells were detected in AS patients and HCs respectively (Fig. 4.11A). Given a SD of 4 within the AS patient cohort, where the “known ($\mu(0)$)” and “unknown $\mu(1)$ ” mean values of the population were 7 and 11 respectively, a sample size of 8 was required. Given an SD of 10 within the HC cohort and using the identical $\mu(0)$ and $\mu(1)$ values, a sample size of 50 was required. Therefore, to determine any potential difference between our cohorts, with respect to the proportion of IFN γ ⁺ CD4⁺ T cells, a sample size of between 8 and 50 individuals would be required.

T cells and other immune cells influence immune responses through secretion of cytokines, which are also important for lineage development, T cell priming, and cell activation. Therefore, the levels of plasma growth factors and cytokines related to these processes were analysed by luminex and ELISA. In contrast to our results suggesting that a higher proportion of circulating IL-17-secreting cells is present in AS patients, we did not observe a corresponding increase in plasma IL-17A concentration (Fig. 4.13A). Similarly, Zhang et al did not observe an increase in plasma IL-17A despite an increase in circulating IL-17⁺ CD4⁺ T cells (530). These findings suggest that Th17 cells, if involved in AS pathogenesis, may not exert their effects through increases in plasma IL-17A. Th17 cells secrete a variety of other cytokines such as IL-6, TNF α , IL-22 and IL-17F that may be involved in disease pathogenesis (635, 636). Of interest, and something that will be partially addressed in Chapter 6, relates to the involvement of AS DCs in driving this potential Th17 phenotype. For example, DCs have been shown to produce IL-6, necessary for the generation of Th17 cells along with TGF β (108, 637). Additionally, Hansel et al report that SLAN⁺ DCs secrete large amounts of the Th17-associated cytokines IL-23 and IL-6, promoting generation of IL-17⁺ IFN γ ⁺ T cells (249). Therefore, the slight increase in CD14⁻ CD16⁺ mononuclear cells, including SLAN⁺ DCs (Fig. 3.7A), in AS patients may contribute to the expansion of Th17 cells in AS patients. However, as the *in vivo* functions of human blood DCs remain obscure, identification of an equivalent tissue resident DC population may help elucidate pathways involved in disease pathogenesis.

As suggested earlier, Th17 cells may contribute to AS pathogenesis via an IL-17 independent mechanism. Th17 cells have been reported to secrete an array of cytokines including IL-6, TNF α and IL-22 (635, 636). Although increased in AS patients, IL-6 and TNF α levels were very low (<30pg – Fig. 4.14A). In fact, a monoclonal antibody that targets and blocks the IL-6R has been reported to be ineffective in AS clinical trials (23).

However, the functional attributes of these cytokines in AS have not been assessed and may still play a pathogenic role in disease progression. Intracellular cytokine staining for IL-6 and TNF α could be performed to assess whether Th17 cells may contribute to plasma levels of these cytokines. In addition, Th17 cells have been shown to excel in the provision of B cell help through induction of antibody production including IgA and IgM, whilst remaining partially refractory to Treg-mediated suppression (120). Therefore, promotion of B cell responses and sustained activation *in vivo* may represent additional pathways through which Th17 cells may mediate disease pathogenesis in an IL-17-independent manner.

As discussed above, AS patient IL-17A levels were not different from those observed in HCs, whilst IL-6 and TNF α were significantly upregulated. Furthermore, IL-23p19 was also significantly elevated in AS patient plasma (Fig. 4.13D). Both IL-6 and IL-23p19 have previously been reported to be upregulated in AS patients (49), supporting data presented here. As both cytokines are involved in the generation and maintenance of Th17 cells in both mice and men (108, 109, 120, 635), these observations lend further support to a pathogenic role for Th17 cells in AS. Therefore, the elevated levels of IL-6, IL-23p19 and TNF α in AS patients could contribute to pathogenic immune responses, potentially through development of Th17 cells. Aside from inflammation and Th17 associated cytokines, no difference in IFN γ (Th1) and IL-10 (Treg) levels were detected between AS patients and HCs.

Further supporting a shift in circulating T cell phenotype of our patient cohort, the Th2 associated cytokine IL-4 was downregulated in AS patients compared to HCs (Fig. 4.13C). However, IL-5 did not correlate with IL-4 as no difference was observed between HCs and AS patients (Fig. 4.13C). These data could suggest that activated Th2 cells known to secrete both IL-4 and IL-5 do not contribute to this observation. Alternatively IL-4-secreting populations, including mast cells, may be reduced in AS patients.

Cytokines are also involved in driving the development of immune populations. Flt3L, a haematopoietic growth factor, is upregulated in AS patient plasma compared to HCs (Fig. 4.14B). To the best of my knowledge, this observation has not previously been described in AS. Given the integral role of Flt3L in the development of DCs (284, 287) and the observation that AS patients have a significantly reduced population of CD1c⁺ cDCs (Fig. 3.4B), plasma Flt3L may be increased in AS patients to promote development of cDCs in order to rectify this deficiency. This idea is supported by the observation that DC subsets

expand in humans *in vivo* following Flt3L administration (572). Further experiments to support or disprove this hypothesis could include enumeration of DC progenitors in blood of AS patients and HCs. If this reduction in CD1c⁺ DCs in AS patients contributes to disease pathogenesis, Flt3L could be a potential target for future therapies. Alternatively, if mature blood cDCs migrate into peripheral tissue, then their presence may be exaggerated within peripheral tissue supporting the need for investigation into the function of blood DCs *in vivo*, and analysis of tissue-resident DC populations in HCs and AS patients including the intestine and skin.

Overall, a differential chemokine receptor profile on activated T cells was observed in AS patients compared to HCs. Specifically, the proportion of CCR6⁺ circulating activated T cells increased, while the proportion of CXCR3⁺ cells decreased in AS patients. A trend towards a higher proportion of IL-17⁺ CCR6⁺ T cells in AS patients' blood was observed, along with elevated levels of the Th17-polarising cytokines, IL-6 and IL-23p19. These results suggest that Th17 cells may play an important role in AS pathogenesis. Interestingly, it was additionally observed that the myeloid cell growth factor Flt3L may be elevated in AS patients to compensate for their loss of CD1c⁺ cDCs.

Our results to date have identified alterations to the circulating myeloid and T cell profile in AS patients. However, I next sought to address their contribution to the inflammatory response within inflamed extra-articular tissues of AS patients. Subsequently, using synovial fluid (SF) samples isolated from the peripheral joints of AS patients, the cDC and T cell subsets residing within this inflamed tissue were characterised.

Chapter 5: Synovial Fluid

5.1 Introduction

Patients with SpA often develop extra-articular manifestations including uveitis and skin inflammation. AS patients, often with peripheral arthritis, can experience build up of synovial fluid (SF) within the joint space. This causes severe pain within the joint and inhibits joint function, whereupon SF is often removed to alleviate these symptoms. Analysis of the cells recruited to the joint, their surface phenotype and the SF cytokine milieu can help elucidate the mechanisms of disease pathology.

The majority of SF studies in AS patients focus on the presence of T cell subsets, their function and the cytokines they produce. Specifically, functional Tregs have been isolated from AS patient SF (548, 549). A variety of Th1 and Th2 associated cytokines have been detected in AS patient SF, including IL-12/IL-23 p40 (531, 638). To date, the presence of conventional and plasmacytoid DCs in AS SF has not been investigated. Unlike AS, several groups have isolated cDCs and pDCs from RA SF, where cDCs have been shown to accumulate within SF, in addition to having a more activated phenotype compared to their blood counterparts (217, 581). As DCs principally induce and direct immune responses, it is important to identify and assess their functions in SF. Therefore, we set out to identify and phenotype cDC and pDC subsets within AS SF. To generate context for the DC data, other cell types such as monocytes and T cells were also studied.

5.2 Patient characteristics

For the SF analyses described in this chapter 4 patient samples were analysed. Details of these patients are shown in Table 5.1.

Table 5.1: Patient characteristics for SF analysis

For the characterisation of SF cDC and pDC subsets, samples from four AS patients were used. ESR, CRP, disease duration and treatment protocol information were available for all AS patients.

ID	Sex	Tissue	Age (yrs)	ESR (mm/hr)	CRP (mg/L)	Duration (yrs)	Treatment
1	Female	Shoulder	68	28	7	32	Adalimumab
2	Male	Knee	50	22	29	13	Etoricoxib, Sulphasalazine

3	Male	Knee	35	5	24	3	Etoricoxib, Sulphasalazine
4	Male	Knee	60	18	36	23	None

Three of the four patients were male, and three SF samples were aspirated from the knee (Table 5.1). When comparing patients 1 and 2 (Fig. 5.7 and Fig. 5.8), several observations regarding inflammatory markers and disease treatment are relevant. AS patient 1, at time of analysis, was receiving anti-TNF α treatment (Adalimumab – Table 5.1). CRP levels were also within the normal range (<10, Dr David McCarey – personal communication). The treatment protocol of AS patient 2 included an NSAID (Etoricoxib) and a DMARD (Sulphasalazine). Values of 22 (ESR) and 29 (CRP) for patient 2 indicate ongoing inflammation. Furthermore, the remaining two AS patients presented with high levels of CRP. Interestingly patient 4, who at time of analysis was not receiving any form of treatment, had long-standing disease with high levels of CRP. These differences, and their potential effects on the DC subsets and cytokines will be discussed below.

5.3 Synovial fluid mononuclear phagocytes

There are no reports describing the myeloid profile of SF isolated from AS patients. Therefore, DC populations in AS patient SF were characterised using the techniques developed to identify blood DCs. To do this, gating strategies used for peripheral blood cDC, monocyte and pDC analysis were adopted to identify similar subsets within SF.

5.3.1 cDCs and monocytes

Two DC subsets were identified in AS patient SF. The gating strategy used to identify these subsets is depicted in Fig. 5.1A. First, cell debris was gated out by FSC-A and SSC-A with doublets subsequently removed according to their FSC-A/FSC-H characteristics (Fig. 5.1A). Dead cells (DAPI⁺) were also excluded from further analysis. Single, live leukocytes were assessed for the expression of LIN markers (CD3, CD15, CD19 and CD56). All LIN⁻ CD14⁻ cells were analysed for co-expression of CD11c and MHC II (Fig. 5.1A). These single DAPI⁻ LIN⁻ CD14⁻ CD11c⁺ MHC II⁺ cells could be subdivided into two cDC populations: CD1c⁺ and CD141⁺ DCs (Fig. 5.1A). Based on their surface marker expression, these two DC subsets appeared to be analogous to the DC populations found in peripheral blood.

To identify monocyte populations within SF, single DAPI⁻ leukocytes were assessed for CD11c and MHC II expression (Fig. 5.1B). The CD11c⁺ MHC II⁺ cells were further analysed for expression of monocyte markers CD14 and CD16 (Fig. 5.1B), and three CD11c⁺ MHC II⁺ subsets were identified based on differential expression of these markers (Fig. 5.1B – populations 1, 2 and 3). Populations 1 and 2 are equivalent to the CD14⁺ monocyte subsets identified in peripheral blood. Population 1 is the CD14⁺ CD16⁻ monocyte fraction, whilst population 2 can be identified as the CD14⁺ CD16⁺ monocyte population (Fig. 5.1B). The CD14⁻ CD16⁺ mononuclear population appears to be absent from SF tissue (Fig. 5.1B). Population 3 consists of the two cDC populations identified in SF and peripheral blood (Fig. 3.1A and Fig. 5.1B).

As discussed in chapter 3, CD14⁻ CD16⁺ mononuclear cells can be subdivided into two populations based on the expression of SLAN. In order to confirm the absence of the CD14⁻ CD16⁺ population in SF, cells were further assessed for the expression of CD16 and the associated SLAN⁺ and SLAN⁻ subsets (Fig. 5.2). Initially, SF monocyte subsets were assessed and compared to blood monocytes analysed on the same day (Fig. 5.2A). When live LIN⁻ CD11c⁺ MHC II⁺ cells were analysed for CD14 and CD16 expression (Fig. 5.2A), no CD14⁻ CD16⁺ cells were observed in the SF sample. Furthermore, CD11c⁺ MHC II⁺ SF cDCs were assessed for the expression of SLAN (Fig. 5.2B). Mouse IgM was used as the isotype control. Most SF CD11c⁺ MHC II⁺ cells lacked expression of SLAN (Fig. 5.2B). However as this experiment did not include a positive control, and since it is known that SLAN⁺ cells exist in blood (Fig. 3.6A), these analyses were subsequently repeated using unmatched blood and SF processed and analysed on the same day. These samples were used to further confirm or reject the presence of any live LIN⁻ SLAN⁺ leukocytes in SF (Fig. 5.2C). Gates were set using the isotype. Peripheral blood was used as a positive control, and as expected, a population of SLAN⁺ cells could be identified (Fig. 5.2C). In contrast, very few live LIN⁻ leukocytes in SF expressed SLAN (Fig. 5.2C). In all these experiments, we were unable to detect definitive populations of CD14⁻ CD16⁺ SLAN⁺ or CD14⁻ CD16⁺ SLAN⁻ mononuclear cells in SF isolated from AS patients (Fig. 5.1 and Fig. 5.2). However, our staining could suggest that a small population of CD16⁻ SLAN⁺ cells exist in SF, however in order to confirm this further analyses would have to be performed.

5.3.2 Plasmacytoid DCs

pDCs are the primary secretors of type I interferons and are key contributors to the immune response against viral infections (639). In order to identify SF pDCs, the gating

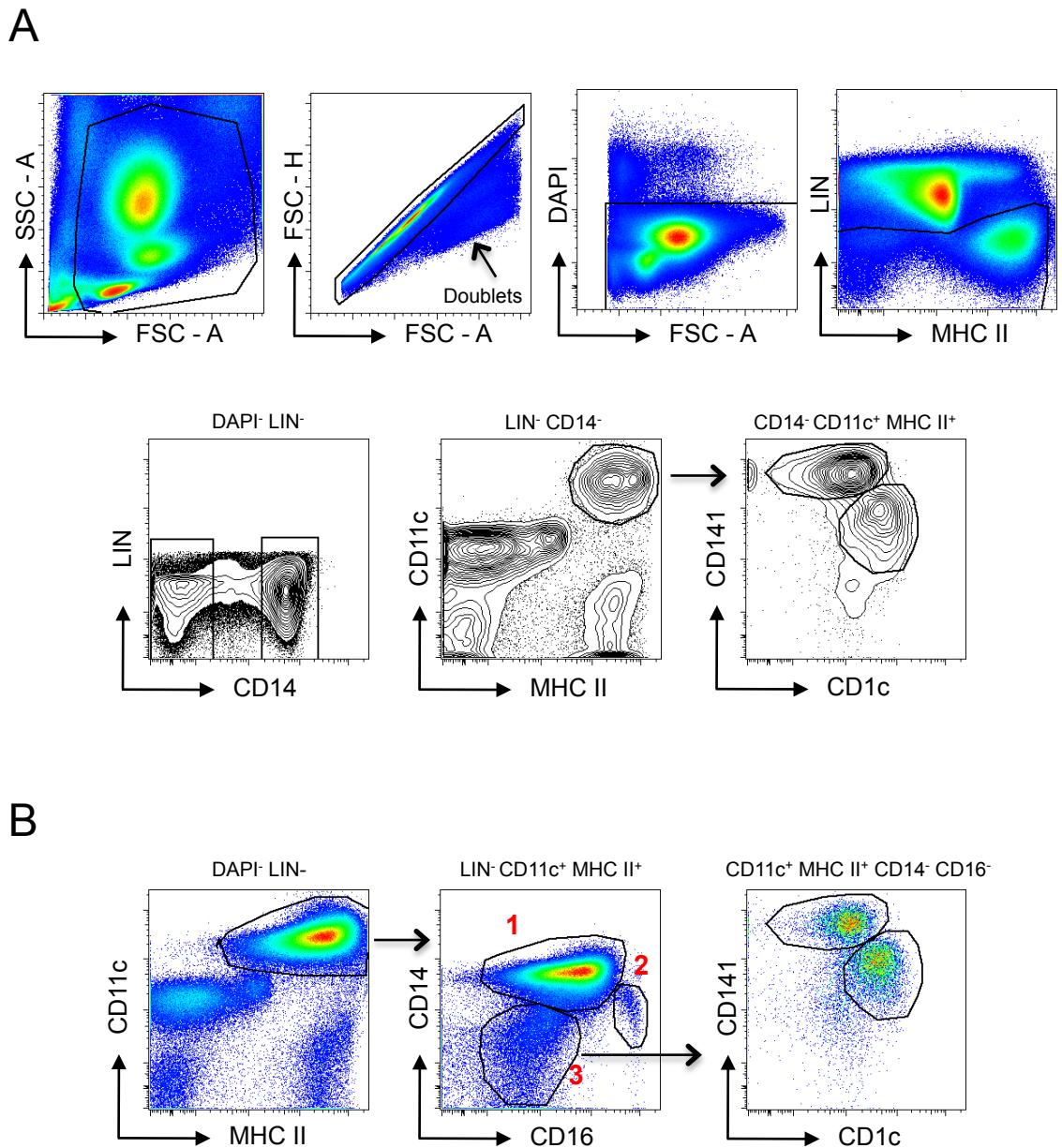


Figure 5.1: Identification of CD141⁺ and CD1c⁺ Synovial Fluid DC Subsets

CD141⁺ and CD1c⁺ DCs can be found in synovial fluid (SF) isolated from AS patients. **(A)** Gating strategy used to identify SF DC subsets. Doublets and dead cells (DAPI⁺) were excluded from analysis. Live single cells that lacked expression of LIN markers were analysed for CD14 expression. CD14⁻ cells co-expressing CD11c and MHC II were divided into CD141⁺ and CD1c⁺ DC subsets. **(B)** Identification of monocytes in SF. Single DAPI⁻ LIN⁻ cells were analysed for CD11c and MHC II expression. LIN⁻ CD11c⁺ MHC II⁺ cells were divided into three subsets: CD14⁺ CD16⁻ (1), CD14⁺ CD16⁺ (2) and CD14⁻ CD16⁻ (3). Subset 3 contained SF DCs – CD141⁺ and CD1c⁺ populations. LIN = CD3, CD15, CD19 and CD56.

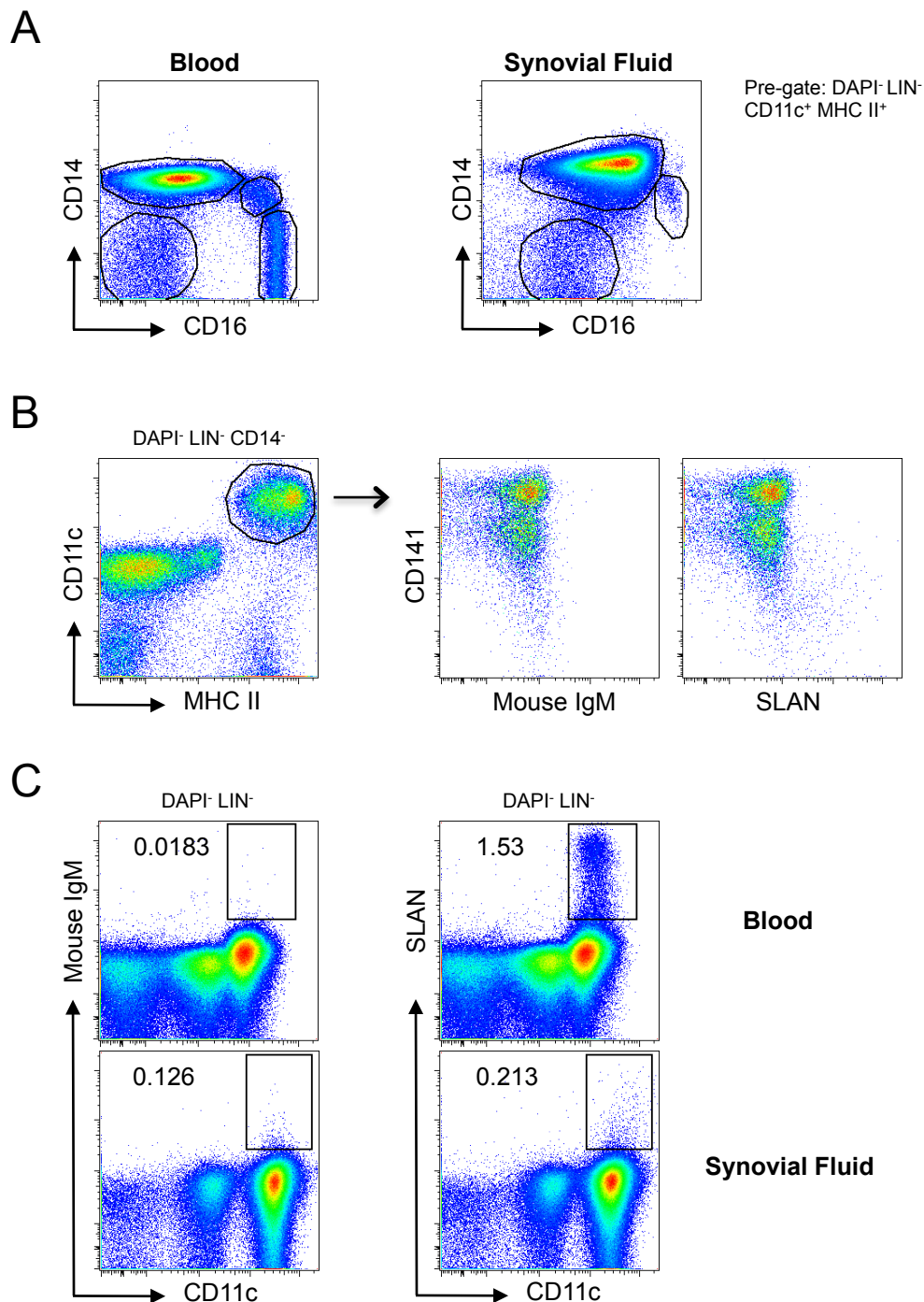


Figure 5.2: Presence of CD16⁺ CD11c⁺ mononuclear cells and SLAN subsets in SF

Absence of CD14⁻ CD16⁺ mononuclear cells and the respective SLAN⁺ and SLAN⁻ subsets from AS SF. SF from one AS patient was assessed for the occurrence of the SLAN⁺ and SLAN⁻ subsets of CD16⁺ mononuclear cells. **(A)** DAPI⁻ LIN⁻ CD11c⁺ MHC II⁺ cells were analysed for the presence of CD16⁺ CD14⁻ cells in HC blood (left) and AS patient SF (right). LIN contains markers against CD3, CD15, CD19 and CD56. **(B)** Total SF DCs (DAPI⁻ LIN⁻ CD14⁻ CD11c⁺ MHC II⁺) were assessed for expression of SLAN. **(C)** Comparison of total mononuclear cells isolated from blood (top) and SF (bottom) cells for the presence of SLAN⁺ cells. Percentages represent the proportion of single, DAPI⁻ LIN⁻ (CD3, CD15, CD19 and CD56) cells used for analysis. Gates were set based on the isotype-matched negative control (left).

strategy used to identify blood pDCs was used. SF pDCs were detected in our cohort of AS patients using the gating strategy shown in Fig. 5.3A. pDCs were identified as single DAPI⁻ LIN⁻ cells, that co-expressed CD123 and MHC II and also expressed the pDC marker CD304 (Fig. 5.3A). To conclude, pDCs (DAPI⁻ LIN⁻ CD123⁺ MHC II⁺ CD304⁺) can be identified in AS patient SF (Fig. 5.3). In addition, quantification of SF pDCs (DAPI⁻ LIN⁻ CD123⁺ MHC II⁺ CD304⁺) was also performed, in terms of percentage of live cells. Approximately 0.2% of total SF live cells are pDCs (Fig. 5.3B), compared to the 0.3% of live cells found in blood (Fig. 3.4C).

5.4 Surface phenotype of cDCs and monocytes

We have identified two cDC subsets, two monocyte subsets and pDCs in AS SF. After identification of these cells, it was important to further characterise their surface phenotype to assess whether SF cDCs and monocytes possessed a surface phenotype similar to their blood counterparts. Thus, CD11b and CD86 expression was assessed on SF cDCs and monocytes (Fig. 5.4). Single live LIN⁻ CD14⁻ CD11c⁺ MHC II⁺ DCs were assessed for CD11b expression (Fig. 5.4A). The CD141⁺ DC subset expressed negligible levels of CD11b whilst the CD1c population homogeneously expressed CD11b (Fig. 5.4A). These findings are similar to the CD11b expression profile on blood cDCs (Fig. 3.16A). Due to the inflammatory environment surrounding SF cDCs, it was also important to assess the activation status of cDCs isolated from this tissue. Therefore, expression of the co-stimulatory molecule CD86 was assessed on both cDC subsets (Fig. 5.4B). Surprisingly, our findings show both cDC subsets were relatively immature, with CD86 absent from the cell surface, when compared to the observed levels of CD86 expression on CD14⁺ CD16⁻ blood monocytes (Fig. 5.4B and 3.14B).

Monocyte subsets – CD14⁺ CD16⁻ and CD14⁺ CD16⁺ - were similarly assessed for CD11b and CD86 expression (Fig. 5.4C and Fig. 5.4D). Similar to blood monocytes (Fig. 3.18A), both CD14⁺ CD16⁻ and CD14⁺ CD16⁺ SF monocyte populations homogeneously expressed high levels of CD11b (Fig. 5.4C). The activation status of these myeloid cell populations was also assessed, and both SF monocyte subsets expressed low levels of CD86 (Fig. 5.4D), although CD14⁺ CD16⁻ monocytes expressed higher levels of CD86 than the CD14⁺ CD16⁺ population. However, this observation was made on the basis of one AS patient and therefore may not be indicative of AS patient SF tissue-resident DCs. Overall, the surface phenotype of SF monocytes, at least in terms of CD11b expression, is similar to that observed in blood.

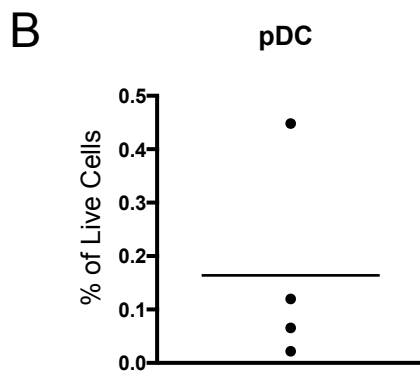
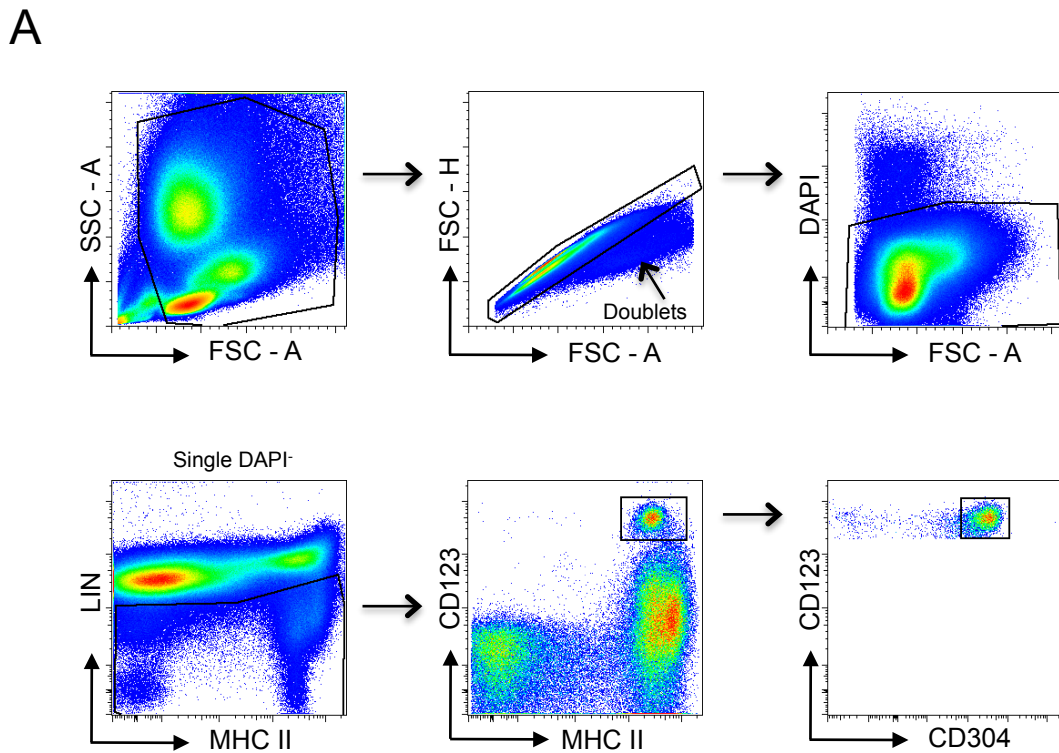


Figure 5.3: pDCs present in AS patient SF

pDCs are present in AS patient SF. Mononuclear cells were isolated from SF as described in chapter 2. **(A)** Gating strategy used to identify SF pDCs. Cell debris was gated out by FSC-A and SSC-A. Doublets were excluded using the FSC-A and SSC-A gate and DAPI⁺ dead cells were also eliminated. Live single cells were analysed for expression of lineage markers (CD3, CD15, CD19 and CD56) and MHC II. LIN⁻ cells were assessed for MHC II and CD123 expression. CD123⁺ MHC II⁺ cells were analysed for CD304 expression; CD123⁺ CD304⁺ MHC II⁺ cells are SF pDCs. **(B)** pDCs were evaluated in terms of % of live cells in AS SF from 4 patients. pDCs (LIN⁻ MHC II⁺ CD123⁺ CD304⁺) were identified as described in A.

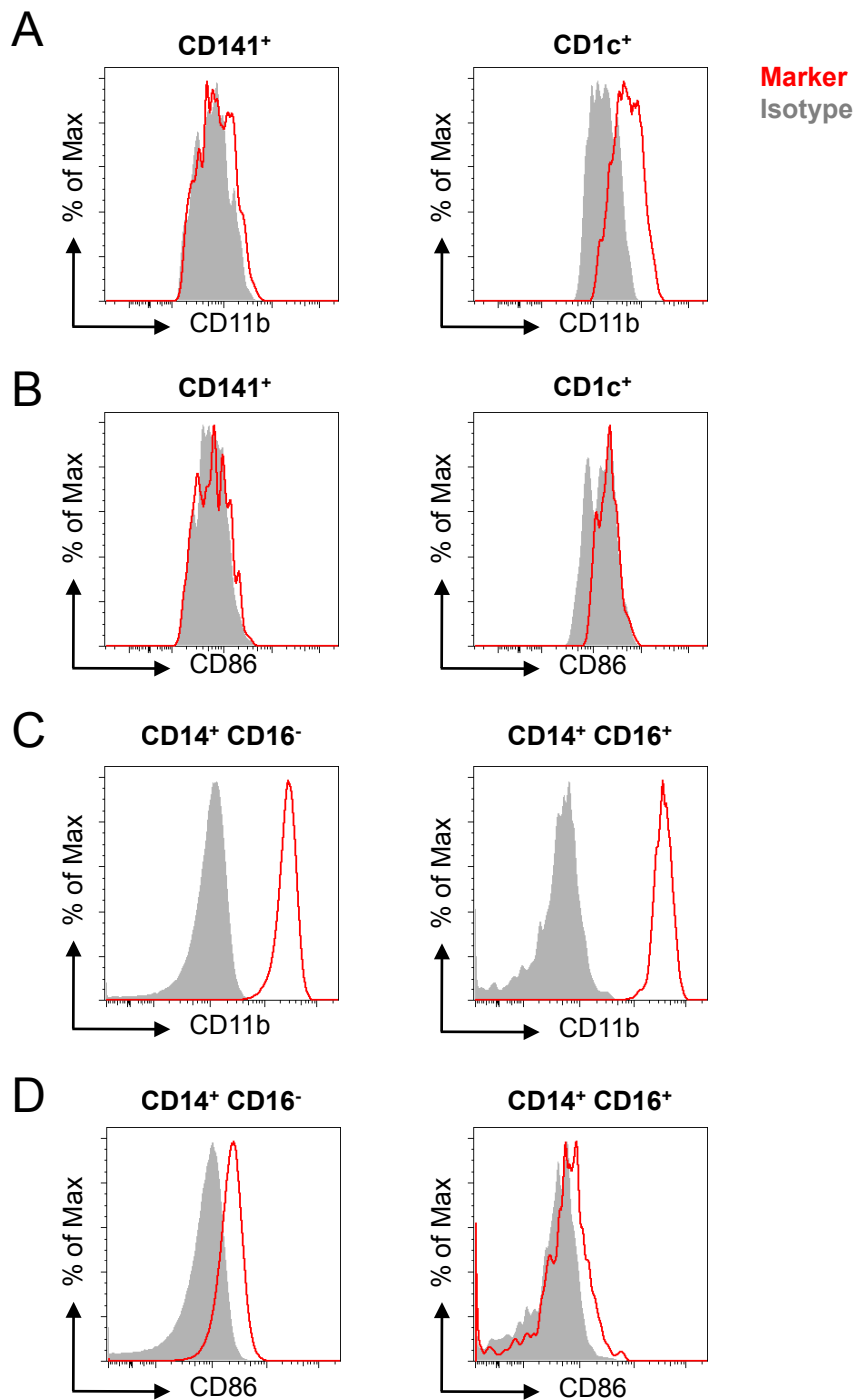


Figure 5.4: Expression of CD11b and CD86 by SF cDC and monocyte subsets

CD86 is minimally expressed on all cDC and monocyte SF subsets. cDC and monocyte subsets were analysed for the expression of CD11b and the activation marker CD86. CD141⁺ (left) and CD1c⁺ (right) SF DC subsets were analysed for expression of CD11b (A) and the co-stimulatory molecule CD86 (B). CD14⁺ CD16⁻ (left) and CD14⁺ CD16⁺ (right) monocytes were assessed for expression of CD11b (C) and CD86 (D). Isotype (Mouse IgG1κ) is depicted in grey shaded histogram. Marker expression for each subset is shown in red.

5.5 Quantification of cDCs

In order to understand the role of cDCs at sites of inflammation, it is important to quantify them within these tissues. The data in Fig. 5.5 are collated from all four AS patient SF samples used in this study. Using the gating strategy presented in Fig. 5.1A, the proportions of CD141⁺ and CD1c⁺ cDCs, among CD11c⁺ MHC II⁺ DCs and total live cells were evaluated (Fig. 5.5A). As in blood (Fig. 3.4), CD1c⁺ DCs in SF, were the major cDC population accounting for approximately 60% of CD14⁻ CD11c⁺ MHC II⁺ cells (Fig. 5.5A). CD141⁺ cDCs in blood represented 1% of CD14⁻ CD11c⁺ MHC II⁺ cells, whereas within SF, this increased to around 30% (Fig. 5.5A). However, it should be noted that we are unable to directly compare blood and SF DC populations in terms percentage of CD11c⁺ MHC II⁺ cells due to the presence of the CD14⁻ CD16⁺ mononuclear population in blood, and their absence from SF. However, it is possible to directly compare blood and SF DCs in terms of percentage of live cells. In SF, each DC population accounted for approximately 1% of total live cells (Fig. 5.5A). This is in contrast to the blood where CD141⁺ and CD1c⁺ DC subsets accounted for approximately 0.02% and 0.6% of live cells, respectively (Fig. 3.4A and Fig. 3.4B). By all measures, CD141⁺ DCs represent a much greater proportion of leukocytes in SF than in blood. Overall, cDCs represent approximately 2% of total live cells isolated from SF aspirated from inflamed joints of AS patients.

5.6 CD4⁺ T cells and chemokine receptor expression

T cells are known to be involved in driving the pathology of AS, partly through their secretion of cytokines and inflammatory molecules (468, 470, 471, 479, 536). Thus, SF CD4⁺ T cells were analysed in terms of maturation (naïve, memory, activated and regulatory T cells) and chemokine receptor expression. The blood CD4⁺ T cell gating strategy (Fig. 4.1A) was adopted to identify naïve (CD45RA⁺ CD25⁻), activated (CD45RA⁻ CD25^{int}), memory (CD45RA⁻ CD25⁻) and Treg (CD45RA⁻ CD25^{hi}) subsets in SF (Fig. 5.6A). Cell debris was excluded from T cell analysis using the FSC-A vs SSC-A profile. Doublets and dead cells (DAPI⁺) were also excluded. Single DAPI⁻ cells were analysed for CD3 and CD4 expression. Cells co-expressing these markers were subdivided on the basis of CD25 and CD45RA expression (Fig. 5.6A). Naïve T cells (CD25⁻ CD45RA⁺) were absent from AS patient SF, although this statement is based on data from one patient (Fig. 5.6A). T cells isolated from AS patient SF could be divided into two populations based on

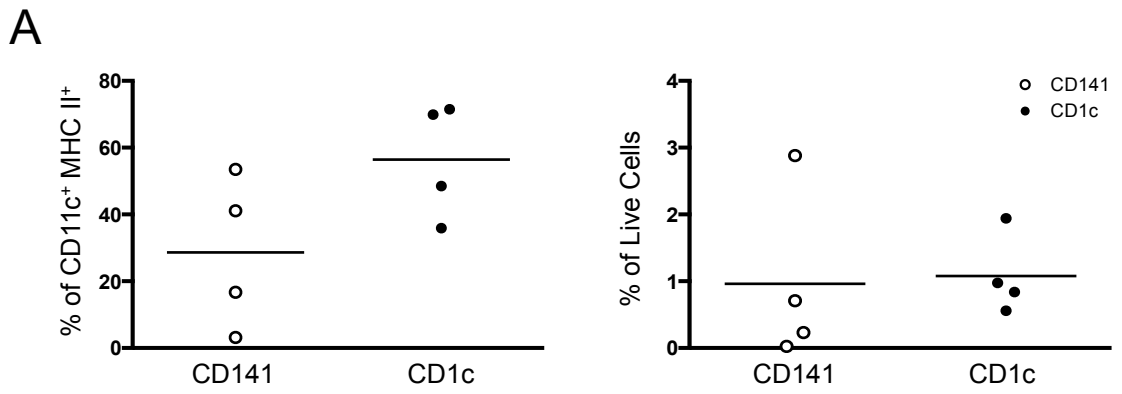


Figure 5.5: Quantification of SF cDC subsets

cDC subsets in SF from AS patients. **(A)** Using the gating strategy in Fig. 5.1A, CD141⁺ and CD1c⁺ DCs were enumerated in the SF of 4 AS patients. Proportion of LIN⁻ CD14⁻ CD11c⁺ MHC II⁺ CD1c⁺ and CD141⁺ DCs were enumerated as % of CD11c⁺ MHC II⁺ (left) and live cells (right). Empty circles – CD141⁺ DCs and filled circles – CD1c⁺ DCs.

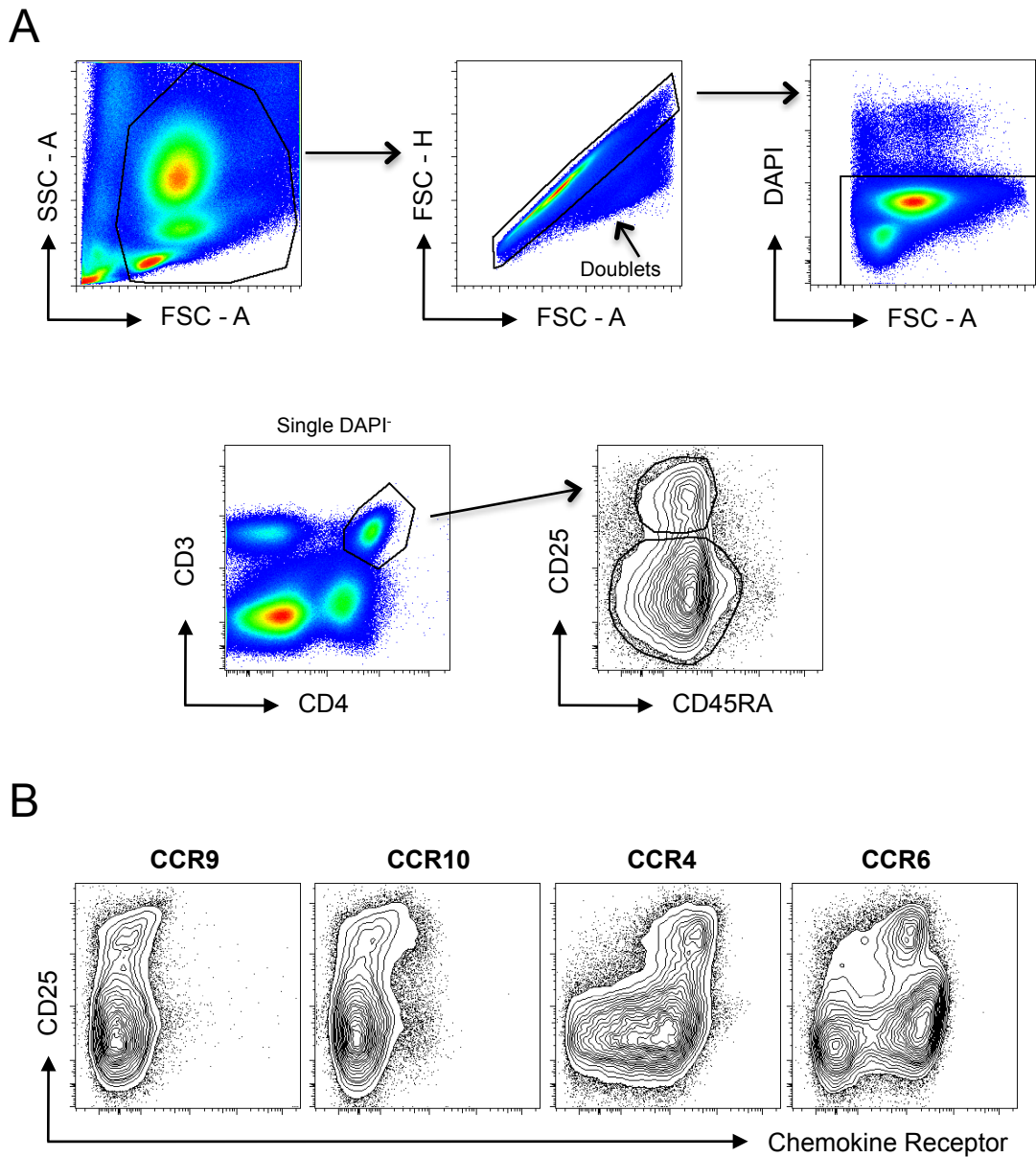


Figure 5.6: CD4⁺ T cells infiltrate AS synovium and express CCR4 and CCR6

CD4⁺ T cells infiltrate AS synovium and express the chemokine receptors CCR4 and CCR6. **(A)** Gating strategy used to analyse T cells subsets in AS SF. Firstly, cell debris was gated out on FSC-A vs SSC-A and doublets were excluded by FSC-A vs FSC-H. Dead cells (DAPI⁺) were removed from analysis. Live single cells were analysed for CD3 and CD4 expression. DAPI⁻ CD3⁺ CD4⁺ T cells were assessed for CD25 and CD45RA expression. **(B)** Chemokine receptor (CCR) expression on SF T cells from one AS patient. CD3⁺ CD4⁺ T cells were analysed for the expression of CCR9, CCR10, CCR4 and CCR6.

CD25 expression: CD25^{lo} CD4⁺ and CD25^{hi} CD4⁺ T cells (Fig. 5.6A). Due to the fact that only one AS patient was assessed for the presence of T cells, further analysis on the identity of CD4⁺ T cells regarding memory, activated or Treg status was not performed.

Chemokine receptor expression can direct migration and tissue localisation of leukocytes (59, 157). Therefore, expression of CCR9, CCR10, CCR4 and CCR6 on CD3⁺ CD4⁺ SF T cells isolated from one AS patient was assessed. The majority of the CD25^{hi} cells expressed both CCR4 and CCR6 (Fig. 5.6B). In addition, a large proportion of the CD25^{lo} T cells also expressed CCR4 and/or CCR6 (Fig. 5.6B). Very few AS SF T cells expressed CCR9 or CCR10 (Fig. 5.6B). Overall, a CD25^{hi} population was identified within SF CD3⁺ CD4⁺ T cells, expressing chemokine receptors CCR4 and CCR6 (Fig. 5.6). This population could be represent tissue equivalents of CD25^{hi} T regs observed in blood (Fig. 4.1).

5.7 Blood and SF cDC and pDC populations

Enumerative and phenotypic comparison of blood DCs with those at sites of inflammation, including the SF, can further elucidate the function and involvement of DCs in AS pathogenesis (217, 640). We therefore analysed, using matched patient blood and SF samples, DC subsets present in blood and SF.

Matched blood and SF samples from two AS patients were analysed on the same day for the presence of cDC and pDC populations (Fig. 5.7). Using the gating strategies described in Fig. 3.1A and Fig. 5.1A, cDC subsets were compared for each AS patient between the two tissues: blood and SF (Fig. 5.7A). Both blood cDC subsets (CD141⁺ and CD1c⁺) could be identified in the SF isolated from AS patients (Fig. 5.7A). When expressed as percentage of live cells, total cDCs represent a larger leukocyte population in SF (4.82% (1) and 0.58% (2)) than in blood (0.024% (1) and 0.06% (2), Fig. 5.7A). Unfortunately, access to matched samples was limited and only two sets of samples were analysed in this way, and thus it is not possible to draw definitive conclusions. Furthermore, the proportions of blood and SF cDC subsets also differed between the two AS patients analysed. CD141⁺ cDCs isolated from the blood of AS patient 1 accounted for 10.4% of total DC, whereas they accounted for only 4.2% in SF. In contrast, 4% of blood cDCs expressed CD141 in AS patient 2 whilst this subset contributed 59.8% to the total SF cDC population (Fig. 5.7A). However, these differences may be attributed to the SF localisation (shoulder vs knee) and gender of the patients used for matched analysis. Overall, cDCs may represent a higher proportion of cells in SF than in the blood.

Blood and SF analysis for pDCs was also performed on these two matched AS samples (Fig. 5.7B). pDCs, identified by the gating strategy described in Fig. 5.3A (DAPI⁻ LIN⁻ CD123⁺ MHC II⁺ CD304⁺), can be found in AS patient SF (Fig. 5.7B). pDCs, as a proportion of total DAPI⁻ LIN⁻ CD123⁺ MHC II⁺ cells, represented a larger leukocyte population in blood compared to SF, for both AS patients (Fig. 5.7B). However, when presented as proportion of total live cells only a slight increase in pDCs in SF compared to blood was observed for AS patient 1 (0.0158% vs 0.0224%), whereas pDCs were much more abundant in the SF in AS patient 2 (0.0149% vs 0.122%, Fig. 5.7B).

5.8 Differences in cytokine profile between blood and SF

Cytokines play many important roles in the development, perpetuation and resolution of immune responses. Consequently, it is of great importance to identify cytokines at sites of inflammation that may be involved in driving disease pathology. Therefore, we set out to determine the presence of SF cytokines and growth factors associated either with T cell subsets (Th1, Th2 and Th17) or inflammation (Fig. 5.8). Specifically, the concentrations of IFN γ , IL-1 β , IL-5, IL-6, IL-10, IL-17A, TNF α , Flt3L and IL-23p19 were measured in the plasma and SF of two patients (Fig. 5.8A and 5.8B). IL-4, IL-12 and GM-CSF levels were also assessed but fell below the limit of detection (data not shown). Low levels (less than 50pg/ml) of IFN γ , IL-1 β , IL-5, IL-10, IL-17A, TNF α and IL-23p19 were observed in both plasma and SF for AS patient 1 (Fig. 5.8A) and AS patient 2 (Fig. 5.8B). Surprisingly, the two most prevalent cytokines in AS patient plasma and SF were IL-6 and Flt3L. However, no overall difference in Flt3L levels in AS patient SF and plasma could be detected, however less Flt3L was detected in the SF of one AS patient compared to plasma (Fig. 5.8B and 5.8C). The most extreme difference observed between AS patient plasma and SF was the presence of IL-6 (Fig. 5.8C). IL-6 concentrations were much higher in AS patient SF than in matched blood samples. Overall, several inflammatory cytokines and growth factors could be detected in AS patient SF (Fig. 5.8). However, Flt3L and IL-6 were detected at the highest concentrations in both blood and SF, with IL-6 levels being higher in AS patient SF.

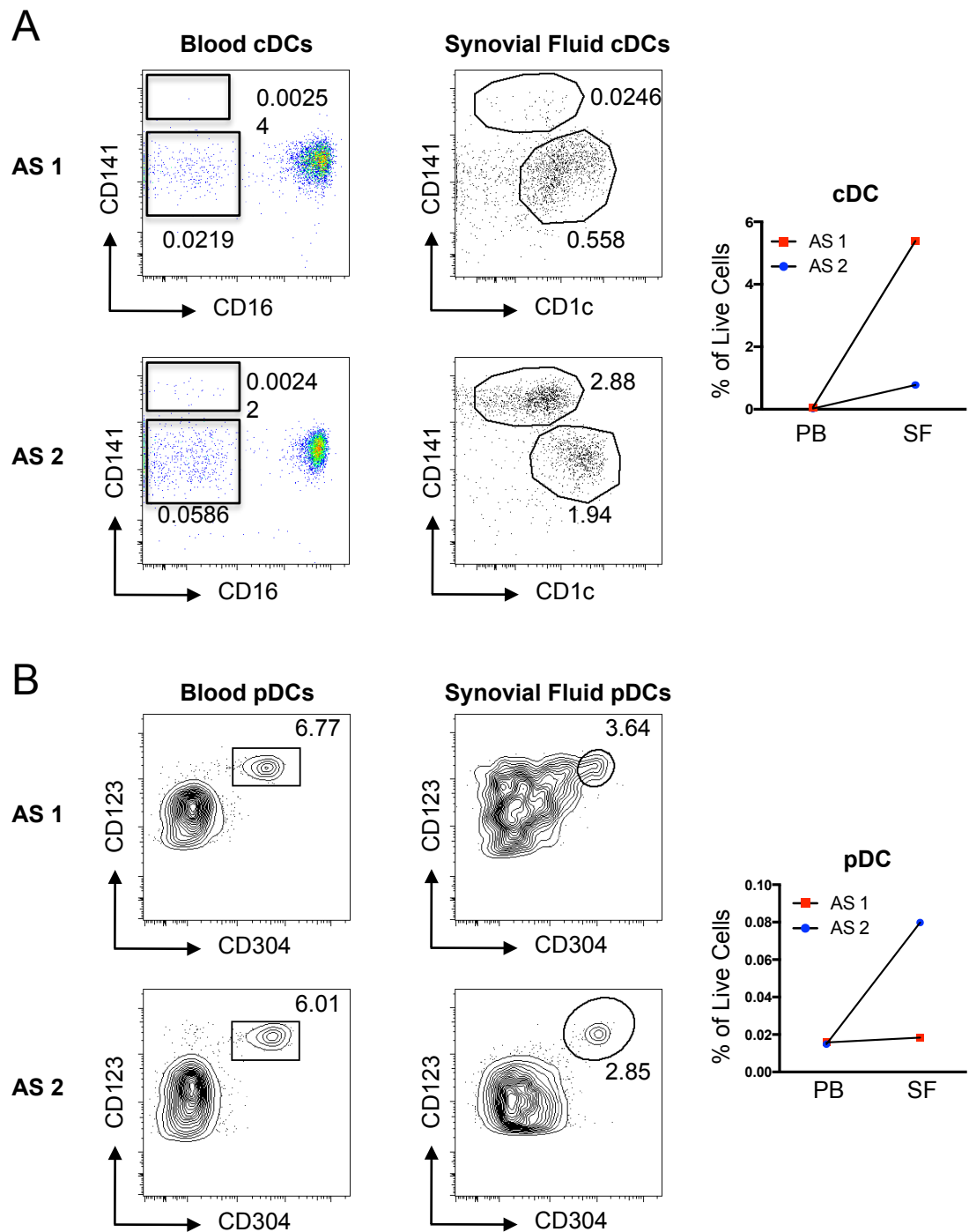


Figure 5.7: Comparison of cDCs and pDCs between peripheral blood and SF

Comparison of cDCs and pDCs in matched peripheral blood (PB) and SF in two AS patients. **(A)** Two AS patients were assessed for the presence of CD141⁺ and CD1c⁺ DCs in blood (left) and SF (centre). Single DAPI⁻ LIN⁻ (CD3/CD15/CD19/CD56) CD14⁻ CD11c⁺ MHC II⁺ cells were subdivided on expression of CD141 and CD16 (blood) or CD141 and CD1c (SF). Percentages represent proportion of live cells. Comparison of blood and SF CD141⁺ and CD1c⁺ DCs - % of live cells (right). **(B)** Presence of pDCs in PB and SF was compared for two AS patients. pDCs were identified as single DAPI⁻ LIN⁻ CD123⁺ MHC II⁺ CD304⁺ cells in both blood (left) and SF (centre). Percentages in contour plots represent proportion of total DAPI⁻ LIN⁻ CD123⁺ MHC II⁺ cells. Comparison of blood and SF DCs as % of live cells (right).

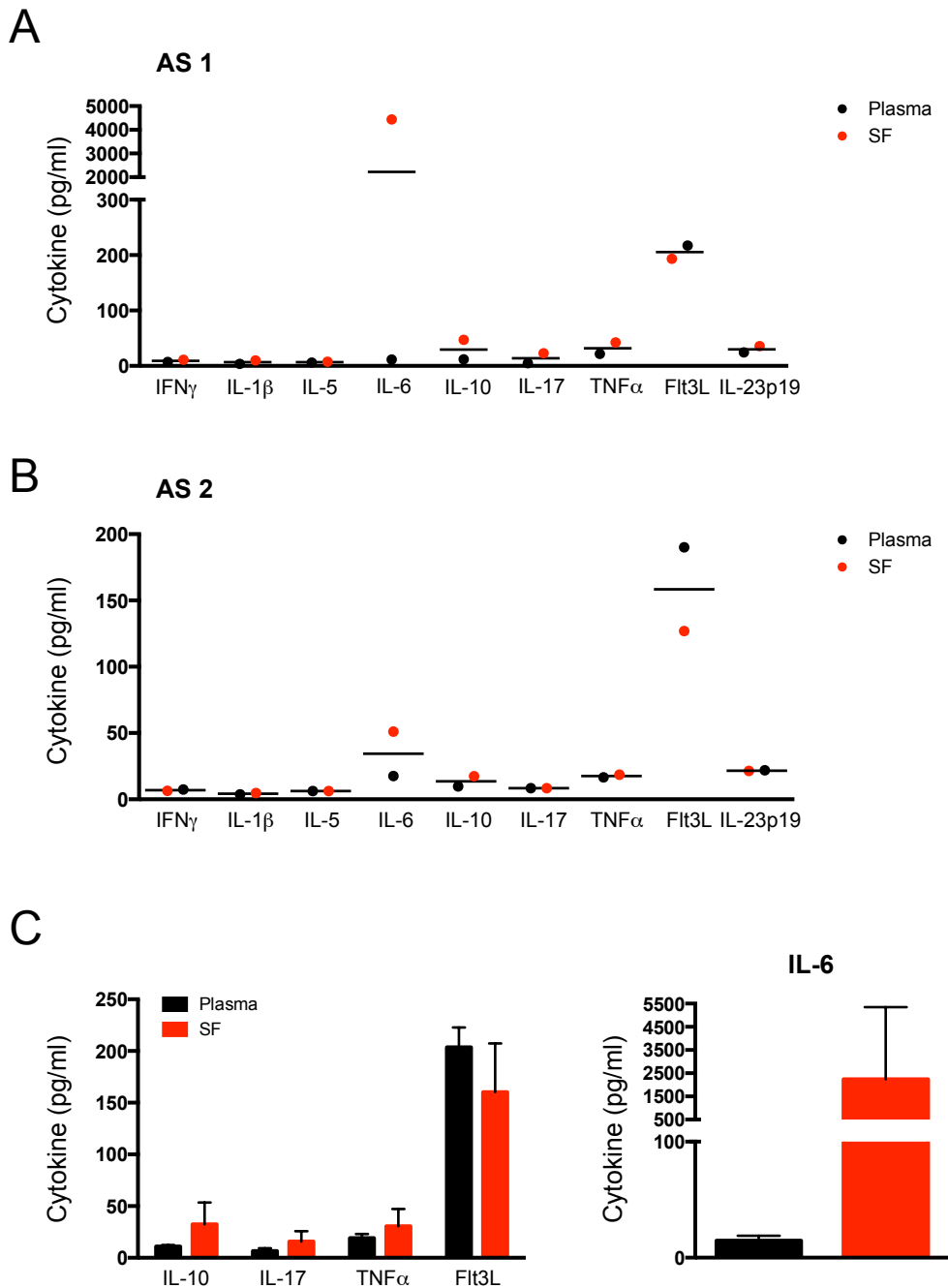


Figure 5.8: Comparison of cytokine levels in AS plasma and SF

IL-6 is highly upregulated in AS patient SF. Using Luminex and ELISA assays, plasma and SF cytokine levels were compared for two AS patients. Levels of specific cytokines were compared between plasma (black) and SF (red) levels for AS patient 1 (A) and AS patient 2 (B). Cytokines measured: IFN γ , IL-1 β , IL-5, IL-6, IL-10, IL-17, TNF α , Fit3L and IL-23p19. (C) Combined data from both AS patients for SF concentrations of IL-10, IL-17, TNF α , Fit3L and IL-6 in plasma (black) and SF (red). Error bars show mean + SD, n = 2 AS patients.

5.9 Discussion

AS pathogenesis is poorly understood. Most groups, including ourselves, use blood populations to delineate AS development. Unfortunately, these studies do not address the inflammatory processes occurring within afflicted tissues. Excitingly, several studies have explored new avenues of research using samples from the intestine (468, 551, 553, 554). Furthermore, SF is occasionally collected from AS patients with lower limb arthritis (4). Although a useful resource, there are caveats that must be considered when analysing SF in order to assess AS pathology. Inflamed synovial joints are more commonly associated with diseases such as RA (641) and are not typical of AS pathology. Therefore, data from peripheral joint SF may not be disease specific or reflect the biological processes occurring within the inflamed SIJs characteristic of AS. Despite this, SF studies may provide immunological information relating to peripheral joint and extra-articular disease manifestations and AS development, improving understanding of this complex disease.

Many AS SF studies focus on T cell antigen reactivity, identification of functional T cell subsets (Tregs and Th17) and presence/role of HLA-B27₂ molecules (502, 540, 549, 615). DCs migrate from sites of inflammation via lymphatics to draining lymph nodes and interact with naïve T cells to induce immune responses, whether they be tolerogenic or pro-inflammatory. They also affect T cell maturation and differentiation, and consequently instruct T cell migration to inflamed tissues. Despite their central role in immune response initiation, no published study has analysed myeloid cell subsets in SF from AS patients. Identifying the cell populations involved in AS disease pathogenesis may facilitate generation of new therapeutics, as has been achieved for RA and ulcerative colitis (UC) (217, 641-645).

Within our small cohort, 75% of patients were male, with SF aspirated from the knee (Table 5.1). Patient 1, receiving anti-TNF α treatment (Adalimumab), had low CRP but high ESR levels. Anti-TNF α treatment may contribute to the low CRP value (646). In contrast, patient 2 received combination therapy and suffered from high levels of inflammation (Table 5.1). Patient 3, who at the time of analysis was not receiving any therapeutics, suffered from severe inflammation. These data support previous observations that treatment strategies may affect the inflammatory status of AS patients (647-649).

Two cDC subsets were identified by surface marker expression in AS SF: CD1c⁺ and CD141⁺ DCs (Fig. 5.2A). Only CD1c⁺ SF DCs expressed CD11b, and this differential

expression of CD11b on cDC subsets is similar to that observed in blood (Fig. 3.16A). Surprisingly, AS SF cDCs appeared to be relatively immature given the negligible levels of surface CD86 detected (Fig. 5.4B). Our results suggest that these subsets are phenotypically similar to the more fully characterised mature blood cDC subsets. Although detailed functional analyses of these subsets was not possible during this study, the relative immaturity of SF cDCs compared to their blood counterparts suggests potential alterations to the functional attributes of DCs residing within inflamed tissues. DC immaturity is often associated with tolerance (329, 580, 596, 597). Therefore, AS DCs in SF might function to inhibit chronic inflammation, potentially through induction of Tregs. Low levels of co-stimulatory molecule expression are additionally associated with DCs capable of antigen uptake, supporting functional antigen presentation properties of AS SF DCs. Interestingly, Jongbloed et al found that following TLR stimulation, RA SF DCs preferentially secreted more tolerogenic IL-10 than their blood counterparts, despite their high expression of CD40 and CD86 (217). These data support the idea that SF DC may have tolerogenic properties. However, this statement is based solely on CD86 expression levels on AS SF DCs, highlighting the need for further functional analyses of SF DCs: antigen presentation, T cell priming and cytokine secretion. Interestingly, the AS patient receiving anti-TNF α therapy had a greater proportion of SF cDCs compared to the patient treated with combination therapy. Thus, SF cDCs may be expanded indirectly through anti-TNF α therapy. Alternatively, SF cDCs may exacerbate peripheral symptoms leading to the requirement for biological therapy. These results highlight the importance to functionally characterise AS SF DCs, to elucidate the disease processes occurring within peripheral joints and extra-articular tissues.

CD1c⁺ cDCs represented approximately 60% of total SF cDCs, with each cDC population representing 1% of total live cells (Fig. 5.5A). Of total live PBMCs, CD1c⁺ DCs greatly outnumbered the CD141⁺ subset. Our matched blood/SF analysis demonstrated that DCs were found at a higher frequency within SF (Fig. 5.7). Taken together, total DCs and the CD141⁺ subset represented a greater proportion of leukocytes within SF. Studies in RA patients revealed a similar increased frequency of SF DC populations (217), but did not investigate the presence and proportion of CD141⁺ DC in RA SF. CD141⁺ cDCs are thought to be equivalent to and share the tolerogenic and cross-presenting properties of murine CD8 α ⁺ DCs (200, 212, 332, 340, 650, 651). Therefore, a preferential increase in SF CD141⁺ DCs might indicate that regulatory processes are being implemented within sites of inflammation. These data suggest that within AS SF, abundant immature DCs may function to inhibit and control ongoing inflammation.

As described above, our studies and others' report accumulation of DCs in SF of inflamed joints. Jongbloed et al suggested that this reflected increased migration of blood DCs into the tissues (217). However, these experiments are unable to elucidate the origin and relationship of blood and SF DCs. Equivalent circulating blood DCs in mouse peripheral blood are difficult to identify (390, 652), and animal studies have suggested that mature DCs do not enter non-lymphoid tissues and peripheral lymph nodes via blood (652, 653). In contrast, Robinson et al propose tissue DC replenishment from human blood populations (216). If mature blood DCs do not migrate into tissue, do precursors seed and differentiate within tissue as occurs in mice (288, 380)? CD34⁺ stem cells may represent circulating human DC progenitors (600, 654). To address this question, isolated blood cDCs could be transferred and tracked using the NOD/SCID mouse model, both under steady state and inflammatory conditions.

Monocytes have been suggested to develop into tissue DCs under inflammatory conditions *in vivo* (227, 228, 655, 656). Furthermore, monocytes isolated from RA SF promote Th17 responses within sites of inflammation (657). Consequently, we set out to identify and phenotypically characterise AS SF monocytes. Two monocyte subsets (CD14⁺ CD16⁻ and CD14⁺ CD16⁺) could be identified in AS SF (Fig. 5.1B). Both subsets expressed high levels of CD11b, similarly to blood (Fig. 5.4C and Fig. 3.18A). As observed for SF cDCs, CD86 expression was very low on both monocyte populations compared to their blood counterparts (Fig. 5.4D and 3.14). This apparent downregulation of CD86 within SF could result from the surrounding cytokine milieu, or indicate a potential anti-inflammatory role for these populations within the inflamed tissue. Our SF cytokine analyses however do not support this hypothesis with regards to an anti-inflammatory cytokine milieu, as only low levels of IL-10 were detected (Fig. 5.8). Interestingly, Evans et al found SF monocytes in RA to express high levels of co-stimulatory molecules CD40 and CD86, and promote Th17 responses (657). It will be important to understand these phenotypic differences between AS and RA to better understand pathology. In addition to DCs, tissue infiltrating monocytes can give rise to tissue macrophages, at least in certain tissues (225). However, macrophage specific markers such as CD206 and CD33 were not included here and CD14⁺ CD11c⁺ MHC II⁺ cells were considered tissue monocytes due to their similarities with blood monocytes. Consequently, we cannot exclude the possibility that these monocyte populations contain macrophages, or are transiting through the macrophage differentiation process.

Blood CD14⁻ CD16⁺ mononuclear cells patrol blood vessels, survey the epithelium and potentially enter inflamed tissues (229, 237, 356). Despite acceptance that CD14⁻ CD16⁺ mononuclear cells contain SLAN⁻ and SLAN⁺ subsets, the functional attributes of these populations in blood and peripheral tissue have not yet been investigated. The distinction between SLAN subsets is important, with evidence suggesting CD14⁻ CD16⁺ SLAN⁺ cells to be DCs (239, 240, 359). We observed a complete absence of CD14⁻ CD16⁺ mononuclear cells from AS SF (Fig. 5.1B and 5.2C). Absence of this population could reflect *in situ* differentiation resulting in loss of CD16 and SLAN expression. SLAN⁺ cells could be detected within AS SF, however this population was very minor. Dermal SLAN⁺ cells have previously been described under inflammatory conditions, suggesting that this potential *in situ* differentiation would be restricted to inflamed tissues (249, 250, 252). Blood SLAN⁺ cells could be cultured *in vitro* in the presence of cytokines that reflect AS SF milieu, with marker expression being assessed over time. Loss of markers including CD16 and SLAN during culture could indicate *in situ* tissue differentiation of SLAN⁺ cells. Furthermore, SLAN expression may not represent functional differentiation given that total CD14⁻ CD16⁺ cells have been described to migrate through blood vasculature and perform surveillance functions (237). If SLAN expression does not infer population distinction then a lack of a distinct SLAN⁺ population is supported through the absence of CD14⁻ CD16⁺ mononuclear cells. SLAN expression may therefore reflect phases of monocyte maturation or differentiation. To address this, CD14⁻ CD16⁺ SLAN^{+/-} subsets could be cultured *in vitro*. Cultures could be supplemented with growth factors and/or cytokines including Flt3L, M-CSF, TGFβ (358) with SLAN expression being monitored over time. These experiments would determine if SLAN^{+/-} subsets represent distinct populations. To complement these studies, functional analyses of blood SLAN⁻ and SLAN⁺ subsets could be performed including T cell proliferation and chemokine receptor induction.

In RA and psoriatic arthritis (PsA), pDCs have been shown to accumulate within joint SF and possess an immature phenotype (217, 640). CD123⁺ CD304⁺ pDCs were identified in all four AS patient samples (Fig. 5.3). In contrast to RA and PsA, pDCs as a proportion of total leukocytes were reduced in SF compared to blood (Fig. 5.5B and Fig. 3.4C), although no consistent difference was observed when represented as frequency of live cells. Consequently, pDCs may not contribute to disease pathogenesis within SF. To assess their role, phenotypic and functional assessments should be performed, including expression of TLR 7 and 9 (219) and type I IFN production. Jongbloed et al observed RA SF pDCs to be immature, but responsive to TLR stimulation (217). Interestingly, pDCs in a patient

receiving combination therapy represented a larger SF leukocyte population than in a patient on anti-TNF α therapy (Fig. 5.7). Anti-TNF α treatment might therefore inhibit expansion or recruitment of SF pDCs. Recent studies suggest that anti-TNF α treatment may inhibit further radiographic disease progression, and thereby potentially implicate pDCs in disease development (557, 558). Future studies using larger patient cohorts to assess the functional capabilities of AS SF pDCs are required to determine the role of these cells in AS pathology.

T cell migration is dependent on upregulation of surface molecules following DC: T cell interactions (468, 479, 536, 658). Specific chemokine receptor profiles are associated with cells infiltrating the synovium in several arthritic diseases (116, 658-660). Consequently, identification and phenotypic analysis of AS SF T cell subsets can help delineate pathways involved in pathology and identify potential therapeutic targets. In addition, these studies may additionally elucidate further roles for DCs in disease pathogenesis through their influence on T cell priming. We identified CD25^{hi} and CD25^{int} CD4⁺ T cell subsets in AS SF (Fig. 5.6A). Insufficient sample numbers precluded analyses of FOXP3, ROR γ t and CD45RO expression, and thus it was not possible to clearly define the T cell subsets in AS SF. Functional circulating FOXP3⁺ cells identified in AS blood suggest that the SF CD25^{hi} population may contain Tregs (548, 661). In addition to identifying T cell populations, analysis of the T cell chemokine receptor profile was performed. Interestingly, CCR4 and CCR6 were co-expressed on all SF CD25^{hi} cells (Fig. 5.6B). As discussed in chapter four, CCR4 and CCR6 are involved in the migration of cells predominantly to the skin and intestine/joint respectively. Of those analysed, CCR4 and CCR6 were the only chemokine receptors detected in SF. Therefore, CCR4 and CCR6 may be involved in migration to or retention within AS SF, and may therefore represent potential therapeutic targets. Maraviroc, a CCR5 antagonist, is approved for clinical use in treatment of individuals infected with human immunodeficiency virus (HIV), supporting the idea that it may be possible to develop therapeutics targeting this type of molecule (662, 663). Furthermore, as discussed previously, CCR6 is expressed on Th17 cells, lending support to the notion that AS is a Th17 mediated disease.

Having identified immature myeloid cell subsets in AS SF, we analysed the cytokine profile of two matched blood and SF samples to assess the contribution of the surrounding cytokine milieu to this observed phenotype. The two dominant cytokines in AS patient plasma and SF were IL-6 and Flt3L (Fig. 5.8). Flt3L is a haematopoietic growth factor known to expand cDCs and pDCs *in vivo* (571, 572). Patient SF Flt3L levels could

promote development of immature myeloid cells to restore tissue homeostasis, given their potential tolerogenic capacity (Fig. 3.4). Alternatively, *in situ* expansion or development of cDC and pDCs may be detrimental to joint function. These hypotheses highlight the need for functional analyses of SF DC. IL-6 was increased in AS patient SF compared to plasma. Additionally, SF IL-6 levels were considerably higher in the patient receiving anti-TNF α treatment compared to the patient receiving DMARD/NSAID combination therapy. High levels of SF IL-6 may contribute to disease pathology through generation of Th17 cells, supported also by the presence of CCR6⁺ cell population in the SF, as discussed above. Consequently, increased IL-6 levels may be indicative of requirement for biological therapy, previously shown to indirectly reduce pro-inflammatory molecules including IL-6 (621). Furthermore, plasma IL-6 has been noted to correlate with RA radiographic progression, supporting a pathogenic role for this molecule (664). Thus, cytokines may contribute to disease pathogenesis through their role in lineage development and cell activation, and they also represent attractive therapeutic candidates: anti-TNF α treatment is a well-established therapy for AS and RA (665-667). Trials in PsA patients suggest that molecules targeting IL-12/23 (668, 669) and IL-17A (670) may provide partial symptomatic relief. Despite these advances, many AS patients remain unresponsive to current therapeutics. Identifying specific molecules associated with AS disease pathogenesis could provide symptomatic relief for this cohort of patients. Our data and that of published studies highlight a role for IL-6 in disease pathogenesis, however anti-IL-6 treatment (Tocilizumab) remains ineffective (23). Further studies are therefore required to assess cytokine function, specifically IL-6 and Flt3L, within AS allowing us to classify the role of Th17 cells, DCs and other immune populations in driving the inflammation observed within peripheral joints and extra-articular tissues of AS patients.

We have identified two cDC subsets, two monocyte populations and pDCs in AS patient SF. CD14⁻ CD16⁺ mononuclear cells were absent from SF, supporting the concept that they function as a blood surveillance population (237, 356). Although the functions of these subsets in AS SF were not assessed, a larger population of cDCs was found in SF than in blood, while pDCs were found in similar proportions in both tissues. Anti-TNF α treatment may influence SF DC populations, although further investigation is required. Given the altered T cell chemokine receptor profile of blood in patients, we examined resident SF CD4⁺ T cells in AS SF. CCR4 and CCR6 may be required to prevent extravasation from or allow entry of CD25^{hi} CD4⁺ T cells to inflamed synovium. IL-17-secreting CD4⁺ T cells express CCR6, indicating a potential role for Th17s in disease pathogenesis given the association between CCR6 expression and the Th17 phenotype.

High levels of IL-6 and Flt3L were also observed in AS SF and may contribute to disease pathology. Overall, observations relating to the cellular infiltrate and cytokine milieu in AS SF were made, but due to the small sample number and lack of functional assessment, follow up studies will be required to understand the immunopathology of AS SF.

Following these investigations identifying and quantifying DC and T cell populations in AS patients, we next aimed to assess DC function in AS patients. In the next chapter, I will address the abilities of individual blood myeloid populations to stimulate T cell proliferation, cytokine production and chemokine receptor expression.

Chapter 6: Functional characterisation of circulating DCs

6.1 Introduction

In previous chapters we have identified populations of DCs and T cells in the blood and SF of AS patients. Analyses of T cell subsets in AS patients revealed differences in the expression of T cell chemokine receptors that may be influenced by interactions with DCs. Previous work from our laboratory identified deficiencies within the DC populations of HLA-B27 TG rats (480). Specifically, loss of CD103⁺ CD11b^{int} CD172a^{lo} DCs correlated with secretion of IL-17 by interacting T cells, potentially driving a pathogenic Th17 response. These results suggest that loss of specific DC populations or alterations to DC function can lead to the induction of aberrant responses. Previous work assessing the function of AS patient DCs has wholly focused on monocyte-derived DCs (moDCs) cultured from monocytes *in vitro* in the presence of GM-CSF and IL-4. These cultures, despite generating considerable cell numbers, generate inflammatory DCs and consequently cannot be considered to truly represent *in vivo* DC populations (545). In addition, both circulating DC populations are not represented within these monocyte-derived cultures. Nevertheless, their findings suggested that moDCs generated from AS patients did not differ in their expression of co-stimulatory molecules and cytokine secretion, including IL-23, although resting moDCs may express less MHC II compared to HC control populations (546, 547). Because the influence of circulating DCs in the induction and control of peripheral immune responses in AS remains unknown, we set out to assess the functions of blood DCs directly isolated from HCs and AS patients.

6.2 Patient characteristics

Patients were recruited from the Glasgow Royal Infirmary AS clinic run by Dr David McCarey and Dr Anne McEntegart. Patient Information regarding disease severity, treatment and duration was collated. Data for the AS patients and HCs used for in the analyses of DC function are summarised in Table 3.1.

Table 6.1: Patient characteristics for DC function experiments

For analysis, 18 AS patients and 11 HCs were used. Patient characteristics were collated and are summarised below. For some parameters, records were not available for all patients. Percentages represent proportion of all patients used in the study. Spinal disease was assessed based on the presence or absence of cervical, thoracic and lumbar involvement. Levels were categorised on the number of sites involved: 1 site = level 1, 2 sites = level 2 and 3 sites = level 3. Combination therapy consists of DMARD and NSAID treatment. N/A = Not applicable. Mean \pm SD is shown.

	AS Patients	Healthy Controls
Age (yrs)	53.3 ± 12.1	46.4 ± 13
Sex – Male/Female	15/3	8/3
Disease Duration (yrs)	26.2 ± 12.8	N/A
B27 – Pos/Neg (% B27⁺)	15/1 (83%)	1/11 (9%)
BASDAI	3.5 ± 2.5	N/A
BASMI	4.7 ± 2.4	N/A
ESR (mm/hr)	11.7 ± 11.2	N/A
CRP (mg/L)	9.7 ± 13.8	N/A
Bilateral Sacroiliitis – No. (%)	17 (94.4%)	N/A
Spinal disease		
Absent – No. (%)	8 (44%)	N/A
Level 1 – No. (%)	4 (22%)	N/A
Level 2 – No. (%)	4 (22%)	N/A
Level 3 – No. (%)	1 (5.6%)	N/A
Extra-articular Disease		
IBD – No. (%)	1 (5.6%)	N/A
Uveitis – No. (%)	0 (0%)	N/A
Psoriasis – No. (%)	1 (5.6%)	N/A
Arthritis – No. (%)	4 (22%)	N/A
Medication		
Nil – No. (%)	5 (27.8%)	N/A
NSAIDs – No. (%)	10 (55.6%)	N/A
Combination – No. (%)	1 (5.6%)	N/A
Biologics – No. (%)	1 (5.6%)	N/A

6.3 Induction of T cell proliferation

DCs prime the adaptive immune response. Several landmark papers in the 1970s identified DCs residing within lymphoid tissues of mice, where their primary function was to stimulate proliferation of naïve T cells (185, 186, 671, 672). As previous studies in AS patients using moDCs have focused on expression of co-stimulatory molecules and

cytokine secretion, we initially set out to examine the outcome of DC: T cell interactions, with an initial read out of T cell proliferation. To do this we used the gold standard assay to assess T cell proliferation following DC interaction: the mixed leukocyte reaction (MLR) (186). Monocytes were included in some MLR experiments as a comparative population. To perform these experiments, we flow sorted DC subsets or monocytes from AS patients and HCs. DCs and monocytes were resuspended at concentrations ranging from 1,500 to 24,000 DCs/100 μ l in complete media and co-cultured with mismatched HC purified naïve CD4⁺ T cells (20,000 cells) for 5 days. T cell proliferation was then assessed by CFSE dilution. The gating strategy used to identify proliferating T cells following culture is depicted in Fig. 6.1. Cell debris, doublets and dead cells (DAPI⁺) were excluded as previously described. Single live cells were analysed for CD4 and CFSE expression. Total CD4⁺ T cells were then assessed for their CFSE level; with the CD4⁺ CFSE^{lo} cells classified as the proliferating CD4⁺ T cell population (Fig. 6.1A). Representative FACS plots obtained for each DC/monocyte population are depicted in Fig. 6.1B. Based on these plots, CD1c⁺ DCs were the most proficient subset at inducing T cell proliferation. CD141⁺ DCs were efficient at inducing T cell proliferation despite a maximum of only 1,500 DCs being available for co-culture with naïve T cells. For each MLR experiment, T cells alone were stimulated with 10 μ g/ml of ConA and proliferation and chemokine receptor induction were assessed as a control (Fig. 6.2A). ConA induced significant levels of T cell proliferation and CXCR3 expression (Fig. 6.2A and 6.2B). Induction of CXCR3 was assessed given the reported association with the Th1 phenotype and given the downregulation of CXCR3 expression on AS patient activated and memory T cells (Fig. 4.8). Following optimisation of the MLR conditions, quantification of multiple MLRs was performed (Fig. 6.2C). No significant differences between AS patients and HCs were observed for MLRs containing the following myeloid populations: CD141⁺ and CD1c⁺ DCs, CD14⁻ CD16⁺ mononuclear cells and CD14⁺ CD16⁻ monocytes (Fig. 6.2C). As DC numbers were diluted, reduced T cell proliferation was observed for each population (Fig. 6.2C). The ability to induce T cell proliferation was compared between all four subsets in AS patients and HCs. When HC DC and monocyte subsets were compared for their ability to induce T cell proliferation, CD1c⁺ DCs were the most efficient population at inducing T cell proliferation with 12,000 DCs inducing approximately 40% proliferation (Fig. 6.3A). Following quantification of 9 independent experiments, 12,000 CD14⁻ CD16⁺ mononuclear cells and 1,500 CD141⁺ DCs induced 25% and 20% T cell proliferation respectively. Of all the subsets, HC monocytes were the poorest inducers of T cell proliferation with approximately ~8% of CD4⁺ T cells showing CFSE dilution following co-culture with 12,000 monocytes (Fig. 6.3A). AS patient myeloid populations induce

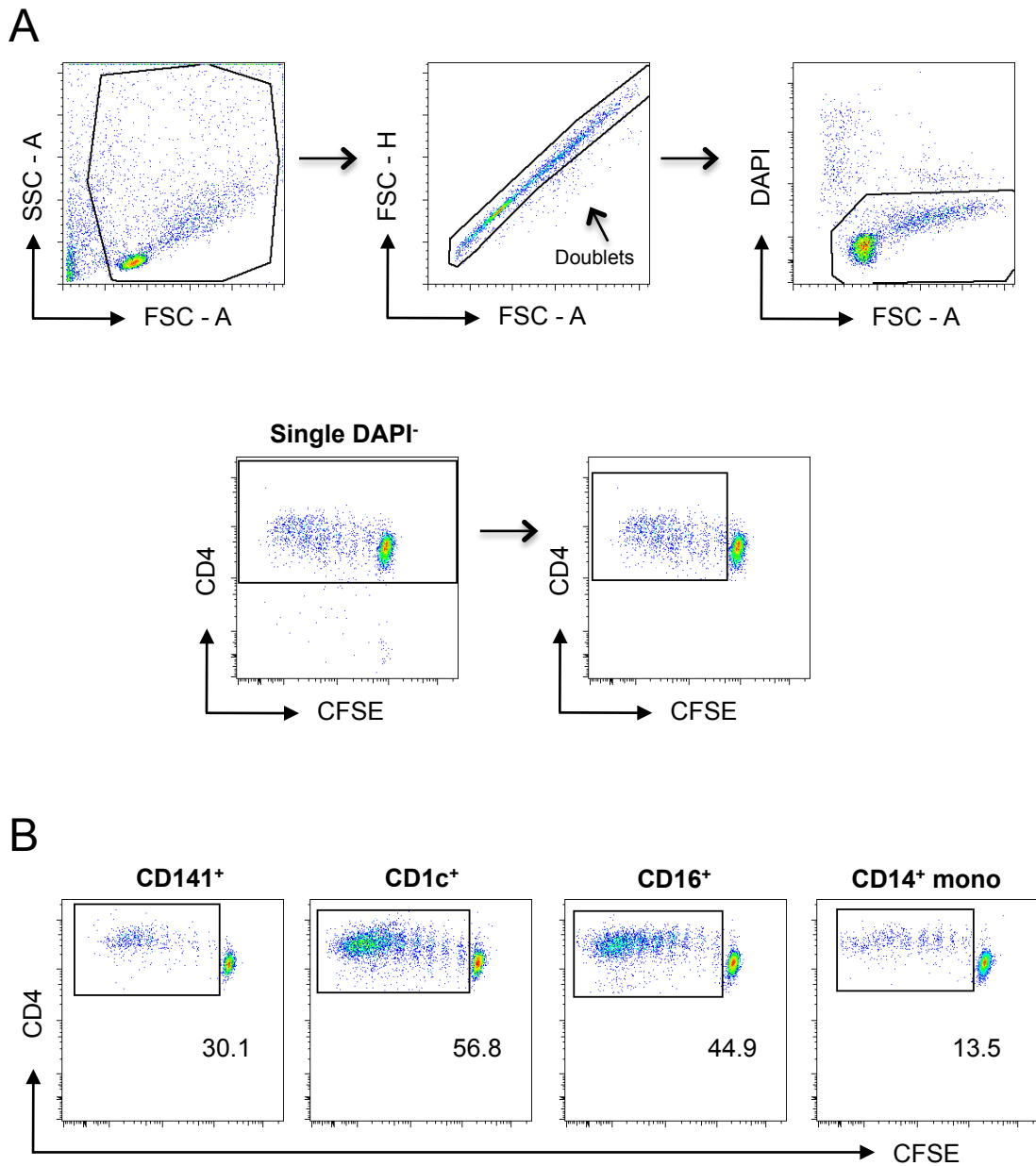


Figure 6.1: Induction of T cell proliferation by blood DC/monocyte subsets

Ability of human blood DC/monocyte subsets to induce naïve T cell proliferation. Naïve CFSE⁺ CD4⁺ T cells were co-cultured with DC/monocyte subsets for 5 days. Proliferation assessed by CFSE dilution. **(A)** Single DAPI⁻ cells were assessed for CD4 expression (bottom – left). The proportion of proliferating CD4⁺ T cells was used for further analysis (bottom – right). **(B)** Characteristic FACS plots of T cell proliferation induced by DC/monocyte subsets: - CD141⁺ DCs (1,500 cells), CD1c⁺ DCs (12,000 cells), CD16⁺ mononuclear cells (12,000 cells) and CD14⁺ monocytes (12,000 cells). Numbers represent % of T cells undergoing proliferation.

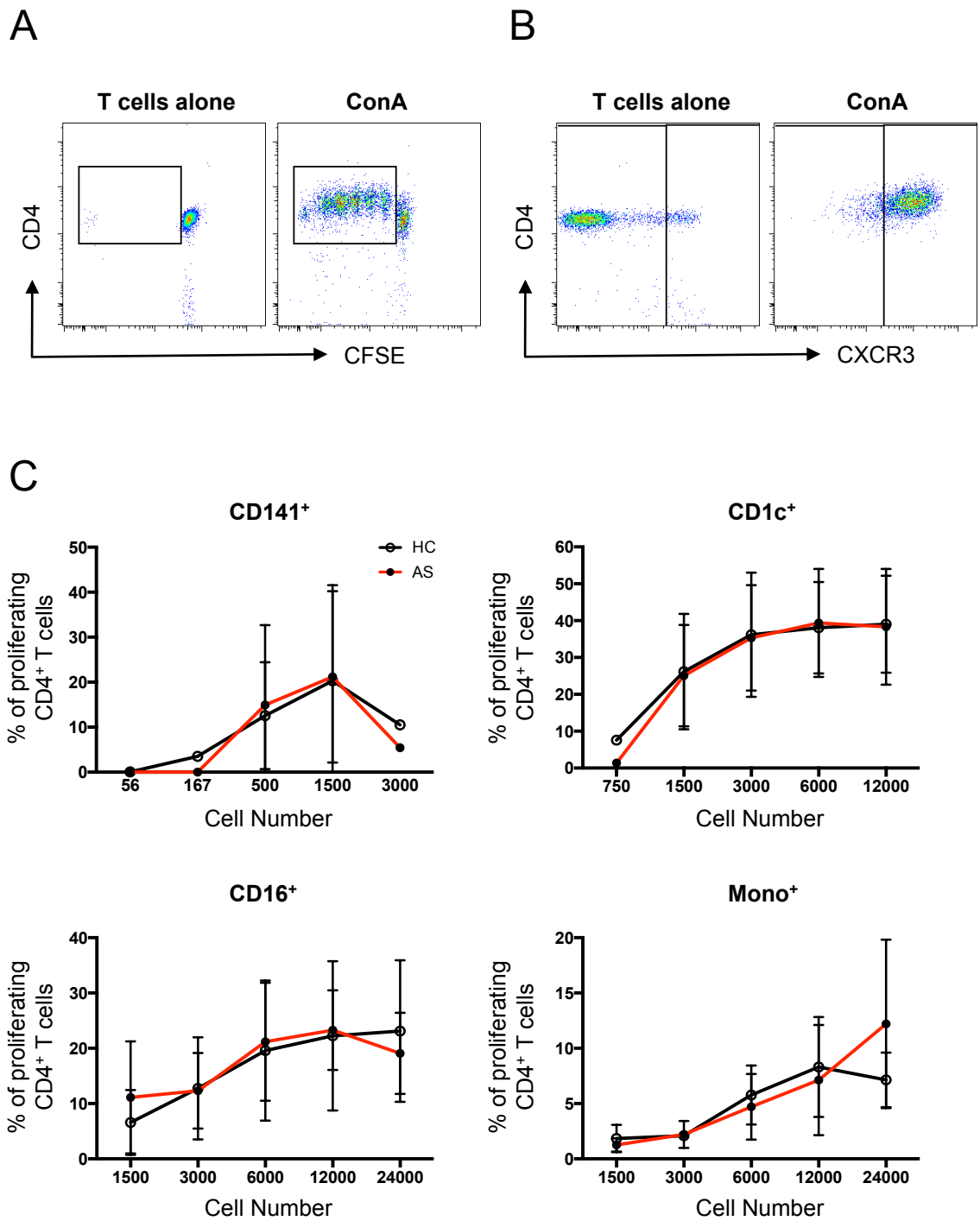
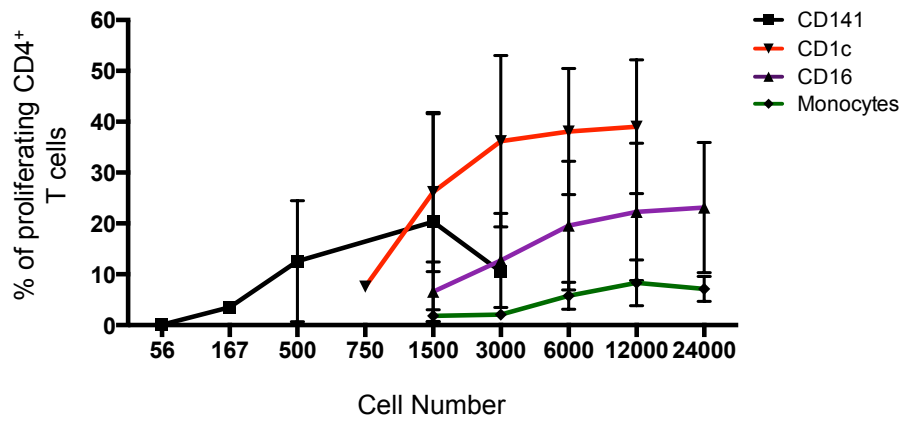


Figure 6.2: T cell proliferation induction by HC and AS blood DC/monocyte subsets

DC/monocytes were cultured with 20,000 naïve CFSE⁺ CD4⁺ T cells for 5 days to assess T cell DC/monocyte function. Proliferation was assessed by CFSE dilution. T cells alone (left) and 10µg/ml concanavalin A (ConA - right) were assed for T cell proliferation (**A**) and chemokine receptor induction. (**B**) Proportions of proliferating T cells for each subset were compared between AS patients (red) and HCs (black). Error bars represent mean +/- SD. Subsets used for analysis: - CD141⁺ DCs (8 HCs, 13 AS patients), CD1c⁺ DCs (10 HCs, 16 AS patients), CD14⁺ CD16⁺ mononuclear cells (9 HC, 15 AS patients) and CD14⁺ monocytes (4 HC, 6 AS patients).

A



B

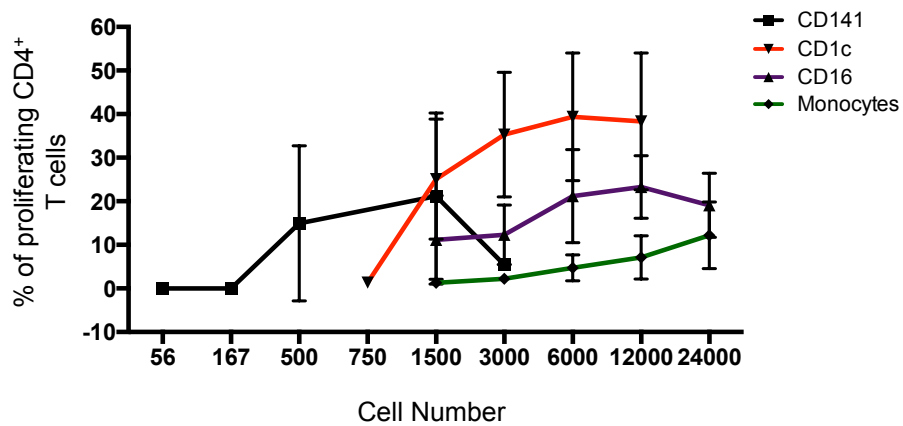


Figure 6.3: Comparison of T cell proliferation by blood DC/monocyte subsets

DC/monocyte subsets have different abilities to induce T cell proliferation. Different numbers of DC/monocytes were cultured with 20,000 naïve CFSE⁺ CD4⁺ T cells for 5 days. T cell proliferation was assessed by CFSE dilution. Proportion of proliferating T cells for HC (A) and AS patient (B) induced by CD141⁺ (green) and CD1c⁺ DCs (red), CD14⁻ CD16⁺ mononuclear cells (purple) and CD14⁺ monocytes was compared. Error bars represent mean +/- SD. Numbers used for analysis: - CD141⁺ DCs (8 HCs/13 AS patients), CD1c⁺ DCs (10 HCs/16 AS patients), CD14⁻ CD16⁺ mononuclear cells (9 HC/15 AS patients) and CD14⁺ monocytes (4 HC/6 AS patients).

proliferation of naïve CD4⁺ T cells at levels indistinguishable from the equivalent HC myeloid populations (Fig. 6.3B).

Overall, no difference was observed between AS patient and HC subsets in their ability to induce T cell stimulation. However, we did observe differences in the ability of the individual subsets to induce T cell proliferation. In our hands, CD1c⁺ DCs were the most proficient subset at inducing proliferation of naïve CD4⁺ T cells. In contrast, monocytes stimulated very little T cell proliferation.

6.4 Upregulation of chemokine receptors

In addition to stimulating proliferation of naïve CD4⁺ T cells, DCs direct T cell migration, development and maturation. Following uptake of pathogenic or harmless antigen DCs migrate from peripheral tissue to the draining lymph node. Following interaction with migrating DCs, differentiated T cells acquire specific molecules assisting cell migration, including chemokine receptors and integrins. Intestinal DCs induce molecules, including CCR9 and $\alpha 4\beta 7$, promoting migration of responding T cells to mucosal tissues (171, 172, 413, 673). Consequently, analyses of circulating T cells in terms of chemokine receptor (CCR) expression can infer the dominant location of T cell priming in steady state and inflammatory conditions. Our results suggested that AS patient DCs preferentially induced CCR6 on interacting CD4⁺ T cells. This observation was accompanied by a reduction in CXCR3 priming. Accordingly we set out to assess the ability of blood DC subsets, isolated from both AS patients and HCs, to induce CCR6 and CXCR3 on the surface of interacting T cells in an MLR setting. To identify CCR⁺ T cells, cell debris, doublets and dead (DAPI⁺) cells were excluded from analysis (Fig. 6.4A). CD4⁺ CFSE^{lo} T cells were subsequently analysed for the expression of chemokine receptors. CCR⁺ cells were compared to the appropriate isotype-matched control. Representative plots of CCR6 expression on CD4⁺ proliferating T cells, following co-culture with CD141⁺ and CD1c⁺ DCs and CD14⁻ CD16⁺ mononuclear cells are depicted in Fig. 6.4B. These demonstrate that, CD141⁺ and CD1c⁺ DCs were the principal inducers of CCR6 on interacting T cells. Quantification of T cell CCR6 upregulation following MLR co-culture with CD141⁺ and CD1c⁺ DCs, CD14⁻ CD16⁺ mononuclear cells and CD14⁺ CD16⁻ monocytes is shown in Fig. 6.5A. Only one MLR co-culture was used to assess CCR6 expression using CD14⁺ CD16⁻ monocytes. AS patient myeloid populations did not significantly differ in their ability to induce CCR6 on interacting CD4⁺ T cells compared to their HC counterparts

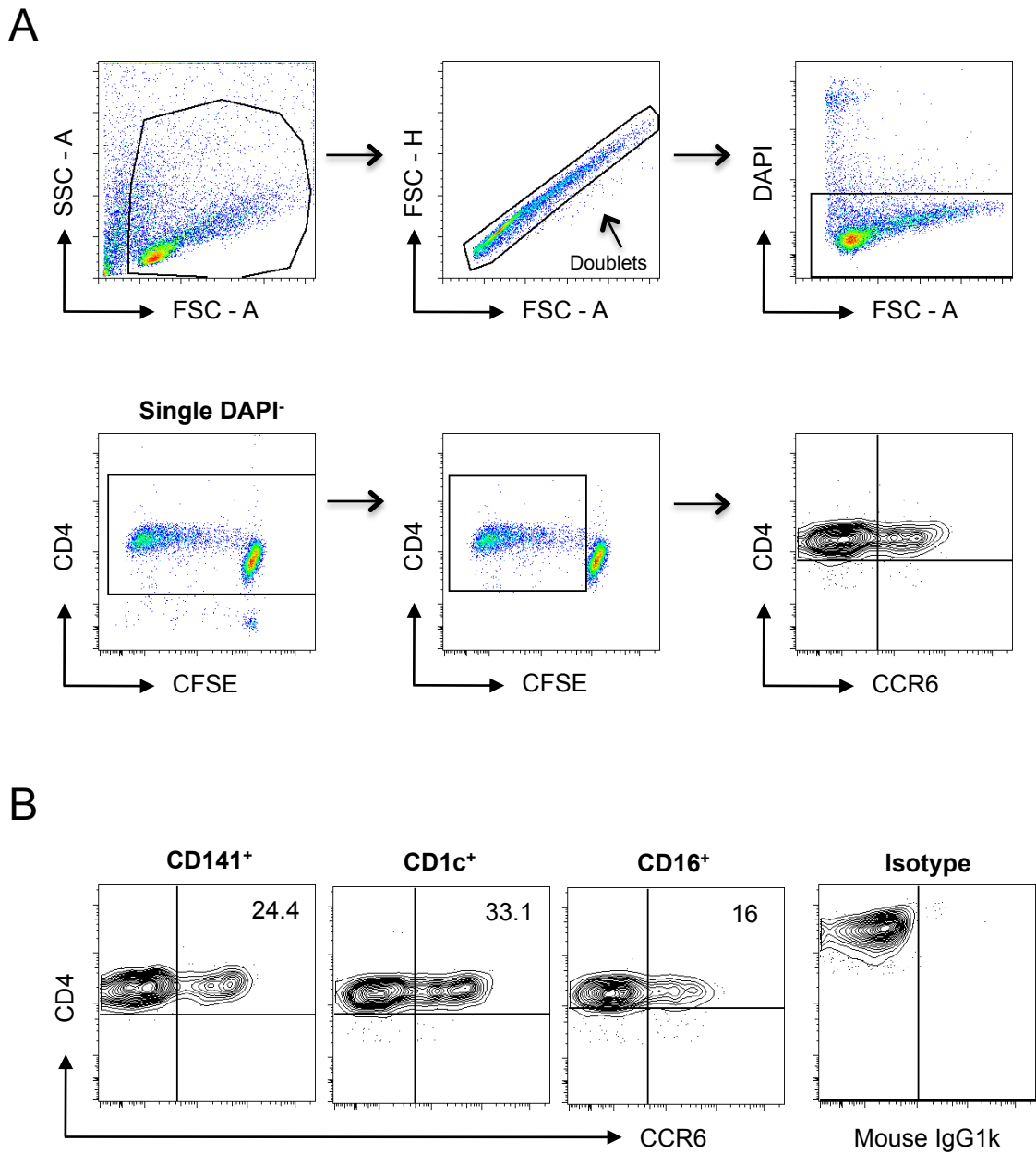


Figure 6.4: Ability of human blood DCs/monocytes to induce T cell homing markers

Capability of DC/monocyte subsets to induce chemokine receptor (CCR) induction. **(A)** Gating strategy to identify proliferating CCR⁺ CD4⁺ T cells after MLR co-culture. Doublets and dead cells were excluded from analysis (top row). Single live cells were then analysed for expression of CD4 (bottom, left). Proliferating CD4⁺ T cells (bottom, centre) were analysed for expression of CCR (bottom, right). **(B)** 1,500 CD141⁺ DCs (left), 12,000 CD1c⁺ DCs (centre, left) and 12,000 CD14⁻ CD16⁺ mononuclear cells (centre, right) are able to induce CCR6. Numbers represent % of CCR6⁺ proliferating T cells. Isotype used to set CCR⁺ gate in some cases (right).

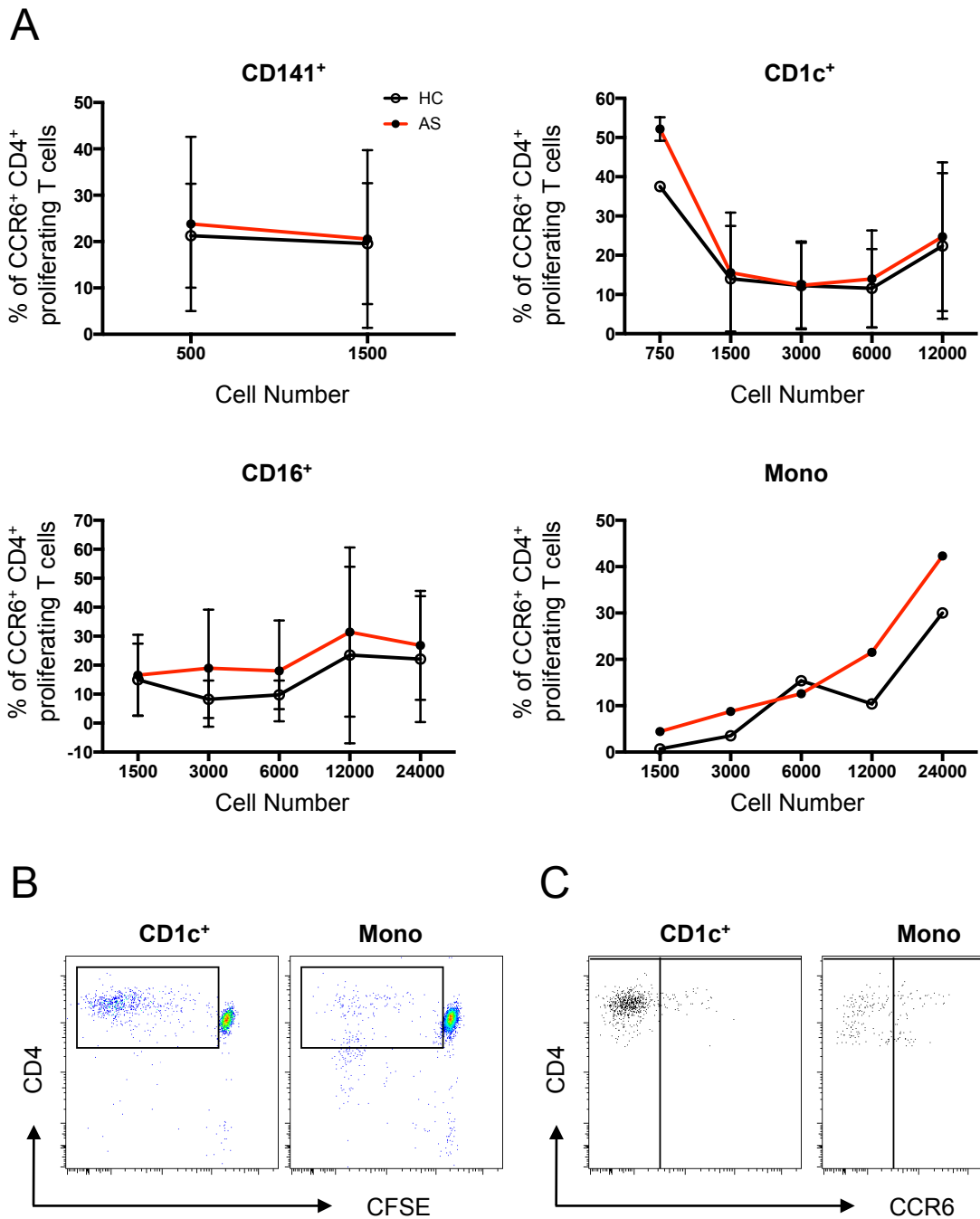


Figure 6.5: CCR6 induction by HC and AS blood DC/monocyte subsets

No difference in the ability of HC (black) and AS patients (red) DC/monocyte subsets to induce CCR6 on interacting T cells in an MLR co-culture system. **(A)** CD141⁺ DCs (4 HC, 6 AS), CD1c⁺ DCs (4 HC, 7 AS), CD14⁻ CD16⁺ mononuclear cells (5 HC, 8 AS) and CD14⁺ monocytes (1 HC, 1 AS) were tested for their ability to induce CCR6. Error bars show mean +/- SD. Ability of 24,000 CD14⁺ monocytes (right) and 12,000 CD1c⁺ DCs (left) to induce T cell proliferation **(B)** and CCR6 induction on interacting T cells **(C)**. Gates were set on isotype.

(Fig. 6.5A). FACS plots depicting the proliferative capacity and CCR induction of CD1c⁺ DCs and CD14⁺ CD16⁻ monocytes are shown in Fig. 6.5B and 6.5C.

We next established the ability of AS patient and HC myeloid cells to induce CXCR3 expression. Representative FACS plots showing proportion of CXCR3⁺ CD4⁺ T cells following MLR co-culture with CD141⁺ and CD1c⁺ DCs, CD14⁻ CD16⁺ mononuclear cells and CD14⁺ CD16⁻ monocytes are presented in Fig. 6.6A. All subsets were capable of inducing CXCR3 expression on proliferating T cells. Interestingly, co-cultures containing all myeloid populations induced 90% of proliferating T cells to express CXCR3. Following co-culture of 1,500 CD141⁺ DCs and 20,000 naïve CD4⁺ T cells, no difference between AS patients and HCs was observed (Fig. 6.6B). Similarly, no difference was observed between AS patient and HC CD1c⁺ DCs, CD14⁻ CD16⁺ mononuclear cells and CD14⁺ CD16⁻ monocytes in their ability to induce CXCR3 expression at any DC: T cell ratio (Fig. 6.6B).

Overall we observed no increase in CCR6 induction by AS patient DCs when compared to their HC counterparts. In addition, no difference in CXCR3 induction was observed between AS patient or HC myeloid subsets.

6.5 Induction of T cell responses

DCs direct T cell differentiation, polarising effector T cell towards Th1/Th2/Th17 or Treg phenotypes. Following MLR co-culture, T cell differentiation can be assessed by measuring the cytokines secreted. Luminex and ELISA technology was used to assess the levels of cytokines secreted from MLR cultures (Fig. 6.7 and 6.8). Cytokines IL-1 β , IL-4, IL-5, IL-6, IL-10, IL-17A, IFN γ , TNF α and the growth factor Flt3L were chosen for analysis because of their association with inflammation, T cell and myeloid populations. Levels of IFN γ (Th1) and IL-4 and IL-5 (Th2) did not differ between HC and AS patients (Fig. 6.7A). However, CD14⁻ CD16⁺ mononuclear cell co-cultures secreted highest levels of both IFN γ and IL-5 (Fig. 6.7A). MLR supernatants obtained from AS patient and HC CD1c⁺ and CD141⁺ DCs and CD14⁻ CD16⁺ mononuclear cell co-cultures contained variable levels of IL-10 and IL-17 (Fig. 6.7A). HC CD1c⁺ and CD141⁺ DC co-cultures may induce elevated levels of IL-10 when compared to AS patients (Fig. 6.7A). HC CD1c⁺ DC co-cultures resulted in the preferential secretion of IL-17A compared to their AS counterparts (Fig. 6.7A). This result is based solely on one HC and two AS patient myeloid co-cultures. Secretion of the inflammatory cytokines IL-1 β , IL-6 and TNF α following AS

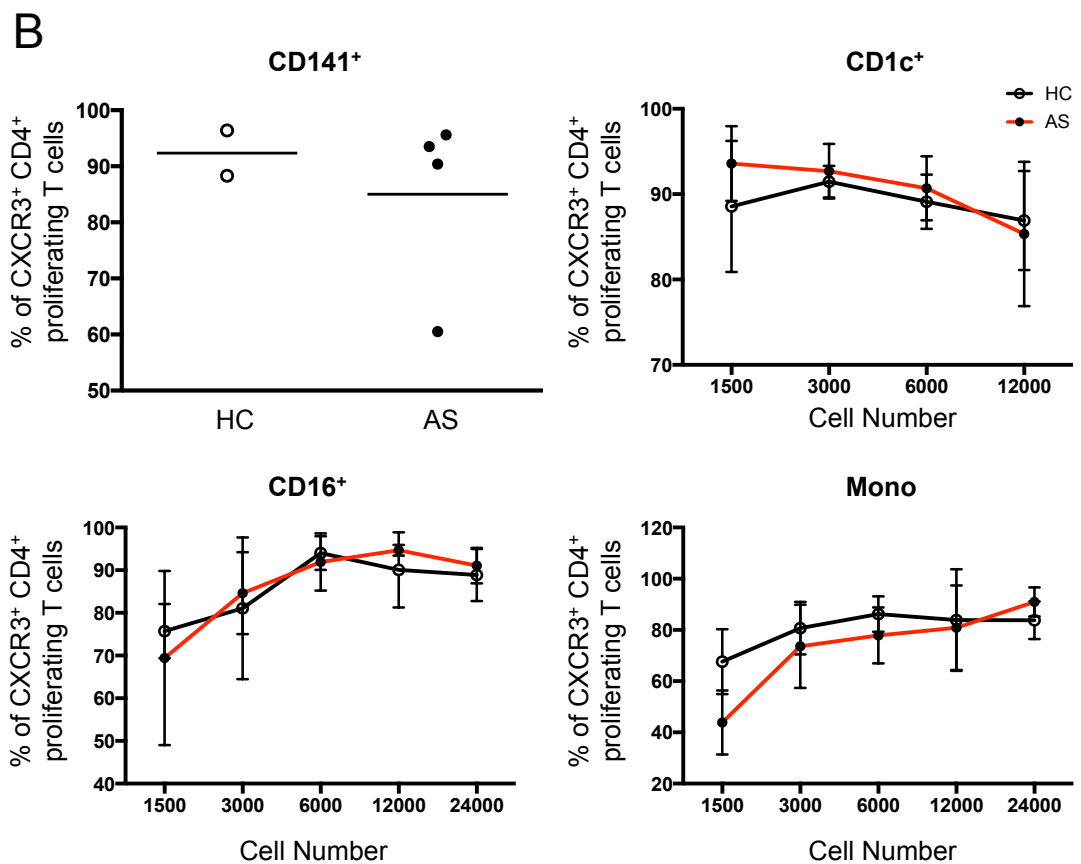
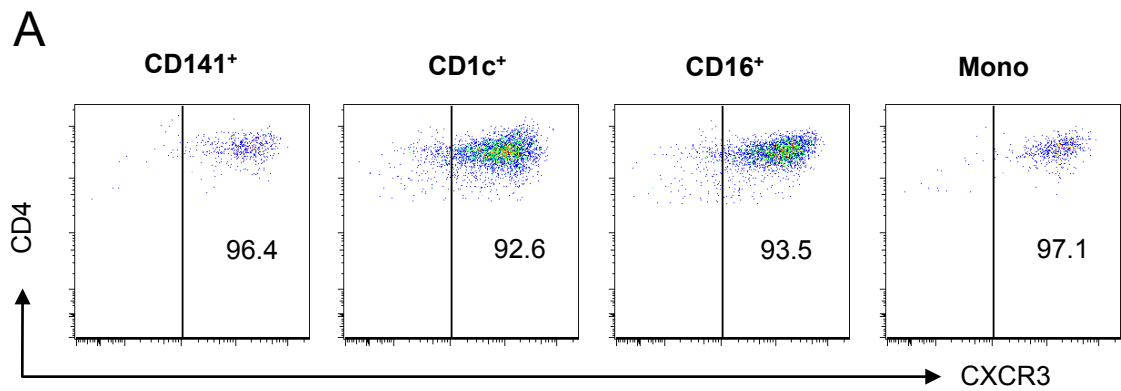


Figure 6.6: CXCR3 induction by HC and AS blood DC/monocyte subsets

No difference in the ability of HC (black) and AS patients (red) DC/monocyte subsets to induce CXCR3 on interacting T cells in an MLR co-culture system. **(A)** Representative FACS plots of CXCR3 induction by HC and AS DC/monocyte subsets. Number represent % of CXCR3⁺ proliferating T cells. **(B)** CD141⁺ DCs (2 HC – empty circles, 4 AS – filled circles), CD1c⁺ DCs (3 HC, 5 AS), CD14⁻ CD16⁺ mononuclear cells (3 HC, 5 AS) and CD14⁺ monocytes (3 HC, 5 AS) were tested for their ability to induce CXCR3. Error bars show mean +/- SD.

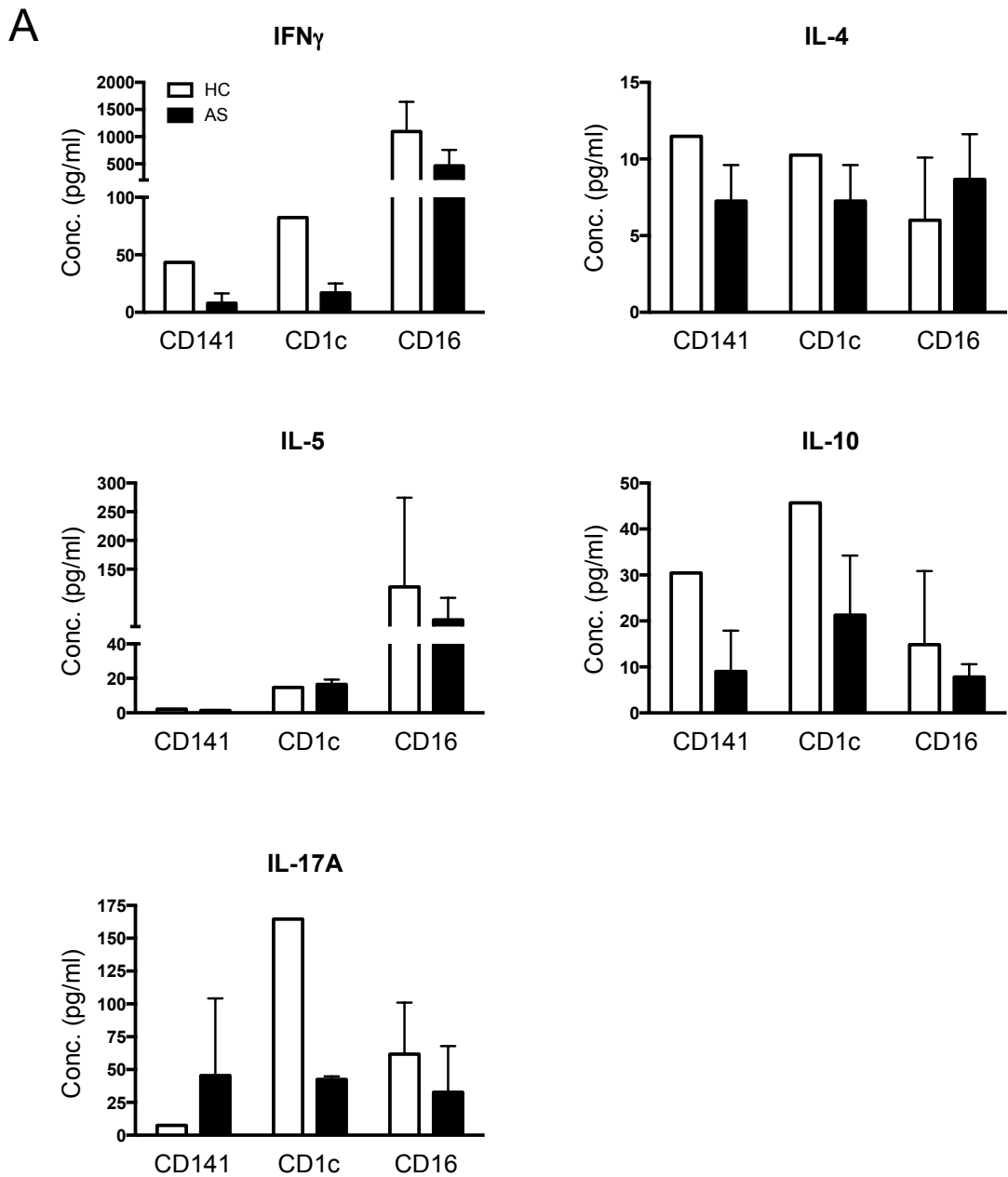


Figure 6.7: Secretion of T cell-associated cytokines following MLR

Secretion of T cell-associated cytokines following co-culture of CD141⁺ and CD1c⁺ DCs and CD14⁻ CD16⁺ mononuclear cells with CD4⁺ CD45RA⁺ naïve T cells. **(A)** Secretion of IFN γ , IL-4, IL-5, IL-10 and IL-17A following myeloid cell co-culture with CD4⁺ naïve T cells for 5 days. Cytokine levels were analysed by Luminex. For co-culture 1,500 CD141⁺ DCs, 12,000 CD1c⁺ DCs and 12,000 CD14⁻ CD16⁺ mononuclear cells were incubated with 20,000 CD4⁺ T cells. For HCs (empty bars) one CD141⁺, one CD1c⁺ and two CD14⁻ CD16⁺ mononuclear cell co-cultures were analysed. The MLR supernatants of two CD141⁺, two CD1c⁺ and 3 CD14⁻ CD16⁺ mononuclear cell AS patient (filled bars) co-cultures were assessed. Error bars represent SD.

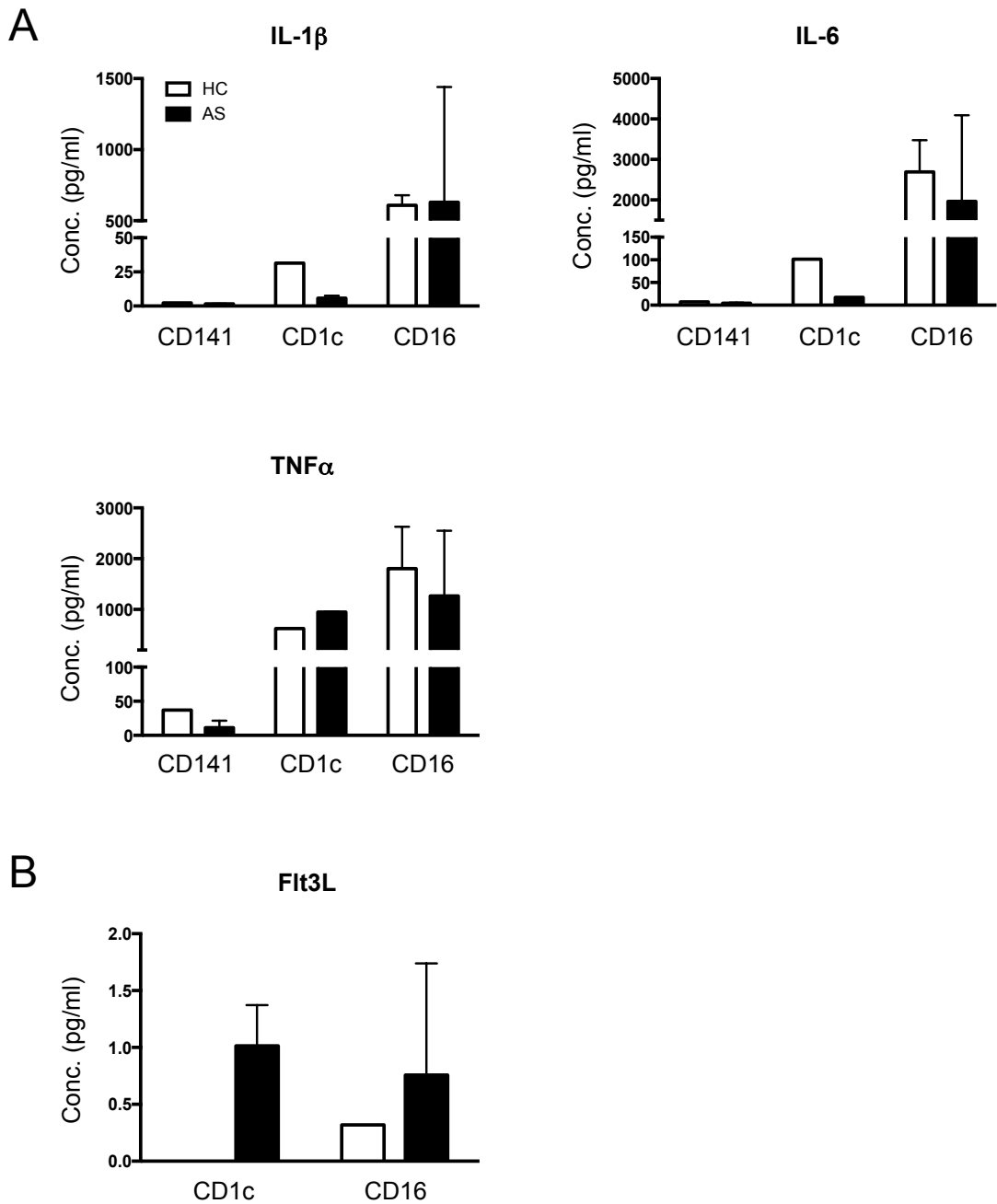


Figure 6.8: Secretion of inflammatory cytokines and growth factors following MLR

Secretion of T cell-associated cytokines following co-culture of CD141⁺ and CD1c⁺ DCs and CD14⁻ CD16⁺ mononuclear cells with CD4⁺ CD45RA⁺ naïve T cells. Secretion of IL-1 β , IL-6 and TNF α (**A**) and Flt3L (**B**) following myeloid cell co-culture with CD4⁺ naïve T cells for 5 days. Cytokine levels were analysed by Luminex. For co-culture 1,500 CD141⁺ DCs, 12,000 CD1c⁺ DCs and 12,000 CD14⁻ CD16⁺ mononuclear cells were incubated with 20,000 CD4⁺ T cells. For HCs (empty bars) one CD141⁺, one CD1c⁺ and two CD14⁻ CD16⁺ mononuclear cell co-cultures were analysed. The MLR supernatants of two CD141⁺, two CD1c⁺ and 3 CD14⁻ CD16⁺ mononuclear cell AS patient (filled bars) co-cultures were assessed. Error bars represent SD.

patient and HC myeloid population co-cultures did not differ between AS patients and HCs (Fig. 6.8A). CD14⁻ CD16⁺ mononuclear co-cultures secreted higher concentrations of IL-1 β and IL-6 than all other myeloid: T cell co-cultures, in both AS patients and HCs (Fig. 6.8A). HC and AS patient CD141⁺ DC: naïve T cell co-cultures secreted the lowest levels of IL-10 (Fig. 6.8A). AS patient and HC CD1c⁺ DC and CD14⁻ CD16⁺ mononuclear MLR supernatants were assessed for the presence of Flt3L (Fig. 6.8B). The single HC CD1c co-culture failed to induce Flt3L production, and only very low levels of Flt3L could be detected in the co-cultures involving AS patient CD1c⁺ DCs and HC and AS patient CD14⁻ CD16⁺ mononuclear cells (Fig. 6.8B). GM-CSF was undetectable in all of the MLR experiments (data not shown). In order to confirm many of these results, these experiments should be repeated.

6.6 Assessment of cell survival

Following analysis of blood DC subsets in AS patient and HC blood, we observed a significant reduction in the proportion of CD1c⁺ DCs as a percentage of CD11c⁺ MHC II⁺ DCs, and an increase in CD14⁻ CD16⁺ mononuclear cells. One hypothesis that may account for this is that AS patient CD1c⁺ DCs may have a reduced lifespan *in vivo*. Consistent with this hypothesis, research using the HLA-B27 TG SpA rat model has suggested a role for ER stress in the development of Th17 responses and SpA (481, 520). Following activation of the ER stress pathway, cells may die by apoptosis. Furthermore, Flt3L induced HLA-B27 TG BM-derived DCs exhibit enhanced caspase-mediated cell death compared to their WT counterparts (480). Therefore because of the reduction of circulating CD1c⁺ DCs in AS patients, and the contribution of ER stress to SpA pathogenesis, we set out to assess survival of AS patient and HC myeloid cells using an *in vitro* assay. CD1c⁺ DCs, CD14⁻ CD16⁺ mononuclear cells and CD14⁺ CD16⁻ monocytes from AS patients and HCs were flow sorted, stained with fluorescent dyes and mixed 1:1. The proportions of live HC and AS cells in the cultures were analysed at 24 and 48 hours later by flow cytometry. Initially, HC cells were stained with CFSE and AS cells were identified using the V450 proliferation dye. No differences were observed in the ratio between AS patient and HC CD1c⁺ DCs and CD14⁻ CD16⁺ mononuclear cells after 24 (Fig. 6.9A) or 48 (Fig. 6.9B) hours. Survival of CD1c⁺ DCs was only assessed after 24 hours. In contrast, cell survival of AS patient CD14⁺ CD16⁻ monocytes appeared to be significantly greater than that of monocytes isolated from a HC at both time points (Fig. 6.9A and 6.9B). Representative FACS plots of monocyte cell survival as assessed by HC: AS ratio are depicted in Fig. 6.9A and 6.9B. These plots confirm that at both 24 and 48

hours, AS patient monocytes outnumbered their HC counterparts. However, to control for the use of different cell proliferation dyes to identify the AS patient and HC myeloid populations, the V450 and CFSE proliferation dyes were swapped between the HC and AS patient subsets, with HC cells now stained with V450 and the AS cells with CFSE. This alteration resulted in reduced survival of AS patient monocytes compared to their HC counterparts (Fig. 6.9C). Together, these results suggest that the survival of AS patient and HC cell subsets using this *in vitro* assay did not differ. Additionally, CFSE was observed to specifically affect survival of CD14⁺ CD16⁻ monocytes.

Quantification of cell death was also performed. For each assay, the proportion of dead cells as defined by FSC and SSC, were converted to a ratio: AS: HC. Once again, initial experiments used CFSE and V450 proliferating dyes to identify HC and AS patient populations respectively. At 24 hours CD1c⁺ DC and CD14⁺ CD16⁻ monocytes isolated from AS patients showed enhanced cell survival compared to that of HC populations (Fig. 6.10A). At 48 hours, survival of AS patient CD14⁺ CD16⁺ mononuclear cells and CD14⁺ CD16⁻ monocytes were again enhanced compared to their HC counterparts (Fig. 6.10A). To control for the effect of these differential dyes, the V450 and CFSE proliferation dyes were swapped between the HC and AS patient subsets. Similar to the results obtained above (Fig. 6.9), a greater proportion of dead cells were observed for all myeloid populations from AS patients (Fig. 6.10B). Specifically enhanced HC survival was observed for CD1c⁺ DC and CD14⁺ CD16⁻ monocytes at 24 hours and CD14⁺ CD16⁻ monocytes at 48 hours (Fig. 6.10B). Representative FACS plots depicting cell death are shown in Fig. 6.10C. At 24 and 48 hours, CD14⁺ CD16⁻ monocytes isolated from AS patients and HCs were assessed for SSC profile. Proportions of live cells are presented.

Our results using this *in vitro* assay suggest that, AS patient myeloid populations do not differ in their survival capacity when compared to HC counterparts. In addition, CFSE was found to induce cell death of flow sorted populations, predominantly CD14⁺ CD16⁻ monocytes.

6.7 ER stress in circulating myeloid populations

Animal model experiments indicate that the unfolded protein response (UPR) induced by ER stress is upregulated in SpA, specifically within myeloid populations (481, 520). However, human studies using monocyte-derived macrophages and PBMCs have so far failed to identify preferential induction of the ER stress pathway in AS (505, 523). Given

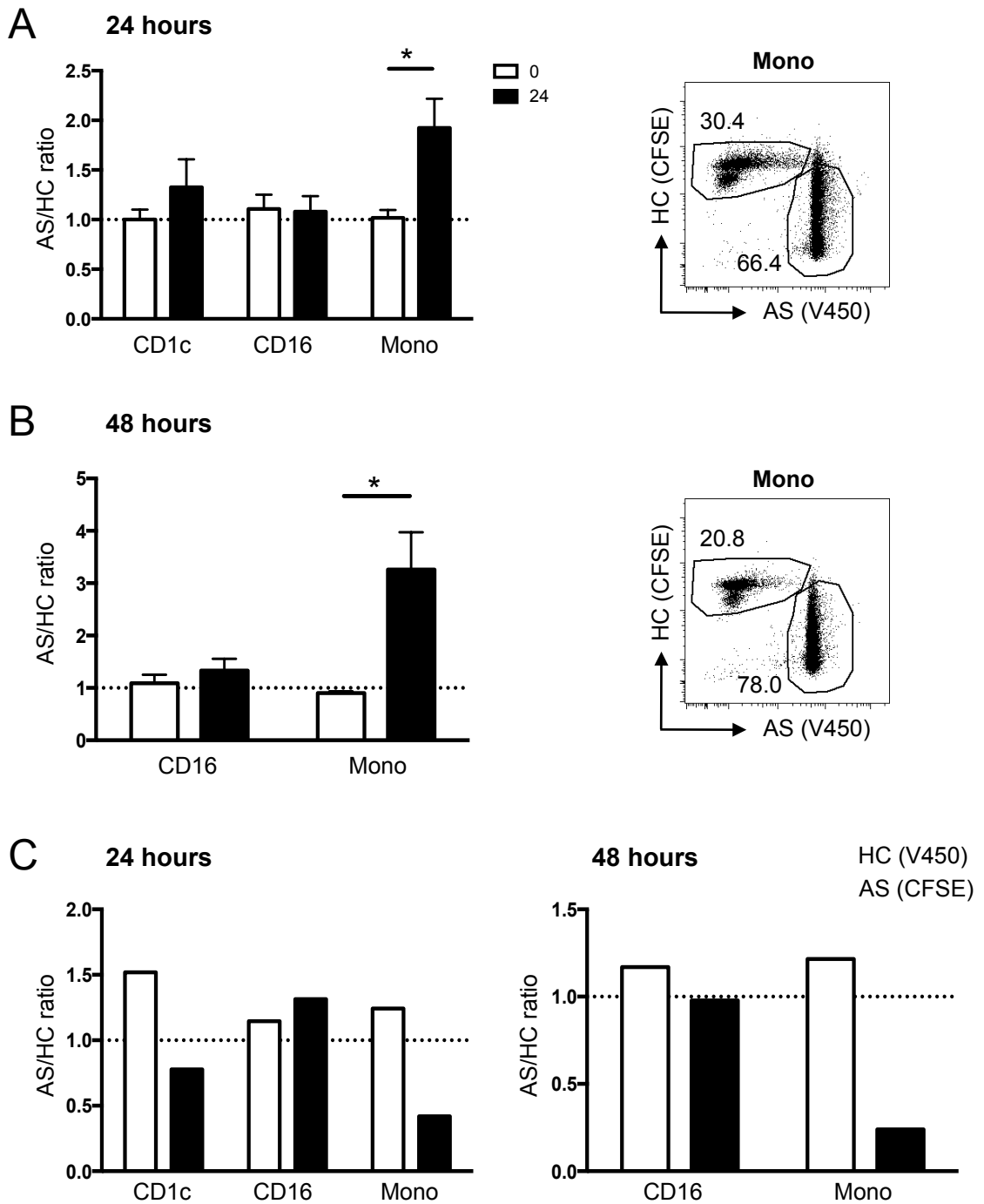


Figure 6.9: Survival of cDC and monocyte subsets isolated from AS patients and HCs

Survival of blood cDC and monocyte subsets. HC (CFSE) and AS (V450) cDC and monocyte subsets, after cell sorting, were mixed 1:1 (dotted line) and cultured for 24 (A) or 48 (B) hours. Cell proportions (AS: HC ratio) analysed at 0 (empty bars) or 24/48 hours (filled bars). Representative FACS plots of monocyte survival at 24 (A – right) and 48 (B – right) hours. Data from 4 independent experiments. Percentages represent proportion of single live cells (FSC vs SSC profile). (C) Cell sorted HC (V450) and AS (CFSE) cDC and monocyte subsets were mixed 1:1 and cultured for 24 (left) or 48 (right) hours. Cell proportions (AS: HC ratio) were analysed at 0 (empty bars) or 24/48 hours (filled bars). CD16⁺ subset contains SLAN⁺ and SLAN⁻ subsets and monocytes are CD14⁺ CD16⁻. One independent experiment. * p = < 0.05, unpaired T test.

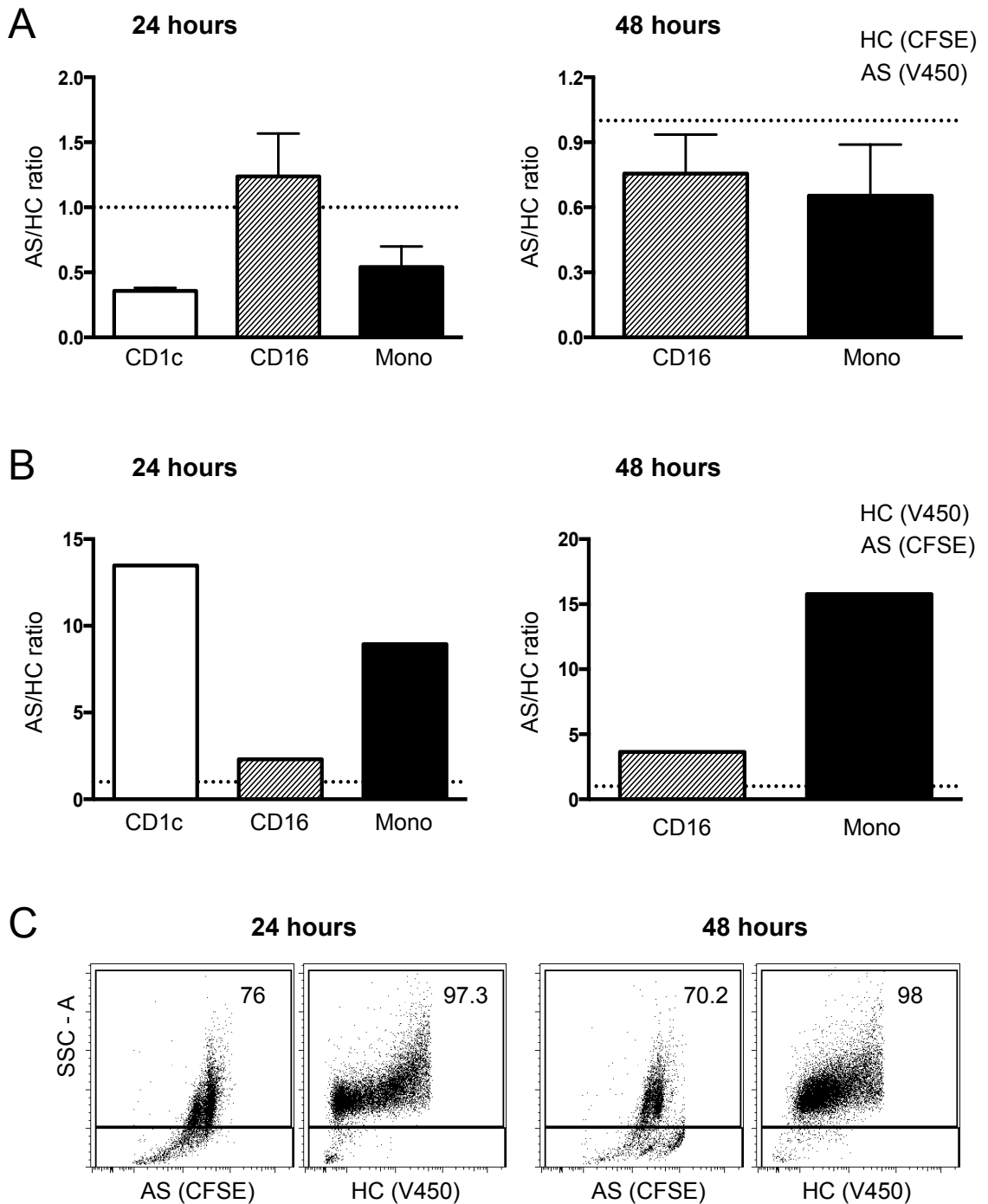


Figure 6.10: Survival of AS patient and HC CD1c, CD16 and monocyte populations

Survival of blood cDC and monocyte subsets. **(A)** HC (CFSE) and AS (V450) cDC and monocyte subsets, after cell sorting, were mixed 1:1 (dotted line) and cultured for 24 (left) or 48 (right) hours. Percent of dead cells was converted to a ratio (AS: HC) and analysed at 0, 24 and 48 hours. Data from 4 independent experiments. **(B)** Cell sorted HC (V450) and AS (CFSE) cDC and monocyte subsets were mixed 1:1 and cultured for 24 (left) or 48 (right) hours. Percentage of dead cells was converted to a ratio (AS: HC) and analysed at 0, 24 and 48 hours. CD16⁺ subset contains SLAN⁺ and SLAN⁻ subsets and monocytes are CD14⁺ CD16⁻. One independent experiment. **(C)** Representative FACS plots of monocyte survival after 24 (left) and 48 (right) hours. Percentages represent proportion of dead cells (FSC vs SSC). One independent experiment.

our expertise in the isolation and characterisation of circulating DC populations, we set out to fully characterise the induction of the ER stress pathway in AS patient and HC CD1c⁺ DCs (Fig. 6.11) and CD14⁻ CD16⁺ mononuclear cells (Fig. 6.12). ER stress can be transmitted through three pathways, each of which was investigated for both myeloid populations. ER stress sensed through PERK activation leads to the phosphorylation of EIF2 α and ATF4. Blood CD1c⁺ DCs isolated from AS patients and HCs did not differ in their expression levels of ATF4, PERK and EIF2 α (Fig. 6.11A). IRE1 activation leads to the splicing of XBP-1, so the levels of unspliced and spliced XBP-1 in AS patient and HC CD1c⁺ DCs were assessed. Unspliced XBP-1 (uXBP-1) and spliced XBP-1 (sXBP-1) levels in CD1c⁺ DCs isolated from both AS patients and HCs were not different (Fig. 6.11B). The third pathway for nuclear transmission of ER stress involves the activation of ATF6. ATF6 was not differentially expressed between CD1c⁺ DCs isolated from AS patients and HCs (Fig. 6.11C). BiP, a chaperone molecule, regulates the activation IRE1, PERK and ATF6 and is released from these ER stress-sensing molecules following ER stress induction. Examination of BiP transcripts in AS patient and HC CD1c⁺ DCs failed to identify differential expression between these populations (Fig. 6.11D).

CD14⁻ CD16⁺ mononuclear cells isolated from AS patients and HCs were also analysed for the expression of genes involved in the ER stress induction pathway. As for CD1c⁺ DCs, genes involved in the PERK (PERK, ATF4 and EIF2 α – Fig. 6.12A), IRE1 (uXBP-1 and sXBP-1 – Fig. 6.12B) and ATF6 (Fig. 6.12C) ER stress pathways were not differentially expressed between CD14⁻ CD16⁺ mononuclear cells isolated from HCs and AS patients. In contrast, BiP expression was elevated in AS patient CD14⁻ CD16⁺ mononuclear cells compared to their HC counterparts (Fig. 6.12D).

In this study, we were unable to assess the induction of the UPR via ER stress in circulating CD141⁺ DCs due to insufficient cells numbers. However, our data suggest that the presence of HLA-B27 in AS patient myeloid DCs and mononuclear cells does not induce ER stress.

6.8 Role of myeloid A20 expression in AS

Deficient expression of A20 (TNFAIP3) specifically within the myeloid compartment of a murine model led to the development of lymphocyte-dependent colitis, arthritis and enthesitis (674). A20 is a protein that negatively regulates NF κ B activation; A20-deficient mice develop severe inflammatory disease (675, 676). A20 is therefore involved in the

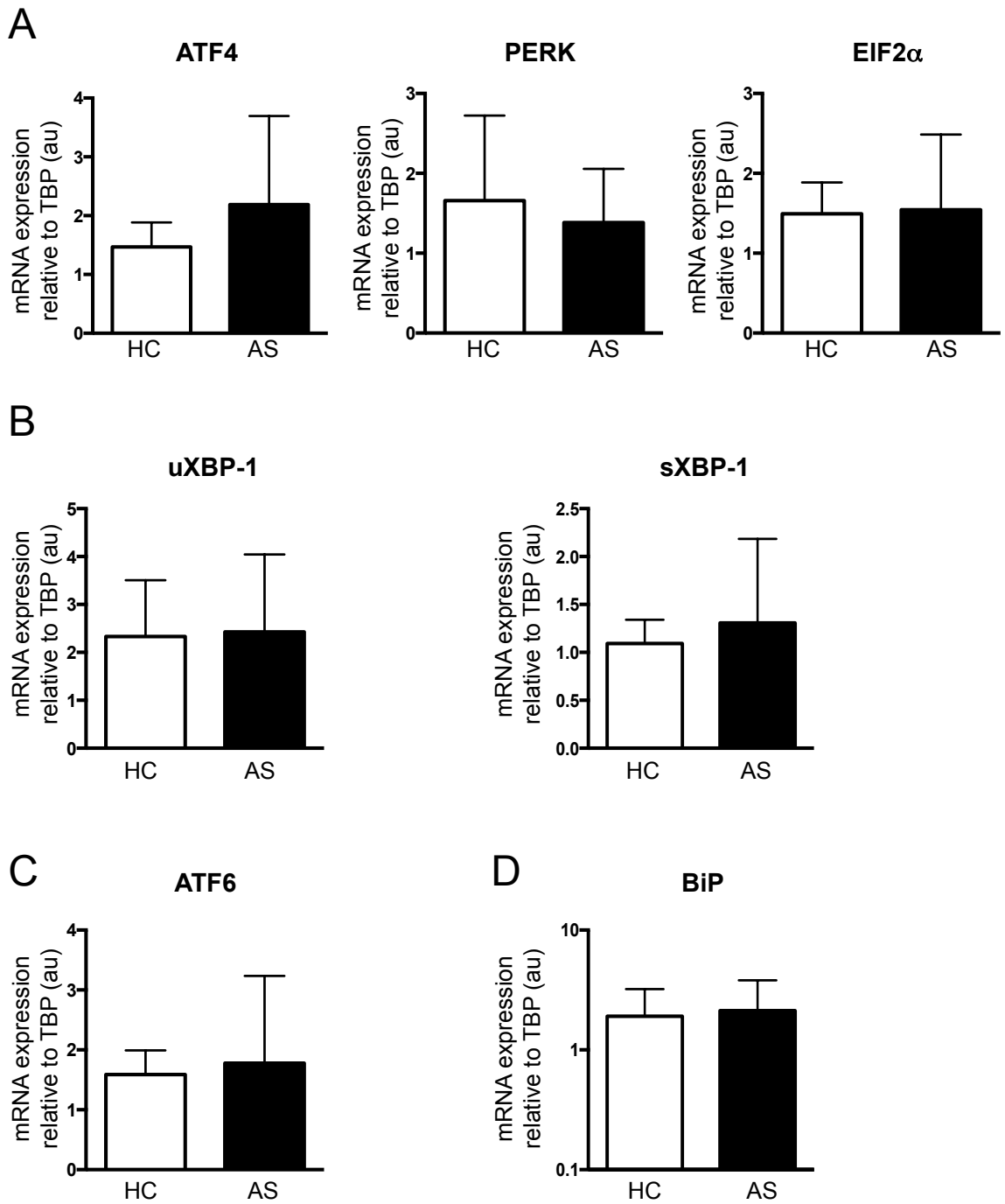


Figure 6.11: Expression of ER stress genes in circulating CD1c⁺ DCs

No evidence of ER stress induction in AS patient circulating CD1c⁺ DCs. Expression of ER stress genes on CD1c⁺ DCs isolated from the blood of AS patients (filled bars) and HCs (empty bars). Gene expression is presented as relative expression compared to that of the endogenous control, TBP: measured in arbitrary units (AU). **(A)** Expression of ATF4, EIF2 α and PERK compared between AS patients and HCs. **(B)** Levels of unspliced XBP-1 (uXBP-1) and spliced XBP-1 (sXBP-1) were compared between AS patients and HCs. Expression of ATF6 **(C)** and BiP **(D)** on CD1c⁺ DCs isolated from AS patients and HCs. For A, B and C, 4 HC and 3 AS patient CD1c⁺ samples were used in analysis. For BiP analysis (D), 13 HCs and 15 AS patient CD1c⁺ DC samples were used. Data normalised to HC CD1c⁺ DCs.

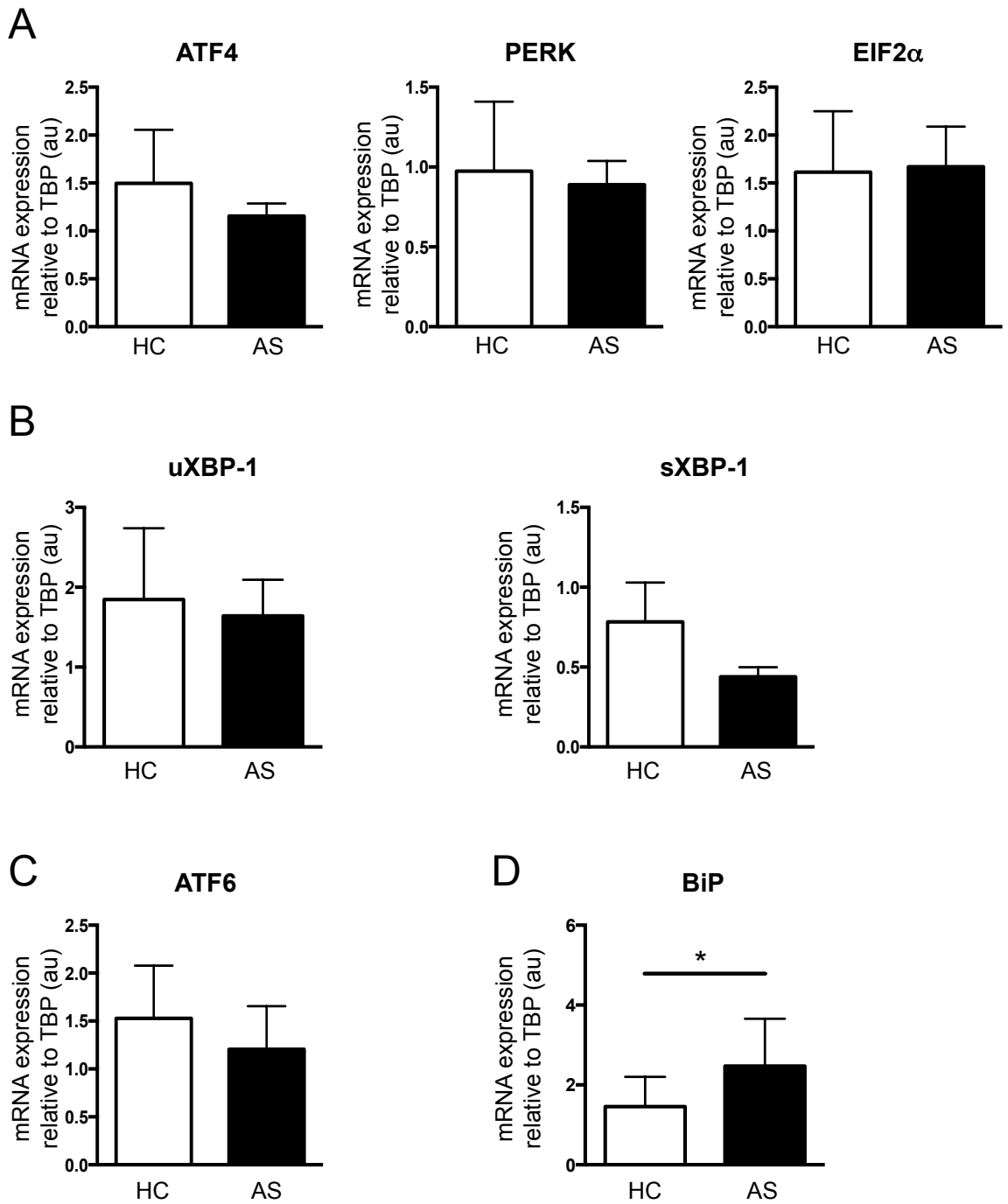


Figure 6.12: Expression of ER stress genes in circulating CD16⁺ mononuclear cells

No evidence of ER stress gene induction within CD16 mononuclear cells isolated from AS patients (filled bars) and HCs (empty bars). Gene expression is presented as relative expression compared to that of the endogenous control, TBP: measured in arbitrary units (AU) and HC CD16⁺ mononuclear cells. **(A)** Expression of ATF4, EIF2 α and PERK compared between AS patients and HCs. **(B)** Levels of unspliced XBP-1 (uXBP-1) and spliced XBP-1 (sXBP-1) were compared between AS patients and HCs. Expression of ATF6 **(C)** and BiP **(D)** on CD16⁺ mononuclear DCs isolated from AS patients and HCs. * $p = <0.05$, Mann-Whitney T test. For A, B and C, 4 HC and 3 AS patient mononuclear samples were analysed. For BiP analysis (D), 10 HCs and 11 AS patient mononuclear samples were used.

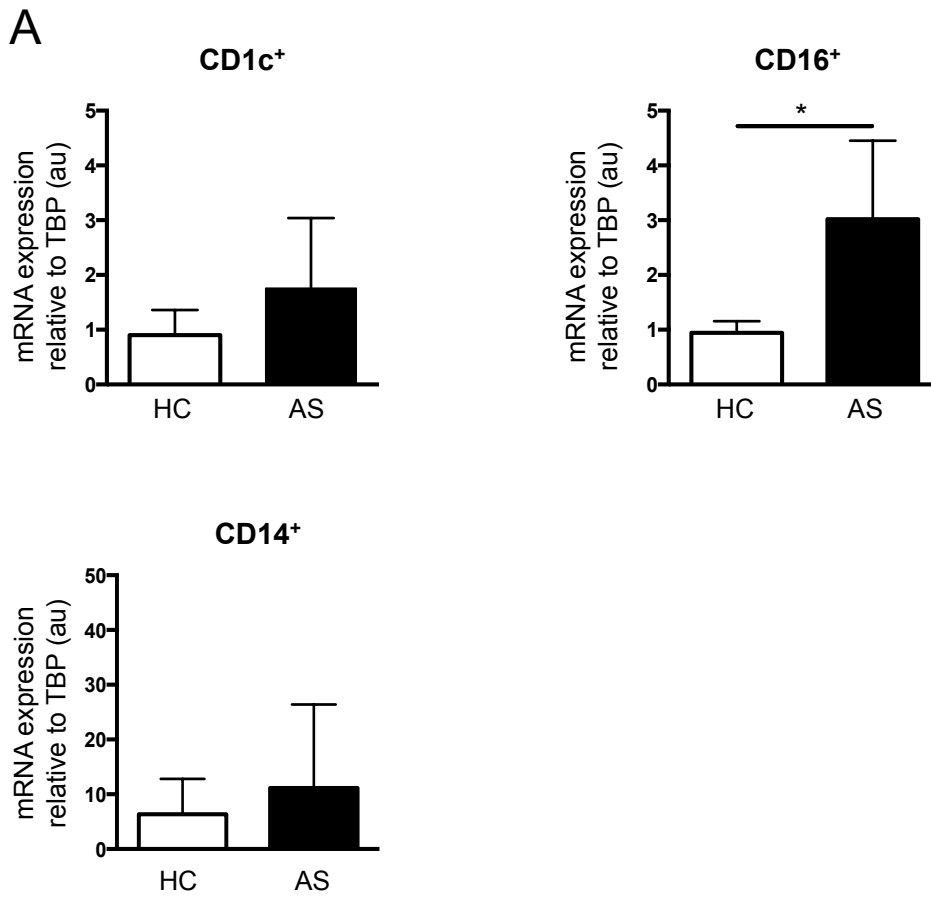


Figure 6.13: Myeloid expression of A20 in AS patients and HCs

CD16⁺ mononuclear cells isolated from AS patients express elevated levels of A20. **(A)** Level of A20 expression in CD1c⁺ DCs (top left), CD14⁻ CD16⁺ mononuclear cells (top right) and CD14⁺ CD16⁺ monocytes isolated from AS patients (filled bars) and HCs (empty bars). For analysis of CD1c⁺ DCs, 7 HCs and 7 AS patients were used for analysis. 4 AS patient and 4 HCs individual CD14⁻ CD16⁺ mononuclear cells and 6 AS patients and 6 HCs were used for gene expression analyses. Gene expression is presented as relative expression compared to that of the endogenous control, TBP: measured in arbitrary units (AU). * p < 0.05, Mann-Whitney T test.

maintenance of immune homeostasis. Coeliac (677) and psoriatic (678, 679) patients have been shown to possess SNPs within the A20 locus, contributing to the genetic make-up of these complex autoimmune diseases. Given the systemic inflammatory nature of AS and the accompanied association with IBD and psoriasis, both of which involve A20 polymorphisms, we set out to establish the expression of A20 within the circulating myeloid populations of AS patients and HCs. Blood CD1c⁺ DCs, CD14⁻ CD16⁺ mononuclear cells and CD14⁺ CD16⁻ monocytes isolated from AS patients and HCs were analysed for the expression of A20 (Fig. 6.13). For both CD1c⁺ DCs and CD14⁺ CD16⁻ mononuclear cells, no difference in the expression of A20 was expressed (Fig. 6.13A). In contrast, A20 expression was elevated in AS patient CD14⁻ CD16⁺ mononuclear cells when compared to HCs (Fig. 6.13A). Our results indicate that A20 is differentially expressed in AS patient CD14⁻ CD16⁺ mononuclear cells, with elevated levels of this regulatory protein being observed.

6.9 Discussion

At the outset of my PhD, we hypothesised that circulating CD141⁺ DCs would be absent or diminished in AS patients, given our observations using the HLA-B27 TG rat SpA model (480). However, we found that AS patients have normal numbers of CD141⁺ DCs.

When examining the DC populations, we identified variations in the circulating myeloid populations of AS patients. A reduction in CD1c⁺ DCs was accompanied by an increase in CD14⁻ CD16⁺ mononuclear cells. In order to understand the contributions of these immune populations to disease pathogenesis, the functions of four circulating myeloid populations were examined: - CD141⁺ and CD1c⁺ DCs, CD14⁻ CD16⁺ mononuclear cells and CD14⁺ CD16⁻ classical monocytes. These investigations have not previously been performed. However, numerous studies have investigated the functional characteristics of these four myeloid populations under steady state conditions. Blood and tissue CD141⁺ DCs are potent inducers of Th1 cells, excel at antigen cross-presentation following TLR3 stimulation, and are the principal inducers of CD8⁺ T cell proliferation (200, 212, 339, 340, 347). In contrast, CD1c⁺ DCs are reported to possess both tolerogenic and immunogenic properties. CD1c⁺ DCs have been shown to secrete IL-10 and express highest levels of the tolerogenic molecule IDO (211). In contrast they have also been reported to induce Th17 differentiation (277). CD14⁻ CD16⁺ mononuclear cells are reported to possess endothelial surveillance properties (237) and are capable of pro-inflammatory Th1 and Th17 induction (249, 252, 346, 359). Finally, classical CD14⁺ CD16⁻ monocytes are highly phagocytic,

express high levels of reactive oxygen species (ROS), lysozyme and are proficient in the induction of T cell proliferation (237). Given the functional attributes of these myeloid populations and their involvement in immune response generation, we set out to establish the functional attributes of AS patient circulating myeloid populations and whether they might be involved in the pathogenesis of this systemic disease.

Patients recruited to this study were mostly male and HLA-B27⁺ (Table 6.1). Again, average disease score levels of approximately 4 for both BASDAI and BASMI categories were observed (Table 6.1). Levels of inflammation were not excessively high, with scores below 10 considered to be applicable to the general population (Dr David McCarey, personal communication). Almost all recruited patients presented with evidence of bilateral sacroiliitis, determined through MRI and X-ray examination. 30% of patients exhibited extra-articular symptoms, with peripheral arthritis the most common. Data were unavailable for one patient (Table 6.1). The majority of the patients were undergoing treatment through NSAID administration. These parameters are characteristic of the general AS population and are similar to the other patient cohorts used in this study. Males were preferentially recruited to the HC cohort, to replicate the bias in the patient cohort. The HCs had a slightly lower average age (53.3 vs 46.4 years). The majority of recruited healthy individuals lacked expression of the disease-associated HLA-B27 molecule (Table 6.1). Overall AS patients included within this study exhibited similar disease profiles to the general AS population.

We assessed the capacity of blood myeloid populations to induce T cell proliferation *ex vivo* using MLRs. All blood myeloid populations examined were capable of stimulating T cell proliferation in a 5-day co-culture with naïve CD4⁺ T cells (Fig. 6.2). However, there were no differences between AS patient and HC populations' ability to drive T cell proliferation, at any DC: T cell ratio (Fig. 6.2). As discussed in chapter 4, AS patients did not possess a higher proportion of circulating effector T cell populations compared to HCs (Fig. 4.2 and 4.3). These observations may be connected given that DCs, as the principal APCs of the immune system, prime and direct T cell responses. Therefore, the similar capabilities of AS patient and HC myeloid populations may be consistent with the lack of change to the circulating effector T cell profile of AS patients. However, it should be noted that this experimental approach does not assess the antigen processing capabilities of AS patient DCs, and those isolated from HCs, as exogenous antigen is not processed and presented via MHC II in this setting. To address this, DCs isolated from tetanus-toxoid

immunised patients and HCs could be incubated with tetanus toxoid and autologous T cells.

Due to the low numbers of CD141⁺ DCs isolated from peripheral blood, it was difficult to fully assess the induction of T cell proliferation by this blood DC subset. However, at the highest possible DC: T cell ratio (1,500 DCs: 20:000 naïve CD4⁺ T cells), CD141⁺ DCs were just as proficient as the CD1c⁺ DC subset in the induction of T cell proliferation in both HCs (Fig. 6.3A) and AS patients (Fig. 6.3B). CD141⁺ DCs have previously been reported to support elevated levels of CD8⁺ T cell proliferation. As SpA diseases are CD8⁺ T cell independent, at least in the HLA-B27 TG rats, the interaction between circulating myeloid populations and CD8⁺ T cells was not assessed in this study. However, our data indicate that CD141⁺ and CD1c⁺ DCs do not differ in their ability to induce CD4⁺ T cell proliferation. Future experiments using greater DC numbers could be performed to substantiate these observations. Both CD14⁻ CD16⁺ mononuclear cells and CD14⁺ CD16⁻ monocytes were less efficient at inducing T cell proliferation than CD1c⁺ DCs in both HCs (Fig. 6.3A) and AS patients (Fig. 6.3B). This observation was maintained at all DC: T cell ratios (Fig. 6.3). Interestingly, CD14⁻ CD16⁺ mononuclear cells were consistently better at driving T cell proliferation than CD14⁺ CD16⁻ monocytes, in both HC (Fig. 6.3A) and AS patient (Fig. 6.3B) myeloid: T cell co-cultures, and at all DC: T cell ratios. Thus, CD14⁻ CD16⁺ mononuclear cells appear functionally distinct from CD14⁺ CD16⁻ monocytes. The CD14⁻ CD16⁺ mononuclear population contains both SLAN⁻ and SLAN⁺ cells (Fig. 3.6A). In this study, the functional properties of these populations were not examined separately. However, given that SLAN⁺ cells are thought to represent a third blood DC subset (240, 249, 250, 359) and DCs possess an enhanced capacity to drive T cell proliferation (Fig. 6.3), functional assessment of the individual populations may delineate their relationship to monocytes and DCs. CD14⁺ CD16⁻ monocytes possess a superior capacity to phagocytose beads (1µm biotinylated YG-Fluospheres) (237). Taken together, these data are consistent with previously reported functional differences between monocyte and dendritic cell populations.

DC: T cell interactions drive T cell proliferation, migration and differentiation. Therefore, we assessed whether AS patient myeloid cells might drive aberrant immune responses through effects on T cell migration and differentiation. To do this, we determined the ability of the four myeloid populations to induce CCR6 and CXCR3 expression on interacting CD4⁺ T cells. CCR6 has been associated with Th17 cells and skin/gut homing, and CXCR3 with Th1 cells. CCR6 and CXCR3 were also chosen for investigation due to

their differential expression on T cells in AS patient blood; an elevated frequency of circulating activated CD4⁺ T cells in AS patients expressed CCR6, with the converse being true for CXCR3. Therefore, we hypothesised that AS patient myeloid populations would induce CCR6 expression on a higher proportion of proliferating T cells, potentially driving Th17 differentiation and therefore contribute to the pathogenesis of AS. In fact, all myeloid populations were capable of CCR6 induction on proliferating CD4⁺ T cells (Fig. 6.5) and no difference in CCR6 induction was observed between AS patient and HC myeloid populations. Around 20% of proliferating CD4⁺ T cells expressed CCR6 following co-culture (Fig. 6.5A). Therefore, AS patient myeloid cells were no more proficient in their ability to drive CCR6 expression than their HC counterparts.

We hypothesised that, given the reduction in circulating CXCR3⁺ T cells, AS patient myeloid populations may be less efficient at driving this T cell phenotype. In fact, all HC and AS patient myeloid populations (CD141⁺ and CD1c⁺ DCs, CD14⁻ CD16⁺ mononuclear cells and CD14⁺ CD16⁻ monocytes) were capable of CXCR3 induction (Fig. 6.6B). However, CXCR3 induction did not differ between AS patient and HC co-cultures (Fig. 6.6B), leading us to reject our hypothesis. Taken together, these data suggest that AS patient myeloid cells do not differ in their ability to drive CCR6 or CXCR3 expression on interacting T cells. Given that the *in vitro* conditions used do not replicate those occurring *in vivo* it would be of interest to perform similar experiments using tissue-resident myeloid cell populations, particularly from AS-affected tissues. Exogenous signals will affect DC/myeloid function; therefore identifying the alternative exogenous signals present in AS and assessing their subsequent impact on DC/myeloid function may help elucidate the immune pathways occurring *in vivo*. Our plasma cytokine data demonstrated that several pro-inflammatory cytokines and Flt3L were dysregulated in AS that could affect DC/myeloid function. It may therefore be interesting to perform T cell: DC cultures in the presence of these cytokines. These experiments would help elucidate whether DCs contribute to the generation of aberrant T cell responses.

Given the association of specific chemokine receptors with specific T cell phenotypes, our data may also indicate that AS patient myeloid populations do not preferentially induce Th17 responses, unlike in HLA-B27 TG rats (480). To address this question, intracellular cytokine staining of the proliferating T cells would need to be performed. We performed preliminary experiments to address this question by examining the cytokines secreted following DC: T cell co-culture (Fig. 6.7 and 6.8). For these experiments, supernatants were collected from CD141⁺ and CD1c⁺ DC, and CD14⁻ CD16⁺ mononuclear cell MLR

cultures with naïve CD4⁺ T cells, and analysed the resulting cytokine and growth factor milieu. Due to the limited sample numbers, it is difficult to draw conclusions, but our data indicate that co-cultures with CD14⁻ CD16⁺ mononuclear cells preferentially secrete IFN γ , IL-5, IL-1 β and IL-6 (Fig. 6.7 and 6.8). Of these cytokines, IL-6 levels were highest, suggesting that these cultures may support Th17 generation, given the involvement of IL-6 in Th17 differentiation in humans (107, 109). MLRs containing CD141⁺ DCs induced secretion of very few cytokines (Fig. 6.7 and 6.8). No difference in the cytokine profiles from these co-culture supernatants were observed between AS patient and HCs. Therefore all myeloid populations were capable of CCR6 induction in the MLR setting, with CD14⁻ CD16⁺ mononuclear co-cultures favouring the production of IL-6 that may promote Th17 generation.

Given the altered circulating myeloid population profile of AS patients, we assessed whether differential cell survival could account for our observations. As proportion of CD11c⁺ MHC II⁺ cells, AS patients had fewer circulating CD1c⁺ DCs (Fig. 3.4B) and more CD14⁻ CD16⁺ mononuclear cells (Fig. 3.7A). Initial experiments suggested that a greater proportion of AS patient DCs died following overnight culture (data not shown). Therefore, we set out to determine if AS patient myeloid populations differed in their survival capacity. We identified selective CFSE toxicity, resulting in increased cell death of blood monocytes (Fig. 6.7C, 6.8B and 6.8C), but no underlying difference in cell survival between the circulating myeloid cells of AS patients and HCs.

Despite more than 40 years of research investigating the association between HLA-B27 and AS development, the pathogenic role of this MHC class I molecule remains elusive. It was postulated that HLA-B27-induced ER stress may be a critical process, largely due to the observed induction of ER stress in myeloid populations of HLA-B27 TG rats, which leads to IL-23 production (481, 511, 520, 522). IL-23 promotes the Th17 phenotype and may therefore promote AS development and pathogenesis in the rats. To date evidence for ER stress induction in human myeloid populations is limited (505, 523, 524). Therefore I aimed to determine the activation of the UPR in circulating myeloid populations isolated from AS patients and HCs, and its potential involvement in AS pathogenesis. We examined the expression of 5 genes involved in the nuclear transduction of ER stress, in addition to the chaperone molecule BiP. CD1c⁺ DCs and CD14⁻ CD16⁺ mononuclear cells isolated from AS patients failed to show evidence of ER stress induction either via the PERK, IRE1 or ATF6 pathways (Fig. 6.11A, 6.11B and 6.11C). These results indicate that HLA-B27 misfolding does not drive ER stress, in myeloid cells, and that this mechanism is

therefore unlikely to contribute to AS pathogenesis. Our data are consistent with previous human studies (505, 523, 524). However, we did observe upregulation of the ER chaperone molecule BiP specifically within AS patient CD14⁻ CD16⁺ mononuclear cells (Fig. 6.11D and 6.12D). However, given that this upregulation of BiP was not associated with increased expression of additional ER stress genes, it is possible that enhanced HLA-B27 misfolding within CD14⁻ CD16⁺ cells results in the activation of alternative stress-associated signalling pathways. A recent study by Ciccia et al found the autophagy process to be upregulated in lamina propria mononuclear cells (LPMCs) isolated from AS patients, instead of the UPR pathway (524). Future analyses could therefore investigate the activation of autophagy, perhaps through expression of genes including autophagy protein 5 (ATG5) and ATG12 in circulating myeloid populations of AS patients.

Our final functional analysis involved expression of A20, otherwise known as TNFAIP3. A20 SNPs are associated with susceptibility to coeliac disease (677) and psoriasis (678, 679). Furthermore, A20 is a negative regulator of NFκB, with expression required for immune homeostasis (675, 676). CD1c⁺ DCs and CD14⁺ CD16⁻ monocytes isolated from AS patients and HCs expressed similar levels of this regulatory gene (Fig. 6.13A). In contrast, CD14⁻ CD16⁺ mononuclear cells isolated from AS patients expressed elevated levels of A20 compared to their HC counterparts (Fig. 6.13A). Given that A20 regulates NFκB expression, CD14⁻ CD16⁺ mononuclear cells isolated from AS patients may exhibit altered cytokine production, which may subsequently affect T cell differentiation and immune response induction. To test this hypothesis, the activation of genes directly targeted by A20 could be investigated, including receptor-interacting protein 1 (RIP1) and TNF receptor-associated factor 6 (TRAF6).

Overall, AS circulating myeloid populations did not differ in their ability to induce T cell proliferation or CCR6/CXCR3 expression compared to their HC counterparts. However, co-culture of AS patient and HC CD14⁻ CD16⁺ mononuclear cells with CD4⁺ T cells induced large quantities of IL-6, required for Th17 differentiation. Furthermore, we failed to detect evidence of ER stress upregulation in the circulating myeloid populations of AS patients, as has been observed in SpA animal models (481, 520, 522).

In order to further delineate the immune pathways involved in the development of AS, we next set out to correlate AS patient clinical parameters with their immunological profile. These correlative analyses are designed to test the effects of therapeutics, disease severity, inflammation and existence of extra-articular symptoms, on circulating immune

populations. These analyses may aid understanding of disease-associated pathways and mechanisms of current therapeutics.

Chapter 7: Comparisons between patient characteristics and immunological parameters

7.1 Introduction

In previous chapters, using clinical samples, differences were identified in the circulating myeloid DC and lymphoid populations of AS patients. The clinical attributes of AS patients differed in terms of their inflammatory status, treatment strategies, disease duration, age, and HLA-B27 status. As each of these factors could influence the patients' immunopathology, it was decided to perform correlative analyses between the patients' clinical attributes and several immunological parameters, as detailed in table 7.2. Due to low numbers of HLA-B27⁺ HCs and HLA-B27⁻ AS patients, the impact of HLA-B27 expression on disease pathogenesis was not analysed, however, the effects of other clinical parameters are assessed in detail. The aim of these analyses was to identify molecules or cell populations associated with AS development. Specifically, we set out to determine if circulating myeloid populations and T lymphocytes in AS patients were affected by specific clinical parameters. Given the involvement of DCs in driving and directing immune responses, it was hypothesised that DC populations would be affected by the ongoing inflammatory response.

7.2 Patient Characteristics

As for previous analyses, clinical factors such as disease score and treatment regimens were recorded during clinical consultation. Collated patient and HC data used for the correlative analyses are summarised in Table 7.1. The majority of analyses used a subgroup of the AS patients described below.

Table 7.1: Clinical characteristics of AS patients and healthy controls

All or a subset of the 50 AS patients and 30 HCs were used for correlative analyses. Patient characteristics are depicted in Table 7.1. Details for each clinical factor were not available for all patients. Subsequently, percentages represent proportion of all patients used in this study. Spinal disease was assessed based on the presence or absence of cervical, thoracic and lumbar involvement. Levels were categorised based on the number of sites affected: 1 site = level 1, 2 sites = level 2 and 3 sites = level 3. Mean \pm SD is shown. N/A = not applicable.

	AS Patients	Healthy Controls
Age (yrs)	54.4 \pm 12.3	40.3 \pm 12.4
Sex – Male/Female	39/11	17/12
Disease Duration (yrs)	28.1 \pm 12.5	N/A
B27 – Pos/Neg (% B27⁺)	46/4 (92%)	6/23 (26%)

BASDAI	4.04 ± 2.24	N/A
BASMI	4 ± 2.58	N/A
ESR (mm/hr)	13.27 ± 12.78	N/A
CRP (mg/L)	6.6 ± 8.76	N/A
Bilateral Sacroiliitis – No. (%)	68%	N/A
Spinal disease		
Absent – No. (%)	5 (10%)	N/A
Level 1 – No. (%)	9 (18%)	N/A
Level 2 – No. (%)	7 (14%)	N/A
Level 3 – No. (%)	7 (14%)	N/A
Extra-articular Disease		
IBD – No. (%)	3 (6%)	N/A
Uveitis – No. (%)	4 (8%)	N/A
Psoriasis – No. (%)	3 (6%)	N/A
Arthritis – No. (%)	8 (16%)	N/A
Medication		
DMARDs – No. (%)	1 (2%)	N/A
NSAIDs – No. (%)	24 (48%)	N/A
Biologics – No. (%)	4 (8%)	N/A
DMARD + NSAID – No. (%)	4 (8%)	N/A
DMARD + Biologic – No. (%)	1 (2%)	N/A
NSAID + Biologic – No. (%)	2 (4%)	N/A

Within the patient cohort, approximately 80% were male with an average age of 55 years. 60% of recruited HCs were male with a slightly lower average age of 40 years. Over 90% of AS patients expressed the MHC class I molecule HLA-B27, whilst 26% of the HC cohort showed similar expression. Patients presented with average disease scores and low levels of inflammation (Table 7.1). Levels below 10 for both inflammatory markers – ESR and CRP – are considered normal for the Glasgow population (Dr David McCarey, personal communication). Approximately 70% of AS patients presented with bilateral sacroiliitis, a characteristic feature of AS (Table 7.1). However, data regarding this disease trait was unavailable for 14 patients, whilst 2 individuals did not exhibit evidence of

sacroiliitis. Data regarding levels of spinal disease was available for only 23 individuals. Of these patients, spinal abnormalities predominantly affected one spinal region, commonly the lumbar or cervical areas. Approximately 35% of AS patients presented with a minimum of one extra-articular manifestation, with peripheral arthritis being the dominant form of affliction (Table 7.1). Data regarding the development of extra-articular manifestations was not available for 10 patients. NSAIDs including ibuprofen and etoricoxib were the most common form of treatment. Overall, the majority of our patient cohort was male and HLA-B27⁺ with low levels of disease severity and inflammation. Correlations between the clinical factors presented in Table 7.1 and several immunological parameters (Table 7.2) are discussed below.

7.3 Correlative analyses

The immunological parameters listed in Table 7.2 were each compared with the several clinical parameters in AS patients: disease treatment and duration, presence of extra-articular manifestations, age, ESR, CRP, BASFI, BASMI and BASDAI.

Table 7.2: Immunological parameters assessed for correlative analyses

Clinical parameters were assessed for their correlation with the immunological factors below: Cytokines detected in patient plasma (pg/ml); myeloid cell and T cell populations analysed in patient blood; chemokine receptors expressed on the surface of circulating CD4⁺ T cells; total PBMC numbers/ml of blood.

Cytokines	Myeloid cells	T cells	Chemokine receptors	Others
IL-1β	CD141	CD4 ⁺	CCR4	PBMC number
IL-4	CD1c	Naïve	CCR6	
IL-5	CD14 ⁻ CD16 ⁺	Memory	CCR9	
IL-6	pDC	Activated	CCR10	
IL-10		Regulatory	CXCR3	
IL-17A				
IL-23p19				
Flt3L				
IFNγ				
TNFα				

For these analyses, all myeloid and T cell populations, except pDCs, were analysed both as proportion of parent population and of live cells. pDCs were assessed only as proportion of

live cells. Expression of chemokine receptors on memory, activated and regulatory CD4⁺ T cell populations were similarly compared both as percentage of total live cells and of total CD4⁺ T cells. Naïve T cells were not included in chemokine receptor analysis. To statistically analyse the patient correlative analyses, linear regression and Kruskal Wallis Spearman correlative tests were performed, followed by the Dunn multiple comparisons post test. Those showing significance are described in more detail and discussed below.

7.4 The influence of disease severity

Many patients are unresponsive to currently available therapeutics, and thus elucidation of immunopathogenic pathways may direct future investigations into new therapeutics. Therefore, this study set out to identify immunological parameters associated with disease severity, treatment regimens and inflammatory status.

The BASDAI and BASMI scales indicate disease severity, and are evaluated between 0-10. The patient cohort here presented with low to average scores, averaging approximately 4 for both measurements. It was hypothesised that changes in disease severity would be associated with changes in blood cell populations. Despite not reaching significance ($p=0.069$), a trend towards an increase in the proportion of circulating activated CD4⁺ T cells with increasing disease severity was observed (Fig. 7.1A). In contrast, the proportion of naïve T cells decreased significantly with an increase in disease score (Fig. 7.1A). Several interesting correlations relating disease severity to chemokine receptor expression were also observed. A significant ($p=0.015$) negative correlation between BASDAI and CCR4⁺ activated T cells (Fig. 7.2A) was seen; as disease severity increased, the proportions of circulating CCR4⁺ CD25^{int} T cells decreased. In addition, the proportion of circulating CCR4 expressing memory T cells also fell with higher BASDAI scores (Fig. 7.2A). In contrast, increased proportions of CCR6⁺ regulatory T cells (CD25^{hi}) correlated with elevated BASMI ($p=0.018$) and BASFI ($p=0.007$) scores (Fig. 7.2B). Additional analyses revealed that the proportion of CXCR3⁺ activated T cells also correlated with increasing disease severity; elevated BASDAI scores were associated with a larger proportion of circulating CXCR3⁺ activated CD4⁺ T cells (Fig. 7.2C). These results suggest an association between increased disease severity and higher proportions of activated circulating T cells with specific chemokine receptor profiles. Analysis of CCR9 or CCR10 expression did not correlate with disease severity.

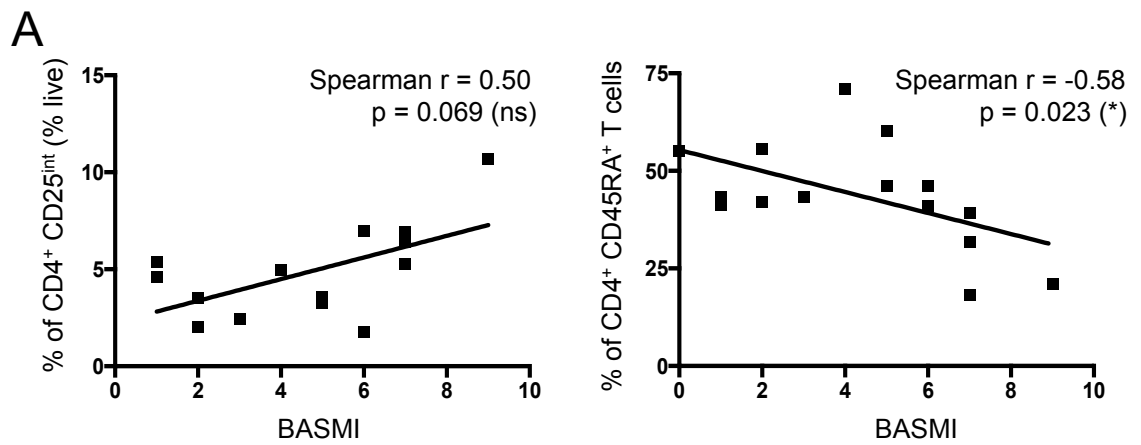


Figure 7.1: T cell proportional correlations with disease severity

Disease severity is associated with a reduction in circulating naïve CD4⁺ T cells. (A) BASMI scores (0-10) were plotted against activated T cells (CD4⁺ CD25^{int} - left), as proportion of live cells and CD4⁺ CD45RA⁺ naïve T cells (right) as proportion of T cells for AS patients (n = 14/15). Linear regression and spearman correlation statistical test were performed for every correlation. * = $p < 0.05$, ns = not significant.

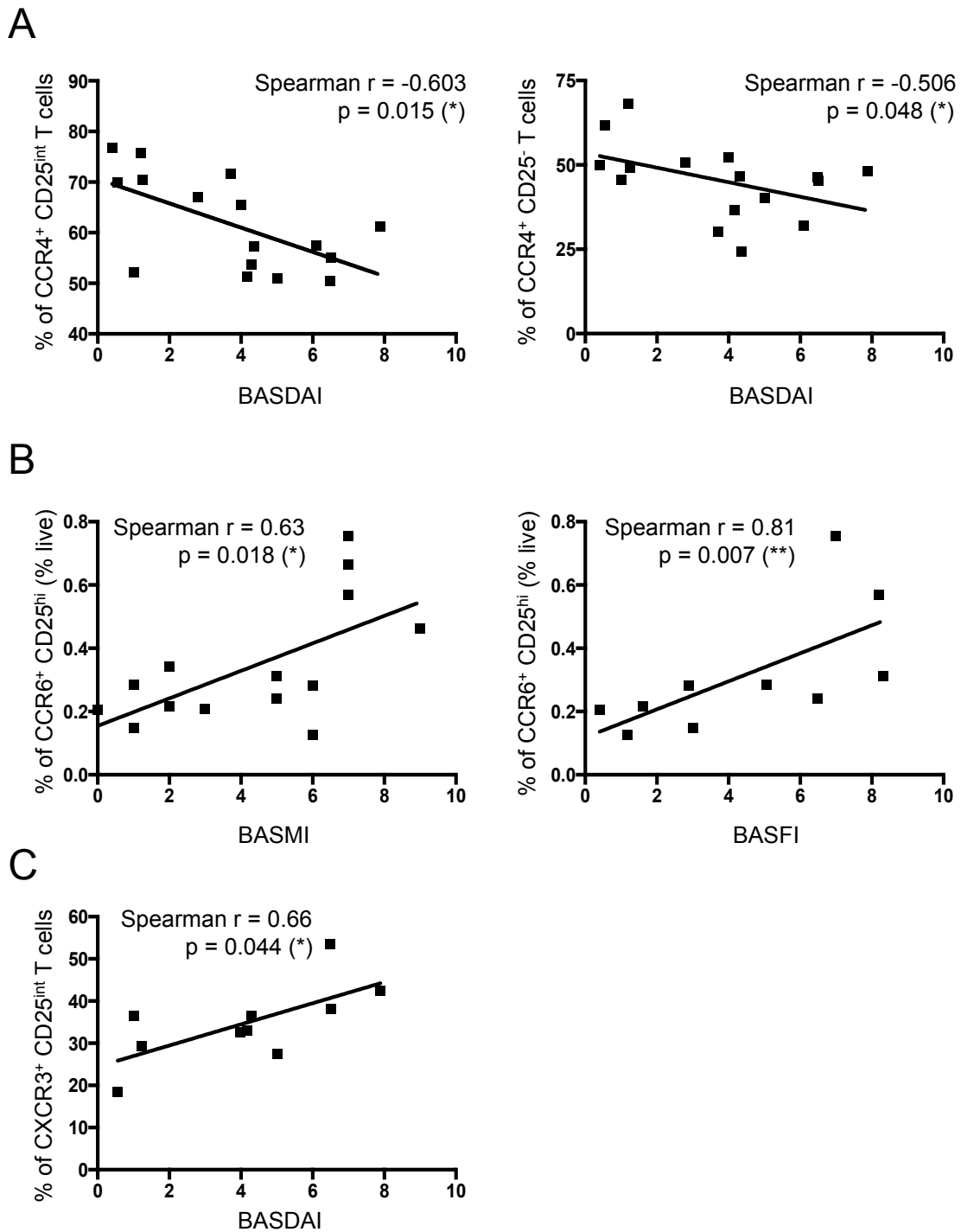


Figure 7.2: CD4⁺ T cell chemokine profile correlations with disease severity

Disease severity is associated with CCR6⁺ activated and regulatory T cells. **(A)** Effect of BASDAI (0-10) on CCR4⁺ activated (left) and memory (right) as proportion of total CD4⁺ T cells. $n = 14-16$. **(B)** CCR6⁺ regulatory T cells, as proportion of live cells were correlated with BASMI (left) and BASFI (right) scores. BASFI scores are rated on a scale of 1-10. $n = 10-12$. **(C)** BASDAI score (0-10) association with percentage of CXCR3⁺ CD25^{int} (activated) T cells as percentage of total T cells, $n = 10$ AS patients. Linear regression and spearman correlation statistical test were performed for every correlation. * = $p < 0.05$, ** = $p < 0.01$.

Correlations between clinical parameters and plasma cytokines reveal that only IL-23p19 correlated with disease activity, with low levels correlating with increased disease activity. Although AS patients had significantly elevated plasma IL-23p19 levels compared to HCs (Fig. 4.13D), a significant ($p=0.017$) negative correlation between elevated BASDAI scores and plasma IL-23p19 levels was observed (Fig. 7.3A). To complement this finding, BASMI and plasma IL-23p19 levels were similarly negatively correlated, despite not reaching significance ($p=0.119$ – Fig. 7.3A). It therefore appears that patients experiencing elevated levels of disease activity have lower levels of systemic IL-23p19. However, only 10 patients were used for these analyses, indicating a requirement for further investigation. Interestingly, higher plasma IL-23p19 levels in AS patients were significantly associated with fewer circulating CCR6⁺ regulatory T cells ($p=0.017$, Fig. 7.3B).

7.5 Effect of inflammation on immunological parameters

The influence of inflammation on immunological parameters including circulating DC and T cell populations and plasma cytokines was also investigated. Of all the factors assessed (Table 7.2), significant correlations were only observed between levels of inflammation and the proportions of specific populations of CCR⁺ CD4⁺ T cells.

Comparison of ESR with the proportion of circulating CCR9⁺ activated CD4⁺ T cells in AS patients revealed a significant ($p=0.004$) positive correlation between these parameters (Fig. 7.4A). Not only were elevated ESR levels associated with a higher proportion of circulating CCR9-expressing activated T cells, but elevated CRP levels also positively correlated with increased proportions of CCR9⁺ activated CD4⁺ T cells in the blood (Fig. 7.4A). This CCR9 correlation with CRP was conserved when CCR9⁺ T cells were analysed either as proportion of total T cells ($p=0.0001$) or of total live cells ($p=0.041$ - Fig. 7.4A). CCR6 expressing cells also correlated with inflammation: in a cohort of 22 patients, the proportions of CCR6⁺ activated CD4⁺ T cells significantly correlated with higher ESR levels (Fig. 7.4B). Furthermore, elevated CRP levels positively correlated with higher proportions of circulating CCR9⁺ memory ($p=0.028$) and regulatory ($p=0.022$) T cell populations (Fig. 7.5A). These data highlight changes to the chemokine receptor profile of circulating T cells in patients with more severe systemic inflammation, and support a role for CCR9⁺ T cells in responding to, or driving, inflammatory processes in patients with AS.

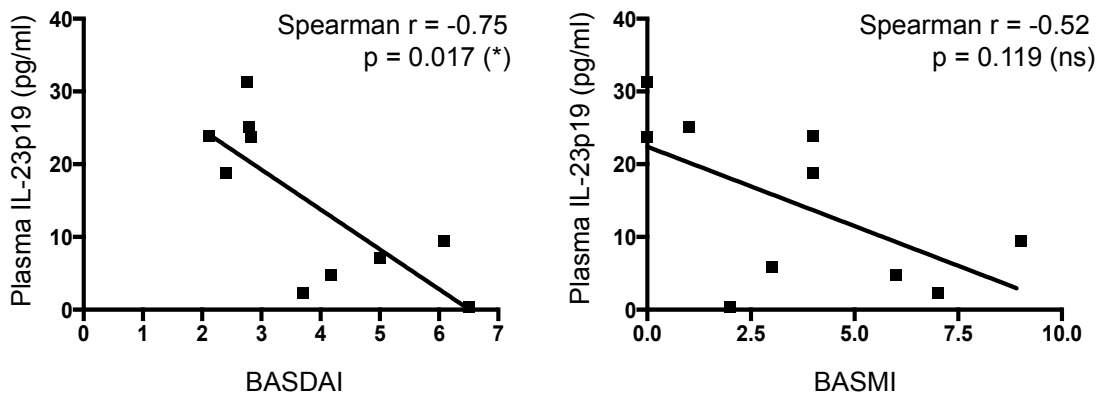
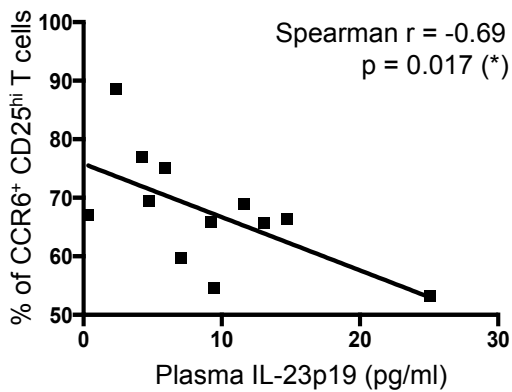
A**B**

Figure 7.3: Immunological correlations related to disease severity and IL-23p19

Disease severity is negatively associated with plasma IL-23p19. **(A)** Levels of plasma IL-23p19, measured by ELISA, were plotted against scores of disease severity: BASDAI (left) and BASMI (right), $n = 10$ AS patients. **(B)** Correlation between CCR6⁺ CD25^{hi} CD4⁺ T cells (regulatory) and plasma IL-23p19 (pg/ml) levels, $n = 12$ AS patients. Linear regression and spearman correlation statistical test were performed for every correlation. * = $p < 0.05$, ns = not significant.

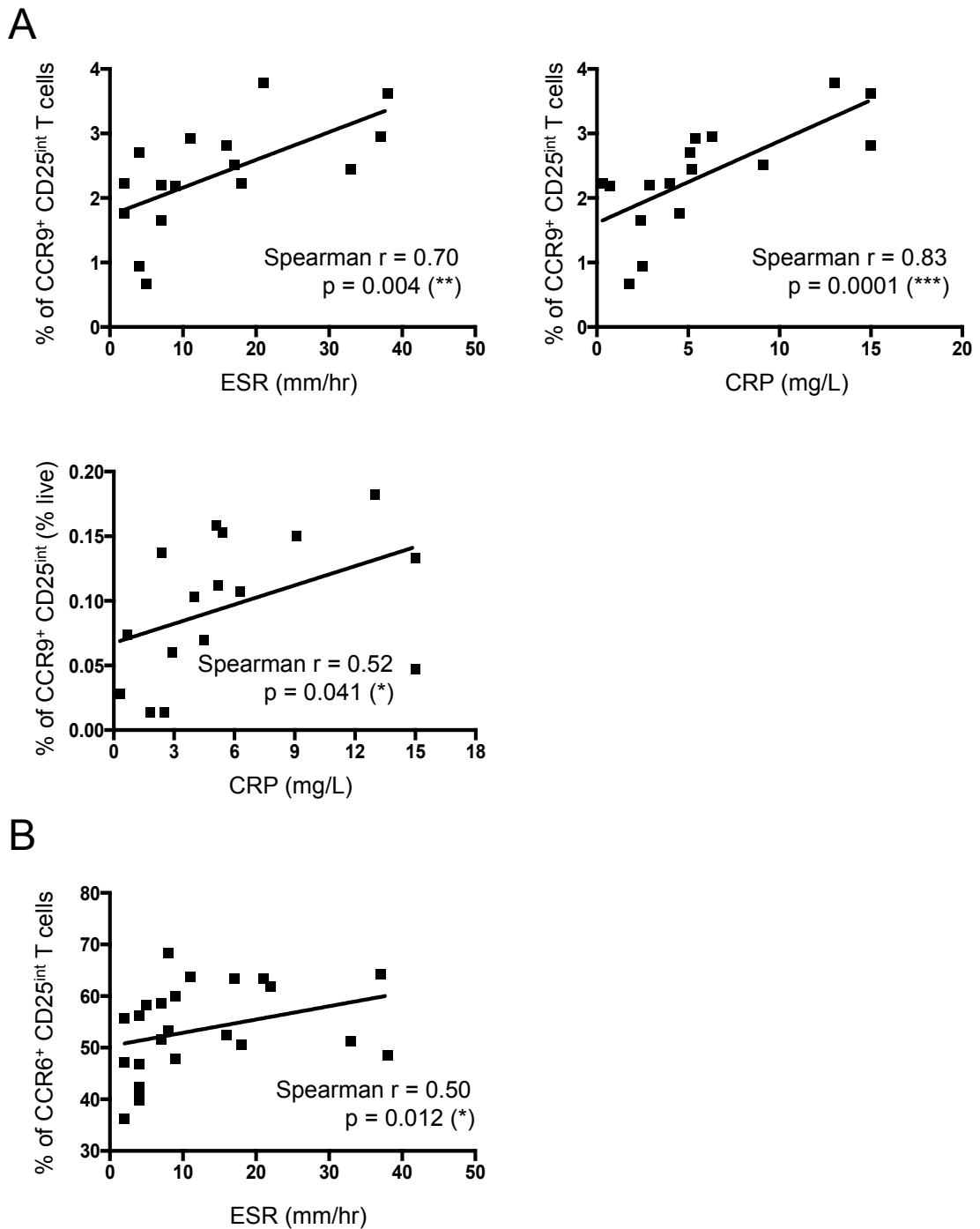


Figure 7.4: Influence of inflammation on activated CD4⁺ T cell chemokine profiles

Elevated levels of inflammation increase proportion of circulating CCR6⁺ and CCR9⁺ activated CD4⁺ T cells. **(A)** Correlation between proportion of circulating CD4⁺ CCR9⁺ CD25^{int} (activated) T cells and ESR (top left) and CRP (top right) as proportion of CD4⁺ T cells and as proportion of live cells (bottom). n = 16 AS patients. **(B)** Assessment of ESR and percentage of circulating activated CD4⁺ CCR6⁺ T cells (CD25^{int}). 22 patients used in analysis. Linear regression and spearman correlation statistical test were performed for every correlation. * = p < 0.05, ** = p < 0.01.

A

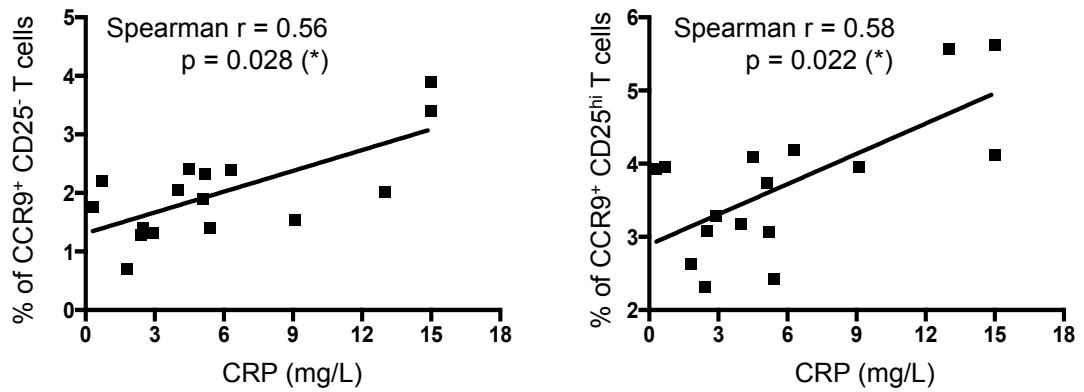


Figure 7.5: CCR9 association with inflammation

Elevated levels of inflammation increase proportion of circulating CCR9⁺ memory and regulatory CD4⁺ T cells. (A) Correlation between proportion of circulating CD4⁺ CCR9⁺ CD25⁻ (memory) T cells and CD4⁺ CCR9⁺ CD25^{hi} (regulatory) T cells CRP (mg/L). n = 16 AS patients. Linear regression and spearman correlation statistical tests were performed for both correlations. * = p < 0.05.

7.6 Disease treatment protocols and plasma cytokines

AS patients were administered a diverse range of therapeutics partially dependent upon their disease activity level, and thus it was investigated if patient therapeutic regimens correlated with the immunological parameters summarised in Table 7.2. Within the patient cohort, six treatment groups were identified: NSAIDs, DMARDs, biologics (anti-TNF α), or combinations of NSAIDs and DMARDs, DMARDs and biologics, and NSAIDs and biologics (Table 7.1). Due to insufficient numbers of samples, the following treatment groups were excluded from these analyses: DMARDs; DMARD and biologics; and NSAIDs and biologics. Consequently, the effect of DMARD treatment on immunological parameters could not be assessed.

HCs, and patients prescribed NSAIDs had significantly fewer circulating CCR4⁺ activated and memory CD4⁺ T cells compared to those receiving biological therapy (Fig. 7.6A). No other alterations to the cellular immune profile of AS patients were associated with disease treatment. As shown in chapter 3, compared to HCs, AS patients had elevated plasma IL-23p19 and TNF α levels (Fig. 3.13D and 3.14A). Accordingly, patients prescribed NSAID therapy had significantly elevated levels of plasma IL-23p19 compared to HCs ($p=0.0183$, Fig. 7.6B). Differences in plasma concentrations of IL-23p19 between HCs and the remaining treatment protocols did not reach significance (Fig. 7.6B). Analysis of plasma TNF α levels revealed that, compared to HCs, patients receiving biological therapy (predominantly adalimumab), had significantly elevated plasma TNF α levels ($p=0.0069$, Fig. 7.6B). No other significant differences were observed. Overall, these results complement our plasma cytokine observations and indicate that different therapeutics, particularly biological therapy, may be associated with specific plasma cytokine profiles and cell populations.

7.7 Influence of extra-articular disease manifestation

Approximately 35% of the patient cohort experienced symptoms of extra-articular disease. In this study, the development of four common comorbidities was recorded: uveitis, psoriasis, IBD, and peripheral arthritis. Due to the small numbers of patients included in each of the individual groups, it was decided to categorise the patients into two groups based on the presence or absence of extra-articular disease. Of the immunological parameters assessed (Table 7.2), only plasma cytokine levels of IL-6 and TNF α , and

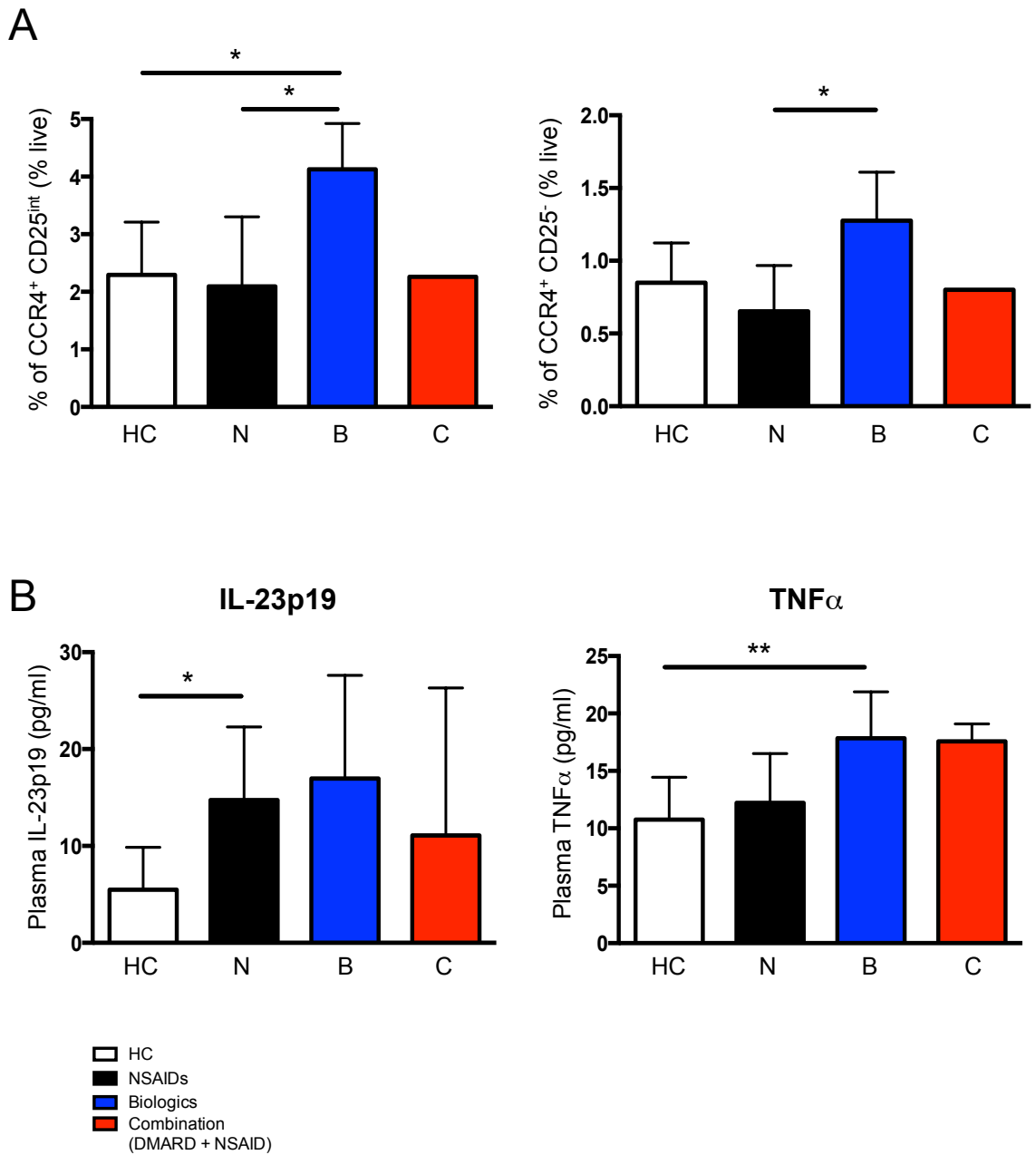


Figure 7.6: Influence of disease treatment strategies on cytokines and chemokines

Patients receiving NSAIDs have higher circulating levels of IL-23p19 compared to HCs. **(A)** Analysis of CCR4⁺ activated (left) and memory (right) T cells, as proportion of live cells, for HCs and AS patients. **(B)** Effect of disease treatment protocols on plasma IL-23p19 (left) and TNF α plasma levels (right). Groups analysed: HCs (HC - empty), NSAIDs (N - black), Biological therapy (B - blue) and combination therapy consisting of DMARDs and NSAIDs (C - red). One-way anova: Kruskal Wallis test with Dunn multiple comparisons performed for statistical analyses. * = $p < 0.05$, ** = $p < 0.01$. 13 HCs, 9 NSAID, 4 biologic and 1 combination treated patients were used for analysis in A. Patient numbers used for IL-23p19 analysis: HC = 17, N = 10, B = 2 and C = 2. Patient numbers used for TNF α analysis: HC: 27, N = 13, B = 4 and C = 2. Mean + SD.

PBMC numbers were significantly associated with the presence or absence of extra-articular disease. Compared to HCs, patients without extra-articular disease had significantly greater numbers of PBMCs/ml of blood (Fig. 7.7A). No difference was observed in PBMCs/ml of blood between HCs and patients with extra-articular disease, and no significant differences were observed between the patient groups. These results support the previous observation that AS patients have a greater number of circulating PBMCs compared to HCs.

Interestingly, patients with extra-articular disease showed significantly elevated plasma IL-6 and TNF α levels compared to HCs (Fig. 7.7B). Both cytokines were previously observed to be upregulated in AS patient plasma (Fig. 4.14A). Additionally, TNF α was significantly elevated in patients without extra-articular disease compared to HCs (Fig. 7.7B). Overall, patients with extra-articular disease showed elevated levels of the inflammatory cytokines IL-6 and TNF α compared to HCs.

7.8 DC related correlations

At the outset of this project, it was hypothesised that CD141⁺ DCs in patients would be altered based on our observations in the HLA-B27 TG SpA rat model (480). Comparisons between HC and AS patient samples disproved this hypothesis, as no differences were seen in the proportions of circulating CD141⁺ DCs. Despite no observed differences in this DC population, some changes were seen in AS patient blood myeloid populations and plasma Flt3L levels, and it was subsequently decided to examine whether these were affected by patient clinical or immunological parameters.

Interestingly, a significantly greater proportion of circulating CD141⁺ DCs, as proportion of total live cells, was observed in older patients (n=31, p=0.022 – Fig. 7.8A). No correlation was detected between age and CD141⁺ DCs within the HC cohort (Fig. 7.8A). These observations indicate that with increasing age, CD141⁺ DCs in AS patients represent a greater proportion of circulating leukocytes. In accordance, despite not reaching significance (p=0.063), a positive correlation was observed in AS patients between disease duration and elevated frequencies of CD141⁺ DCs (Fig. 7.8B). Additionally, the proportion of CD141⁺ DCs among live cells increased with BASDAI scores (Fig. 7.8B). This correlation reached significance (p=0.014). Taken together these results suggest that with long-term disease and increased disease severity, the proportion of circulating CD141⁺ DCs in patients increases.

Given that DCs direct immune response perpetuation through priming of T cells, we set out to identify relationships between specific DC populations and the T cell phenotype profiles observed in AS patients. It was hypothesised that the observed differences in AS patient myeloid populations and T cells would correlate with altered plasma cytokine profiles. However, analyses performed disproved this hypothesis (data not shown) - no significant relationships between these factors were observed. Unexpectedly, a correlation between AS patient CD141⁺ DCs and circulating CCR6⁺ activated T cells was observed, with increased CD141⁺ DCs (% of CD11c⁺ MHC II⁺) associated with an increase in the proportion of activated CCR6 expressing T cells (Fig. 7.8C). This correlation reached significance (p=0.016). Additional analyses of correlations between circulating DCs and age were performed, and they revealed that the proportion of CD1c⁺ DCs in AS patients also increased with age, although no association with disease duration was observed (Fig. 7.9A, data not shown). No significant correlation between age and CD14⁻ CD16⁺ mononuclear cells was observed in AS patients (Fig. 7.9A). In contrast, age was observed to have no effect on HC circulating CD14⁻ CD16⁺ and CD1c⁺ populations (Fig. 7.9B). Overall, changes in the proportion of CD141⁺ DCs appear to correlate with several factors in AS patients including age, disease duration and disease severity.

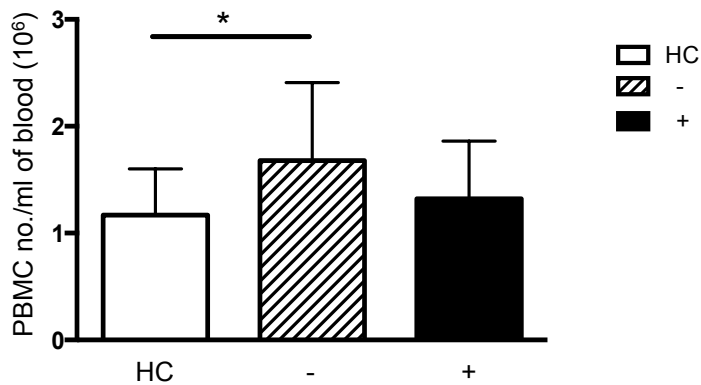
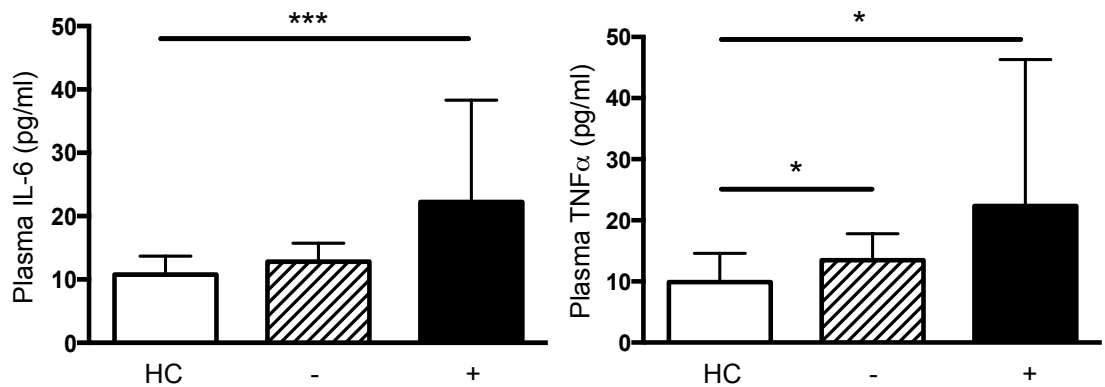
A**B**

Figure 7.7: Influence of extra-articular manifestations on immunological parameters

AS patients who have developed extra-articular manifestations exhibit elevated plasma levels of IL-6 and TNF α . **(A)** Comparison of HCs (empty bars), patients without extra-articular disease (-/hashed bars) and patients with extra-articular manifestations (+/filled bars) were compared regarding total PBMC number/ml of blood. Extra-articular manifestations include: IBD, psoriasis, uveitis and peripheral arthritis. **(B)** Plasma IL-6 (left) and TNF α (right) levels were measured in HCs and AS patients with or without extra-articular disease. One-way anova: Kruskal Wallis test with Dunn multiple comparisons performed for statistical analyses. * = $p < 0.05$, *** = $p < 0.001$. For analysis, 24-33 HCs, 18-20 patients without extra-articular disease and 9-13 patients with extra-articular disease were used. Mean + SD.

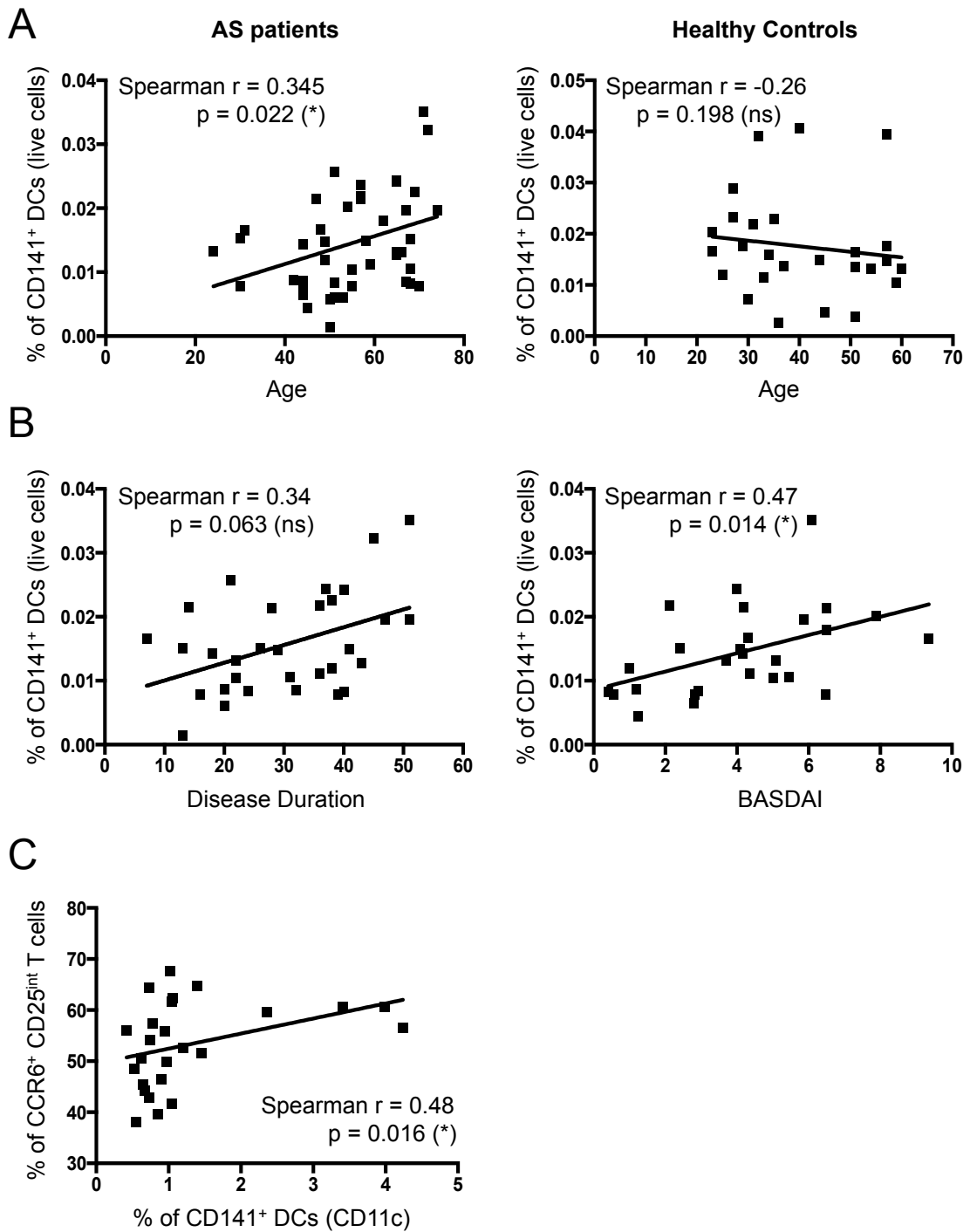
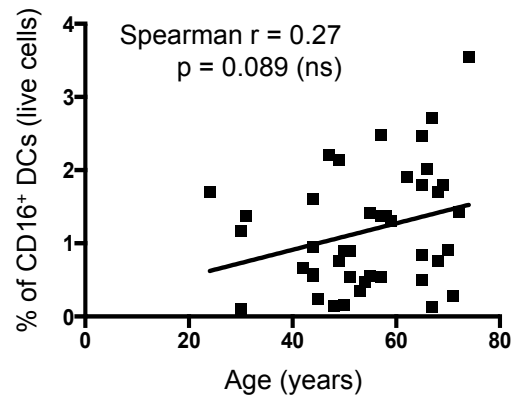
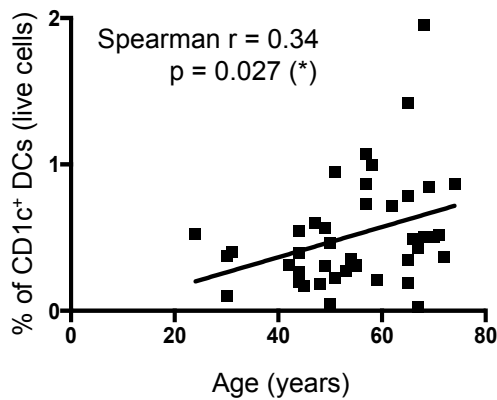


Figure 7.8: Influence of clinical and immunological factors on CD141⁺ DCs

CD141⁺ DCs in AS patients are positively associated with disease severity and age. **(A)** Association between age and circulating CD141⁺ DCs in HCs (left) and AS patients (right). For analysis, 26 HCs and 44 AS patients were used. **(B)** Effect of disease duration (years - left) and BASDAI (right) on proportion of circulating CD141⁺ DCs in AS patients, as proportion of live cells (n = 27-31). **(C)** Association between % of CD141⁺ DCs of total CD11c⁺ MHC II⁺ cells and % of CCR6⁺ activated T cells. 25 patients used for analysis. Linear regression and spearman correlation statistical tests were used to assess significance of correlations. * = $p < 0.05$, ns = not significant.

A AS patients



B Healthy Controls

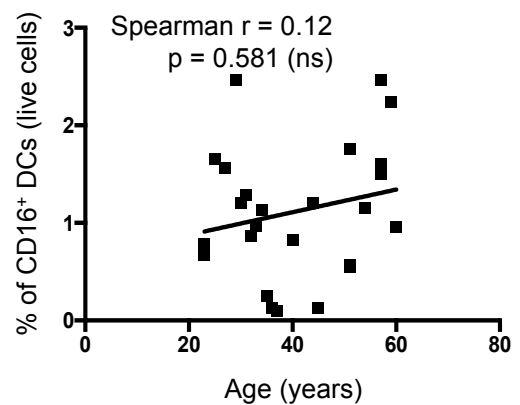
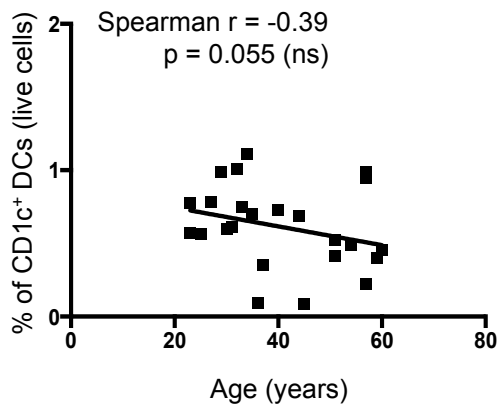


Figure 7.9: Influence of age on DC populations in AS patient and HCs

CD1c⁺ DCs increase with age in AS patients. Correlation between proportion of circulating CD16⁺ mononuclear cells (left) and CD1c⁺ DCs (right) with age (years) in AS patients (**A**) and HCs (**B**). For all analyses, 42 AS patients and 25 HCs were used. Linear regression and spearman correlation statistical test were performed for every correlation. * = $p < 0.05$, ** = $p < 0.01$.

7.9 Discussion

The focus of this PhD project was to understand the role of DCs in AS pathogenesis. With only slight differences noted in the proportions of circulating DC populations between AS patients and HCs, other cell types were also investigated, including T cells and monocytes. Subsequently, differences in the T cell chemokine receptor and plasma cytokine profiles of AS patients were identified. To fully comprehend the relationships between the observed altered immunological profiles and disease development, there is a need to understand how immunological parameters and patient clinical characteristics are related (Table 7.2). Consequently, the impact of several clinical and immunological parameters was assessed on circulating cell populations and plasma cytokine levels in patients.

Comparison of the HC and AS patient cohorts revealed several disparities. Approximately 15 years separated the average ages of the AS patient and HC cohorts and analyses presented here suggest that age influences immunological parameters. Furthermore, there was an unintentional bias towards female and HLA-B27⁺ individuals within the HC cohort. As AS is predominantly associated with a young male population, this HC cohort does not sufficiently replicate this gender bias. Furthermore, the proportion of HLA-B27⁺ HC individuals is five times that of the general Caucasian population (508). The institutional ethics required HCs to be recruited from within the Institute of Infection, Immunity and Inflammation at the University of Glasgow. This resulted in a limited pool of eligible candidates. Consequently differences in age, gender and HLA-B27 expression should be considered when directly comparing HC and AS patient cohorts.

Most patients were treated with NSAIDs. Only 8% of patients received biologics, predominantly anti-TNF α . Compared to HCs, patients receiving biological therapeutics had elevated levels of plasma TNF α (Fig. 7.6B). This observation could suggest that TNF α , a marker of inflammation, could be used to assess progression between treatment regimens. Following etanercept treatment in AS patients, *ex vivo* stimulated cells have been shown to be capable of enhanced TNF α secretion (562, 680). Longitudinal studies could be performed to assess patient immunological responses to different treatment strategies, including naïve patients who have not yet experienced therapeutic benefit. Unfortunately, no treatment-naïve patients were recruited during this study. Information regarding medication prescribed to HCs was not recorded, and thus due to the prevalence of NSAIDs it is possible that HCs at time of recruitment were actively self-administering

NSAIDs. It would therefore be useful to record such details for HCs recruited to future studies to further elucidate the effect of NSAIDs.

Disease severity, determined by degree of joint pain, stiffness and fatigue might be influenced by numerous factors including current therapeutics and development of extra-articular manifestations. Patients with higher levels of disease severity tended to have a greater proportion of circulating activated T cells, with fewer expressing CCR4 (Fig. 7.2A). The chemokine receptor profile of these circulating T cells was additionally altered in AS patients in terms of CCR6 and CXCR3. Blood CCR6⁺ regulatory (Fig. 7.2B) and CXCR3⁺ activated CD4⁺ T cells (Fig. 7.2C) were observed to increase with disease score. CD4⁺ T cells are thought to contribute to human pathogenesis and are essential for disease development in HLA-B27 TG rats (181, 470, 471, 495, 530). A greater proportion of circulating activated T cells may indicate enhanced clonal expansion, and these activated T cells propagate immune responses and therefore potentially contribute to disease pathogenesis. These observations could indicate that T cell migration patterns change during disease. Alternatively, given that chemokine receptors are associated with specific T cell phenotypes, CCR6 with Th17, CCR4 with Th2, and CXCR3 with Th1, these results may imply skewing of the CD4⁺ T cell response during disease development. These associations imply that Th1 effector cells and CCR6⁺ Tregs may contribute to disease progression and pathogenesis. These results are consistent with previous publications regarding the involvement of Th1 cells in disease development (526, 527, 532). However, as only 14 patients were included in this analysis, it will be important to corroborate these results using a larger cohort. That being said, the correlation between increased disease severity and proportions of CCR6⁺ regulatory T cells was observed using both BASMI and BASFI assessments (Fig. 7.2B), adding credence to this particular observation. Overall, these results suggest that CCR6, CCR4 and CXCR3 expressing CD4⁺ T cells may be contributing to AS pathogenesis.

The idea that T cell migration changes in AS is supported by the observation presented in chapter 5 that AS SF-resident T cells predominantly express CCR4 and CCR6 (Fig. 5.6B). Thus, enhanced migration of activated CCR4⁺ T cells to tissues including SF and skin, could account for the observed decrease in the proportion of circulating CCR4⁺ cells. The opposite appears to be true for CCR6 expressing cells; elevated BASMI and BASFI scores were associated with a greater proportion of circulating CCR6⁺ regulatory T cells. Changes to the systemic inflammatory environment and location of T cell priming associated with increased disease severity may affect the chemokine receptor profile of circulating T cell

populations. CCR4 mediates skin migration of infiltrating leukocytes, whilst CXCR3 aids leukocyte entry into inflamed tissues (173, 175, 182, 183, 614, 627).

CCR6 is involved in directing migration of lymphocytes to the intestine. It is expressed on Th17 cells, with the largest population of tissue resident Th17 cells in mice located within the intestine (681, 682). Additionally, resident Th17 populations have been identified in human intestinal tissue (683). However, Th17 cells have not been demonstrated to play a role in AS intestinal pathogenesis, and indeed Ciccia et al found IL-17 not to be associated with subclinical intestinal inflammation in AS patients (551). Nevertheless, the increase in CCR6 expression among CD4⁺ T cells may implicate the intestine in AS pathogenesis. To assess this proposal, investigation of intestinal homing markers not analysed in this study, including $\alpha 4\beta 7$, would be important. Furthermore, it would be interesting to categorise patients based on their specific extra-articular disease manifestations, enabling identification of the origins of T cell priming associated with specific disease phenotypes.

As described previously, elevated IL-23p19 levels in AS patient plasma were observed compared to HCs (Fig. 4.13D). The recent literature suggests a high association between AS, Th17 cells and the IL-23R (39, 181, 495, 538, 684). It was therefore interesting that patients with higher BASDAI and BASMI scores generally had low levels of plasma IL-23 (Fig. 7.3A), suggesting a degree of IL-23-mediated protection, despite the requirement for IL-23 in the maintenance of Th17 cells (112), believed to be pathogenic in AS. Surprisingly, AS patients with highest systemic levels of IL-23p19 had low levels of circulating CCR6⁺ regulatory T cells (Fig. 7.3B). These correlative data suggest that the protection afforded by IL-23 is not mediated through induction/function of CCR6⁺ Tregs. Although, inflamed patients exhibited a higher proportion of circulating CCR6⁺ activated T cells (Fig. 7.4B), insinuating their involvement in the perpetuation of systemic inflammation in AS patients.

Several experimental considerations need to be taken into account when determining the role of IL-23 in disease development: levels of detectable IL-23p19 in AS patient and HC plasma were very low (<30pg/ml) and may be below level of accurate detection (Fig. 4.13D), and only 10 patients were available for analysis (Fig. 7.3). Therefore it will be important to further assess the influence of disease severity and inflammation on plasma IL-23p19 and CCR6⁺ CD4⁺ T cells using a larger patient cohort. However these correlations allow us to draw several conclusions: IL-23 may in fact be protective through inhibition of disease progression; IL-23 in AS may not function to maintain Th17 cells *in*

vivo; and inflammation in AS patients may be perpetuated by CCR6⁺ activated T cells or may be driven from mucosa-associated tissues.

While the aetiology of AS remains unclear, there are clear associations between the intestinal environment and the development of disease. HLA-B27 TG rats raised in germ-free conditions do not develop SpA-like symptoms (444). There is also a strong association between IBD and AS (4, 13). Correlative analyses between clinical and immunological parameters have provided support for this hypothesis. For instance, it was observed that elevated frequencies of circulating CCR9⁺ cells were associated with increased ESR and CRP levels (Fig. 7.4A). This observation held true for circulating activated, memory and regulatory CCR9⁺ CD4⁺ T cell populations (Fig. 7.4 and 7.5). These correlations strongly suggest an association between inflammation and circulating CCR9⁺ CD4⁺ T cell populations. Activation of T cells by intestinal DCs preferentially induces CCR9, important for intestinal homing of activated T cells (171). The association between CCR9 and markers of inflammation indicate that systemic inflammation may be initiated from the intestine. It would therefore be interesting to group patients depending on their extra-articular disease symptoms and assess their chemokine receptor expression profiles. These analyses would determine whether CCR9 involvement was specific to AS IBD sufferers or involved in systemic AS disease pathogenesis. The cohort here did permit categorisation of patients based on the presence or absence of extra-articular involvement. No AS patients with IBD were included in the correlative analyses relating CCR9, ESR and CRP, suggesting that the association between CCR9 and inflammation may not be specific to AS IBD sufferers, and therefore may be characteristic of the general AS population. Furthermore, analyses of gut-resident immune populations, specifically DCs and T cells may elucidate the role and function of these intestinal populations in driving systemic disease. It may therefore be of interest to investigate circulating CCR9⁺ populations to elucidate any potential role for the intestine in disease initiation and development.

These observations, and published studies, suggest that ESR and CRP do not correlate with disease activity in AS patients (685, 686). Therefore it is perhaps unjust to directly compare disease activity with levels of systemic inflammation with relation to immunological parameters. Biological molecules including cytokines and growth factors may be more representative of disease severity. IL-6 is an attractive candidate for such a biological disease marker, with lower plasma IL-6 levels correlating with reduced disease score in AS (525, 561, 687). However, no correlations were detected between ESR, disease severity and IL-6 in this study.

Immunological correlations associated with different treatment regimens may identify the modes of action of current therapeutics, or the immunological processes involved in disease activity. Dombrecht et al observed reduced circulating activated CD4⁺ T cells following anti-TNF α treatment (622). However, no correlations between treatment regimens and T cell proportional parameters were detected. Despite the fact that no difference was observed between AS patients and HCs in the circulating CCR4⁺ T cells subsets (Fig. 4.7), anti-TNF α treated patients had a significantly higher proportion of CCR4⁺ activated and memory CD4⁺ T cells compared to HCs and NSAID treated patients (Fig. 7.6A). The increase in CCR4⁺ activated and memory T cells in anti-TNF α treated patients could reflect a change in the cytokine milieu, thereby promoting a shift in the balance towards the CCR4 associated Th2 phenotype. However, no elevated levels of IL-4 and IL-5 were detected to support this idea (Fig. 4.13C). In fact, no significant reductions in plasma cytokines were observed following anti-TNF α therapy. These results suggest that biological therapy (anti-TNF α) may increase circulating CCR4⁺ T cell populations, although further investigation is required given that a maximum of 4 patients were included in the biological group. To fully address the mode of action for these varied regimens, comparison with naïve patients would be beneficial.

As previously discussed, categorisation of patients according to extra-articular disease status may illuminate pathogenic processes. The cohort contained only 50 AS patients, preventing comprehensive analyses of individual extra-articular disease manifestations. It was possible, however, to analyse patient groups defined by the presence or absence of extra-articular symptoms. Interestingly, plasma IL-6 and TNF α levels were elevated in patients with extra-articular disease (Fig. 7.7B). These results indicate that patients with extra-articular disease have a higher degree of systemic inflammation than HCs and AS patients with only spinal disease. Conversely, patients without extra-articular involvement had more PBMCs per ml of blood compared to HCs (Fig. 7.7A). These results suggest that the immunological profiles of patients with and without extra-articular disease may be different.

As described above, the initial hypothesis was developed from the observation that the rat DC analogue of the human CD141⁺ DC population was absent from HLA-B27 TG animals (480). However, no difference in the proportion of circulating CD141⁺ DCs was observed in AS patients compared to HCs (Fig. 3.4A). However, direct comparisons between human blood and rat intestinal findings may be inappropriate given the differences in cell origin and function between human blood DCs and their counterparts in rat tissues. Therefore, in

future, the aim is to examine CD141⁺ DCs in patient intestinal tissue. In the correlative analysis, several CD141⁺ DC associated observations were identified. Interestingly, AS patients have a higher proportion of CD141⁺ and CD1c⁺ DCs as they age (Fig. 7.8A and 7.9A). Similar correlations in HCs were not observed (Fig. 7.8A and 7.9B). Additionally, elevated disease scores (BASDAI) were associated with higher proportions of circulating CD141⁺ DCs (Fig. 7.8B). Taken together, these results suggest that the proportion of CD141⁺ DCs increases with disease progression. Recent evidence suggests that CD141⁺ DCs in the skin may be tolerogenic, secreting IL-10 and inducing Tregs (332). CD141⁺ DCs may therefore increase in AS patients as disease progresses to control pathogenic T cell responses. Alternatively, AS CD141⁺ DCs may promote disease activity. It should be noted however that correlations between inflammation, Flt3L concentrations and CD141⁺ DCs were not observed (data not shown). In future, functional investigations of this subset in HCs and AS patients may be fundamental to understanding disease pathogenesis.

To address the biological consequence of CD141⁺ DCs in disease pathogenesis, correlations between immunological parameters and CD141⁺ DCs were examined. Interestingly, an increase in CD141⁺ DCs was associated with a higher proportion of circulating CCR6⁺ activated CD4⁺ T cells (Fig. 7.8C). This observation might indicate that CD141⁺ promote CCR6⁺ T cell responses. As IL-17-secreting Th17 cells predominantly express CCR6 (Fig. 4.10D), CD141⁺ DCs in AS patients could promote disease development through this pathogenic subset. However, AS patient blood CD141⁺ DCs did not differ in their ability to induce T cell proliferation or CCR6 compared to HCs (Fig. 6.2C and 6.5A). To establish if a direct relationship exists between CCR6⁺ activated T cells and CD141⁺ DCs, DCs isolated from peripheral/extra-articular tissue should be assessed for their ability to induce T cell proliferation and chemokine receptor induction.

In conclusion, several correlations between clinical parameters and the immunological profile of AS patients have been identified. Of note, elevated inflammatory markers were associated with greater proportions of circulating CCR9⁺ activated T cells suggesting intestinal involvement in inflammatory processes. Th17 cells may be involved in disease perpetuation; elevated proportions of CCR6⁺ regulatory cells correlate with disease severity. However the role of plasma IL-23p19 appears to be more complicated than was initially imagined. Interestingly, the proportion of AS patient CD141⁺ DCs increased with age, disease duration and disease severity suggesting CD141⁺ DC involvement in late stage disease. It is therefore important to establish the function of this population in AS.

Following observations that intestinal migrating DC populations were altered in SpA rats, and the strong association between CCR9 expression and intestinal inflammation in AS patients, I set out to establish techniques to isolate and functionally analyse DC and T cell subsets from human intestinal specimens. Following optimisation of these protocols, the aim is to apply these techniques to intestinal biopsy samples from AS patients, in order to better understand the connections between the intestine and disease development.

Chapter 8: Intestinal Phagocytes

8.1 Introduction

Diseases belonging to the SpA family, including AS, PsA and ReA (688) share many genetic and pathophysiological factors. AS, like other SpA family members, is often associated with development of extra-articular clinical manifestations including uveitis, psoriasis, arthritis and IBD (4, 619, 620, 688). The link between AS and intestinal pathology is particularly strong. For instance, it has been shown that approximately 50% of Crohn's patients expressing HLA-B27 eventually develop AS (4, 440). In addition, approximately 50% of AS patients not clinically diagnosed with CD have subclinical intestinal inflammation, detectable at colonoscopy (4, 13, 441). These studies suggest a connection between the intestine and AS pathogenesis, and are supported by experiments using HLA-B27 TG animals where germ-free animals fail to develop SpA symptoms (444). In addition, the Milling lab has previously shown that HLA-B27 TG rats lack a subset of 'tolerogenic' CD11b^{int} CD103⁺ CD172a^{lo} intestinal DCs and that this absence correlated with exaggerated Th17 type responses (480). Therefore, understanding the link between intestinal inflammation and AS may provide information that will facilitate the generation of effective, targeted therapies.

DCs are the bridge between innate and adaptive immunity, and are directly responsible for inducing tolerance towards self-antigens and commensal bacteria, whilst directing robust protective immunity against harmful pathogens. When these processes become dysregulated in genetically susceptible individuals, aberrant responses directed against commensal bacteria may develop, resulting in the development of IBD including CD and UC (689). Previous studies have implicated mononuclear phagocytes (MP) with altered behaviour in the development of IBD (225, 425, 690-693). Specifically, these studies have identified altered activation status, TLR expression, cytokine secretion, NOD2 polymorphisms and NFκB dysregulation of MP of IBD patients (225, 234, 403, 404, 427, 692, 694-697). However it should be noted that many of these studies simply used co-expression of CD11c and MHC II to identify intestinal DCs, an approach now considered insufficient for distinguishing between different MP populations in most non-lymphoid tissues (225, 234). This is due to the realisation that many surface markers regarded as 'DC-specific', such as CD11c and MHC II, are in fact expressed by multiple cell types including tissue macrophages. For example, although 'pro-inflammatory' MHC II⁺ CD172a⁺ "DCs" have been suggested to accumulate in the colonic mucosa of Crohn's patients (698), macrophages were not excluded from these analyses and thus it remains unclear whether these truly represent bona fide DC. In contrast to IBD where intestinal

‘DCs’ have been studied, intestinal DCs in AS patients have not been investigated. This is somewhat surprising given the strong association between intestinal inflammation and AS.

Recent data indicate that the addition of antibodies specific for CD64 enable rigorous discrimination of tissue macrophages from DCs in both mouse and man (225, 234). However, to the best of my knowledge, this method of discrimination and DC identification has not yet been applied to the setting of human IBD. Therefore we aimed to apply this identification strategy in an attempt to understand more fully the role of intestinal DCs in AS development. Specifically, our objective was to identify any phenotypic and/or functional differences in DC subsets isolated from AS patient intestinal tissue, or alterations in their abundance compared to those in HCs. Unfortunately, during the course of my PhD I did not receive any intestinal samples from HLA-B27⁺ or HLA-B27⁻ AS patients. However with the tissue samples we did receive, I developed methods to characterise intestinal cDC, macrophage and T cell populations from HCs and IBD patients. I developed efficient purification techniques and performed precise phenotypic analyses. These will be applied to AS patient intestinal samples in the future, with the aim of understanding the link between intestinal inflammation and AS pathogenesis.

8.2 Patient characteristics

Intestinal tissue samples were provided by and collected from the Biorepository NHSGGC at the Southern General Hospital. All tissue samples were processed within 3 hours following surgery. Several patient characteristics were provided for every fresh tissue sample and are detailed in Table 8.1.

Table 8.1: Patient characteristics for intestinal tissue specimens

In total, 15 intestinal tissue samples were processed for analysis. Surgical resections included specimens of colonic and small intestinal tissue. Health status refers to whether the processed tissue specimen was healthy (normal) or diseased. Diseased tissue was isolated from patients suffering from CD or UC.

Tissue Type	Health Status	Sample No.	Sex (M/F)	Average age (yrs)
Colon	Normal	9	5/4	65.1
	Diseased	4	2/2	35.5
Small Intestine	Normal	2	0/2	60.5
	Diseased	0	N/A	N/A

The majority of samples processed were colonic surgical resections from male HCs undergoing surgery to remove tumour tissue. The average age for HC tissue collection was >60yrs for both tissue types. Diseased patients tended to be younger with an average age of 35.5yrs. Three of the four diseased colonic tissue samples were isolated from UC patients and the remaining patient suffered from CD. Approximately 80% of HC individuals were suffering from intestinal adenocarcinoma. Unfortunately, we did not receive any inflamed SI samples, meaning that I could not carry out a direct comparison of the inflammatory infiltrate present in the small intestinal lamina propria (SILP) versus the colon. In the end, the majority of tissue samples were utilised for the optimisation of tissue digestion protocols in order to achieve high cell yields and viability, and to avoid enzymatic cleavage of specific surface markers.

8.3 Isolation of intestinal phagocytes

Published protocols to isolate mononuclear populations from human intestinal tissue vary greatly. Several groups use “walk-out” assays, where migratory cells leave intact intestinal tissue following overnight culture at 37°C (405, 699, 700). However, the majority of investigators enzymatically digest tissue to isolate specific populations, although the enzyme cocktails used differ dramatically (225, 427, 690). Within our department, the laboratory group led by Professor Allan Mowat have developed and refined protocols for the enzymatic digestion of intestinal tissues in mice. Therefore, we initially assessed the suitability of these protocols for the isolation of DCs and macrophages from human intestinal samples. To begin with, we used a combination of collagenase V (0.85mg/ml), collagenase D (1.25mg/ml), dispase (1mg/ml) and DNase (0.03mg/ml), which is used routinely by the Mowat laboratory to isolate murine colonic leukocytes. Following epithelial layer removal, tissue was digested until completely disintegrated. Remaining cells were subsequently analysed using flow cytometry to identify cDC subsets. To identify intestinal (colonic) cDCs, a gating strategy similar to that for blood DC characterisation was adopted (Fig. 8.1A). Firstly, cell debris and aggregates were gated out using their FSC and SSC properties (Fig. 8.1A). Intestinal leukocytes were then identified amongst live colonic isolates by their expression of the common leukocyte antigen, CD45 (Fig. 8.1A). T- and B-lymphocytes, as well as neutrophils and NK cells were gated out by selecting leukocytes lacking the lineage (LIN) markers CD3, CD15, CD19 and CD56 (Fig. 8.1A). LIN⁻ cells were further assessed for the expression of CD14, and CD14⁺ cells were excluded from cDC analysis as CD14 has been shown to identify cells of the monocyte/macrophage lineage (225, 425, 427, 691). Following exclusion of CD14⁺ cells,

live CD45⁺ LIN⁻ CD14⁻ cells were analysed for co-expression of CD11c and MHC II (Fig. 8.1B). This revealed a distinct population of CD11c⁺ MHC II⁺ cells in which DC subsets could be identified on the basis of CD141 and CD1c expression (Fig. 8.1B and 8.1C).

Because tissue samples were routinely delivered late in the afternoon, we wanted to assess the feasibility of storing the tissue overnight and performing the isolation and analysis the following day. We therefore stored whole tissue overnight at 4°C, digested the following day and assessed the viability of the LP isolates retrieved (Fig. 8.1C). Although the viability of isolated cells after overnight storage was satisfactory, CD141⁺ DCs could not be detected (data not shown). Therefore, in all subsequent analyses we performed digestion of intestinal tissue immediately upon collection.

However it became apparent that several markers used in blood cDC and monocyte analysis were not expressed on cells isolated from intestinal tissue using the protocol (digest A) described above. For example, expression of CX3CR1 by intestinal macrophages (7AAD⁻ CD45⁺ LIN⁻ MHC II⁺ CD14⁺) isolated from the duodenum of a HC was surprisingly low given that these cells have been reported to express high levels of this chemokine receptor (Fig. 8.2A) (427, 701). In addition, CD16⁺ cells could not be detected within the 7AAD⁻ CD45⁺ LIN⁻ CD14⁻ CD11c⁺ MHC II⁺ population, but were abundant in the same population in blood (Fig. 8.2B). However, it should be noted that despite their absence amongst CD11c⁺ MHC II⁺ DCs, CD16⁺ cells could be detected amongst total leukocytes (Fig. 8.2C and 3.1A). Indeed, healthy duodenal tissue appeared to contain CD45⁺ LIN⁺ CD16⁺ and CD45⁺ LIN⁻ CD16⁺ cell populations, when compared with a CD16 FMO (Fig. 8.2C). To determine whether the absence of specific markers was the result of enzymatic cleavage, expression of CX3CR1 and CD16 by freshly isolated PBMCs was compared with PBMCs that had been incubated for 45 minutes in the presence of the digestive enzymes (Fig. 8.2D and 8.2E). In contrast to freshly isolated PBMCs, CX3CR1 expression on DAPI⁻ LIN⁻ CD14⁺ cells was absent on PBMCs following enzymatic digestion (Fig. 8.2D). Within circulating DAPI⁻ LIN⁻ CD14⁻ CD11c⁺ MHC II⁺ cells, CD14⁻ CD16⁺ mononuclear cells could be detected. However following enzymatic digestion, expression of CD16 on this population was degraded (Fig. 8.2E). We concluded that the enzymatic cocktail (digest A) including collagenase V, collagenase D, dispase and DNase caused loss of CD16 and CX3CR1 from the surface of cell populations.

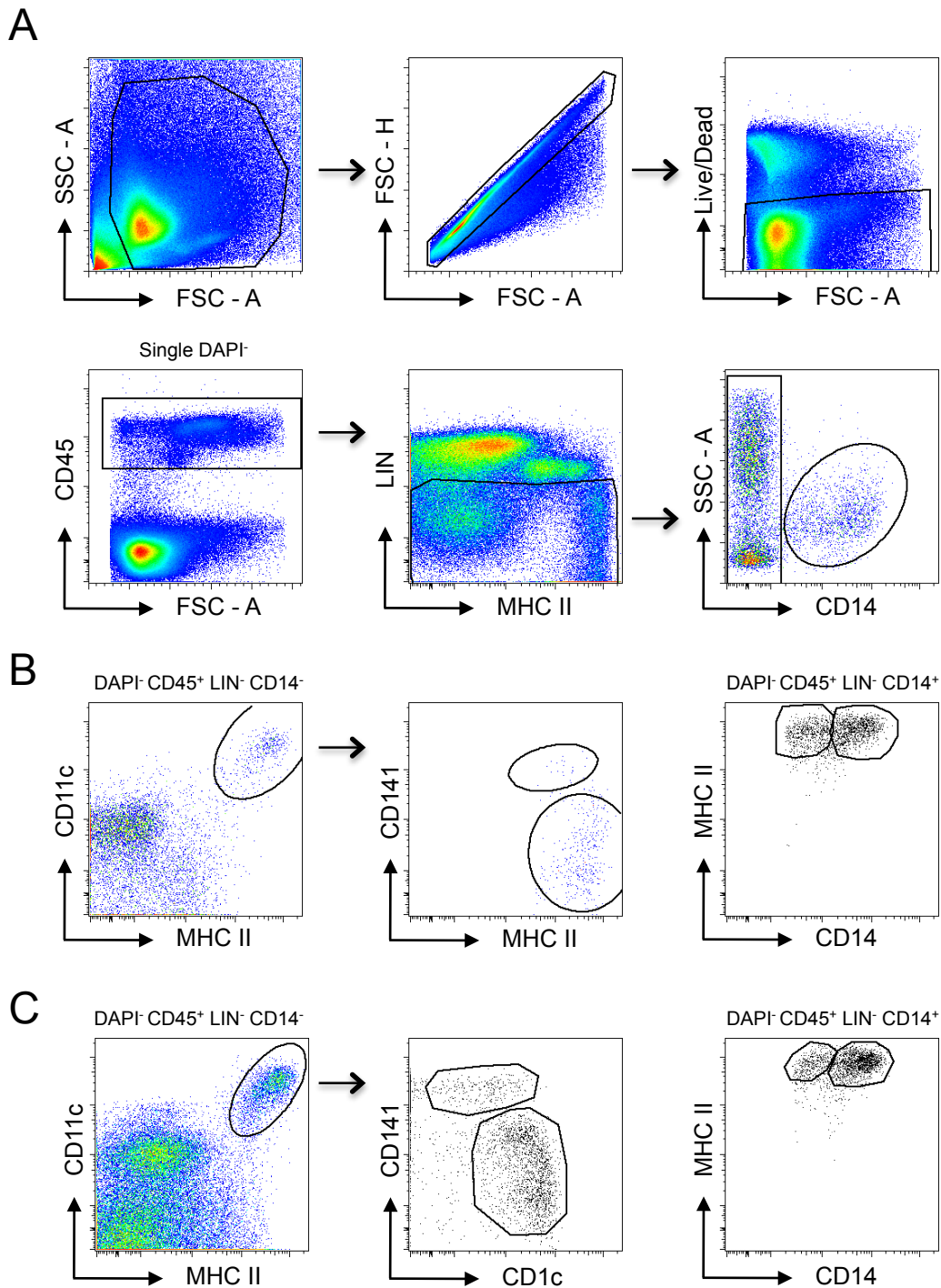


Figure 8.1: Initial gating strategy for identification of intestinal phagocyte subsets

Isolation of intestinal phagocytic subsets from HCs using digest A. **(A)** Colonic tissue was digested using digest A: Collagenase V (0.85mg/ml), Collagenase D (1.25mg/ml), Dispase (1mg/ml) and DNase (0.03mg/ml). Gating strategy to identify intestinal phagocytes: - After gating out cell debris, single cells were selected by their FSC-A vs FSC-H profile and dead cells were excluded with live CD45⁺ cells used for further analysis. Lineage⁺ (CD3, CD15, CD19 and CD56) cells were excluded. LIN⁻ cells were subdivided on CD14 expression. cDC and macrophage subsets were identified in colonic tissue processed immediately **(B)** or 24 hours later **(C)**. DAPI⁻ CD45⁺ LIN⁻ CD14⁻ CD11c⁺ MHC II⁺ cells contained CD141⁺ and CD1c⁺ subsets. DAPI⁻ CD45⁺ LIN⁻ CD14⁺ CD11c⁺ MHC II⁺ cells are intestinal macrophages, subdivided into CD14^{lo} and CD14^{hi} populations.

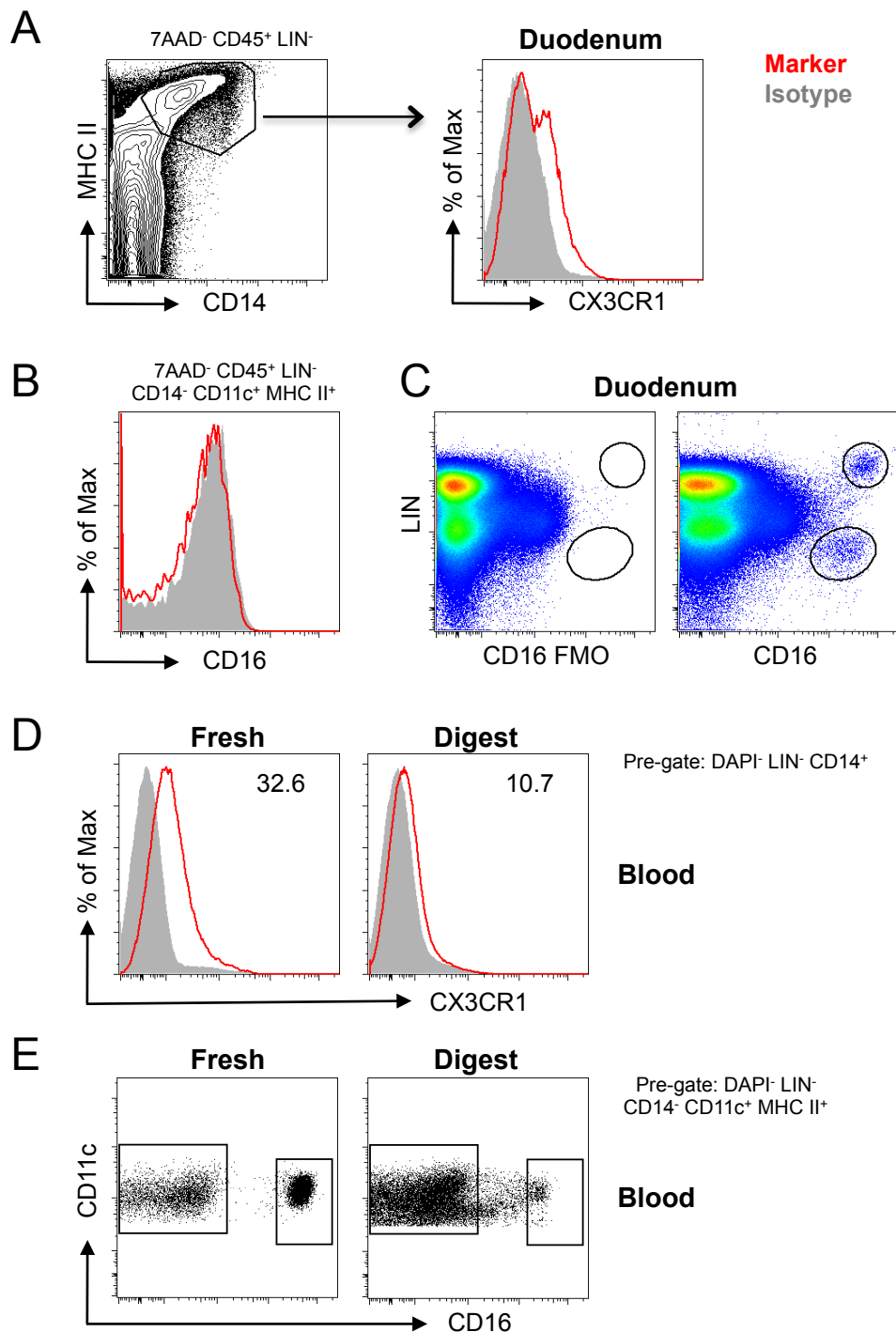


Figure 8.2: Cleavage of CX3CR1 and CD16 by enzymatic digestion

CX3CR1 and CD16 markers were cleaved following enzymatic digestion with digest A: collagenase V (0.85mg/ml), collagenase D (1.25mg/ml), dispase (1mg/ml) and DNase (0.03mg/ml). (A) CX3CR1 expression on live CD45⁺ LIN⁻ MHC II⁺ CD14⁺ cells isolated from duodenal tissue. Isotype (filled histograms), markers (red). (B) CD16 expression on total HC duodenal DCs (Live CD45⁺ LIN⁻ CD14⁻ CD11c⁺ MHC II⁺). (C) Total 7AAD⁻ CD45⁺ cells were subdivided on LIN and CD16 expression (right). CD16⁺ populations were identified based on the CD16 FMO. (D) Expression of surface CX3CR1 on PBMCs freshly isolated (left) or following enzymatic digestion (right). Live (DAPI⁻ LIN⁻ CD14⁺ cells were used for analysis (E) CD16 expression on DAPI⁻ LIN⁻ CD14⁻ CD11c⁺ MHC II⁺ cells freshly isolated (left) or after enzymatic digestion (right).

These results prompted us to adapt the original enzymatic digestion protocol. We next set out to test the suitability of two other enzyme cocktails: collagenase D together with DNase (digest 1), and liberase plus DNase (digest 2 - Fig. 8.3). We incubated PBMCs with each enzyme mix and then assessed CX3CR1 expression. Unlike in previous experiments, CX3CR1 on total live cells was expressed at similar levels under all conditions (Fig. 8.3A). Furthermore, all subsets of DCs (CD141⁺ cDCs and CD1c⁺ cDCs), as well as CD14⁻ CD16⁺ mononuclear cells could be identified amongst total live LIN⁻ CD14⁻ CD11c⁺ MHC II⁺ cells (Fig. 8.3B). It should be noted however that marginal CD16 cleavage was apparent following enzymatic digestion (digests 1 and 2 - Fig. 8.3B). To further assess cleavage of CD16, total 7AAD⁻ cells were analysed for expression of the monocyte markers CD14 and CD16 (Fig. 8.3C). CD14⁺ CD16⁻ and CD14⁺ CD16⁺ monocyte populations were present under all conditions. However, a small population expressing highest levels of CD16 could not be detected following digestion with liberase and DNase (digest 2 - Fig. 8.3C). This observation was further confirmed when analysing total live cells for expression of CD16 and CD11c (Fig. 8.3D). Based on these results, we decided to test whether the digest 1 enzyme cocktail (collagenase D (1mg/ml) and DNase (0.03mg/ml)) was sufficient for digesting colonic tissue. Unfortunately, this enzyme cocktail failed to efficiently digest tissue. Therefore, in a final attempt to find a suitable enzyme cocktail, collagenase D and DNase was supplemented with collagenase VIII (1mg/ml) and dispase (1mg/ml - referred to as digest B). This new enzyme cocktail efficiently digested intestinal tissue and CD16 expression did not fall following digestion, compared to the initial enzyme digest formula (digest A - Fig. 8.4A). For example, 0.988% of live CD45⁺ cells expressed CD16 and LIN (digest B), compared to just 0.0763% using the initial protocol (digest A). Using this optimised enzyme combination, we set out to ascertain the presence of CD14⁻ CD16⁺ mononuclear cells within extra-articular tissues, given the dubiety regarding their classification and function as previously described (Chapter 3). Very few LIN⁻ CD16⁺ cells were observed within healthy colonic tissue (0.026%), leading us to conclude that CD11c⁺ MHC II⁺ CD14⁻ CD16⁺ mononuclear cells were largely absent from intestinal tissue (Fig. 8.4A). Unfortunately, CX3CR1 expression on cDCs, as well as CD14⁺ MHC II⁺ cells, did not differ between the two digestion protocols (Fig. 8.4B). Therefore, we cannot exclude the possibility that our adapted enzyme protocol (digest B) cleaves CX3CR1 from the cell surface. In addition to CD16 and CX3CR1 expression, we analysed expression of CD64 and CD11c on total cDCs and CD14⁺ MHC II⁺ macrophages (Fig. 8.4C and 8.4D). Expression of CD64 (Fig. 8.4C) and CD11c (Fig. 8.4D) did not differ between digestion protocols. All populations expressed relatively high levels of CD64 (Fig. 8.4C) and CD11c (Fig. 8.4D). Based on our findings,

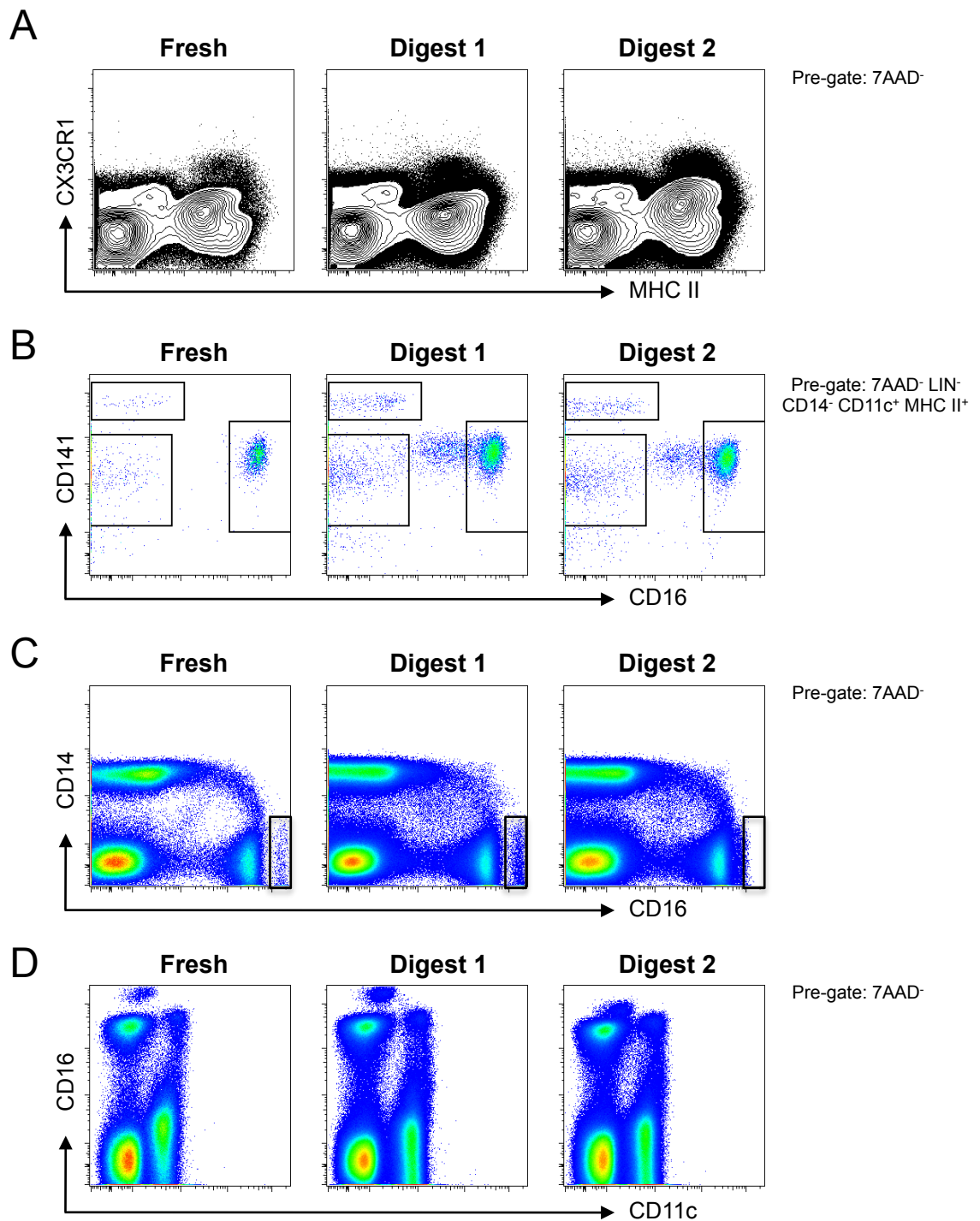


Figure 8.3: Marker expression is dependent on enzymatic digestion conditions

Freshly isolated PBMCs or PBMCs digested with digest 1 (collagenase D (1mg/ml) and DNase (0.03mg/ml, centre)) or digest 2 (liberase (0.4WU/ml) and DNase (0.03mg/ml, right)) were examined for CX3CR1 and CD16 expression. **(A)** Total live (7AAD⁻) cells were analysed for CX3CR1 and MHC II expression. **(B)** Blood DCs (7AAD⁻ LIN⁻ CD14⁻ CD11c⁺ MHC II⁺) were divided based on CD141 and CD16 expression. **(C)** Live (7AAD⁻) cells were assessed for CD14 and CD16 expression to identify monocyte subsets. **(D)** Total live cells were analysed for CD16 and CD11c expression to identify PBMC CD16⁺ subsets.

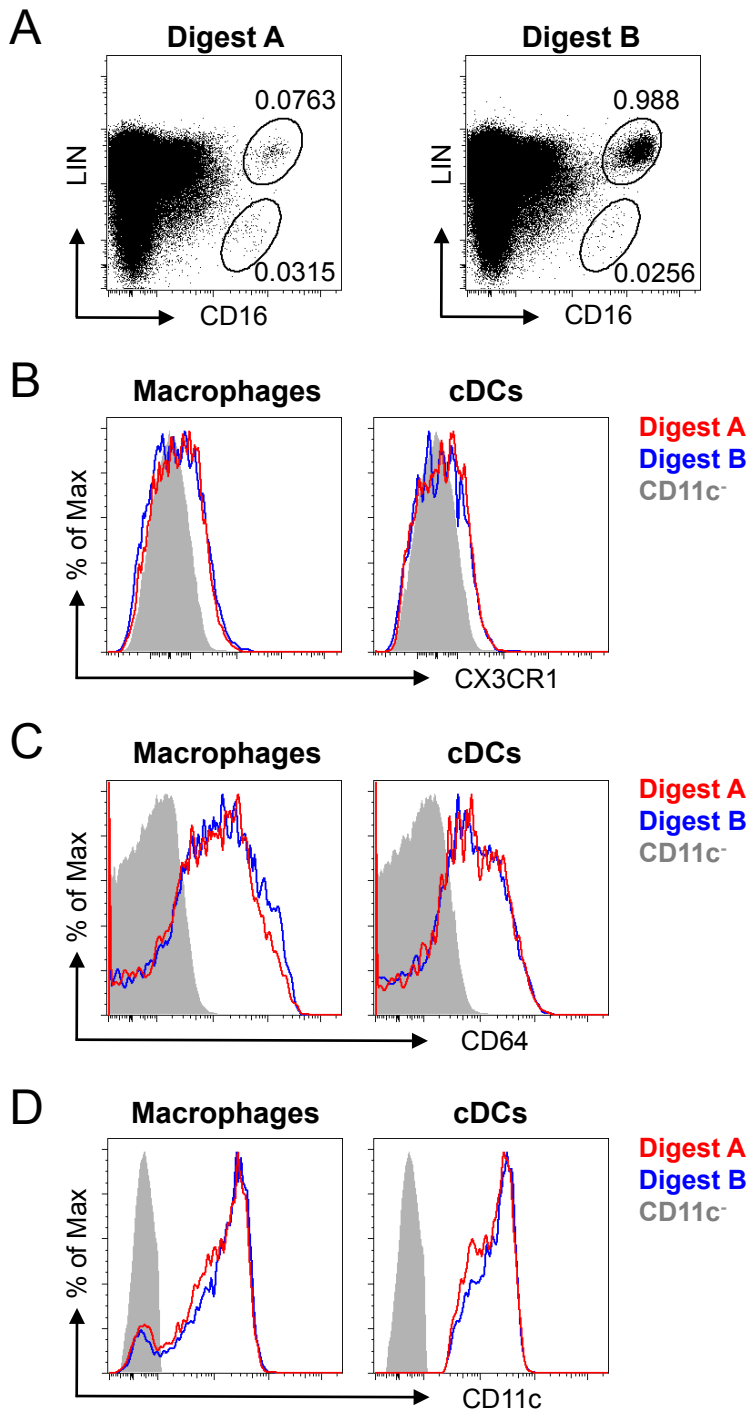


Figure 8.4: Surface marker expression following enzymatic digestion

Colonic macrophage and cDC populations were analysed for the expression of CD16, CX3CR1, CD64 and CD11c under different enzymatic digestion conditions. Digest A (red) involves collagenase V (0.85mg/ml), collagenase D (1.25mg/ml), dispase (1mg/ml) and DNase (0.03mg/ml). Digest B (blue) includes the following enzymes: collagenase VIII, collagenase D, dispase and DNase. (A) Total 7AAD⁻ CD45⁺ cells amongst colonic isolates were assessed for LIN (CD3, CD15, CD19 and CD56) and CD16 expression. Percentages reflect proportion of parent population. Total live CD45⁺ LIN⁻ CD14⁺ MHC II⁺ macrophages (left) and CD14⁻ cDCs (right) were analysed for the expression of CX3CR1 (B), CD64 (C) and CD11c (D) under the different enzymatic digestion conditions. CD11c⁻ cells (grey histogram) were used as a control population.

we decided to use our digest B enzyme cocktail (collagenase D, collagenase VIII, dispase and DNase) in all subsequent experiments involving human intestinal tissue, despite the uncertainty relating to CX3CR1 expression.

CD14⁻ CD16⁺ mononuclear cells in blood express SLAN and so to verify our original observation that CD14⁻ CD16⁺ mononuclear cells are essentially absent from healthy human intestinal mucosa, total single live CD45⁺ cells were analysed for the expression of SLAN (Fig. 8.5A) and CD16 (Fig. 8.5B). Very few SLAN⁺ cells could be identified, some of which expressed CD11c and MHC II. No clear populations could be identified from the FSC-A and SSC-A profile, suggesting that the few apparent SLAN⁺ cells may have been dead or the product of non-specific antibody binding (Fig. 8.5A). Furthermore, despite the identification of two populations expressing CD16 (Fig. 8.5B), neither population appeared to contain genuine CD16⁺ mononuclear cells. The LIN⁻ CD16⁺ population did not express CD11c and MHC II while the LIN⁺ CD16⁺ population appeared to be granulocytic, based on its FSC-A and SSC-A characteristics (Fig. 8.5B). Our results suggest that CD14⁻ CD16⁺ mononuclear cells are rare in steady state human intestine.

During these experiments, it became evident that exclusion of cells expressing LIN markers was not required for identification of intestinal cDCs. Therefore a revised gating strategy was used in the following experiments. This involved the exclusion of cell debris, doublets and dead cells as previously described, before selecting CD45-expressing leukocytes, which were subsequently analysed for expression of CD14 to exclude macrophages (Fig. 8.6A). Live CD45⁺ CD14⁻ cells that co-expressed CD11c and MHC II, at this point were considered cDCs. However, to assess contamination of this population with LIN⁺ (CD3, CD15, CD19 and CD56) cells, 7AAD⁻ CD45⁺ CD14⁻ CD11c⁺ MHC II⁺ cells were assessed for expression of LIN and MHC II, and back-gated on total 7AAD⁻ CD45⁺ cells (Fig. 8.6B). The gate confirms that all cDCs are contained within the LIN⁻ population. Consequently, LIN markers were no longer required and were not included in subsequent cDC analyses.

8.4 Identification of intestinal cDCs

Following development of the digestion and staining protocols, we set out to identify cDC populations in human intestinal samples. Comparisons between mouse and human DC subsets to date have suggested that mouse CD103⁺ CD8⁺ DCs may be equivalent to CD141⁺ human DCs, whereas CD1c⁺ cDCs correspond to mouse splenic CD4⁺ DCs

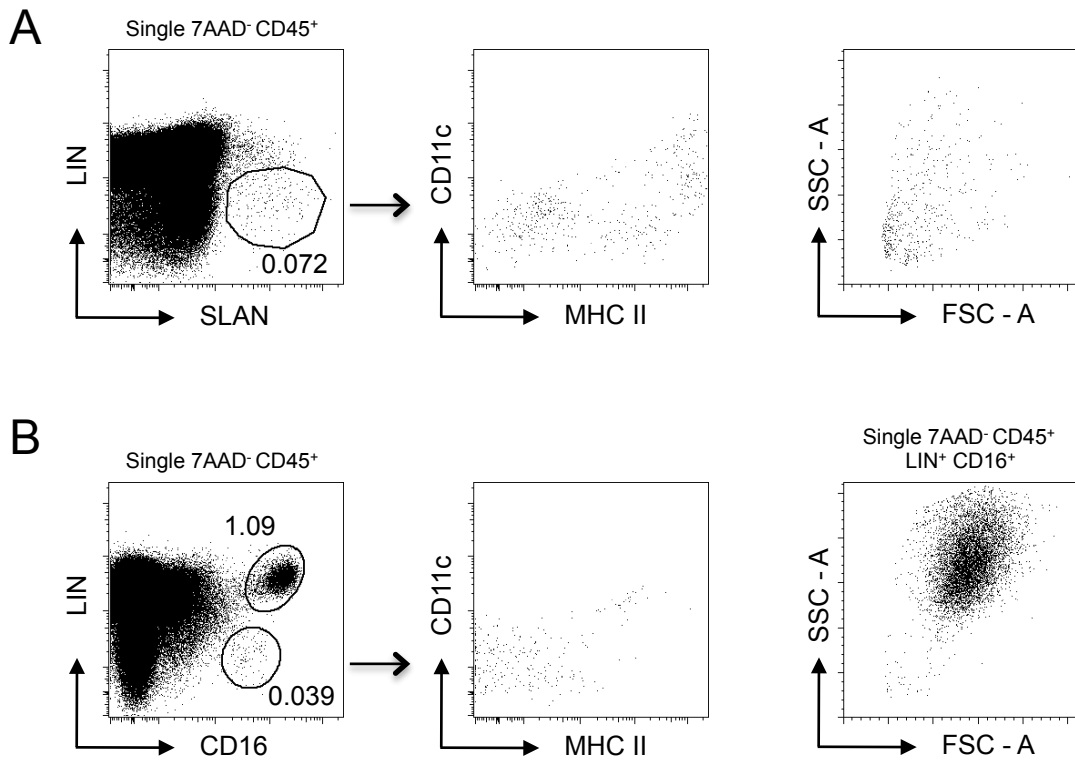


Figure 8.5: Identification of CD14⁻ CD16⁺ intestinal mononuclear cells

CD14⁻ CD16⁺ mononuclear cells do not enter colonic mucosa under steady state conditions. **(A)** Single 7AAD⁻ CD45⁺ cells were analysed for expression of LIN (CD3, CD15, CD19 and CD56) and SLAN. SLAN⁺ LIN⁻ cells were assessed for expression of CD11c and MHC II (centre), and FSC-A and SSC-A profiles (right). Percentages represent proportion of parent population. **(B)** Total single live CD45⁺ leukocytes were analysed for the expression of LIN and CD16. LIN⁻ CD16⁺ cells were analysed for expression of CD11c and MHC II (centre). LIN⁺ CD16⁺ cells were back-gated on FSC-A and SSC-A (right). Data from a single experiment using colonic tissue isolated from one HC.

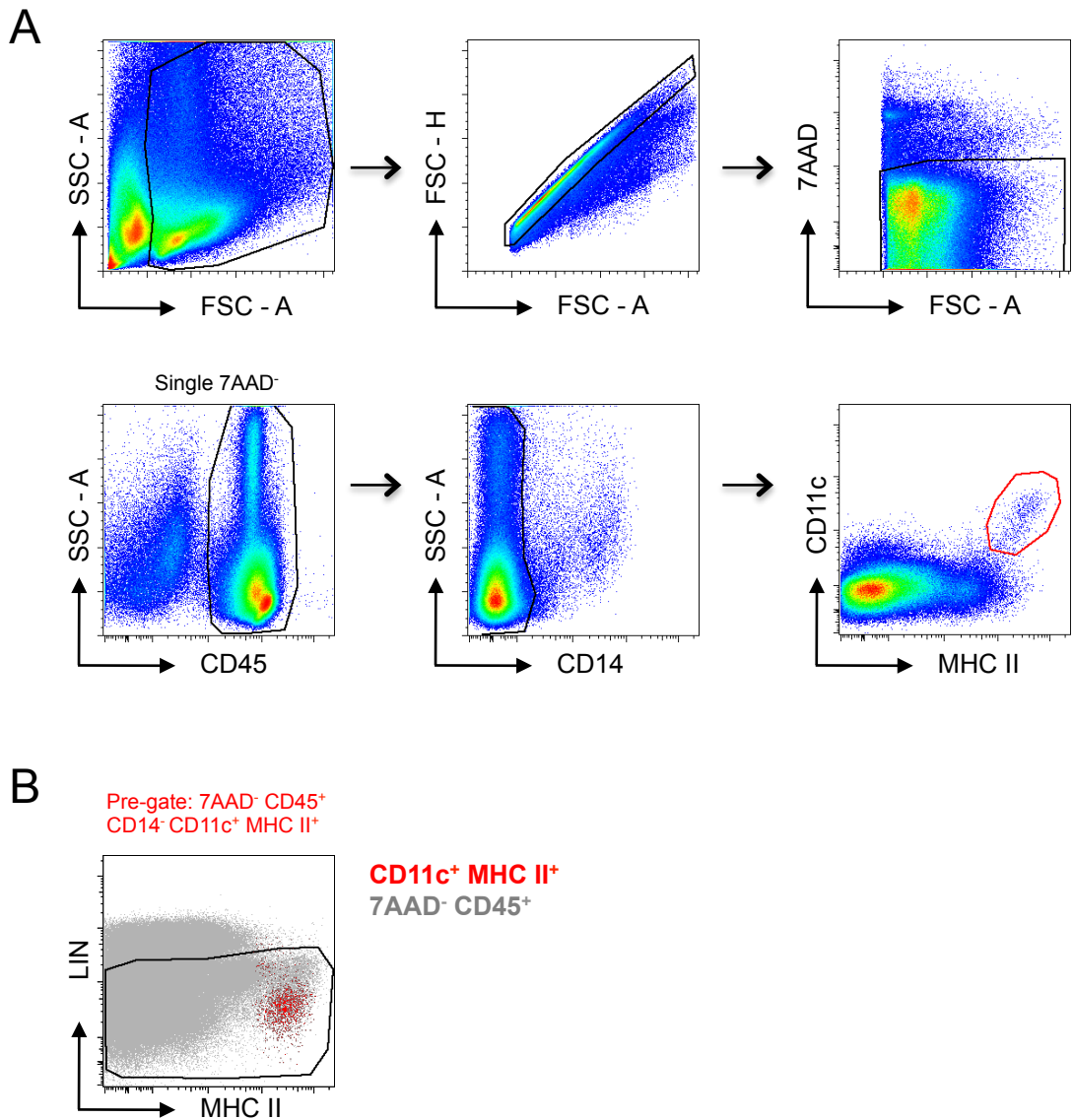


Figure 8.6: Lineage exclusion not required for the identification of intestinal cDCs

Live CD45⁺ CD14⁻ CD11c⁺ MHC II⁺ cells lack expression of LIN markers. **(A)** Cell debris and aggregates were gated out on FSC and SSC characteristics, and live cells selected as 7AAD⁻. Single live (7AAD⁻) cells were analysed for expression of CD45. CD45⁺ CD14⁻ cells were further assessed for co-expression of CD11c and MHC II, and were classified as DCs. **(B)** DCs (red) were backgated for LIN and MHC II expression. Total 7AAD⁻ CD45⁺ cells are used as staining comparison (grey). Gate depicts cells included within LIN⁻ fraction.

(200, 203, 212, 277, 340, 393). These species comparative analyses shape the investigative field of human disease research and that of therapeutic development. However, additional functional and phenotypic analyses of human immune populations are required to substantiate these functional and phenotypic relationships. As described above, analysis of human intestinal DC subsets under resting and inflammatory conditions has not been performed in detail. In mice, recently published data where contaminating macrophages are excluded through the use of specific cell population markers (e.g. CD64), identifies four populations of intestinal cDC based on expression of CD103 and CD11b (234, 389). Jaensson et al identified LIN⁻ CD11c⁺ MHC II⁺ CD103⁺ DCs in human MLNs capable of inducing the gut homing markers CCR9 and $\alpha 4\beta 7$ on responding CD8⁺ T cells (274). Similarly, Persson et al identified CD103⁺ cDCs in small intestinal tissue isolated from HCs (275), however this study did not consider the possibility of CD103⁻ cDCs existing in the mucosa. Therefore, in addition to the traditional blood/tissue cDC markers CD1c and CD141, we included CD103 in our staining protocol to try to identify all the intestinal DC subsets, including any potential CD103⁻ DCs (203, 210, 265, 271, 340, 702). The gating strategy adopted to identify human intestinal cDC subsets is depicted in Fig. 8.7. CD64⁺ CD14⁺ cells amongst live leukocytes were excluded from analysis due to their classification as macrophages. Live CD45⁺ CD14⁻ CD64⁻ cells expressing CD11c and MHC II were considered to be human intestinal DCs (Fig. 8.7A). As stated above, murine intestinal DCs are identified through CD103 and CD11b expression (389). However, low expression of CD11b on blood DCs directed us to use SIRP α for identification of human intestinal DC populations, given their reported co-expression. This cell population can be subdivided into 4 distinct populations based on expression of CD103 and SIRP α (Fig. 8.7A): CD103⁺ SIRP α ⁺ (red), CD103⁺ SIRP α ⁻ (blue), CD103⁻ SIRP α ⁺ (green) and CD103⁻ SIRP α ⁻ cDC subsets (orange). In blood, we and others can identify CD141⁺ (BDCA-3) and CD1c⁺ (BDCA-1) cDC populations (202, 203, 209, 210, 393, 576). Thus, we analysed CD141 and CD1c expression on all four populations of human intestinal DC to align these newly identified populations with those found in blood. The CD103⁻ SIRP α ⁻ population was distinctly heterogeneous for CD141 expression, whereas CD103⁺ SIRP α ⁺ and CD103⁻ SIRP α ⁺ DCs expressed intermediate levels of this surface marker (Fig. 8.7B). Importantly, CD103⁺ SIRP α ⁻ DC expressed uniformly high levels of CD141 (Fig. 8.7B). CD1c expression was observed to correlate with SIRP α expression on DC populations (Fig. 8.7B). Therefore, only the CD103⁺ SIRP α ⁺ and CD103⁻ SIRP α ⁺ subsets expressed significant levels of CD1c. The CD103⁻ SIRP α ⁻ subset was heterogeneous for expression of CD1c (Fig. 8.7B). Overall we have identified four populations of intestinal DC that differ in their surface marker expression of CD103, SIRP α , CD1c and CD141.

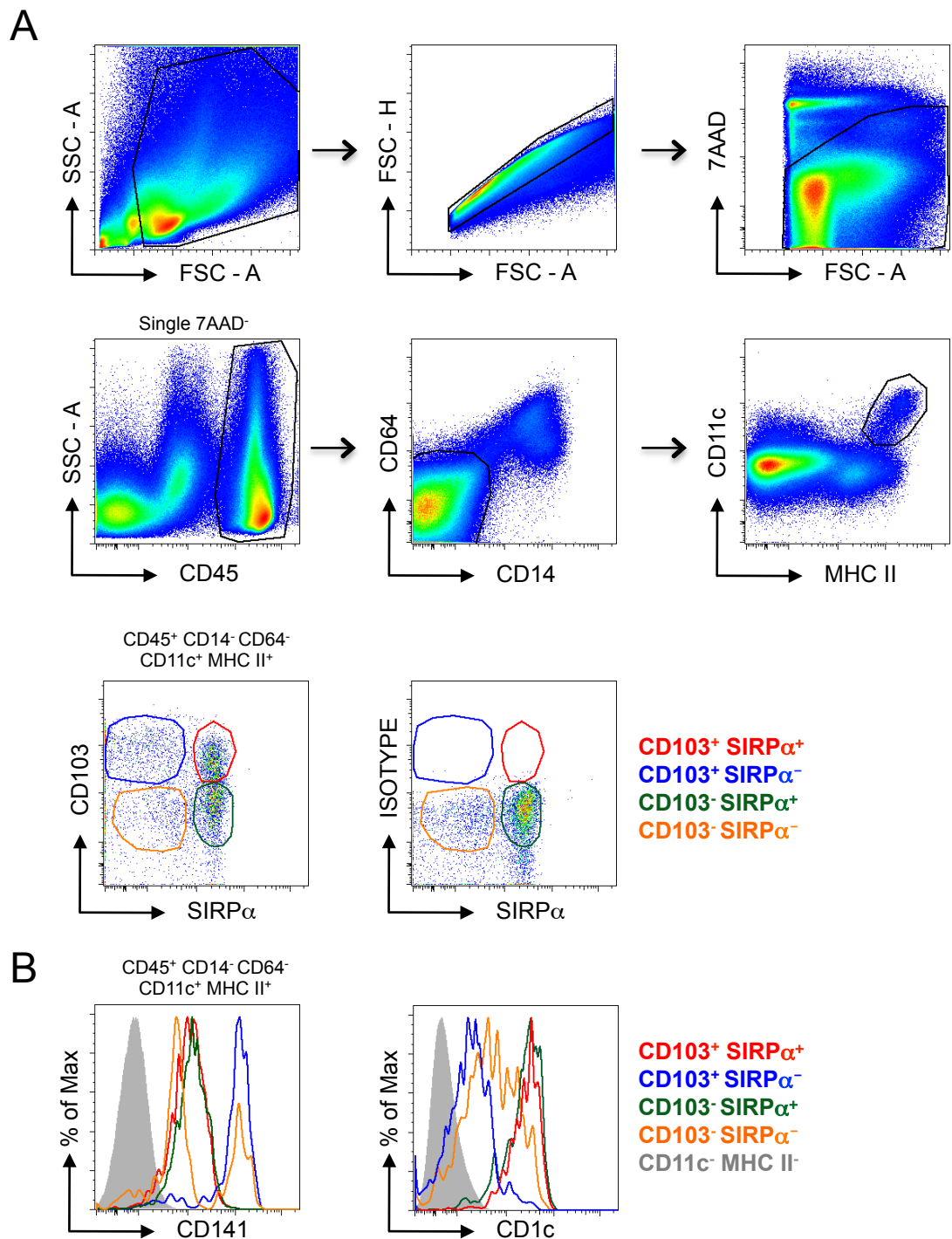


Figure 8.7: Identification of intestinal cDC subsets

Four intestinal cDC subsets can be identified based on the expression of CD103, CD141, SIRP α and CD1c. **(A)** Gating strategy used to identify intestinal cDC subsets digested using the enzymatic cocktail (digest 2): collagenase VIII, collagenase D, dispase and DNase. Doublets and live cells (7AAD⁻) were excluded from further analysis. Single live CD45⁺ cells were assessed for expression of CD14 and CD64. LIN⁻ CD14⁻ CD64⁻ cells were analysed for CD11c and MHC II expression. CD11c⁺ MHC II⁺ cells were assessed for expression of CD103 and SIRP α . cDC gates were set based on CD103 isotype. **(B)** Expression of CD141 (left) and CD1c (right) on CD103⁻ and SIRP α -defined cDC subsets. 7AAD⁻ CD45⁺ CD11c⁻ MHC II⁻ cells were used as controls for marker expression. Data are representative of four individual experiments.

8.5 Steady state vs inflammation

Having established reliable protocols for the identification of intestinal DC populations, we wished to ascertain whether there were any differences in these populations between HCs, HLA-B27⁺ and HLA-B27⁻ AS patients. However, the only tissue available was colonic and duodenal tissue from HCs, UC and CD patients. Representative histological sections of colonic tissue isolated from a UC patient are presented in Fig. 8.8. These transverse and longitudinal sections demonstrate the presence of intestinal inflammation in our UC samples, as evidenced by elongated crypts (Fig. 8.8A), epithelial erosions, cellular infiltrate (Fig. 8.8B) and numerous goblet cells (Fig. 8.8C). Unfortunately uninflamed specimens were not available to act as control sections.

Using the gating strategy described in Fig. 8.7A, cDC populations digested from colonic tissue isolated from a HC and a CD patient were identified and compared. As before, four populations could be identified amongst CD11c⁺ MHC II⁺ cells on the basis of CD103 and SIRP α expression in healthy colon (Fig. 8.9A). Importantly, all four populations of cDC were present in inflamed CD colon, albeit at different proportions (Fig. 8.9A). Within inflamed intestinal tissue, CD103⁺ SIRP α ⁺ cDCs appear to be diminished compared with HCs (Fig. 8.9A). In addition, the proportion of the CD103⁻ SIRP α ⁻ population was increased in CD tissue compared with the HC. The remaining cDC populations (CD103⁻ SIRP α ⁺ and CD103⁺ SIRP α ⁻) remained comparatively stable. The results here suggested that colonic cDC populations may be altered in CD. However given that these observations compared only one HC with one CD sample, these experiments would need to be repeated to establish whether these alterations are reproducible.

8.6 Expression of CCR2 by intestinal DC populations

During these experiments, a PhD student in Prof Mowat's laboratory (Charlotte Scott) was examining the phenotype, function and ontogeny of murine intestinal DCs. Interestingly, she observed differential CCR2 expression on mouse intestinal DC subsets. Specifically, she found that intestinal CD103⁻ CD11b⁺ DCs were heterogeneous for CCR2 expression. Therefore, I set out to examine CCR2 expression on human intestinal DC subsets. In HC colonic tissue, CCR2 was expressed at varying levels on all DC subsets except the CD103⁺ SIRP α ⁻ population (Fig. 8.9B). For both the CD103⁻ SIRP α ⁺ and CD103⁺ SIRP α ⁺ populations, CCR2 expression was heterogeneous (Fig. 8.9B). Interestingly, the CD103⁻

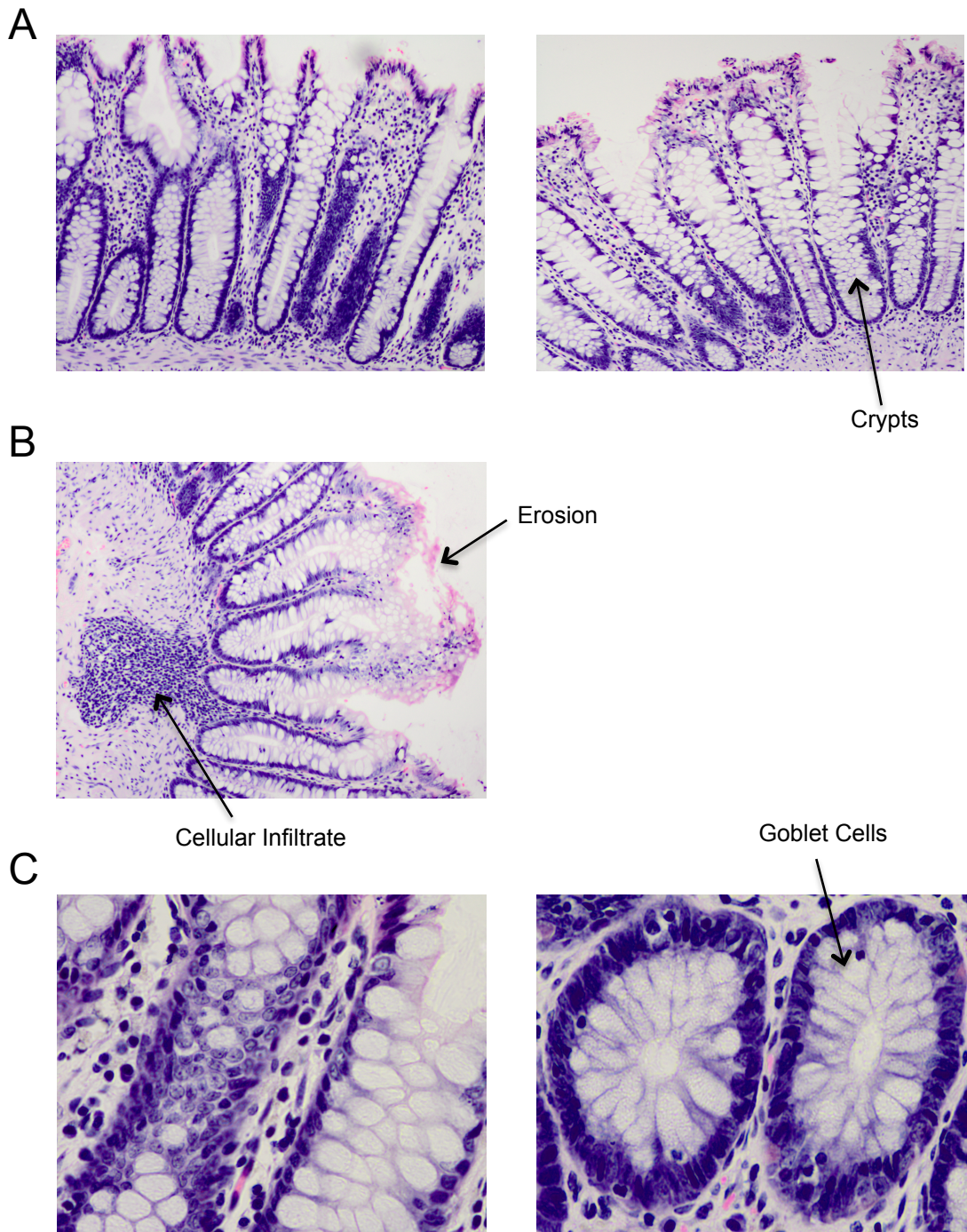


Figure 8.8: Histology of colonic tissue from an Ulcerative Colitis patient

Histological sections of colonic tissue removed from an ulcerative colitis (UC) patient show signs of crypt hyperplasia, erosions and cellular infiltrate. (A) Sections of colonic UC tissue show elongation of crypts. Pictures taken at 10X magnification. (B) Evidence of erosions and cellular infiltrate in colonic tissue from a UC patient. Pictures taken at 10X magnification. (C) Sections at 40X magnification of colonic tissue from a UC patient. Goblet cells appear to be numerous within colonic crypts. Arrows indicate points of interest.

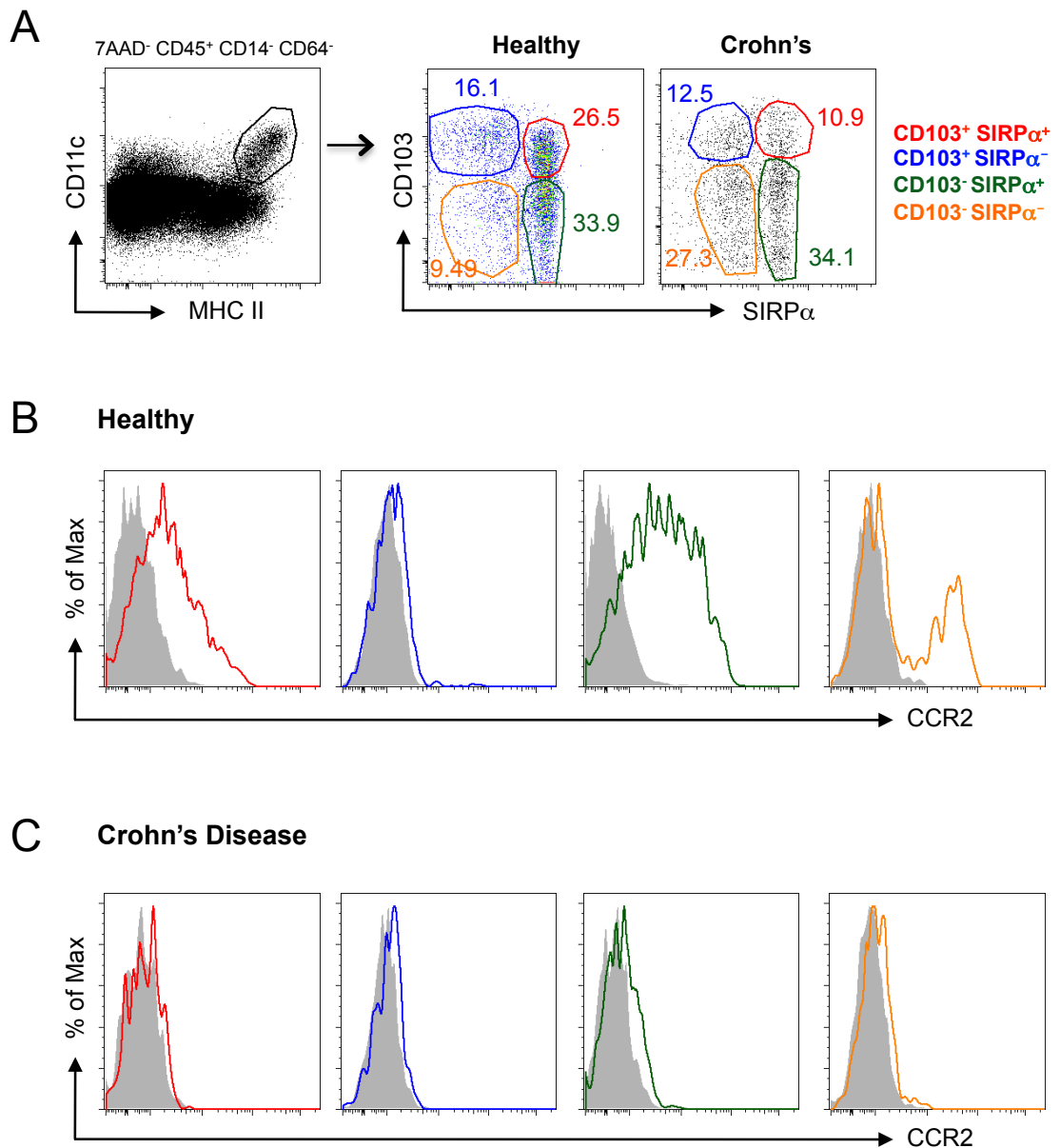


Figure 8.9: Expression of CCR2 by cDC subsets from steady state and inflamed colon

CD103⁺ SIRP α ⁻ intestinal DCs lack expression of CCR2. **(A)** Identification of colonic cDC populations in a HC (centre) and a Crohn's patient (right). 7AAD⁻ CD45⁺ CD14⁻ CD64⁻ CD11c⁺ MHC II⁺ cells were subdivided into four cDC populations based on CD103 and SIRP α expression. Percentages represent proportion of CD11c⁺ MHC II⁺ cells. Histograms depict CCR2 expression on each intestinal cDC subset from a HC **(B)** and a Crohn's disease patient **(C)**: CD103⁺ SIRP α ⁺, CD103⁺ SIRP α ⁻, CD103⁻ SIRP α ⁺ and CD103⁻ SIRP α ⁻. CCR2 isotype = mouse IgG2b. Data are representative of 3 individual tissue samples.

SIRP α ⁻ DC subset appeared distinctly bimodal for CCR2 expression (Fig. 8.9B). This staining pattern was replicated in three independent experiments using HC intestinal tissue. We can therefore conclusively say that all human DC intestinal populations, except the CD103⁺ SIRP α ⁻ population, express CCR2. In addition, CCR2 expression on DC subsets isolated from one CD sample was assessed. In contrast to HCs, all DC subsets lacked expression of CCR2 (Fig. 8.9C). This comparison is based only on one HC sample and one CD patient. However, these results suggest that CCR2 is differentially expressed on intestinal DC subsets and may be altered in the presence of inflammation.

8.7 Intestinal macrophages

It has recently be shown in mice that Ly6C^{hi} blood monocytes can give rise to both ‘resident’ and pro-inflammatory macrophages in the intestine (225, 234). Under steady state conditions Ly6C^{hi} monocytes give rise to resident, anti-inflammatory macrophages identified by their unusually high expression of CX3CR1. In contrast, during inflammation this process is disrupted leading to the accumulation of pro-inflammatory CX3CR1^{int} macrophages (225). In addition, two macrophage populations were identified in the human small intestine that may correlate with macrophage populations in mice: CD14^{lo} and CD14^{hi} subsets (225). Based on these findings we set out to identify macrophage populations in colonic tissue of HCs and CD patients. The gating strategy used to identify macrophage subsets is depicted in Fig. 8.10. Macrophages were identified amongst CD45⁺ LIN⁻ (CD3, CD15, CD19 and CD56) cells as CD206⁺ cells (Fig. 8.10A). Within this population, two colonic macrophage subsets could be identified: CD14^{hi} and CD14^{lo}. Both populations were next analysed for the expression of a variety of markers previously reported to be expressed by intestinal macrophages including CD11c, MHC II, CD33 and CD209. Whereas both subsets highly expressed CD206, MHC II and CD33 (Fig. 8.10B), the CD14^{hi} population expressed CD64 at higher levels than CD14^{lo} macrophages (Fig. 8.10B). CD209 (also known as DC-SIGN) has previously been reported to be preferentially expressed on immature human DCs (703, 704), with current studies focusing on CD209 as a potential target for DC therapeutics (705). However, in our hands we found expression of CD209 to be higher on both intestinal macrophage populations than on total CD14⁻ CD64⁻ CD11c⁺ MHC II⁺ DCs (Fig. 8.10C). In addition, CD14^{hi} macrophages appeared to have lower levels of CD11c compared to both CD14^{lo} macrophages and total CD14⁻ CD64⁻ CD11c⁺ MHC II⁺ DC (Fig. 8.10C). To the best of my knowledge, this is the most comprehensive analysis of human intestinal macrophages to date. These data emphasise the need for inclusion of phenotypic markers to allow discrimination of CD11c⁺

MHC II⁺ macrophages from CD11c⁺ MHC II⁺ DC. Furthermore, we have identified two populations of colonic macrophages that differ in their expression of CD11c and CD64.

8.8 Macrophages in inflammation

To prepare for future studies of intestinal tissue from AS patients, we aimed to analyse the proportions of colonic macrophage populations under steady state and inflammatory conditions. Our results suggest that proportions of both colonic macrophage populations change following inflammation in CD (Fig. 8.11A). In our hands, CD14^{hi} macrophages dominated in healthy colonic tissue, representing ~10% of all 7AAD⁻ CD45⁺ LIN⁻ cells, compared with ~1.3% occupied by CD14^{lo}. Again this distribution of intestinal macrophages is representative of three independent experiments using HC intestinal tissue. Under inflammatory conditions, the proportion of CD14^{hi} colonic macrophages appeared to decrease (Fig. 8.11A). In the CD sample, CD14^{hi} macrophages represented 3.9% of total live CD45⁺ LIN⁻ cells compared to 10% for the HC CD14^{hi} population. In addition, we noted the accumulation of CD45⁺ LIN⁻ CD206⁻ CD14⁺ cells in CD (2.64%), which were essentially absent in the healthy mucosa (0.386%). This population could represent infiltrating monocytes and will be discussed later (Fig. 8.11A). Due to the expansion of this CD206⁻ CD14⁺ population in CD, we next determined expression of several macrophage/myeloid markers including CD11c, MHC II, CD33 and CD64 on all three populations (Fig. 8.11B). CD206⁻ CD14⁺ cells uniformly expressed CD64 and expressed CD11c and CD33 at similar levels to CD14^{hi} and CD14^{lo} macrophages. However these CD206⁻ CD14⁺ cells expressed MHC II at lower levels than the other macrophage populations (Fig. 8.11B).

In addition to changes in the macrophage populations, there were other changes in the CD45⁺ LIN⁻ compartment. Notably, a population of CD11c⁺ MHC II⁻ cells expanded markedly in CD compared to HC tissue (Fig. 8.11C).

In summary, following identification of CD14^{hi} and CD14^{lo} intestinal macrophages, we observed differences in the proportions of colonic macrophage subsets in CD, although this observation was only based on one HC and one CD sample.

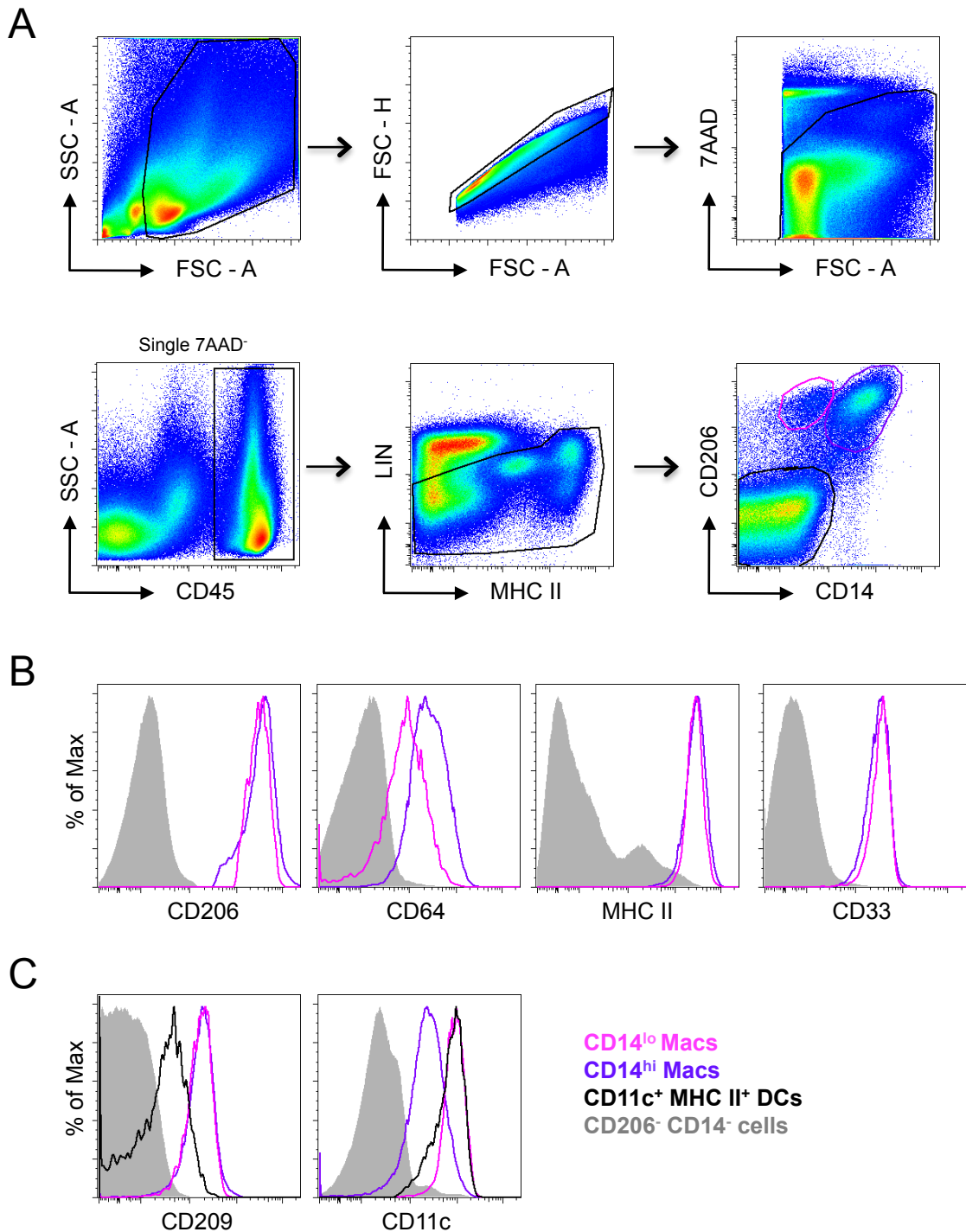


Figure 8.10: Identification of intestinal macrophages in healthy colon

Intestinal macrophage populations express varying levels of CD14. **(A)** Gating strategy to identify intestinal macrophages. Cells debris was excluded based on FSC vs SSC characteristics. CD45⁺ leukocytes were identified within the single 7AAD⁻ population. CD45⁺ cells were analysed for expression of lineage (CD3, CD15, CD19 and CD56) and MHC II. LIN⁻ cells were then subdivided based on CD206 and CD14 expression. **(B)** Histograms depict expression of CD206, CD64, MHC II and CD33 on CD14^{hi} (purple) and CD14^{lo} (pink) macrophages. Single 7AAD⁻ CD45⁺ LIN⁻ CD206⁻ CD14⁻ cells were used as a control population (grey). **(C)** CD209 and CD11c expression on CD14^{hi} and CD14^{lo} macrophages and CD45⁺ CD11c⁺ MHC II⁺ CD14⁻ DCs (black). All expression data except CD33 (Crohn's) was from a HC. Data representative of 7 independent tissue samples.

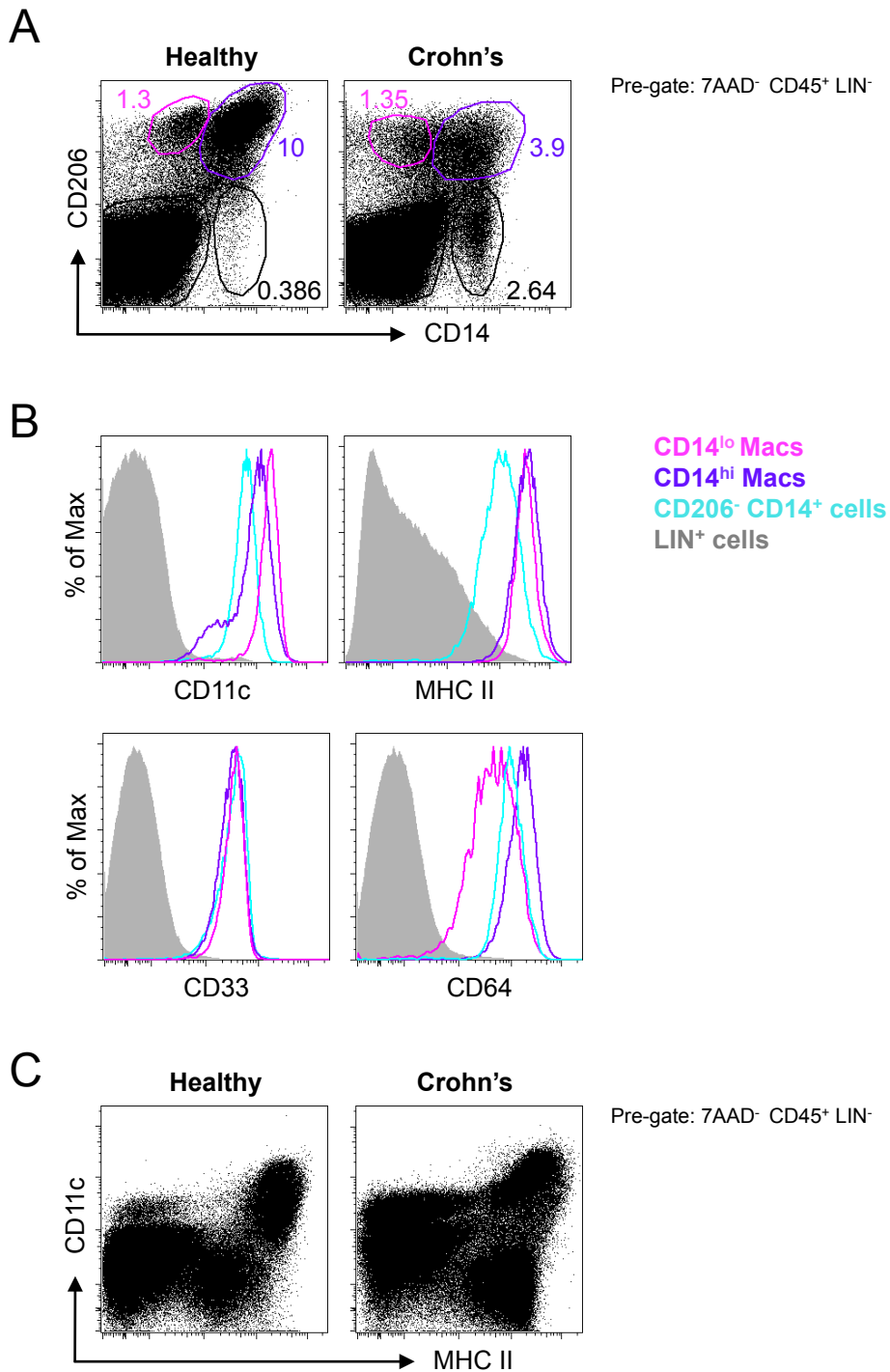


Figure 8.11: Macrophages in steady state and Crohn's disease

CD206⁻ CD14⁺ cells infiltrate intestinal tissue isolated from a Crohn's patient. **(A)** Comparison of intestinal macrophage populations in a HC (left) and a Crohn's patient (right). Single 7AAD⁻ CD45⁺ LIN⁻ cells were assessed for the expression of CD206 and CD14. LIN = CD3, CD15, CD19 and CD56. Percentages represent proportion of LIN⁻ cells. **(B)** Expression of CD11c, MHC II, CD33 and CD64 on CD14^{hi} macrophages (purple), CD14^{lo} macrophages (pink) and CD206⁻ CD14⁺ cells (light blue) from a Crohn's patient. LIN⁺ cells were used as a control population for marker expression. **(C)** Total live CD45⁺ LIN⁻ cells were assessed for expression of CD11c and MHC II in a HC (left) and a Crohn's patient (right).

8.9 *In vivo* turnover of intestinal macrophages

Unpublished results from the Mowat laboratory (Calum Bain and Alberto Bravo) identified differences in the proliferation of intestinal macrophage populations during development in mice (unpublished observations). We therefore set up a collaboration to investigate the proliferative capabilities of intestinal macrophage populations in humans. Ki67 is a nuclear antigen expressed exclusively by cells in active cell cycle and can be detected by intracellular antibody staining. Therefore we examined the expression of Ki67 by intestinal macrophages from healthy and inflamed mucosa. To ensure we could detect Ki67 expression by colonic isolates, we first examined the expression by total live leukocytes. Only 0.427% of CD206⁻ cells expressed Ki67 in the steady state (Fig. 8.12A). In contrast, 4.67% of live CD45⁺ CD206⁻ colonic cells from inflamed tissue expressed Ki67 (Fig. 8.12A). These results suggest that proliferation of immune populations is enhanced in the presence of inflammation and additionally indicate that our Ki67 staining protocol accurately identifies proliferating cells. We next examined the proliferation potential of the CD206⁺ macrophage subsets and CD206⁻ CD14⁺ cells directly (Fig. 8.12B and 8.12C). Neither CD14^{hi} macrophages nor the CD206⁻ CD14⁺ population proliferate rapidly *in vivo* in the steady state (Fig. 8.12B) or during inflammatory conditions (Fig. 8.12C). In contrast, the CD14^{lo} macrophage subset both in the HC (Fig. 8.12B) and CD tissue (Fig. 8.12C) showed some proliferation (~5%). These results are representative of three independent experiments using HC intestinal tissue. To the best of my knowledge, the proliferative capacity of human intestinal macrophage populations has not previously been described. These findings predominantly corroborate those observations in the murine studies and therefore we hope to include these data in a future manuscript (Calum Bain and Alberto Bravo, unpublished observations).

Although we were unable to definitively assess *in vivo* proliferation of intestinal DC subsets due to the lack of appropriate markers, we examined CD45⁺ LIN⁻ CD11c⁺ CD14⁻ CD206⁻ cells that may represent DCs. These cells showed levels of Ki67 expression similar to that of CD14^{lo} macrophages (Fig. 8.12D). Thus putative DCs and CD14^{lo} macrophages appear to turnover *in situ*.

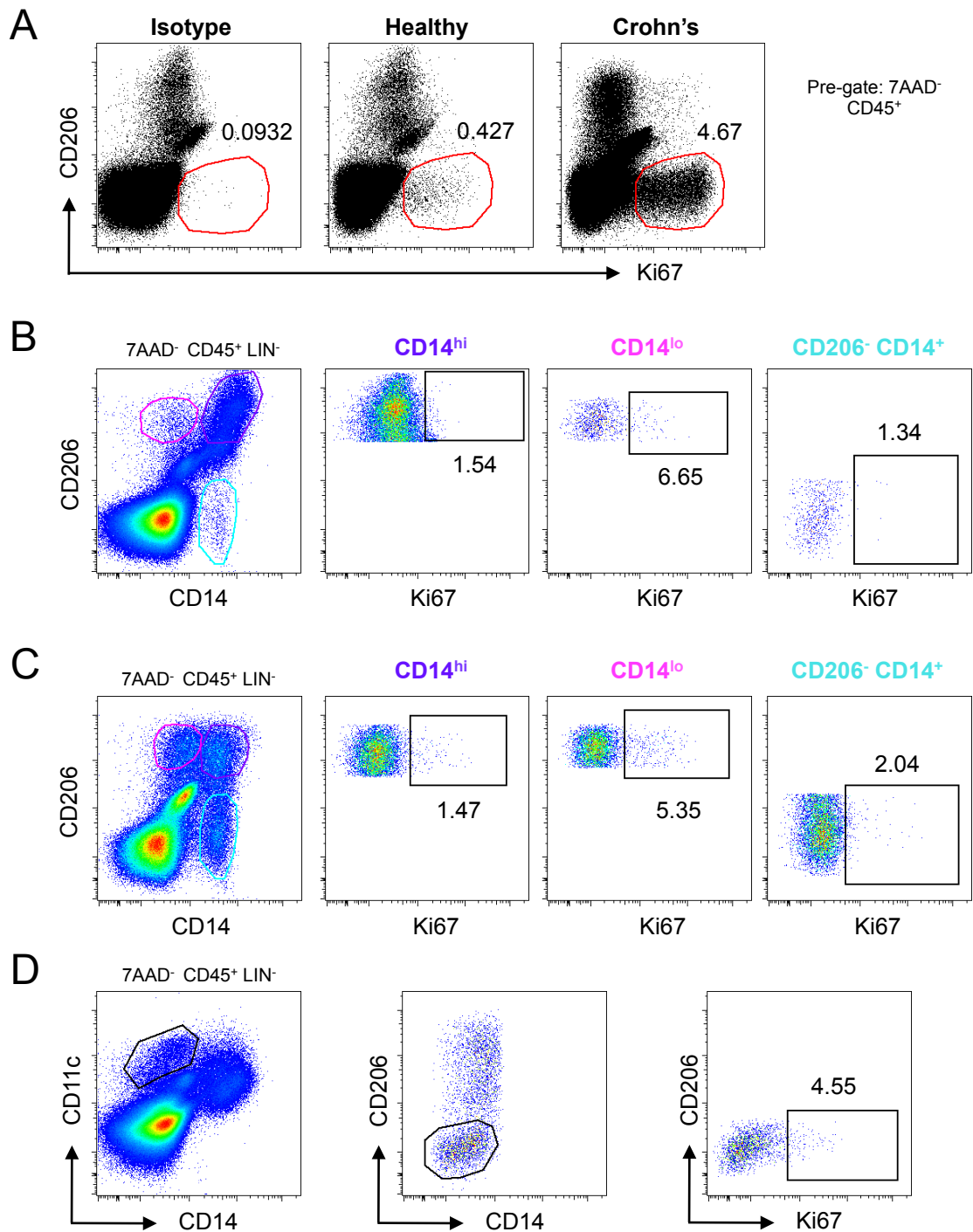


Figure 8.12: Macrophage subset proliferation potential from HC and inflamed colon

Colonic macrophages do not proliferate *in vivo*. **(A)** Ki67 staining was used to assess cell proliferation *in vivo* on total single 7AAD⁻ CD45⁺ cells isolated from a HC (centre) and a Crohn's patient (left). Ki67 isotype was used to set Ki67⁺ gate (red). Percentages represent proportion of parent population. Analysis of Ki67 on macrophage subsets from a HC **(B)** and a Crohn's patient **(C)**. Live CD45⁺ LIN⁻ cells were subdivided into CD14^{lo} (pink) and CD14^{hi} (purple) macrophages and CD206⁻ CD14⁺ (light blue) cells and assessed for Ki67. Percentages represent proportion of Ki67⁺ cells within each subset. **(D)** Live CD45⁺ LIN⁻ cells were analysed for CD11c and CD14 expression. CD11c⁺ CD14⁻ CD206⁻ cells were assessed for Ki67. Percentage represents proportion of dividing cells within subset. Data representative of 3 independent experiments.

8.10 Discussion

The majority of AS studies focus on blood due to ease of tissue access and recruitment of HCs. Using blood, we have identified small differences in the proportions of circulating immune populations in AS patients compared to HCs: a reduction of CD1c⁺ cDCs accompanied by an increase in CD14⁻ CD16⁺ mononuclear cells and differential expression of chemokine receptors on CD4⁺ T cells (Chapter 3 and 4). However, blood profiling is insufficient to fully characterise and understand the immune pathways involved in AS development. In contrast, use of disease-affected tissue can aid elucidation of the precise mechanisms involved and thereby improve our understanding of disease pathology and generation of disease specific therapies. The main sites of inflammation and aberrant bone processes in AS are within the spine and SIJs (4). However access to spinal tissue is limited. Consequently, most studies investigating AS pathogenesis through the use of extra-articular and peripheral tissues focus on SF and the intestine. We have identified DCs, CCR4⁺ and CCR6⁺ CD4⁺ T cells and described the cytokine milieu within the SF of AS patients (Chapter 5). However, excess joint SF is often associated with lower limb peripheral arthritis in AS patients, meaning that the ongoing inflammatory processes within AS SF may, in fact, be more characteristic of RA pathogenesis.

Data from animal models and patients suggest a connection between the intestine and AS pathogenesis. Taurog et al observed alleviation of intestinal and joint pathology in HLA-B27 TG rats when housed in germ-free conditions (444). In Crohn's patients, 50% of those expressing the MHC class I molecule HLA-B27 developed AS (4, 440). In addition, the study by Van Praet et al reported that 50% of their SpA cohort presented with evidence of subclinical gut inflammation (441, 706). Furthermore, intestinal inflammation has been observed to correlate with disease severity (441, 706). These studies suggest that intestinal inflammation, joint pathology and AS pathogenesis are inextricably linked.

Intestinal studies in AS patients have focused on cytokine expression, T cell subsets (Tregs), NK cells and a basic characterisation of cellular infiltrate (551-554, 707). No study to date has investigated and characterised the intestinal DC populations in AS patients. This is surprising given their primary role in inducing and directing immune responses. This statement is confounded through the use of overlapping myeloid markers, difficulties in isolating significant cell numbers and limited tissue availability. Using our knowledge of blood DCs and mouse intestinal DC subsets, we aimed to analyse intestinal DC populations in AS patients and HCs. Starting from our observation that CD172a^{lo}

migratory intestinal DCs were absent in the HLA-B27 TG rats, we hypothesised that intestinal CD141⁺ DCs would be absent from AS intestinal tissue, and that this defect would contribute to disease pathogenesis and development. In the time available to perform these studies I have developed techniques for the analysis of human intestinal DC populations, which have contributed to two important projects. These results are herein described. Unfortunately I did not receive any AS patient intestinal samples or those from HLA-B27⁺ IBD patients, and have therefore not been able to test my hypothesis. However, using HC and IBD intestinal tissue samples, we developed techniques to successfully isolate immune populations, including DCs and macrophages, from human intestinal surgical resections. Following successful isolation, we performed preliminary comparisons of the DC and macrophage populations residing within HC and IBD intestinal tissue. In contrast to AS, numerous studies have identified and quantified the DC populations present in UC and CD intestinal tissue. For instance, DCs present within the inflamed mucosa of CD patients have been found to accumulate and congregate with T cells and express higher levels of CD40, TLR2 and TLR4 (404, 694, 695, 698). Recently, cell specific markers have been identified that enable greater distinction between macrophage and DC populations. These markers include CD64 (225, 234). It is now clear that groups previously thought to be investigating IBD ‘DC’ biology have unintentionally been isolating and characterising mixed populations of DCs and macrophages. Therefore, in addition to refining intestinal cell isolation protocols, we performed experiments investigating DC and macrophage subsets in the human intestine under steady state and inflammatory conditions.

The majority of HC intestinal tissue used in this study was excised from patients suffering with intestinal adenocarcinoma. Healthy tissue surrounding the tumour was used for analysis, however we are unable to exclude the possibility that this HC tissue was actively inflamed. Therefore when performing correlative analysis between HCs and IBD patients, the health status of HCs must be taken into consideration. To eliminate this uncertainty in future studies, histological analysis could be performed on all tissue samples.

Intestinal cell populations were initially isolated using a protocol developed by the laboratory of Professor Allan Mowat. However this protocol was found to induce cleavage of at least two cell surface markers used to identify mononuclear populations in blood, CD16 and CX3CR1 (Fig. 8.2D and 8.2E). In blood, CD14⁻ CD16⁺ mononuclear cells were slightly increased in AS patients compared to HCs (Fig. 3.7A). It was therefore vital to adapt the isolation protocol to identify and functionally assess the role, if any, played by

CD14⁻ CD16⁺ mononuclear cells within inflamed tissues. Alterations to the enzyme cocktail, specifically the replacement of collagenase V with collagenase VIII, resulted in efficient tissue digestion without degradation of CD16 (Fig. 8.4A). Despite these protocol alterations, CX3CR1 expression remained difficult to detect following digestion (Fig. 8.4B). This could either signify that CX3CR1 is expressed at low levels within the human intestine, or that CX3CR1 is still cleaved by the enzyme cocktail. As published studies have detected CX3CR1 expression on CD14⁺ intestinal mononuclear cells (427, 701), the latter option is the more plausible explanation. If CX3CR1 expression data are required for further characterisation of immune populations, this protocol will have to be adapted. Overall, we successfully developed a protocol for the isolation of intestinal immune populations, which did not induce cleavage of the majority of DC and macrophage markers, excluding CX3CR1.

Using this adapted protocol, we repeated our experiments to detect CD14⁻ CD16⁺ mononuclear cells in the human intestine under steady state conditions. The results indicate that in the absence of inflammation, CD14⁻ CD16⁺ cells do not enter the intestinal mucosa (Fig. 8.5B). In blood, this CD14⁻ CD16⁺ population is heterogeneous, as discussed above, containing both SLAN⁺ and SLAN⁻ cells. CD16 has been shown to be rapidly shed, in a protease-dependent manner, from the surface of maturing SLAN⁺ DCs (588). To exclude the possibility that intestinal migration of this mononuclear population may be associated with CD16 downregulation, we analysed total live cells for expression of SLAN. Somewhat surprisingly, we were unable to clearly identify a distinct SLAN⁺ population in the human intestine under steady state conditions (Fig. 8.5A). However, this analysis was performed using only one HC colonic tissue sample; further experiments are clearly necessary. These data are further complicated because the CD14⁻ CD16⁺ population is not definitively characterised. CD14⁻ CD16⁺ SLAN⁻ cells are described as putative monocytes, whilst SLAN⁺ cells may represent a population of DCs (229, 237, 239). Comparison of these findings with analogous murine studies supports the idea that CD14⁻ CD16⁺ populations may be absent from peripheral and/or extra-articular tissue under steady state conditions; their proposed function is as a blood vessel surveillance population in the steady state (229, 237, 248, 356). Inflammation may alter migration of this blood CD14⁻ CD16⁺ population, leading to accumulation within inflamed tissues and potential involvement in disease pathogenesis (223, 237). Therefore, characterisation of CD14⁻ CD16⁺ mononuclear cells under inflammatory conditions should be performed to elucidate the function and identity of this subset in humans. However, our data suggest that both

subsets (SLAN⁻ and SLAN⁺) of the CD14⁻ CD16⁺ population do not enter intestinal mucosa under resting conditions, supporting their proposed role in blood surveillance.

If CD14⁻ CD16⁺ SLAN⁺ cells represent a third human DC subset, then our data indicate that this subset does not develop within or migrate to the intestinal mucosa under steady state conditions. Several groups have identified SLAN⁺ cells in healthy skin by immunohistochemistry, but these skin-residing SLAN⁺ cells lacked expression of CD11c (249, 250), and are therefore unlikely to represent tissue equivalents of the blood CD14⁻ CD16⁺ SLAN⁺ cells. The apparent exclusion of SLAN⁺ cells from the intestinal mucosa may be the result of intestinal conditioning. Several intestinal myeloid populations have been shown to be refractory to stimulation (424, 436, 708-710), thereby preventing generation of aberrant responses to harmless antigens. This anti-inflammatory environment in the intestine may also inhibit *in situ* development of the potentially inflammatory SLAN⁺ DC population. Inflammation affects the development of the murine intestinal macrophages (225); inflammation may affect *in situ* development of SLAN⁺ DCs in tissues. To support this hypothesis, SLAN⁺ cells have been identified in inflamed human tonsil, psoriatic skin, PPs and CD ileal mucosa (249-252). The majority of these studies depend on single stain immunohistochemistry, hindering characterisation of these SLAN⁺ cells. However these data may indicate that during inflammation, DC precursors seeding peripheral tissue may acquire the ability to generate CD14⁻ CD16⁺ SLAN⁺ DCs. Thus, the observed increase in circulating CD14⁻ CD16⁺ cells in AS patients, may be the result of increased development of this cell population under inflammatory conditions in peripheral tissues of patients.

We next set out to examine the cDC populations (CD141⁺ and CD1c⁺) in human intestinal mucosa. Recent advances in murine DC classification have led to the identification of four DC populations based on expression of CD103 and CD11b (234, 389). Jaensson et al also identified CD103⁺ DCs in the human MLN (274). The recent use of CD64 as a macrophage-specific marker in mice and men (225, 234) has highlighted the heterogeneity of the populations previously considered to be homogenous populations of DCs or macrophages. Using a combination of these markers, we set out to characterise human intestinal DC populations. Through definitive exclusion of macrophages (CD64⁺ and CD14⁺), we have now identified four intestinal DC subsets, based on their expression of cell surface markers CD103 and SIRP α : CD103⁺ SIRP α ⁻, CD103⁺ SIRP α ⁺, CD103⁻ SIRP α ⁻ and CD103⁻ SIRP α ⁺ populations (Fig. 8.7A). Due to the low expression of CD11b on CD1c⁺ blood DCs, we used SIRP α expression instead of CD11b to identify DC

populations (Fig. 3.16A). To the best of my knowledge, DC subsets characterised using these markers have not previously been described in human peripheral tissue. To align these subsets with the mature circulating DC populations in humans, CD141 and CD1c expression was assessed. CD1c was found to be predominantly co-expressed with SIRP α (Fig. 8.7B). As all murine lymph-migrating CD11b⁺ DCs also expressed SIRP α (389), it is not surprising that intestinal equivalents of the circulating human CD11b⁺ DC population (CD1c⁺ DCs) similarly express SIRP α . CD103⁺ SIRP α ⁻ DCs were the only DC subset to homogeneously express CD141 (Fig. 8.7B). This supports the idea that human CD141⁺ DCs are analogous to the murine CD103⁺ SIRP α ⁻ non-lymphoid and lymphoid CD8 α ⁺ DC populations (222, 334, 380). Additionally, the CD103⁻ SIRP α ⁻ population was observed to be heterogeneous for CD141 and CD1c expression (Fig. 8.7B). It is therefore interesting to speculate that this CD103⁻ SIRP α ⁻ population could either contain multiple populations that may be subdivided on markers not yet analysed. Further analysis of human intestinal DC subsets is required to fully characterise these populations.

In CD we observed a reduction in the CD103⁺ SIRP α ⁺ DC population, accompanied by an increase in the CD103⁻ SIRP α ⁻ DC subset (Fig. 8.9A). However, this comparison is based on one HC and one CD patient and further study is required using additional samples. Furthermore, as these were proportional differences they may be influenced by the presence of other leukocytes that accumulate during inflammation. However, if this observation were conserved, it would open interesting avenues for understanding the role of human intestinal DCs in IBD pathogenesis.

Despite limited availability of samples, further surface phenotyping of these novel human intestinal DC subsets was performed, specifically in relation to their expression of CCR2. As discussed, work from the Mowat group uncovered heterogeneity in CCR2 expression in murine intestinal DCs (Charlotte Scott, unpublished data). Furthermore, the CCR2⁺ and CCR2⁻ populations displayed different functions. Specifically, murine CD103⁻ CD11b⁺ DCs could be subdivided on the basis of CCR2 expression, with the CCR2⁺ subset preferentially inducing IL-17A production from interacting antigen-specific T cells (Charlotte Scott, unpublished data). In addition, CCR2^{-/-} mice are less able to induce Th17 responses. Consequently, I aimed to establish whether this heterogeneity also existed in human intestinal DC subsets. Interestingly, all intestinal DC subsets except the CD103⁺ SIRP α ⁻ DC population exhibited signs of heterogeneity with respect to CCR2 expression (Fig. 8.9B). Strikingly within the CD103⁻ SIRP α ⁻ subset, as for CD141, two distinct subsets could be differentiated by CCR2 expression levels. These data have been combined

with the data from the murine CCR2 DC data, and have been submitted for publication. Surprisingly in CD, we observed a complete lack of CCR2 expression on all DC subsets (Fig. 8.9C).

The role of CCR2 on these DC subsets remains elusive. Jimenez et al have postulated that CCR2 expression on Langerhans cells is required for complete maturation, migration and cytokine secretion (711). In addition, thymic SIRP α ⁺ DCs have been suggested to induce negative selection, migration and antigen uptake in a CCR2 dependent manner (712, 713). It will therefore be important to perform further experiments to establish the role of CCR2 on steady state DCs, and on DCs in inflamed tissues.

Overall, we have established a protocol for the successful isolation of immune populations from intestinal surgical resections from HCs and IBD patients. Using this protocol, we have for the first time identified at least 4 intestinal DC subsets based on the expression of CD103 and SIRP α . In addition, our preliminary results suggest that CCR2 is differentially expressed within human intestinal DC subsets.

Inflammatory/classical monocytes (Ly6C^{hi}) have recently been shown develop into intestinal macrophages in mice under both steady state and inflammatory conditions (225, 234). Blood monocyte contribution to tissue macrophage development appears to be unique to the gut as recent reports have suggested that the majority of tissue macrophage populations are maintained independent of blood monocytes (714, 715). The fate of newly extravasated monocytes in the gut mucosa appears to be dependent on the context of the environment into which they arrive. For instance, during intestinal inflammation monocyte maturation is disrupted, leading to a shift in the balance between resident and pro-inflammatory macrophage populations (225). Additionally, Bain et al observed equivalent processes occurring in human small intestinal tissue, with accumulation of CD14^{hi} macrophages in inflammation (225). Based on this data, we examined macrophage populations residing in colonic tissue under steady state and pro-inflammatory conditions. Early work suggested that only inflammatory macrophages within human intestinal mucosa expressed CD14 (423, 424, 716). However, several recent studies have identified CD14^{lo} macrophages in resting and inflammatory mucosal tissue (225, 234, 427, 691). In our hands, we could identify two intestinal macrophage populations based on expression of CD206 and CD14: CD14^{hi} CD206⁺ and CD14^{lo} CD206⁺ subsets (Fig. 8.10A). Both subsets expressed high levels of MHC II, CD33 and CD209 (Fig. 8.10B). Interestingly CD209 (DC-SIGN) is regarded as a DC-associated marker and consequently thought to be a

potential candidate for DC targeting (704, 705, 717). However, we observed higher expression of CD209 on both intestinal macrophage populations compared with total DCs (Fig. 8.10C). This observation could have important consequences for the efficiency of DC targeting. However this macrophage surface phenotyping is based on limited samples and so it is important that further studies are carried out. Both populations expressed CD64, recently shown to discriminate between DCs and macrophages in mice and men (Fig. 8.10B) (225, 234). In contrast to Bain et al where CD14^{lo} macrophages were found to lack CD11c expression, in our hands CD14^{hi} macrophages expressed lower levels of CD11c compared to CD14^{lo} macrophages and DCs.

Another interesting discrepancy between the two studies refers to the abundance of the individual macrophage subsets. Bain et al found the CD14^{lo} population in HC small intestinal tissue to dominate over the CD14^{hi} subset, with expansion of the CD14^{hi} population being observed in CD patients (225). These observations suggest that the CD14^{hi} population may represent the pro-inflammatory human macrophage population and would agree with previous studies showing that intestinal CD14⁺ macrophages only exist under inflammatory conditions (425, 427). Although referred to as ‘proinflammatory’, the precise functions of human intestinal macrophage populations have not yet been elucidated. In addition, our studies consistently (n=3) found the CD14^{hi} subset to represent the largest intestinal macrophage population in HC colonic tissue (Fig. 8.11A).

These disparities could reflect differences between macrophage tissue localisation. Tissue samples used by both studies differ not only in terms of anatomical location (colon vs small intestine) but also in terms of tissue processing. Both studies involved removal of muscle and fat layers, however differences in tissue processing could affect the proportion of isolated immune populations. The functions of these subsets as previously discussed remain unknown. Therefore understanding the roles of these populations in resting and inflammatory conditions may help elucidate these apparent differences. If CD14^{hi} macrophages are equivalent to the CX3CR1^{int} mouse pro-inflammatory subset (225), our results could suggest that HC tissue used in our studies may not be truly representative of steady state conditions. As previously stated, the study by Bain et al characterised populations isolated from the small intestine (225). In contrast, the majority of our studies were performed using colonic populations. Therefore anatomical location of immune populations could alter cell function. The colon harbours more commensal bacteria compared to the small intestine (718, 719). The presence of bacteria may affect cell function and phenotype. Given their expansion in disease, one could postulate that within

the small intestine, CD14^{hi} macrophages are the proinflammatory population that are outnumbered in the steady state by the CD14^{lo} resident population (225). In contrast, we observed domination of the CD14^{hi} subset in HC colonic tissue. Given the increased bacterial load and the need to prevent generation of aberrant responses to commensal bacteria, colonic CD14^{hi} macrophages may represent the resident, refractory population in contrast to the small intestine. These tissue differences highlight the requirement for functional characterisation of both CD14^{lo} and CD14^{hi} macrophages in the colon and small intestine. Furthermore, the role of intestinal flora on human intestinal macrophage populations remains an interesting avenue of research. Therefore several factors may contribute to the difference between these studies, emphasising the need for further investigation.

When analysing macrophage populations under inflammatory conditions, we observed expansion or infiltration of a population of CD206⁻ CD14⁺ cells within CD mucosa compared to HC tissue (Fig. 8.11A). This population expressed high levels of CD11c, CD64 and CD33, to the same level observed on 'resident' macrophage subsets (Fig. 8.11B). However, these cells did express slightly lower levels of MHC II. This surface phenotype corresponds to that of blood monocytes. Grimm et al demonstrated that CD14⁺ blood monocytes in IBD patients migrated to the inflamed mucosa (690). Therefore, our observed CD206⁻ CD14⁺ population could represent infiltrating monocytes in the process of differentiating into inflammatory macrophages, which may contribute to the perpetuation of IBD. In CD, although the CD14^{hi} population appeared to dominate (Fig. 8.11A), the comparative difference between CD14^{lo} and CD14^{hi} macrophages was not as great as that observed in the steady state. This observation, although only based on one CD patient again highlights the need for further investigation. Again, expansion of other leukocyte populations may affect the proportional analyses of these populations.

As stated previously, intestinal macrophages are unique in their development from circulating blood monocytes. Langerhans cell (LC) precursors in mice have recently been shown to seed the epidermis and mature into LCs, undergo rapid initial proliferation with continual low level proliferation being observed throughout life (720, 721). With regards to the development of tissue-resident macrophage populations, lung alveolar macrophages, kupffer cells and CNS-resident microglia appear to adopt similar replenishment mechanisms *in situ*, as described for LCs (589, 722-724). Members of Prof Mowat's laboratory investigating macrophage development in mice have generated data suggesting that intestinal macrophages lose the ability to proliferate *in situ* during development from

the neonatal period into adulthood (Calum Bain and Alberto Bravo, unpublished observations). Subsequently we set out to replicate their findings by assessing the proliferative capacity of intestinal macrophages in adults. CD14^{hi} macrophages did not proliferate *in vivo* (Fig. 8.12B). In contrast, the CD14^{lo} population exhibited very low levels of proliferation (Fig. 8.12B). These results suggest that macrophages in humans may turnover *in situ*, although further experiments will have to be performed to confirm this analysis. It would be interesting to study macrophage proliferation in colonic and small intestinal tissue due to the observed differences regarding macrophage populations previously described between tissue locations.

Overall, to the best of my knowledge we have identified and defined four populations of intestinal DC subsets. Initial studies suggest that these populations may be altered in IBD patients based on proportional analysis and expression of CCR2. Interestingly, we identified two macrophage populations in human intestinal mucosa, which may differ in function and phenotype depending on anatomical location and ability to proliferate *in vivo*. Following successful identification of DCs, macrophages and T cells, we hope to apply these techniques to AS patients in order to elucidate mechanisms and tissues involved in disease pathogenesis.

Chapter 9: Final discussion

9.1 General discussion

The aim of my PhD project was to investigate the immunopathogenesis of AS, focusing on the phenotype and function of circulating DCs to elucidate their role in this systemic, inflammatory disease. We hypothesised that human CD141⁺ DCs would be absent or diminished in AS patients, given that HLA-B27 TG SpA rats lack the equivalent DC subset (480). Our results led us to reject our initial hypothesis. However, our investigations of AS immunopathogenesis have elucidated several immunological pathways that may contribute to the development and perpetuation of AS.

Firstly, alterations to the proportions of circulating myeloid populations in AS patients may perpetuate aberrant immune responses. Our cohort of AS patients had significantly elevated levels of circulating CCR6⁺ activated T cells, and plasma IL-6 and IL-23, both involved in generation and maintenance of Th17 cells *in vivo* (107, 109, 112). These data, and the observation that most IL-17-secreting cells express CCR6, implicate Th17 involvement in disease pathogenesis. In AS patients, a significantly reduced proportion of their CD11c⁺ MHC II⁺ cells were of the CD1c⁺ DC subset. This was accompanied by an increase in total CD14⁻ CD16⁺ mononuclear cells. Functional analyses of these populations revealed an inherent ability of both subsets to induce CCR6 on interacting CD4⁺ T cells. Complementing this observation, preliminary data suggests that co-cultures containing CD14⁻ CD16⁺ mononuclear cells and allogeneic CD4⁺ T cells preferentially induce high levels of IL-6 production. Our data therefore indicate that in AS patients, a shift in their myeloid immune populations towards the CCR6-inducing CD14⁻ CD16⁺ mononuclear population may contribute to the induction of T cell-mediated pathogenesis through an IL-6-dependent induction of a Th17 phenotype (Fig. 9.1).

AS is a systemic inflammatory disease for which the aetiology remains elusive. Patient data and experimental results from HLA-B27 TG rats reveal an intriguing relationship between AS, the intestine and disease pathogenesis. Of the 90% of AS patients that fail to develop overt IBD, at least 50% display evidence of subclinical intestinal inflammation (4, 13, 441). Furthermore, HLA-B27 TG rats maintained under germ-free conditions do not develop SpA-like symptoms. These observations suggest a link between intestinal inflammation and disease pathogenesis. We provide an immunological basis for this relationship. We observed elevated levels of systemic inflammation, as determined by ESR and CRP, to be associated with a higher proportion of circulating CCR9⁺ and CCR6⁺ activated T cells. Both CCR9 and CCR6 mediate homing of immune populations to

mucosal tissues, particularly the intestine (171, 172, 176, 413). Our results indicate that systemic inflammation in AS patients is either driven from the intestine, or drives activated T cells to the intestine. Given that no correlations between disease severity and these CCR⁺ T populations were observed, this intestinal-linked systemic inflammation in AS patients may be transitory.

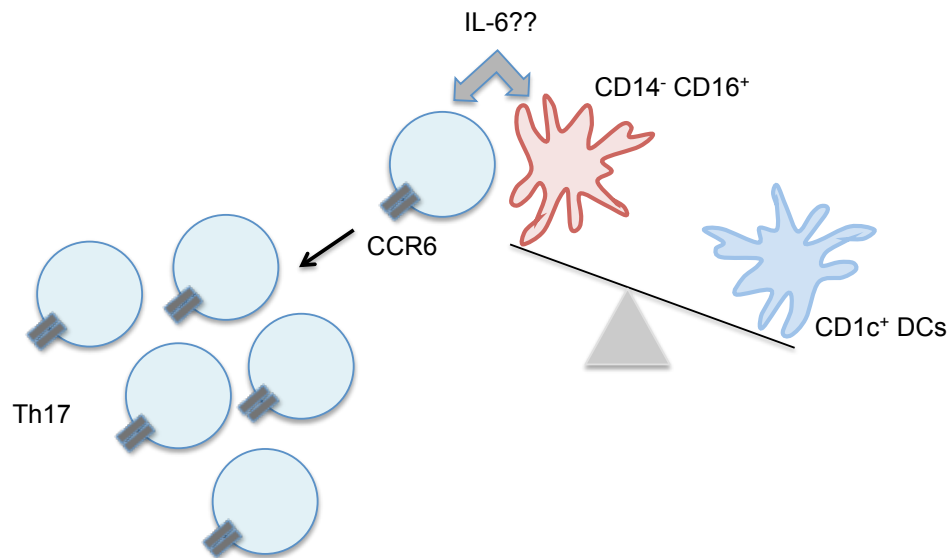


Figure 9.1: Role of DCs in disease pathogenesis

Circulating myeloid populations in AS patients are altered. Circulating CD14⁻ CD16⁺ mononuclear cells are increased in patient blood compared to CD1c⁺ DCs. CD14⁻ CD16⁺ mononuclear cell interactions with CD4⁺ T cells result in IL-6 secretion and CCR6 induction. These conditions support the generation of Th17 cells, presumed to be pathogenic in AS.

Many AS patient studies focus on the involvement of Th17 cells in disease pathogenesis. This emphasis has been fostered by numerous studies indicating promotion of aberrant Th17 responses in both humans (527, 528, 530) and HLA-B27 TG rats (479, 480). However, direct functional evidence regarding their contribution to human disease pathogenesis is negligible. Furthermore, analysis of extra-articular tissue involvement in AS patients reveals little involvement of IL-17-secreting lymphocytes in disease (540, 551). Our correlative analyses and immunological profiling of AS patients suggest a role for IL-23 in AS pathogenesis unconnected with maintenance of Th17 cells (112). Based on our data, we hypothesise that IL-23 may even be protective in AS (Fig. 9.2).

AS patients with elevated levels of circulating IL-23 have low levels of disease severity, suggesting that IL-23 may inhibit disease progression. Given this observation, we propose the following model: HLA-B27-induced loss of intestinal barrier integrity in AS patients promotes development of gut inflammation. The subsequent immune response is driven

innately by IL-23, and protective immunity depends upon engagement of the IL-23R on macrophages, neutrophils, T cells, DCs and numerous other immune populations. These IL-23-driven populations function to restore the integrity of the mucosal barrier, eradicate any potentially harmful pathogen and contain the potentially pathogenic inflammatory response in a Treg independent manner. However, if an adaptive immune response is developed, then disease progresses in an IL-23-independent manner. A side effect of this detrimental T cell response relates to the generation of intestinal-homing CCR6⁺ Tregs; Patients with elevated proportions of circulating CCR6-expressing Tregs were observed to be those patients with highest disease scores (BASMI and BASFI).

Overall, our data indicate that induction of intestinal responses, involving Treg priming within the MLN, promote disease progression in AS. Alternatively, when the intestinal immune response is dominated by IL-23, and in the absence of Tregs, patients are protected from disease progression. These differential outcomes may be determined by an individuals' genetic profile; compared to protected IL-23^{hi} patients, AS patients with low plasma IL-23 levels may have a distinct genetic background with specific SNPs that contribute to the loss of immune control and disease progression. Several other distinct factors may also contribute to this switch from regulation to disease progression. In addition, our data clearly highlight a pathway that connects intestinally activated T cells with systemic inflammation, which is uncoupled from overall disease progression.

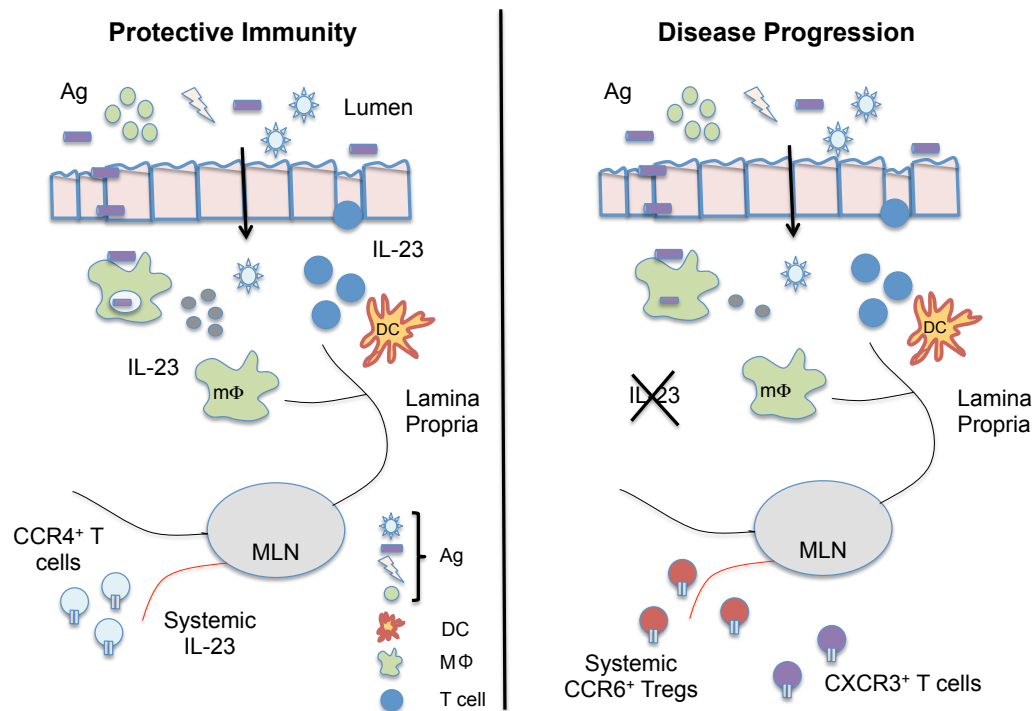


Figure 9.2: Immunopathogenesis of AS

Diagram depicting a potential mechanism for disease progression. Patients with low disease severity have high circulating levels of IL-23 that may provide protection by an undefined mechanism. In the absence of IL-23, a pathogenic adaptive immune response develops. This response generates CCR6⁺ Tregs that fail to control disease progression. mΦ = macrophage, DC = dendritic cell, MLN = mesenteric lymph node, Ag = antigen.

9.2 Conclusion

To date, no study has investigated the involvement of circulating DCs in the immunopathogenesis of AS. Therefore, the data presented here contribute significantly to our understanding of AS. Specifically, we observed alterations to the circulating myeloid profile of AS patients, which may promote the induction of aberrant immune responses through induction of CCR6 and secretion of IL-6. Furthermore, this study highlights the importance of the intestinal environment in driving systemic inflammation and indicates the potential for intestine-driven disease progression. In the future, we would aim to fully characterise the involvement of the intestinal immune system in the development and perpetuation of AS, through assessment of the functional attributes of tissue-resident DCs. Furthermore, investigation of the functions of IL-23 in the intestinal immune response may elucidate mechanisms of disease pathogenesis and aid development of future AS-targeted therapies.

References

1. Moll, J. M., I. Haslock, I. F. Macrae, and V. Wright. 1974. Associations between ankylosing spondylitis, psoriatic arthritis, Reiter's disease, the intestinal arthropathies, and Behcet's syndrome. *Medicine (Baltimore)* 53: 343–364.
2. Zochling, J., J. Brandt, and J. Braun. 2005. The current concept of spondyloarthritis with special emphasis on undifferentiated spondyloarthritis. *Rheumatology (Oxford)* 44: 1483–1491.
3. Dougados, M., and D. Baeten. 2011. Spondyloarthritis. *Lancet* 377: 2127–2137.
4. Braun, J., and J. Sieper. 2007. Ankylosing spondylitis. *Lancet* 369: 1379–1390.
5. D'Agostino, M. A., and I. Olivieri. 2006. Enthesitis. *Best Pract Res Clin Rheumatol* 20: 473–486.
6. Lautermann, D., and J. Braun. 2002. Ankylosing spondylitis--cardiac manifestations. *Clin Exp Rheumatol* 20: S11–5.
7. Rudwaleit, M., D. van der Heijde, R. Landewé, N. Akkoc, J. Brandt, C. T. Chou, M. Dougados, F. Huang, J. Gu, Y. Kirazli, F. Van Den Bosch, I. Olivieri, E. Roussou, S. Scarpato, I. J. Sørensen, R. Valle-Oñate, U. Weber, J. Wei, and J. Sieper. 2011. The Assessment of SpondyloArthritis International Society classification criteria for peripheral spondyloarthritis and for spondyloarthritis in general. *Ann Rheum Dis* 70: 25–31.
8. Rudwaleit, M., D. van der Heijde, R. Landewé, J. Listing, N. Akkoc, J. Brandt, J. Braun, C. T. Chou, E. Collantes-Estevez, M. Dougados, F. Huang, J. Gu, M. A. Khan, Y. Kirazli, W. P. Maksymowych, H. Mielants, I. J. Sørensen, S. Ozgocmen, E. Roussou, R. Valle-Oñate, U. Weber, J. Wei, and J. Sieper. 2009. The development of Assessment of SpondyloArthritis international Society classification criteria for axial spondyloarthritis (part II): validation and final selection. *Ann Rheum Dis* 68: 777–783.
9. Kim, T.-H., W.-S. Uhm, and R. D. Inman. 2005. Pathogenesis of ankylosing spondylitis and reactive arthritis. *Curr Opin Rheumatol* 17: 400–405.
10. Little, H., D. R. Swinson, and B. Cruickshank. 1976. Upward subluxation of the axis in ankylosing spondylitis. A clinical pathologic report. *Am. J. Med.* 60: 279–285.
11. Thomas, G. P., and M. A. Brown. 2010. Genetics and genomics of ankylosing spondylitis. *Immunol Rev* 233: 162–180.
12. Vander Cruyssen, B., C. Ribbens, A. Boonen, H. Mielants, K. de Vlam, J. Lenaerts, S. Steinfeld, F. Van den Bosch, L. Dewulf, and N. Vastesaeger. 2007. The epidemiology of ankylosing spondylitis and the commencement of anti-TNF therapy in daily rheumatology practice. *Ann Rheum Dis* 66: 1072–1077.
13. De Vos, M., C. Cuvelier, H. Mielants, E. Veys, F. Barbier, and A. Elewaut. 1989. Ileocolonoscopy in seronegative spondylarthropathy. *Gastroenterology* 96: 339–344.
14. Ball, J. 1971. Enthesopathy of rheumatoid and ankylosing spondylitis. *Ann Rheum Dis* 30: 213–223.
15. Gerster, J. C., T. L. Vischer, A. Bennani, and G. H. Fallet. 1977. The painful heel. Comparative study in rheumatoid arthritis, ankylosing spondylitis, Reiter's syndrome, and generalized osteoarthritis. *Ann Rheum Dis* 36: 343–348.
16. Ball, J. 1983. The enthesopathy of ankylosing spondylitis. *Br. J. Rheumatol.* 22: 25–28.
17. Schett, G. 2012. Independent development of inflammation and new bone formation in ankylosing spondylitis. *Arthritis Rheum* n/a–n/a.
18. Elewaut, D., and G. Schett. 2012. The development of ankylosis in ankylosing spondylitis is largely dependent on inflammation. *Arthritis Rheum*.
19. van der Heijde, D., R. Landewé, S. Einstein, P. Ory, D. Vosse, L. Ni, S.-L. Lin, W. Tsuji, and J. C. Davis. 2008. Radiographic progression of ankylosing spondylitis after up to two years of treatment with etanercept. *Arthritis Rheum* 58: 1324–1331.
20. van der Heijde, D., D. Salonen, B. N. Weissman, R. Landewé, W. P. Maksymowych, H. Kupper, S. Ballal, E. Gibson, R. Wong, Canadian (M03-606) study group, ATLAS

- study group. 2009. Assessment of radiographic progression in the spines of patients with ankylosing spondylitis treated with adalimumab for up to 2 years. *Arthritis Res Ther* 11: R127.
21. Maksymowych, W. P., P. Chiowchanwisawakit, T. Clare, S. J. Pedersen, M. Østergaard, and R. G. W. Lambert. 2009. Inflammatory lesions of the spine on magnetic resonance imaging predict the development of new syndesmophytes in ankylosing spondylitis: evidence of a relationship between inflammation and new bone formation. *Arthritis Rheum* 60: 93–102.
22. Baraliakos, X., J. Listing, M. Rudwaleit, J. Brandt, J. Sieper, and J. Braun. 2005. Radiographic progression in patients with ankylosing spondylitis after 2 years of treatment with the tumour necrosis factor alpha antibody infliximab. *Ann Rheum Dis* 64: 1462–1466.
23. Sieper, J., B. Porter-Brown, L. Thompson, O. Harari, and M. Dougados. 2013. Assessment of short-term symptomatic efficacy of tocilizumab in ankylosing spondylitis: results of randomised, placebo-controlled trials. *Ann Rheum Dis*.
24. Brewerton, D. A., F. D. Hart, A. Nicholls, M. Caffrey, D. C. James, and R. D. Sturrock. 1973. Ankylosing spondylitis and HL-A 27. *Lancet* 1: 904–907.
25. Caffrey, M. F., and D. C. James. 1973. Human lymphocyte antigen association in ankylosing spondylitis. *Nature* 242: 121.
26. Brown, M. A., L. G. Kennedy, A. J. MacGregor, C. Darke, E. Duncan, J. L. Shatford, A. Taylor, A. Calin, and P. Wordsworth. 1997. Susceptibility to ankylosing spondylitis in twins: the role of genes, HLA, and the environment. *Arthritis Rheum* 40: 1823–1828.
27. Brown, M. A. 2009. Genetics and the pathogenesis of ankylosing spondylitis. *Curr Opin Rheumatol* 21: 318–323.
28. Brown, M. A. 2010. Genetics of ankylosing spondylitis. *Curr Opin Rheumatol* 22: 126–132.
29. MacLean, I. L., S. Iqbal, P. Woo, A. C. Keat, R. A. Hughes, G. H. Kingsley, and S. C. Knight. 1993. HLA-B27 subtypes in the spondarthropathies. *Clin Exp Immunol* 91: 214–219.
30. Armas, J. B., S. Gonzalez, J. Martinez-Borra, F. Laranjeira, E. Ribeiro, J. Correia, M. L. Ferreira, M. Toste, A. López-Vazquez, and C. López-Larrea. 1999. Susceptibility to ankylosing spondylitis is independent of the Bw4 and Bw6 epitopes of HLA-B27 alleles. *Tissue Antigens* 53: 237–243.
31. López-Larrea, C., K. Sujirachato, N. K. Mehra, P. Chiewsilp, D. Isarangkura, U. Kanga, O. Dominguez, E. Coto, M. Penã, and F. Setiën. 1995. HLA-B27 subtypes in Asian patients with ankylosing spondylitis. Evidence for new associations. *Tissue Antigens* 45: 169–176.
32. Gonzalez-Roces, S., M. V. Alvarez, S. Gonzalez, A. Dieye, H. Makni, D. G. Woodfield, L. Housan, V. Konenkov, M. C. Abbadí, N. Grunnet, E. Coto, and C. López-Larrea. 1997. HLA-B27 polymorphism and worldwide susceptibility to ankylosing spondylitis. *Tissue Antigens* 49: 116–123.
33. García, F., D. Rognan, J. R. Lamas, A. Marina, and J. A. López de Castro. 1998. An HLA-B27 polymorphism (B*2710) that is critical for T-cell recognition has limited effects on peptide specificity. *Tissue Antigens* 51: 1–9.
34. García-Fernández, S., S. Gonzalez, A. Miña Blanco, J. Martinez-Borra, M. Blanco-Gelaz, A. López-Vazquez, and C. López-Larrea. 2001. New insights regarding HLA-B27 diversity in the Asian population. *Tissue Antigens* 58: 259–262.
35. Tamouza, R., I. Mansour, N. Bouguacha, S. Klayme, K. Djouadi, S. Laoussadi, M. Azoury, N. Dulphy, R. Ramasawmy, R. Krishnamoorthy, A. Toubert, R. Naman, and D. Charron. 2001. A new HLA-B*27 allele (B*2719) identified in a Lebanese patient affected with ankylosing spondylitis. *Tissue Antigens* 58: 30–33.
36. Brown, M. A., K. D. Pile, L. G. Kennedy, A. Calin, C. Darke, J. Bell, B. P. Wordsworth, and F. Cornélis. 1996. HLA class I associations of ankylosing spondylitis in the white population in the United Kingdom. *Ann Rheum Dis* 55: 268–270.

37. Cauli, A., A. Vacca, A. Mameli, G. Passiu, M. T. Fiorillo, R. Sorrentino, and A. Mathieu. 2007. A Sardinian patient with ankylosing spondylitis and HLA-B*2709 co-occurring with HLA-B*1403. *Arthritis Rheum* 56: 2807–2809.
38. D'Amato, M., M. T. Fiorillo, C. Carcassi, A. Mathieu, A. Zuccarelli, P. P. Bitti, R. Tosi, and R. Sorrentino. 1995. Relevance of residue 116 of HLA-B27 in determining susceptibility to ankylosing spondylitis. *Eur J Immunol* 25: 3199–3201.
39. Wellcome Trust Case Control Consortium, Australo-Anglo-American Spondylitis Consortium (TASC), P. R. Burton, D. G. Clayton, L. R. Cardon, N. Craddock, P. Deloukas, A. Duncanson, D. P. Kwiatkowski, M. I. McCarthy, W. H. Ouwehand, N. J. Samani, J. A. Todd, P. Donnelly, J. C. Barrett, D. Davison, D. Easton, D. M. Evans, H.-T. Leung, J. L. Marchini, A. P. Morris, C. C. A. Spencer, M. D. Tobin, A. P. Attwood, J. P. Boorman, B. Cant, U. Everson, J. M. Hussey, J. D. Jolley, A. S. Knight, K. Koch, E. Meech, S. Nutland, C. V. Prowse, H. E. Stevens, N. C. Taylor, G. R. Walters, N. M. Walker, N. A. Watkins, T. Winzer, R. W. Jones, W. L. McArdle, S. M. Ring, D. P. Strachan, M. Pembrey, G. Breen, D. St Clair, S. Caesar, K. Gordon-Smith, L. Jones, C. Fraser, E. K. Green, D. Grozeva, M. L. Hamshere, P. A. Holmans, I. R. Jones, G. Kirov, V. Moskivina, I. Nikolov, M. C. O'Donovan, M. J. Owen, D. A. Collier, A. Elkin, A. Farmer, R. Williamson, P. McGuffin, A. H. Young, I. N. Ferrier, S. G. Ball, A. J. Balmforth, J. H. Barrett, T. D. Bishop, M. M. Iles, A. Maqbool, N. Yuldasheva, A. S. Hall, P. S. Braund, R. J. Dixon, M. Mangino, S. Stevens, J. R. Thompson, F. Bredin, M. Tremelling, M. Parkes, H. Drummond, C. W. Lees, E. R. Nimmo, J. Satsangi, S. A. Fisher, A. Forbes, C. M. Lewis, C. M. Onnie, N. J. Prescott, J. Sanderson, C. G. Matthew, J. Barbour, M. K. Mohiuddin, C. E. Todhunter, J. C. Mansfield, T. Ahmad, F. R. Cummings, D. P. Jewell, J. Webster, M. J. Brown, M. G. Lathrop, J. Connell, A. Dominiczak, C. A. B. Marciano, B. Burke, R. Dobson, J. Gungadoo, K. L. Lee, P. B. Munroe, S. J. Newhouse, A. Onipinla, C. Wallace, M. Xue, M. Caulfield, M. Farrall, A. Barton, Biologics in RA Genetics and Genomics Study Syndicate (BRAGGS) Steering Committee, I. N. Bruce, H. Donovan, S. Eyre, P. D. Gilbert, S. L. Hilder, A. M. Hinks, S. L. John, C. Potter, A. J. Silman, D. P. M. Symmons, W. Thomson, J. Worthington, D. B. Dunger, B. Widmer, T. M. Frayling, R. M. Freathy, H. Lango, J. R. B. Perry, B. M. Shields, M. N. Weedon, A. T. Hattersley, G. A. Hitman, M. Walker, K. S. Elliott, C. J. Groves, C. M. Lindgren, N. W. Rayner, N. J. Timpson, E. Zeggini, M. Newport, G. Sirugo, E. Lyons, F. Vannberg, A. V. S. Hill, L. A. Bradbury, C. Farrar, J. J. Pointon, P. Wordsworth, M. A. Brown, J. A. Franklyn, J. M. Heward, M. J. Simmonds, S. C. L. Gough, S. Seal, Breast Cancer Susceptibility Collaboration (UK), M. R. Stratton, N. Rahman, M. Ban, A. Goris, S. J. Sawcer, A. Compston, D. Conway, M. Jallow, M. Newport, G. Sirugo, K. A. Rockett, S. J. Bumpstead, A. Chaney, K. Downes, M. J. R. Ghorri, R. Gwilliam, S. E. Hunt, M. Inouye, A. Keniry, E. King, R. McGinnis, S. Potter, R. Ravindrarajah, P. Whittaker, C. Widdén, D. Withers, N. J. Cardin, D. Davison, T. Ferreira, J. Pereira-Gale, I. B. Hallgrimsdóttir, B. N. Howie, Z. Su, Y. Y. Teo, D. Vukcevic, D. Bentley, M. A. Brown, A. Compston, M. Farrall, A. S. Hall, A. T. Hattersley, A. V. S. Hill, M. Parkes, M. Pembrey, M. R. Stratton, S. L. Mitchell, P. R. Newby, O. J. Brand, J. Carr-Smith, S. H. S. Pearce, R. McGinnis, A. Keniry, P. Deloukas, J. D. Reveille, X. Zhou, A.-M. Sims, A. Dowling, J. Taylor, T. Doan, J. C. Davis, L. Savage, M. M. Ward, T. L. Learch, M. H. Weisman, and M. Brown. 2007. Association scan of 14,500 nonsynonymous SNPs in four diseases identifies autoimmunity variants. *Nat. Genet.* 39: 1329–1337.
40. Australo-Anglo-American Spondyloarthritis Consortium (TASC), J. D. Reveille, A.-M. Sims, P. Danoy, D. M. Evans, P. Leo, J. J. Pointon, R. Jin, X. Zhou, L. A. Bradbury, L. H. Appleton, J. C. Davis, L. Diekman, T. Doan, A. Dowling, R. Duan, E. L. Duncan, C. Farrar, J. Hadler, D. Harvey, T. Karaderi, R. Mogg, E. Pomeroy, K. Pryce, J. Taylor, L. Savage, P. Deloukas, V. Kumanduri, L. Peltonen, S. M. Ring, P. Whittaker, E. Glazov, G. P. Thomas, W. P. Maksymowycz, R. D. Inman, M. M. Ward, M. A. Stone, M. H. Weisman, B. P. Wordsworth, and M. A. Brown. 2010. Genome-wide association study of

- ankylosing spondylitis identifies non-MHC susceptibility loci. *Nat. Genet.* 42: 123–127.
41. Danoy, P., K. Pryce, J. Hadler, L. A. Bradbury, C. Farrar, J. Pointon, Australo-Anglo-American Spondyloarthritis Consortium, M. Ward, M. Weisman, J. D. Reveille, B. P. Wordsworth, M. A. Stone, Spondyloarthritis Research Consortium of Canada, W. P. Maksymowych, P. Rahman, D. Gladman, R. D. Inman, and M. A. Brown. 2010. Association of variants at 1q32 and STAT3 with ankylosing spondylitis suggests genetic overlap with Crohn's disease. *PLoS Genet.* 6: e1001195.
42. Davidson, S. I., Y. Liu, P. A. Danoy, X. Wu, G. P. Thomas, L. Jiang, L. Sun, N. Wang, J. Han, H. Han, Australo-Anglo-American Spondyloarthritis Consortium, P. M. Visscher, M. A. Brown, and H. Xu. 2011. Association of STAT3 and TNFRSF1A with ankylosing spondylitis in Han Chinese. *Ann Rheum Dis* 70: 289–292.
43. Duerr, R. H., K. D. Taylor, S. R. Brant, J. D. Rioux, M. S. Silverberg, M. J. Daly, A. H. Steinhart, C. Abraham, M. Regueiro, A. Griffiths, T. Dassopoulos, A. Bitton, H. Yang, S. Targan, L. W. Datta, E. O. Kistner, L. P. Schumm, A. T. Lee, P. K. Gregersen, M. M. Barmada, J. I. Rotter, D. L. Nicolae, and J. H. Cho. 2006. A genome-wide association study identifies IL23R as an inflammatory bowel disease gene. *Science* 314: 1461–1463.
44. Cargill, M., M. Cargill, S. J. Schrodi, S. J. Schrodi, M. Chang, M. Chang, V. E. Garcia, V. E. Garcia, R. Brandon, R. Brandon, K. P. Callis, K. P. Callis, N. Matsunami, N. Matsunami, K. G. Ardlie, K. G. Ardlie, D. Civello, D. Civello, J. J. Catanese, J. J. Catanese, D. U. Leong, D. U. Leong, J. M. Panko, J. M. Panko, L. B. McAllister, L. B. McAllister, C. B. Hansen, C. B. Hansen, J. Papenfuss, J. Papenfuss, S. M. Prescott, S. M. Prescott, T. J. White, T. J. White, M. F. Leppert, M. F. Leppert, G. G. Krueger, G. G. Krueger, A. B. Begovich, and A. B. Begovich. 2007. A large-scale genetic association study confirms IL12B and leads to the identification of IL23R as psoriasis-risk genes. 80: 273–290.
45. Evans, D. M., C. C. A. Spencer, J. J. Pointon, Z. Su, D. Harvey, G. Kochan, U. Oppermann, U. Opperman, A. Dilthey, M. Pirinen, M. A. Stone, L. Appleton, L. Moutsianas, L. Moutsianis, S. Leslie, T. Wordsworth, T. J. Kenna, T. Karaderi, G. P. Thomas, M. M. Ward, M. H. Weisman, C. Farrar, L. A. Bradbury, P. Danoy, R. D. Inman, W. Maksymowych, D. Gladman, P. Rahman, Spondyloarthritis Research Consortium of Canada (SPARCC), A. Morgan, H. Marzo-Ortega, P. Bowness, K. Gaffney, J. S. H. Gaston, M. Smith, J. Bruges-Armas, A.-R. Couto, R. Sorrentino, F. Paladini, M. A. Ferreira, H. Xu, Y. Liu, L. Jiang, C. Lopez-Larrea, R. Díaz-Peña, A. López-Vázquez, T. Zayats, G. Band, C. Bellenguez, H. Blackburn, J. M. Blackwell, E. Bramon, S. J. Bumpstead, J. P. Casas, A. Corvin, N. Craddock, P. Deloukas, S. Dronov, A. Duncanson, S. Edkins, C. Freeman, M. Gillman, E. Gray, R. Gwilliam, N. Hammond, S. E. Hunt, J. Jankowski, A. Jayakumar, C. Langford, J. Liddle, H. S. Markus, C. G. Mathew, O. T. McCann, M. I. McCarthy, C. N. A. Palmer, L. Peltonen, R. Plomin, S. C. Potter, A. Rautanen, R. Ravindrarajah, M. Ricketts, N. Samani, S. J. Sawcer, A. Strange, R. C. Trembath, A. C. Viswanathan, M. Waller, P. Weston, P. Whittaker, S. Widaa, N. W. Wood, G. McVean, J. D. Reveille, B. P. Wordsworth, M. A. Brown, P. Donnelly, Australo-Anglo-American Spondyloarthritis Consortium (TASC), Wellcome Trust Case Control Consortium 2 (WTCCC2). 2011. Interaction between ERAP1 and HLA-B27 in ankylosing spondylitis implicates peptide handling in the mechanism for HLA-B27 in disease susceptibility. *Nat. Genet.* 43: 761–767.
46. Cui, X., F. N. Rouhani, F. Hawari, and S. J. Levine. 2003. Shedding of the type II IL-1 decoy receptor requires a multifunctional aminopeptidase, aminopeptidase regulator of TNF receptor type 1 shedding. *J Immunol* 171: 6814–6819.
47. Chan, A. T., S. D. Kollnberger, L. R. Wedderburn, and P. Bowness. 2005. Expansion and enhanced survival of natural killer cells expressing the killer immunoglobulin-like receptor KIR3DL2 in spondylarthritis. *Arthritis Rheum* 52: 3586–3595.
48. Pappu, B. P., A. Borodovsky, T. S. Zheng, X. Yang, P. Wu, X. Dong, S. Weng, B. Browning, M. L. Scott, L. Ma, L. Su, Q. Tian, P. Schneider, R. A. Flavell, C. Dong, and L.

- C. Burkly. 2008. TL1A-DR3 interaction regulates Th17 cell function and Th17-mediated autoimmune disease. *Journal of Experimental Medicine* 205: 1049–1062.
49. Taylan, A., I. Sari, D. L. Kozaci, A. Yuksel, S. Bilge, Y. Yildiz, G. Sop, I. Coker, N. Gunay, and N. Akkoc. 2011. Evaluation of the T helper 17 axis in ankylosing spondylitis. *Rheumatol Int.*
50. Yamazaki, K., D. McGovern, J. Ragoussis, M. Paolucci, H. Butler, D. Jewell, L. Cardon, M. Takazoe, T. Tanaka, T. Ichimori, S. Saito, A. Sekine, A. Iida, A. Takahashi, T. Tsunoda, M. Lathrop, and Y. Nakamura. 2005. Single nucleotide polymorphisms in TNFSF15 confer susceptibility to Crohn's disease. *Hum. Mol. Genet.* 14: 3499–3506.
51. LeibundGut-Landmann, S., O. Gross, M. J. Robinson, F. Osorio, E. C. Slack, S. V. Tsoni, E. Schweighoffer, V. Tybulewicz, G. D. Brown, J. Ruland, and C. Reis e Sousa. 2007. Syk- and CARD9-dependent coupling of innate immunity to the induction of T helper cells that produce interleukin 17. *Nat Immunol* 8: 630–638.
52. Itohara, S., N. Nakanishi, O. Kanagawa, R. Kubo, and S. Tonegawa. 1989. Monoclonal antibodies specific to native murine T-cell receptor gamma delta: analysis of gamma delta T cells during thymic ontogeny and in peripheral lymphoid organs. *Proc Natl Acad Sci USA* 86: 5094–5098.
53. Janeway, C. A. 1988. T-cell development. Accessories or coreceptors? *Nature* 335: 208–210.
54. Starr, T. K., S. C. Jameson, and K. A. Hogquist. 2003. Positive and negative selection of T cells. *Annu Rev Immunol* 21: 139–176.
55. De Rosa, S. C., L. A. Herzenberg, L. A. Herzenberg, and M. Roederer. 2001. 11-color, 13-parameter flow cytometry: identification of human naive T cells by phenotype, function, and T-cell receptor diversity. *Nat. Med.* 7: 245–248.
56. Picker, L. J., J. R. Treer, B. Ferguson-Darnell, P. A. Collins, D. Buck, and L. W. Terstappen. 1993. Control of lymphocyte recirculation in man. I. Differential regulation of the peripheral lymph node homing receptor L-selectin on T cells during the virgin to memory cell transition. *J Immunol* 150: 1105–1121.
57. Catalina, M. D., M. C. Carroll, H. Arizpe, A. Takashima, P. Estess, and M. H. Siegelman. 1996. The route of antigen entry determines the requirement for L-selectin during immune responses. *J Exp Med* 184: 2341–2351.
58. Steeber, D. A., P. Engel, A. S. Miller, M. P. Sheetz, and T. F. Tedder. 1997. Ligation of L-selectin through conserved regions within the lectin domain activates signal transduction pathways and integrin function in human, mouse, and rat leukocytes. *J Immunol* 159: 952–963.
59. Butcher, E. C., and L. J. Picker. 1996. Lymphocyte homing and homeostasis. *Science* 272: 60–66.
60. Zhu, J., and W. E. Paul. 2008. CD4 T cells: fates, functions, and faults. *Blood* 112: 1557–1569.
61. Smith, K. A., S. Gillis, P. E. Baker, D. McKenzie, and F. W. Ruscetti. 1979. T-cell growth factor-mediated T-cell proliferation. *Ann. N. Y. Acad. Sci.* 332: 423–432.
62. Leonard, W. J., J. M. Depper, T. Uchiyama, K. A. Smith, T. A. Waldmann, and W. C. Greene. 1982. A monoclonal antibody that appears to recognize the receptor for human T-cell growth factor; partial characterization of the receptor. *Nature* 300: 267–269.
63. Robb, R. J., A. Munck, and K. A. Smith. 1981. T cell growth factor receptors. Quantitation, specificity, and biological relevance. *J Exp Med* 154: 1455–1474.
64. Hamann, D., P. A. Baars, B. Hooibrink, and R. W. van Lier. 1996. Heterogeneity of the human CD4+ T-cell population: two distinct CD4+ T-cell subsets characterized by coexpression of CD45RA and CD45RO isoforms. *Blood* 88: 3513–3521.
65. Itoh, M., T. Takahashi, N. Sakaguchi, Y. Kuniyasu, J. Shimizu, F. Otsuka, and S. Sakaguchi. 1999. Thymus and autoimmunity: production of CD25+CD4+ naturally anergic and suppressive T cells as a key function of the thymus in maintaining immunologic self-tolerance. *J Immunol* 162: 5317–5326.

66. Dieckmann, D., H. Plottner, S. Berchtold, T. Berger, and G. Schuler. 2001. Ex vivo isolation and characterization of CD4(+)CD25(+) T cells with regulatory properties from human blood. *J Exp Med* 193: 1303–1310.
67. Annunziato, F., L. Cosmi, F. Liotta, E. Lazzeri, R. Manetti, V. Vanini, P. Romagnani, E. Maggi, and S. Romagnani. 2002. Phenotype, localization, and mechanism of suppression of CD4(+)CD25(+) human thymocytes. *J Exp Med* 196: 379–387.
68. Fehérvári, Z., and S. Sakaguchi. 2004. Development and function of CD25+CD4+ regulatory T cells. *Curr Opin Immunol* 16: 203–208.
69. Jonuleit, H., E. Schmitt, M. Stassen, A. Tuettgenberg, J. Knop, and A. H. Enk. 2001. Identification and functional characterization of human CD4(+)CD25(+) T cells with regulatory properties isolated from peripheral blood. *J Exp Med* 193: 1285–1294.
70. Chen, W., W. Jin, N. Hardegen, K.-J. Lei, L. Li, N. Marinos, G. McGrady, and S. M. Wahl. 2003. Conversion of peripheral CD4+CD25- naive T cells to CD4+CD25+ regulatory T cells by TGF-beta induction of transcription factor Foxp3. *J Exp Med* 198: 1875–1886.
71. Groux, H., A. O'Garra, M. Bigler, M. Rouleau, S. Antonenko, J. E. de Vries, and M. G. Roncarolo. 1997. A CD4+ T-cell subset inhibits antigen-specific T-cell responses and prevents colitis. *Nature* 389: 737–742.
72. Wakkach, A., F. Cottrez, and H. Groux. 2001. Differentiation of regulatory T cells 1 is induced by CD2 costimulation. *J Immunol* 167: 3107–3113.
73. Farber, D. L. 2000. T Cell Memory: Heterogeneity and Mechanisms. *Clinical Immunology* 95: 173–181.
74. Sallusto, F., D. Lenig, R. Förster, M. Lipp, and A. Lanzavecchia. 1999. Two subsets of memory T lymphocytes with distinct homing potentials and effector functions. *Nature* 401: 708–712.
75. Lanzavecchia, A., and F. Sallusto. 2005. Understanding the generation and function of memory T cell subsets. *Curr Opin Immunol* 17: 326–332.
76. Mosmann, T. R., H. Cherwinski, M. W. Bond, M. A. Giedlin, and R. L. Coffman. 1986. Two types of murine helper T cell clone. I. Definition according to profiles of lymphokine activities and secreted proteins. *J Immunol* 136: 2348–2357.
77. Del Prete, G. F., M. De Carli, C. Mastromauro, R. Biagiotti, D. Macchia, P. Falagiani, M. Ricci, and S. Romagnani. 1991. Purified protein derivative of *Mycobacterium tuberculosis* and excretory-secretory antigen(s) of *Toxocara canis* expand in vitro human T cells with stable and opposite (type 1 T helper or type 2 T helper) profile of cytokine production. *J Clin Invest* 88: 346–350.
78. Mosmann, T. R., and S. Sad. 1996. The expanding universe of T-cell subsets: Th1, Th2 and more. *Immunol Today* 17: 138–146.
79. Zurawski, G., and J. E. de Vries. 1994. Interleukin 13, an interleukin 4-like cytokine that acts on monocytes and B cells, but not on T cells. *Immunol Today* 15: 19–26.
80. Mosmann, T. R., and R. L. Coffman. 1989. TH1 and TH2 cells: different patterns of lymphokine secretion lead to different functional properties. *Annu Rev Immunol* 7: 145–173.
81. Pace, J. L., S. W. Russell, B. A. Torres, H. M. Johnson, and P. W. Gray. 1983. Recombinant mouse gamma interferon induces the priming step in macrophage activation for tumor cell killing. *J Immunol* 130: 2011–2013.
82. Murray, H. W., G. L. Spitalny, and C. F. Nathan. 1985. Activation of mouse peritoneal macrophages in vitro and in vivo by interferon-gamma. *J Immunol* 134: 1619–1622.
83. Szabo, S. J., S. T. Kim, G. L. Costa, X. Zhang, C. G. Fathman, and L. H. Glimcher. 2000. A novel transcription factor, T-bet, directs Th1 lineage commitment. *Cell* 100: 655–669.
84. Letimier, F. A., N. Passini, S. Gasparian, E. Bianchi, and L. Rogge. 2007. Chromatin remodeling by the SWI/SNF-like BAF complex and STAT4 activation synergistically induce IL-12Rbeta2 expression during human Th1 cell differentiation. *EMBO J.* 26: 1292–

1302.

85. Afkarian, M., J. R. Sedy, J. Yang, N. G. Jacobson, N. Cereb, S. Y. Yang, T. L. Murphy, and K. M. Murphy. 2002. T-bet is a STAT1-induced regulator of IL-12R expression in naïve CD4⁺ T cells. *Nat Immunol* 3: 549–557.
86. Jacobson, N. G., S. J. Szabo, R. M. Weber-Nordt, Z. Zhong, R. D. Schreiber, J. E. Darnell, and K. M. Murphy. 1995. Interleukin 12 signaling in T helper type 1 (Th1) cells involves tyrosine phosphorylation of signal transducer and activator of transcription (Stat)3 and Stat4. *J Exp Med* 181: 1755–1762.
87. Bacon, C. M., E. F. Petricoin, J. R. Ortaldo, R. C. Rees, A. C. Lerner, J. A. Johnston, and J. J. O'Shea. 1995. Interleukin 12 induces tyrosine phosphorylation and activation of STAT4 in human lymphocytes. *Proc Natl Acad Sci USA* 92: 7307–7311.
88. Athie-Morales, V., H. H. Smits, D. A. Cantrell, and C. M. U. Hilkens. 2004. Sustained IL-12 signaling is required for Th1 development. *J Immunol* 172: 61–69.
89. Hsieh, C. S., S. E. Macatonia, C. S. Tripp, S. F. Wolf, A. O'Garra, and K. M. Murphy. 1993. Development of TH1 CD4⁺ T cells through IL-12 produced by Listeria-induced macrophages. *Science* 260: 547–549.
90. Takeda, A., S. Hamano, A. Yamanaka, T. Hanada, T. Ishibashi, T. W. Mak, A. Yoshimura, and H. Yoshida. 2003. Cutting edge: role of IL-27/WSX-1 signaling for induction of T-bet through activation of STAT1 during initial Th1 commitment. *J Immunol* 170: 4886–4890.
91. Lucas, S., N. Ghilardi, J. Li, and F. J. de Sauvage. 2003. IL-27 regulates IL-12 responsiveness of naïve CD4⁺ T cells through Stat1-dependent and -independent mechanisms. *Proc Natl Acad Sci USA* 100: 15047–15052.
92. Szabo, S. J., A. S. Dighe, U. Gubler, and K. M. Murphy. 1997. Regulation of the interleukin (IL)-12R beta 2 subunit expression in developing T helper 1 (Th1) and Th2 cells. *J Exp Med* 185: 817–824.
93. Ma, X., J. M. Chow, G. Gri, G. Carra, F. Gerosa, S. F. Wolf, R. Dzialo, and G. Trinchieri. 1996. The interleukin 12 p40 gene promoter is primed by interferon gamma in monocytic cells. *J Exp Med* 183: 147–157.
94. Zheng, W., and R. A. Flavell. 1997. The transcription factor GATA-3 is necessary and sufficient for Th2 cytokine gene expression in CD4 T cells. *Cell* 89: 587–596.
95. Zhang, D. H., L. Cohn, P. Ray, K. Bottomly, and A. Ray. 1997. Transcription factor GATA-3 is differentially expressed in murine Th1 and Th2 cells and controls Th2-specific expression of the interleukin-5 gene. *J Biol Chem* 272: 21597–21603.
96. Tahvanainen, J., M. Pykäläinen, T. Kallonen, H. Lähteenmäki, O. Rasool, and R. Lahesmaa. 2006. Enrichment of nucleofected primary human CD4⁺ T cells: a novel and efficient method for studying gene function and role in human primary T helper cell differentiation. *J. Immunol. Methods* 310: 30–39.
97. Lund, R. J., M. Löytömäki, T. Naumanen, C. Dixon, Z. Chen, H. Ahlfors, S. Tuomela, J. Tahvanainen, J. Scheinin, T. Henttinen, O. Rasool, and R. Lahesmaa. 2007. Genome-wide identification of novel genes involved in early Th1 and Th2 cell differentiation. *J Immunol* 178: 3648–3660.
98. Ouyang, W., S. H. Ranganath, K. Weindel, D. Bhattacharya, T. L. Murphy, W. C. Sha, and K. M. Murphy. 1998. Inhibition of Th1 development mediated by GATA-3 through an IL-4-independent mechanism. *Immunity* 9: 745–755.
99. Hsieh, C. S., A. B. Heimberger, J. S. Gold, A. O'Garra, and K. M. Murphy. 1992. Differential regulation of T helper phenotype development by interleukins 4 and 10 in an alpha beta T-cell-receptor transgenic system. *Proc Natl Acad Sci USA* 89: 6065–6069.
100. Cote-Sierra, J., G. Foucras, L. Guo, L. Chiodetti, H. A. Young, J. Hu-Li, J. Zhu, and W. E. Paul. 2004. Interleukin 2 plays a central role in Th2 differentiation. *Proc Natl Acad Sci USA* 101: 3880–3885.
101. Nelms, K., A. D. Keegan, J. Zamorano, J. J. Ryan, and W. E. Paul. 1999. The IL-4 receptor: signaling mechanisms and biologic functions. *Annu Rev Immunol* 17: 701–738.

102. Fiorentino, D. F., A. Zlotnik, P. Vieira, T. R. Mosmann, M. Howard, K. W. Moore, and A. O'Garra. 1991. IL-10 acts on the antigen-presenting cell to inhibit cytokine production by Th1 cells. *J Immunol* 146: 3444–3451.
103. Cua, D. J., J. Sherlock, Y. Chen, C. A. Murphy, B. Joyce, B. Seymour, L. Lucian, W. To, S. Kwan, T. Churakova, S. Zurawski, M. Wiekowski, S. A. Lira, D. Gorman, R. A. Kastelein, and J. D. Sedgwick. 2003. Interleukin-23 rather than interleukin-12 is the critical cytokine for autoimmune inflammation of the brain. *Nature* 421: 744–748.
104. Murphy, C. A., C. L. Langrish, Y. Chen, W. Blumenschein, T. McClanahan, R. A. Kastelein, J. D. Sedgwick, and D. J. Cua. 2003. Divergent pro- and antiinflammatory roles for IL-23 and IL-12 in joint autoimmune inflammation. *J Exp Med* 198: 1951–1957.
105. Langrish, C. L., Y. Chen, W. M. Blumenschein, J. Mattson, B. Basham, J. D. Sedgwick, T. McClanahan, R. A. Kastelein, and D. J. Cua. 2005. IL-23 drives a pathogenic T cell population that induces autoimmune inflammation. *J Exp Med* 201: 233–240.
106. Harrington, L. E., R. D. Hatton, P. R. Mangan, H. Turner, T. L. Murphy, K. M. Murphy, and C. T. Weaver. 2005. Interleukin 17-producing CD4⁺ effector T cells develop via a lineage distinct from the T helper type 1 and 2 lineages. *Nat Immunol* 6: 1123–1132.
107. Wilson, N. J., K. Boniface, J. R. Chan, B. S. McKenzie, W. M. Blumenschein, J. D. Mattson, B. Basham, K. Smith, T. Chen, F. Morel, J.-C. Lecron, R. A. Kastelein, D. J. Cua, T. K. McClanahan, E. P. Bowman, and R. de Waal Malefyt. 2007. Development, cytokine profile and function of human interleukin 17-producing helper T cells. *Nat Immunol* 8: 950–957.
108. Bettelli, E., Y. Carrier, W. Gao, T. Korn, T. B. Strom, M. Oukka, H. L. Weiner, and V. K. Kuchroo. 2006. Reciprocal developmental pathways for the generation of pathogenic effector TH17 and regulatory T cells. *Nature* 441: 235–238.
109. Acosta-Rodriguez, E. V., G. Napolitani, A. Lanzavecchia, and F. Sallusto. 2007. Interleukins 1 β and 6 but not transforming growth factor- β are essential for the differentiation of interleukin 17-producing human T helper cells. *Nat Immunol* 8: 942–949.
110. Ivanov, I. I., B. S. McKenzie, L. Zhou, C. E. Tadokoro, A. Lepelley, J. J. Lafaille, D. J. Cua, and D. R. Littman. 2006. The orphan nuclear receptor ROR γ directs the differentiation program of proinflammatory IL-17⁺ T helper cells. *Cell* 126: 1121–1133.
111. Milner, J. D., J. M. Brenchley, A. Laurence, A. F. Freeman, B. J. Hill, K. M. Elias, Y. Kanno, C. Spalding, H. Z. Elloumi, M. L. Paulson, J. Davis, A. Hsu, A. I. Asher, J. O'Shea, S. M. Holland, W. E. Paul, and D. C. Douek. 2008. Impaired T(H)17 cell differentiation in subjects with autosomal dominant hyper-IgE syndrome. *Nature* 452: 773–776.
112. Stritesky, G. L., N. Yeh, and M. H. Kaplan. 2008. IL-23 promotes maintenance but not commitment to the Th17 lineage. *The Journal of Immunology* 181: 5948–5955.
113. Fujino, S., A. Andoh, S. Bamba, A. Ogawa, K. Hata, Y. Araki, T. Bamba, and Y. Fujiyama. 2003. Increased expression of interleukin 17 in inflammatory bowel disease. *Gut* 52: 65–70.
114. Weaver, C. T., R. D. Hatton, P. R. Mangan, and L. E. Harrington. 2007. IL-17 family cytokines and the expanding diversity of effector T cell lineages. *Annu Rev Immunol* 25: 821–852.
115. Nistala, K., S. Adams, H. Cambrook, S. Ursu, B. Olivito, W. de Jager, J. G. Evans, R. Cimaz, M. Bajaj-Elliott, and L. R. Wedderburn. 2010. Th17 plasticity in human autoimmune arthritis is driven by the inflammatory environment. *Proc Natl Acad Sci USA* 107: 14751–14756.
116. Nistala, K., H. Moncrieffe, K. R. Newton, H. Varsani, P. Hunter, and L. R. Wedderburn. 2008. Interleukin-17-producing T cells are enriched in the joints of children with arthritis, but have a reciprocal relationship to regulatory T cell numbers. *Arthritis Rheum* 58: 875–887.
117. Lee, Y. K., H. Turner, C. L. Maynard, J. R. Oliver, D. Chen, C. O. Elson, and C. T. Weaver. 2009. Late developmental plasticity in the T helper 17 lineage. *Immunity* 30: 92–

107.

118. Bending, D., H. De la Peña, M. Veldhoen, J. M. Phillips, C. Uyttenhove, B. Stockinger, and A. Cooke. 2009. Highly purified Th17 cells from BDC2.5NOD mice convert into Th1-like cells in NOD/SCID recipient mice. *J Clin Invest* 119: 565–572.
119. Mucida, D., Y. Park, G. Kim, O. Turovskaya, I. Scott, M. Kronenberg, and H. Cheroutre. 2007. Reciprocal TH17 and regulatory T cell differentiation mediated by retinoic acid. *Science* 317: 256–260.
120. Annunziato, F., L. Cosmi, V. Santarlasci, L. Maggi, F. Liotta, B. Mazzinghi, E. Parente, L. Fili, S. Ferri, F. Frosali, F. Giudici, P. Romagnani, P. Parronchi, F. Tonelli, E. Maggi, and S. Romagnani. 2007. Phenotypic and functional features of human Th17 cells. *J Exp Med* 204: 1849–1861.
121. Jiang, S., and C. Dong. 2013. A complex issue on CD4(+) T-cell subsets. *Immunol Rev* 252: 5–11.
122. Dardalhon, V., A. Awasthi, H. Kwon, G. Galileos, W. Gao, R. A. Sobel, M. Mitsdoerffer, T. B. Strom, W. Elyaman, I.-C. Ho, S. Khoury, M. Oukka, and V. K. Kuchroo. 2008. IL-4 inhibits TGF-beta-induced Foxp3+ T cells and, together with TGF-beta, generates IL-9+ IL-10+ Foxp3(-) effector T cells. *Nat Immunol* 9: 1347–1355.
123. Veldhoen, M., C. Uyttenhove, J. van Snick, H. Helmby, A. Westendorf, J. Buer, B. Martin, C. Wilhelm, and B. Stockinger. 2008. Transforming growth factor-beta “reprograms” the differentiation of T helper 2 cells and promotes an interleukin 9-producing subset. *Nat Immunol* 9: 1341–1346.
124. Chang, H.-C., S. Sehra, R. Goswami, W. Yao, Q. Yu, G. L. Stritesky, R. Jabeen, C. McKinley, A.-N. Ahyi, L. Han, E. T. Nguyen, M. J. Robertson, N. B. Perumal, R. S. Tepper, S. L. Nutt, and M. H. Kaplan. 2010. The transcription factor PU.1 is required for the development of IL-9-producing T cells and allergic inflammation. *Nat Immunol* 11: 527–534.
125. Staudt, V., E. Bothur, M. Klein, K. Lingnau, S. Reuter, N. Grebe, B. Gerlitzki, M. Hoffmann, A. Ulges, C. Taube, N. Dehzad, M. Becker, M. Stassen, A. Steinborn, M. Lohoff, H. Schild, E. Schmitt, and T. Bopp. 2010. Interferon-regulatory factor 4 is essential for the developmental program of T helper 9 cells. *Immunity* 33: 192–202.
126. Jones, C. P., L. G. Gregory, B. Causton, G. A. Campbell, and C. M. Lloyd. 2012. Activin A and TGF- β promote T(H)9 cell-mediated pulmonary allergic pathology. *J Allergy Clin. Immunol.* 129: 1000–10.e3.
127. Kaplan, M. H., Y. L. Sun, T. Hoey, and M. J. Grusby. 1996. Impaired IL-12 responses and enhanced development of Th2 cells in Stat4-deficient mice. *Nature* 382: 174–177.
128. Trifari, S., C. D. Kaplan, E. H. Tran, N. K. Crellin, and H. Spits. 2009. Identification of a human helper T cell population that has abundant production of interleukin 22 and is distinct from T(H)-17, T(H)1 and T(H)2 cells. *Nat Immunol* 10: 864–871.
129. Eyerich, S., K. Eyerich, D. Pennino, T. Carbone, F. Nasorri, S. Pallotta, F. Cianfarani, T. Odorisio, C. Traidl-Hoffmann, H. Behrendt, S. R. Durham, C. B. Schmidt-Weber, and A. Cavani. 2009. Th22 cells represent a distinct human T cell subset involved in epidermal immunity and remodeling. *J Clin Invest* 119: 3573–3585.
130. Duhon, T., R. Geiger, D. Jarrossay, A. Lanzavecchia, and F. Sallusto. 2009. Production of interleukin 22 but not interleukin 17 by a subset of human skin-homing memory T cells. *Nat Immunol* 10: 857–863.
131. Mitchison, N. A. 1971. The carrier effect in the secondary response to hapten-protein conjugates. II. Cellular cooperation. *Eur J Immunol* 1: 18–27.
132. Yu, D., S. Rao, L. M. Tsai, S. K. Lee, Y. He, E. L. Sutcliffe, M. Srivastava, M. Linterman, L. Zheng, N. Simpson, J. I. Ellyard, I. A. Parish, C. S. Ma, Q.-J. Li, C. R. Parish, C. R. Mackay, and C. G. Vinuesa. 2009. The transcriptional repressor Bcl-6 directs T follicular helper cell lineage commitment. *Immunity* 31: 457–468.
133. Nurieva, R. I., Y. Chung, D. Hwang, X. O. Yang, H. S. Kang, L. Ma, Y.-H. Wang, S.

- S. Watowich, A. M. Jetten, Q. Tian, and C. Dong. 2008. Generation of T follicular helper cells is mediated by interleukin-21 but independent of T helper 1, 2, or 17 cell lineages. *Immunity* 29: 138–149.
134. Dinarello, C. A. 2007. Historical insights into cytokines. *Eur J Immunol* 37 Suppl 1: S34–45.
135. Arai, K. I., F. Lee, A. Miyajima, S. Miyatake, N. Arai, and T. Yokota. 1990. Cytokines: coordinators of immune and inflammatory responses. *Annu. Rev. Biochem.* 59: 783–836.
136. McInnes, I. B. 2013. Cytokines. Part 3: 367–377.
137. Vigne, S., G. Palmer, C. Lamacchia, P. Martin, D. Talabot-Ayer, E. Rodriguez, F. Ronchi, F. Sallusto, H. Dinh, J. E. Sims, and C. Gabay. 2011. IL-36R ligands are potent regulators of dendritic and T cells. *Blood* 118: 5813–5823.
138. Acosta-Rodriguez, E. V., L. Rivino, J. Geginat, D. Jarrossay, M. Gattorno, A. Lanzavecchia, F. Sallusto, and G. Napolitani. 2007. Surface phenotype and antigenic specificity of human interleukin 17-producing T helper memory cells. *Nat Immunol* 8: 639–646.
139. Durum, S. K., J. A. Schmidt, and J. J. Oppenheim. 1985. Interleukin 1: an immunological perspective. *Annu Rev Immunol* 3: 263–287.
140. Van Snick, J. 1990. Interleukin-6: an overview. *Annu Rev Immunol* 8: 253–278.
141. Pfeffer, K. 2003. Biological functions of tumor necrosis factor cytokines and their receptors. *Cytokine Growth Factor Rev.* 14: 185–191.
142. Paul, W. E., and J. Ohara. 1987. B-cell stimulatory factor-1/interleukin 4. *Annu Rev Immunol* 5: 429–459.
143. Sanderson, C. J. 1992. Interleukin-5, eosinophils, and disease. *Blood* 79: 3101–3109.
144. Moore, K. W., R. de Waal Malefyt, R. L. Coffman, and A. O'Garra. 2001. Interleukin-10 and the interleukin-10 receptor. *Annu Rev Immunol* 19: 683–765.
145. Trinchieri, G. 1995. Interleukin-12: a proinflammatory cytokine with immunoregulatory functions that bridge innate resistance and antigen-specific adaptive immunity. *Annu Rev Immunol* 13: 251–276.
146. Wynn, T. A. 2003. IL-13 effector functions. *Annu Rev Immunol* 21: 425–456.
147. Gaffen, S. L. 2008. An overview of IL-17 function and signaling. *Cytokine* 43: 402–407.
148. Chang, S. H., and C. Dong. 2009. IL-17F: regulation, signaling and function in inflammation. *Cytokine* 46: 7–11.
149. Honda, K. 2012. IL-22 from T cells: better late than never. *Immunity* 37: 952–954.
150. McGeachy, M. J., Y. Chen, C. M. Tato, A. Laurence, B. Joyce-Shaikh, W. M. Blumenschein, T. K. McClanahan, J. J. O'Shea, and D. J. Cua. 2009. The interleukin 23 receptor is essential for the terminal differentiation of interleukin 17-producing effector T helper cells in vivo. *Nat Immunol* 10: 314–324.
151. Schroder, K., P. J. Hertzog, T. Ravasi, and D. A. Hume. 2004. Interferon-gamma: an overview of signals, mechanisms and functions. *J Leukoc Biol* 75: 163–189.
152. Taylor, A. W. 2009. Review of the activation of TGF-beta in immunity. *J Leukoc Biol* 85: 29–33.
153. Hamilton, J. A. 2002. GM-CSF in inflammation and autoimmunity. *Trends Immunol.* 23: 403–408.
154. Karsunky, H., M. Merad, A. Cozzio, I. L. Weissman, and M. G. Manz. 2003. Flt3 ligand regulates dendritic cell development from Flt3+ lymphoid and myeloid-committed progenitors to Flt3+ dendritic cells in vivo. *J Exp Med* 198: 305–313.
155. Saito, Y., C. S. Boddupalli, C. Borsotti, and M. G. Manz. 2013. Dendritic cell homeostasis is maintained by nonhematopoietic and T-cell-produced Flt3-ligand in steady state and during immune responses. *Eur J Immunol* 43: 1651–1658.
156. Zlotnik, A., and O. Yoshie. 2000. Chemokines: a new classification system and their role in immunity. *Immunity* 12: 121–127.

157. Baggiolini, M., A. Walz, and S. L. Kunkel. 1989. Neutrophil-activating peptide-1/interleukin 8, a novel cytokine that activates neutrophils. *J Clin Invest* 84: 1045–1049.
158. Zlotnik, A., O. Yoshie, and H. Nomiya. 2006. The chemokine and chemokine receptor superfamilies and their molecular evolution. *Genome Biol* 7: 243.
159. Baggiolini, M. 1998. Chemokines and leukocyte traffic. *Nature* 392: 565–568.
160. Moser, B., and P. Loetscher. 2001. Lymphocyte traffic control by chemokines. *Nat Immunol* 2: 123–128.
161. Yoshie, O., T. Imai, and H. Nomiya. 1997. Novel lymphocyte-specific CC chemokines and their receptors. *J Leukoc Biol* 62: 634–644.
162. Sallusto, F., C. R. Mackay, and A. Lanzavecchia. 2000. The role of chemokine receptors in primary, effector, and memory immune responses. *Annu Rev Immunol* 18: 593–620.
163. Bockaert, J., and J. P. Pin. 1999. Molecular tinkering of G protein-coupled receptors: an evolutionary success. *EMBO J* 18: 1723–1729.
164. Journot, L., D. Spengler, C. Pantaloni, A. Dumuis, M. Sebben, and J. Bockaert. 1994. The PACAP receptor: generation by alternative splicing of functional diversity among G protein-coupled receptors in nerve cells. *Semin. Cell Biol* 5: 263–272.
165. Pantaloni, C., P. Brabet, B. Bilanges, A. Dumuis, S. Houssami, D. Spengler, J. Bockaert, and L. Journot. 1996. Alternative splicing in the N-terminal extracellular domain of the pituitary adenylate cyclase-activating polypeptide (PACAP) receptor modulates receptor selectivity and relative potencies of PACAP-27 and PACAP-38 in phospholipase C activation. *J Biol Chem* 271: 22146–22151.
166. Mellado, M., J. M. Rodríguez-Frade, A. J. Vila-Coro, S. Fernández, A. Martín de Ana, D. R. Jones, J. L. Torán, and C. Martínez-A. 2001. Chemokine receptor homo- or heterodimerization activates distinct signaling pathways. *EMBO J* 20: 2497–2507.
167. Curnock, A. P., M. K. Logan, and S. G. Ward. 2002. Chemokine signalling: pivoting around multiple phosphoinositide 3-kinases. *Immunology* 105: 125–136.
168. Luster, A. D. 1998. Chemokines--chemotactic cytokines that mediate inflammation. *N. Engl. J. Med.* 338: 436–445.
169. Cyster, J. G., and C. C. Goodnow. 1995. Pertussis toxin inhibits migration of B and T lymphocytes into splenic white pulp cords. *J Exp Med* 182: 581–586.
170. Laudanna, C., J. J. Campbell, and E. C. Butcher. 1996. Role of Rho in chemoattractant-activated leukocyte adhesion through integrins. *Science* 271: 981–983.
171. Johansson-Lindbom, B., M. Svensson, M.-A. Wurbel, B. Malissen, G. Márquez, and W. Agace. 2003. Selective generation of gut tropic T cells in gut-associated lymphoid tissue (GALT): requirement for GALT dendritic cells and adjuvant. *J Exp Med* 198: 963–969.
172. Mora, J. R., M. R. Bono, N. Manjunath, W. Weninger, L. L. Cavanagh, M. Roseblatt, and U. H. von Andrian. 2003. Selective imprinting of gut-homing T cells by Peyer's patch dendritic cells. *Nature* 424: 88–93.
173. Soler, D., T. L. Humphreys, S. M. Spinola, and J. J. Campbell. 2003. CCR4 versus CCR10 in human cutaneous TH lymphocyte trafficking. *Blood* 101: 1677–1682.
174. Morales, J., B. Homey, A. P. Vicari, S. Hudak, E. Oldham, J. Hedrick, R. Orozco, N. G. Copeland, N. A. Jenkins, L. M. McEvoy, and A. Zlotnik. 1999. CTACK, a skin-associated chemokine that preferentially attracts skin-homing memory T cells. *Proc Natl Acad Sci USA* 96: 14470–14475.
175. Campbell, J. J., G. Haraldsen, J. Pan, J. Rottman, S. Qin, P. Ponath, D. P. Andrew, R. Warnke, N. Ruffing, N. Kassam, L. Wu, and E. C. Butcher. 1999. The chemokine receptor CCR4 in vascular recognition by cutaneous but not intestinal memory T cells. *Nature* 400: 776–780.
176. Iwasaki, A., and B. L. Kelsall. 2000. Localization of distinct Peyer's patch dendritic cell subsets and their recruitment by chemokines macrophage inflammatory protein (MIP)-3alpha, MIP-3beta, and secondary lymphoid organ chemokine. *J Exp Med* 191: 1381–

1394.

177. Wurbel, M.-A., M. G. McIntire, P. Dwyer, and E. Fiebiger. 2011. CCL25/CCR9 interactions regulate large intestinal inflammation in a murine model of acute colitis. *PLoS ONE* 6: e16442.
178. Tarnowski, M., R. Liu, M. Wysoczynski, J. Ratajczak, M. Kucia, and M. Z. Ratajczak. 2010. CXCR7: a new SDF-1-binding receptor in contrast to normal CD34(+) progenitors is functional and is expressed at higher level in human malignant hematopoietic cells. *Eur. J. Haematol.* 85: 472–483.
179. Hardtke, S., L. Ohl, and R. Förster. 2005. Balanced expression of CXCR5 and CCR7 on follicular T helper cells determines their transient positioning to lymph node follicles and is essential for efficient B-cell help. *Blood* 106: 1924–1931.
180. Hirota, K., H. Yoshitomi, M. Hashimoto, S. Maeda, S. Teradaira, N. Sugimoto, T. Yamaguchi, T. Nomura, H. Ito, T. Nakamura, N. Sakaguchi, and S. Sakaguchi. 2007. Preferential recruitment of CCR6-expressing Th17 cells to inflamed joints via CCL20 in rheumatoid arthritis and its animal model. *Journal of Experimental Medicine* 204: 2803–2812.
181. Shen, H., J. C. Goodall, and J. S. Hill Gaston. 2009. Frequency and phenotype of peripheral blood Th17 cells in ankylosing spondylitis and rheumatoid arthritis. *Arthritis Rheum* 60: 1647–1656.
182. Syrbe, U., J. Siveke, and A. Hamann. 1999. Th1/Th2 subsets: distinct differences in homing and chemokine receptor expression? *Springer Semin. Immunopathol.* 21: 263–285.
183. Sallusto, F., D. Lenig, C. R. Mackay, and A. Lanzavecchia. 1998. Flexible programs of chemokine receptor expression on human polarized T helper 1 and 2 lymphocytes. *J Exp Med* 187: 875–883.
184. Banchereau, J., and R. M. Steinman. 1998. Dendritic cells and the control of immunity. *Nature* 392: 245–252.
185. Steinman, R. M., and Z. A. Cohn. 1973. Identification of a novel cell type in peripheral lymphoid organs of mice. I. Morphology, quantitation, tissue distribution. *J Exp Med* 137: 1142–1162.
186. Steinman, R. M., and M. D. Witmer. 1978. Lymphoid dendritic cells are potent stimulators of the primary mixed leukocyte reaction in mice. *Proc Natl Acad Sci USA* 75: 5132–5136.
187. Schulz, O., E. Jaensson, E. K. Persson, X. Liu, T. Worbs, W. W. Agace, and O. Pabst. 2009. Intestinal CD103+, but not CX3CR1+, antigen sampling cells migrate in lymph and serve classical dendritic cell functions. *Journal of Experimental Medicine* 206: 3101–3114.
188. Pugh, C. W., G. G. MacPherson, and H. W. Steer. 1983. Characterization of nonlymphoid cells derived from rat peripheral lymph. *J Exp Med* 157: 1758–1779.
189. Akbari, O., R. H. DeKruyff, and D. T. Umetsu. 2001. Pulmonary dendritic cells producing IL-10 mediate tolerance induced by respiratory exposure to antigen. *Nat Immunol* 2: 725–731.
190. Lutz, M. B., and G. Schuler. 2002. Immature, semi-mature and fully mature dendritic cells: which signals induce tolerance or immunity? *Trends Immunol.* 23: 445–449.
191. Lutz, M. B., N. A. Kukutsch, M. Menges, S. Rössner, and G. Schuler. 2000. Culture of bone marrow cells in GM-CSF plus high doses of lipopolysaccharide generates exclusively immature dendritic cells which induce alloantigen-specific CD4 T cell anergy in vitro. *Eur J Immunol* 30: 1048–1052.
192. Rescigno, M., and A. Di Sabatino. 2009. Dendritic cells in intestinal homeostasis and disease. *J Clin Invest* 119: 2441–2450.
193. Lande, R., and M. Gilliet. 2010. Plasmacytoid dendritic cells: key players in the initiation and regulation of immune responses. *Ann. N. Y. Acad. Sci.* 1183: 89–103.
194. Siegal, F. P., N. Kadowaki, M. Shodell, P. A. Fitzgerald-Bocarsly, K. Shah, S. Ho, S. Antonenko, and Y. J. Liu. 1999. The nature of the principal type 1 interferon-producing cells in human blood. *Science* 284: 1835–1837.

195. Grouard, G., M. C. Rissoan, L. Filgueira, I. Durand, J. Banchereau, and Y. J. Liu. 1997. The enigmatic plasmacytoid T cells develop into dendritic cells with interleukin (IL)-3 and CD40-ligand. *J Exp Med* 185: 1101–1111.
196. Vinh, D. C., S. Y. Patel, G. Uzel, V. L. Anderson, A. F. Freeman, K. N. Olivier, C. Spalding, S. Hughes, S. Pittaluga, M. Raffeld, L. R. Sorbara, H. Z. Elloumi, D. B. Kuhns, M. L. Turner, E. W. Cowen, D. Fink, D. Long-Priel, A. P. Hsu, L. Ding, M. L. Paulson, A. R. Whitney, E. P. Sampaio, D. M. Frucht, F. R. DeLeo, and S. M. Holland. 2010. Autosomal dominant and sporadic monocytopenia with susceptibility to mycobacteria, fungi, papillomaviruses, and myelodysplasia. *Blood* 115: 1519–1529.
197. Bigley, V., M. Haniffa, S. Doulatov, X.-N. Wang, R. Dickinson, N. McGovern, L. Jardine, S. Pagan, I. Dimmick, I. Chua, J. Wallis, J. Lordan, C. Morgan, D. S. Kumararatne, R. Doffinger, M. van der Burg, J. van Dongen, A. Cant, J. E. Dick, S. Hambleton, and M. Collin. 2011. The human syndrome of dendritic cell, monocyte, B and NK lymphoid deficiency. *J Exp Med* 208: 227–234.
198. Hambleton, S., S. Salem, J. Bustamante, V. Bigley, S. Boisson-Dupuis, J. Azevedo, A. Fortin, M. Haniffa, L. Ceron-Gutierrez, C. M. Bacon, G. Menon, C. Trouillet, D. McDonald, P. Carey, F. Ginhoux, L. Alsina, T. J. Zumwalt, X.-F. Kong, D. Kumararatne, K. Butler, M. Hubeau, J. Feinberg, S. Al-Muhsen, A. Cant, L. Abel, D. Chaussabel, R. Doffinger, E. Talesnik, A. Grumach, A. Duarte, K. Abarca, D. Moraes-Vasconcelos, D. Burk, A. Berghuis, F. Geissmann, M. Collin, J.-L. Casanova, and P. Gros. 2011. IRF8 mutations and human dendritic-cell immunodeficiency. *N. Engl. J. Med.* 365: 127–138.
199. Emile, J. F., F. Geissmann, O. C. Martin, I. Radford-Weiss, Y. Lepelletier, B. Heymer, T. Espanol, K. B. de Santes, Y. Bertrand, N. Brousse, J. L. Casanova, and A. Fischer. 2000. Langerhans cell deficiency in reticular dysgenesis. *Blood* 96: 58–62.
200. Jongbloed, S. L., A. J. Kassianos, K. J. McDonald, G. J. Clark, X. Ju, C. E. Angel, C.-J. J. Chen, P. R. Dunbar, R. B. Wadley, V. Jeet, A. J. E. Vulink, D. N. J. Hart, and K. J. Radford. 2010. Human CD141+ (BDCA-3)+ dendritic cells (DCs) represent a unique myeloid DC subset that cross-presents necrotic cell antigens. *J Exp Med* 207: 1247–1260.
201. Hart, D. N. 1997. Dendritic cells: unique leukocyte populations which control the primary immune response. *Blood* 90: 3245–3287.
202. Dzionek, A., A. Fuchs, P. Schmidt, S. Cremer, M. Zysk, S. Miltenyi, D. W. Buck, and J. Schmitz. 2000. BDCA-2, BDCA-3, and BDCA-4: three markers for distinct subsets of dendritic cells in human peripheral blood. *J Immunol* 165: 6037–6046.
203. Poulin, L. F., M. Salio, E. Griessinger, F. Anjos-Afonso, L. Craciun, J.-L. Chen, A. M. Keller, O. Joffre, S. Zelenay, E. Nye, A. Le Moine, F. Faure, V. Donckier, D. Sancho, V. Cerundolo, D. Bonnet, and C. Reis e Sousa. 2010. Characterization of human DNGR-1+ BDCA3+ leukocytes as putative equivalents of mouse CD8alpha+ dendritic cells. *J Exp Med* 207: 1261–1271.
204. O'Doherty, U., M. Peng, S. Gezelter, W. J. Swiggard, M. Betjes, N. Bhardwaj, and R. M. Steinman. 1994. Human blood contains two subsets of dendritic cells, one immunologically mature and the other immature. *Immunology* 82: 487–493.
205. Strobl, H., C. Scheinecker, E. Riedl, B. Csmarits, C. Bello-Fernandez, W. F. Pickl, O. Majdic, and W. Knapp. 1998. Identification of CD68+lin- peripheral blood cells with dendritic precursor characteristics. *J Immunol* 161: 740–748.
206. Palucka, K., J. Banchereau, and I. Mellman. 2010. Designing vaccines based on biology of human dendritic cell subsets. *Immunity* 33: 464–478.
207. Ziegler-Heitbrock, L., P. Ancuta, S. Crowe, M. Dalod, V. Grau, D. N. Hart, P. J. M. Leenen, Y.-J. Liu, G. Macpherson, G. J. Randolph, J. Scherberich, J. Schmitz, K. Shortman, S. Sozzani, H. Strobl, M. Zembala, J. M. Austyn, and M. B. Lutz. 2010. Nomenclature of monocytes and dendritic cells in blood. *Blood* 116: e74–80.
208. Ju, X., G. Clark, and D. N. J. Hart. 2010. *Review of Human DC Subtypes*. Humana Press; :3–20.
209. MacDonald, K. P. A., D. J. Munster, G. J. Clark, A. Dzionek, J. Schmitz, and D. N. J.

- Hart. 2002. Characterization of human blood dendritic cell subsets. *Blood* 100: 4512–4520.
210. Lindstedt, M., K. Lundberg, and C. A. K. Borrebaeck. 2005. Gene family clustering identifies functionally associated subsets of human in vivo blood and tonsillar dendritic cells. *J Immunol* 175: 4839–4846.
211. Kassianos, A. J., M. Y. Hardy, X. Ju, D. Vijayan, Y. Ding, A. J. E. Vulink, K. J. McDonald, S. L. Jongbloed, R. B. Wadley, C. Wells, D. N. J. Hart, and K. J. Radford. 2012. Human CD1c (BDCA-1)⁺ myeloid dendritic cells secrete IL-10 and display an immuno-regulatory phenotype and function in response to *Escherichia coli*. *Eur J Immunol* 42: 1512–1522.
212. Bachem, A., S. Güttler, E. Hartung, F. Ebstein, M. Schaefer, A. Tannert, A. Salama, K. Movassaghi, C. Opitz, H. W. Mages, V. Henn, P.-M. Kloetzel, S. Gurka, and R. A. Kroczek. 2010. Superior antigen cross-presentation and XCR1 expression define human CD11c⁺CD141⁺ cells as homologues of mouse CD8⁺ dendritic cells. *J Exp Med* 207: 1273–1281.
213. Hémond, C., A. Neel, M. Heslan, C. Braudeau, and R. Josien. 2013. Human blood mDC subsets exhibit distinct TLR repertoire and responsiveness. *J Leukoc Biol* 93: 599–609.
214. Galibert, L., G. S. Diemer, Z. Liu, R. S. Johnson, J. L. Smith, T. Walzer, M. R. Comeau, C. T. Rauch, M. F. Wolfson, R. A. Sorensen, A.-R. Van der Vuurst de Vries, D. G. Branstetter, R. M. Koelling, J. Scholler, W. C. Fanslow, P. R. Baum, J. M. Derry, and W. Yan. 2005. Nectin-like protein 2 defines a subset of T-cell zone dendritic cells and is a ligand for class-I-restricted T-cell-associated molecule. *J Biol Chem* 280: 21955–21964.
215. Caminschi, I., A. I. Proietto, F. Ahmet, S. Kitsoulis, J. Shin Teh, J. C. Y. Lo, A. Rizzitelli, L. Wu, D. Vremec, S. L. H. van Dommelen, I. K. Campbell, E. Maraskovsky, H. Braley, G. M. Davey, P. Mottram, N. van de Velde, K. Jensen, A. M. Lew, M. D. Wright, W. R. Heath, K. Shortman, and M. H. Lahoud. 2008. The dendritic cell subtype-restricted C-type lectin Clec9A is a target for vaccine enhancement. *Blood* 112: 3264–3273.
216. Robinson, S. P., S. Patterson, N. English, D. Davies, S. C. Knight, and C. D. Reid. 1999. Human peripheral blood contains two distinct lineages of dendritic cells. *Eur J Immunol* 29: 2769–2778.
217. Jongbloed, S. L., M. C. Lebre, A. R. Fraser, J. A. Gracie, R. D. Sturrock, P. P. Tak, and I. B. McInnes. 2006. Enumeration and phenotypical analysis of distinct dendritic cell subsets in psoriatic arthritis and rheumatoid arthritis. *Arthritis Res Ther* 8: R15.
218. Bruno, L., P. Res, M. Dessing, M. Cella, and H. Spits. 1997. Identification of a committed T cell precursor population in adult human peripheral blood. *J Exp Med* 185: 875–884.
219. Krug, A., A. Towarowski, S. Britsch, S. Rothenfusser, V. Hornung, R. Bals, T. Giese, H. Engelmann, S. Endres, A. M. Krieg, and G. Hartmann. 2001. Toll-like receptor expression reveals CpG DNA as a unique microbial stimulus for plasmacytoid dendritic cells which synergizes with CD40 ligand to induce high amounts of IL-12. *Eur J Immunol* 31: 3026–3037.
220. Sozzani, S., W. Vermi, A. Del Prete, and F. Facchetti. 2010. Trafficking properties of plasmacytoid dendritic cells in health and disease. *Trends Immunol.* 31: 270–277.
221. Cao, W., D. B. Rosen, T. Ito, L. Bover, M. Bao, G. Watanabe, Z. Yao, L. Zhang, L. L. Lanier, and Y.-J. Liu. 2006. Plasmacytoid dendritic cell-specific receptor ILT7-Fc epsilonRI gamma inhibits Toll-like receptor-induced interferon production. *J Exp Med* 203: 1399–1405.
222. Merad, M., P. Sathe, J. Helft, J. Miller, and A. Mortha. 2013. The dendritic cell lineage: ontogeny and function of dendritic cells and their subsets in the steady state and the inflamed setting. *Annu Rev Immunol* 31: 563–604.
223. Auffray, C., M. H. Sieweke, and F. Geissmann. 2009. Blood monocytes: development, heterogeneity, and relationship with dendritic cells. *Annu Rev Immunol* 27: 669–692.

224. Gordon, S., and P. R. Taylor. 2005. Monocyte and macrophage heterogeneity. *Nat Rev Immunol* 5: 953–964.
225. Bain, C. C., C. L. Scott, H. Uronen-Hansson, S. Gudjonsson, O. Jansson, O. Grip, M. Williams, B. Malissen, W. W. Agace, and A. M. Mowat. 2012. Resident and pro-inflammatory macrophages in the colon represent alternative context-dependent fates of the same Ly6C(hi) monocyte precursors. *Mucosal Immunol*.
226. Rivollier, A., J. He, A. Kole, V. Valatas, and B. L. Kelsall. 2012. Inflammation switches the differentiation program of Ly6Chi monocytes from antiinflammatory macrophages to inflammatory dendritic cells in the colon. *Journal of Experimental Medicine* 209: 139–155.
227. León, B., M. López-Bravo, and C. Ardavin. 2007. Monocyte-derived dendritic cells formed at the infection site control the induction of protective T helper 1 responses against *Leishmania*. *Immunity* 26: 519–531.
228. Serbina, N. V., T. P. Salazar-Mather, C. A. Biron, W. A. Kuziel, and E. G. Pamer. 2003. TNF/iNOS-Producing Dendritic Cells Mediate Innate Immune Defense against Bacterial Infection. *Immunity* 19: 59–70.
229. Geissmann, F., S. Jung, and D. R. Littman. 2003. Blood monocytes consist of two principal subsets with distinct migratory properties. *Immunity* 19: 71–82.
230. Naik, S. H., D. Metcalf, A. van Nieuwenhuijze, I. Wicks, L. Wu, M. O'Keeffe, and K. Shortman. 2006. Intrasplenic steady-state dendritic cell precursors that are distinct from monocytes. *Nat Immunol* 7: 663–671.
231. Grage-Griebenow, E., H. D. Flad, and M. Ernst. 2001. Heterogeneity of human peripheral blood monocyte subsets. *J Leukoc Biol* 69: 11–20.
232. Grage-Griebenow, E., H. D. Flad, M. Ernst, M. Bzowska, J. Skrzeczyńska, and J. Pryjma. 2000. Human MO subsets as defined by expression of CD64 and CD16 differ in phagocytic activity and generation of oxygen intermediates. *Immunobiology* 202: 42–50.
233. Ziegler-Heitbrock, L. 2006. The CD14⁺ CD16⁺ blood monocytes: their role in infection and inflammation. *J Leukoc Biol* 81: 584–592.
234. Tamoutounour, S., S. Henri, H. Lelouard, B. de Bovis, C. de Haar, C. J. van der Woude, A. M. Woltman, Y. Reyat, D. Bonnet, D. Sichien, C. C. Bain, A. M. Mowat, C. Reis e Sousa, L. F. Poulin, B. Malissen, and M. Williams. 2012. CD64 distinguishes macrophages from dendritic cells in the gut and reveals the Th1-inducing role of mesenteric lymph node macrophages during colitis. *Eur J Immunol* 42: 3150–3166.
235. Ziegler-Heitbrock, H. W., B. Passlick, and D. Flieger. 1988. The monoclonal antimonocyte antibody My4 stains B lymphocytes and two distinct monocyte subsets in human peripheral blood. *Hybridoma* 7: 521–527.
236. Passlick, B., D. Flieger, and H. W. Ziegler-Heitbrock. 1989. Identification and characterization of a novel monocyte subpopulation in human peripheral blood. *Blood* 74: 2527–2534.
237. Cros, J., N. Cagnard, K. Woollard, N. Patey, S.-Y. Zhang, B. Senechal, A. Puel, S. K. Biswas, D. Moshous, C. Picard, J.-P. Jais, D. D'Cruz, J.-L. Casanova, C. Trouillet, and F. Geissmann. 2010. Human CD14^{dim} monocytes patrol and sense nucleic acids and viruses via TLR7 and TLR8 receptors. *Immunity* 33: 375–386.
238. Geissmann, F., C. Auffray, R. Palframan, C. Wirrig, A. Ciocca, L. Campisi, E. Narni-Mancinelli, and G. Lauvau. 2008. Blood monocytes: distinct subsets, how they relate to dendritic cells, and their possible roles in the regulation of T-cell responses. *Immunol. Cell Biol.* 86: 398–408.
239. Schäkel, K., R. Kannagi, B. Kniep, Y. Goto, C. Mitsuoka, J. Zwirner, A. Soruri, M. von Kietzell, and E. Rieber. 2002. 6-Sulfo LacNAc, a novel carbohydrate modification of PSGL-1, defines an inflammatory type of human dendritic cells. *Immunity* 17: 289–301.
240. Schäkel, K., E. Mayer, C. Federle, M. Schmitz, G. Riethmüller, and E. P. Rieber. 1998. A novel dendritic cell population in human blood: one-step immunomagnetic isolation by a specific mAb (M-DC8) and in vitro priming of cytotoxic T lymphocytes. *Eur*

J Immunol 28: 4084–4093.

241. Frenette, P. S., R. C. Johnson, R. O. Hynes, and D. D. Wagner. 1995. Platelets roll on stimulated endothelium in vivo: an interaction mediated by endothelial P-selectin. *Proc Natl Acad Sci USA* 92: 7450–7454.
242. Geng, J. G., M. P. Bevilacqua, K. L. Moore, T. M. McIntyre, S. M. Prescott, J. M. Kim, G. A. Bliss, G. A. Zimmerman, and R. P. McEver. 1990. Rapid neutrophil adhesion to activated endothelium mediated by GMP-140. *Nature* 343: 757–760.
243. Larsen, E., A. Celi, G. E. Gilbert, B. C. Furie, J. K. Erban, R. Bonfanti, D. D. Wagner, and B. Furie. 1989. PADGEM protein: a receptor that mediates the interaction of activated platelets with neutrophils and monocytes. *Cell* 59: 305–312.
244. Thieblemont, N., L. Weiss, H. M. Sadeghi, C. Estcourt, and N. Haeffner-Cavaillon. 1995. CD14^{low}CD16^{high}: a cytokine-producing monocyte subset which expands during human immunodeficiency virus infection. *Eur J Immunol* 25: 3418–3424.
245. Backé, E., R. Schwarting, J. Gerdes, M. Ernst, and H. Stein. 1991. Ber-MAC3: new monoclonal antibody that defines human monocyte/macrophage differentiation antigen. *J. Clin. Pathol.* 44: 936–945.
246. Fogg, D. K., C. Sibon, C. Miled, S. Jung, P. Aucouturier, D. R. Littman, A. Cumano, and F. Geissmann. 2006. A clonogenic bone marrow progenitor specific for macrophages and dendritic cells. *Science* 311: 83–87.
247. Jung, S., J. Aliberti, P. Graemmel, M. J. Sunshine, G. W. Kreutzberg, A. Sher, and D. R. Littman. 2000. Analysis of fractalkine receptor CX(3)CR1 function by targeted deletion and green fluorescent protein reporter gene insertion. *Mol. Cell. Biol.* 20: 4106–4114.
248. Carlin, L. M., E. G. Stamatides, C. Auffray, R. N. Hanna, L. Glover, G. Vizcay-Barrena, C. C. Hedrick, H. T. Cook, S. Diebold, and F. Geissmann. 2013. Nr4a1-dependent Ly6C(low) monocytes monitor endothelial cells and orchestrate their disposal. *Cell* 153: 362–375.
249. Hänsel, A., C. Günther, J. Ingwersen, J. Starke, M. Schmitz, M. Bachmann, M. Meurer, E. P. Rieber, and K. Schäkel. 2011. Human slan (6-sulfo LacNAc) dendritic cells are inflammatory dermal dendritic cells in psoriasis and drive strong TH17/TH1 T-cell responses. *J. Allergy Clin. Immunol.* 127: 787–94.e1–9.
250. Günther, C., J. Starke, N. Zimmermann, and K. Schäkel. 2012. Human 6-sulfo LacNAc (slan) dendritic cells are a major population of dermal dendritic cells in steady state and inflammation. *Clin. Exp. Dermatol.* 37: 169–176.
251. de Baey, A., I. Mende, G. Baretton, A. Greiner, W. H. Hartl, P. A. Baeuerle, and H. M. Diepolder. 2003. A subset of human dendritic cells in the T cell area of mucosa-associated lymphoid tissue with a high potential to produce TNF-alpha. *J Immunol* 170: 5089–5094.
252. Hänsel, A., C. Günther, W. Baran, M. Bidier, H.-M. Lorenz, M. Schmitz, M. Bachmann, T. Döbel, A. H. Enk, and K. Schäkel. 2013. Human 6-sulfo LacNAc (slan) dendritic cells have molecular and functional features of an important pro-inflammatory cell type in lupus erythematosus. *J. Autoimmun.* 40: 1–8.
253. Williams, K. A., D. N. Hart, J. W. Fabre, and P. J. Morris. 1980. Distribution and quantitation of HLA-ABC and DR (Ia) antigens on human kidney and other tissues. *Transplantation* 29: 274–279.
254. Velásquez-Lopera, M. M., L. A. Correa, and L. F. García. 2008. Human spleen contains different subsets of dendritic cells and regulatory T lymphocytes. *Clin Exp Immunol* 154: 107–114.
255. McIlroy, D., C. Troadec, F. Grassi, A. Samri, B. Barrou, B. Autran, P. Debré, J. Feuillard, and A. Hosmalin. 2001. Investigation of human spleen dendritic cell phenotype and distribution reveals evidence of in vivo activation in a subset of organ donors. *Blood* 97: 3470–3477.
256. Res, P. C., F. Couwenberg, F. A. Vyth-Dreese, and H. Spits. 1999. Expression of pTalpha mRNA in a committed dendritic cell precursor in the human thymus. *Blood* 94:

2647–2657.

257. Res, P., E. Martínez-Cáceres, A. Cristina Jaleco, F. Staal, E. Noteboom, K. Weijer, and H. Spits. 1996. CD34+CD38dim cells in the human thymus can differentiate into T, natural killer, and dendritic cells but are distinct from pluripotent stem cells. *Blood* 87: 5196–5206.
258. Evans, V. A., P. U. Cameron, and S. R. Lewin. 2008. Human thymic dendritic cells: Regulators of T cell development in health and HIV-1 infection. *Clinical Immunology* 126: 1–12.
259. Bendriss-Vermare, N., C. Barthélémy, I. Durand, C. Bruand, C. Dezutter-Dambuyant, N. Moulian, S. Berrih-Aknin, C. Caux, G. Trinchieri, and F. Brière. 2001. Human thymus contains IFN- α -producing CD11c(-), myeloid CD11c(+), and mature interdigitating dendritic cells. *J Clin Invest* 107: 835–844.
260. Vandenabeele, S., H. Hochrein, N. Mavaddat, K. Winkel, and K. Shortman. 2001. Human thymus contains 2 distinct dendritic cell populations. *Blood* 97: 1733–1741.
261. Schmitt, C., H. Fohrer, S. Beaudet, P. Palmer, M. J. Alpha, B. Canque, J. C. Gluckman, and A. H. Dalloul. 2000. Identification of mature and immature human thymic dendritic cells that differentially express HLA-DR and interleukin-3 receptor in vivo. *J Leukoc Biol* 68: 836–844.
262. Gurney, K. B., A. D. Colantonio, B. Blom, H. Spits, and C. H. Uittenbogaart. 2004. Endogenous IFN- α production by plasmacytoid dendritic cells exerts an antiviral effect on thymic HIV-1 infection. *J Immunol* 173: 7269–7276.
263. Summers, K. L., B. D. Hock, J. L. McKenzie, and D. N. Hart. 2001. Phenotypic characterization of five dendritic cell subsets in human tonsils. *Am J Pathol* 159: 285–295.
264. Segura, E., M. Durand, and S. Amigorena. 2013. Similar antigen cross-presentation capacity and phagocytic functions in all freshly isolated human lymphoid organ-resident dendritic cells. *Journal of Experimental Medicine* 210: 1035–1047.
265. Segura, E., J. Valladeau-Guilemond, M.-H. Donnadieu, X. Sastre-Garau, V. Soumelis, and S. Amigorena. 2012. Characterization of resident and migratory dendritic cells in human lymph nodes. *J Exp Med* 209: 653–660.
266. Valladeau, J., and S. Saeland. 2005. Cutaneous dendritic cells. *Semin. Immunol.* 17: 273–283.
267. Nestle, F. O., X. G. Zheng, C. B. Thompson, L. A. Turka, and B. J. Nickoloff. 1993. Characterization of dermal dendritic cells obtained from normal human skin reveals phenotypic and functionally distinctive subsets. *J Immunol* 151: 6535–6545.
268. Klechevsky, E., R. Morita, M. Liu, Y. Cao, S. Coquery, L. Thompson-Snipes, F. Briere, D. Chaussabel, G. Zurawski, A. K. Palucka, Y. Reiter, J. Banchereau, and H. Ueno. 2008. Functional specializations of human epidermal Langerhans cells and CD14+ dermal dendritic cells. *Immunity* 29: 497–510.
269. Ebner, S., Z. Ehammer, S. Holzmann, P. Schwingshackl, M. Forstner, P. Stoitzner, G. M. Huemer, P. Fritsch, and N. Romani. 2004. Expression of C-type lectin receptors by subsets of dendritic cells in human skin. *Int. Immunol.* 16: 877–887.
270. Verstege, M. I., F. J. W. ten Kate, S. M. Reinartz, C. M. van Drunen, F. J. M. Slors, W. A. Bemelman, F. A. Vyth-Dreese, and A. A. te Velde. 2008. Dendritic cell populations in colon and mesenteric lymph nodes of patients with Crohn's disease. *J. Histochem. Cytochem.* 56: 233–241.
271. Dillon, S. M., L. M. Rogers, R. Howe, L. A. Hostetler, J. Buhrman, M. D. McCarter, and C. C. Wilson. 2010. Human intestinal lamina propria CD11c+ dendritic cells display an activated phenotype at steady state and produce IL-23 in response to TLR7/8 stimulation. *The Journal of Immunology* 184: 6612–6621.
272. Poulin, L. F., Y. Reyrol, H. Uronen-Hansson, B. U. Schraml, D. Sancho, K. M. Murphy, U. K. Håkansson, L. F. Moita, W. W. Agace, D. Bonnet, and C. Reis e Sousa. 2012. DNDR-1 is a specific and universal marker of mouse and human Batf3-dependent dendritic cells in lymphoid and nonlymphoid tissues. *Blood* 119: 6052–6062.

273. Ráki, M., A.-C. R. Beitnes, K. E. A. Lundin, J. Jahnsen, F. L. Jahnsen, and L. M. Sollid. 2013. Plasmacytoid dendritic cells are scarcely represented in the human gut mucosa and are not recruited to the celiac lesion. *Mucosal Immunol*.
274. Jaensson, E., H. Uronen-Hansson, O. Pabst, B. Eksteen, J. Tian, J. L. Coombes, P.-L. Berg, T. Davidsson, F. Powrie, B. Johansson-Lindbom, and W. W. Agace. 2008. Small intestinal CD103+ dendritic cells display unique functional properties that are conserved between mice and humans. *Journal of Experimental Medicine* 205: 2139–2149.
275. Persson, E. K., H. Uronen-Hansson, M. Semmrich, A. Rivollier, K. Hägerbrand, J. Marsal, S. Gudjonsson, U. Håkansson, B. Reizis, K. Kotarsky, and W. W. Agace. 2013. IRF4 Transcription-Factor-Dependent CD103+CD11b+ Dendritic Cells Drive Mucosal T Helper 17 Cell Differentiation. *Immunity* 38: 958–969.
276. Beitnes, A.-C. R., M. Ráki, K. E. A. Lundin, J. Jahnsen, L. M. Sollid, and F. L. Jahnsen. 2011. Density of CD163+ CD11c+ dendritic cells increases and CD103+ dendritic cells decreases in the coeliac lesion. *Scand J Immunol* 74: 186–194.
277. Schlitzer, A., N. McGovern, P. Teo, T. Zelante, K. Atarashi, D. Low, A. W. S. Ho, P. See, A. Shin, P. S. Wasan, G. Hoeffel, B. Malleret, A. Heiseke, S. Chew, L. Jardine, H. A. Purvis, C. M. U. Hilkens, J. Tam, M. Poidinger, E. R. Stanley, A. B. Krug, L. Renia, B. Sivasankar, L. G. Ng, M. Collin, P. Ricciardi-Castagnoli, K. Honda, M. Haniffa, and F. Ginhoux. 2013. IRF4 transcription factor-dependent CD11b+ dendritic cells in human and mouse control mucosal IL-17 cytokine responses. *Immunity* 38: 970–983.
278. Masten, B. J., G. K. Olson, C. A. Tarleton, C. Rund, M. Schuyler, R. Mehran, T. Archibeque, and M. F. Lipscomb. 2006. Characterization of myeloid and plasmacytoid dendritic cells in human lung. *J Immunol* 177: 7784–7793.
279. Geissmann, F., M. G. Manz, S. Jung, M. H. Sieweke, M. Merad, and K. Ley. 2010. Development of monocytes, macrophages, and dendritic cells. *Science* 327: 656–661.
280. Kamath, A. T., S. Henri, F. Battye, D. F. Tough, and K. Shortman. 2002. Developmental kinetics and lifespan of dendritic cells in mouse lymphoid organs. *Blood* 100: 1734–1741.
281. Manz, M. G., T. Miyamoto, K. Akashi, and I. L. Weissman. 2002. Prospective isolation of human clonogenic common myeloid progenitors. *Proc Natl Acad Sci USA* 99: 11872–11877.
282. Chicha, L., D. Jarrossay, and M. G. Manz. 2004. Clonal type I interferon-producing and dendritic cell precursors are contained in both human lymphoid and myeloid progenitor populations. *J Exp Med* 200: 1519–1524.
283. Akashi, K., D. Traver, T. Miyamoto, and I. L. Weissman. 2000. A clonogenic common myeloid progenitor that gives rise to all myeloid lineages. *Nature* 404: 193–197.
284. McKenna, H. J., K. L. Stocking, R. E. Miller, K. Brasel, T. De Smedt, E. Maraskovsky, C. R. Maliszewski, D. H. Lynch, J. Smith, B. Pulendran, E. R. Roux, M. Teepe, S. D. Lyman, and J. J. Peschon. 2000. Mice lacking flt3 ligand have deficient hematopoiesis affecting hematopoietic progenitor cells, dendritic cells, and natural killer cells. *Blood* 95: 3489–3497.
285. Mebius, R. E., T. Miyamoto, J. Christensen, J. Domen, T. Cupedo, I. L. Weissman, and K. Akashi. 2001. The fetal liver counterpart of adult common lymphoid progenitors gives rise to all lymphoid lineages, CD45+CD4+CD3- cells, as well as macrophages. *J Immunol* 166: 6593–6601.
286. Naik, S. H., P. Sathe, H.-Y. Park, D. Metcalf, A. I. Proietto, A. Dakic, S. Carotta, M. O'Keefe, M. Bahlo, A. Papenfuss, J.-Y. Kwak, L. Wu, and K. Shortman. 2007. Development of plasmacytoid and conventional dendritic cell subtypes from single precursor cells derived in vitro and in vivo. *Nat Immunol* 8: 1217–1226.
287. Onai, N., A. Obata-Onai, M. A. Schmid, and M. G. Manz. 2007. Flt3 in regulation of type I interferon-producing cell and dendritic cell development. *Ann. N. Y. Acad. Sci.* 1106: 253–261.
288. Liu, K., G. D. Vitoria, T. A. Schwickert, P. Guernonprez, M. M. Meredith, K. Yao,

- F.-F. Chu, G. J. Randolph, A. Y. Rudensky, and M. Nussenzweig. 2009. In vivo analysis of dendritic cell development and homeostasis. *Science* 324: 392–397.
289. Diao, J., E. Winter, C. Cantin, W. Chen, L. Xu, D. Kelvin, J. Phillips, and M. S. Cattral. 2006. In situ replication of immediate dendritic cell (DC) precursors contributes to conventional DC homeostasis in lymphoid tissue. *J Immunol* 176: 7196–7206.
290. Ishikawa, F., H. Niiro, T. Iino, S. Yoshida, N. Saito, S. Onohara, T. Miyamoto, H. Minagawa, S.-I. Fujii, L. D. Shultz, M. Harada, and K. Akashi. 2007. The developmental program of human dendritic cells is operated independently of conventional myeloid and lymphoid pathways. *Blood* 110: 3591–3660.
291. Schotte, R., M. Nagasawa, K. Weijer, H. Spits, and B. Blom. 2004. The ETS transcription factor Spi-B is required for human plasmacytoid dendritic cell development. *J Exp Med* 200: 1503–1509.
292. Spits, H., F. Couwenberg, A. Q. Bakker, K. Weijer, and C. H. Uittenbogaart. 2000. Id2 and Id3 inhibit development of CD34(+) stem cells into predendritic cell (pre-DC)2 but not into pre-DC1. Evidence for a lymphoid origin of pre-DC2. *J Exp Med* 192: 1775–1784.
293. Corcoran, L., I. Ferrero, D. Vremec, K. Lucas, J. Waithman, M. O'Keefe, L. Wu, A. Wilson, and K. Shortman. 2003. The lymphoid past of mouse plasmacytoid cells and thymic dendritic cells. *J Immunol* 170: 4926–4932.
294. Blom, B., S. Ho, S. Antonenko, and Y. J. Liu. 2000. Generation of interferon alpha-producing predendritic cell (Pre-DC)2 from human CD34(+) hematopoietic stem cells. *J Exp Med* 192: 1785–1796.
295. Chen, W., S. Antonenko, J. M. Sederstrom, X. Liang, A. S. H. Chan, H. Kanzler, B. Blom, B. R. Blazar, and Y.-J. Liu. 2004. Thrombopoietin cooperates with FLT3-ligand in the generation of plasmacytoid dendritic cell precursors from human hematopoietic progenitors. *Blood* 103: 2547–2553.
296. Gilliet, M., A. Boonstra, C. Paturel, S. Antonenko, X.-L. Xu, G. Trinchieri, A. O'Garra, and Y.-J. Liu. 2002. The development of murine plasmacytoid dendritic cell precursors is differentially regulated by FLT3-ligand and granulocyte/macrophage colony-stimulating factor. *J Exp Med* 195: 953–958.
297. Cisse, B., M. L. Caton, M. Lehner, T. Maeda, S. Scheu, R. Locksley, D. Holmberg, C. Zweier, N. S. den Hollander, S. G. Kant, W. Holter, A. Rauch, Y. Zhuang, and B. Reizis. 2008. Transcription factor E2-2 is an essential and specific regulator of plasmacytoid dendritic cell development. *Cell* 135: 37–48.
298. Bell, D., J. W. Young, and J. Banchemreau. 1999. Dendritic cells. *Adv. Immunol.* 72: 255–324.
299. Steinman, R. M., K. Inaba, S. Turley, P. Pierre, and I. Mellman. 1999. Antigen capture, processing, and presentation by dendritic cells: recent cell biological studies. *Hum Immunol* 60: 562–567.
300. Sallusto, F., M. Cella, C. Danieli, and A. Lanzavecchia. 1995. Dendritic cells use macropinocytosis and the mannose receptor to concentrate macromolecules in the major histocompatibility complex class II compartment: downregulation by cytokines and bacterial products. *J Exp Med* 182: 389–400.
301. Inaba, K., M. Inaba, M. Naito, and R. M. Steinman. 1993. Dendritic cell progenitors phagocytose particulates, including bacillus Calmette-Guerin organisms, and sensitize mice to mycobacterial antigens in vivo. *J Exp Med* 178: 479–488.
302. Bieber, T. 1997. Fc epsilon RI-expressing antigen-presenting cells: new players in the atopic game. *Immunol Today* 18: 311–313.
303. Fanger, N. A., K. Wardwell, L. Shen, T. F. Tedder, and P. M. Guyre. 1996. Type I (CD64) and type II (CD32) Fc gamma receptor-mediated phagocytosis by human blood dendritic cells. *J Immunol* 157: 541–548.
304. Jiang, W., W. J. Swiggard, C. Heufler, M. Peng, A. Mirza, R. M. Steinman, and M. C. Nussenzweig. 1995. The receptor DEC-205 expressed by dendritic cells and thymic epithelial cells is involved in antigen processing. *Nature* 375: 151–155.

305. Savill, J., I. Dransfield, C. Gregory, and C. Haslett. 2002. A blast from the past: clearance of apoptotic cells regulates immune responses. *Nat Rev Immunol* 2: 965–975.
306. Buus, S., A. Sette, S. M. Colon, D. M. Jenis, and H. M. Grey. 1986. Isolation and characterization of antigen-Ia complexes involved in T cell recognition. *Cell* 47: 1071–1077.
307. Joffre, O. P., E. Segura, A. Savina, and S. Amigorena. 2012. Cross-presentation by dendritic cells. *Nat Rev Immunol* 12: 557–569.
308. Maupin-Furlow, J. 2011. Proteasomes and protein conjugation across domains of life. *Nat Rev Micro*.
309. Kisselev, A. F., T. N. Akopian, K. M. Woo, and A. L. Goldberg. 1999. The sizes of peptides generated from protein by mammalian 26 and 20 S proteasomes. Implications for understanding the degradative mechanism and antigen presentation. *J Biol Chem* 274: 3363–3371.
310. Serwold, T., F. Gonzalez, J. Kim, R. Jacob, and N. Shastri. 2002. ERAAP customizes peptides for MHC class I molecules in the endoplasmic reticulum. *Nature* 419: 480–483.
311. Blum, J. S., P. A. Wearsch, and P. Cresswell. 2013. Pathways of antigen processing. *Annu Rev Immunol* 31: 443–473.
312. Townsend, A., and J. Trowsdale. 1993. The transporters associated with antigen presentation. *Semin. Cell Biol.* 4: 53–61.
313. Sadasivan, B., P. J. Lehner, B. Ortmann, T. Spies, and P. Cresswell. 1996. Roles for calreticulin and a novel glycoprotein, tapasin, in the interaction of MHC class I molecules with TAP. *Immunity* 5: 103–114.
314. Landsverk, O. J. B., O. Bakke, and T. F. Gregers. 2009. MHC II and the endocytic pathway: regulation by invariant chain. *Scand J Immunol* 70: 184–193.
315. Huotari, J., and A. Helenius. 2011. Endosome maturation. *EMBO J.* 30: 3481–3500.
316. Bikoff, E. K., L. Y. Huang, V. Episkopou, J. van Meerwijk, R. N. Germain, and E. J. Robertson. 1993. Defective major histocompatibility complex class II assembly, transport, peptide acquisition, and CD4+ T cell selection in mice lacking invariant chain expression. *J Exp Med* 177: 1699–1712.
317. Anderson, M. S., and J. Miller. 1992. Invariant chain can function as a chaperone protein for class II major histocompatibility complex molecules. *Proc Natl Acad Sci USA* 89: 2282–2286.
318. Riberdy, J. M., J. R. Newcomb, M. J. Surman, J. A. Barbosa, and P. Cresswell. 1992. HLA-DR molecules from an antigen-processing mutant cell line are associated with invariant chain peptides. *Nature* 360: 474–477.
319. Denzin, L. K., and P. Cresswell. 1995. HLA-DM induces CLIP dissociation from MHC class II alpha beta dimers and facilitates peptide loading. *Cell* 82: 155–165.
320. Jung, S., D. Unutmaz, P. Wong, G.-I. Sano, K. De los Santos, T. Sparwasser, S. Wu, S. Vuthoori, K. Ko, F. Zavala, E. G. Pamer, D. R. Littman, and R. A. Lang. 2002. In vivo depletion of CD11c+ dendritic cells abrogates priming of CD8+ T cells by exogenous cell-associated antigens. *Immunity* 17: 211–220.
321. Förster, R., A. Schubel, D. Breitfeld, E. Kremmer, I. Renner-Müller, E. Wolf, and M. Lipp. 1999. CCR7 coordinates the primary immune response by establishing functional microenvironments in secondary lymphoid organs. *Cell* 99: 23–33.
322. Grakoui, A., S. K. Bromley, C. Sumen, M. M. Davis, A. S. Shaw, P. M. Allen, and M. L. Dustin. 1999. The immunological synapse: a molecular machine controlling T cell activation. *Science* 285: 221–227.
323. Paul, W. E., and R. A. Seder. 1994. Lymphocyte responses and cytokines. *Cell* 76: 241–251.
324. Krummel, M. F., and M. D. Cahalan. 2010. The immunological synapse: a dynamic platform for local signaling. *J. Clin. Immunol.* 30: 364–372.
325. Huppa, J. B., and M. M. Davis. 2003. T-cell-antigen recognition and the immunological synapse. *Nat Rev Immunol* 3: 973–983.

326. Huppa, J. B., M. Gleimer, C. Sumen, and M. M. Davis. 2003. Continuous T cell receptor signaling required for synapse maintenance and full effector potential. *Nat Immunol* 4: 749–755.
327. Feske, S., J. Giltman, R. Dolmetsch, L. M. Staudt, and A. Rao. 2001. Gene regulation mediated by calcium signals in T lymphocytes. *Nat Immunol* 2: 316–324.
328. Dieu-Nosjean, M. C., A. Vicari, S. Lebecque, and C. Caux. 1999. Regulation of dendritic cell trafficking: a process that involves the participation of selective chemokines. *J Leukoc Biol* 66: 252–262.
329. Hawiger, D., K. Inaba, Y. Dorsett, M. Guo, K. Mahnke, M. Rivera, J. V. Ravetch, R. M. Steinman, and M. C. Nussenzweig. 2001. Dendritic cells induce peripheral T cell unresponsiveness under steady state conditions in vivo. *J Exp Med* 194: 769–779.
330. Menges, M., S. Rössner, C. Voigtländer, H. Schindler, N. A. Kukutsch, C. Bogdan, K. Erb, G. Schuler, and M. B. Lutz. 2002. Repetitive injections of dendritic cells matured with tumor necrosis factor alpha induce antigen-specific protection of mice from autoimmunity. *J Exp Med* 195: 15–21.
331. Liu, K., T. Iyoda, M. Saternus, Y. Kimura, K. Inaba, and R. M. Steinman. 2002. Immune tolerance after delivery of dying cells to dendritic cells in situ. *J Exp Med* 196: 1091–1097.
332. Chu, C.-C., N. Ali, P. Karagiannis, P. Di Meglio, A. Skowera, L. Napolitano, G. Barinaga, K. Grysb, E. Sharif-Paghaleh, S. N. Karagiannis, M. Peakman, G. Lombardi, and F. O. Nestle. 2012. Resident CD141 (BDCA3)+ dendritic cells in human skin produce IL-10 and induce regulatory T cells that suppress skin inflammation. *J Exp Med* 209: 935–945.
333. Persson, E. K., C. L. Scott, A. M. Mowat, and W. W. Agace. 2013. Dendritic cell subsets in the intestinal lamina propria: Ontogeny and function. *Eur J Immunol*.
334. Edelson, B. T., W. Kc, R. Juang, M. Kohyama, L. A. Benoit, P. A. Klekotka, C. Moon, J. C. Albring, W. Ise, D. G. Michael, D. Bhattacharya, T. S. Stappenbeck, M. J. Holtzman, S.-S. J. Sung, T. L. Murphy, K. Hildner, and K. M. Murphy. 2010. Peripheral CD103+ dendritic cells form a unified subset developmentally related to CD8alpha+ conventional dendritic cells. *Journal of Experimental Medicine* 207: 823–836.
335. Munn, D. H., M. D. Sharma, J. R. Lee, K. G. Jhaver, T. S. Johnson, D. B. Keskin, B. Marshall, P. Chandler, S. J. Antonia, R. Burgess, C. L. Slingluff, and A. L. Mellor. 2002. Potential regulatory function of human dendritic cells expressing indoleamine 2,3-dioxygenase. *Science* 297: 1867–1870.
336. Le Bon, A., and D. F. Tough. 2008. Type I interferon as a stimulus for cross-priming. *Cytokine Growth Factor Rev.* 19: 33–40.
337. Schulz, O., S. S. Diebold, M. Chen, T. I. Näslund, M. A. Nolte, L. Alexopoulou, Y.-T. Azuma, R. A. Flavell, P. Liljeström, and C. Reis e Sousa. 2005. Toll-like receptor 3 promotes cross-priming to virus-infected cells. *Nature* 433: 887–892.
338. Sancho, D., O. P. Joffre, A. M. Keller, N. C. Rogers, D. Martínez, P. Hernanz-Falcón, I. Rosewell, and C. Reis e Sousa. 2009. Identification of a dendritic cell receptor that couples sensing of necrosis to immunity. *Nature* 458: 899–903.
339. Crozat, K., R. Guiton, V. Contreras, V. Feuillet, C.-A. Dutertre, E. Ventre, T.-P. Vu Manh, T. Baranek, A. K. Storset, J. Marvel, P. Boudinot, A. Hosmalin, I. Schwartz-Cornil, and M. Dalod. 2010. The XC chemokine receptor 1 is a conserved selective marker of mammalian cells homologous to mouse CD8alpha+ dendritic cells. *J Exp Med* 207: 1283–1292.
340. Haniffa, M., A. Shin, V. Bigley, N. McGovern, P. Teo, P. See, P. S. Wasan, X.-N. Wang, F. Malinarich, B. Malleret, A. Larbi, P. Tan, H. Zhao, M. Poidinger, S. Pagan, S. Cookson, R. Dickinson, I. Dimmick, R. F. Jarrett, L. Renia, J. Tam, C. Song, J. Connolly, J. K. Y. Chan, A. Gehring, A. Bertolotti, M. Collin, and F. Ginhoux. 2012. Human Tissues Contain CD141(hi) Cross-Presenting Dendritic Cells with Functional Homology to Mouse CD103(+) Nonlymphoid Dendritic Cells. *Immunity* 37: 60–73.

341. Meixlsperger, S., C. S. Leung, P. C. Ramer, M. Pack, L. D. Vanoaica, G. Breton, S. Pascolo, A. M. Salazar, A. Dzionek, J. Schmitz, R. M. Steinman, and C. Munz. 2013. CD141+ dendritic cells produce prominent amounts of IFN- α after dsRNA recognition and can be targeted via DEC-205 in humanized mice. *Blood*.
342. Lauterbach, H., B. Bathke, S. Gilles, C. Traidl-Hoffmann, C. A. Lubber, G. Fejer, M. A. Freudenberg, G. M. Davey, D. Vremec, A. Kallies, L. Wu, K. Shortman, P. Chaplin, M. Suter, M. O'Keefe, and H. Hochrein. 2010. Mouse CD8 α + DCs and human BDCA3+ DCs are major producers of IFN-lambda in response to poly IC. *Journal of Experimental Medicine* 207: 2703–2717.
343. Haan, den, J. M., S. M. Lehar, and M. J. Bevan. 2000. CD8(+) but not CD8(-) dendritic cells cross-prime cytotoxic T cells in vivo. *J Exp Med* 192: 1685–1696.
344. Iyoda, T., S. Shimoyama, K. Liu, Y. Omatsu, Y. Akiyama, Y. Maeda, K. Takahara, R. M. Steinman, and K. Inaba. 2002. The CD8+ dendritic cell subset selectively endocytoses dying cells in culture and in vivo. *J Exp Med* 195: 1289–1302.
345. Schulz, O., and C. Reis e Sousa. 2002. Cross-presentation of cell-associated antigens by CD8 α + dendritic cells is attributable to their ability to internalize dead cells. *Immunology* 107: 183–189.
346. Piccioli, D., S. Tavarini, E. Borgogni, V. Steri, S. Nuti, C. Sammicheli, M. Bardelli, D. Montagna, F. Locatelli, and A. Wack. 2007. Functional specialization of human circulating CD16 and CD1c myeloid dendritic-cell subsets. *Blood* 109: 5371–5379.
347. Yu, C. I., C. Becker, Y. Wang, F. Marches, J. Helft, M. Leboeuf, E. Anguiano, S. Pourpe, K. Goller, V. Pascual, J. Banchereau, M. Merad, and K. Palucka. 2013. Human CD1c(+) Dendritic Cells Drive the Differentiation of CD103(+) CD8(+) Mucosal Effector T Cells via the Cytokine TGF- β . *Immunity* 38: 818–830.
348. Cepek, K. L., S. K. Shaw, C. M. Parker, G. J. Russell, J. S. Morrow, D. L. Rimm, and M. B. Brenner. 1994. Adhesion between epithelial cells and T lymphocytes mediated by E-cadherin and the alpha E beta 7 integrin. *Nature* 372: 190–193.
349. Coombes, J. L., K. R. R. Siddiqui, C. V. Arancibia-Carcamo, J. Hall, C.-M. Sun, Y. Belkaid, and F. Powrie. 2007. A functionally specialized population of mucosal CD103+ DCs induces Foxp3+ regulatory T cells via a TGF-beta and retinoic acid-dependent mechanism. 204: 1757–1764.
350. Benson, M. J., K. Pino-Lagos, M. Roseblatt, and R. J. Noelle. 2007. All-trans retinoic acid mediates enhanced T reg cell growth, differentiation, and gut homing in the face of high levels of co-stimulation. *J Exp Med* 204: 1765–1774.
351. Sun, C.-M., J. A. Hall, R. B. Blank, N. Bouladoux, M. Oukka, J. R. Mora, and Y. Belkaid. 2007. Small intestine lamina propria dendritic cells promote de novo generation of Foxp3 T reg cells via retinoic acid. *J Exp Med* 204: 1775–1785.
352. Sato, T., T. Kitawaki, H. Fujita, M. Iwata, T. Iyoda, K. Inaba, T. Ohteki, S. Hasegawa, K. Kawada, Y. Sakai, H. Ikeuchi, H. Nakase, A. Niwa, A. Takaori-Kondo, and N. Kadowaki. 2013. Human CD1c+ Myeloid Dendritic Cells Acquire a High Level of Retinoic Acid-Producing Capacity in Response to Vitamin D3. *The Journal of Immunology*.
353. Belge, K.-U., F. Dayyani, A. Horelt, M. Siedlar, M. Frankenberger, B. Frankenberger, T. Espevik, and L. Ziegler-Heitbrock. 2002. The proinflammatory CD14+CD16+DR++ monocytes are a major source of TNF. *J Immunol* 168: 3536–3542.
354. Zhao, C., H. Zhang, W.-C. Wong, X. Sem, H. Han, S.-M. Ong, Y.-C. Tan, W.-H. Yeap, C.-S. Gan, K.-Q. Ng, M. B.-C. Koh, P. Kourilsky, S.-K. Sze, and S.-C. Wong. 2009. Identification of novel functional differences in monocyte subsets using proteomic and transcriptomic methods. *J. Proteome Res.* 8: 4028–4038.
355. Rossol, M., S. Kraus, M. Pierer, C. Baerwald, and U. Wagner. 2012. The CD14(bright) CD16+ monocyte subset is expanded in rheumatoid arthritis and promotes expansion of the Th17 cell population. *Arthritis Rheum* 64: 671–677.
356. Auffray, C., D. Fogg, M. Garfa, G. Elain, O. Join-Lambert, S. Kayal, S. Sarnacki, A.

- Cumano, G. Lauvau, and F. Geissmann. 2007. Monitoring of blood vessels and tissues by a population of monocytes with patrolling behavior. *Science* 317: 666–670.
357. Jähnisch, H., R. Wehner, A. Tunger, A. Kunze, S. Oehrl, K. Schäkel, J. Rohayem, M. Bornhäuser, T. Tonn, M. Bachmann, and M. Schmitz. 2013. TLR7/8 agonists trigger immunostimulatory properties of human 6-sulfo LacNAc dendritic cells. *Cancer Lett.* 335: 119–127.
358. Randolph, G. J., G. Sanchez-Schmitz, R. M. Liebman, and K. Schäkel. 2002. The CD16(+) (FcγRIII(+)) subset of human monocytes preferentially becomes migratory dendritic cells in a model tissue setting. *J Exp Med* 196: 517–527.
359. Schäkel, K., M. von Kietzell, A. Hänsel, A. Ebling, L. Schulze, M. Haase, C. Semmler, M. Sarfati, A. N. Barclay, G. J. Randolph, M. Meurer, and E. P. Rieber. 2006. Human 6-sulfo LacNAc-expressing dendritic cells are principal producers of early interleukin-12 and are controlled by erythrocytes. *Immunity* 24: 767–777.
360. Wehner, R., B. Löbel, M. Bornhäuser, K. Schäkel, M. Cartellieri, M. Bachmann, E. P. Rieber, and M. Schmitz. 2009. Reciprocal activating interaction between 6-sulfo LacNAc+ dendritic cells and NK cells. *Int J Cancer* 124: 358–366.
361. Cella, M., D. Jarrossay, F. Facchetti, O. Alebardi, H. Nakajima, A. Lanzavecchia, and M. Colonna. 1999. Plasmacytoid monocytes migrate to inflamed lymph nodes and produce large amounts of type I interferon. *Nat. Med.* 5: 919–923.
362. Ito, T., Y.-H. Wang, and Y.-J. Liu. 2005. Plasmacytoid dendritic cell precursors/type I interferon-producing cells sense viral infection by Toll-like receptor (TLR) 7 and TLR9. *Springer Semin. Immunopathol.* 26: 221–229.
363. Kolumam, G. A., S. Thomas, L. J. Thompson, J. Sprent, and K. Murali-Krishna. 2005. Type I interferons act directly on CD8 T cells to allow clonal expansion and memory formation in response to viral infection. *J Exp Med* 202: 637–650.
364. Marrack, P., J. Kappler, and T. Mitchell. 1999. Type I interferons keep activated T cells alive. *J Exp Med* 189: 521–530.
365. Mescher, M. F., J. M. Curtsinger, P. Agarwal, K. A. Casey, M. Gerner, C. D. Hammerbeck, F. Popescu, and Z. Xiao. 2006. Signals required for programming effector and memory development by CD8+ T cells. *Immunol Rev* 211: 81–92.
366. Penna, G., M. Vulcano, A. Roncari, F. Facchetti, S. Sozzani, and L. Adorini. 2002. Cutting edge: differential chemokine production by myeloid and plasmacytoid dendritic cells. *J Immunol* 169: 6673–6676.
367. Decalf, J., S. Fernandes, R. Longman, M. Ahloulay, F. Audat, F. Lefrerre, C. M. Rice, S. Pol, and M. L. Albert. 2007. Plasmacytoid dendritic cells initiate a complex chemokine and cytokine network and are a viable drug target in chronic HCV patients. *J Exp Med* 204: 2423–2437.
368. Villadangos, J. A., and L. Young. 2008. Antigen-presentation properties of plasmacytoid dendritic cells. *Immunity* 29: 352–361.
369. Hoeffel, G., A.-C. Ripoche, D. Matheoud, M. Nascimbeni, N. Escriou, P. Lebon, F. Heshmati, J.-G. Guillet, M. Gannagé, S. Caillat-Zucman, N. Casartelli, O. Schwartz, H. De la Salle, D. Hanau, A. Hosmalin, and C. Marañón. 2007. Antigen crosspresentation by human plasmacytoid dendritic cells. *Immunity* 27: 481–492.
370. Turnbull, E., and G. Macpherson. 2001. Immunobiology of dendritic cells in the rat. *Immunol Rev* 184: 58–68.
371. Liu, L., M. Zhang, C. Jenkins, and G. G. MacPherson. 1998. Dendritic cell heterogeneity in vivo: two functionally different dendritic cell populations in rat intestinal lymph can be distinguished by CD4 expression. *J Immunol* 161: 1146–1155.
372. Huang, F. P., N. Platt, M. Wykes, J. R. Major, T. J. Powell, C. D. Jenkins, and G. G. MacPherson. 2000. A discrete subpopulation of dendritic cells transports apoptotic intestinal epithelial cells to T cell areas of mesenteric lymph nodes. *J Exp Med* 191: 435–444.
373. Milling, S. W. F., C. D. Jenkins, U. Yrliid, V. Cerovic, H. Edmond, V. McDonald, M.

- Nassar, and G. Macpherson. 2009. Steady-state migrating intestinal dendritic cells induce potent inflammatory responses in naive CD4⁺ T cells. *Mucosal Immunol* 2: 156–165.
374. Yrlid, U., V. Cerovic, S. Milling, C. D. Jenkins, L. S. Klavinskis, and G. G. MacPherson. 2006. A distinct subset of intestinal dendritic cells responds selectively to oral TLR7/8 stimulation. *Eur J Immunol* 36: 2639–2648.
375. Cerovic, V., C. D. Jenkins, A. G. C. Barnes, S. W. F. Milling, G. G. MacPherson, and L. S. Klavinskis. 2009. Hyporesponsiveness of intestinal dendritic cells to TLR stimulation is limited to TLR4. *J Immunol* 182: 2405–2415.
376. Trinité, B., C. Voisine, H. Yagita, and R. Josien. 2000. A subset of cytolytic dendritic cells in rat. *J Immunol* 165: 4202–4208.
377. Hubert, F.-X., C. Voisine, C. Louvet, M. Heslan, and R. Josien. 2004. Rat plasmacytoid dendritic cells are an abundant subset of MHC class II⁺ CD4⁺CD11b-OX62⁻ and type I IFN-producing cells that exhibit selective expression of Toll-like receptors 7 and 9 and strong responsiveness to CpG. *J Immunol* 172: 7485–7494.
378. Waskow, C., K. Liu, G. Darrasse-Jeze, P. Guermonprez, F. Ginhoux, M. Merad, T. Shengelia, K. Yao, and M. Nussenzweig. 2008. The receptor tyrosine kinase Flt3 is required for dendritic cell development in peripheral lymphoid tissues. *Nat Immunol* 9: 676–683.
379. Hildner, K., B. T. Edelson, W. E. Purtha, M. Diamond, H. Matsushita, M. Kohyama, B. Calderon, B. U. Schraml, E. R. Unanue, M. S. Diamond, R. D. Schreiber, T. L. Murphy, and K. M. Murphy. 2008. Batf3 deficiency reveals a critical role for CD8 α ⁺ dendritic cells in cytotoxic T cell immunity. *Science* 322: 1097–1100.
380. Ginhoux, F., K. Liu, J. Helft, M. Bogunovic, M. Greter, D. Hashimoto, J. Price, N. Yin, J. Bromberg, S. A. Lira, E. R. Stanley, M. Nussenzweig, and M. Merad. 2009. The origin and development of nonlymphoid tissue CD103⁺ DCs. *Journal of Experimental Medicine* 206: 3115–3130.
381. Hacker, C., R. D. Kirsch, X.-S. Ju, T. Hieronymus, T. C. Gust, C. Kuhl, T. Jorgas, S. M. Kurz, S. Rose-John, Y. Yokota, and M. Zenke. 2003. Transcriptional profiling identifies Id2 function in dendritic cell development. *Nat Immunol* 4: 380–386.
382. Kusunoki, T., M. Sugai, T. Katakai, Y. Omatsu, T. Iyoda, K. Inaba, T. Nakahata, A. Shimizu, and Y. Yokota. 2003. TH2 dominance and defective development of a CD8⁺ dendritic cell subset in Id2-deficient mice. *J. Allergy Clin. Immunol.* 111: 136–142.
383. Dudziak, D., A. O. Kamphorst, G. F. Heidkamp, V. R. Buchholz, C. Trumpfheller, S. Yamazaki, C. Cheong, K. Liu, H.-W. Lee, C. G. Park, R. M. Steinman, and M. C. Nussenzweig. 2007. Differential antigen processing by dendritic cell subsets in vivo. *Science* 315: 107–111.
384. Maldonado-López, R., T. De Smedt, P. Michel, J. Godfroid, B. Pajak, C. Heirman, K. Thielemans, O. Leo, J. Urbain, and M. Moser. 1999. CD8 α ⁺ and CD8 α ⁻ subclasses of dendritic cells direct the development of distinct T helper cells in vivo. *J Exp Med* 189: 587–592.
385. Hochrein, H., K. Shortman, D. Vremec, B. Scott, P. Hertzog, and M. O’Keeffe. 2001. Differential production of IL-12, IFN- α , and IFN- γ by mouse dendritic cell subsets. *J Immunol* 166: 5448–5455.
386. Qiu, C.-H., Y. Miyake, H. Kaise, H. Kitamura, O. Ohara, and M. Tanaka. 2009. Novel subset of CD8 α ⁺ dendritic cells localized in the marginal zone is responsible for tolerance to cell-associated antigens. *The Journal of Immunology* 182: 4127–4136.
387. Anderson, K. L., H. Perkin, C. D. Surh, S. Venturini, R. A. Maki, and B. E. Torbett. 2000. Transcription factor PU.1 is necessary for development of thymic and myeloid progenitor-derived dendritic cells. *J Immunol* 164: 1855–1861.
388. Caton, M. L., M. R. Smith-Raska, and B. Reizis. 2007. Notch-RBP-J signaling controls the homeostasis of CD8⁻ dendritic cells in the spleen. *J Exp Med* 204: 1653–1664.
389. Cerovic, V., S. A. Houston, C. L. Scott, A. Aumeunier, U. Yrlid, A. M. Mowat, and S. W. F. Milling. 2013. Intestinal CD103(-) dendritic cells migrate in lymph and prime

- effector T cells. *Mucosal Immunol* 6: 104–113.
390. O'Keefe, M., H. Hochrein, D. Vremec, B. Scott, P. Hertzog, L. Tatarczuch, and K. Shortman. 2003. Dendritic cell precursor populations of mouse blood: identification of the murine homologues of human blood plasmacytoid pre-DC2 and CD11c⁺ DC1 precursors. *Blood* 101: 1453–1459.
391. Asselin-Paturel, C., A. Boonstra, M. Dalod, I. Durand, N. Yessaad, C. Dezutter-Dambuyant, A. Vicari, A. O'Garra, C. Biron, F. Brière, and G. Trinchieri. 2001. Mouse type I IFN-producing cells are immature APCs with plasmacytoid morphology. *Nat Immunol* 2: 1144–1150.
392. Nakano, H., M. Yanagita, and M. D. Gunn. 2001. CD11c(+)B220(+)Gr-1(+) cells in mouse lymph nodes and spleen display characteristics of plasmacytoid dendritic cells. *J Exp Med* 194: 1171–1178.
393. Robbins, S. H., T. Walzer, D. Dembélé, C. Thibault, A. Defays, G. Bessou, H. Xu, E. Vivier, M. Sellars, P. Pierre, F. R. Sharp, S. Chan, P. Kastner, and M. Dalod. 2008. Novel insights into the relationships between dendritic cell subsets in human and mouse revealed by genome-wide expression profiling. *Genome Biol* 9: R17.
394. Villadangos, J. A., and K. Shortman. 2010. Found in translation: the human equivalent of mouse CD8⁺ dendritic cells. *J Exp Med* 207: 1131–1134.
395. Macpherson, A. J., E. Slack, M. B. Geuking, and K. D. McCoy. 2009. The mucosal firewalls against commensal intestinal microbes. *Semin Immunopathol* 31: 145–149.
396. Mowat, A. M., and J. L. Viney. 1997. The anatomical basis of intestinal immunity. *Immunol Rev* 156: 145–166.
397. Macpherson, A. J., and N. L. Harris. 2004. Interactions between commensal intestinal bacteria and the immune system. *Nat Rev Immunol* 4: 478–485.
398. Guy-Grand, D., and P. Vassalli. 1993. Gut intraepithelial T lymphocytes. *Curr Opin Immunol* 5: 247–252.
399. Breese, E., C. P. Braegger, C. J. Corrigan, J. A. Walker-Smith, and T. T. MacDonald. 1993. Interleukin-2- and interferon-gamma-secreting T cells in normal and diseased human intestinal mucosa. *Immunology* 78: 127–131.
400. al-Dawoud, A., I. Nakshabendi, A. Foulis, and A. M. Mowat. 1992. Immunohistochemical analysis of mucosal gamma-interferon production in coeliac disease. *Gut* 33: 1482–1486.
401. Guy-Grand, D., N. Cerf-Bensussan, B. Malissen, M. Malassis-Seris, C. Briottet, and P. Vassalli. 1991. Two gut intraepithelial CD8⁺ lymphocyte populations with different T cell receptors: a role for the gut epithelium in T cell differentiation. *J Exp Med* 173: 471–481.
402. Guy-Grand, D., B. Cuénod-Jabri, M. Malassis-Seris, F. Selz, and P. Vassalli. 1996. Complexity of the mouse gut T cell immune system: identification of two distinct natural killer T cell intraepithelial lineages. *Eur J Immunol* 26: 2248–2256.
403. Stagg, A. J., A. L. Hart, S. C. Knight, and M. A. Kamm. 2003. The dendritic cell: its role in intestinal inflammation and relationship with gut bacteria. *Gut* 52: 1522–1529.
404. Hart, A. L., H. O. Al-Hassi, R. J. Rigby, S. J. Bell, A. V. Emmanuel, S. C. Knight, M. A. Kamm, and A. J. Stagg. 2005. Characteristics of intestinal dendritic cells in inflammatory bowel diseases. *Gastroenterology* 129: 50–65.
405. Bell, S. J., R. Rigby, N. English, S. D. Mann, S. C. Knight, M. A. Kamm, and A. J. Stagg. 2001. Migration and maturation of human colonic dendritic cells. *J Immunol* 166: 4958–4967.
406. Ma, X., J. Sun, E. Papasavvas, H. Riemann, S. Robertson, J. Marshall, R. T. Bailer, A. Moore, R. P. Donnelly, G. Trinchieri, and L. J. Montaner. 2000. Inhibition of IL-12 production in human monocyte-derived macrophages by TNF. *J Immunol* 164: 1722–1729.
407. Zakharova, M., and H. K. Ziegler. 2005. Paradoxical anti-inflammatory actions of TNF-alpha: inhibition of IL-12 and IL-23 via TNF receptor 1 in macrophages and dendritic cells. *J Immunol* 175: 5024–5033.

408. Kobayashi, M., M.-N. Kweon, H. Kuwata, R. D. Schreiber, H. Kiyono, K. Takeda, and S. Akira. 2003. Toll-like receptor-dependent production of IL-12p40 causes chronic enterocolitis in myeloid cell-specific Stat3-deficient mice. *J Clin Invest* 111: 1297–1308.
409. Takeda, K., B. E. Clausen, T. Kaisho, T. Tsujimura, N. Terada, I. Förster, and S. Akira. 1999. Enhanced Th1 activity and development of chronic enterocolitis in mice devoid of Stat3 in macrophages and neutrophils. *Immunity* 10: 39–49.
410. Grivennikov, S., E. Karin, J. Terzic, D. Mucida, G.-Y. Yu, S. Vallabhapurapu, J. Scheller, S. Rose-John, H. Cheroutre, L. Eckmann, and M. Karin. 2009. IL-6 and Stat3 are required for survival of intestinal epithelial cells and development of colitis-associated cancer. *Cancer Cell* 15: 103–113.
411. Jarry, A., C. Bossard, C. Bou-Hanna, D. Masson, E. Espaze, M. G. Denis, and C. L. Laboisse. 2008. Mucosal IL-10 and TGF-beta play crucial roles in preventing LPS-driven, IFN-gamma-mediated epithelial damage in human colon explants. *J Clin Invest* 118: 1132–1142.
412. Monteleone, I., A. M. Platt, E. Jaensson, W. W. Agace, and A. M. Mowat. 2008. IL-10-dependent partial refractoriness to Toll-like receptor stimulation modulates gut mucosal dendritic cell function. *Eur J Immunol* 38: 1533–1547.
413. Stagg, A. J., M. A. Kamm, and S. C. Knight. 2002. Intestinal dendritic cells increase T cell expression of alpha4beta7 integrin. *Eur J Immunol* 32: 1445–1454.
414. Rimoldi, M., M. Chieppa, V. Salucci, F. Avogadri, A. Sonzogni, G. M. Sampietro, A. Nespoli, G. Viale, P. Allavena, and M. Rescigno. 2005. Intestinal immune homeostasis is regulated by the crosstalk between epithelial cells and dendritic cells. *Nat Immunol* 6: 507–514.
415. Iwasaki, A., and B. L. Kelsall. 1999. Freshly isolated Peyer's patch, but not spleen, dendritic cells produce interleukin 10 and induce the differentiation of T helper type 2 cells. *J Exp Med* 190: 229–239.
416. Iwasaki, A., and B. L. Kelsall. 2001. Unique functions of CD11b+, CD8 alpha+, and double-negative Peyer's patch dendritic cells. *J Immunol* 166: 4884–4890.
417. Annacker, O., J. L. Coombes, V. Malmström, H. H. Uhlig, T. Bourne, B. Johansson-Lindbom, W. W. Agace, C. M. Parker, and F. Powrie. 2005. Essential role for CD103 in the T cell-mediated regulation of experimental colitis. *J Exp Med* 202: 1051–1061.
418. Macpherson, A. J., and T. Uhr. 2004. Induction of protective IgA by intestinal dendritic cells carrying commensal bacteria. *Science* 303: 1662–1665.
419. Sato, A., M. Hashiguchi, E. Toda, A. Iwasaki, S. Hachimura, and S. Kaminogawa. 2003. CD11b+ Peyer's patch dendritic cells secrete IL-6 and induce IgA secretion from naive B cells. *J Immunol* 171: 3684–3690.
420. Badami, E., C. Sorini, M. Coccia, V. Usuelli, L. Molteni, A. M. Bolla, M. Scavini, A. Mariani, C. King, E. Bosi, and M. Falcone. 2011. Defective differentiation of regulatory FoxP3+ T cells by small-intestinal dendritic cells in patients with type 1 diabetes. *Diabetes* 60: 2120–2124.
421. Matteoli, G., E. Mazzini, I. D. Iliev, E. Mileti, F. Fallarino, P. Puccetti, M. Chieppa, and M. Rescigno. 2010. Gut CD103+ dendritic cells express indoleamine 2,3-dioxygenase which influences T regulatory/T effector cell balance and oral tolerance induction. *Gut* 59: 595–604.
422. Kaser, A., O. Ludwiczek, S. Holzmann, A. R. Moschen, G. Weiss, B. Enrich, I. Graziadei, S. Dunzendorfer, C. J. Wiedermann, E. Mürzl, E. Grasl, Z. Jasarevic, N. Romani, F. A. Offner, and H. Tilg. 2004. Increased expression of CCL20 in human inflammatory bowel disease. *J. Clin. Immunol.* 24: 74–85.
423. Smith, P. D., E. N. Janoff, M. Mosteller-Barnum, M. Merger, J. M. Orenstein, J. F. Kearney, and M. F. Graham. 1997. Isolation and purification of CD14-negative mucosal macrophages from normal human small intestine. *J. Immunol. Methods* 202: 1–11.
424. Smythies, L. E., M. Sellers, R. H. Clements, M. Mosteller-Barnum, G. Meng, W. H. Benjamin, J. M. Orenstein, and P. D. Smith. 2005. Human intestinal macrophages display

- profound inflammatory anergy despite avid phagocytic and bacteriocidal activity. *J Clin Invest* 115: 66–75.
425. Grimm, M. C., P. Pavli, E. Van de Pol, and W. F. Doe. 1995. Evidence for a CD14+ population of monocytes in inflammatory bowel disease mucosa--implications for pathogenesis. *Clin Exp Immunol* 100: 291–297.
426. Smith, P. D., L. E. Smythies, M. Mosteller-Barnum, D. A. Sibley, M. W. Russell, M. Merger, M. T. Sellers, J. M. Orenstein, T. Shimada, M. F. Graham, and H. Kubagawa. 2001. Intestinal macrophages lack CD14 and CD89 and consequently are down-regulated for LPS- and IgA-mediated activities. *J Immunol* 167: 2651–2656.
427. Kamada, N., T. Hisamatsu, S. Okamoto, H. Chinen, T. Kobayashi, T. Sato, A. Sakuraba, M. T. Kitazume, A. Sugita, K. Koganei, K. S. Akagawa, and T. Hibi. 2008. Unique CD14 intestinal macrophages contribute to the pathogenesis of Crohn disease via IL-23/IFN-gamma axis. *J Clin Invest* 118: 2269–2280.
428. Smith, P. D., L. E. Smythies, R. Shen, T. Greenwell-Wild, M. Gliozzi, and S. M. Wahl. 2011. Intestinal macrophages and response to microbial encroachment. *Mucosal Immunol* 4: 31–42.
429. Rescigno, M., M. Urbano, B. Valzasina, M. Francolini, G. Rotta, R. Bonasio, F. Granucci, J. P. Kraehenbuhl, and P. Ricciardi-Castagnoli. 2001. Dendritic cells express tight junction proteins and penetrate gut epithelial monolayers to sample bacteria. *Nat Immunol* 2: 361–367.
430. Niess, J. H., S. Brand, X. Gu, L. Landsman, S. Jung, B. A. McCormick, J. M. Vyas, M. Boes, H. L. Ploegh, J. G. Fox, D. R. Littman, and H.-C. Reinecker. 2005. CX3CR1-mediated dendritic cell access to the intestinal lumen and bacterial clearance. *Science* 307: 254–258.
431. Pull, S. L., J. M. Doherty, J. C. Mills, J. I. Gordon, and T. S. Stappenbeck. 2005. Activated macrophages are an adaptive element of the colonic epithelial progenitor niche necessary for regenerative responses to injury. *Proc Natl Acad Sci USA* 102: 99–104.
432. Morteau, O., S. G. Morham, R. Sellon, L. A. Dieleman, R. Langenbach, O. Smithies, and R. B. Sartor. 2000. Impaired mucosal defense to acute colonic injury in mice lacking cyclooxygenase-1 or cyclooxygenase-2. *J Clin Invest* 105: 469–478.
433. Hadis, U., B. Wahl, O. Schulz, M. Hardtke-Wolenski, A. Schippers, N. Wagner, W. Müller, T. Sparwasser, R. Förster, and O. Pabst. 2011. Intestinal tolerance requires gut homing and expansion of FoxP3+ regulatory T cells in the lamina propria. *Immunity* 34: 237–246.
434. Bain, C. C., and A. M. Mowat. 2011. Intestinal macrophages - specialised adaptation to a unique environment. *Eur J Immunol* 41: 2494–2498.
435. Mahida, Y. R., K. C. Wu, and D. P. Jewell. 1989. Respiratory burst activity of intestinal macrophages in normal and inflammatory bowel disease. *Gut* 30: 1362–1370.
436. Smythies, L. E., R. Shen, D. Bimczok, L. Novak, R. H. Clements, D. E. Eckhoff, P. Bouchard, M. D. George, W. K. Hu, S. Dandekar, and P. D. Smith. 2010. Inflammation anergy in human intestinal macrophages is due to Smad-induced IkappaBalpha expression and NF-kappaB inactivation. *J Biol Chem* 285: 19593–19604.
437. Snelgrove, R. J., J. Goulding, A. M. Didierlaurent, D. Lyonga, S. Vekaria, L. Edwards, E. Gwyer, J. D. Sedgwick, A. N. Barclay, and T. Hussell. 2008. A critical function for CD200 in lung immune homeostasis and the severity of influenza infection. *Nat Immunol* 9: 1074–1083.
438. Bain, C. C., and A. M. Mowat. 2012. CD200 receptor and macrophage function in the intestine. *Immunobiology* 217: 643–651.
439. Kayama, H., Y. Ueda, Y. Sawa, S. G. Jeon, J. S. Ma, R. Okumura, A. Kubo, M. Ishii, T. Okazaki, M. Murakami, M. Yamamoto, H. Yagita, and K. Takeda. 2012. Intestinal CX3C chemokine receptor 1(high) (CX3CR1(high)) myeloid cells prevent T-cell-dependent colitis. *Proc Natl Acad Sci USA* 109: 5010–5015.
440. Purrmann, J., H. Zeidler, J. Bertrams, E. Juli, S. Cleveland, W. Berges, R. Gemsa, C.

- Specker, and H. E. Reis. 1988. HLA antigens in ankylosing spondylitis associated with Crohn's disease. Increased frequency of the HLA phenotype B27,B44. *J Rheumatol* 15: 1658–1661.
441. Van Praet, L., F. E. Van den Bosch, P. Jacques, P. Carron, L. Jans, R. Colman, E. Glorieus, H. Peeters, H. Mielants, M. De Vos, C. Cuvelier, and D. Elewaut. 2013. Microscopic gut inflammation in axial spondyloarthritis: a multiparametric predictive model. *Ann Rheum Dis* 72: 414–417.
442. Hascelik, G., B. Oz, N. Olmez, A. Memis, G. Yoruk, B. Unsal, and N. Ekinici. 2009. Association of macroscopic gut inflammation with disease activity, functional status and quality of life in ankylosing spondylitis. *Rheumatol Int* 29: 755–758.
443. Brophy, S., S. Pavy, P. Lewis, G. Taylor, L. Bradbury, D. Robertson, C. Lovell, and A. Calin. 2001. Inflammatory eye, skin, and bowel disease in spondyloarthritis: genetic, phenotypic, and environmental factors. *J Rheumatol* 28: 2667–2673.
444. Taurog, J. D., J. A. Richardson, J. T. Croft, W. A. Simmons, M. Zhou, J. L. Fernández-Sueiro, E. Balish, and R. E. Hammer. 1994. The germfree state prevents development of gut and joint inflammatory disease in HLA-B27 transgenic rats. *J Exp Med* 180: 2359–2364.
445. Stebbings, S., K. Munro, M. A. Simon, G. Tannock, J. Highton, H. Harmsen, G. Welling, P. Seksik, J. Dore, G. Grame, and A. Tilsala-Timisjarvi. 2002. Comparison of the faecal microflora of patients with ankylosing spondylitis and controls using molecular methods of analysis. *Rheumatology (Oxford)* 41: 1395–1401.
446. Smith, J. A., E. Märker-Hermann, and R. A. Colbert. 2006. Pathogenesis of ankylosing spondylitis: current concepts. *Best Pract Res Clin Rheumatol* 20: 571–591.
447. François, R. J., D. L. Gardner, E. J. Degrave, and E. G. Bywaters. 2000. Histopathologic evidence that sacroiliitis in ankylosing spondylitis is not merely enthesitis. *Arthritis Rheum* 43: 2011–2024.
448. Tam, L.-S., J. Gu, and D. Yu. 2010. Pathogenesis of ankylosing spondylitis. *Nat Rev Rheumatol* 6: 399–405.
449. McGonagle, D., M. A. Khan, H. Marzo-Ortega, P. O'Connor, W. Gibbon, and P. Emery. 1999. Enthesitis in spondyloarthropathy. *Curr Opin Rheumatol* 11: 244–250.
450. McGonagle, D., W. Gibbon, P. O'Connor, M. Green, C. Pease, and P. Emery. 1998. Characteristic magnetic resonance imaging enthesal changes of knee synovitis in spondylarthropathy. *Arthritis Rheum* 41: 694–700.
451. Braun, J., M. Bollow, L. Neure, E. Seipelt, F. Seyrekbasan, H. Herbst, U. Eggens, A. Distler, and J. Sieper. 1995. Use of immunohistologic and in situ hybridization techniques in the examination of sacroiliac joint biopsy specimens from patients with ankylosing spondylitis. *Arthritis Rheum* 38: 499–505.
452. Bollow, M., T. Fischer, H. Reissauer, M. Backhaus, J. Sieper, B. Hamm, and J. Braun. 2000. Quantitative analyses of sacroiliac biopsies in spondyloarthropathies: T cells and macrophages predominate in early and active sacroiliitis- cellularity correlates with the degree of enhancement detected by magnetic resonance imaging. *Ann Rheum Dis* 59: 135–140.
453. Baeten, D. 2000. Comparative study of the synovial histology in rheumatoid arthritis, spondyloarthropathy, and osteoarthritis: influence of disease duration and activity. *Ann Rheum Dis* 59: 945–953.
454. Baeten, D., P. Demetter, C. A. Cuvelier, E. Kruithof, N. Van Damme, M. De Vos, E. M. Veys, and F. De Keyser. 2002. Macrophages expressing the scavenger receptor CD163: a link between immune alterations of the gut and synovial inflammation in spondyloarthropathy. *J Pathol* 196: 343–350.
455. Demetter, P., M. De Vos, J. A. Van Huysse, D. Baeten, L. Ferdinande, H. Peeters, H. Mielants, E. M. Veys, F. De Keyser, and C. A. Cuvelier. 2005. Colon mucosa of patients both with spondyloarthritis and Crohn's disease is enriched with macrophages expressing the scavenger receptor CD163. *Ann Rheum Dis* 64: 321–324.

456. McGonagle, D., H. Marzo-Ortega, P. O'Connor, W. Gibbon, P. Hawkey, K. Henshaw, and P. Emery. 2002. Histological assessment of the early enthesitis lesion in spondyloarthritis. *Ann Rheum Dis* 61: 534–537.
457. Laloux, L., M. C. Voisin, J. Allain, N. Martin, L. Kerboull, X. Chevalier, and P. Claudepierre. 2001. Immunohistological study of entheses in spondyloarthropathies: comparison in rheumatoid arthritis and osteoarthritis. *Ann Rheum Dis* 60: 316–321.
458. Hammer, R. E., S. D. Maika, J. A. Richardson, J. P. Tang, and J. D. Taurog. 1990. Spontaneous inflammatory disease in transgenic rats expressing HLA-B27 and human beta 2m: an animal model of HLA-B27-associated human disorders. *Cell* 63: 1099–1112.
459. Tran, T. M., M. L. Dorris, N. Satumtira, J. A. Richardson, R. E. Hammer, J. Shang, and J. D. Taurog. 2006. Additional human beta2-microglobulin curbs HLA-B27 misfolding and promotes arthritis and spondylitis without colitis in male HLA-B27-transgenic rats. *Arthritis Rheum* 54: 1317–1327.
460. Braem, K., and R. J. Lories. 2012. Insights into the pathophysiology of ankylosing spondylitis: contributions from animal models. *Joint Bone Spine* 79: 243–248.
461. Kontoyiannis, D., M. Pasparakis, T. T. Pizarro, F. Cominelli, and G. Kollias. 1999. Impaired on/off regulation of TNF biosynthesis in mice lacking TNF AU-rich elements: implications for joint and gut-associated immunopathologies. *Immunity* 10: 387–398.
462. Hayer, S., B. Niederreiter, I. Nagelreiter, J. Smolen, and K. Redlich. 2010. Interleukin 6 is not a crucial regulator in an animal model of tumour necrosis factor-mediated bilateral sacroiliitis. *Ann Rheum Dis* 69: 1403–1406.
463. Bárdos, T., Z. Szabó, M. Czipri, C. Vermes, M. Tunyogi-Csapó, R. M. Urban, K. Mikecz, and T. T. Glant. 2005. A longitudinal study on an autoimmune murine model of ankylosing spondylitis. *Ann Rheum Dis* 64: 981–987.
464. Maksymowych, W. P. 2000. Ankylosing spondylitis--at the interface of bone and cartilage. *J Rheumatol* 27: 2295–2301.
465. Lories, R. J. U., P. Matthys, K. de Vlam, I. Derese, and F. P. Luyten. 2004. Ankylosing enthesitis, dactylitis, and onychopariostitis in male DBA/1 mice: a model of psoriatic arthritis. *Ann Rheum Dis* 63: 595–598.
466. Lories, R. J. U., I. Derese, and F. P. Luyten. 2005. Modulation of bone morphogenetic protein signaling inhibits the onset and progression of ankylosing enthesitis. *J Clin Invest* 115: 1571–1579.
467. Mahowald, M. L., H. Krug, and J. Taurog. 1988. Progressive ankylosis in mice. An animal model of spondylarthropathy. I. Clinical and radiographic findings. *Arthritis Rheum* 31: 1390–1399.
468. Sherlock, J. P., B. Joyce-Shaikh, S. P. Turner, C.-C. Chao, M. Sathe, J. Grein, D. M. Gorman, E. P. Bowman, T. K. McClanahan, J. H. Yearley, G. Eberl, C. D. Buckley, R. A. Kastelein, R. H. Pierce, D. M. Laface, and D. J. Cua. 2012. IL-23 induces spondyloarthritis by acting on ROR- γ t(+) CD3(+)CD4(-)CD8(-) enthesal resident T cells. *Nat. Med.* 18: 1069–1076.
469. Qian, B.-F., S. L. Tonkonogy, F. Hoentjen, L. A. Dieleman, and R. B. Sartor. 2005. Dysregulated luminal bacterial antigen-specific T-cell responses and antigen-presenting cell function in HLA-B27 transgenic rats with chronic colitis. *Immunology* 116: 112–121.
470. Breban, M., J. L. Fernández-Sueiro, J. A. Richardson, R. R. Hadavand, S. D. Maika, R. E. Hammer, and J. D. Taurog. 1996. T cells, but not thymic exposure to HLA-B27, are required for the inflammatory disease of HLA-B27 transgenic rats. *J Immunol* 156: 794–803.
471. May, E., M. L. Dorris, N. Satumtira, I. Iqbal, M. I. Rehman, E. Lightfoot, and J. D. Taurog. 2003. CD8 alpha beta T cells are not essential to the pathogenesis of arthritis or colitis in HLA-B27 transgenic rats. *J Immunol* 170: 1099–1105.
472. Taurog, J. D., M. L. Dorris, N. Satumtira, T. M. Tran, R. Sharma, R. Dressel, J. van den Brandt, and H. M. Reichardt. 2009. Spondylarthritis in HLA-B27/human beta2-microglobulin-transgenic rats is not prevented by lack of CD8. *Arthritis Rheum* 60: 1977–

1984.

473. Hoentjen, F., S. L. Tonkonogy, B. Liu, R. B. Sartor, J. D. Taurog, and L. A. Dieleman. 2006. Adoptive transfer of nontransgenic mesenteric lymph node cells induces colitis in athymic HLA-B27 transgenic nude rats. *Clin Exp Immunol* 143: 474–483.
474. Breban, M., R. E. Hammer, J. A. Richardson, and J. D. Taurog. 1993. Transfer of the inflammatory disease of HLA-B27 transgenic rats by bone marrow engraftment. *J Exp Med* 178: 1607–1616.
475. Fert, I., S. Glatigny, C. Poulain, N. Satumtira, M. L. Dorris, J. D. Taurog, and M. Breban. 2008. Correlation between dendritic cell functional defect and spondylarthritis phenotypes in HLA-B27/HUMAN beta2-microglobulin-transgenic rat lines. *Arthritis Rheum* 58: 3425–3429.
476. Hacquard-Bouder, C., G. Falgarone, A. Bosquet, F. Smaoui, D. Monnet, M. Ittah, and M. Breban. 2004. Defective costimulatory function is a striking feature of antigen-presenting cells in an HLA-B27-transgenic rat model of spondylarthropathy. *Arthritis Rheum* 50: 1624–1635.
477. Dhaenens, M., I. Fert, S. Glatigny, S. Haerinck, C. Poulain, E. Donnadieu, C. Hacquard-Bouder, C. André, D. Elewaut, D. Deforce, and M. Breban. 2009. Dendritic cells from spondylarthritis-prone HLA-B27-transgenic rats display altered cytoskeletal dynamics, class II major histocompatibility complex expression, and viability. *Arthritis Rheum* 60: 2622–2632.
478. Hacquard-Bouder, C., M.-S. Chimenti, B. Giquel, E. Donnadieu, I. Fert, A. Schmitt, C. André, and M. Breban. 2007. Alteration of antigen-independent immunologic synapse formation between dendritic cells from HLA-B27-transgenic rats and CD4+ T cells: selective impairment of costimulatory molecule engagement by mature HLA-B27. *Arthritis Rheum* 56: 1478–1489.
479. Glatigny, S., I. Fert, M. A. Blaton, R. J. Lories, L. M. Araujo, G. Chiocchia, and M. Breban. 2012. Proinflammatory Th17 cells are expanded and induced by dendritic cells in spondylarthritis-prone HLA-B27-transgenic rats. *Arthritis Rheum* 64: 110–120.
480. Utriainen, L., D. Firmin, P. Wright, V. Cerovic, M. Breban, I. McInnes, and S. Milling. 2012. Expression of HLA-B27 causes loss of migratory dendritic cells in a Rat model of spondyloarthritis. *Arthritis Rheum*.
481. DeLay, M. L., M. J. Turner, E. I. Klenk, J. A. Smith, D. P. Sowders, and R. A. Colbert. 2009. HLA-B27 misfolding and the unfolded protein response augment interleukin-23 production and are associated with Th17 activation in transgenic rats. *Arthritis Rheum* 60: 2633–2643.
482. Taurog, J. D., S. D. Maika, N. Satumtira, M. L. Dorris, I. L. McLean, H. Yanagisawa, A. Sayad, A. J. Stagg, G. M. Fox, A. Lê O'Brien, M. Rehman, M. Zhou, A. L. Weiner, J. B. Splawski, J. A. Richardson, and R. E. Hammer. 1999. Inflammatory disease in HLA-B27 transgenic rats. *Immunol Rev* 169: 209–223.
483. Ebringer, R., D. Cooke, D. R. Cawdell, P. Cowling, and A. Ebringer. 1977. Ankylosing spondylitis: klebsiella and HL-A B27. *Rheumatol Rehabil* 16: 190–196.
484. Mäki-Ikola, O., M. Penttinen, R. Von Essen, C. Gripenberg-Lerche, H. Isomäki, and K. Granfors. 1997. IgM, IgG and IgA class enterobacterial antibodies in serum and synovial fluid in patients with ankylosing spondylitis and rheumatoid arthritis. *Br. J. Rheumatol.* 36: 1051–1053.
485. Rashid, T., and A. Ebringer. 2007. Ankylosing spondylitis is linked to Klebsiella--the evidence. *Clin. Rheumatol.* 26: 858–864.
486. Stone, M. A., U. Payne, C. Schentag, P. Rahman, C. Pacheco-Tena, and R. D. Inman. 2004. Comparative immune responses to candidate arthritogenic bacteria do not confirm a dominant role for Klebsiella pneumonia in the pathogenesis of familial ankylosing spondylitis. *Rheumatology (Oxford)* 43: 148–155.
487. Schwimbeck, P. L., D. T. Yu, and M. B. Oldstone. 1987. Autoantibodies to HLA B27 in the sera of HLA B27 patients with ankylosing spondylitis and Reiter's syndrome.

- Molecular mimicry with *Klebsiella pneumoniae* as potential mechanism of autoimmune disease. *J Exp Med* 166: 173–181.
488. Fielder, M., S. J. Pirt, I. Tarpey, C. Wilson, P. Cunningham, C. Ettelaie, A. Binder, S. Bansal, and A. Ebringer. 1995. Molecular mimicry and ankylosing spondylitis: possible role of a novel sequence in pullulanase of *Klebsiella pneumoniae*. *FEBS Lett.* 369: 243–248.
489. Ramos, M., I. Alvarez, L. Sesma, A. Logean, D. Rognan, and J. A. López de Castro. 2002. Molecular mimicry of an HLA-B27-derived ligand of arthritis-linked subtypes with chlamydial proteins. *J Biol Chem* 277: 37573–37581.
490. Ben Dror, L., E. Barnea, I. Beer, M. Mann, and A. Admon. 2010. The HLA-B*2705 peptidome. *Arthritis Rheum* 62: 420–429.
491. Hülsmeier, M., M. T. Fiorillo, F. Bettosini, R. Sorrentino, W. Saenger, A. Ziegler, and B. Uchanska-Ziegler. 2004. Dual, HLA-B27 subtype-dependent conformation of a self-peptide. *J Exp Med* 199: 271–281.
492. Fiorillo, M. T., C. Rückert, M. Hülsmeier, R. Sorrentino, W. Saenger, A. Ziegler, and B. Uchanska-Ziegler. 2005. Allele-dependent similarity between viral and self-peptide presentation by HLA-B27 subtypes. *J Biol Chem* 280: 2962–2971.
493. López de Castro, J. A. 2007. HLA-B27 and the pathogenesis of spondyloarthropathies. *Immunol Lett* 108: 27–33.
494. Peh, C. A., S. R. Burrows, M. Barnden, R. Khanna, P. Cresswell, D. J. Moss, and J. McCluskey. 1998. HLA-B27-restricted antigen presentation in the absence of tapasin reveals polymorphism in mechanisms of HLA class I peptide loading. *Immunity* 8: 531–542.
495. Bowness, P., A. Ridley, J. Shaw, A. T. Chan, I. Wong-Baeza, M. Fleming, F. Cummings, A. McMichael, and S. Kollnberger. 2011. Th17 cells expressing KIR3DL2+ and responsive to HLA-B27 homodimers are increased in ankylosing spondylitis. *The Journal of Immunology* 186: 2672–2680.
496. Bird, L. A., C. A. Peh, S. Kollnberger, T. Elliott, A. J. McMichael, and P. Bowness. 2003. Lymphoblastoid cells express HLA-B27 homodimers both intracellularly and at the cell surface following endosomal recycling. *Eur J Immunol* 33: 748–759.
497. Allen, R. L., C. A. O'Callaghan, A. J. McMichael, and P. Bowness. 1999. Cutting edge: HLA-B27 can form a novel beta 2-microglobulin-free heavy chain homodimer structure. *J Immunol* 162: 5045–5048.
498. Chatzikyriakidou, A., P. V. Voulgari, and A. A. Drosos. 2011. What is the role of HLA-B27 in spondyloarthropathies? *Autoimmun Rev* 10: 464–468.
499. Allen, R. L., T. Raine, A. Haude, J. Trowsdale, and M. J. Wilson. 2001. Leukocyte receptor complex-encoded immunomodulatory receptors show differing specificity for alternative HLA-B27 structures. *J Immunol* 167: 5543–5547.
500. Kollnberger, S., L. Bird, M.-Y. Sun, C. Retiere, V. M. Braud, A. McMichael, and P. Bowness. 2002. Cell-surface expression and immune receptor recognition of HLA-B27 homodimers. *Arthritis Rheum* 46: 2972–2982.
501. Ugolini, S., C. Arpin, N. Anfossi, T. Walzer, A. Cambiaggi, R. Förster, M. Lipp, R. E. Toes, C. J. Melief, J. Marvel, and E. Vivier. 2001. Involvement of inhibitory NKRs in the survival of a subset of memory-phenotype CD8+ T cells. *Nat Immunol* 2: 430–435.
502. Payeli, S. K., S. Kollnberger, O. Marroquin Belaunzaran, M. Thiel, K. McHugh, J. Giles, J. Shaw, S. Kleber, A. Ridley, I. Wong-Baeza, S. Keidel, K. Kuroki, K. Maenaka, A. Wadle, C. Renner, and P. Bowness. 2012. Inhibiting HLA-B27 homodimer-driven immune cell inflammation in spondylarthritis. *Arthritis Rheum* 64: 3139–3149.
503. McHugh, K., O. Rysnik, S. Kollnberger, J. Shaw, L. Utriainen, M. H. Al-Mossawi, S. Payeli, O. Marroquin, S. Milling, C. Renner, and P. Bowness. 2013. Expression of aberrant HLA-B27 molecules is dependent on B27 dosage and peptide supply. *Ann Rheum Dis*.
504. Santos, S. G., S. Lynch, E. C. Campbell, A. N. Antoniou, and S. J. Powis. 2008. Induction of HLA-B27 heavy chain homodimer formation after activation in dendritic

cells. *Arthritis Res Ther* 10: R100.

505. Campbell, E. C., F. Fettke, S. Bhat, K. D. Morley, and S. J. Powis. 2011. Expression of MHC class I dimers and ERAP1 in an ankylosing spondylitis patient cohort.

Immunology 133: 379–385.

506. Vázquez, M. N., and J. A. López de Castro. 2005. Similar cell surface expression of beta2-microglobulin-free heavy chains by HLA-B27 subtypes differentially associated with ankylosing spondylitis. *Arthritis Rheum* 52: 3290–3299.

507. Uchanska-Ziegler, B., and A. Ziegler. 2003. Ankylosing spondylitis: a beta2m-deposition disease? *Trends Immunol.* 24: 73–76.

508. Colbert, R. A., M. L. DeLay, E. I. Klenk, and G. Layh-Schmitt. 2010. From HLA-B27 to spondyloarthritis: a journey through the ER. *Immunol Rev* 233: 181–202.

509. Dangoria, N. S., M. L. DeLay, D. J. Kingsbury, J. P. Mear, B. Uchanska-Ziegler, A. Ziegler, and R. A. Colbert. 2002. HLA-B27 misfolding is associated with aberrant intermolecular disulfide bond formation (dimerization) in the endoplasmic reticulum. *J Biol Chem* 277: 23459–23468.

510. Mear, J. P., K. L. Schreiber, C. Münz, X. Zhu, S. Stevanović, H. G. Rammensee, S. L. Rowland-Jones, and R. A. Colbert. 1999. Misfolding of HLA-B27 as a result of its B pocket suggests a novel mechanism for its role in susceptibility to spondyloarthropathies. *J Immunol* 163: 6665–6670.

511. Tran, T. M., N. Satumtira, M. L. Dorris, E. May, A. Wang, E. Furuta, and J. D. Taurog. 2004. HLA-B27 in transgenic rats forms disulfide-linked heavy chain oligomers and multimers that bind to the chaperone BiP. *J Immunol* 172: 5110–5119.

512. Antoniou, A. N., S. Ford, J. D. Taurog, G. W. Butcher, and S. J. Powis. 2004. Formation of HLA-B27 homodimers and their relationship to assembly kinetics. *J Biol Chem* 279: 8895–8902.

513. Schröder, M., and R. J. Kaufman. 2005. The mammalian unfolded protein response. *Annu. Rev. Biochem.* 74: 739–789.

514. Kozutsumi, Y., M. Segal, K. Normington, M. J. Gething, and J. Sambrook. 1988. The presence of malfolded proteins in the endoplasmic reticulum signals the induction of glucose-regulated proteins. *Nature* 332: 462–464.

515. Dorner, A. J., L. C. Wasley, and R. J. Kaufman. 1992. Overexpression of GRP78 mitigates stress induction of glucose regulated proteins and blocks secretion of selective proteins in Chinese hamster ovary cells. *EMBO J.* 11: 1563–1571.

516. Travers, K. J., C. K. Patil, L. Wodicka, D. J. Lockhart, J. S. Weissman, and P. Walter. 2000. Functional and genomic analyses reveal an essential coordination between the unfolded protein response and ER-associated degradation. *Cell* 101: 249–258.

517. Ogata, M., S.-I. Hino, A. Saito, K. Morikawa, S. Kondo, S. Kanemoto, T. Murakami, M. Taniguchi, I. Tanii, K. Yoshinaga, S. Shiosaka, J. A. Hammarback, F. Urano, and K. Imaizumi. 2006. Autophagy is activated for cell survival after endoplasmic reticulum stress. *Mol. Cell. Biol.* 26: 9220–9231.

518. Yorimitsu, T., U. Nair, Z. Yang, and D. J. Klionsky. 2006. Endoplasmic reticulum stress triggers autophagy. *J Biol Chem* 281: 30299–30304.

519. Schröder, M. 2008. Endoplasmic reticulum stress responses. *Cell. Mol. Life Sci.* 65: 862–894.

520. Turner, M. J., D. P. Sowders, M. L. DeLay, R. Mohapatra, S. Bai, J. A. Smith, J. R. Brandewie, J. D. Taurog, and R. A. Colbert. 2005. HLA-B27 misfolding in transgenic rats is associated with activation of the unfolded protein response. *J Immunol* 175: 2438–2448.

521. Bogaert, S., M. De Vos, K. Olievier, H. Peeters, D. Elewaut, B. Lambrecht, P. Pouliot, and D. Laukens. 2011. Involvement of endoplasmic reticulum stress in inflammatory bowel disease: a different implication for colonic and ileal disease? *PLoS ONE* 6: e25589.

522. Turner, M. J., M. L. DeLay, S. Bai, E. Klenk, and R. A. Colbert. 2007. HLA-B27 up-regulation causes accumulation of misfolded heavy chains and correlates with the

- magnitude of the unfolded protein response in transgenic rats: Implications for the pathogenesis of spondylarthritis-like disease. *Arthritis Rheum* 56: 215–223.
523. Zeng, L., M. J. Lindstrom, and J. A. Smith. 2011. Ankylosing spondylitis macrophage production of higher levels of interleukin-23 in response to lipopolysaccharide without induction of a significant unfolded protein response. *Arthritis Rheum* 63: 3807–3817.
524. Ciccica, F., A. Accardo-Palumbo, A. Rizzo, G. Guggino, S. Raimondo, A. Giardina, A. Cannizzaro, R. A. Colbert, R. Alessandro, and G. Triolo. 2013. Evidence that autophagy, but not the unfolded protein response, regulates the expression of IL-23 in the gut of patients with ankylosing spondylitis and subclinical gut inflammation. *Ann Rheum Dis*.
525. Gratacós, J., A. Collado, X. Filella, R. Sanmartí, J. Cañete, J. Llena, R. Molina, A. Ballesta, and J. Muñoz-Gómez. 1994. Serum cytokines (IL-6, TNF-alpha, IL-1 beta and IFN-gamma) in ankylosing spondylitis: a close correlation between serum IL-6 and disease activity and severity. *Br. J. Rheumatol.* 33: 927–931.
526. Bal, A., E. Unlu, G. Bahar, E. Aydog, E. Eksioglu, and R. Yorgancioglu. 2007. Comparison of serum IL-1 beta, sIL-2R, IL-6, and TNF-alpha levels with disease activity parameters in ankylosing spondylitis. *Clin. Rheumatol.* 26: 211–215.
527. Limón-Camacho, L., M. I. Vargas-Rojas, J. Vázquez-Mellado, J. Casasola-Vargas, J. F. Moctezuma, R. Burgos-Vargas, and L. Llorente. 2012. In vivo peripheral blood proinflammatory T cells in patients with ankylosing spondylitis. *J Rheumatol* 39: 830–835.
528. Wang, X., Z. Lin, Q. Wei, Y. Jiang, and J. Gu. 2009. Expression of IL-23 and IL-17 and effect of IL-23 on IL-17 production in ankylosing spondylitis. *Rheumatol Int* 29: 1343–1347.
529. Mei, Y., F. Pan, J. Gao, R. Ge, Z. Duan, Z. Zeng, F. Liao, G. Xia, S. Wang, S. Xu, J. Xu, L. Zhang, and D. Ye. 2011. Increased serum IL-17 and IL-23 in the patient with ankylosing spondylitis. *Clin. Rheumatol.* 30: 269–273.
530. Zhang, L., Y.-G. Li, Y.-H. Li, L. Qi, X.-G. Liu, C.-Z. Yuan, N.-W. Hu, D.-X. Ma, Z.-F. Li, Q. Yang, W. Li, and J.-M. Li. 2012. Increased frequencies of Th22 cells as well as Th17 cells in the peripheral blood of patients with ankylosing spondylitis and rheumatoid arthritis. *PLoS ONE* 7: e31000.
531. Wendling, D., J.-P. Cedoz, and E. Racadot. 2009. Serum and synovial fluid levels of p40 IL12/23 in spondyloarthropathy patients. *Clin. Rheumatol.* 28: 187–190.
532. Yang, P. T., H. Kasai, L. J. Zhao, W. G. Xiao, F. Tanabe, and M. Ito. 2004. Increased CCR4 expression on circulating CD4(+) T cells in ankylosing spondylitis, rheumatoid arthritis and systemic lupus erythematosus. *Clin Exp Immunol* 138: 342–347.
533. Duftner, C., C. Goldberger, A. Falkenbach, R. Würzner, B. Falkensammer, K. P. Pfeiffer, E. Maerker-Hermann, and M. Schirmer. 2003. Prevalence, clinical relevance and characterization of circulating cytotoxic CD4+CD28- T cells in ankylosing spondylitis. *Arthritis Res Ther* 5: R292–300.
534. Zhang, L., L. B. Jarvis, H. J. Baek, and J. S. H. Gaston. 2009. Regulatory IL4+CD8+ T cells in patients with ankylosing spondylitis and healthy controls. *Ann Rheum Dis* 68: 1345–1351.
535. Szalay, B., G. Mészáros, Á. Cseh, L. Ács, M. Deák, L. Kovács, B. Vásárhelyi, and A. Balog. 2012. Adaptive immunity in ankylosing spondylitis: phenotype and functional alterations of T-cells before and during infliximab therapy. *Clin. Dev. Immunol.* 2012: 808724.
536. Kenna, T. J., S. I. Davidson, R. Duan, L. A. Bradbury, J. McFarlane, M. Smith, H. Weedon, S. Street, R. Thomas, G. P. Thomas, and M. A. Brown. 2012. Enrichment of circulating interleukin-17-secreting interleukin-23 receptor-positive γ/δ T cells in patients with active ankylosing spondylitis. *Arthritis Rheum* 64: 1420–1429.
537. Lin, Q., Z. Lin, J. Gu, F. Huang, T. Li, Q. Wei, Z. Liao, S. Cao, Y. Jiang, and J. Huang. 2010. Abnormal high-expression of CD154 on T lymphocytes of ankylosing spondylitis patients is down-regulated by etanercept treatment. *Rheumatol Int* 30: 317–323.
538. Jandus, C., G. Bioley, J.-P. Rivals, J. Dudler, D. Speiser, and P. Romero. 2008.

- Increased numbers of circulating polyfunctional Th17 memory cells in patients with seronegative spondylarthritides. *Arthritis Rheum* 58: 2307–2317.
539. Xueyi, L., C. Lina, W. Zhenbiao, H. Qing, L. Qiang, and P. Zhu. 2013. Levels of circulating Th17 cells and regulatory T cells in ankylosing spondylitis patients with an inadequate response to anti-TNF- α therapy. *J. Clin. Immunol.* 33: 151–161.
540. Appel, H., R. Maier, P. Wu, R. Scheer, A. Hempfing, R. Kayser, A. Thiel, A. Radbruch, C. Loddenkemper, and J. Sieper. 2011. Analysis of IL-17(+) cells in facet joints of patients with spondyloarthritis suggests that the innate immune pathway might be of greater relevance than the Th17-mediated adaptive immune response. *Arthritis Res Ther* 13: R95.
541. Yang, X.-Y., H.-Y. Wang, X.-Y. Zhao, L.-J. Wang, Q.-H. Lv, and Q.-Q. Wang. 2013. Th22, but not Th17 might be a good index to predict the tissue involvement of systemic lupus erythematosus. *J. Clin. Immunol.* 33: 767–774.
542. Kagami, S., H. L. Rizzo, J. J. Lee, Y. Koguchi, and A. Blauvelt. 2010. Circulating Th17, Th22, and Th1 cells are increased in psoriasis. *J. Invest. Dermatol.* 130: 1373–1383.
543. Zhao, S.-S., J.-W. Hu, J. Wang, X.-J. Lou, and L.-L. Zhou. 2011. Inverse correlation between CD4⁺ CD25^{high} CD127^{low}/- regulatory T-cells and serum immunoglobulin A in patients with new-onset ankylosing spondylitis. *J. Int. Med. Res.* 39: 1968–1974.
544. Wright, C., M. Edelmann, K. diGleria, S. Kollnberger, H. Kramer, S. McGowan, K. McHugh, S. Taylor, B. Kessler, and P. Bowness. 2009. Ankylosing spondylitis monocytes show upregulation of proteins involved in inflammation and the ubiquitin proteasome pathway. *Ann Rheum Dis* 68: 1626–1632.
545. Xu, Y., Y. Zhan, A. M. Lew, S. H. Naik, and M. H. Kershaw. 2007. Differential development of murine dendritic cells by GM-CSF versus Flt3 ligand has implications for inflammation and trafficking. *J Immunol* 179: 7577–7584.
546. Slobodin, G., A. Kessel, N. Kofman, E. Toubi, I. Rosner, and M. Odeh. 2012. Phenotype of resting and activated monocyte-derived dendritic cells grown from peripheral blood of patients with ankylosing spondylitis. *Inflammation* 35: 772–775.
547. PREVOSTO, C., J. C. Goodall, and J. S. Hill Gaston. 2012. Cytokine Secretion by Pathogen Recognition Receptor-stimulated Dendritic Cells in Rheumatoid Arthritis and Ankylosing Spondylitis. *J Rheumatol* 39: 1918–1928.
548. Cao, D., R. van Vollenhoven, L. Klareskog, C. Trollmo, and V. Malmström. 2004. CD25^{bright}CD4⁺ regulatory T cells are enriched in inflamed joints of patients with chronic rheumatic disease. *Arthritis Res Ther* 6: R335–46.
549. Appel, H., P. Wu, R. Scheer, C. Kedor, B. Sawitzki, A. Thiel, A. Radbruch, J. Sieper, and U. Syrbe. 2011. Synovial and peripheral blood CD4⁺FoxP3⁺ T cells in spondyloarthritis. *J Rheumatol* 38: 2445–2451.
550. Appel, H., R. Maier, J. Bleil, A. Hempfing, C. Loddenkemper, U. Schlichting, U. Syrbe, and J. Sieper. 2013. In situ analysis of IL-23 and IL-12 positive cells in the spine of patients with ankylosing spondylitis. *Arthritis Rheum.*
551. Ciccìa, F., M. Bombardieri, A. Principato, A. Giardina, C. Tripodo, R. Porcasi, S. Peralta, V. Franco, E. Giardina, A. Craxi, C. Pitzalis, and G. Triolo. 2009. Overexpression of interleukin-23, but not interleukin-17, as an immunologic signature of subclinical intestinal inflammation in ankylosing spondylitis. *Arthritis Rheum* 60: 955–965.
552. Ciccìa, F., A. Rizzo, A. Accardo-Palumbo, A. Giardina, M. Bombardieri, G. Guggino, S. Taverna, G. D. Leo, R. Alessandro, and G. Triolo. 2012. Increased expression of interleukin-32 in the inflamed ileum of ankylosing spondylitis patients. *Rheumatology (Oxford)* 51: 1966–1972.
553. Ciccìa, F., A. Accardo-Palumbo, A. Giardina, P. Di Maggio, A. Principato, M. Bombardieri, A. Rizzo, R. Alessandro, A. Ferrante, S. Principe, S. Peralta, F. Conte, S. Drago, A. Craxi, G. De Leo, and G. Triolo. 2010. Expansion of intestinal CD4⁺CD25^(high) Treg cells in patients with ankylosing spondylitis: a putative role for interleukin-10 in preventing intestinal Th17 response. *Arthritis Rheum* 62: 3625–3634.

554. Ciccia, F., A. Accardo-Palumbo, R. Alessandro, A. Rizzo, S. Principe, S. Peralta, F. Raiata, A. Giardina, G. De Leo, and G. Triolo. 2011. Interleukin-22 and IL-22-producing NKp44(+) NK cells in the subclinical gut inflammation of patients with ankylosing spondylitis. *Arthritis Rheum*.
555. Roychowdhury, B., S. Bintley-Bagot, D. Y. Bulgen, R. N. Thompson, E. J. Tunn, and R. J. Moots. 2002. Is methotrexate effective in ankylosing spondylitis? *Rheumatology (Oxford)* 41: 1330–1332.
556. Braun, J., R. van den Berg, X. Baraliakos, H. Boehm, R. Burgos-Vargas, E. Collantes-Estevez, H. Dagfinrud, B. Dijkmans, M. Dougados, P. Emery, P. Geher, M. Hammoudeh, R. D. Inman, M. Jongkees, M. A. Khan, U. Kiltz, T. Kvien, M. Leirisalo-Repo, W. P. Maksymowych, I. Olivieri, K. Pavelka, J. Sieper, E. Stanislawska-Biernat, D. Wendling, S. Ozgocmen, C. van Drogen, B. van Royen, and D. van der Heijde. 2011. 2010 update of the ASAS/EULAR recommendations for the management of ankylosing spondylitis. In vol. 70. 896–904.
557. Haroon, N., R. D. Inman, T. J. Learch, M. H. Weisman, M. Lee, M. H. Rahbar, M. M. Ward, J. D. Reveille, and L. S. Gensler. 2013. The Impact of TNF-inhibitors on radiographic progression in Ankylosing Spondylitis. *Arthritis Rheum*.
558. Konsta, M., P. P. Sfikakis, V. K. Bournia, D. Karras, and A. Iliopoulos. 2013. Absence of radiographic progression of hip arthritis during infliximab treatment for ankylosing spondylitis. *Clin. Rheumatol.* 32: 1229–1232.
559. Gorman, J. D., K. E. Sack, and J. C. Davis. 2002. Treatment of ankylosing spondylitis by inhibition of tumor necrosis factor alpha. *N. Engl. J. Med.* 346: 1349–1356.
560. Braun, J., J. Sieper, M. Breban, E. Collantes-Estevez, J. Davis, R. Inman, H. Marzo-Ortega, and H. Mielants. 2002. Anti-tumour necrosis factor alpha therapy for ankylosing spondylitis: international experience. *Ann Rheum Dis* 61 Suppl 3: iii51–60.
561. Brandt, J., H. Haibel, D. Cornely, W. Golder, J. Gonzalez, J. Reddig, W. Thriene, J. Sieper, and J. Braun. 2000. Successful treatment of active ankylosing spondylitis with the anti-tumor necrosis factor alpha monoclonal antibody infliximab. *Arthritis Rheum* 43: 1346–1352.
562. Zou, J., M. Rudwaleit, J. Brandt, A. Thiel, J. Braun, and J. Sieper. 2003. Up regulation of the production of tumour necrosis factor alpha and interferon gamma by T cells in ankylosing spondylitis during treatment with etanercept. *Ann Rheum Dis* 62: 561–564.
563. Wenink, M. H., K. C. M. Santegoets, J. Butcher, L. van Bon, F. G. M. Lamers-Karnebeek, W. B. van den Berg, P. L. C. M. van Riel, I. B. McInnes, and T. R. D. J. Radstake. 2011. Impaired dendritic cell proinflammatory cytokine production in psoriatic arthritis. *Arthritis Rheum* 63: 3313–3322.
564. Walsh, L., P. Davies, and B. McConkey. 1979. Relationship between erythrocyte sedimentation rate and serum C-reactive protein in rheumatoid arthritis. *Ann Rheum Dis* 38: 362–363.
565. Ingersoll, M. A., R. Spanbroek, C. Lottaz, E. L. Gautier, M. Frankenberger, R. Hoffmann, R. Lang, M. Haniffa, M. Collin, F. Tacke, A. J. R. Habenicht, L. Ziegler-Heitbrock, and G. J. Randolph. 2010. Comparison of gene expression profiles between human and mouse monocyte subsets. *Blood* 115: e10–e19.
566. Strauss-Ayali, D., S. M. Conrad, and D. M. Mosser. 2007. Monocyte subpopulations and their differentiation patterns during infection. *J Leukoc Biol* 82: 244–252.
567. Ziegler-Heitbrock, H. W., M. Ströbel, D. Kieper, G. Fingerle, T. Schlunck, I. Petersmann, J. Ellwart, M. Blumenstein, and J. G. Haas. 1992. Differential expression of cytokines in human blood monocyte subpopulations. *Blood* 79: 503–511.
568. Weber, C., K. U. Belge, P. von Hundelshausen, G. Draude, B. Steppich, M. Mack, M. Frankenberger, K. S. Weber, and H. W. Ziegler-Heitbrock. 2000. Differential chemokine receptor expression and function in human monocyte subpopulations. *J Leukoc Biol* 67: 699–704.

569. Banchereau, J., F. Brière, C. Caux, J. Davoust, S. Lebecque, Y. J. Liu, B. Pulendran, and K. Palucka. 2000. Immunobiology of dendritic cells. *Annu Rev Immunol* 18: 767–811.
570. Naik, S. H., A. I. Proietto, N. S. Wilson, A. Dakic, P. Schnorrer, M. Fuchsberger, M. H. Lahoud, M. O'Keeffe, Q.-X. Shao, W.-F. Chen, J. A. Villadangos, K. Shortman, and L. Wu. 2005. Cutting edge: generation of splenic CD8⁺ and CD8⁻ dendritic cell equivalents in Fms-like tyrosine kinase 3 ligand bone marrow cultures. *J Immunol* 174: 6592–6597.
571. Maraskovsky, E., E. Daro, E. Roux, M. Teepe, C. R. Maliszewski, J. Hoek, D. Caron, M. E. Lebsack, and H. J. McKenna. 2000. In vivo generation of human dendritic cell subsets by Flt3 ligand. *Blood* 96: 878–884.
572. Pulendran, B., J. Banchereau, S. Burkeholder, E. Kraus, E. Guinet, C. Chalouni, D. Caron, C. Maliszewski, J. Davoust, J. Fay, and K. Palucka. 2000. Flt3-ligand and granulocyte colony-stimulating factor mobilize distinct human dendritic cell subsets in vivo. *J Immunol* 165: 566–572.
573. Sasmono, R. T., D. Oceandy, J. W. Pollard, W. Tong, P. Pavli, B. J. Wainwright, M. C. Ostrowski, S. R. Himes, and D. A. Hume. 2003. A macrophage colony-stimulating factor receptor-green fluorescent protein transgene is expressed throughout the mononuclear phagocyte system of the mouse. *Blood* 101: 1155–1163.
574. Wiktor-Jedrzejczak, W., and S. Gordon. 1996. Cytokine regulation of the macrophage (M phi) system studied using the colony stimulating factor-1-deficient op/op mouse. *Physiol. Rev.* 76: 927–947.
575. Meredith, M. M., K. Liu, G. Darrasse-Jeze, A. O. Kamphorst, H. A. Schreiber, P. Guermonprez, J. Idoyaga, C. Cheong, K.-H. Yao, R. E. Niec, and M. C. Nussenzweig. 2012. Expression of the zinc finger transcription factor zDC (Zbtb46, Btbd4) defines the classical dendritic cell lineage. *J Exp Med* 209: 1153–1165.
576. Crozat, K., R. Guiton, M. Williams, S. Henri, T. Baranek, I. Schwartz-Cornil, B. Malissen, and M. Dalod. 2010. Comparative genomics as a tool to reveal functional equivalences between human and mouse dendritic cell subsets. *Immunol Rev* 234: 177–198.
577. Giannoukakis, N., B. Phillips, D. Finegold, J. Harnaha, and M. Trucco. 2011. Phase I (safety) study of autologous tolerogenic dendritic cells in type 1 diabetic patients. *Diabetes Care* 34: 2026–2032.
578. Lu, W., L. C. Arraes, W. T. Ferreira, and J.-M. Andrieu. 2004. Therapeutic dendritic-cell vaccine for chronic HIV-1 infection. *Nat. Med.* 10: 1359–1365.
579. Banchereau, J., A. K. Palucka, M. Dhodapkar, S. Burkeholder, N. Taquet, A. Rolland, S. Taquet, S. Coquery, K. M. Wittkowski, N. Bhardwaj, L. Pineiro, R. Steinman, and J. Fay. 2001. Immune and clinical responses in patients with metastatic melanoma to CD34(+) progenitor-derived dendritic cell vaccine. *Cancer Res.* 61: 6451–6458.
580. Hilkens, C. M. U., and J. D. Isaacs. 2013. Tolerogenic dendritic cell therapy for rheumatoid arthritis: where are we now? *Clin Exp Immunol* 172: 148–157.
581. Takakubo, Y., M. Takagi, K. Maeda, Y. Tamaki, A. Sasaki, T. Asano, S. Fukushima, Y. Kiyoshige, H. Orui, T. Ogino, and M. Yamakawa. 2008. Distribution of myeloid dendritic cells and plasmacytoid dendritic cells in the synovial tissues of rheumatoid arthritis. *J Rheumatol* 35: 1919–1931.
582. Lebre, M. C., S. L. Jongbloed, S. W. Tas, T. J. M. Smeets, I. B. McInnes, and P. P. Tak. 2008. Rheumatoid arthritis synovium contains two subsets of CD83-DC-LAMP-dendritic cells with distinct cytokine profiles. *Am J Pathol* 172: 940–950.
583. Kavousanaki, M., A. Makrigiannakis, D. Boumpas, and P. Verginis. 2010. Novel role of plasmacytoid dendritic cells in humans: induction of interleukin-10-producing Treg cells by plasmacytoid dendritic cells in patients with rheumatoid arthritis responding to therapy. *Arthritis Rheum* 62: 53–63.
584. Gerl, V., A. Lischka, D. Panne, P. Grossmann, R. Berthold, B. F. Hoyer, R. Biesen, A. Bruns, T. Alexander, A. Jacobi, T. Dörner, G.-R. Burmester, A. Radbruch, and F. Hiepe. 2010. Blood dendritic cells in systemic lupus erythematosus exhibit altered

- activation state and chemokine receptor function. *Ann Rheum Dis* 69: 1370–1377.
585. Henriques, A., L. Inês, T. Carvalheiro, M. Couto, A. Andrade, S. Pedreiro, P. Laranjeira, J. M. Morgado, M. L. Pais, J. A. P. da Silva, and A. Paiva. 2012. Functional characterization of peripheral blood dendritic cells and monocytes in systemic lupus erythematosus. *Rheumatol Int* 32: 863–869.
586. Pang, L., L. Wang, T. Suo, H. Hao, X. Fang, J. Jia, F. Huang, and J. Tang. 2008. Tumor necrosis factor-alpha blockade leads to decreased peripheral T cell reactivity and increased dendritic cell number in peripheral blood of patients with ankylosing spondylitis. *J Rheumatol* 35: 2220–2228.
587. Ancuta, P., K.-Y. Liu, V. Misra, V. S. Wacliche, A. Gosselin, X. Zhou, and D. Gabuzda. 2009. Transcriptional profiling reveals developmental relationship and distinct biological functions of CD16+ and CD16- monocyte subsets. *BMC Genomics* 10: 403.
588. Döbel, T., A. Kunze, J. Babatz, K. Tränkner, A. Ludwig, M. Schmitz, A. Enk, and K. Schäkel. 2013. FcγRIII (CD16) equips immature 6-sulfo LacNAc-expressing dendritic cells (sIaDCs) with a unique capacity to handle IgG-complexed antigens. *Blood*.
589. Yona, S., K.-W. Kim, Y. Wolf, A. Mildner, D. Varol, M. Breker, D. Strauss-Ayali, S. Viukov, M. Guilliams, A. Misharin, D. A. Hume, H. Perlman, B. Malissen, E. Zelzer, and S. Jung. 2013. Fate mapping reveals origins and dynamics of monocytes and tissue macrophages under homeostasis. *Immunity* 38: 79–91.
590. Palframan, R. T., S. Jung, G. Cheng, W. Weninger, Y. Luo, M. Dorf, D. R. Littman, B. J. Rollins, H. Zweerink, A. Rot, and U. H. von Andrian. 2001. Inflammatory chemokine transport and presentation in HEV: a remote control mechanism for monocyte recruitment to lymph nodes in inflamed tissues. *J Exp Med* 194: 1361–1373.
591. Varol, C., A. Vallon-Eberhard, E. Elinav, T. Aychek, Y. Shapira, H. Luche, H. J. Fehling, W.-D. Hardt, G. Shakhar, and S. Jung. 2009. Intestinal lamina propria dendritic cell subsets have different origin and functions. *Immunity* 31: 502–512.
592. Bogunovic, M., F. Ginhoux, J. Helft, L. Shang, D. Hashimoto, M. Greter, K. Liu, C. Jakubzick, M. A. Ingersoll, M. Leboeuf, E. R. Stanley, M. Nussenzweig, S. A. Lira, G. J. Randolph, and M. Merad. 2009. Origin of the lamina propria dendritic cell network. *Immunity* 31: 513–525.
593. Randolph, G. J., K. Inaba, D. F. Robbiani, R. M. Steinman, and W. A. Muller. 1999. Differentiation of phagocytic monocytes into lymph node dendritic cells in vivo. *Immunity* 11: 753–761.
594. Weissman, D., Y. Li, J. Ananworanich, L. J. Zhou, J. Adelsberger, T. F. Tedder, M. Baseler, and A. S. Fauci. 1995. Three populations of cells with dendritic morphology exist in peripheral blood, only one of which is infectable with human immunodeficiency virus type 1. *Proc Natl Acad Sci USA* 92: 826–830.
595. Verdijk, P., P. A. van Veelen, A. H. de Ru, P. J. Hensbergen, K. Mizuno, H. K. Koerten, F. Koning, C. P. Tensen, and A. M. Mommaas. 2004. Morphological changes during dendritic cell maturation correlate with cofilin activation and translocation to the cell membrane. *Eur J Immunol* 34: 156–164.
596. Jonuleit, H., E. Schmitt, G. Schuler, J. Knop, and A. H. Enk. 2000. Induction of interleukin 10-producing, nonproliferating CD4(+) T cells with regulatory properties by repetitive stimulation with allogeneic immature human dendritic cells. *J Exp Med* 192: 1213–1222.
597. Probst, H. C., J. Lagnel, G. Kollias, and M. van den Broek. 2003. Inducible transgenic mice reveal resting dendritic cells as potent inducers of CD8+ T cell tolerance. *Immunity* 18: 713–720.
598. Hernandez, M. G. H., L. Shen, and K. L. Rock. 2007. CD40-CD40 ligand interaction between dendritic cells and CD8+ T cells is needed to stimulate maximal T cell responses in the absence of CD4+ T cell help. *J Immunol* 178: 2844–2852.
599. Watowich, S. S., and Y.-J. Liu. 2010. Mechanisms regulating dendritic cell specification and development. *Immunol Rev* 238: 76–92.

600. Proietto, A. I., D. Mittag, A. W. Roberts, N. Sprigg, and L. Wu. 2012. The equivalents of human blood and spleen dendritic cell subtypes can be generated in vitro from human CD34(+) stem cells in the presence of fms-like tyrosine kinase 3 ligand and thrombopoietin. *Cell. Mol. Immunol.* 9: 446–454.
601. Langlet, C., S. Tamoutounour, S. Henri, H. Luche, L. Ardouin, C. Grégoire, B. Malissen, and M. Guilliams. 2012. CD64 expression distinguishes monocyte-derived and conventional dendritic cells and reveals their distinct role during intramuscular immunization. *The Journal of Immunology* 188: 1751–1760.
602. Stanley, E. R., K. L. Berg, D. B. Einstein, P. S. Lee, F. J. Pixley, Y. Wang, and Y. G. Yeung. 1997. Biology and action of colony--stimulating factor-1. *Mol. Reprod. Dev.* 46: 4–10.
603. Satpathy, A. T., W. Kc, J. C. Albring, B. T. Edelson, N. M. Kretzer, D. Bhattacharya, T. L. Murphy, and K. M. Murphy. 2012. Zbtb46 expression distinguishes classical dendritic cells and their committed progenitors from other immune lineages. *J Exp Med* 209: 1135–1152.
604. Gautier, E. L., T. Shay, J. Miller, M. Greter, C. Jakubzick, S. Ivanov, J. Helft, A. Chow, K. G. Elpek, S. Gordonov, A. R. Mazloom, A. Ma'ayan, W.-J. Chua, T. H. Hansen, S. J. Turley, M. Merad, G. J. Randolph, Immunological Genome Consortium. 2012. Gene-expression profiles and transcriptional regulatory pathways that underlie the identity and diversity of mouse tissue macrophages. *Nat Immunol* 13: 1118–1128.
605. Miller, J. C., B. D. Brown, T. Shay, E. L. Gautier, V. Jojic, A. Cohain, G. Pandey, M. Leboeuf, K. G. Elpek, J. Helft, D. Hashimoto, A. Chow, J. Price, M. Greter, M. Bogunovic, A. Bellemare-Pelletier, P. S. Frenette, G. J. Randolph, S. J. Turley, M. Merad, Immunological Genome Consortium. 2012. Deciphering the transcriptional network of the dendritic cell lineage. *Nat Immunol* 13: 888–899.
606. Baek, H. J., L. Zhang, L. B. Jarvis, and J. S. H. Gaston. 2008. Increased IL-4+ CD8+ T cells in peripheral blood and autoreactive CD8+ T cell lines of patients with inflammatory arthritis. *Rheumatology (Oxford)* 47: 795–803.
607. Sakaguchi, S., T. Yamaguchi, T. Nomura, and M. Ono. 2008. Regulatory T cells and immune tolerance. *Cell* 133: 775–787.
608. Johansson-Lindbom, B., and W. W. Agace. 2007. Generation of gut-homing T cells and their localization to the small intestinal mucosa. *Immunol Rev* 215: 226–242.
609. Mora, J. R., G. Cheng, D. Picarella, M. Briskin, N. Buchanan, and U. H. von Andrian. 2005. Reciprocal and dynamic control of CD8 T cell homing by dendritic cells from skin- and gut-associated lymphoid tissues. *J Exp Med* 201: 303–316.
610. Homey, B., H. Alenius, A. Müller, H. Soto, E. P. Bowman, W. Yuan, L. McEvoy, A. I. Lauerma, T. Assmann, E. Bünemann, M. Lehto, H. Wolff, D. Yen, H. Marxhausen, W. To, J. Sedgwick, T. Ruzicka, P. Lehmann, and A. Zlotnik. 2002. CCL27-CCR10 interactions regulate T cell-mediated skin inflammation. *Nat. Med.* 8: 157–165.
611. Pan, J., E. J. Kunkel, U. Gossler, N. Lazarus, P. Langdon, K. Broadwell, M. A. Vierra, M. C. Genovese, E. C. Butcher, and D. Soler. 2000. A novel chemokine ligand for CCR10 and CCR3 expressed by epithelial cells in mucosal tissues. *J Immunol* 165: 2943–2949.
612. Salmi, M., and S. Jalkanen. 2005. Lymphocyte homing to the gut: attraction, adhesion, and commitment. *Immunol Rev* 206: 100–113.
613. Varona, R., V. Cadenas, J. Flores, C. Martínez-A, and G. Márquez. 2003. CCR6 has a non-redundant role in the development of inflammatory bowel disease. *Eur J Immunol* 33: 2937–2946.
614. Groom, J. R., and A. D. Luster. 2011. CXCR3 in T cell function. *Exp. Cell Res.* 317: 620–631.
615. Syrbe, U., R. Scheer, P. Wu, and J. Sieper. 2012. Differential synovial Th1 cell reactivity towards Escherichia coli antigens in patients with ankylosing spondylitis and rheumatoid arthritis. *Ann Rheum Dis* 71: 1573–1576.

616. Ergin, A., U. Syrbe, R. Scheer, A. Thiel, T. Adam, K. Büsow, R. Duchmann, M. Zeitz, and J. Sieper. 2011. Impaired peripheral Th1 CD4+ T cell response to Escherichia coli proteins in patients with Crohn's disease and ankylosing spondylitis. *J. Clin. Immunol.* 31: 998–1009.
617. Atagunduz, P., H. Appel, W. Kuon, P. Wu, A. Thiel, P.-M. Kloetzel, and J. Sieper. 2005. HLA-B27-restricted CD8+ T cell response to cartilage-derived self peptides in ankylosing spondylitis. *Arthritis Rheum* 52: 892–901.
618. Bidad, K., E. Salehi, A. Jamshidi, A. A. Saboor-Yaraghi, M. Oraei, A. Meysamie, M. Mahmoudi, and M. H. Nicknam. 2013. Effect of All-transretinoic Acid on Th17 and T Regulatory Cell Subsets in Patients with Ankylosing Spondylitis. *J Rheumatol.*
619. Martin, T. M., J. R. Smith, and J. T. Rosenbaum. 2002. Anterior uveitis: current concepts of pathogenesis and interactions with the spondyloarthropathies. *Curr Opin Rheumatol* 14: 337–341.
620. Sampaio-Barros, P. D., R. A. Conde, R. Bonfiglioli, M. B. Bértolo, and A. M. Samara. 2006. Characterization and outcome of uveitis in 350 patients with spondyloarthropathies. *Rheumatol Int* 26: 1143–1146.
621. Charles, P., M. J. Elliott, D. Davis, A. Potter, J. R. Kalden, C. Antoni, F. C. Breedveld, J. S. Smolen, G. Eberl, K. deWoody, M. Feldmann, and R. N. Maini. 1999. Regulation of cytokines, cytokine inhibitors, and acute-phase proteins following anti-TNF- α therapy in rheumatoid arthritis. *J Immunol* 163: 1521–1528.
622. Dombrecht, E. J., N. E. Aerts, A. J. Schuerwegh, M. M. Hagendorens, D. G. Ebo, J. F. Van Offel, C. H. Bridts, W. J. Stevens, and L. S. De Clerck. 2006. Influence of anti-tumor necrosis factor therapy (Adalimumab) on regulatory T cells and dendritic cells in rheumatoid arthritis. *Clin Exp Rheumatol* 24: 31–37.
623. Dejaco, C., C. Duftner, A. Klauser, and M. Schirmer. 2010. Altered T-cell subtypes in spondyloarthritis, rheumatoid arthritis and polymyalgia rheumatica. *Rheumatol Int* 30: 297–303.
624. Wu, Y., M. Ren, R. Yang, X. Liang, Y. Ma, Y. Tang, L. Huang, J. Ye, K. Chen, P. Wang, and H. Shen. 2011. Reduced immunomodulation potential of bone marrow-derived mesenchymal stem cells induced CCR4+CCR6+ Th/Treg cell subset imbalance in ankylosing spondylitis. *Arthritis Res Ther* 13: R29.
625. Poddubnyy, D. A., E. Märker-Hermann, W. Kaluza-Schilling, H. Zeidler, J. Braun, J. Listing, J. Sieper, and M. Rudwaleit. 2011. Relation of HLA-B27, tumor necrosis factor- α promoter gene polymorphisms, and T cell cytokine production in ankylosing Spondylitis -- a comprehensive genotype-phenotype analysis from an observational cohort. *J Rheumatol* 38: 2436–2441.
626. Ehrenstein, M. R., J. G. Evans, A. Singh, S. Moore, G. Warnes, D. A. Isenberg, and C. Mauri. 2004. Compromised function of regulatory T cells in rheumatoid arthritis and reversal by anti-TNF α therapy. *J Exp Med* 200: 277–285.
627. Ruth, J. H., J. B. Rottman, K. J. Katschke, S. Qin, L. Wu, G. LaRosa, P. Ponath, R. M. Pope, and A. E. Koch. 2001. Selective lymphocyte chemokine receptor expression in the rheumatoid joint. *Arthritis Rheum* 44: 2750–2760.
628. Hirahara, K., L. Liu, R. A. Clark, K.-I. Yamanaka, R. C. Fuhlbrigge, and T. S. Kupper. 2006. The majority of human peripheral blood CD4+CD25^{high}Foxp3⁺ regulatory T cells bear functional skin-homing receptors. *J Immunol* 177: 4488–4494.
629. Iellem, A., M. Mariani, R. Lang, H. Recalde, P. Panina-Bordignon, F. Sinigaglia, and D. D'Ambrosio. 2001. Unique chemotactic response profile and specific expression of chemokine receptors CCR4 and CCR8 by CD4(+)CD25(+) regulatory T cells. *J Exp Med* 194: 847–853.
630. GOWANS, J. L., and E. J. KNIGHT. 1964. THE ROUTE OF RE-CIRCULATION OF LYMPHOCYTES IN THE RAT. *Proc. R. Soc. Lond., B, Biol. Sci.* 159: 257–282.
631. Andrian, von, U. H., and T. R. Mempel. 2003. Homing and cellular traffic in lymph nodes. *Nat Rev Immunol* 3: 867–878.

632. Mandl, J. N., R. Liou, F. Klauschen, N. Vrisekoop, J. P. Monteiro, A. J. Yates, A. Y. Huang, and R. N. Germain. 2012. Quantification of lymph node transit times reveals differences in antigen surveillance strategies of naive CD4⁺ and CD8⁺ T cells. *Proc Natl Acad Sci USA* 109: 18036–18041.
633. Shen, H., J. C. Goodall, and J. S. H. Gaston. 2010. Frequency and phenotype of T helper 17 cells in peripheral blood and synovial fluid of patients with reactive arthritis. *J Rheumatol* 37: 2096–2099.
634. Wedderburn, L. R., N. Robinson, A. Patel, H. Varsani, and P. Woo. 2000. Selective recruitment of polarized T cells expressing CCR5 and CXCR3 to the inflamed joints of children with juvenile idiopathic arthritis. *Arthritis Rheum* 43: 765–774.
635. Annunziato, F., L. Cosmi, F. Liotta, E. Maggi, and S. Romagnani. 2012. Defining the human T helper 17 cell phenotype. *Trends Immunol.* 33: 505–512.
636. Weaver, C. T., L. E. Harrington, P. R. Mangan, M. Gavrieli, and K. M. Murphy. 2006. Th17: an effector CD4 T cell lineage with regulatory T cell ties. *Immunity* 24: 677–688.
637. Korn, T., E. Bettelli, W. Gao, A. Awasthi, A. Jäger, T. B. Strom, M. Oukka, and V. K. Kuchroo. 2007. IL-21 initiates an alternative pathway to induce proinflammatory T(H)17 cells. *Nature* 448: 484–487.
638. Cañete, J. D., S. E. Martínez, J. Farrés, R. Sanmartí, M. Blay, A. Gómez, G. Salvador, and J. Muñoz-Gómez. 2000. Differential Th1/Th2 cytokine patterns in chronic arthritis: interferon gamma is highly expressed in synovium of rheumatoid arthritis compared with seronegative spondyloarthropathies. *Ann Rheum Dis* 59: 263–268.
639. Perussia, B., V. Fanning, and G. Trinchieri. 1985. A leukocyte subset bearing HLA-DR antigens is responsible for in vitro alpha interferon production in response to viruses. *Nat. Immun. Cell Growth Regul.* 4: 120–137.
640. Lande, R., E. Giacomini, B. Serafini, B. Rosicarelli, G. D. Sebastiani, G. Minisola, U. Tarantino, V. Riccieri, G. Valesini, and E. M. Coccia. 2004. Characterization and recruitment of plasmacytoid dendritic cells in synovial fluid and tissue of patients with chronic inflammatory arthritis. *J Immunol* 173: 2815–2824.
641. McInnes, I. B., and G. Schett. 2011. The pathogenesis of rheumatoid arthritis. *N. Engl. J. Med.* 365: 2205–2219.
642. Seyler, T. M., Y. W. Park, S. Takemura, R. J. Bram, P. J. Kurtin, J. J. Goronzy, and C. M. Weyand. 2005. BLYS and APRIL in rheumatoid arthritis. *J Clin Invest* 115: 3083–3092.
643. Edwards, J. C. W., L. Szczepanski, J. Szechinski, A. Filipowicz-Sosnowska, P. Emery, D. R. Close, R. M. Stevens, and T. Shaw. 2004. Efficacy of B-cell-targeted therapy with rituximab in patients with rheumatoid arthritis. *N. Engl. J. Med.* 350: 2572–2581.
644. Sartor, R. B. 2006. Mechanisms of disease: pathogenesis of Crohn's disease and ulcerative colitis. *Nat Clin Pract Gastroenterol Hepatol* 3: 390–407.
645. Duchmann, R., I. Kaiser, E. Hermann, W. Mayet, K. Ewe, and K. H. Meyer zum Büschenfelde. 1995. Tolerance exists towards resident intestinal flora but is broken in active inflammatory bowel disease (IBD). *Clin Exp Immunol* 102: 448–455.
646. Elliott, M. J., R. N. Maini, M. Feldmann, A. Long-Fox, P. Charles, P. Katsikis, F. M. Brennan, J. Walker, H. Bijl, and J. Ghayeb. 1993. Treatment of rheumatoid arthritis with chimeric monoclonal antibodies to tumor necrosis factor alpha. *Arthritis Rheum* 36: 1681–1690.
647. Arends, S., E. Brouwer, E. van der Veer, H. Groen, M. K. Leijnsma, P. M. Houtman, T. L. Th A Jansen, C. G. M. Kallenberg, and A. Spoorenberg. 2011. Baseline predictors of response and discontinuation of tumor necrosis factor-alpha blocking therapy in ankylosing spondylitis: a prospective longitudinal observational cohort study. *Arthritis Res Ther* 13: R94.
648. de Vries, M. K., I. C. van Eijk, I. E. van der Horst-Bruinsma, M. J. L. Peters, M. T. Nurmohamed, B. A. C. Dijkmans, B. P. C. Hazenberg, and G. J. Wolbink. 2009.

- Erythrocyte sedimentation rate, C-reactive protein level, and serum amyloid a protein for patient selection and monitoring of anti-tumor necrosis factor treatment in ankylosing spondylitis. *Arthritis Rheum* 61: 1484–1490.
649. Fraser, S. M., and R. D. Sturrock. 1990. Evaluation of sulphasalazine in ankylosing spondylitis--an interventional study. *Br. J. Rheumatol.* 29: 37–39.
650. Shortman, K., and W. R. Heath. 2010. The CD8+ dendritic cell subset. *Immunol Rev* 234: 18–31.
651. Huysamen, C., J. A. Willment, K. M. Dennehy, and G. D. Brown. 2008. CLEC9A is a novel activation C-type lectin-like receptor expressed on BDCA3+ dendritic cells and a subset of monocytes. *J Biol Chem* 283: 16693–16701.
652. Kupiec-Weglinski, J. W., J. M. Austyn, and P. J. Morris. 1988. Migration patterns of dendritic cells in the mouse. Traffic from the blood, and T cell-dependent and -independent entry to lymphoid tissues. *J Exp Med* 167: 632–645.
653. Randolph, G. J., J. Ochando, and S. Partida-Sánchez. 2008. Migration of dendritic cell subsets and their precursors. *Annu Rev Immunol* 26: 293–316.
654. Romani, N., S. Gruner, D. Brang, E. Kämpgen, A. Lenz, B. Trockenbacher, G. Konwalinka, P. O. Fritsch, R. M. Steinman, and G. Schuler. 1994. Proliferating dendritic cell progenitors in human blood. *J Exp Med* 180: 83–93.
655. Guilliams, M., K. Movahedi, T. Bosschaerts, T. VandenDriessche, M. K. Chuah, M. Hérin, A. Acosta-Sanchez, L. Ma, M. Moser, J. A. Van Ginderachter, L. Brys, P. De Baetselier, and A. Beschin. 2009. IL-10 dampens TNF/inducible nitric oxide synthase-producing dendritic cell-mediated pathogenicity during parasitic infection. *The Journal of Immunology* 182: 1107–1118.
656. Kim, T. S., and T. J. Braciale. 2009. Respiratory dendritic cell subsets differ in their capacity to support the induction of virus-specific cytotoxic CD8+ T cell responses. *PLoS ONE* 4: e4204.
657. Evans, H. G., N. J. Gullick, S. Kelly, C. Pitzalis, G. M. Lord, B. W. Kirkham, and L. S. Taams. 2009. In vivo activated monocytes from the site of inflammation in humans specifically promote Th17 responses. *Proc Natl Acad Sci USA* 106: 6232–6237.
658. Schmutz, C., A. Cartwright, H. Williams, O. Haworth, J. H. H. Williams, A. Filer, M. Salmon, C. D. Buckley, and J. Middleton. 2010. Monocytes/macrophages express chemokine receptor CCR9 in rheumatoid arthritis and CCL25 stimulates their differentiation. *Arthritis Res Ther* 12: R161.
659. O'Boyle, G., C. R. J. Fox, H. R. Walden, J. D. P. Willet, E. R. Mavin, D. W. Hine, J. M. Palmer, C. E. Barker, C. A. Lamb, S. Ali, and J. A. Kirby. 2012. Chemokine receptor CXCR3 agonist prevents human T-cell migration in a humanized model of arthritic inflammation. *Proc Natl Acad Sci USA* 109: 4598–4603.
660. Issekutz, A. C., P. J. Quinn, B. Lang, S. Ramsey, A. M. Huber, D. Rowter, M. Karkada, and T. B. Issekutz. 2011. Coexpression of chemokine receptors CCR5, CXCR3, and CCR4 and ligands for P- and E-selectin on T lymphocytes of patients with juvenile idiopathic arthritis. *Arthritis Rheum* 63: 3467–3476.
661. Wright, P., L. Utriainen, and S. Milling. 2013. Dendritic cells and regulatory T cells in spondyloarthritis. *Curr Opin Rheumatol* 25: 440–447.
662. Gilliam, B. L., D. J. Riedel, and R. R. Redfield. 2010. Clinical use of CCR5 inhibitors in HIV and beyond. *J Transl Med* 9: S9–14.
663. Saag, M., J. Goodrich, G. Fätkenheuer, B. Clotet, N. Clumeck, J. Sullivan, M. Westby, E. van der Ryst, H. Mayer, A4001029 Study Group. 2009. A double-blind, placebo-controlled trial of maraviroc in treatment-experienced patients infected with non-R5 HIV-1. *J Infect. Dis.* 199: 1638–1647.
664. Nishina, N., Y. Kaneko, H. Kameda, M. Kuwana, and T. Takeuchi. 2013. Reduction of plasma IL-6 but not TNF- α by methotrexate in patients with early rheumatoid arthritis: a potential biomarker for radiographic progression. *Clin. Rheumatol.*
665. Braun, J., and J. Sieper. 2002. Therapy of ankylosing spondylitis and other

- spondyloarthritides: established medical treatment, anti-TNF-alpha therapy and other novel approaches. *Arthritis Res.* 4: 307–321.
666. Braun, J., J. Brandt, J. Listing, A. Zink, R. Alten, W. Golder, E. Gromnica-Ihle, H. Kellner, A. Krause, M. Schneider, H. Sörensen, H. Zeidler, W. Thriene, and J. Sieper. 2002. Treatment of active ankylosing spondylitis with infliximab: a randomised controlled multicentre trial. *Lancet* 359: 1187–1193.
667. Elliott, M. J., R. N. Maini, M. Feldmann, J. R. Kalden, C. Antoni, J. S. Smolen, B. Leeb, F. C. Breedveld, J. D. Macfarlane, and H. Bijl. 1994. Randomised double-blind comparison of chimeric monoclonal antibody to tumour necrosis factor alpha (cA2) versus placebo in rheumatoid arthritis. *Lancet* 344: 1105–1110.
668. Gottlieb, A., A. Menter, A. Mendelsohn, Y.-K. Shen, S. Li, C. Guzzo, S. Fretzin, R. Kunyetz, and A. Kavanaugh. 2009. Ustekinumab, a human interleukin 12/23 monoclonal antibody, for psoriatic arthritis: randomised, double-blind, placebo-controlled, crossover trial. *Lancet* 373: 633–640.
669. McInnes, I. B., A. Kavanaugh, A. B. Gottlieb, L. Puig, P. Rahman, C. Ritchlin, C. Brodmerkel, S. Li, Y. Wang, A. M. Mendelsohn, M. K. Doyle, on behalf of the PSUMMIT 1 Study Group. 2013. Efficacy and safety of ustekinumab in patients with active psoriatic arthritis: 1 year results of the phase 3, multicentre, double-blind, placebo-controlled PSUMMIT 1 trial. *Lancet*.
670. McInnes, I. B., J. Sieper, J. Braun, P. Emery, D. van der Heijde, J. D. Isaacs, G. Dahmen, J. Wollenhaupt, H. Schulze-Koops, J. Kogan, S. Ma, M. M. Schumacher, A. P. Bertolino, W. Hueber, and P. P. Tak. 2013. Efficacy and safety of secukinumab, a fully human anti-interleukin-17A monoclonal antibody, in patients with moderate-to-severe psoriatic arthritis: a 24-week, randomised, double-blind, placebo-controlled, phase II proof-of-concept trial. *Ann Rheum Dis*.
671. Sunshine, G. H., D. R. Katz, and M. Feldmann. 1980. Dendritic cells induce T cell proliferation to synthetic antigens under Ir gene control. *J Exp Med* 152: 1817–1822.
672. Nussenzweig, M. C., R. M. Steinman, B. Gutchinov, and Z. A. Cohn. 1980. Dendritic cells are accessory cells for the development of anti-trinitrophenyl cytotoxic T lymphocytes. *J Exp Med* 152: 1070–1084.
673. Johansson-Lindbom, B., M. Svensson, O. Pabst, C. Palmqvist, G. Márquez, R. Förster, and W. W. Agace. 2005. Functional specialization of gut CD103+ dendritic cells in the regulation of tissue-selective T cell homing. *J Exp Med* 202: 1063–1073.
674. Hammer, G. E., E. E. Turer, K. E. Taylor, C. J. Fang, R. Advincula, S. Oshima, J. Barrera, E. J. Huang, B. Hou, B. A. Malynn, B. Reizis, A. DeFranco, L. A. Criswell, M. C. Nakamura, and A. Ma. 2011. Expression of A20 by dendritic cells preserves immune homeostasis and prevents colitis and spondyloarthritis. *Nat Immunol* 12: 1184–1193.
675. Lee, E. G. 2000. Failure to Regulate TNF-Induced NF-kappa B and Cell Death Responses in A20-Deficient Mice. *Science* 289: 2350–2354.
676. Turer, E. E., R. M. Tavares, E. Mortier, O. Hitotsumatsu, R. Advincula, B. Lee, N. Shifrin, B. A. Malynn, and A. Ma. 2008. Homeostatic MyD88-dependent signals cause lethal inflammation in the absence of A20. *Journal of Experimental Medicine* 205: 451–464.
677. Trynka, G., A. Zhernakova, J. Romanos, L. Franke, K. A. Hunt, G. Turner, M. Bruinenberg, G. A. Heap, M. Platteel, A. W. Ryan, C. de Kovel, G. K. T. Holmes, P. D. Howdle, J. R. F. Walters, D. S. Sanders, C. J. J. Mulder, M. L. Mearin, W. H. M. Verbeek, V. Trimble, F. M. Stevens, D. Kelleher, D. Barisani, M. T. Bardella, R. McManus, D. A. van Heel, and C. Wijmenga. 2009. Coeliac disease-associated risk variants in TNFAIP3 and REL implicate altered NF-kappaB signalling. *Gut* 58: 1078–1083.
678. Nair, R. P., K. C. Duffin, C. Helms, J. Ding, P. E. Stuart, D. Goldgar, J. E. Gudjonsson, Y. Li, T. Tejasvi, B.-J. Feng, A. Ruether, S. Schreiber, M. Weichenthal, D. Gladman, P. Rahman, S. J. Schrodi, S. Prahalad, S. L. Guthery, J. Fischer, W. Liao, P.-Y. Kwok, A. Menter, G. M. Lathrop, C. A. Wise, A. B. Begovich, J. J. Voorhees, J. T. Elder,

- G. G. Krueger, A. M. Bowcock, G. R. Abecasis, Collaborative Association Study of Psoriasis. 2009. Genome-wide scan reveals association of psoriasis with IL-23 and NF-kappaB pathways. *Nat. Genet.* 41: 199–204.
679. Elder, J. T. 2009. Genome-wide association scan yields new insights into the immunopathogenesis of psoriasis. *Genes Immun.* 10: 201–209.
680. Zou, J. X., J. Braun, and J. Sieper. 2002. Immunological basis for the use of TNFalpha-blocking agents in ankylosing spondylitis and immunological changes during treatment. *Clin Exp Rheumatol* 20: S34–7.
681. Wang, C., S. G. Kang, J. Lee, Z. Sun, and C. H. Kim. 2009. The roles of CCR6 in migration of Th17 cells and regulation of effector T-cell balance in the gut. *Mucosal Immunol* 2: 173–183.
682. Schutyser, E., S. Struyf, and J. Van Damme. 2003. The CC chemokine CCL20 and its receptor CCR6. *Cytokine Growth Factor Rev.* 14: 409–426.
683. Kleinschek, M. A., K. Boniface, S. Sadekova, J. Grein, E. E. Murphy, S. P. Turner, L. Raskin, B. Desai, W. A. Faubion, R. de Waal Malefyt, R. H. Pierce, T. McClanahan, and R. A. Kastelein. 2009. Circulating and gut-resident human Th17 cells express CD161 and promote intestinal inflammation. *Journal of Experimental Medicine* 206: 525–534.
684. Karaderi, T., D. Harvey, C. Farrar, L. H. Appleton, M. A. Stone, R. D. Sturrock, M. A. Brown, P. Wordsworth, and J. J. Pointon. 2009. Association between the interleukin 23 receptor and ankylosing spondylitis is confirmed by a new UK case-control study and meta-analysis of published series. *Rheumatology (Oxford)* 48: 386–389.
685. Song, I. H., M. Rudwaleit, J. Listing, and J. Sieper. 2009. Comparison of the Bath Ankylosing Spondylitis Disease Activity Index and a modified version of the index in assessing disease activity in patients with ankylosing spondylitis without peripheral manifestations. *Ann Rheum Dis* 68: 1701–1707.
686. Spoorenberg, A., D. van der Heijde, E. de Klerk, M. Dougados, K. de Vlam, H. Mielants, H. van der Tempel, and S. van der Linden. 1999. Relative value of erythrocyte sedimentation rate and C-reactive protein in assessment of disease activity in ankylosing spondylitis. *J Rheumatol* 26: 980–984.
687. Visvanathan, S., C. Wagner, J. C. Marini, D. Baker, T. Gathany, J. Han, D. van der Heijde, and J. Braun. 2008. Inflammatory biomarkers, disease activity and spinal disease measures in patients with ankylosing spondylitis after treatment with infliximab. *Ann Rheum Dis* 67: 511–517.
688. Baeten, D., F. De Keyser, N. Van Damme, E. M. Veys, and H. Mielants. 2002. Influence of the gut and cytokine patterns in spondyloarthropathy. *Clin Exp Rheumatol* 20: S38–42.
689. Cho, J. H. 2008. The genetics and immunopathogenesis of inflammatory bowel disease. *Nat Rev Immunol* 8: 458–466.
690. Grimm, M. C., W. E. Pullman, G. M. Bennett, P. J. Sullivan, P. Pavli, and W. F. Doe. 1995. Direct evidence of monocyte recruitment to inflammatory bowel disease mucosa. *J. Gastroenterol. Hepatol.* 10: 387–395.
691. Kamada, N., T. Hisamatsu, H. Honda, T. Kobayashi, H. Chinen, M. T. Kitazume, T. Takayama, S. Okamoto, K. Koganei, A. Sugita, T. Kanai, and T. Hibi. 2009. Human CD14+ macrophages in intestinal lamina propria exhibit potent antigen-presenting ability. *The Journal of Immunology* 183: 1724–1731.
692. Baumgart, D. C., S. Thomas, I. Przesdzing, D. Metzke, C. Bielecki, S. M. Lehmann, S. Lehnardt, Y. Dörffel, A. Sturm, A. Scheffold, J. Schmitz, and A. Radbruch. 2009. Exaggerated inflammatory response of primary human myeloid dendritic cells to lipopolysaccharide in patients with inflammatory bowel disease. *Clin Exp Immunol* 157: 423–436.
693. Platt, A. M., C. C. Bain, Y. Bordon, D. P. Sester, and A. M. Mowat. 2010. An independent subset of TLR expressing CCR2-dependent macrophages promotes colonic inflammation. *The Journal of Immunology* 184: 6843–6854.

694. Baumgart, D. C., D. Metzke, O. Guckelberger, A. Pascher, C. Grötzing, I. Przesdzin, Y. Dörffel, J. Schmitz, and S. Thomas. 2011. Aberrant plasmacytoid dendritic cell distribution and function in patients with Crohn's disease and ulcerative colitis. *Clin Exp Immunol* 166: 46–54.
695. Middel, P., D. Raddatz, B. Gunawan, F. Haller, and H.-J. Radzun. 2006. Increased number of mature dendritic cells in Crohn's disease: evidence for a chemokine mediated retention mechanism. *Gut* 55: 220–227.
696. Hugot, J. P., M. Chamaillard, H. Zouali, S. Lesage, J. P. Cézard, J. Belaiche, S. Almer, C. Tysk, C. A. O'Morain, M. Gassull, V. Binder, Y. Finkel, A. Cortot, R. Modigliani, P. Laurent-Puig, C. Gower-Rousseau, J. Macry, J. F. Colombel, M. Sahbatou, and G. Thomas. 2001. Association of NOD2 leucine-rich repeat variants with susceptibility to Crohn's disease. *Nature* 411: 599–603.
697. Schreiber, S., S. Nikolaus, and J. Hampe. 1998. Activation of nuclear factor kappa B inflammatory bowel disease. *Gut* 42: 477–484.
698. Baba, N., V. Q. Van, K. Wakahara, M. Rubio, G. Fortin, B. Panzini, G. Soucy, R. Wassef, C. Richard, R. Tamaz, R. Lahaie, E. J. Bernard, Y. Caussignac, R. Leduc, R. Lougnarath, C. Bergeron, M. A. Racicot, F. Bergeron, M. A. Panzini, P. Demetter, D. Franchimont, K. Schäkel, G. Weckbecker, F. Kolbinger, C. Heusser, T. Huber, K. Welzenbach, and M. Sarfati. 2013. CD47 fusion protein targets CD172a+ cells in Crohn's disease and dampens the production of IL-1 and TNF. *Journal of Experimental Medicine* 210: 1251–1263.
699. Bernardo, D., S. Vallejo-Díez, E. R. Mann, H. O. Al-Hassi, B. Martínez-Abad, E. Montalvillo, C. T. Tee, A. U. Muruganathan, H. Núñez, S. T. C. Peake, A. L. Hart, L. Fernández-Salazar, J. A. Garrote, E. Arranz, and S. C. Knight. 2012. IL-6 promotes immune responses in human ulcerative colitis and induces a skin-homing phenotype in the dendritic cells and Tcells they stimulate. *Eur J Immunol* 42: 1337–1353.
700. Mahida, Y. R., A. M. Galvin, T. Gray, S. Makh, M. E. McAlindon, H. F. Sewell, and D. K. Podolsky. 1997. Migration of human intestinal lamina propria lymphocytes, macrophages and eosinophils following the loss of surface epithelial cells. *Clin Exp Immunol* 109: 377–386.
701. Candia, E., D. Díaz-Jiménez, P. Langjahr, L. E. Núñez, M. de la Fuente, N. Farfán, F. López-Kostner, M. Abedrapo, M. Alvarez-Lobos, G. Pinedo, C. J. Beltrán, C. González, M.-J. González, R. Quera, and M. A. Hermoso. 2012. Increased production of soluble TLR2 by lamina propria mononuclear cells from ulcerative colitis patients. *Immunobiology* 217: 634–642.
702. Mittag, D., A. I. Proietto, T. Loudovaris, S. I. Mannering, D. Vremec, K. Shortman, L. Wu, and L. C. Harrison. 2011. Human Dendritic Cell Subsets from Spleen and Blood Are Similar in Phenotype and Function but Modified by Donor Health Status. *The Journal of Immunology* 186: 6207–6217.
703. Geijtenbeek, T. G. H., R. Torensma, S. J. van Vliet, G. C. F. van Duijnhoven, G. J. Adema, Y. van Kooyk, and C. G. Figdor. 2000. Geijtenbeek, T.B.H. 100: 575–585.
704. Soilleux, E. J., L. S. Morris, G. Leslie, J. Chehimi, Q. Luo, E. Levroney, J. Trowsdale, L. J. Montaner, R. W. Doms, D. Weissman, N. Coleman, and B. Lee. 2002. Constitutive and induced expression of DC-SIGN on dendritic cell and macrophage subpopulations in situ and in vitro. *J Leukoc Biol* 71: 445–457.
705. Hesse, C., W. Ginter, T. Förg, C. T. Mayer, A. M. Baru, C. Arnold-Schrauf, W. W. J. Unger, H. Kalay, Y. van Kooyk, L. Berod, and T. Sparwasser. 2013. In vivo targeting of human DC-SIGN drastically enhances CD8(+) T-cell-mediated protective immunity. *Eur J Immunol*.
706. Laukens, D., H. Peeters, B. V. Cruyssen, T. Boonefaes, D. Elewaut, F. De Keyser, H. Mielants, C. Cuvelier, E. M. Veys, K. Knecht, P. Van Hummelen, E. Remaut, L. Steidler, M. De Vos, and P. Rottiers. 2006. Altered gut transcriptome in spondyloarthritis. *Ann Rheum Dis* 65: 1293–1300.

707. Lamarque, D., J. T. V. Nhieu, M. Breban, C. Bernardeau, N. Martin-Garcia, Z. Szepes, J.-C. Delchier, B. Whittle, and P. Claudepierre. 2003. Lymphocytic infiltration and expression of inducible nitric oxide synthase in human duodenal and colonic mucosa is a characteristic feature of ankylosing spondylitis. *J Rheumatol* 30: 2428–2436.
708. Hedl, M., J. Li, J. H. Cho, and C. Abraham. 2007. Chronic stimulation of Nod2 mediates tolerance to bacterial products. *Proc Natl Acad Sci USA* 104: 19440–19445.
709. Mahida, Y. R., S. Patel, P. Gionchetti, D. Vaux, and D. P. Jewell. 1989. Macrophage subpopulations in lamina propria of normal and inflamed colon and terminal ileum. *Gut* 30: 826–834.
710. Kamada, N., T. Hisamatsu, S. Okamoto, T. Sato, K. Matsuoka, K. Arai, T. Nakai, A. Hasegawa, N. Inoue, N. Watanabe, K. S. Akagawa, and T. Hibi. 2005. Abnormally differentiated subsets of intestinal macrophage play a key role in Th1-dominant chronic colitis through excess production of IL-12 and IL-23 in response to bacteria. *J Immunol* 175: 6900–6908.
711. Jimenez, F., M. P. Quinones, H. G. Martinez, C. A. Estrada, K. Clark, E. Garavito, J. Ibarra, P. C. Melby, and S. S. Ahuja. 2010. CCR2 plays a critical role in dendritic cell maturation: possible role of CCL2 and NF-kappa B. *The Journal of Immunology* 184: 5571–5581.
712. Baba, T., Y. Nakamoto, and N. Mukaida. 2009. Crucial contribution of thymic Sirp alpha+ conventional dendritic cells to central tolerance against blood-borne antigens in a CCR2-dependent manner. *The Journal of Immunology* 183: 3053–3063.
713. Baba, T., M. E. S. Badr, U. Tomaru, A. Ishizu, and N. Mukaida. 2012. Novel process of intrathymic tumor-immune tolerance through CCR2-mediated recruitment of Sirpα+ dendritic cells: a murine model. *PLoS ONE* 7: e41154.
714. Hashimoto, D., A. Chow, C. Noizat, P. Teo, M. B. Beasley, M. Leboeuf, C. D. Becker, P. See, J. Price, D. Lucas, M. Greter, A. Mortha, S. W. Boyer, E. C. Forsberg, M. Tanaka, N. Van Rooijen, A. García-Sastre, E. R. Stanley, F. Ginhoux, P. S. Frenette, and M. Merad. 2013. Tissue-resident macrophages self-maintain locally throughout adult life with minimal contribution from circulating monocytes. *Immunity* 38: 792–804.
715. Schulz, C., E. G. Perdiguero, L. Chorro, H. Szabo-Rogers, N. Cagnard, K. Kierdorf, M. Prinz, B. Wu, S. E. W. Jacobsen, J. W. Pollard, J. Frampton, K. J. Liu, and F. Geissmann. 2012. A Lineage of Myeloid Cells Independent of Myb and Hematopoietic Stem Cells. *Science* 336: 86–90.
716. Allison, M. C., and L. W. Poulter. 1991. Changes in phenotypically distinct mucosal macrophage populations may be a prerequisite for the development of inflammatory bowel disease. *Clin Exp Immunol* 85: 504–509.
717. Hosszu, K. K., A. Valentino, U. Vinayagasundaram, R. Vinayagasundaram, M. G. Joyce, Y. Ji, E. I. B. Peerschke, and B. Ghebrehiwet. 2012. DC-SIGN, C1q, and gC1qR form a trimolecular receptor complex on the surface of monocyte-derived immature dendritic cells. *Blood* 120: 1228–1236.
718. Simon, G. L., and S. L. Gorbach. 1984. Intestinal flora in health and disease. *Gastroenterology* 86: 174–193.
719. GUARNER, F., and J. MALAGELADA. 2003. Gut flora in health and disease. *The Lancet* 361: 512–519.
720. Chorro, L., A. Sarde, M. Li, K. J. Woollard, P. Chambon, B. Malissen, A. Kissenpfennig, J.-B. Barbaroux, R. Groves, and F. Geissmann. 2009. Langerhans cell (LC) proliferation mediates neonatal development, homeostasis, and inflammation-associated expansion of the epidermal LC network. *Journal of Experimental Medicine* 206: 3089–3100.
721. Hoeffel, G., Y. Wang, M. Greter, P. See, P. Teo, B. Malleret, M. Leboeuf, D. Low, G. Oller, F. Almeida, S. H. Y. Choy, M. Grisotto, L. Renia, S. J. Conway, E. R. Stanley, J. K. Y. Chan, L. G. Ng, I. M. Samokhvalov, M. Merad, and F. Ginhoux. 2012. Adult Langerhans cells derive predominantly from embryonic fetal liver monocytes with a minor

- contribution of yolk sac-derived macrophages. *Journal of Experimental Medicine* 209: 1167–1181.
722. Ajami, B., J. L. Bennett, C. Krieger, W. Tetzlaff, and F. M. V. Rossi. 2007. Local self-renewal can sustain CNS microglia maintenance and function throughout adult life. *Nat. Neurosci.* 10: 1538–1543.
723. Ginhoux, F., M. Greter, M. Leboeuf, S. Nandi, P. See, S. Gokhan, M. F. Mehler, S. J. Conway, L. G. Ng, E. R. Stanley, I. M. Samokhvalov, and M. Merad. 2010. Fate mapping analysis reveals that adult microglia derive from primitive macrophages. *Science* 330: 841–845.
724. Guilliams, M., I. De Kler, S. Henri, S. Post, L. Vanhoutte, S. De Prijck, K. Deswarte, B. Malissen, H. Hammad, and B. N. Lambrecht. 2013. Alveolar macrophages develop from fetal monocytes that differentiate into long-lived cells in the first week of life via GM-CSF. *Journal of Experimental Medicine*.